FINAL REPORT SUBMITTED TO THE BANK
BY THE PROJECT TEAM

RAINS-ASIA:
AN ASSESSMENT MODEL FOR AIR POLLUTION IN ASIA

Wes Foell, Markus Amann, Greg Carmichael, Michael Chadwick, Jean-Paul Hettelingh, Leen Hordijk, Zhao Dianwu (eds.)

Report on the World Bank Sponsored Project
"Acid Rain and Emission Reductions in Asia"

December 1995

FINAL REPORT SUBMITTED TO THE BANK
BY THE PROJECT TEAM

RAINS-ASIA: AN ASSESSMENT MODEL FOR AIR POLLUTION IN ASIA

Wes Foell, Markus Amann, Greg Carmichael, Michael Chadwick, Jean-Paul Hettelingh, Leen Hordijk, Zhao Dianwu (eds.)

Report on the World Bank Sponsored Project
"Acid Rain and Emission Reductions in Asia"

December 1995

ACKNOWLEDGMENTS

The RAINS-Asia program is a collaborative effort involving several research institutions in Asia, Europe and North America (see **Chapter I** for a complete list of participating institutions). This effort was supported with active participation from Ministries and agencies in Asian countries.

This report is prepared by the project team. The project team members are Wesley Foell and Collin Green of Resource Management Associates, Wisconsin, USA; Gregory Carmichael of the University of Iowa, USA; Jean-Paul Hettelingh of the National Institute of Public Health and the Environment, Netherlands; Leen Hordijk of the Center for Environmental Studies, Netherlands; and Markus Amann of the International Institute for Applied Systems Analysis, Austria.

The RAINS-Asia report and model were peer-reviewed by an international team of scientists: H. Dovland of the Norwegian Institute for Air Research, Norway; R.K. Pachauri of the Tata Energy Research Institute, India; B. Lübkert-Alcamo from the National Institute for Public Health and the Environment, Netherlands; B. Schärer from the Federal Environmental Agency, Germany; D. M. Whelpdale from the Atmospheric Environment Service, Canada; H. Ueda from Kyushu University, Japan; K. Bull from the Institute of Terrestrial Ecology, United Kingdom; Sijin Lee from Kyong-gi University, Republic of Korea; K.C. Moon from the Korean Institute of Science and Technology, Korea; and S. Seki from the Environment Agency, Japan. Special acknowledgments are due to the Internal Steering Committee at the World Bank, consisting of Anil Malhotra, Dennis Anderson, Arun Sanghvi, Todd Johnson, Carl-Heinz Mumme, Joseph Gilling, Mudassar Imran, Achilles Adamantiades, and Charles Feinstein. The task managers for the program are Jitendra Shah at the World Bank (with overall management guidance from Maritta Koch-Weser), and Ali Azimi at the Asian Development Bank (with overall management guidance from Bindu Lohani). Margret Gottsleben of IIASA, Marianne Weismann and Peter de Smet, of RIVM-CCE are acknowledged for editing and lay out of the final report.

The RAINS-Asia program was developed with the assistance of grants from the Royal Norwegian Ministry of Foreign Affairs, the Norwegian Consultant Trust Funds, the Netherlands Consultant Trust Funds, the Swedish Consultant Trust Funds, the Asian Development Bank, and in-kind contributions from participating institutions.

TABLE OF CONTENTS

1. INTRODUCTION

Authors:
Leen Hordijk, Wes Foell, Jitendra Shah

1.1 Acid rain in Asia: the problem I-1
1.2 Project history I-7
1.3 Goal of the projects I-8
1.4 Terms of Reference for the Program I-9
A. Energy and emissions module I-9
B. Atmospheric transport and deposition module I-10
C. Ecosystem sensitivity evaluation and mapping I-11
D. Critical load evaluation and model integration modules I-11
E. Asian countries data collection and institutional development I-13
1.5 Major meetings and workshops held during the project I-14
1.6 Team and network in Asia I-14
References I-17

2. INTEGRATED ASSESSMENT

Authors:
Markus Amann, Janusz Cofala, Leen Hordijk

2.1 Introduction II-1
2.2 Integrated assessment of air pollution in Asia II-1
2.3 Relevant policy questions II-2
2.4 The concept of integrated assessment of air pollution in Asia II-3
2.5 The RAINS model - an overview II-6
The Regional Energy Scenario Generator (RESGEN) Module II-8
Energy and Emission (ENEM) Module II-9
Atmospheric Transport and Deposition (ATMOS) Sub-Module II-10
Environmental Impact and Critical Loads (IMPACT) Module II-10
2.6 Implementation II-11

3. ENERGY MODULE

Authors: Collin Green, John Legler, Ashok Sarkar, Wes Foell

With contributions from: Markus Amann, Janusz Cofala, Torleif Haugland, Ram Shrestha, and Sribas Bhattacharya

3.1 Introduction III-1
3.1.1 Background III-1
3.1.2 Specific Objectives III-3
3.1.3 Major Capabilities and the Use of RESGEN III-6

3.2 Overview of Methodology III-8
3.2.1 General Discussion III-8
Regions III-9
3.2.2 General Structure of RESGEN III-14
3.2.3 Detailed Discussion III-16
Sectoral end-use energy consumption III-16
Residential sector
Commercial sector
Agricultural sector
Industrial sector
Transportation sector
Energy supply sector III-21
Electricity generation sector
3.3 RESGEN and RAINS-ASIA Databases III-26
3.3.1 Institutional Process III-26
3.3.2 Data Requirements III-27
Scope III-27
Geographic Definitions
Temporal Definitions
Database Description of the RESGEN Databases III-28
Socioeconomic Database
Energy Database
Fuel Characteristics Data
Large Point Source Data for Power Plants
3.3.3 Status of Regional Database III-29

3.4 Energy Scenario Assumptions III-32
3.4.1 Socioeconomic Factors III-32
Population III-32
Gross Domestic Product III-32
3.4.2 Technology III-38
3.4.3 Fuel Types III-38
3.4.4 Regional (Subcountry) Fuel Allocation Assumptions III-38
3.4.5 Power Supply Assumptions III-40

3.5 Energy/Economic Analysis III-41

3.5.1 Overview III-41
3.5.2 China country description III-41
3.5.3 India country description III-43
3.5.4 Indonesia country description III-44
3.5.5 South Korea country description III-46
3.5.6 Gas Trade in Asia III-47

3.6 Energy Scenario Results III-47

3.7 Summary and Conclusions III-60

3.8 References III-62

4. MISSIONS AND CONTROL

Authors:
David Streets, Markus Amann, Neelo Bhatti, Janusz Cofala, Collin Green

4.1 Introduction IV-1
4.2 The gridded emissions inventory (1987-88) IV-3
4.2.1 Methodology and assumptions IV-4
4.2.2 National emissions totals IV-9
4.3 Current and future emissions in ENEM IV-14
4.3.1 Methodology, data, and assumptions IV-14
4.3.2 Regional and national emission totals IV-20
4.4 Technical emission control options and costs IV-24
4.4.1 Low sulfur fuels and fuel desulfurization IV-26
4.4.2 Desulfurization during or after combustion IV-27
4.4.3 Control of process emissions IV-34
4.4.4 Cost curves for SO_2 reduction IV-35
4.6 Conclusions and recommendations IV-37
REFERENCES IV-38

5. ATMOS MODULE
LONG RANGE TRANSPORT AND DEPOSITION OF SULFUR IN ASIA

Authors:
Gregory R. Carmichael and Richard L. Arndt

5.1 Summary V-1
5.2 Overview of ATMOS sub-project V-1
5.3. Acid deposition modeling V-2
5.3.1 Overview V-2
5.3.2 Modeling framework V-3
5.3.3 Policy issues V-6

5.4 Acid deposition modeling for Asia V-6
5.4.1 Description of the ATMOS model V-7
5.4.2 Transport calculation V-7
5.4.3 Concentration/deposition calculations V-10
5.4.4 Parameters used in model V-13
5.4.5 Input data V-15
5.4.6 Outputs V-20
5.5 ATMOS modeling results V-20
5.5.1 Sulfur deposition V-20
5.5.2 Source-receptor relationships V-24
5.5.3 Surface concentrations V-33
5.5.4 Preliminary model evaluation V-42
5.6 Monitoring and focal center activities V-42
5.6.1 Monitoring sulfur dioxide in East Asia V-42
5.6.2 Monitoring results V-43
5.6.3 Collaborations and focal center activities V-50
5.7 Other modeling activities V-52
5.7.1 Calcium deposition V-55
5.8 Uncertainty V-56
5.9 References V-57

6. ASSESSMENT OF ENVIRONMENTAL EFFECTS OF ACIDIC DEPOSITION

J.-P. Hettelingh, M.J. Chadwick, H. Sverdrup, D. Zhao (eds.)

6.1 Introduction VI-1
6.1.1 Direct and indirect effects VI-2
6.1.2 Critical load approach VI-4
6.1.3 The RAINS-ASIA IMPACT project VI-6
6.1.4 Organization of the chapter VI-7
6.2 Establishing sensitivity criteria for Asian ecosystems using two approaches VI-7
6.2.1 Introduction VI-7
6.2.2 Steady state mass balance approach VI-8
6.2.3 Data for the derivation of BC/Al ratios VI-9
6.2.4 The basis of the relative sensitivity approach VI-17
6.3 Background data and mapping the sensitivity in Asia VI-28
6.3.1 Introduction VI-28
6.3.2 Background for the sensitivity mapping VI-28
6.3.3 Data for sensitivity and critical load mapping VI-29
6.3.4 Mapping sensitivity in Asia VI-40
6.4 Computation and mapping of critical loads in Asia VI-45
6.4.1 Introduction VI-45
6.4.2 The Steady State Mass Balance Model VI-46
6.4.3 Results VI-49
6.5 Conclusions and recommendations VI-52
6.6 References VI-59

7. SCENARIOS OF FUTURE ACIDIFICATION IN ASIA: EXPLORATORY CALCULATIONS

Authors:
Markus Amann, Janusz Cofala

7.1 Introduction VII-1
7.2 Energy pathways VII-2
7.3 A reference emission scenario: base case energy path without additional measures to control emissions VII-4
7.3.1 Sulfur deposition VII-7
7.3.2 Achievement of critical loads for acid deposition VII-8
7.4 Exploring the technical potential for reducing SO_2 emissions: The BAT (Best Available Technology) scenario VII-12
7.5 An advanced emission control technology (ACT) scenario VII-14
7.6 A 'basic control technology' (BCT) scenario VII-17
7.7 A scenario with local applications of advanced technologies (LACT) VII-21
7.8 Relocation of plants in sensitive regions VII-25
7.9 Implications of the energy efficiency pathway VII-30
7.10 Conclusions VII-31
References VII-33

ANNEXES

Annex 1 CRITICAL BC/A1 RATIOS

Annex 2 DATA PRODUCTION AND RELIABILITY; RELATIVE BUFFERING RATES AND ESTIMATED WEATHERING RATES

Annex 3 APPLICATION AND EVALUATION OF CRITICAL LOAD METHODS FOR ACID DEPOSITION IN GUNMA, JAPAN

Annex 4 APPLICATION OF CRITICAL LOADS IN CHINA

Annex 5 SUMMARY REPORT OF IMPACT WORKSHOPS HELD AT RCEES, BEIJING.

RAINS-ASIA:
AN ASSESSMENT MODEL FOR AIR POLLUTION IN ASIA

Chapter 1

Introduction

Leen Hordijk, Wes Foell, Jitendra Shah

Report on the World Bank Sponsored Project
"Acid Rain and Emission Reductions in Asia"

December 1995

1. INTRODUCTION

Authors:
Leen Hordijk, Wes Foell, Jitendra Shah

TABLE OF CONTENTS

1.1 Acid rain in Asia: the problem I-1
1.2 Project history I-7
1.3 Goal of the projects I-8
1.4 Terms of Reference for the Program I-9
  A. Energy and emissions module I-9
  B. Atmospheric transport and deposition module I-10
  C. Ecosystem sensitivity evaluation and mapping I-11
  D. Critical load evaluation and model integration modules I-11
  E. Asian countries data collection and institutional development I-13
1.5 Major meetings and workshops held during the project I-14
1.6 Team and network in Asia I-14
References I-17

LIST OF TABLES

Table 1.1 Current and projected SO_2 emissions by region I-2
Table 1.2 Vulnerability of various Asian regions to acid deposition risk factors I-6

LIST OF FIGURES

Figure 1.1 Summary of Acid Deposition in Asia (Bhatti et al., 1991) I-4

1. INTRODUCTION

Authors:
Leen Hordijk, Wes Foell, Jitendra Shah

1.1 Acid rain in Asia: the problem

What is acid rain? Acid Rain is a term used to describe the result of atmospheric chemical reactions of pollutants such as SO_x and NO_x with naturally occurring atmospheric water and oxygen. The popular term "Acid Rain" includes both the wet deposition and dry deposition (SO_2 gas) on the environment. Anthropogenic emissions of acid rain precursors occur during the combustion of fossil fuels, especially coal, for energy production in the power, transport, industrial and residential and commercial sectors. The impacts of these emissions are felt at the local, national and regional scales, via air quality deterioration at the local level, and via the impacts of acid rain on ecosystems at the national and regional levels.

Acid rain has been an issue of widespread concern in Europe and North America for more than 15 years. Because of the heavy utilization of fossil fuels in industrial countries in the second half of this century, the acidity of rain has increased markedly, damaging lakes, soils, forests, and materials in many countries. In response, a number of countries have carried out major programs of monitoring, damage assessment, modeling, and analysis of various technical and economic strategies for mitigating the effects of acid deposition.

Although policy-makers in Europe and North America are still attempting to resolve issues related to the choice and implementation of acid rain control strategies, progress has clearly been made in decreasing acid deposition. This progress is based on a number of steps, including energy conservation and efficiency improvements, a shift away from using fossil fuels containing large quantities of acid rain precursors, deployment of emission control technologies, and existing or anticipated national and regional laws and agreements. In the Asia region, emissions of acid rain precursors are currently at high levels and expected to increase further given the rapid growth in energy consumption.

Growth in energy consumption in Asia. Many Asian countries have experienced rapid economic growth during the last two decades and this trend is expected to continue. Accompanying rapid economic growth is a gargantuan appetite for energy. At current growth rates, Asian energy demand is doubling every twelve years -- as compared to the world average of every twenty-eight years. The demand for electricity is growing even faster: two to three times faster than GDP for most of the rapidly industrializing East Asian countries and up to two times faster for most of South Asia. The amount of new investment being planned in the Asian power sector during the 1990s is two-thirds of all the power-related investments being made in the development world during this period. Over 80 percent of all energy is derived from fossil fuels and 95 percent from fossil and biomass fuels. Coal is the dominant energy source (58 percent in East Asia, and 39 percent in South Asia), and is expanding at 6.5 percent per year, a rate which exceeds regional economic growth.

Local impacts of emissions. Local air pollution is becoming a serious problem and high pollutant deposition levels are being measured in an increasing number of locations (Rodhe et al., 1988; Bhatti et al., 1991). Most of the air pollution problems identified in the nations of Asia are confined to localized areas of high emissions, usually associated with the densely populated metropolitan regions such as Bangkok, Beijing, Bombay, Calcutta, Delhi, Hong Kong, Jakarta, Kuala Lumpur, Manila, Shenyang, and Seoul and pollutant concentrations in most of these cities regularly exceed the World Health Organization (WHO) recommended limits for particulate matter and sometime for SO_2. Additional monitoring in these areas may uncover a more widespread pollution problem than is presently observed.

Transboundary impacts of emissions. The projected development of fossil fuel energy systems (mostly involving coal combustion), would entail greatly increased emissions of a wide range of substances of concern including, most prominently, acidifying compounds and greenhouse gases (Foell and Green, 1991). Because these would likely be emitted from large energy facilities with high stacks, they could decrease local effects but increase the long-range transport of these acidifying substances to potentially sensitive geographical areas. Table 1.1 shows the current and projected emissions of sulphur dioxide (SO_2) for Europe, USA, and Asia . The total projected SO_2 emissions for the Asian countries in 2000 and 2010 are 54 and 76 million tons, respectively. These estimates far exceed the estimated emissions of North America and Eastern/Western Europe combined.

Table 1.1 Current and projected SO_2 emissions by region

Region/country	1990	2000	2010
Europe	38	22	14
USA	21	15	14
Asia	34	53	78
China	22	34	48
India	4.5	6.6	10.9
Other	7.5	12.4	19.1

Sources:

Europe: Cofala, J., Schöpp, W., 1995: Assessing Future Acidification in Europe. Note prepared for the 15th Meeting of the UN/ECE Task Force on Integrated Assessment Modelling, May 1995, The Hague. IIASA, Laxenburg, Austria.

USA: Estimates obtained from National Acid Precipitation Assessment Program (NAPAP) Integrated Assesment. Draft Sept. 1990.

Asia: Reference scenario from Chapter 7 of this report.

Acid rain in Asia. Figure 1.1 gives an overview of the acid rain situation in Asia as estimated before the start of this study (Bhatti et al., 1991). Relative sulfur dioxide emissions in 1985 by country or region are indicated by vertical bars. Emissions are significant in China, India, Japan, and the Koreas and are small but growing very rapidly in several other countries of South and Southeast Asia. Deposition patterns of emissions are largely determined by wind flow patterns, shown by arrows in the figure. In winter (January) the flow is generally from the land mass to the ocean, while in summer (July) the reverse occurs. Typical monitored values of pH are shown in the circles. Low pH values, (e.g., 4.5) occur in Japan and Southern China where emissions are large; elsewhere the pH values are 6 to 7. Because of the paucity of monitoring sites, the probability of low pH's at other unsuspected locations is high.

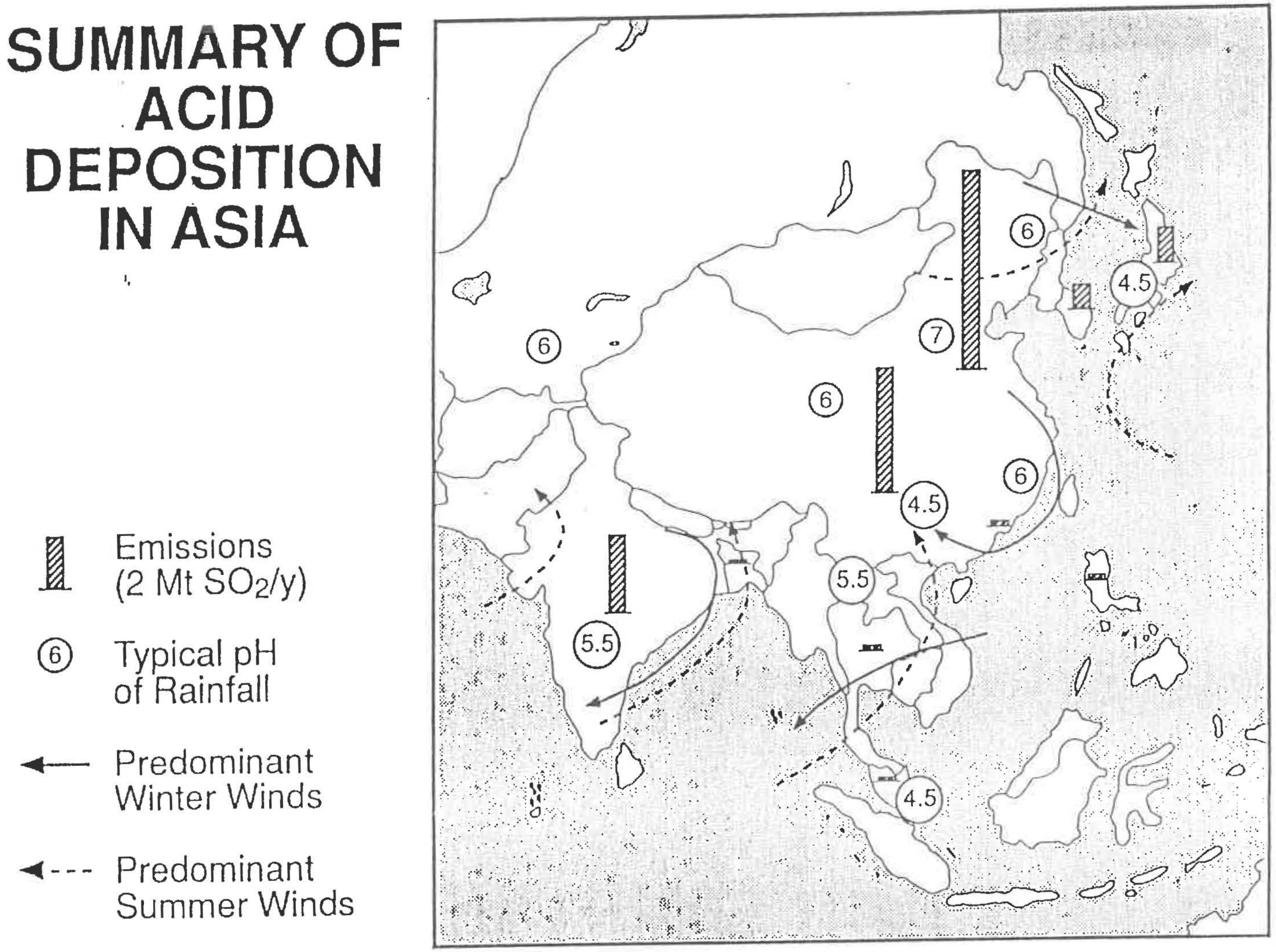

Figure 1.1 Summary of Acid Deposition in Asia (Bhatti et al., 1991)

Status of research. In Asia, where recognition of this phenomenon is just beginning, very little research has been conducted on the levels and impacts of acid deposition. However, available monitoring data show that the acidity of rainfall has been rising dramatically in some areas of the region. The degree to which this increased acidity is affecting Asian ecosystems is unknown at present. However, given the North American and European experience, impacts can be expected to be significant. Some of the ecosystems of the Asia region are similar to those found in areas of North America and Europe where the majority of the research on acid deposition impacts has been conducted. Thus, in some cases it should be possible to extrapolate the potential effects found in these western nations to the corresponding ecosystems of Asia. However, many other environments in Asia are very different from those for which acid deposition impacts have been studied, and research will have to be conducted to analyze and assess the relative vulnerability of these various anthropogenic and natural environments to acidic inputs.

Nevertheless, based on knowledge of the various components (i.e., soils, flora, fauna, climate, etc.) of the ecosystems in question, their relative vulnerability to acidic inputs and their distribution in the Asian region, it is possible to attempt to predict the potential effects of acidic deposition (Bhatti et al., 1991). For a given area to be at high risk from acidification, a number of conditions must be present simultaneously. First, the area must be receiving or at risk of receiving high levels of deposition. Second, the soils of the area must be sensitive to acidification, and the area must have vegetation, fauna, aquatic organisms, man-made materials and/or large human populations vulnerable to increased inputs of acidity. One attempt to assess these risks for the Asian region showed Japan, Korea, Southern China, and the mountainous regions of South-east Asia with the mountain zones of Southwestern India to be at greatest risk (Bhatti et al., 1991) (see Table 1.2).

In most Asian countries there does not seem to be either a strong scientific or a public constituency to address the potentially serious problems in the future for long-range transport and deposition of sulfur and nitrogen species, and for the consequent damage to ecosystems, health, and materials.

In addition to their global implications, the long-term and regional/local implications of these atmospheric emissions touch not only the natural environment, but also have far-reaching implications for important commercial and cultural activities such as forestry, agriculture, and tourism. The political ramifications of transboundary environmental pollution in Asia are also likely to be serious.

Table 1.2 Vulnerability of various Asian regions to acid deposition risk factors

	High emis-sions		High deposition		Sensitive soils	Sensitive vegetation and materials	High risk
Region	Current	Future	Current	Future			
NE China	X	X		X		X	
Japan, Korea			X (winter mostly)	X (winter mostly)	X	X	X
S China		X	X (winter mostly)	X (winter mostly)	X	X	X
SE Asia	X	X	X (local areas, summer mostly)	X (local areas, summer mostly)	X (mountain areas)	X (mountain areas)	X (mountain areas)
SE Asian islands	X	X	X (isolated, local)	X (isolated, local)	X (mountain areas)		
N India	X	X		X (summer)		X (Himalayan foothills)	
SW India			(borderline acidity)	X (winter)	X	X (mountain areas)	(borderline in mountain areas)
NE India		X		X (summer)	X		
Sri Lanka, Maldives			(borderline acidity)	X (winter)			
Siberia, N Mongolia				X (summer)		X	

Why RAINS-ASIA? In light of this outlook, the time has come to develop an integrated program of assessment and policy analysis for the purpose of analyzing long-term strategies for acid rain problems at national and at Asia-wide levels. A key component of such a program entails the application of the analytic and policy development experience gained in the West to this emerging issue in Asia. An analytical tool has been built to help decision-makers project future trends in emissions, estimate the regional consequences for acid deposition levels, evaluate the vulnerability of natural and artificial systems, and estimate the costs and effectiveness of alternative mitigative actions that might be taken. Such a policy analysis exercise can start to raise environmental awareness in the region and begin a dialogue that could help ameliorate (or prevent the worsening of) an environmental problem in the early stages.

The role of the World Bank. World Bank involvement would help the ongoing process of assisting countries in the Asia region incorporate environmental considerations into the developing strategies. The Bank is active at the national levels through assistance to countries to prepare and implement National Environmental Action Plans, and at the global level through partnership in the Global Environmental Facility. Increasingly, the Bank is beginning to assist countries work together to understand the causes and impacts of regional or common environmental problems and explore mitigatory options, as a means to facilitating countries meet their obligations under international or regional treaties. Further, by using RAINS-ASIA, the Bank should be able to minimize the acid rain related environmental consequences of its work in the power and industrial sectors in Asia, and adopt a environmentally proactive development strategy.

1.2 Project history

This project has its institutional genesis in 1989. At that time there was a small but growing recognition of the potential air pollution problems resulting from the massive growth of fossil fuel use in Asia. In response to the above concern, an effort to explore mechanisms to bring together a group of prominent scientists to assess the magnitude of the problem and to recommend needed actions began. This resulted in the convening of a small group of international specialists on acid rain at Asian Institute of Technology (AIT) in Bangkok, Thailand in November, 1989, with the financial support of the U.S. Department of Energy. The objectives of this small workshop were to assess the status of existing or potential acid rain issues in several Asian countries; to review relevant experiences in Europe and North America; and if appropriate, to begin to plan and design a follow-up research/action program.

First conference in 1989. The AIT workshop brought together a considerable body of international knowledge and experience dealing with acid rain problems. The participants were chosen to represent the entire spectrum of issues and expertise, ranging from energy technologies and pollutant emissions, all the way through the cause-effect chain to the ultimate damage of natural and manmade systems. Participants from Asia included specialists from several of the Asia countries with greatest concerns about acid rain, including China, India, Thailand, Indonesia, and Korea, the United Nations Environmental Program (UNEP), and several energy/environment scientists from AIT.

As a result of its review of the current and future situation in Asia, the workshop concluded that acid deposition had the potential to cause significant damage in Asia. In China there already appeared to be considerable evidence of the effects. The participants were greatly concerned by the implications of the planned initiatives for accelerated development of massive fossil-fuel energy systems in many Asia nations, which could entail greatly increased emission of acid deposition precursors. Because these would likely be emitted from large energy facilities with high stacks they could increase the transport of these acidifying substances to sensitive geographical areas.

Based on the above conclusions, the Workshop participants recommended the development of an intensified monitoring program in Asia and the development of a program for research on pollutant transportation/transformation and on the impact of acid depositions on natural and man-made systems. In addition the participants strongly recommended that an integrative program of assessment and policy analysis be developed for the purpose of analyzing long-term strategies for acid rain problems at national and Asia-wide levels. This initial conference became the first of a series of "Annual Conferences on Acid Rain and Emissions Reduction in Asia".

Second conference on Acid Rain. In November 1990, an expanded group of prominent experts attended a "Second Annual Conference on Acid Rain and Emissions Reduction in Asia" at AIT under the broader sponsorship of the U.S. Department of Energy, the World Bank, UNEP, and ESCAP. It had the objective of reviewing the problem in more depth, and if appropriate, to lay out a detailed program and plan of action. At this conference, several papers were presented and discussed (AIT 1990) which provided a further quantified understanding of the current status and potential of the acid rain problem in Asia. Major results included: (1) a survey paper (Bhatti, et al. 1991) which gave a broad perspective of the issues; and, (2) the first Asia-wide estimate of acid precursors through the year 2010 (Foell and Green, 1991).

Based on the discussions at this Conference, a phased integrated policy analysis framework was planned. The plan included personnel and resource requirements, schedules, institutional statements of interest and responsibilities from approximately 14 institutions through Asia, Europe, and North America. In the addition, for the first time, the conference produced a Proceedings, containing several papers presented at the conference (Foell and Sharma, 1991). A major outcome and follow-up of this conference was a growing awareness of the potential acidification and air pollution problems in Asia. This included increased interest within national governments and research organizations, as well as in the international community, including UNEP, ESCAP, ADB and the World Bank.

<u>World Bank - Asian Development Bank involvement</u>. In early 1991 the World Bank expressed interest in a project which focussed on the development of a policy-oriented assessment tool to address acid rain related issues. Based on the earlier discussions the possibility of adapting to Asia the RAINS model, developed by IIASA for acid rain assessment in Europe was explored. At the third annual conference, held at AIT in November 1991, with environmental officials of the World Bank and ADB in attendance, detailed project plans and agreements were developed for a so-called RAINS-ASIA project. Using the RAINS model as the analytical framework for the project, the conference produced a specific written proposal to the two multilateral banks as discussed below. In addition a Conference Proceedings was published laying out major technical frameworks for the anticipated research (Foell and Green, 1992).

1.3 Goal of the projects

In recent years, integrated assessment models have been utilized for international negotiations on acid rain. The purpose of these models is to provide negotiators or regulators with a full regional picture of the problems associated with the entire causal process from energy systems and emissions through to the ultimate impact on natural and man-made systems. The model user can analyze the regional and national implications of various scenarios, which include options for energy use, control strategies, and mitigation policies. Such an effort for the acid rain problem in Europe has led to the Regional Acidification INformation and Simulation (RAINS-EUROPE) model.This model has increasingly been used for policy analysis under the Convention on Long-range Transboundary Air Pollution (United Nations, Geneva). Most recently the RAINS-EUROPE model has been used in the negotiations that led to the signing of the Second Sulfur Protocol. This Protocol contains SO_2 emission reduction requirements for the 33 Signatories which have largely been based on calculations with RAINS-EUROPE.

In 1992 the World Bank commissioned several research institutes to develop the first phase of a complete assessment methodology of the acid rain impacts for Asia, as done for Europe. To achieve this goal in phase 1 of the project, the experience collected in the construction and use of the RAINS-EUROPE model was used to create RAINS-ASIA. Additional expertise on the specific Asian situation was added to the research team. RAINS-ASIA was aimed to be an integrated acid rain and emissions policy analysis model for the development of national and regional policy perspectives in Asia. The model design includes the entire causal chain from energy systems and emissions through to the ultimate impact on natural and man-made systems.

Similar to the RAINS model for Europe, RAINS-ASIA consists of three modules, each describing a part of the cause-effect chain. The modular structure of RAINS-ASIA will allow for easy replacement of individual modules when knowledge progresses. The four basic modules of the RAINS model are:

1. Regional Energy Scenario Generation Module (RESGEN)
2. Energy and emissions module (ENEM)
3. Atmospheric module (ATMOS)
4. Impacts module (IMPACT)

The RAINS-ASIA model covers the countries of East, South, and South-East Asia, with particular focus on China, India, Thailand, and North and South Korea (10^o South to 55^o North in latitude and 60^o to 150^o East in longitude). The temporal range of all the model is 1990 - 2020 with time resolution of one year. RAINS-ASIA has been implemented on a PC.

In addition, the Regional Energy Scenario Generator (RESGEN) has been developed. RESGEN output is directly linked to RAINS-ASIA.

1.4 Terms of Reference for the Program

The development of the RAINS-ASIA model took place as a collaborative effort involving several international institutions. The RAINS-ASIA program included development of several components:

(a) Energy and Emissions Module and Energy Economic Analysis;
(b) Atmospheric Transport and Deposition Module;
(c) Ecosystem Sensitivity Evaluation and Mapping for Asia;
(d) Critical Load Evaluation and Model Integration Modules; and,
(e) Asian Countries Data Collection and Institutional Development.

Separate consulting contracts were prepared for each of these components. The first four components were funded through the World Bank while a separate contract for the fifth component was prepared by the Asian Development Bank (ADB). This report is for the model development projects financed by the World Bank. The results of ADB Asian Countries data gathering effort project through AIT has been reported in a separate report.

A. ENERGY AND EMISSIONS MODULE

The Energy and Emissions module development for RAINS-ASIA included:

(i) Development of a policy-based energy/emissions module for front-end interfacing with

RAINS-ASIA. The model structure shall be based on the definition of the regions of interest and the level of sub-country analysis necessary to produce the required gridded energy and emission data for baseline and scenario emission inventories.

(ii) Construct a detailed protocol to define the methodology for data collection of country and sub-country specific data on Asian energy and economic systems.

(iii) Create a preliminary emissions inventory for the Asian region for a base year on the basis of 1^{0} by 1^{0} grid resolution. This emissions inventory shall differentiate between the location of point and area sources as needed for the atmospheric transport calculations and shall try to incorporate season variations in emission patterns.

(iv) Integrate all appropriate collected and assimilated data into the energy/emissions model.

(v) Develop baseline and future energy/emission scenarios, based on the revised regional sub-country energy/emissions model. This includes initial model runs, model testing, and development of the baseline energy/emissions scenario.

Energy/Economic Analysis

The Energy/Economic Analysis for RAINS-ASIA included the following:

(i) Provide important national information on which to base a thorough analysis of the potential for energy conservation, efficiency and fuel substitution;

(ii) Apply a "top-down" econometric model of energy and emission to a few Asian countries, particularly China, India, S.Korea and Indonesia;

(iii) Identify and evaluate information needed for the development of alternative scenarios and develop insight into the analysis of economic impacts of efficiency improvements and fuel substitutions; and,

(iv) Initiate an analysis at macro scale of the institutional, financial and resource constraints to fuel substitution and energy sector development.

B. ATMOSPHERIC TRANSPORT AND DEPOSITION MODULE

The Atmospheric transport and deposition sub-module development for RAINS-ASIA included:

(i) Develop an acid deposition dispersion model for use in Asia. The Asian domain shall consist of the window bounded by 10^{0} South to 55^{0} North latitude, and 60^{0} to 160^{0} East longitude and should treat emissions from elevated sources.

(ii) Select model parameters (dry deposition velocities, reaction rates, dispersion parameters) which are appropriate for Asian applications. Asia specific parameters must take into account high levels of dust, and tropical conditions. Sensitivity calculations shall be performed to identify key input parameters.

(iii) Select base year for calculation of annual deposition. Special attention to be paid to select representative meteorological conditions.

(iv) Calculate annual sulfur deposition (wet, dry and total) on a grid to grid basis for a complete annual cycle. Sulfur dioxide and sulfate surface concentrations shall also be calculated.

(v) Develop appropriate post processing tools to calculate the transfer matrices needed by the RAINS model, calculate country-to-country matrices, and display the data on regional and sub-regional basis.

(vi) Identify observational data in Asia on sulfur dioxide and sulfate ambient concentrations, and precipitation sulfate, for use in model verification. Preliminary model performance evaluation shall be initiated.

(vii) Obtain data on the base-cation composition of anthropogenic and natural aerosol components in Asian countries. Locate regions of natural emissions and identify seasonal dependence. This information shall be used in future studies estimating base-cation deposition in Asia.

(viii) Establish a network of scientists and principal contacts in Asia to coordinate the development and application of the atmospheric model in Asia.

(ix) Deliver the dispersion model for use as tool to study long range transport of air pollutants in the Asia region. This model shall be used outside of the RAINS-ASIA model.

C. ECOSYSTEM SENSITIVITY EVALUATION AND MAPPING

The development of an Ecosystem Sensitivity Evaluation and Mapping for Asia module for RAINS-ASIA and included:

(i) Enhancement of data collection, digitization, GIS manipulation and production of interim maps for review and assessment. Activities will include: collection of maps and digital data; land use data; soil type, geology, precipitation, evaporation, and GIS manipulation; and methodology refinement.

(ii) Organize a scoping meeting on the final methodology including establishment of sensitivity and critical load relationship criteria.

(iii) Participate in workshops to discuss sensitivity mapping and assignment of critical loads for the region.

(iv) Coordinate with other components including critical load maps preparation.

D. CRITICAL LOAD EVALUATION AND MODEL INTEGRATION MODULES

The work on the Critical Load Evaluation module for RAINS-ASIA included the following:

(i) The sensitivity of Asian ecosystems shall be described by means of preliminary computed critical loads. A review and contacting of the Asian institutes for the exchange of methodologies, maps and data for critical load evaluation shall be initialized during the project;

(ii) Expansion of the application of critical load assessment methodology in Asia in collaboration with Asian scientists working on other components. The methodology for the computation of critical loads in Asia shall be examined using existing data which will be digitized and made available through other project component, and data from China, Japan, and Korea if available and appropriate. The results of this effort shall be disseminated for review of the methodology including background maps developed under another component of the project;

(iii) Organize a scoping meeting on the final critical load assessment methodology and carry out preliminary evaluation of critical loads and maps for the region;

(iv) Compute critical loads for grid cells in Asia and, if appropriate, use sensitivity classes for the verification and regional extrapolation of the computed critical loads. The result of this activity shall be an applicable map of critical loads which can then be incorporated into RAINS-ASIA;

(v) Disseminate critical loads maps to other consultants and organizations;

(vi) Conduct a workshop to evaluate and review the results of the critical load and background maps; and

(vii) Submit the critical loads map to the Model integration task manager for incorporation into RAINS-ASIA.

Model Integration

The Model Integration module consisted of the following tasks:

(i) The RAINS-ASIA model will consist of several modules. The linkage among all modules shall be established under this component. The RAINS-EUROPE model shall be modified to accommodate the changes necessary to implement RAINS-ASIA. Cooperation and coordination with other consultants will be a key to the success of this component;

(ii) Redefine the region of interest from Europe to Asia by developing a grid matrix and geographic map for the Asian region and integrate this matrix and map into the RAINS format;

(iii) Input Asian technological information on combustion and control technologies and adapt the RAINS-EUROPE cost functions for Asia;

(iv) Adapt base year emissions inventory and baseline scenario to reflect the needs of modeling for Asia;

(v) Change the RAINS-EUROPE user interface to meet the Asian policy requirements;

(vi) The RAINS model is capable of assessing scenarios such as emission level changes through technical measures or alterations in energy consumption patterns. A preliminary energy scenario shall be incorporated from the other components to illustrate the operation of RAINS-ASIA;

(vii) Deposition patterns and first assessments of these patterns by comparison to critical loads shall be computed and displayed geographically. Emission and energy scenarios shall be displayed graphically; and,

(viii) A manual for RAINS-ASIA shall be developed.

E. ASIAN COUNTRIES DATA COLLECTION AND INSTITUTIONAL DEVELOPMENT

Work under this task included collection of data on socio-economic indicators and energy characteristics (see Chapter 3.3), monitoring sulfur dioxide in East Asia (see Chapter 5.6), and organizing an IMPACT task meeting (see Chapter 6, Annex 5). This work was carried out under a separate contract from the Asian Development Bank.

Workshops planned in Terms of Reference

Three major workshops to coordinate various components were planned during for the project. These activities are described below.

(i) Task Group & Project Coordination/Progress Workshop, Four months after project start To be held in Asia. The first major workshop is planned at the end of the fourth month of the project. This workshop shall serve two specific purposes: working group meetings for the four components and a project coordination meeting. At this meeting, the methodologies of the working groups shall be discussed and finalized, critical data gaps shall be identified, and task-specific activities refined as necessary.

(ii) Model Integration Workshop, Nine months after project start. After nine months, the preliminary individual RAINS-ASIA components shall be delivered to the model integration team. At this workshop, the individual components shall be presented to the group, and these components shall be interfaced within the RAINS-ASIA model. All protocols regarding units, formats, and component details shall be discussed at this time. The plans for testing the assembled RAINS-ASIA model, and finalization of the base case RAINS-ASIA simulation, shall be determined at this meeting.

(iii) Preliminary Results and Program Progress Meeting, twelve months after project start. This project conference, held in the twelfth month of the project, shall be to review the first complete initial results using RAINS-ASIA. This meeting shall contain all key members of the project team. Results from the four major components shall be reported, along with the integrated RAINS-ASIA products. Further developments, refinement in the type and display of model outputs, plans for additional model testing, and final selection of scenarios shall be discussed at this time.

1.5 Major meetings and workshops held during the project

The project has met several times to discuss progress and interact with scientists from Asian countries. A brief overview of the project meetings is listed below. Apart from these meetings, the various tasks leaders met with Asian scientists to improve input and discuss tentative results. These meetings are discussed in the respective chapters in this report.

June 1992: Start of the project (kick-off meeting); timetable; definition of final products (Madison, Wisconsin, USA)

November 1992: 4th Annual Conference on Acid Rain and Emissions in Asia (Bangkok, Thailand)

April 1993: Integration meeting; interim results of sub-modules; first version of the software (Laxenburg, Austria)

September 1993: Presentation of interim report to the World Bank Task Managers (Washington, D.C., USA)

February and July 1994: Integration meeting; second version of software; scenario development (Laxenburg, Austria)

October 1994: Scenario development and final report meeting (Beijing, China)

November 1994: Symposium on Acid Rain and Emissions in Asia (Bangkok, Thailand)

May 1995: Peer Review Meeting (Washington, D.C., USA)

1.6 Team and network in Asia

This project has been carried out by a team of experts from Asia, Europe and the United States. This broad-based effort has been co-coordinated by the Asia Technical Department of the World Bank and the Asian Development Bank. The project has been organized into four major tasks: Energy and Emissions; Transport, Deposition and Monitoring; Ecosystem Sensitivity; and Integration. Each task involved a team of Asian and European/USA scientists. For each task there is an Asian project leader and focal center(s) to support the development of the RAINS-ASIA model and to facilitate networking among scientists and analysts in Asia. A unique team of experts from Europe and the United States, has been assembled for the project. The team members were specifically selected for their extensive experience and dedication to the subject of acid rain in Asia. Participating institutes for the project:

Contract Management:

World Bank	--	Jitendra Shah
Asian Development Bank	--	Ali Azimi

Project Management:

USA/Europe	Leen Hordijk, Wageningen Agricultural University, Netherlands Wesley K. Foell, Resource Management Associates, USA	
ASIA	S.C. Bhattacharya and R.M. Shrestha, Asian Institute of Technology, Thailand	

Energy and Emissions Module:

USA/Europe	Project Leader:	Wesley K. Foell, Resource Management Associates, USA
	Institutions:	Resource Management Associates, USA Argonne National Laboratory, USA ECON Energy, Norway
Asia	Project Leaders:	S.C. Bhattacharya and R.M. Shrestha, AIT
	Focal Points:	
	Japan -	University of Tokyo
	India -	Tata Energy Research Institute
	China -	Research Center for Eco-Environmental Sciences
	Thailand -	Dept. of Energy Development and Promotion
	Bangladesh -	Bangladesh Council of Scientific and Industrial Research
	Indonesia -	Institute of Technology at Bandung
	Philippines -	Department of Energy
	Pakistan -	Pakistan Atomic Energy Commission
	Myanmar -	Ministry of Energy
	Vietnam -	Institute of Energy
	South Korea -	Korean Institute of Energy Economics
	Malaysia -	University Sains Malaysia, Penang

Atmospheric Transport and Deposition Module:

USA/Europe	Project Leader:	Greg Carmichael, University of Iowa, USA
Asia	Project Leader:	Manju Mohan, Indian Institute of Technology, India
	Institutions:	
	Japan -	Central Research Institute Electric Power Industry
	-	Kyushu University
	Hong Kong -	Royal Observatory
	South Korea -	Ajuo University
	South Korea -	Korean Institute of Science and Technology
	China -	Research Center for Eco Environmental Sciences
	Monitoring Network Collaborators:	
	India -	Indian Institute of Technology

Nepal	-	Nepal Meteorological Services
South Korea	-	Ajou University
Thailand	-	Environmental Research and Training Center
Malaysia	-	Malaysia Meteorological Agency
Indonesia	-	Institute of Technology at Bandung
Taiwan	-	Taiwan National University
Hong Kong	-	Hong Kong Polytechnic
Vietnam	-	Institute of Chemistry, Hanoi
Bangladesh	-	Jahangirnagar University
China	-	Research Center for Eco-Environmental Sciences
Sweden	-	Swedish Environment Research Institute

Impacts Module:

USA/Europe Project Leader: Jean-Paul Hettelingh, RIVM, Netherlands

Institutions:

Stockholm Environment Institute, England
University of Lund, Sweden
GEODAN, Netherlands

Asia Project Leader: Zhao Dianwu, Research Center for Eco-Environmental Sciences, Beijing, China

Institutions:

South Korea	-	Kyong-gi University
Bangladesh	-	Jahangirnagar University
Japan	-	National Institute for Environmental Studies
Vietnam	-	Institute of Chemistry, Center for Research of Vietnam
Taiwan	-	Taiwan National University

Integration of RAINS-ASIA

USA/Europe Project Leader: Markus Amann, IIASA. Austria

Other Institutions from which individuals have participated in the Project

Thailand	-	King Monkuts Institute of Technology, Thonburi
	-	Electric Generating Authority of Thailand
	-	Thailand Development Research Institute
Australia	-	University of Technology Sydney, CSIRO
USA	-	Oak Ridge National Laboratory; East-West Center
International	-	UNEP
	-	ESCAP

References

Bhatti, N., D.G. Streets, W.K. Foell, 1991, Acid rain in Asia, in: Foell and Sharma (1991), pp. 5-33.

Bhatti, N. and D.G. Streets, 1992, Preliminary grid-by-grid SO_2 emissions inventory for Asia, in Foell and Green (1992), pp. 87-94.

Foell, W.K. and C.W Green, 1991, Acid rain in Asia: an economic, energy and emissions overview, in: Foell and Sharma (1991), pp. 123-145.

Foell, W.K. and C.W. Green (eds), 1992, *Third Annual Conference on Acid Rain and Emissions in Asia*, November 1991, AIT, Bangkok, 277 pp.

Foell, W.K. and D. Sharma, 1991, *Second Annual Conference on Acid Rain and Emissions in Asia*, November 1990, AIT, Bangkok, 253 pp.

Rodhe, H., E. Cowling, I.E. Galbally, J.N. Galloway, and R. Herrera, 1988, Acidification and regional air pollution in the tropics, in: H. Rodhe and R. Herrera (eds), *Acidification in Tropical Countries*, SCOPE 36, Wiley and Sons, Chichester, UK.

RAINS-ASIA:
AN ASSESSMENT MODEL FOR AIR POLLUTION IN ASIA

Chapter 2

Integrated Assessment

Markus Amann, Janusz Cofala, Leen Hordijk

Report on the World Bank Sponsored Project
"Acid Rain and Emission Reductions in Asia"

December 1995

2. INTEGRATED ASSESSMENT

Authors:
Markus Amann, Janusz Cofala, Leen Hordijk

TABLE OF CONTENTS

2.1 Introduction II-1
2.2 Integrated assessment of air pollution in Asia II-1
2.3 Relevant policy questions II-2
2.4 The concept of integrated assessment of air pollution in Asia II-3
2.5 The RAINS model - an overview II-6
The Regional Energy Scenario Generator (RESGEN) Module . II-8
Energy and Emission (ENEM) Module II-9
Atmospheric Transport and Deposition (ATMOS) Sub-Module II-10
Environmental Impact and Critical Loads (IMPACT) Module . II-10
2.6 Implementation II-11

LIST OF FIGURES

Figure 1. Flowchart of RAINS-Asia II-5
Figure 2. Study domain of RAINS-Asia II-7

2. INTEGRATED ASSESSMENT

Authors:
Markus Amann, Janusz Cofala, Leen Hordijk

2.1 Introduction

An analysis of acid rain (or of any other environmental policy issue) can be carried out in several ways. In general one can distinguish between "a single issue" analysis and an integrated analysis. The first kind is often used to determine if and how much acid rain contributes to forest damage in a particular area, to analyze the deposition pattern of emissions from a number of sources, or to make a cost-effectiveness analysis of the possible options to reduce the emissions of a given source. This "single issue" analysis has proven to be of great value to enhance better understanding of the problems related to acid rain.

In many countries in Europe and North America, large multi-year and multi-million dollar research programs have been carried out from which analyses of this have been drawn. However, next to this type of analysis the need was felt in some countries to develop a more comprehensive analysis of all aspects of acid rain. This analysis is denoted as Integrated Assessment (IA). This analysis would be particularly useful if expensive abatement programs were to be developed that would have a large effect on various economic sectors of the country or would even affect the country's international competing position.

Although integrated assessment is more than 'operating an integrated model', it is frequently so that IA has been identified with building a large model. We would like to stress that in our view IA is a process rather than a model building effort alone. The model is one of the tools for IA, certainly not the IA itself. However, one of the major steps is frequently the construction of an integrated model.

2.2 Integrated assessment of air pollution in Asia

In large parts of Asia, air quality is rapidly decreasing. Impacts are most visible on a local scale at some hot spots: In 1990, 12 of the 15 most polluted cities in the world (i.e., highest levels of particulate matter) were in Asia, imposing significant threats to human health. However, air pollution is not only a local problem; many pollutants (such as sulfur dioxide or nitrogen compounds) stay in the atmosphere several days before they are deposited on the earth's surface. During this time wind moves the air and thereby also the pollution over distances of several hundreds to thousands of kilometers, dispersing emissions over large areas. Many sensitive ecosystems in Asia face now, after the sharp increase of emissions experienced in the last decade, an excess of their tolerable exposure limits to pollution, which ultimately will result in significant damage to these (natural and agricultural) ecosystems, for example in southwest China.

At an early stage such latent impacts and injuries are difficult to identify. However, if nothing is done the current pace of economic development in this region will be accompanied by a strong growth of emissions and wide-spread damage will only be a question of time. An early detection of the upcoming problem will enable the consideration of a full range of countermeasures - out of which the most cost-effective could be selected to avoid costly damage.

The analysis and finally the proper choice of measures, however, is a complex task. Many different aspects should be taken into account:

- the future dynamics of economic growth in different regions
- the planned strategies to satisfy the implied demand for energy
- the associated emissions of air pollutants
- the available technical options and the costs of reducing emissions
- the spatial dispersion of emissions through the atmosphere
- the regional sensitivities of ecosystems (such as agricultural crops, natural forests, etc.) and human health towards air pollution
- the practical implementation of strategies (setting technological standards, economic incentive instruments, etc.)

Restricting the scope to a few single aspects from the list above may provide an incomplete or even wrong analysis. An integrative view considering the full variety of aspects is essential for the correct understanding of the air pollution problem and for developing cost-effective strategies to reduce the problem.

Integrated assessment models help to structure the problem in a consistent way. Such models apply confirmed scientific evidence of the various disciplines to the specific situation in a region (based on reviewed high quality data bases). By putting the various aspects into relation to each other such models are valuable tools for gaining insight into costs and benefits of alternative approaches to reduce impacts of air pollution. Therefore, they are most useful both on the national level (e.g., in exploring environmental impacts of future power expansion plans or in the process of preparing decisions on the site of new emission sources) and on the international level when considering international cooperative solutions to avoid or reduce environmental problems caused by air pollution.

2.3 Relevant policy questions

Air pollution may be viewed from a variety of angles with different questions posed to an assessment analysis. There is an interest in obtaining answers to questions of general nature, such as

- What will be the emissions in the future ?
- How do they depend on the pace and structure of economic development ?
- Could the anticipated emissions eventually cause threats to sensitive ecosystems ?
- If they are of concern, which ecosystems in which regions are endangered ?
- What are the technical options to control emissions ?
- And how much would it cost ?
- Are there options other than emission control technologies to keep emissions at an acceptable level, e.g., improvements of energy efficiency?

In practice, interest is often not only focused on questions of such general nature, but poses the same questions for a specific region. Obviously, answers will depend crucially on the country or region under consideration, i.e., the answers might be different in different parts of Asia. A regional model covering all of Asia with a uniform, consistent and internationally accepted methodology will not only provide site-specific answers in the national context, but also important information on international problems such as:

- What is the impact of emissions of a certain country on its neighbors?
- To what extent can strategies focusing solely on domestic emissions solve the air pollution problem in a country?
- What are the gains to be made by international cooperation?

Before devoting attention to transboundary pollution problems, however, most countries tend to focus their interest more on domestic policies. Integrated assessment could also some of the questions arising in such a context:

- Where are the sensitive ecosystems in a country?
- Which (present and future) emission sources make contributions to sulfur deposition at these locations?
- To what extent can emission control measures alleviate the exposure?
- At what cost?
- What are the acidification impacts of national power expansion plans (considering also the development in neighboring countries?
- If a specific (future) emission source (such as a planned power station) puts significant load on sensitive ecosystems, are there any ways to prevent the problem by moving the location to less sensitive sites?
- Or by installation of flue gas treatment at these locations?
- To what extent can emission control measures elevate the exposure?
- At what cost?
- Which potential problems could be avoided by low energy strategies?
- etc.

Integrated assessment models have been developed to provide information on many aspects of a particular problem, and thereby enable the user to generate answers to the types of questions listed above.

2.4 The concept of integrated assessment of air pollution in Asia

To provide a tool for the integrated assessment of air pollution in Asia, as a first step the general air pollution problem has been confined to the acidification problem, primarily caused by emissions of sulfur dioxide (SO_2). The assessment framework includes the major relationships and (physical) linkages between the activities causing emissions, the technical and economic characteristics of the emission sources and the technical and economic potential for control, the atmospheric dispersion of sulfur compounds and the regional sensitivities of natural and managed ecosystems towards deposition of sulfur. A series of models covering the various aspects of the acidification problem are implemented on a computer in a user-friendly way to enable also inexperienced users to operate the assessment framework and to gain basic insight into the air pollution problem in Asia. Without any doubt all of the problem areas mentioned above are extremely complex subjects to explore, involving a large variety of influencing factors. Detailed models have been created to describe:

- the dynamics of future energy consumption,
- atmospheric dispersion of pollutants, and
- acidification of soils under the specific conditions prevailing in the region.

Details on each of these models are provided in the respective sections of this report. Based on voluminous data sets these models have been implemented for Asia and represent current up-to-date information on the various aspects of the pollution problem

Integration of all aspects maintaining the full range of details for each sector is difficult to implement and would result in an unmanageable conglomerate of models and data. To create a practical tool for strategy analysis, a crucial step in the model development was the identification of a simple representation of the relations between the policy input variable of the modules (e.g., economic development for the energy module, annual emissions of the atmospheric module and deposition for the impact module) and the output variables (annual emissions of the energy module, deposition of the atmospheric module and protection of an ecosystem for the impact module). For the final implementation of the integrated tool, these simple relationships are then connected with each other into an overall assessment framework allowing the comparative analysis of alternative energy and emission reduction strategies.

Another important feature of the implementation is its user-friendliness. This means that the model is operational on standard personal computers. The model uses standard user interfaces similar to Microsoft Windows. The individual modules are set up in such a way that inexperienced users are guided through the logical sequence of steps necessary for creating and evaluating emission control scenarios. On-line 'help' is available to the user at any time to quickly receive advice on available options and further procedures. Special attention has been devoted to the graphical representation of model results (e.g., time development of emissions, deposition patterns, protection of ecosystems, etc.). Consequently, the model is not only a tool for the actual analysis of air pollution control strategies, but has also an important educational function in transfer of knowledge to a wide audience in the region.

Although the model is basically intended to provide a general picture of the air pollution problem in Asia, limitations had to be accepted when developing a first version. Most notably, its initial implementation focuses mainly on the potential acidification problem in Asia, and excludes other air pollution-related problems, such as urban air quality, global climate change, tropospheric ozone and others. Consequently, the project's first phase focused on capturing the major pathways of sulfur dioxide (SO_2) emissions, ignoring for the moment the potential contributions to the acidification problem made by nitrogen oxides and ammonia. Similarly, other pollutants' species causing different problems (CO_2, particulate matter, volatile organic compounds, etc.) are excluded as well from the first model version.

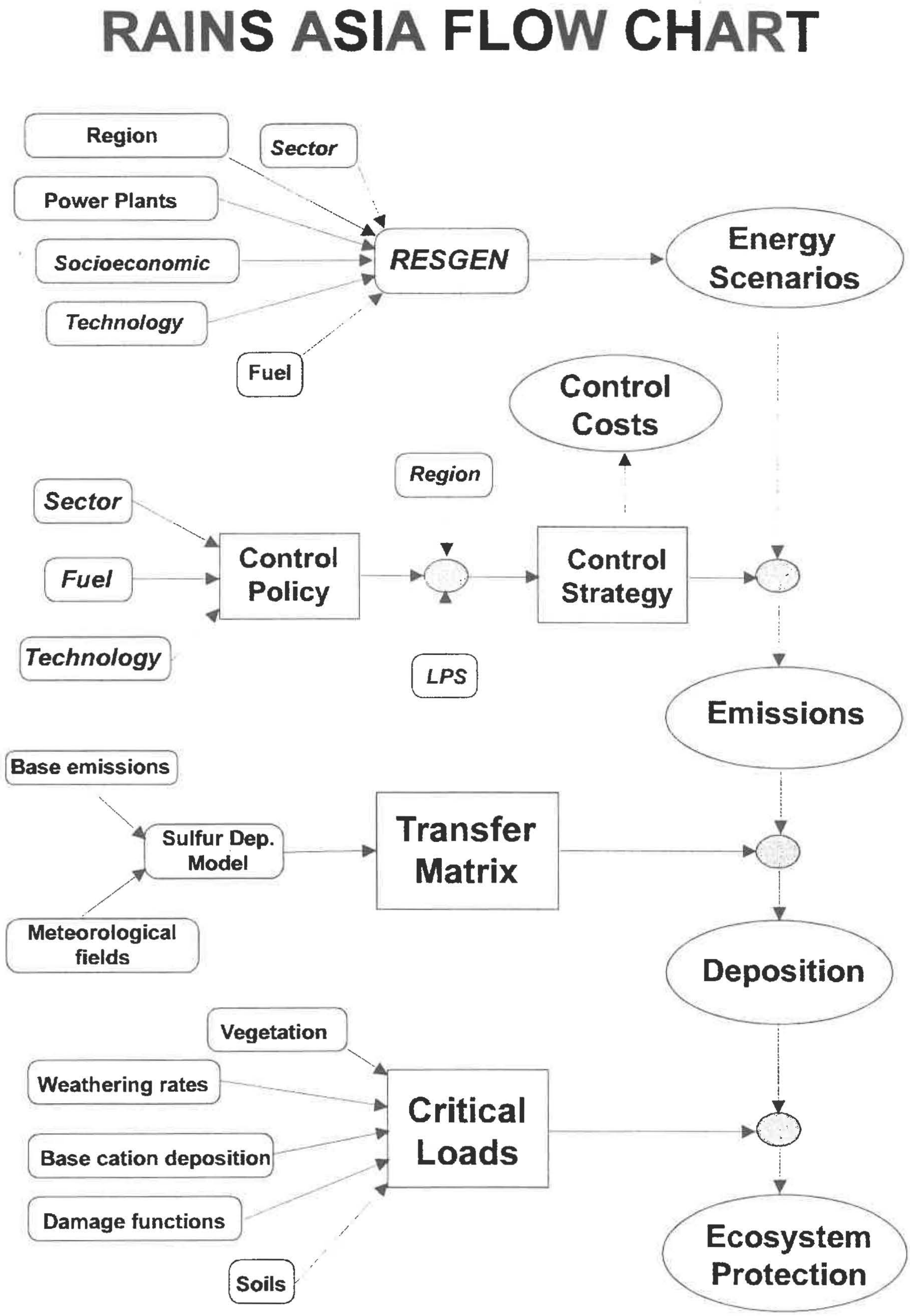

Figure 1. Flow chart of RAINS-Asia

Despite the wide range of facets of the acidification problem considered in the model, some limitations had to be accepted also. To keep the first implementation managable, the model restricts itself to the description of the major physical flows of sulfur in the biosphere. A number of economic aspects intrinsically linked with the air pollution problem, such as the potential role of economic instruments for reducing emissions or the monetary benefit evaluation of avoided environmental damage, have not been incorporated into the current analysis. It is important to note, however, that the framework describing the physical flows of sulfur emissions, available now after the first phase, provides a unique and indispensable basis for any future analysis of such aspects.

2.5 The RAINS model - an overview

The initial version of the 'Regional Air Pollution INformation and Simulation' (RAINS)-model was developed as a tool for the integrated assessment of alternative strategies to reduce acid deposition in Europe (Alcamo et al., 1990). The model has found prominent application as a scientific support tool during the international negotiations on the new sulfur protocol to the Convention on Long-range Transboundary Air Pollution (Amann, 1993; Hordijk, 1991). Recently, a protocol was signed by 33 countries committing themselves to (country-specific) emission reduction obligations as calculated with the RAINS model.

For purpose of study in Asia, the model has been extensively modified and further developed (version RAINS 7.0) to be applicable to this region of the world, provided that appropriate databases are prepared. The RAINS 7.0 model describes the pathways of emissions and mechanisms of acidification in the environment for sulfur dioxide, which is a major acidifying component. The structure of the model is presented in Figure 1. The various sub-models are organized into four modules, each of which addresses a different part of the air pollution/acidification process:

1) the Regional Energy Scenario Generator (RESGEN) module, which estimates energy consumption parameters based on socioeconomic and technological assumption

2) the Energy and Emissions (ENEM) module, which uses these scenarios to calculate sulfur emissions and the costs of selected control strategies

3) the Deposition and Critical Loads (DEP) module, which consists of

4) the ATMOS atmospheric transport and deposition submodule, which calculates the levels and patterns of sulfur deposition resulting from a given emission scenario

5) the IMPACT module, which calculates ecosystem critical loads and their environmental effects, based on these sulfur deposition patterns.

To capture the full spatial scope of the problem (the long-range characteristics of sulfur dioxide transport in the atmosphere), the geographical model domain covers Asia from 60° E to 160° E and 60° N to 10° S (see Figure 2). Although the model's geographic

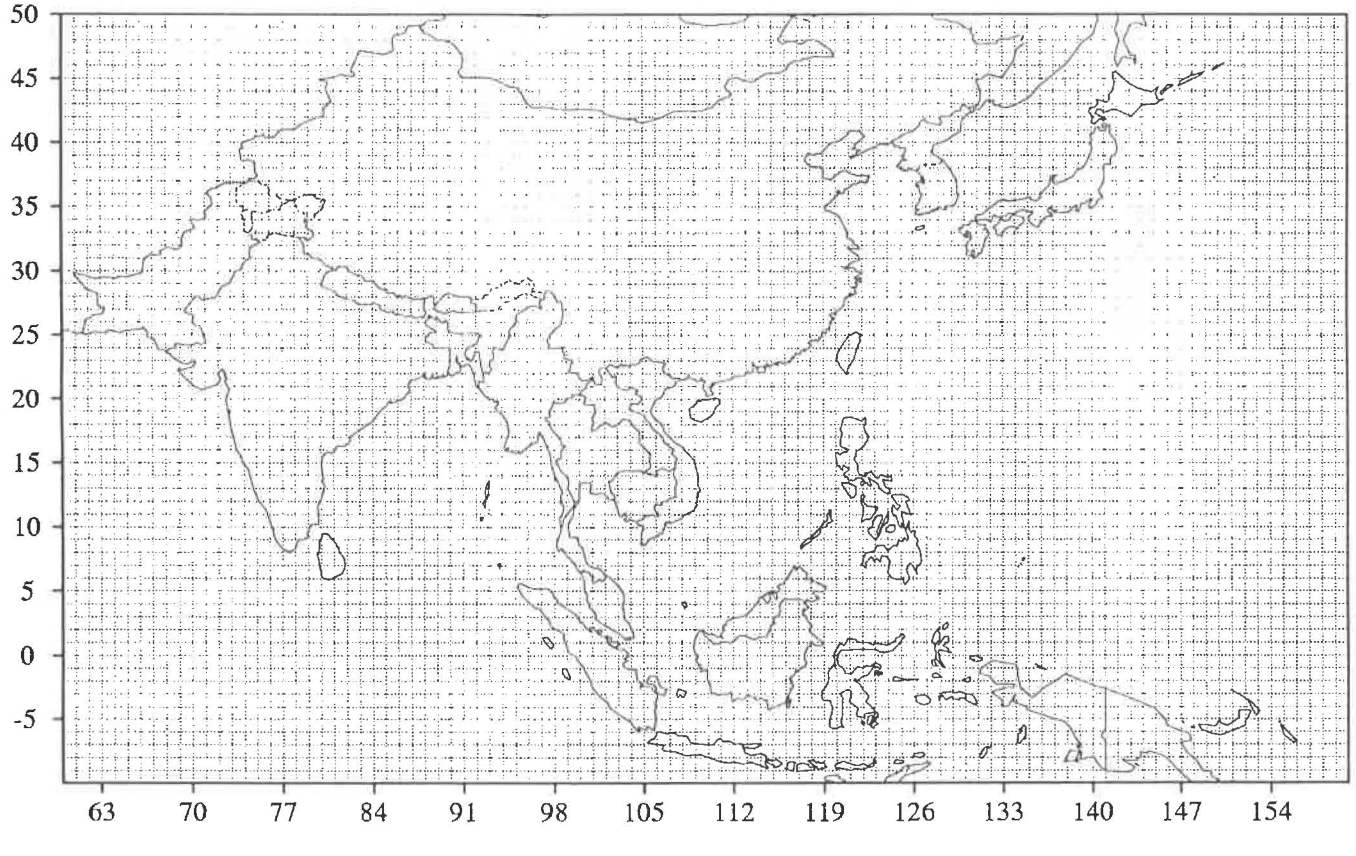

Figure 2. Study domain of RAINS-Asia

scope is broad, it is nevertheless detailed in coverage, treating individually a total of 94 separate regions in 23 countries. Twenty-two of these regions are major metropolitan areas, while international sea lanes constitute one region. The model uses 1990 data as a base year, and calculates future energy levels, emissions, and environmental impacts through the year 2020 in ten-year time steps.

The major data bases in the model have the following dimensions:
- 6 end-use consumption sectors
- 17 fuel types
- 355 large point sources of emissions
- 31 ecosystem types

The Regional Energy Scenario Generator (RESGEN) Module

The RESGEN module estimates present and future energy supply and sectoral energy consumption for a wide variety of socioeconomic and technological assumptions. It incorporates an elaborate database on energy demand and supply for the 94 regions for the base year (1990) and necessary information to develop scenarios up to the year 2020. Given a set of specifications concerning current and future conditions (using either the extensive socioeconomic data base in the model, or from user-specified assumptions and energy data), RESGEN calculates energy scenarios for the period 1990 to 2020.

In this module, energy consumption is disaggregated into industrial, transportation, residential, commercial, agricultural, and "other" sectors. The description of the energy supply and transformation system distinguishes the major sources of emissions, including electricity generation, oil refining, and other energy sector operations with combustion of fossil fuel.
This framework can be used for rough estimates of future energy demand- and supply trends for a variety of socio-economic and technical assumptions, but cannot substitute for more detailed analysis of energy development.

Using RESGEN, a user can select, review, and modify a number of key parameters at the sub-country (regional) level, including:

- socioeconomic data: rates of population growth and GDP growth (broken into three components: industrial, agricultural, and commercial/other).

- growth rates of energy demand among the six end-use sectors

- energy intensity: i.e., the energy demand per unit of output for each of the six end-use sectors

- mix of fuels used in each sector: Since SO_2 emissions are highly dependent on the type and characteristics of the fuel(s) used, the model considers a total of 17 different fuel types, including various qualities of coal, other solid fuels, fuel oil, natural gas, renewable sources, hydro, and nuclear.

- fuel characteristics, such as the sulfur content of various fuels.

- electricity supply systems characteristics, including the size, technology, and location of individual power plants

A major component of the work in the development of RESGEN was the creation of the national and regional energy data base, drawn heavily from the contributions from the Asia network of research institutions established for the project.

Energy and Emission (ENEM) Module

The Energy and Emissions (ENEM) module of the RAINS-Asia module uses the information on energy demand, types of fuels used and location of major sources of emissions developed by the RESGEN module, and estimates the resulting amounts and patterns of SO_2 emissions, and the costs of various control options.

With ENEM, the model user can calculate SO_2 emissions and investigate a number of different emissions control options, focussing on reducing the sulfur contained in fuel, either before, during, or after combustion. Emissions are separated into low-level (area) sources and high-level (large point sources). The user can select emissions control techniques to be applied to particular large point sources, in specific economic sectors, or in certain geographical regions.

The following control measures are included:

- use of low sulfur coal, either from naturally occurring low-sulfur coal types, or by some degree of coal washing

- use of low-sulfur heavy fuel oil, either from low-sulfur crude or oil desulfurized during refining

- use of diesel oil (gasoil) with lower sulfur content

- desulfurization during the combustion process (e.g., limestone injection or fluidized bed combustion processes)

- desulfurization of the flue gas after combustion

Regional and national potentials for emission control and the associated costs are estimated on the basis of detailed data on the most commonly-used emission control technologies. The cost evaluation is based on the international operating experience of pollution control equipment by extrapolating it to the country-specific situation of application. Important country-specific factors with strong impact on abatement costs are the characteristic sulfur content of fuels, plant capacity utilization regimes, boiler sizes, etc. These cost estimates for specific fuel types, economic sectors and abatement technologies are combined with the projected pattern of energy consumption. The RAINS model provides "national cost curves" that rank the abatement measures according to their cost-effectiveness. Due to country-specific factors such as energy use patterns and technical infrastructure, national cost curves show significant differences among countries.

Atmospheric Transport and Deposition (ATMOS) Sub-Module

The ATMOS suv-module provides estimates of ambient levels of acid precursors and acid deposition loading throughout the region under study as a function of changing emissions. The projection of acid deposition for future emissions scenarios is based on a transfer matrix for long range transport, which is calculated by using an atmospheric transport/deposition model.

For Asia the deposition fields are calculated with the National Oceanic and Atmospheric Administration (NOAA) BAT (Branching Atmospheric Trajectory) model. BAT is a three-layer model which calculates the dry and wet deposition of SO_2 and sulfate from a particular source, as the pollutant is transported by the meteorological fields. The amount of deposition is calculated along the trajectories determined by the meteorological conditions. Running these trajectories for an entire year allows calculation of annual deposition throughout the region resulting from a particular source. Repeating the calculation for all sources allows the total deposition from the regional emissions to be calculated.

As inputs, the BAT model requires the area and point source emission rates of SO_2 (from ENEM), meteorological winds and temperature, precipitation rates, and estimates of the dispersion coefficients, dry deposition velocities, and wet scavenging coefficients. The BAT model calculates the chemical conversion rates based on simple first-order rate constants, the dry deposition rate as a function of the surface concentrations and the dry deposition velocity, and the wet scavenging as a simple function of precipitation rate. The BAT model is run for each elevated (high stack) and low level (area) source estimated by the ENEM module. Sulfur deposition is calculated on the grid, and the contribution of each source to the grid is calculated.

The results are aggregated to provide source/receptor information for each of the 94 sub-regions, the acid deposition patterns in the study region, and further aggregated to provide country-to-country source/receptor information.

Environmental Impact and Critical Loads (IMPACT) Sub-Module

The IMPACT sub-module assesses the sensitivity of various ecosystems (their "critical loads") to acidic deposition, and compares this information to the deposition data generated by the ATMOS module. Critical loads are in essence the maximum long-term deposition levels which can be tolerated without damage. This process identifies the most sensitive areas which are at greatest risk of damage (e.g., yield loss, growth reduction, and change of biodiversity). By estimating critical loads for various regions and ecosystems, and comparing these natural sensitivities to deposition levels, the IMPACT module allows users to assess the environmental effects of different energy and emission scenarios, answering questions such as:

- What regions and ecosystems are most sensitive to acid deposition?

- What is the geographic scope and extent of ecosystem damage which results from a particular energy scenario?

- What environmental benefits would be realized if a particular emission control strategy were implemented?

Two complementary approaches are used to estimate critical loads for a wide variety of different ecosystems: the definition of relative sensitivity classes, and the steady-state mass balance method. The objective of applying two methodologies was to:

- consider a large number of biogeochemical factors to determine the sensitivity of ecosystems,

- assess the reliability of each method by comparing the broad geographical distribution of results from each method, and

- extend the geographical scope of the assessment of ecosystem sensitivity to include areas where data are insufficient to calculate critical load values directly.

2.6 Implementation

The first of the above modules, RESGEN, is available as a DOS-based user-friendly software package for use on a PC. It provides a powerful tool for the user to create a wide range of scenarios and to export them conveniently into the RAINS-Asia model. It can also be used as a stand-alone regional energy scenario generator, independent of its ability to export data to RAINS-Asia.

The outputs of the other three modules, ENEM, ATMOS, and IMPACT, described above, are combined together into a microcomputer-based policy analysis model, RAINS 7.0. The model allows users to describe emissions in current and future years on regional, country or sub-country basis, follow these emissions through the acid deposition processes, and assess the potential of those emissions to impact critical ecosystems.

RAINS-ASIA:
AN ASSESSMENT MODEL FOR AIR POLLUTION IN ASIA

Chapter 3

Energy Module

Collin Green, John Legler, Ashok Sarkar, Wes Foell

With contributions from: Markus Amann, Janusz Cofala, Torleif Haugland, Ram Shrestha, and Sribas Bhattacharya

Report on the World Bank Sponsored Project
"Acid Rain and Emission Reductions in Asia"

December 1995

3. ENERGY MODULE

Authors: Collin Green, John Legler, Ashok Sarkar, Wes Foell

With contributions from: Markus Amann, Janusz Cofala, Torleif Haugland, Ram Shrestha, and Sribas Bhattacharya

TABLE OF CONTENTS

3.1 Introduction III-1
3.1.1 Background III-1
3.1.2 Specific Objectives III-3
3.1.3 Major Capabilities and the Use of RESGEN III-6

3.2 Overview of Methodology III-8
3.2.1 General Discussion III-8
Regions III-9
3.2.2 General Structure of RESGEN III-14
3.2.3 Detailed Discussion III-16
Sectoral end-use energy consumption III-16
Residential sector
Commercial sector
Agricultural sector
Industrial sector
Transportation sector
Energy supply sector III-21
Electricity generation sector
3.3 RESGEN and RAINS-ASIA Databases III-26
3.3.1 Institutional Process III-26
3.3.2 Data Requirements III-27
Scope III-27
Geographic Definitions
Temporal Definitions
Database Description of the RESGEN Databases III-28
Socioeconomic Database
Energy Database
Fuel Characteristics Data
Large Point Source Data for Power Plants
3.3.3 Status of Regional Database III-29

3.4 Energy Scenario Assumptions III-32
3.4.1 Socioeconomic Factors III-32
Population III-32
Gross Domestic Product III-32
3.4.2 Technology III-38
3.4.3 Fuel Types III-38
3.4.4 Regional (Subcountry) Fuel Allocation Assumptions III-38

3.4.4 Regional (Subcountry) Fuel Allocation Assumptions III-38
3.4.5 Power Supply Assumptions III-40

3.5 Energy/Economic Analysis III-41
3.5.1 Overview III-41
3.5.2 China country description III-41
3.5.3 India country description III-43
3.5.4 Indonesia country description III-44
3.5.5 South Korea country description III-46
3.5.6 Gas Trade in Asia III-47

3.6 Energy Scenario Results III-47

3.7 Summary and Conclusions III-60

3.8 References III-62

LIST OF TABLES

Table 3.1 Names of the 12 National Contact Persons III-5
Table 3.2 Country and Region Names and Abbreviations III-10
Table 3.3 Fuel Types and Brief Descriptions III-30
Table 3.4 Base Year (1990) National Primary Energy Consumption Data Source Comparison III-31
Table 3.5 Base Case Population Scenario Assumptions: National Totals III-34
Table 3.6 Base Case Gross Domestic Product Scenario Assumptions: National Totals III-35
Table 3.7 Industrial Energy Intensity Assumptions for the Base Case III-39
Table 3.8 Total Energy Consumption by Country [Petajoules/year] III-49
Table 3.9 Total Energy Consumption by Region III-51
Table 3.10 Primary Fuel Consumption in the Asia Region [in Petajoules] III-54

LIST OF FIGURES

Figure 3.1 Structure of RAINS-ASIA III-2
Figure 3.2 Map of the Geographic Regions of Asia III-13
Figure 3.3 Overall Flow of Information in RESGEN III-15
Figure 3.4 Map of Large Point Sources (LPS) in Asia III-23
Figure 3.5 Asia Primary Energy Consumption III-50
Figure 3.6 Asia Primary Fuel Consumption – Base Case III-55
Figure 3.7 Asia Primary Fuel Consumption – Low Scenario III-56
Figure 3.8 Asia Primary Energy Intensities III-57
Figure 3.9 Asia Energy Intensities by Sector III-58

LIST OF ACRONYMS

AAGR	Average Annual Growth Rate
ADB	Asian Development Bank
AIT	Asian Institute of Technology
EJ	Exajoules
GDP	Gross Domestic Product
GJ	Gigajoules
GRP	Gross Regional Product
GW	Gigawatts
IEA	International Energy Agency
IIASA	International Institute for Applied Systems Analysis
LNG	Liquid Natural Gas
LPS	Large Point Source(s)
NCP	National Contact Person
PJ	Petajoules
RESGEN	Regional Energy Scenario Generator
SE	Socioeconomic

3. ENERGY MODULE

Authors: Collin Green, John Legler, Ashok Sarkar, Wes Foell

With contributions from: Markus Amann, Janusz Cofala, Torlief Haugland, Ram Shrestha, and Sribas Bhattacharya

3.1. Introduction

3.1.1 Background

Energy policies and energy technologies are a primary driving force behind the problems arising from air pollution emissions in Asia. It is, therefore, important that RAINS-ASIA® have an energy module designed to examine a broad range of policy and technology scenarios at the regional, national, and international levels. *Figure 3.1* depicts the RAINS-ASIA flow chart; the energy module component described in this section is highlighted in gray.

In particular, because of the spatial nature of dispersion of energy-related air pollutants, an analytical framework that will permit subcountry analysis, i.e., regional analysis, needs to be established. Thus, one of the major distinguishing characteristics of the Energy Module is its regional disaggregation. For the past two years work on the module has focussed on the regional aspect of the analysis. This is the first time there has been an effort of this magnitude to carry out regional energy analysis on an Asia-wide basis.

Policy issues strongly shaped the design of the energy module and its requisite database. One major set of policy questions relates to how changes in the energy demand of various components of the economy in any given country, and in Asia as a whole, alter acid deposition patterns. Thus, the energy module contains six end-use energy sectors: residential, commercial, industrial, transportation, agriculture, and non-energy use of fuels. There are two energy conversion sectors: electric utilities and non-electric energy, such as petroleum refineries. Development policies that affect energy use in any of these sectors may have significant effects on the pattern and quantities of future acid deposition.

Another set of policy questions relates to energy supply management and emission controls. Emissions can be reduced by strategies such as increasing the efficiencies of energy use, shifting to fuels with lower emissions, or implementing emission control measures. The module permits the user to examine, at the sector level, the effects of energy demand changes, energy supply management policies, and technological control policies.

Still another set of policy questions relates to the spatial distribution of economic activity, energy facilities, and emissions. With the module, scenarios of future energy use can be made on the smallest subcountry scale that the current database permits. This provides the basis for assigning the responsibilities for the acid deposition to specific regions and will help identify energy strategies for reducing deposition below critical levels for important regions. The Energy Module explicitly identifies large point sources of emissions at specific locations in Asia. Therefore, the location of energy facilities, e.g., power plants, is amenable to analysis within the RAINS-ASIA framework.

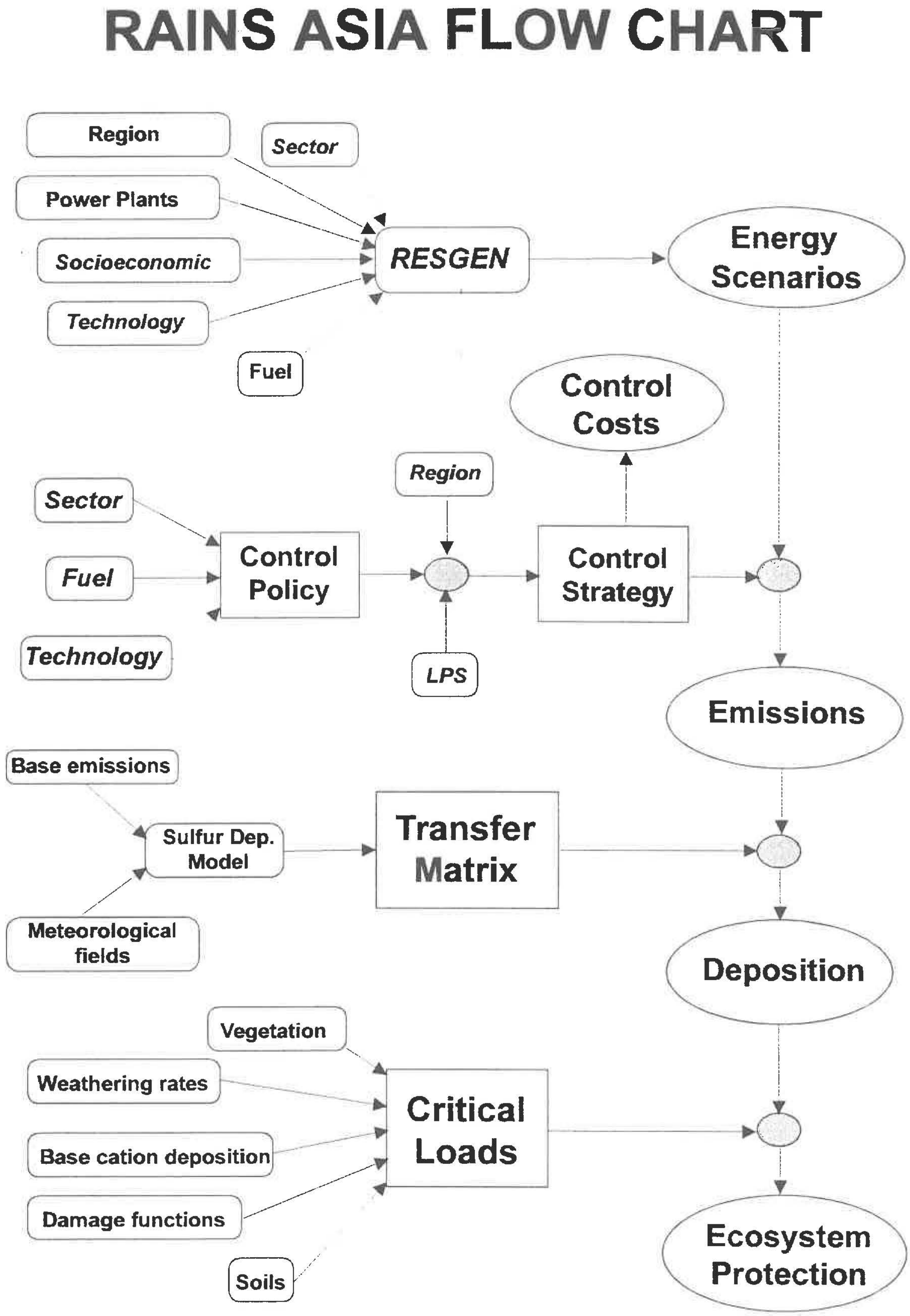

Figure 3.1 Structure of RAINS-ASIA

The year 1990 was chosen as the Base Year. This choice was based on the availability of key socioeconomic and energy data. Time intervals of ten years are used in the analysis, extending through the year 2020. The thirty-year horizon (1990, 2000, 2010, 2020) is consistent with the five- to ten-year implementation periods for major energy facility investments (e.g., power plants). It also extends over a time period during which expected growth of economic activity and population is likely to raise energy consumption in Asian countries to the same range as that of today's highly industrialized nations.

The general design of the Energy Module is based on an earlier country-specific, five-sector energy/emissions module developed by Foell and Green for 13 major developing countries in Asia, (Foell and Green, 1991). In that framework, national atmospheric emissions were linked to energy in a "bottom-up" approach. The present module is a regionalized modification of that approach. The software implemented in the FOXPRO® language is called RESGEN®, the Regional Energy Scenario Generator.

3.1.2 Specific Objectives

The specific objective of the Energy Module is to generate regional energy scenarios with an output format consistent with the spatial- and time-dependent input data requirements of RAINS-ASIA. As shown in *Figure 3.1,* RESGEN interfaces directly with RAINS-ASIA by providing the input files for the energy scenarios to be analyzed. The achievement of this specific objective required the following subtasks:

- The establishment, with the assistance of the Asian Institute of Technology (AIT), of a RAINS-ASIA Energy Network of research institutions to collaborate in the development of a regional energy and emissions database and energy scenario development.

  Because of the new and unique nature of the energy module and its associated regional databases and resultant scenarios, it was decided to develop a network of collaborating research institutions in Asia. AIT, under contract to the Asian Development Bank, played the main role in establishing this network and in coordinating the collection the databases. This network served not only to facilitate the data-collection process in the countries, but also served as a convenient vehicle for establishing ties to key institutions and potential RAINS-ASIA users. Twelve Asian institutions are participating in the RAINS-ASIA Energy Network. These institutions are listed in *Table 3.1.*

- The development, in conjunction with AIT and the RAINS-ASIA Energy Network, of a regional socioeconomic and energy database for the twenty-three Asian countries.

  The specification of regional energy scenarios required a new regional database which is consistent with the spatial- and time-dependent input data requirements of RAINS-ASIA. Because many of the countries in Asia do not have regional (subcountry) information readily available in a convenient, standardized format, the project had to devote special attention to the creation of this database. A set of 94 subcountry regions are defined for Asia, including 22 megacities (metropolitan areas with populations greater than two million) and one region representing the international shipping routes (sea lanes) of Asia.

- The development, with the assistance of AIT, of two Asia-wide socioeconomic/energy scenarios: a Base Case scenario and a Low Energy scenario.

Integration and assimilation of Asian regional energy consumption, large point sources, and socioeconomic data for scenario development is a continuing process. In Phase I of the project, two energy scenarios were developed, based on information from the RAINS-ASIA Energy Network. The scenarios are a Base Case Energy Scenario and an alternative Low Emissions Energy Scenario.

- The design, programming, and testing of a user-friendly Regional Energy Scenario GENerator (RESGEN).

  RESGEN has been developed in the ©FOXPRO database language for generating regional energy scenarios and converting the output files of these scenarios into the specific databases required by RAINS-ASIA. RESGEN estimates energy use for six end-use sectors and two energy conversion sectors, for 23 countries plus one region for international shipping lanes, and for seventeen fuel types. A methodology based on regional population and gross regional product (GRP) distributions is used to allocate energy use to the land-based subcountry regions within the respective countries. The scenario generator produces an inventory of present and future large point sources (LPS) at latitude and longitude coordinates. User-friendly software has been developed for handling, reviewing, and modifying the large regional databases associated with the use of RESGEN.

Table 3.1 Names of the 12 National Contact Persons

1. **Prof. Hajime Akimoto**
Research Center for Advanced Science and Technology,
University of Tokyo
JAPAN

2. **Dr. R.K. Pachauri**
Tata Energy Research Institute
INDIA

3. **Prof. Zhao Dianwu**
Research Center for Eco-Environment Sciences,
Academia Sinica
CHINA

4. **Dr. M. Soedomo**
Energy and Environment Section,
Section for Research on Energy Institute Teknologi Bandung
INDONESIA

5. **Dr. Lim Koon Ong**
Associate Professor and Deputy Dean,
School of Physics,
University Sains Malaysia,
MALAYSIA

6. **Dr. A.M. Khan**
Pakistan Atomic Energy Commission,
PAKISTAN

7. **Ms. C.C. Cabacang**
Department of Energy
PNPC Complex
PHILIPPINES

8. **Dr. Itthi Bijayendrayodhin**
Department of Energy Development and Promotion (DEDP),
THAILAND

9. **Dr. Muhammad Eusuf**
Member (Science and Technology)
Bangladesh Council of Scientific and Industrial Research,
BANGLADESH

10. **Dr. D.N. Tung**
Thermal Power Department
Institute of Energy
VIETNAM

11. **Dr. Hoesung Lee**
Korean Institute of Energy Economics and Promotion
REPUBLIC OF KOREA

12. **U Soe Myint**
Director, General Energy Planning Department
Ministry of Energy
Yangoon
MYANMAR

3.1.3 Major Capabilities and the Use of RESGEN

RESGEN allows the user to change the input components within its framework for the purpose of creating new scenarios. With the goal of meeting the specific objectives discussed in section 3.1.2 above, RESGEN has been designed to address the following issues within its framework:

- Ability to change socioeconomic parameters
- Ability to change sectoral energy demand intensities
- Ability to change sectoral fuel fractions
- Ability to add, delete, or move large point sources

A brief summary of the main options in the RESGEN model follows. A complete description of the options and the use of the RESGEN model is presented in the RESGEN software manual (Legler, *et. al.* 1995).

Socioeconomic Module

Socioeconomic (SE) assumptions provide the basis for the development of energy/supply scenarios. SE assumptions are developed on a country basis. Within each Country SE Assumption exists subnational details (for those countries with more than one region). Both the national and subnational SE assumptions are important in RESGEN in the development of regional energy scenarios.

Input options available to the user for the development of an SE scenario include:

1) Growth rates of national and regional population.
2) Growth rates of gross domestic product (GDP) and regional domestic product (GRP).
3) Sectoral fractions of GDP and GRP for the commercial, agricultural, and industrial sectors.

End-use Demand Module

End-use demand scenarios are first developed at the national level and are linked to a specific SE scenario. Allocation of energy demand to the regional level is accomplished by relating the growth in regional sectoral energy consumption to the growth in regional socioeconomic parameters. Energy consumption is disaggregated into six end-use sectors. The RESGEN program allows the user to develop a separate energy demand scenario for each sector. Sectoral energy demand scenarios are developed by relating sectoral energy demand to the development of sectoral energy intensity and an SE scenario.

Input options available to the user for the development of a sectoral energy demand scenario include:

1) Sectoral Energy Intensities
   National energy use in petajoules (PJ) is calculated by entering an energy intensity for each sector and for each of the scenario years 2000, 2010, and 2020. These

energy intensities are multiplied by a socioeconomic factor (e.g., population is the socioeconomic factor for the residential sector) which gives national sectoral energy use.

2) Sectoral Fuel Fractions
National sectoral energy use is disaggregated into 15 fuels by inputting fuel fractions for each of the sectors for each of the years 2000, 2010, and 2020.

Electricity Supply Module

The electricity supply module is demand driven. The demand for electricity is met by specifying the electricity generation fuel mix at the national level and, subsequently, specifying the electricity generation by specific LPS and regionally disbursed area generation sources.

The main input options available to the user for the development of electricity supply scenarios are:

1) The electricity generation plan
The three major input assumptions which form the electricity generation plan are: own use and transmission and distribution losses, net electricity import or export, and the electricity generation fuel mix.

2) Development of LPS and area generation sources.
The major input assumptions include the contribution to total electricity generation by LPS and the specific location, capacity, efficiency, and input fuels of each LPS. Parameters that pertain to area sources which may also be modified to include regional distribution of non-fossil electricity generation, regional distribution of electricity generation area sources, and the electricity generation efficiency of area sources.

Thus the RESGEN model provides a user-friendly method for creating new energy scenarios for direct input to RAINS-ASIA. New energy scenarios can be developed by modifying either of the two existing reference scenarios developed as part of this Project - the Base Case energy scenario and the Low energy scenario - or by developing new energy scenarios from alternative, user-supplied assumptions. An export option in RESGEN creates all the relevant energy and fuel characteristics databases required as inputs by RAINS-ASIA and writes these files in the appropriate target RAINS-ASIA directory. Upon launching RAIN-ASIA, the new energy scenario from RESGEN may then be selected and initialized in the RAINS-ASIA program, and the analysis of emissions and environmental impacts can be initiated.

3.2 Overview of Methodology

3.2.1 General Discussion

This section provides a description of the methodology used by the Energy Module to create regional energy databases and to generate regional energy scenarios. RESGEN utilizes a simulation approach for generating regional energy scenarios. A simulation structure was chosen for several reasons. First, it provides a great deal of flexibility in both the modeling process and in its application to policy analysis. In a large interdisciplinary and multi-institutional project such as RAINS-ASIA, this flexibility is extremely important. Second, the simulation structure lends itself to the scenario-generation approach that is useful in addressing questions of the "what-if" type.

Initially, considerable attention was given to choosing the appropriate level of detail in the analysis of sectoral energy consumption. Although it would have been possible to individually analyze a large number of end-use energy consumption processes and include them in RESGEN, it was decided that this level of detail would necessitate an unreasonable effort to collect the requisite data at the regional level. Thus, the sectoral analysis was carried out on an aggregated basis, using an energy intensity coefficient or a per capita energy-use coefficient.

The goal of RESGEN is to estimate energy consumption contributing to emissions of SO_2 on a subcountry scale. The RESGEN model covers 23 Asian countries, plus a single area representing the international sea lanes. Because the location of SO_2 emissions is an important consideration in calculating acid deposition, the model resolves these countries into 94 subcountry regions (largely corresponding to internal administrative and geographic boundaries) and 355 LPS. A map of the 94 regions is shown in *Figure 3.2* and described in *Table 3.2*. A map showing the locations of the 355 LPS is shown in *Figure 3.4* Output from the model consists of regional and LPS energy consumption scenarios for each country. This information is available for input to the RAINS-ASIA model, where emissions of SO_2 are computed, acidic deposition is calculated, and environmental impacts are assessed. RESGEN, in tandem with RAINS-ASIA, allows policy makers considerable flexibility to explore a range of subcountry, national, and international policy options to control or mitigate acid deposition impacts.

While there are other highly detailed sectoral energy demand models, e.g. MEDEE-S (REDP, 1989) and WISE (Foell, *et al.*, 1981), these models typically require a vast amount of highly disaggregated input data for each country or subcountry region. The effort required to gather spatially disaggregated data of this type is not justified for the purposes of this model at this time. However, in the future, the results of more detailed energy analysis could possibly be used as direct input to RESGEN.

Within the framework of RESGEN, the following components of the energy system are explicitly defined and specified in the scenarios:

- Socioeconomic activity (population and sectoral economic output)
- End-use sectoral energy demand

- Energy conversion and supply systems, including large power plants
- Primary energy sources, e.g., fuel types and characteristics.

Regions

The geographic scope of the model is Asia, which is here defined to include 23 countries and the international sea lanes (*Table 3.2* and *Figure 3.2*). The countries have been further subdivided into a total of 94 subcountry regions which roughly correspond to administrative and/or political boundaries within each country. Of these 94 regions, 22 are large metropolitan areas with current populations near or in excess of two million inhabitants. China, with 27 regions (mostly based on province boundaries) and India, with 20 regions (mostly based on state boundaries) account for approximately half of the regions. Most of the remaining countries are composed of one region.

Table 3.2 Country and Region Names and Abbreviations*

Country Name (Group)	Country Abbreviation	Region Name	Region Abbreviation
BANGLADESH/B	BANG	*DHAKA*	DHAK
		REST OF COUNTRY	REST
BHUTAN/C	BHUT	WHOLE COUNTRY	BHUT
BRUNEI/C	BRUN	WHOLE COUNTRY	BRUN
CAMBODIA/C	CAMB	WHOLE COUNTRY	CAMB
CHINA/A	CHIN	*BEIJING*	BEIJ
		CHONGQING	CHON
		FUJIAN	FUJI
		GUANGDONG-HAINAN	GUAH
		GUANGXI	GUAX
		GUANGZHOU	GUAZ
		GUIYANG	GUIY
		GUIZHOU	GUIZ
		HEBEI-ANHUI-HENAH	HEHE
		HUBEI	HUBE
		HUNAN	HUNA
		INNER MONGOLIA:NEI MONGOL-NINGXIA	IMON
		JIANGSU	JINU
		JIANGXI	JINX
		NE PLAIN:HEILONGJIANG-JILIN-LIAONING	NEPL
		SHANGHAI	SHAN
		SHENYANG	SHEN
		SHAANXI-GANSU	SHGA
		SHANDONG	SHND
		SHANXI	SHNX
		SICHUAN	SICH
		TAIYUAN	TAIY
		TIANJIN	TIAN
		WEST: TIBET-QINGHAI-XINJIANG UYGUR	WEST
		WUHAN	WUHA
		YUNNAN	YUNN
		ZHEJIANG	ZHEJ
HONG KONG/C	HONG	WHOLE COUNTRY	HONG
INDIA/A	INDI	ANDHRA PRADESH	ANPR
		WEST BENGAL	BENG
		BIHAR	BIHA
		BOMBAY	BOMB
		CALCUTTA	CALC
		DELHI	DELH
		E.HIMALAYAS:ASSAM-NE HIGHLAND	EHIM

Country Name (Group)	Country Abbreviation	Region Name	Region Abbreviation
		GUJARAT	GUJA
INDIA/A	INDI	HARYANA	HARY
		KARNATAKA-GOA	KARN
		KERALA	KERA
		MADRAS	MADR
		MAHARASHTRA-DADRA-NAGAR HAVELI-DAMAN-DIU	MAHA
		MADHYA PRADESH	MAPR
		ORISSA	ORIS
		PUNJAB-CHANDIGARH	PUNJ
		RAJASTHAN	RAJA
		TAMIL NADU-PONDICHERRY	TAMI
		UTTAR PRADESH	UTPR
		W.HIMALAYAS:JAMMU-KASHMIR-HIMACHAL PRADESH	WHIM
INDONESIA/A	INDO	*JAKARTA*	JAKA
		JAVA	JAVA
		REST OF COUNTRY	REST
		SUMATRA	SUMA
JAPAN/A	JAPA	CHUGOKU-SHIKOKU	CHSH
		CHUBU	CHUB
		HOKKAIDO-TOHOKU	HOTO
		KANTO	KANT
		KINKI	KINK
		KYUSHU-OKINAWA	KYOK
KOREA-NORTH/C	KORN	WHOLE COUNTRY	KORN
KOREA-SOUTH/A	KORS	NORTH	NORT
		PUSAN	PUSA
		SEOUL-INCHON	SEOI
		SOUTH	SOUT
LAOS/C	LAOS	WHOLE COUNTRY	LAOS
MALAYSIA/B	MALA	*KUALA LUMPUR*	KUAL
		PENINSULAR MALAYSIA	PENM
		SARAWAK-SABAH	SASA
MONGOLIA/C	MONG	WHOLE COUNTRY	MONG
MYANMAR/B	MYAN	WHOLE COUNTRY	MYAN
NEPAL/C	NEPA	WHOLE COUNTRY	NEPA
PAKISTAN/B	PAKI	*KARACHI*	KARA
		LAHORE	LAHO
		NW FRONTIER PROVINCES-BALUCHISTAN	NMWP
		PUNJAB	PUNJ

Country Name (Group)	Country Abbreviation	Region Name	Region Abbreviation
		SIND	SIND
PHILIPPINES/B	PHIL	BICOL-VISAYAS-MINDANAO	BVMI
		LUZON	LUZO
		METRO MANILA	MANI
SEALANES	SEAL	INTERNATIONAL SHIPPING ROUTES	SEAL
SINGAPORE/C	SING	WHOLE COUNTRY	SING
SRI LANKA/C	SRIL	WHOLE COUNTRY	SRIL
TAIWAN/C	TAIW	WHOLE COUNTRY	TAIW
THAILAND/B	THAI	*BANGKOK METROPOLITAN REGION*	BANG
		CENTRAL VALLEY	CVAL
		NE PLATEAU	NEPL
		N HIGHLANDS	NHIG
		S PENINSULA	SPEN
VIETNAM//B	VIET	NORTH: RED RIVER DELTA-HANOI	NORT
		SOUTH: MEKONG RIVER DELTA-HO CHI MINH CITY	SOUT

* NOTES The 22 italicized entries under "Region Name" represent urban areas.

Group A: This group contains the five Asian countries which have the largest present or potential emissions of SO_2. Data for each country were gathered by a National Contact Person member of the Trans-Asia Energy Network.

Group B: This group contains the next seven countries with significant SO_2 emissions. Data were also gathered for each country by a National Contact Person member of the RAINS-ASIA Energy Network.

Group C: The final group of countries in Asia are all single-region countries. Data collection and database development were less involved, and national published statistics could be relied upon for the majority of the data. For this reason, these countries were not represented in the Network by a National Contact Person. AIT assumed the responsibility for the database development for these countries.

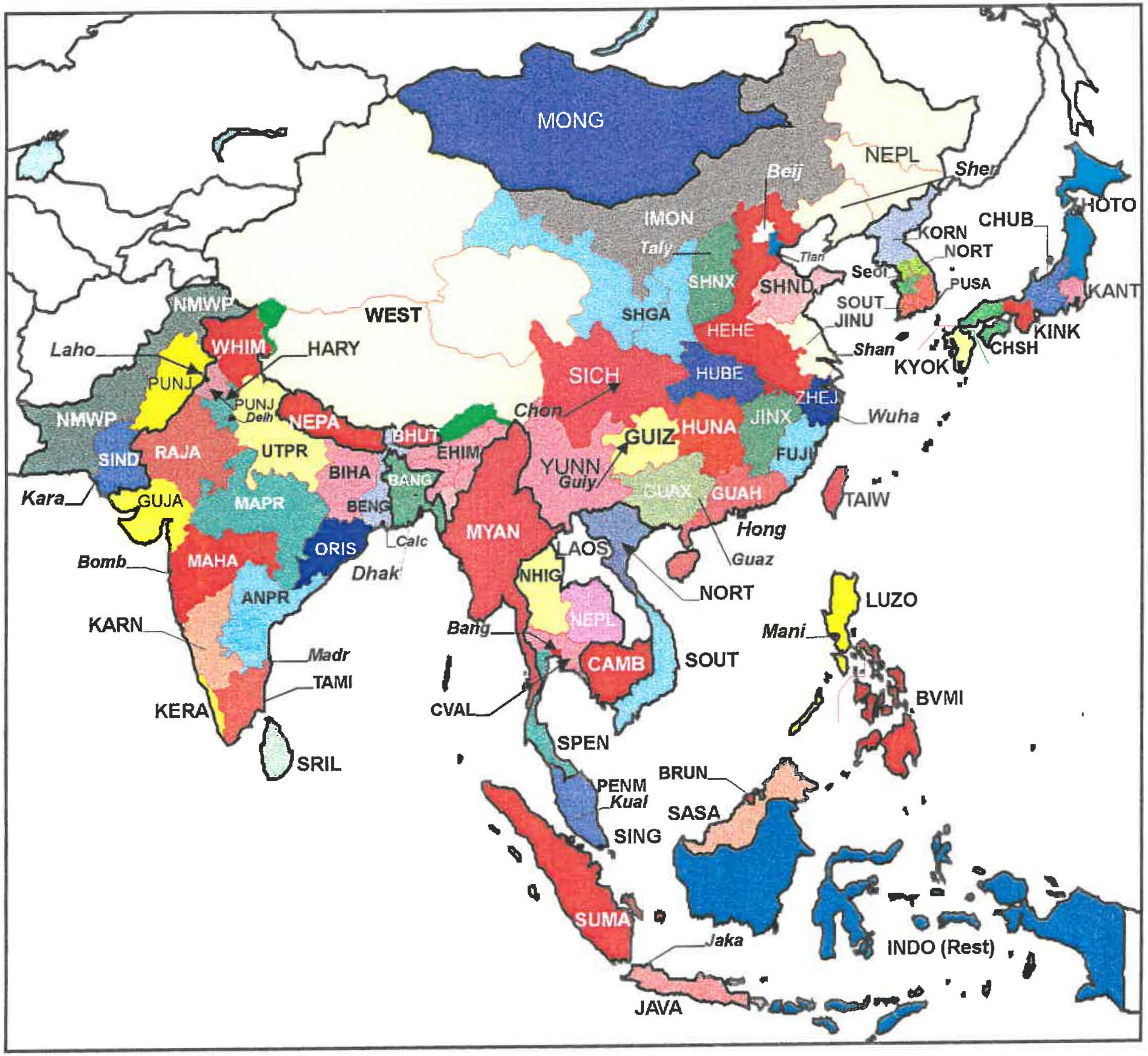

GUIDE
See Table 3.1 for country and region names.
Region abbreviations - in all capitals, for example:
LUZO
Megacity abbreviations - Italicized and first letter capitalized, for example:
Bang

Figure 3.2 Map of the Geographic Regions of Asia

3.2.2 General Structure of RESGEN

Figure 3.3 shows a schematic of the RESGEN model. The figure highlights the links between the various input parameters and how they are used to compute regional and LPS energy consumption. It should be noted that throughout the model, energy supply is assumed to meet energy demand; in other words, the model is demand constrained, not supply constrained. National energy scenarios for each sector are developed at the country level. Fuel consumption is then apportioned to subcountry regions using historical regional distributions, and regional socioeconomic projections.

The following is a discussion of the important factors and procedural steps used in the development of regional energy scenarios.

- National socioeconomic information is the input to a national energy demand model which is structured according to the six end-use energy sectors.

- National sectoral energy demand is calculated according to the scenario assumptions relating to technology.

- Energy use is then apportioned to the subcountry regions, based upon regional socioeconomic base-year data and future regional socioeconomic scenarios.

- Regional sectoral energy use is disaggregated into individual fuel types, according to regional fuel fractions of the base year and future sectoral fuel mix assumptions.

- The outputs of the energy demand analysis define the energy supply requirements. Energy supply is assumed to meet energy demand. Electricity generation is the only supply component analyzed in detail, because it plays the largest role in air pollution emissions. Major power plants are represented as LPS. Demand for electricity, aggregated at the national level, determines the requirement for future electricity generating plants.

- Power plants of specific types, fuels, and sizes are located at predefined locations, identified by specific latitude and longitude coordinates.

- Remaining electricity demand is assumed to be met by small, dispersed electricity generating sources whose fuel mix and regional distribution is controlled by the user.

- The resulting energy scenario, defined by the above seven steps, includes data points for the base year (1990) and for the scenario years 2000, 2010, and 2020. The output data are converted to databases in the requisite RAINS-ASIA format.

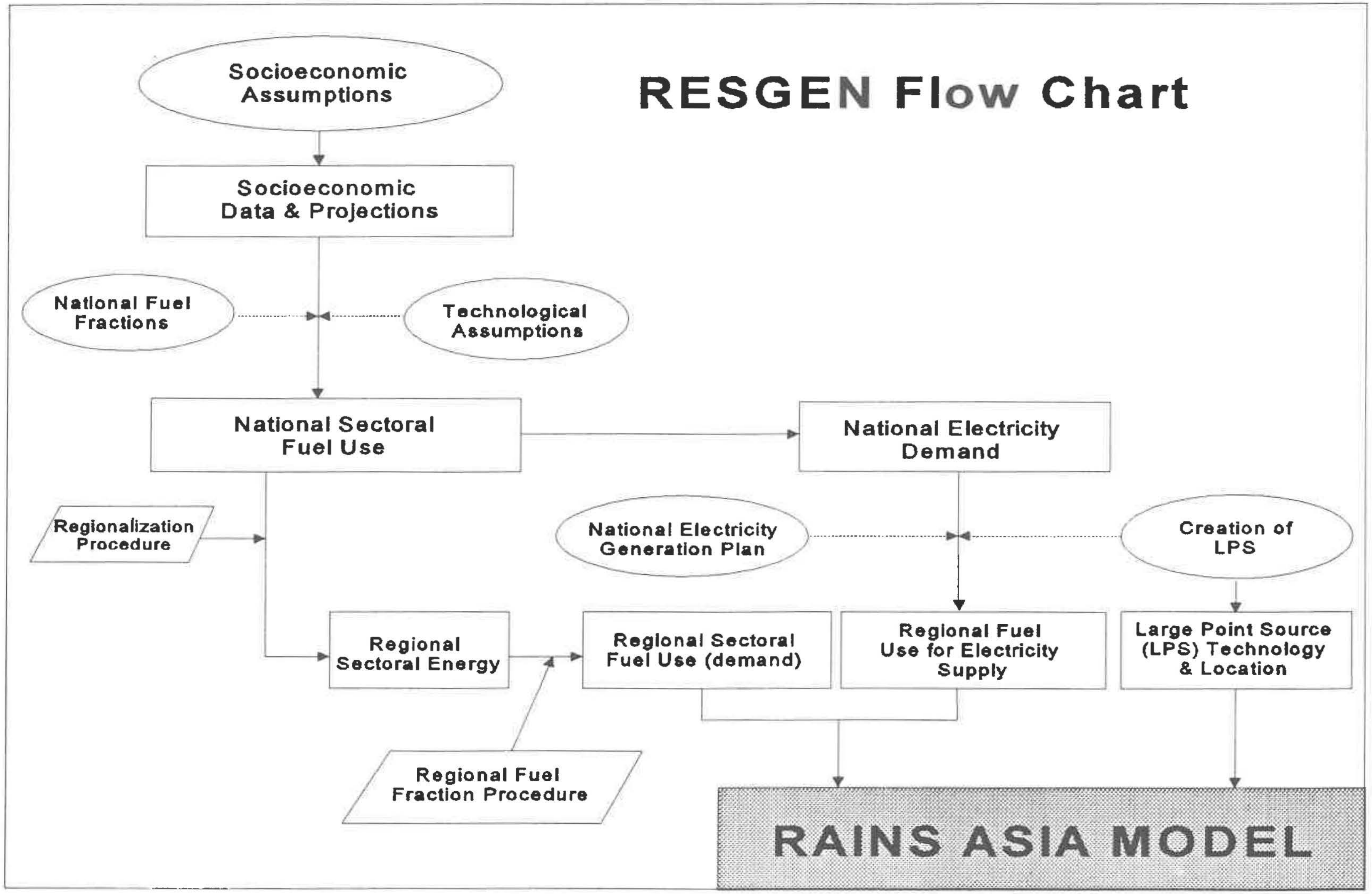

Figure 3.3 Overall Flow of Information in RESGEN

3.2.3 Detailed Discussion

Sectoral end-use energy consumption

Sectoral energy consumption is disaggregated into six end-use energy consumption sectors which are residential, commercial, agricultural, industrial, transportation, and non-energy. Each end-use energy sector is modeled in a similar way.

Sectoral end-use energy demand is given by :

$$ED_{jkt} = SE_{jkt} \times EI_{jk}|_{t-t_s} \times evolEI_{jkt} \tag{1}$$

where:

j = country index.
k = sectoral index.
t = time index (t_s represents the time step for calculations).
ED = sectoral end-use energy demand.
SE = socioeconomic variable (e.g., population, GDP).
EI = sector energy intensity.
evolEI = evolution of the sector energy intensity over the period ($t-t_s$) to t expressed as (1 + the average annual rate of change).

Fuel type fractions are determined for the base year from national level sectoral energy use data. Estimates of future sectoral fuel use are based on trends and/or assumptions about future population and economic growth, sectoral distribution of economic growth, urbanization rates, changes in energy intensity, and changes within the fuel fractions.

Sectoral energy use by fuel type is given by:

$$EU_{jkft} = ED_{jkt} \times FF_{jkft} \tag{2}$$

where:

j = country index.
k = sectoral index.
t = time index (t_s represents the time step for calculations).
f = fuel type index (e.g., diesel, hard coal, natural gas, etc.).
EU = energy use by fuel type.
FF = fuel fraction.

National sectoral energy use figures are allocated to sub-country regions according to the socioeconomic parameter believed to be best correlated with energy consumption. Two major assumptions in this process are that the regional fuel fraction variable in the future (FF_{jklft}) will be similar to the base-year regional fuel fractions, and differences in energy intensities will continue to reflect differences present in the base year.

Regional (subcountry region) fuel use is given by:

$$EU_{jklft} = EU_{jklt} \times FF_{jklft} \tag{3}$$

subject to:

$$\sum_f FF_f \big|_{jklt} = 1 \quad ; \quad \sum_l FF_l \big|_{jkft} = 1 \tag{4}$$

where:

$$FF_{jklft} = \frac{EU_{jklft}}{EU_{jklt}} \tag{5}$$

$$EU_{jklt} = EU_{jkt} \times SEF_{jklt} \tag{6}$$

and:

j = country index.
k = sectoral index.
l = region index.
SEF = socioeconomic-based regional fraction, defined as:

$$SEF_{jklt} = \frac{SE_{jklt}}{SE_{jkt}} \tag{7}$$

Discussion of the major end-use energy sectors follows.

Residential sector

Estimates of residential energy consumption are based on population and per capita residential energy intensity forecasts. Rural and urban households are aggregated. National energy demand in future years for residential energy is estimated as the product of population and the annual residential energy intensity (i.e., the energy used in residential applications per individual, per year). Estimates of future residential energy use are based on trends and/or assumptions concerning future population growth, urbanization rates, changes in the residential energy intensity, and changes within the fuel fractions. Although energy intensities are functions of household income level, the efficiency of residential appliances, the pattern of appliance use, and other direct and indirect factors, these are not considered explicitly in the model.

National residential energy use figures are allocated to subcountry regions based on the percent of total population in each region and the base-year, residential fuel-use distribution.

Regional energy intensities are assumed to change proportionally to changes in the national-level residential energy intensity.

The residential model is useful in examining the following types of questions related to future energy/emissions patterns:

- What are the effects of increasing standards of living (represented by increases in per capita energy consumption) on energy use and emissions? How would the energy use and emissions levels change if per capita energy use increased to levels found in industrialized countries?

- What are the effects, on energy use and emissions, of policies encouraging fuel substitution, such as rural electrification programs?

Commercial sector

The key variable in the commercial sector model is gross income generated by the commercial and service sectors. National commercial sector energy demand is estimated from its gross domestic product and a commercial sector energy intensity (i.e., the energy required by the commercial sector to produce a unit of commercial sector GDP). As with residential energy intensity, commercial energy intensity incorporates a variety of detailed direct and indirect factors, such as building type, that are not considered explicitly in the model. Fuel-mix fractions for the base year are determined from national level, commercial energy-use data. Estimates of future commercial fuel use are based on trends and/or assumptions about future commercial sector GDP growth, changes in the commercial energy intensity, and changes in the sector's fuel mix.

National commercial energy use figures are allocated to subcountry regions based on the percent of total commercial GDP in each region and the base year commercial fuel use distribution. Energy intensities for each region are assumed to change proportionally to changes in the commercial energy intensity at the national level.

The commercial sector model is useful in examining the following types of policy questions:

- To what degree do changes in the rate of economic growth affect commercial energy use and emissions?

- In combination with the other "intermediate" sectors (e.g., agriculture and industry), how might gross sectoral shifts in economic output affect emission patterns?

- How might policies to encourage energy efficiency and/or fuel shifts to lower emission fuels affect emissions?

Agricultural sector

The agricultural sector is modeled similarly to the commercial sector. The key variable in the agricultural model is gross income generated by agricultural production. National energy demand is estimated from input data on the agricultural sector's share of GDP and an agricultural sector energy intensity (i.e., the energy required by the agricultural sector to produce a singularity of agricultural GDP). As with both the residential and commercial energy intensities, the agricultural energy intensity incorporates a variety of direct and indirect factors, such as efficiency differences depending on farm size and management, that are not considered explicitly in the model. From national-level agricultural energy use data, fuel fractions are determined for the base year. Estimates of future agricultural energy use are based on trends and/or assumptions about future agricultural sector GDP growth, changes in the agricultural energy intensity, and changes in the fuel fractions.

National agricultural energy use figures are allocated to subcountry regions based on percent of total agricultural GDP in each region. Agricultural energy intensities for each region are assumed to change proportionally to the changes in the national-level agricultural energy intensity.

The agricultural sector model is useful in examining the following types of policy questions:

- To what degree do changes in the rate of economic growth affect commercial energy use and emissions?

- How might policies to encourage energy efficiency and/or fuel substitution by lower emission fuels affect emissions from the agricultural sector?

Industrial sector

The key variable in the industrial model is the share of GDP generated by industry. In this initial version of RESGEN, all industries are aggregated into a single industry.

National industrial energy demand is calculated from industrial gross domestic product and an industrial energy intensity (i.e., the energy required by industry to produce a unit of industrial output). As with the previously discussed sectors, the industrial energy intensity combines, into one coefficient, a whole set of technological and non-technological factors, such as differences in process efficiencies and energy management, which are not considered explicitly in the model.

From national industrial energy-use data, fuel fractions are determined for the base year. Estimates of future industrial energy use are based on trends and/or assumptions about future industrial GDP growth, changes in the industrial energy intensities, and changes in the fuel fractions.

National industrial energy-use figures are allocated to subcountry regions based on the fraction of total national industrial GDP within each region.

The industrial energy model will be useful in addressing several key policy questions such as:

- What are the effects on energy use and emissions of policies encouraging fuel substitution, such as increased use of electricity and/or natural gas?

- To what degree can emissions be reduced by the introduction of energy efficiency improvement and demand-side management?

- To what degree do changes in the rate of economic growth affect industrial energy use and SO_2 emissions?

Transportation sector

The transportation model follows the same methodology as the sectors described above. The key variable used to estimate transportation energy use is population. Data on national transportation energy use by fuel type in the Base Year and population scenarios provide the information used to calculate future national energy demand for transportation. Because economic forces undoubtedly play a large role in the development of the freight transportation sector, their influence on future energy consumption must be taken into consideration by the user when developing future scenarios for the transportation energy intensity. Using national transportation energy-use data, fuel fractions are determined for scenario years based on historical trends and assumptions about the fuel mix in future years.

National transportation energy-use figures are allocated to subcountry regions based on the percent of total population in each region. Transportation energy intensities are assumed to change proportionally to the national-level transportation energy intensity.

The transportation sector model is useful in examining several key types of policy questions including:

- How do changes in the rate of population growth and the intensity of transportation energy consumption affect emissions?

- How might policies to encourage energy efficiency and/or alternative modes of transportation affect emissions?

Non-energy use

Energy consumption in this sector includes the consumption of lubricants, heavy oil fractions (e.g. asphalt for road construction), and fuel used as chemical feed stocks. Non-energy consumption implies that these fuels are consumed by processes other than combustion, and thus, consumption of the fuels in the sector does not contribute to emissions of SO_2. Because the growth of fuel consumption for this sector is more strongly linked to the development of specific industries than to the development of GDP, the fuel consumption in the non-energy sector is input exogenously by the model user for each scenario year.

Energy supply sector

Electricity generation sector

The electricity generation sector is characterized by the assumption that demand will determine supply. Demand for electricity is aggregated at the country level and is estimated by summing the electricity demand for each of the end-use energy sectors. Development of scenarios depicting future electricity generation systems requires detailed data on the present electricity system (e.g., existing plant locations and types, plant capacities, conversion efficiency, capacity factors, age, expected lifetime, and data regarding system transmission/distribution losses).

Future electric generation scenarios are developed by an iterative process. First, future trends in system-wide characteristics including primary fuel mix, auxiliary power consumption, imports/exports of power, and electricity grid transmission and distribution losses are defined. Second, future plants are either selected from a list of LPS electric generation technologies, or the capacity of existing generating plants is expanded. The data that define the future power plants include input fuel type, capacity, capacity factor, conversion efficiency, and expected lifetime. In future years plants are added to the system until electric demand and fuel mix targets are reached.

The geographic location of new plant capacity is a scenario variable. Thus, electric supply planning data can be utilized to determine the sites, and perhaps types, of generating plants. Based on the constraints imposed by the atmospheric source-receptor transfer matrix in RAINS-ASIA, there is a maximum of 332 unique locations for large point sources in the model and a total of 355 LPS (some LPS share locations). These locations are shown on the map in *Figure 3.4.*

If specific information regarding the location of future plants is not available, or the locations are not included in the list of available LPS location, simplifying assumptions are necessary to locate the new capacity additions within the country. The simplest method employed is the "expanding plant model" where future capacity is assumed to be added to existing capacity. Another option is to assume that additional fuel consumption for electricity generation is not due to LPS, but "area" generating sources. In this instance, primary fuel consumption for electricity generation is allocated to specific regions and assumed to be uniformly distributed across each region.

1) National electricity demand

$$NElD_{jt} = \sum_{k} EU_{jkf_e t} \tag{8}$$

where:

- EU = energy use by fuel type
- f_e = fuel index for electricity.
- j = country index.
- k = sectoral index.

t = time index (t_s represents the time step for calculations).
NElD = national electricity demand.

2) Required electricity generation to meet demand

$$REIGEN_{jt} = [NElD_{jt} \div (1 - SYSLOSS_{jt})] -/+ IMPEXP_{jt} \qquad (9)$$

where:

REIGEN = electricity generation required to meet demand.
SYSLOSS = system losses + auxiliary consumption (fraction of net generation).
IMPEXP = net import (-) or export (+) of electricity

3a) Electric generation by existing LPS capacities

$$ELPSGEN_{jpt} = (OP_p \times ELPSCAP_{jpt} \times ELPSCF_{jpt}) \qquad (10)$$

where:

p = LPS plant index.
ELPSGEN = electricity generation by existing LPS plant.
OP = operation index; = 1, for $t < t_{retire}$
= 0, otherwise.
ELPSCAP = existing LPS plant capacity.
ELPSCF = existing LPS plant capacity factor.

3b) Electric generation by existing non-LPS (area sources) capacities

$$EAREAGEN_{jlt} = EAREACAP_{jlt} \times EAREACF_{jt} \qquad (11)$$

where:

EAREAGEN = generation by existing non-LPS plants.
EAREACAP = total existing non-LPS plant capacity for each region.
EAREACF = average existing non-LPS plant capacity factor.

4a) Electric generation by new LPS capacities

$$NLPSGEN_{jpt} = (OP_p \times NLPSCAP_{jpt} \times NLPSCF_{jpt}) \qquad (12)$$

where:

p = LPS plant index.
NLPSGEN = electricity generation by new LPS plants.
OP = operation index; = 1, for $t_{start} \leq t \leq t_{retire}$
= 0, otherwise.
NLPSCAP = new LPS plant capacity.
NLPSCF = new LPS plant capacity factor.

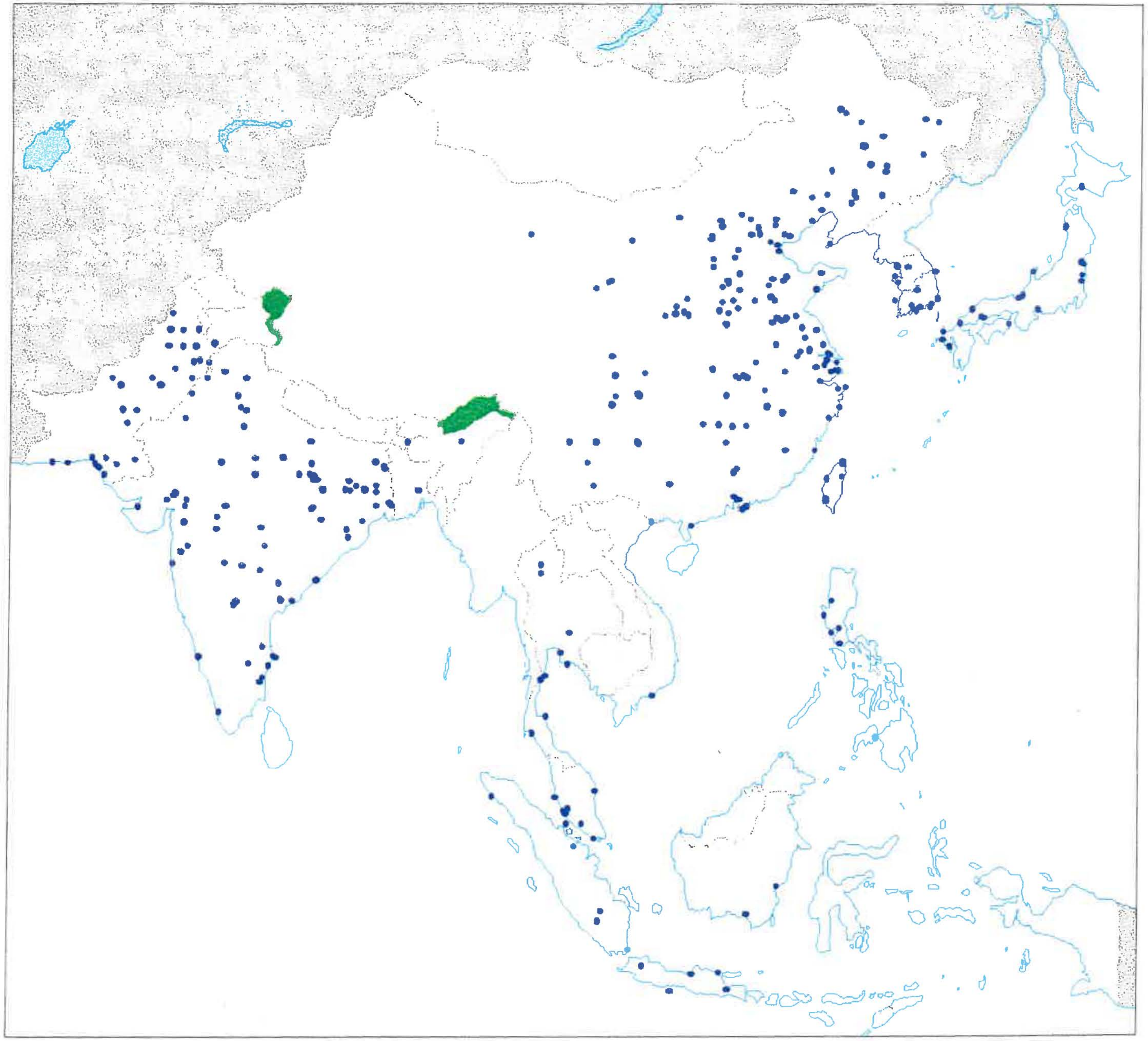

Figure 3.4 Map of Large Point Sources (LPS) in Asia

4b) Electric generation by new non-LPS (area sources) capacities

$$NAREAGEN_{jlt} = NAREACAP_{jlt} \times NAREACF_{jt} \tag{13}$$

where:

NAREAGEN = generation by new non-LPS plants.
NAREACAP = total new non-LPS plant capacity for each region.
NAREACF = average new non-LPS plant capacity factor.

5) Additional new generation required to meet demand

$$\begin{aligned} ADDGEN_{jt} = {} & REIGEN_{jt} - \sum_{p} (ELPSGEN_{jpt} + NLPSGEN_{jpt}) \\ & - \sum_{l} (EAREAGEN_{jlt} + NAREAGEN_{jlt}) \end{aligned} \tag{14}$$

where:
ADDGEN = additional new generation required

6) Allocate additional new required generation to generation fuel types

$$ADDGEN_{jft} = ADDGEN_{jt} \times ELFrac_{jft} \tag{15}$$

where:
ADDGEN = additional new generation by generation fuel type
ELFrac = generation fuel fraction for electric generation, and

$$\sum_{f} ELFrac_{jft} = 1 \tag{16}$$

7) Selection of new LPS plants and/or new LPS capacity to add to existing LPS plants

New LPS or capacity expansions at existing LPS are added by an iterative process. First, a location is chosen from the available site list. Second, a new LPS plant type is selected from a database of possible "LPS reference plants". Input data required to define each plant are: fuel type, unit capacity, number of units, plant capacity factor, age/lifetime, auxiliary consumption, and plant efficiency. Additional capacity can be added to an existing LPS by increasing the number of units added in a given year. However, only one type of plant may be added to a given LPS each year.

LPS plants or capacities are added until the desired generation fuel mix is achieved and the electricity demand is met. If, however, the new LPS generating capacity is insufficient to meet electricity demand, the shortfall is met by assuming the requirements are small non-LPS (area sources) facilities. These small, non-LPS facilities' aggregate-generation fuel mix achieves the goal of the total-generation fuel mix specified in the variable array ELFrac. The regional location of these small area sources is user-specified.

8) New area source generation by primary fuel type

$$NAREAGEN_{jflt} = (ADDGEN_{jft} - \sum_{p} NLPSGEN_{jpft}) \times NAREAFrac_{jlft} \qquad \textbf{(17)}$$

where:

p ⊂ l,	for all plants, p, found in region, l.
NAREAGEN =	new area source generation by primary fuel type
NLPSGEN =	electricity generation by new LPS plants added iteratively from the list of reference plants.
NAREAFrac =	regional generation fraction for non-LPS electric generation, for which

$$\sum_{l} NAREAFrac_{jlft} = 1 \quad ; \quad \sum_{f} NAREAfrac_{jlft} = 1 \qquad \textbf{(18)}$$

9) Primary fuel use for electric generation

$$\begin{aligned} PEU_{jft} = & \sum_{p} (ELPSGEN_{jpft} \times HR_p) + \sum_{l} (EAREAGEN_{jlft} \times HR_j) \\ & + \sum_{p} (NLPSGEN_{jpft} \times HR_p) + \sum_{l} (NAREAGEN_{jlft} \times HR_{jt}) \end{aligned} \qquad \textbf{(19)}$$

where:

PEU =	primary energy use by fuel type for electricity generation.
HR =	average heat rate for LPS and non-LPS.

3.3 RESGEN and RAINS-ASIA Databases

The generation of regional energy scenarios in Asia has required the development of a unique regional database. Because many of the countries in Asia do not have regional (subcountry) information readily available, this database had to be created.

3.3.1 Institutional Process

AIT, Resource Management Associates (RMA), and the International Institute for Applied Systems Analysis (IIASA) had the main responsibility for creation of the databases used in this project. The four major elements of the data base for each country are:

- Socioeconomic Database
- Energy Database
- Fuel Characteristics Database
- Large Point Source Database.

The modeling approach followed by the RAINS-ASIA project required "regional" or sub-country data. Because of the new and unique nature of these regional databases and resultant scenarios, a network of collaborating Asian research institutions was needed to assist in collecting data and developing the databases. AIT, under contract to ADB, played the main role in the establishment of this network and in the coordination of the primary data collection, and database creation. This network, the RAINS-ASIA Energy Network, serves not only to facilitate the data collection process in the countries, but also serves as a convenient vehicle for establishing ties to key institutions and potential RAINS-ASIA users.

Twelve Asian institutions actively participate in the network. For identification purposes, each country's representative in the network is referred to as the National Contact Person (NCP). Refer to *Table 3.1* for the names of the 12 National Contact Persons and their respective institutions.

The initial databases developed for the project to date are the result of an inter-institutional process. Each country database was created in a sequential process, generally beginning with the collection efforts of the NCP. Intermediate data processing and modification were carried out by AIT, RMA, and IIASA. The process included considerable feedback and iteration between the organizations.

- Initial country databases were produced by the NCP and submitted to AIT. For most of the countries, these databases were developed in the form of a hard copy of documented and referenced reports, tables and appendices.

- These databases were input by AIT into spreadsheets and reviewed for consistency with other published data. These data are published in the ADB report *Acid Ran and Emissions Reductions in Asia* (AIT, 1995).

- The socioeconomic, energy and fuel characteristics databases developed by AIT were transformed into a form consistent with the structure needed by RESGEN (RMA, 1993) and were sent to RMA for review and further modification. The LPS databases were transmitted to IIASA where these data were supplemented with data from the International Energy Agency (IEA) Asia Coal Data Base (Maude, *et al.*, 1994) and input in to a format consistent with the RAINS-ASIA data requirements. These data were then transmitted to RMA.

- These workable, secondary databases were used as inputs to RESGEN and provide the basis for the development of regional energy scenarios for the RAINS-ASIA model.

3.3.2 Data Requirements

The Energy Module of the RAINS-ASIA model is very data-intensive. As described in Chapter 2 and shown on the main RAINS-ASIA flow chart (*Figure 3.1*), the country databases are comprised of two main types of data: Base Year data and Scenario data. IIASA has produced an internal Working Paper which describes the field-by-field database content and format required as input to the RAINS-ASIA model (Bertok, *et al*, 1993). RMA has written a follow-up document which assists the data collector in interpreting the IIASA document and provides specification for additional data as required by the RESGEN energy scenario generator (RMA, 1993). The discussion below briefly summarizes these detailed reports.

Scope

Geographic Definitions

The complete RAINS-ASIA database consists of a total of twenty-three (23) country databases and one database for international shipping lanes. The countries included in the database are shown in *Table 3.2*.

Data for each of the 23 countries and the international shipping lanes is stored at the disaggregated regional level. The 94 regions in RAINS-ASIA were defined in collaboration with the members of the RAINS-ASIA Energy Network, AIT, and representatives from the World Bank and ADB. The regions were chosen using the following criteria:

- Alignment with administrative or geographic boundaries within countries

- Level of present and potential future emissions

- Separate identification of fast-growing and/or very large urban agglomerations (Megacities)

- Total manageable number of regions to be approximately 100.

Ninety-three regions are land-based and represent a whole or part of one of the countries listed in *Table 3.2*; the 94^{th} region is reserved for international shipping lanes. A complete listing of the regions included in RAINS-ASIA and their associated countries is also shown in that table.

Temporal Definitions

Data for RAINS-ASIA are reported for one base year and three scenario years:

Base Year: 1990
Scenario Years: 2000, 2010, 2020

Some historical data pertaining to the time-period for the construction of boilers at Large Point Sources is reported for time-periods prior to 1990. For a more detailed explanation see Bertok, *et al.* (1993). Projected values for years between the scenario years are determined for data presentation purposes by linear interpolation.

Database Description of the RESGEN Databases

Socioeconomic Database

Regional databases were developed for population and GDP. Population data were collected for historic years at 1980 and 1990. Regional projections and population figures were provided by AIT and the RAINS-ASIA Energy Network for the scenario years 2000, 2010, and 2020.

GDP and GRP are disaggregated into three sectors: industry, agriculture, and commercial/other. GRP databases for each sector were collected for historic years at 1980 and 1990. Sectoral GRP projections were provided by AIT and the RAINS-ASIA Energy Network for the scenario years 2000, 2010, and 2020.

Energy Database

Fuel and Sector Definitions - A total of 17 different fuel types are considered. These fuel types along with a brief description are listed in *Table 3.3.*

Energy data are classified into eight major categories. These categories include the major energy supply and consumption sectors of the economy, and data are commonly available for these classifications in most published energy statistics. The major categories considered are:

- Fuel Conversion and Loss
- Power Plants
- Residential
- Commercial/Other
- Agricultural
- Transportation
- Industry
- Non-energy Use

Fuel Characteristics Data

Sulfur dioxide emissions from fuels are highly dependent on fuel quality. Regional-level fuel characteristics databases were developed for each of the 23 countries. The fuel characteristics are needed to calculate emissions from area sources (i.e., non-point sources and small point sources). Data collected on fuel characteristics includes: the calorific value and sulfur content and the percent of the original sulfur in the fuel retained in the ash following combustion for the solid fuels. Fuel characteristics are collected separately for each energy sector where fuel is combusted (i.e., fuel characteristics are not collected for the non-energy use and fuel conversion and loss categories).

Large Point Source Data for Power Plants

In general, an LPS is any emission source, at a fixed location, for which individual data are collected. Specifically, for the development of this database, a large point source is defined as an emitting complex with:

- total electric output capacity $\geq$ 300 MW_e [electric power plants], or
- total thermal input capacity $\geq$ 900 MW_{th} [industrial plants], or
- annual SO_2 emissions greater than 20,000 metric tons.

The above LPS definition is arbitrary, and was chosen only to limit the number of existing LPS modeled to about 355. The data collected for the LPS database are detailed and comprehensive. For a complete description of these data, consult Bertok, *et al.* (1993).

3.3.3 Status of Regional Database

A workable regional database has been created for Asia and used successfully to create regional energy scenarios with the RESGEN model. This represents the first subregional, Asia-wide database of its type. It provides a foundation for future RAINS-ASIA applications and case studies. The quality of the data varies somewhat from country to country. Comparison of national aggregations of the AIT-developed Base Year regional databases with other sources of national statistics (e.g., IEA and ADB data) shows that, for some countries, additional work is required to develop consistency between official national energy statistics and the regional database (see *Table 3.4*). An iterative process of evaluation and revision of the databases is underway within the RAINS-ASIA Energy Network. It is recommended that additional work of this type be carried out concurrently with any further studies undertaken.

Table 3.3 Fuel Types and Brief Descriptions

Fuel	Fuel Code
Brown coal/lignite, high quality	BC1
Brown coal/lignite, low quality	BC2
Hard coal, high quality	HC1
Hard coal, medium quality	HC2
Hard coal, low quality	HC3
Derived coal (coke, briquettes)	DC
Other solids, low sulphur	OS1
Other solids, high sulphur	OS2
Heavy Fuel oil	HF
Medium distillates (diesel oil, light fuel oil)	MD
Light fractions (gasoline, kerosene, naphthas, LPG)	LF
Natural Gas	GAS
Renewables	REN
Hydro	HYD
Nuclear	NUC
Electricity	ELE
Heat (steam and hot water)	HT

NOTE: The two categories for other solids include biomass fuels such as firewood, plant residue, charcoal, and animal wastes as well as garbage for incineration. In countries such as India or Bangladesh, "OS1" is used for wood and vegetable waste and "OS2" is used for dung.

The "Renewables" category includes solar, small-scale hydro, wind, geothermal, etc. Because these fuels do not emit SO_2, biomass fuels are included in OS1 or OS2.

Table 3.4 Base Year (1990) National Primary Energy Consumption Data Source Comparison [all data in PJ]

Country	RAINS-ASIA		IEA		ADB
	Total	Commercial	Total	Commercial	Commercial
BANG	805.3	306.3	307.2	327.9	168.3
BHUT	22.5	1.6	na	na	na
BRUN	61.8	61.1	na	86.8	86.0
CAMB	101.0	51.0	na	na	na
CHIN	30254.7	30254.7	29909.2	29300.1	27369.2
HONG	422.1	421.4	427.9	440.9	438.6
INDI	15811.7	7424.7	8331.0	10573.5	7825.8
INDO	3793.2	2439.4	2290.1	3283.9	1845.8
JAPA	17865.5	17865.5	na	15869.9	15867.9
KORN	1764.1	1764.1	na	1843.5	1803.7
KORS	3593.9	3560.5	3810.3	3538.0	3510.2
LAOS	38.1	5.1	na	na	na
MALA	1059.8	998.0	780.4	799.8	709.5
MONG	151.1	140.3	na	na	na
MYAN	309.2	63.9	80.7	274.3	85.8
NEPA	269.6	21.5	17.2	194.9	15.4
PAKI	1435.6	1131.3	1274.1	1328.2	1044.6
PHIL	585.1	585.1	643.5	1035.7	664.7
SEAL	163.0	163.0	na	na	na
SING	342.4	342.4	na	407.5	407.5
SRIL	190.3	82.8	89.1	176.7	87.2
TAIW	2094.0	2094.0	2126.9	2104.6	2104.6
THAI	1688.5	1192.0	1254.6	17987.1	17468.7
VIET	771.8	287.1	297.3	555.3	309.7
TOTALS	83594.3	71256.8	51639.5	90128.6	81813.2

NOTES: "Total" includes biomass; "Commercial" does not include biomass.
See Table 3.2 for country abbreviations.

3.4 Energy Scenario Assumptions

3.4.1 Socioeconomic Factors

Socioeconomic factors are used to estimate the national energy demand for each end-use sector and to apportion end-use fuel consumption to the regional level. The two major types of socioeconomic variables considered are population and GDP.

All energy scenarios are developed from socioeconomic scenarios. A socioeconomic scenario consists of a set of assumptions regarding the regional growth of population and GDP over the time period from 1990 to 2020.

Population

Regional population scenarios are developed through exogenous assumptions of the annual growth rates of total regional population for three time periods: 1990 to 2000, 2000 to 2010, and 2010 to 2020. The use of region-based assumptions for population allows the model to simulate shifts in the distribution of national population such as those exemplified by urban migration. Population data at the regionally disaggregated level required by RESGEN was not available through internationally recognized sources such as the United Nations or the World Bank. As a result, the data and assumptions used to develop the base-case regional and national (shown in *Table 3.5*) population scenarios for each country were obtained through the RAINS-ASIA Energy Network.

Gross Domestic Product

GDP is disaggregated into three sectoral components: industry, agriculture, and commercial/ other. This level of economic aggregation is necessary to capture the structural shifts in the economies of many developing countries. Currently, many developing countries in Asia are experiencing rapid industrialization while agricultural output remains essentially stable. As these economies develop over the next several decades, it is anticipated that the contribution of the services sector to the total economic production will rise, and industry will decline slightly (see *Table 3.6*). Economic developments will profoundly impact the overall intensities and the resulting SO_2 emissions.

GRP scenarios are developed for each of the three sectors for each region. Exogenous assumptions regarding the annual growth rates of each region's sectoral GRP are developed for three time periods: 1990 to 2000, 2000 to 2010, and 2010 to 2020. The use of region-based economic assumptions allow the model to simulate differing levels of economic growth and industrialization regionally. Flexibility in implementing these types of assumptions is useful to policy makers interested in exploring targeted regional economic and industrial expansion plans such as the *special economic zones* in China. Finally, national-level GDP is calculated by aggregating the sectoral GRP values of each region. The data and assumptions used to develop the base case regional and national economic scenarios for each country were obtained through the RAINS-ASIA Energy Network.

Although the socioeconomic scenario development process is an approximation, it adequately provides the spatial accuracy required for regionally allocating emission sources for the long-range transport calculations. When completed, the impacts of the population and GDP assumptions combine to provide a consistent regional socioeconomic scenario for each country. This socioeconomic scenario is then used to provide the basis for an energy demand scenario.

Table 3.5 Base Case Population Scenario Assumptions: National Totals

NOTE: POP = Population in millions AAGR = Average Annual Growth Rate

Country	1990 Base Year	2000		2010		2020	
		POP	*AAGR*	POP	*AAGR*	POP	*AAGR*
BANG	106.12	126.00	*1.73%*	148.00	*1.62%*	170.00	*1.40%*
BHUT	1.43	1.94	*3.10%*	2.47	*2.44%*	3.07	*2.20%*
BRUN	0.25	0.32	*2.50%*	0.40	*2.26%*	0.48	*1.84%*
CAMB	8.57	11.32	*2.82%*	14.80	*2.72%*	19.40	*2.74%*
CHIN	1171.94	1324.48	*1.23%*	1453.42	*0.93%*	1535.44	*0.55%*
HONG	5.80	6.04	*0.41%*	6.44	*0.64%*	6.86	*0.63%*
INDI	847.18	1048.27	*2.15%*	1294.04	*2.13%*	1597.43	*2.13%*
INDO	192.05	228.22	*1.74%*	263.47	*1.45%*	296.30	*1.18%*
JAPA	123.50	126.80	*0.26%*	128.99	*0.17%*	126.89	*-0.16%*
KORN	21.77	26.11	*1.83%*	29.32	*1.17%*	31.92	*0.85%*
KORS	42.87	46.79	*0.88%*	49.68	*0.60%*	50.58	*0.18%*
LAOS	4.14	5.59	*3.05%*	7.20	*2.56%*	8.71	*1.92%*
MALA	17.75	24.56	*3.30%*	31.36	*2.47%*	39.95	*2.45%*
MONG	2.12	2.68	*2.37%*	3.30	*2.10%*	4.27	*2.61%*
MYAN	40.78	49.10	*1.87%*	58.47	*1.76%*	68.54	*1.60%*
NEPL	18.92	24.12	*2.46%*	30.76	*2.46%*	39.22	*2.46%*
PAKI	110.40	145.90	*2.83%*	187.00	*2.51%*	239.80	*2.52%*
PHIL	60.68	75.22	*2.17%*	87.20	*1.49%*	94.68	*0.83%*
SING	2.71	3.00	*1.02%*	3.24	*0.77%*	3.50	*0.77%*
SRIL	16.99	19.38	*1.32%*	21.45	*1.02%*	23.75	*1.02%*
TAIW	20.20	23.23	*1.41%*	25.56	*0.96%*	25.57	*0.00%*
THAI	56.30	64.11	*1.31%*	71.11	*1.04%*	77.86	*0.91%*
VIET	65.18	80.50	*2.13%*	91.00	*1.23%*	108.69	*1.79%*
TOTAL	**2937.65**	**3463.68**	***1.66%***	**4008.68**	***1.47%***	**4572.91**	***1.33%***

NOTE: Country abbreviations are defined in Table 3.2.

Table 3.6 Base Case Gross Domestic Product Scenario Assumptions: National Totals

NOTE:GDP is expressed in Billions of 1990 $US AAGR = Average Annual Growth Rate

Country	Economic Sector	Base Year 1990GDP	2000		2010		2020	
			GDP	*AAGR*	GDP	*AAGR*	GDP	*AAGR*
BANG	Industry	3.56	5.47	*4.39%*	11.90	*8.08%*	24.25	*7.38%*
	Agriculture	8.24	16.42	*7.14%*	23.80	*3.78%*	33.95	*3.62%*
	Commerc/other	10.60	14.60	*3.25%*	23.80	*5.01%*	38.80	*5.01%*
	TOTAL	**22.40**	**36.49**	***5.00%***	**59.50**	***5.01%***	**97.00**	***5.01%***
BHUT	Industry	0.09	0.16	*5.92%*	0.29	*6.13%*	0.52	*6.01%*
	Agriculture	0.13	0.23	*5.87%*	0.41	*5.95%*	0.75	*6.23%*
	Commerc/other	0.09	0.16	*5.92%*	0.29	*6.13%*	0.53	*6.22%*
	TOTAL	**0.31**	**0.55**	***5.90%***	**0.99**	***6.05%***	**1.80**	***6.16%***
BRUN	Industry	0.13	0.15	*1.44%*	0.26	*5.65%*	0.41	*4.66%*
	Agriculture	0.07	0.10	*3.63%*	0.17	*5.45%*	0.27	*4.73%*
	Commerc/other	1.87	2.76	*3.97%*	4.78	*5.65%*	7.42	*4.50%*
	TOTAL	**2.07**	**3.01**	***3.81%***	**5.21**	***5.64%***	**8.10**	***4.51%***
CAMB	Industry	0.30	0.66	*8.20%*	1.18	*5.98%*	1.93	*5.04%*
	Agriculture	0.51	1.13	*8.28%*	2.03	*6.03%*	3.31	*5.01%*
	Commerc/other	0.75	1.66	*8.27%*	2.97	*5.99%*	4.84	*5.00%*
	TOTAL	**1.56**	**3.45**	***8.26%***	**6.18**	***6.00%***	**10.08**	***5.01%***
CHIN	Industry	146.18	326.21	*8.36%*	594.39	*6.18%*	1019.10	*5.54%*
	Agriculture	90.07	159.65	*5.89%*	215.06	*3.02%*	334.15	*4.51%*
	Commerc/other	84.94	262.00	*11.92%*	587.62	*8.41%*	1023.25	*5.70%*
	TOTAL	**321.19**	**747.86**	***8.82%***	**1,397.07**	***6.45%***	**2376.50**	***5.46%***
HONG	Industry	29.95	50.62	*5.39%*	70.87	*3.42%*	119.77	*5.39%*
	Agriculture	0.19	0.32	*5.35%*	0.45	*3.47%*	0.76	*5.38%*
	Commerc/other	39.96	67.53	*5.39%*	94.55	*3.42%*	159.78	*5.39%*
	TOTAL	**70.10**	**118.47**	***5.39%***	**165.87**	***3.42%***	**280.31**	***5.39%***
INDI	Industry	69.98	108.50	*4.48%*	204.50	*6.54%*	387.40	*6.60%*
	Agriculture	65.69	106.64	*4.96%*	152.41	*3.64%*	218.04	*3.65%*
	Commerc/other	72.90	182.24	*9.60%*	343.95	*6.56%*	649.91	*6.57%*
	TOTAL	**208.57**	**397.38**	***6.66%***	**700.86**	***5.84%***	**1,255.35**	***6.00%***
INDO	Industry	56.57	94.25	*5.24%*	135.28	*3.68%*	194.85	*3.72%*
	Agriculture	22.36	30.22	*3.06%*	36.73	*1.97%*	43.61	*1.73%*
	Commerc/other	54.47	95.65	*5.79%*	138.95	*3.80%*	200.81	*3.75%*
	TOTAL	**133.40**	**220.12**	***5.14%***	**310.96**	***3.52%***	**439.27**	***3.51%***
JAPA	Industry	1151.53	1548.12	*3.00%*	1943.97	*2.30%*	2438.93	*2.29%*
	Agriculture	64.95	77.20	*1.74%*	73.40	*-0.50%*	71.23	*-0.30%*
	Commerc/other	1189.10	2786.62	*8.89%*	3716.42	*2.92%*	4877.85	*2.76%*
	TOTAL	**2,405.58**	**4,411.94**	***6.25%***	**5,733.79**	***2.66%***	**7,388.01**	***2.57%***

Country	Economic Sector	Base Year 1990GDP	2000		2010		2020	
			GDP	*AAGR*	GDP	*AAGR*	GDP	*AAGR*
KORN	Industry	12.74	14.94	*1.61%*	17.75	*1.74%*	21.88	*2.11%*
	Agriculture	7.87	7.28	*-0.78%*	6.43	*-1.23%*	7.14	*1.05%*
	Commerc/other	7.39	11.97	*4.94%*	17.58	*3.92%*	21.98	*2.26%*
	TOTAL	**28.00**	**34.19**	***2.02%***	**41.76**	***2.02%***	**51.00**	***2.02%***
KORS	Industry	110.21	225.69	*7.43%*	398.50	*5.85%*	600.48	*4.19%*
	Agriculture	22.03	26.90	*2.02%*	33.16	*2.11%*	37.84	*1.33%*
	Commerc/other	121.43	231.03	*6.64%*	394.43	*5.49%*	590.58	*4.12%*
	TOTAL	**253.67**	**483.62**	***6.67%***	**826.09**	***5.50%***	**1228.90**	***4.05%***
LAOS	Industry	0.15	0.23	*4.37%*	0.33	*3.68%*	0.48	*3.82%*
	Agriculture	0.50	0.73	*3.86%*	1.06	*3.80%*	1.56	*3.94%*
	Commerc/other	0.21	0.31	*3.97%*	0.46	*4.03%*	0.68	*3.99%*
	TOTAL	**0.86**	**1.27**	***3.98%***	**1.85**	***3.83%***	**2.72**	***3.93%***
MALA	Industry	11.58	30.55	*10.19%*	70.66	*8.75%*	146.34	*7.55%*
	Agriculture	5.43	7.05	*2.65%*	8.24	*1.57%*	14.16	*5.56%*
	Commerc/other	12.30	21.15	*5.57%*	38.86	*6.27%*	75.52	*6.87%*
	TOTAL	**29.31**	**58.75**	***7.20%***	**117.76**	***7.20%***	**236.02**	***7.20%***
MONG	Industry	0.91	1.55	*5.47%*	2.64	*5.47%*	4.49	*5.45%*
	Agriculture	0.32	0.55	*5.57%*	0.94	*5.51%*	1.59	*5.40%*
	Commerc/other	0.63	1.07	*5.44%*	1.82	*5.46%*	3.10	*5.47%*
	TOTAL	**1.86**	**3.17**	***5.48%***	**5.40**	***5.47%***	**9.18**	***5.45%***
MYAN	Industry	2.33	3.45	*4.00%*	5.14	*4.07%*	7.56	*3.93%*
	Agriculture	13.46	16.82	*2.25%*	21.03	*2.26%*	26.28	*2.25%*
	Commerc/other	7.46	9.70	*2.66%*	12.61	*2.66%*	16.40	*2.66%*
	TOTAL	**23.25**	**29.97**	***2.57%***	**38.78**	***2.61%***	**50.24**	***2.62%***
NEPA	Industry	0.38	0.67	*5.84%*	1.19	*5.91%*	2.10	*5.84%*
	Agriculture	1.63	2.51	*4.41%*	3.87	*4.42%*	5.95	*4.40%*
	Commerc/other	0.91	1.37	*4.18%*	2.05	*4.11%*	3.03	*3.98%*
	TOTAL	**2.92**	**4.55**	***4.54%***	**7.11**	***4.56%***	**11.08**	***4.54%***
PAKI	Industry	8.92	18.07	*7.31%*	36.18	*7.19%*	71.63	*7.07%*
	Agriculture	9.21	13.58	*3.96%*	19.66	*3.77%*	28.08	*3.63%*
	Commerc/other	17.31	31.81	*6.27%*	57.79	*6.15%*	103.79	*6.03%*
	TOTAL	**35.44**	**63.46**	***6.00%***	**113.63**	***6.00%***	**203.50**	***6.00%***
PHIL	Industry	19.46	24.85	*2.48%*	63.07	*9.76%*	80.25	*2.44%*
	Agriculture	8.51	11.51	*3.07%*	16.86	*3.89%*	11.91	*-3.42%*
	Commerc/other	9.34	34.33	*13.90%*	86.95	*9.74%*	93.32	*0.71%*
	TOTAL	**37.31**	**70.69**	***6.60%***	**166.88**	***8.97%***	**185.48**	***1.06%***
SING	Industry	10.96	23.21	*7.79%*	45.10	*6.87%*	72.35	*4.84%*
	Agriculture	0.09	0.06	*-3.97%*	0.05	*-1.81%*	0.04	*-2.21%*
	Commerc/other	19.90	39.46	*7.09%*	72.97	*6.34%*	117.06	*4.84%*

Country	Economic Sector	Base Year 1990GDP	2000		2010		2020	
			GDP	*AAGR*	GDP	*AAGR*	GDP	*AAGR*
	TOTAL	**30.95**	**62.73**	*7.32%*	**118.12**	***6.53%***	**189.45**	***4.84%***
SRIL	Industry	1.92	2.79	*3.81%*	3.64	*2.70%*	4.75	*2.70%*
	Agriculture	1.79	2.60	*3.80%*	3.39	*2.69%*	4.42	*2.69%*
	Commerc/other	3.88	5.63	*3.79%*	7.34	*2.69%*	9.59	*2.71%*
	TOTAL	**7.59**	**11.02**	***3.80%***	**14.37**	***2.69%***	**18.76**	***2.70%***
TAIW	Industry	65.76	92.12	*3.43%*	156.44	*5.44%*	215.03	*3.23%*
	Agriculture	6.53	6.28	*-0.39%*	11.17	*5.93%*	16.54	*4.00%*
	Commerc/other	83.17	110.96	*2.92%*	204.86	*6.32%*	319.78	*4.55%*
	TOTAL	**155.46**	**209.36**	*3.02%*	**372.47**	***5.93%***	**551.35**	***4.00%***
THAI	Industry	30.22	64.49	*7.87%*	120.45	*6.45%*	207.24	*5.58%*
	Agriculture	11.04	14.96	*3.09%*	19.21	*2.53%*	22.49	*1.59%*
	Commerc/other	45.09	95.31	*7.77%*	171.77	*6.07%*	218.74	*2.45%*
	TOTAL	**86.35**	**174.76**	***7.30%***	**311.43**	***5.95%***	**448.47**	***3.71%***
VIET	Industry	2.60	7.87	*11.71%*	23.09	*11.36%*	55.97	*9.26%*
	Agriculture	4.69	86.60	*33.86%*	13.50	*-16.96%*	21.75	*4.88%*
	Commerc/other	5.67	15.33	*10.46%*	39.30	*9.87%*	86.66	*8.23%*
	TOTAL	**12.96**	**109.80**	*23.82%*	**75.89**	***-3.63%***	**164.38**	***8.04%***
ALL ASIA TOTALS	**Industry**	**1,736.43**	**2,644.62**	*4.30%*	**3,906.82**	***3.98%***	**5,677.71**	***3.81%***
	Agriculture	**334.27**	**574.38**	*5.56%*	**643.82**	***1.15%***	**883.33**	***3.21%***
	Commerc/othe r	**1,789.37**	**4,022.65**	*8.44%*	**6,022.12**	***4.12%***	**8,623.42**	***3.66%***
	TOTAL	**3,871.11**	**7,256.61**	*6.49%*	**10,591.97**	***3.85%***	**15,206.95**	***3.68%***

NOTE: Country abbreviations are defined in Table 3.2

3.4.2 Technology

Technological factors related to energy use are incorporated primarily in energy intensities, which are used to indicate sector-wide levels of energy demand per unit of socioeconomic activity. The energy intensities contain a wide variety of technological and behavioral information that is difficult to quantify separately without a much more detailed subsectoral, end-use energy data base. For example, changes in the industrial energy intensity reflect efficiency improvements in industrial equipment and processes, shifts in output between different industrial sectors, in-plant management schemes for energy conservation, etc. The energy intensity indicators are developed at the national level. Assumptions concerning their future evolution are reflected in each scenario. A sample of the industrial energy intensity assumptions are presented in *Table 3.7.*

3.4.3 Fuel Types

There are seventeen types of fuels contained in the model framework. A detailed list of these fuel types is given in *Table 3.3*. Disaggregation of energy into such a great number of fuels is done for several reasons. First, the emissions of SO_2 from the combustion of fossil fuels are highly dependent on the characteristics of the fuel. Explicit consideration of the major fuels responsible for SO_2 emissions [six types of coal, three types of liquid fuels (oil), and two types of other solid fuels] decreases the uncertainty associated with calculating emissions using a single emission factor per type of fuel. Second, flexibility in representing a wide variety of fuels simplifies the process of representing official country energy plans in the model. Scenario assumptions regarding fuel consumption are made on a sectoral basis for each country and scenario year.

Data on fuel characteristics of each of these fuels have been compiled by the RAINS-ASIA Energy Network. These data include: higher heating value (PJ/tcn), sulfur content (%), and sulfur retention in ash following combustion (fraction of original sulfur present). These fuel characteristics are used in the RAINS-ASIA model to calculate the uncontrolled emission factors for SO_2 from each fuel for each region. Additional information on these parameters is presented in Chapter 4.

3.4.4 Regional (Subcountry) Fuel Allocation Assumptions

Regional socioeconomic data and projections as well as historic regional fuel distributions are used to allocate future estimates of national fuel demand to the regions. Sites of significant energy consumption in energy conversion, such as large power plants, are located geographically as LPS by specific latitude and longitude coordinates for existing plants, capacity expansions, and new power plants. The allocation procedure for energy consumption varies for each energy demand sector, according to the socioeconomic parameter believed to be best-correlated with energy consumption. For example, end-use residential energy consumption is distributed to the regions in proportion to the distribution of population, while industrial energy consumption follows the distribution of industrial GRP.

Table 3.7 Industrial Energy Intensity Assumptions for the Base Case

Note: INDEI = Industrial Energy Efficiency in Gigajoules per $1,000(US 1990) Industrial GDP AAGR = Average Annual Growth Rate

Country	Base Year 1990	2000		2010		2020	
		INDEI	AAGR	INDEI	AAGR	INDEI	AAGR
BANG	40.79	32.00	-2.40%	25.00	-2.44%	20.00	-2.21%
BHUT	2.16	12.39	19.09%	12.36	-0.02%	12.37	0.01%
BRUN	18.41	20.00	0.83%	21.00	0.49%	22.00	0.47%
CAMB	66.67	50.00	-2.84%	45.00	-1.05%	40.00	-1.17%
CHIN	109.85	81.00	-3.00%	60.00	-2.96%	44.20	-3.01%
HONG	1.48	1.34	-0.99%	1.34	0.00%	1.10	-1.95%
INDI	40.83	35.00	-1.53%	29.00	-1.86%	24.00	-1.87%
INDO	9.81	11.00	1.15%	12.00	0.87%	13.00	0.80%
JAPA	4.78	4.0	-1.77%	3.37	-1.70%	2.85	-1.66%
KORN	85.48	120.70	3.51%	139.90	1.49%	158.00	1.22%
KORS	11.53	9.50	-1.92%	8.00	-1.70%	6.70	-1.76%
LAOS	9.87	11.00	1.09%	13.00	1.68%	15.00	1.44%
MALA	19.39	16.00	-1.90%	13.00	-2.06%	11.00	-1.66%
MONG	46.22	35.00	-2.74%	27.00	-2.56%	21.00	-2.48%
MYAN	5.07	5.0	-0.14%	4.8	-0.41%	4.5	-0.64%
NEPL	17.53	17.40	-0.07%	17.20	-0.12%	17.00	-0.12%
PAKI	30.71	27.50	-1.10%	24.50	-1.15%	22.0	-1.07%
PHIL	7.27	9.8	3.03%	7.00	-3.31%	10.00	3.63%
SING	13.21	12.00	-0.96%	11.00	-0.87%	10.00	-0.95%
SRIL	10.01	17.74	5.89%	17.64	-0.06%	17.83	0.11%
TAIW	10.43	11.00	0.53%	9.00	-1.99%	9.00	0.00%
THAI	12.41	11.40	-0.85%	10.70	-0.63%	10.30	-0.38%
VIET	60.42	24.45	-8.65%	20.00	-1.99%	18.00	-1.05%
ASIA AVERAGE	17.06	17.14	0.05%	15.91	-0.74%	14.56	-0.88%

NOTE: Country abbreviations are defined in Table 3.2

3.4.5 Power Supply Assumptions

The assumptions that characterize future electricity supply can be grouped into three general categories: system-wide, electricity generation, and LPS. System-wide assumptions include parameters such as the percentage of generated electricity lost in transmission and distribution, the own-use percentage of auxiliary consumption, and the level of international imports or exports of electricity to neighboring countries. These assumptions have been developed individually for each of the 23 countries covered in the model.

Auxiliary consumption as well as transmission and distribution losses are significant problems for many of the developing countries in Asia. Several countries, including Bangladesh, China, India, Indonesia, and Pakistan, have total electricity losses exceeding 15%. Base Case assumptions for the future assume no change or only moderate improvement of 1% per year in this parameter. The Low Energy scenario assumes that improvements in these losses will take place at the rate of 1% - 2% per year.

The electricity generation fuel mix for the Base Case scenario was taken from published reports on power sector development plans for most of the major countries and information provided through the RAINS-ASIA Energy Network. Although official plans often do not extend beyond 2000 or 2010, the trends developed in these plans were continued through the year 2020 to develop the Base Case.

For the development of the Low energy scenario, it was assumed that the electricity savings realized in the end-use sectors would be translated to capacity reductions in the electricity supply sector according to the following rule. For the Low energy scenario, capacity additions of high-emission fuels such as lignite and hard coal are curtailed first until electricity supply and demand are again in balance. If these fuels were not available for reductions, oil-fired capacity was removed. This fuel phase-out scheme helps demonstrate the potential for SO_2 emissions reduction.

The model disaggregates electricity production into two categories: LPS and area sources. Emissions from LPS are assigned specific latitude and longitude coordinates within a specific region. Area-source electricity production is assumed to be generated by small, dispersed plants or plants which have low SO_2 emission characteristics (e.g., hydro, nuclear, natural gas, and some oil-fired plants). As with the other area-emission sources, emissions from area electricity generating sources are dispersed across the region to which they are assigned.

The model identifies 355 LPS at 332 unique locations. Eighty percent of the LPS are located in three countries: China (133), India (47), and Japan (19). The distribution and location of the 355 LPS sites is shown in *Figure 3.4*. A complete listing of the LPS can be found in the model. The development of the LPS scenarios for both the Base Case and Low scenarios were derived from several data sources, including the RAINS-ASIA Energy Network; Mannini, *et al*, 1990; Maude, *et al*, 1994; and ADB, 1993. In most situations, assumptions regarding LPS, beyond published planning horizons (typically 2010 and 2020), were based on the judgement of the RAINS-ASIA team regarding expansion possibilities of existing plant sites.

3.5 Energy/Economic Analysis

3.5.1 Overview

The building of the energy scenarios, as described in section 3.2, follows a "bottom-up" approach. Price and macroeconomic assumptions are introduced only implicitly into the analysis, rather than in an overall economic framework. To give an additional foundation and perspective to the scenario generation process, the Norwegian firm ECON conducted analytical work relevant to the energy-efficiency and fuel-substitution potential for some of the major energy-consuming countries. In addition, ECON carried out a "top-down" analytical approach, based upon an energy model ECON-ENERGY.

Both ECON's "bottom-up" and "top-down" work provided valuable input into the scenario generation process. Although they provided information at the national level only, that information was based on detailed technical- and economics-based analyses of energy efficiency and fuel substitution potentials. This analysis was done primarily to provide background for four major developing Asian countries; i.e., China, India, Indonesia, and South Korea. Together, they represent close to 90% of fossil fuel consumption in Asia, excluding Japan. The results of the analysis have also proven useful for scenario generation work for the other countries. The ECON work provided a complementary analysis which helped establish the scenario assumptions and parameters on energy efficiency. In addition, the ECON work provided a description of actual and planned systems of natural gas trade in the Asian region, including both liquid natural gas (LNG) and pipeline trade. This work is described in detail in a separate report (ECON, 1994) and is briefly summarized below.

3.5.2 China country description

Primary energy demand in China is dominated by coal, not only for electricity generation but also for industry. Oil use is constrained, and private transportation is very limited. Natural gas has only limited use in China and nuclear was not yet included in energy supplies in 1990. Of the vast hydro resources in China, only about 10% are exploited.

The aggregate energy intensity in China is higher than in any other large country. It was 2.5 times the level in India in 1990 and 3.5 – 4 times higher than levels in Indonesia and South Korea. There is a trend toward a lower energy intensity in China. From 1978 to 1990, the average GDP growth rate was 9%, while primary energy consumption grew 4.5% per annum. Technological improvements, including improvements in managerial procedures, account for some of the decline in the energy intensity. However, the most important factor in this decline is the structural change of the economy, including changes in the composition of foreign trade.

The current and future structure of China's energy use is largely determined by the available indigenous resources. Coal is the most abundant domestic energy source, and it will continue to play a dominant role in the total supply picture. While hydropower is an important energy source, earlier expectations for oil and natural gas finds have proved too optimistic. In 1992, coal production was 1,130 million tonnes representing nearly 30% of world production. The attractiveness of coal is based on a vast resource base and low extraction costs. Coal supplies are, however, hampered by an inadequate infrastructure, and the railway system presents a chronic bottleneck in the coal supply system. Plans for further expansion of the railway system are ambitious, but transport may remain as much of a problem for the coal supply system over the next decade as it was in the 1980s.

Natural gas has been produced primarily to cover local use. In recent years, some encouraging new discoveries have been made, and a doubling of production by 2000 seems feasible. However, natural gas will still remain a minor product in the Chinese energy balance.

Exploiting the large hydro potential involves confronting a number of environmental factors including silting of river deltas and the erosion and silting of dams. Furthermore, several of the proposed large projects could involve farmland flooding and forced migration of large numbers of people.

While two nuclear plants have recently become operational, plans for building more have been scaled down compared to the ambitions of the early 1980's. The major obstacle to the development of nuclear power is the investment required.

The average thermal efficiency of China's coal-fired power plants is about 29%. This is due both to continued use of out-of-date technology and to plant sizes, which are too small to capture economies of scale. A major part of the capacity, added as recently as the 1980s, is well below international efficiency standards, again, largely due to plant size. Transmission losses in China are estimated to be around 15% - slightly worse than the best of the developing countries (e.g., Brazil and South Korea at 12-13%) and significantly better than the worst. Losses in the rural parts of the system vary dramatically and have not been systematically monitored. Broad estimates indicate that losses in the rural areas (33%) are more than twice the losses in urban areas (15%).

China has a substantial potential for improvements in industrial energy efficiency. The most important energy consuming sectors - iron and steel, cement, and chemicals - all have a much higher specific energy consumption than observed in developed countries. These sectors' relatively low energy efficiency is linked to the quality of equipment and the size of plants, resulting in a relatively low quality of product produced. This is also the case for other less energy intensive industries. Main energy consuming equipment such as boilers and electric motors have much lower efficiency than could be obtained by using advanced international technology. For the existing industry as a whole, an average energy intensity reduction of about 30% could be reached over the forecast period (to 2020). In addition, the growth in industrial production will be highest for sectors having a much smaller energy intensity than the current average. The combination of a change in the sector composition of the economy and efficiency improvements within each industry could result in a reduction of the industrial energy intensity of up to 60% of the 1990 level by 2020.

Commercial energy use has been growing at a rate of about 4.5% per annum in the 1980's. Much of the growth is due to the substitution of coal for biomass fuels in rural areas. Coal is the dominant fuel for urban space heating and cooking in China. Efficiencies of coal use for cooking and heating are generally low. Even urban houses are poorly insulated and there is an inherent waste in using coal in cooking stoves. Cooking stoves are often kept alight continuously. Improved design of stoves as well as better coal/briquette quality could improve efficiency. Applying higher insulation standards in new buildings would significantly improve energy efficiency.

Transportation in China is dominated by rail, and coal use represents a high share of total energy consumption. Economic reforms in the 1980's resulted in rapid increases in both passenger and freight transportation. However, the level of per capita energy demand for transport in China remains extremely low. Railway construction has been the major task of transportation development over the past decade, with an emphasis on shifting from coal-steam to diesel and electric locomotives. There is scope for considerable improvement in the technical efficiency throughout the transportation system in China; there is also the potential for a substantial increase in both the demand for transportation and in transportation energy intensity as personal incomes rise and restrictions on private vehicle purchases are eased.

3.5.3 India country description

India's energy use is also coal-dominated, but to a lesser extent than in China. Coal is the primary fuel in electricity generation but has less importance in industry. The demand for oil for transportation is more important than in China. Industry oil use is also more widespread. Most of the natural gas is used in chemicals industry for fertilizer production. An important energy source in India is biomass, which was not included in the ECON analysis. Forty-five percent of all energy consumption is biomass. The aggregate energy intensity increased moderately during the 1970s, while a downward trend was observed in the 1980s. Energy intensity in industry and in the commercial/residential sector declined steadily throughout the 1970s and 1980s.

The overall performance of Indian electricity utilities is relatively poor. This is due to inadequate management and staffing qualifications and the weak financial situation of the utilities. Conversion losses in thermal power stations are considerable because of frequent start-up and shut-down and low-load factors. Average transmission and distribution losses in Indian utilities increased from 16% in 1971 to 19% in 1985 and have since stabilized at this level. Apart from pilferage, the most important reasons for the high losses are inadequate investments in transmission and distribution systems and a high share of low-voltage lines. Efficiency improvements could be obtained by better managerial practices, by amelioration in the coal supply systems, and by measures to increase the load factors.

The energy-intensive sectors of India's industry - iron and steel, aluminum, cement, and fertilizers - have been growing rapidly. Energy demand in these sectors accounts for about 60% of total industrial energy demand. Because most energy-intensive industries are using energy inefficiently, there exists a significant opportunity for efficiency improvements. Lack of proper instrumentation and control systems, poor capacity utilization, erratic power supply from state grids, and outdated equipment are the major reasons for industrial inefficiency. The potential for improving the energy efficiency of the energy-intensive sectors is on the order of 40% - 50%.

In India, the growth in energy used by the residential/commercial sector has been stronger than in China, because of a continued substitution of non-commercial fuels with oil (primarily kerosene) for cooking. The role of non-commercial fuels, particularly animal dung, has traditionally been much more important in India than in China. Total commercial energy requirements in the household sector show a strong correlation with GDP. Electricity and petroleum consumption have increased at rates greater than GDP growth.

Total freight transportation in India has grown at an average of 5.4% per year over the past two decades, whereas passenger traffic has grown at a yearly average of 6.8% over the same period. Rail-based traffic for both freight and passengers has been steadily decreasing. As in China, there has been an active policy over the past two decades to shift from energy intensive coal-based locomotives to those powered by diesel fuel and electricity. While private ownership of cars is still rare in India, there has been a recent surge in the number of two-wheelers. The fuel efficiency of India's truck and car fleet is very low compared to those of developed countries. This can be expected to change as India begins to open the vehicle market to foreign joint ventures.

India has the potential to increase its use of natural gas. Most natural gas reserves and production facilities are located offshore in two major areas close to the Western coast (Bombay High and South Basin). The gas fields are connected to the 1,900 km pipeline system running through the western and northern parts of the country. In consideration of the reserves available, the current production potential, and the volumes of gas currently being flared, there is scope for natural gas replacing oil and coal in many applications.

The hydro potential, which is economically exploitable, is 84 gigawatts (GW). Some 12 GW have already been developed, and an additional 7 GW are under development. The hydro electric share of total electricity generation has declined markedly from 45% in 1965 to 28% in 1991. It is likely that this decline is because its gestation period is considerably longer than that of thermal capacity.

Currently India has nine nuclear units with a total capacity of 1.7 GW. The original target of an expansion to 10 GW by year 2000 has been abandoned in favor of a more modest target of 5.7 GW of nuclear capacity by the turn of the century. However, even this target may be too optimistic in view of the shortage of state funds for new electricity-generation capacity.
All coal deliveries for power generation are from domestic sources. For economic and environmental reasons, however, imports of steam coal for new power stations near the coast are being considered.

3.5.4 Indonesia country description

Indonesia has an per capita income which is higher than in China and India, but it is less industrialized and has a lower energy intensity. Oil is the dominant fuel both in electricity generation and in industry. In addition natural gas plays an important role. The aggregate energy intensity in Indonesia increased in the 1970s through the beginning of the 1980s. Since then, the energy intensity has remained almost stable. The intensity in 1990 is about 70% higher than it was in 1971. It is, however, still 30% lower than in India and less than one-third of the level in China, measured at official exchange rates. Growth in energy consumption has been driven primarily by a rapid industrialization and by large investments in infrastructure. Electricity demand grew quickly in the 1980s. Substitution of non-commercial fuels by commercial fuels has also played an important role in the increase of energy intensity.

Because Indonesia has built most of its power plants recently, electricity is generated efficiently. Despite growth in the contribution from coal and natural gas, oil still accounts for an important share in power generation. Transmission and distribution losses remain high. In the 1975-1985 period, losses averaged between 21% and 25%. Because Indonesia consists of a string of islands, the country lacks an integrated national electricity grid. The government- owned utility has made an effort to extend electricity supplies to rural as well as urban areas. Investments in upgrading the transmission and distribution system could reduce losses. On the other hand, increased rural electrification tends to increase losses, in particular in the distribution grid. Some reductions in average losses are expected, but the reductions will be relatively small in the period approaching 2000, due to substantial extensions of the rural grids. In the longer term, when the targeted rural electrification has been achieved, the improvements in the technical performance of the transmission and distribution grids could gain more weight in reducing average losses.

The most important energy consuming sectors of Indonesia's industry are fertilizers, iron and steel, cement, sugar, and textiles. Important potentials exist for reducing the energy intensity of industry. It has been estimated that efficiency improvements in the iron and steel industry could increase steel production from 1.3 million tonnes in 1989 to 2.5 million tonnes by the end of the decade, without increasing natural gas use. The fertilizer industry, which accounts for about half of the natural gas use in Indonesia, has the potential of improving its efficiency by 30% - 40%.

In Indonesia, the average urban household consumes four times more commercial fuels and 15 times more electricity than the average rural household. Rural homes, however, consume nine times more biomass. Low-income households in cities still draw most of their energy from biomass. Total energy demand in the residential/commercial sector increased 5.5% per annum in the 1980s, with the strongest growth in electricity demand.

Per capita transport energy consumption in Indonesia is very low. In 1986, motorbikes and mopeds accounted for 70% of the vehicle fleet in Indonesia. Automobile ownership is still low. The main goal of transportation policy is to improve the road transportation capacity in order to keep pace with the needs of rapid industrialization and to extend the road network to the peripheral areas of the country. In order to preserve the supply of oil for export, private passenger transportation is discouraged by means of a high tax on gasoline.

Natural gas is the most important energy source when considering substitution with a less polluting fuel. The recoverable proven and potential reserves of gas are about 91 trillion cubic feet. About 57% of the production is devoted to LNG, which is exported. Domestic sales account for about 14% of the gross production - the balance being flaring or own-use by operators. Natural gas, apart from LNG, has been treated as a by-product of oil exploration. Domestic gas sales are promoted by the government which directs the state-owned oil and gas producer to supply gas to a few major industries at prices below cost. Fertilizer, steel, and cement industries dominate the domestic use of gas. A number of small and medium-sized fields which could, in principle, supply the domestic market have not yet been developed. Expansion of domestic gas utilization is justified by the relatively low economic costs of developing some of these fields.

The electricity utility is planning to increase hydropower capacity from the 2,300 MW in 1992 to about 6,800 MW in 2004. Total hydropower potential has been estimated at 75,000 MW for the country as a whole

3.5.5 South Korea country description

In South Korea, rapid economic growth and industrialization has resulted in an equally rapid growth in energy demand. The most notable changes in the fuel mix since the early 1980s are the growth in the share of oil, the introduction of nuclear power on a large scale, and the onset of liquid natural gas importation. In the electricity sector, policies have been directed at a diversification of the fuel mix from oil to nuclear power, natural gas, and coal. Nuclear now represents 48% of total electricity generation against 9% in 1980, LNG represents 9% (0% in 1980), and coal, of which most is imported steam coal, represents 18% (6% in 1980). During the 1970s, energy consumption grew at a rate of more than 10% per annum, while the GDP growth rate was 8% leading to an increase in energy intensity. Since the second oil price shock in 1979, energy intensity has been declining.

There has been a profound restructuring of the energy use for electricity generation in South Korea. Nuclear power has experienced a rapid expansion and now accounts for 48% of total power generation. LNG imports started in 1986 and gas now accounts for 9% of power generation. Large-scale coal use in electricity generation is a relatively new phenomenon. Because of the rapid expansion in the electricity capacity, and because investments in new plants have been concentrated on large-scale projects, the overall thermal efficiency of the system is relatively high. Transmission and distribution losses are small, around 6%. Transmission distances are short, and there is a high concentration of population and industry.

South Korea's industrial sector dominates its energy use. Between 1975 and 1990 total energy use increased 3.5 times. Growth of industrial production has been high and concentrated on energy-intensive sectors, particularly in the 1970s. In the 1980s, production growth was slower and concentrated on the less energy-intensive segments of industry. It is likely that industrial production growth will occur primarily in the least energy-intensive sectors. This, in combination with energy efficiency improvements in particular industries will result in a decline in South Korea's aggregate industrial energy intensity.

Rapid economic growth in South Korea has been followed by a noticeable shift in the residential/commercial sector energy consumption from low-quality fuels such as anthracite and firewood, to oil products, town gas, and electricity. Government promotion of district heating systems in the largest cities will contribute to energy efficiency improvements. Increased penetration of natural gas for heating will reduce the energy intensity of the residential sector, because of its higher efficiency compared to other fuels.

Private car ownership is increasing rapidly in South Korea, driven by strong growth in real personal incomes and the removal of restrictions on private car purchases. While the efficiency of the vehicle fleet is very good, the transportation energy per capita will likely increase substantially as the suppressed demand for personal transportation is absorbed.

There has been a major shift in the energy mix away from oil to nuclear power, coal, and

LNG in power generation. Nuclear plants under construction and committed to be constructed will double the nuclear capacity by 2000. Additional nuclear capacities are planned to come on-stream after 2000. Because of environmental considerations and the desire to reduce dependence on oil, there is a planned increase in the use of natural gas for power generation in industry and in the residential sector.

3.5.6 Gas Trade in Asia

Strong economic growth in parts of Asia combined with an increasing awareness of the environmental problems, is already leading to increased demand for gas in the region, and will continue to do so in the foreseeable future. Until pipeline systems are designed and built, this means that the already dominant position that Asia holds in LNG trade, accounting for close to three quarters of world trade, will grow even stronger. Both regional pipeline systems and LNG trade require massive investments and have considerable lead times. Several pipeline projects for gas to India and to China from the Middle East (where gas reserves are abundant) are being considered. In East Asia, several major pipeline project proposals are under examination. Some of those can be seen as parts of a future giant regional grid. Considerable growth in LNG trade is probable due to the strong increase in energy demand and the uncertainty surrounding major pipeline projects in the region. New finds and expansion of existing fields in the region may provide a considerable share of the consumption increases, but it is generally believed that an increase in imports from the Middle East is also necessary.

3.6 Energy Scenario Results

The previous sections of this chapter have summarized the RAINS-ASIA Energy Module. Two energy scenarios have been developed using the RESGEN model to demonstrate the methodology and to provide input to RAINS-ASIA for the purpose of calculating SO_2 emissions scenarios, acid deposition scenarios, and the anticipated impact of these scenarios on the Asian environment. These scenarios and results are described in subsequent chapters.

The Base Case energy scenario is based, as much as possible, upon official country projections of energy consumption. While it is clear that "official" country projections of energy consumption are often exaggerated or optimistic forecasts, the RAINS-ASIA team felt it was important to include these forecasts in the model scenarios in order to demonstrate the potential environmental consequences of such scenarios, thus gaining the confidence of government energy and environmental planning agencies. When the necessary data were unavailable at the level required by RESGEN, business-as-usual trends were followed. In this case it was assumed that each country would follow the existing energy policies, without introducing additional measures to improve the quality of the environment, such as energy efficiency measures of fuel substitution to reduce emissions of acidifying pollutants.

The Low energy scenario demonstrates an energy pathway which incorporates reductions in energy intensities and fuel substitution. This scenario explores the possible reduction of emissions through a strong effort to use energy more efficiently and a shift to lower-emission fuels in the power sector. The efficiency improvements deemed possible through 2020 are based on general improvements in technology and on the experiences of industrialized countries during the period 1973 - 1983, as they responded to the sharp rise in energy prices. The purpose of the Low energy scenario is to demonstrate the importance and potential of energy efficiency and fuel substitution in reducing emissions.

The results of the Base Case and Low energy scenarios are displayed in *Table 3.8* and *Figure 3.5* for each of the 23 countries and the sea lanes, and *Table 3.9* for all 94 regions. For the Base Case, energy consumption grows at an average rate of 4.0% per year over the 30-year period. The average annual rate of growth is stronger in the first period (4.5%) than in the subsequent two periods (3.8%). In aggregate, total energy consumption in Asia would be approximately 130 Exajoules (EJ) in the year 2000 and 275 EJ by 2020.

Notable in these results is the continued dominance of China and India in the regional energy consumption totals. In 1990, China and India accounted for approximately 55% of the total regional energy consumption. By 2020, this percentage has risen to 60% for the Base Case. The total contribution of Japan, however, decreases dramatically from 21% in 1990 to 11% in 2020. The contributions of the other Asian countries remain relatively stable, at a few percent or less, over the 30-year period.

Primary fuel consumption for the two scenarios is shown in *Table 3.10* and *Figures 3.6 and 3.7*. The share of coal in primary energy was about 41% in 1990 and is projected to remain reasonably stable in the Base Case throughout the 30-year period. Thus by 2020, total coal consumption in the Base Case will more than triple, reaching 110 EJ, or about 3.75 billion tons. The consumption of natural gas will increase nearly five-fold reaching 9% of total primary energy by 2020. While the consumption of biomass fuels will continue to rise modestly over the period studied, its contribution to primary energy will decrease from 15% in 1990 to 8% in 2020.

Although the Low energy scenario incorporates assumptions regarding the implementation of significant energy efficiency improvements, energy growth in the region remains at relatively high levels. Energy growth rates for all three periods average 3.1% per year, with the strongest growth rates experienced in the first period (3.2%). However, the Low energy scenario results in significant net energy savings of 15 EJ below the Base Case in 2000, and 67 EJ in 2020; this results in an 11% and 24% savings, respectively.

Consumption of coal in the Low energy scenario in 2020 is 76 EJ (about 2.59 billion tons), a 31% reduction in total coal consumption from the Base Case. This reduction is due to the combined effects of assumptions of improved energy efficiency and to fuel substitution in the power generation sector away from coal to low-emission fuels such as hydro, nuclear, and natural gas.

Figures 3.8 and 3.9 give additional insight into the energy growth in the two scenarios by displaying the sectoral and total primary energy intensities over the scenario period. In *Figure 3.8*, the domestic and transport intensities are expressed as annual per capita energy consumption. For the industrial sector, the intensity figures are expressed as annual energy use per unit of industrial output (measured in GDP). For both figures, all values are normalized, with the 1990 intensity equal to one.

Table 3.8 Total Energy Consumption by Country [Petajoules/year]

COUNTRY	1990	2000		2010		2020	
		Base	Low	Base	Low	Base	Low
BANG	805	1062	1019	1554	1427	2363	1965
BHUT	22	31	30	41	40	58	56
BRUN	62	130	122	171	149	229	178
CAMB	101	183	161	354	258	757	454
CHIN	30255	50527	43438	73518	59131	101016	75348
HONG	422	662	619	912	762	1211	980
INDI	15812	22908	20192	36932	29764	63621	48367
INDO	3793	6247	5878	9250	7768	13684	10138
JAPA	17866	22606	20187	25679	20913	28809	21535
KORN	1764	3186	2862	4980	3923	7910	5455
KORS	3594	6264	5814	9497	7794	13448	9743
LAOS	38	56	55	82	79	121	108
MALA	1060	1953	1928	3475	3186	6031	4686
MONG	151	193	178	260	212	361	266
MYAN	309	426	421	577	567	737	719
NEPL	270	357	336	467	425	615	514
PAKI	1436	2531	2359	4353	3910	7361	6391
PHIL	585	1082	948	1921	1820	3113	2401
SEAL	163	208	208	266	266	343	343
SING	342	645	641	1130	1061	1731	1522
SRIL	190	399	285	502	372	632	435
TAIW	2094	3334	2910	4796	4241	6843	5771
THAI	1688	3292	2902	5693	4482	9326	6697
VIET	772	1186	1176	2118	1926	3801	3359
TOTAL	**83594**	**129468**	**114669**	**188528**	**154476**	**274121**	**207431**

NOTE: Country abbreviations are defined in Table 3.2

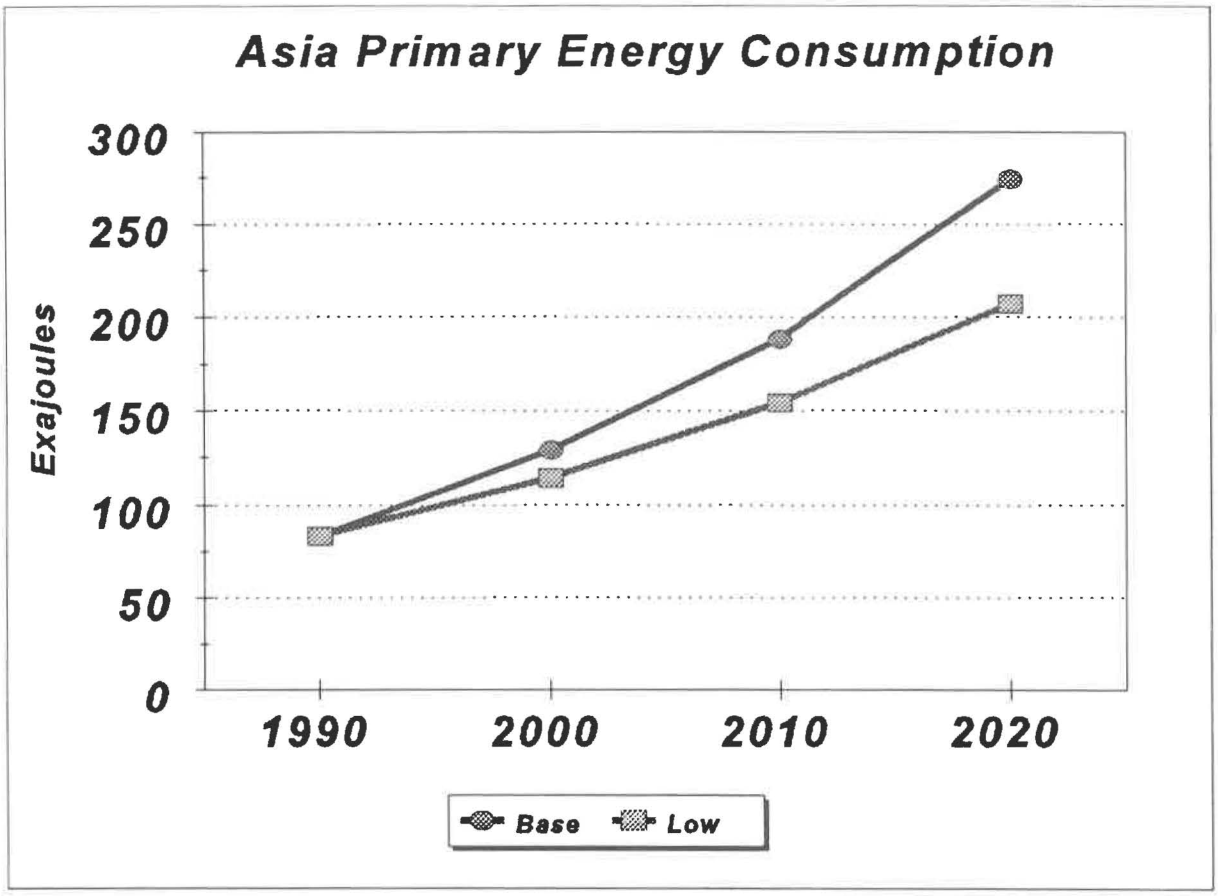

Figure 3.5 Asia Primary Energy Consumption

Table 3.9 Total Energy Consumption by Region (in Petajoules)

COUNTRY	REGION	1990	2000		2010		2020	
			Base	Low	Base	Low	Base	Low
BANG	*DHAK*	140	243	233	405	372	612	502
	REST	665	819	786	1149	1055	1751	1463
BHUT	WHOL	22	31	30	41	40	58	56
BRUN	WHOL	62	130	122	171	149	229	178
CAMB	WHOL	101	183	161	354	258	757	454
CHIN	*BEIJ*	730	1272	1068	1809	1443	2561	1899
	CHON	412	697	605	1032	821	1403	1035
	FUJI	571	958	856	1296	1089	1769	1395
	GUAH	1135	2007	1725	3295	2633	4690	3513
	GUAX	627	1322	1140	1923	1565	2586	1964
	GUAZ	395	610	535	877	713	1120	810
	GUIY	192	267	233	353	290	453	352
	GUIZ	462	759	677	1090	907	1512	1157
	HEHE	4627	7435	6405	11092	8904	14259	10618
	HUBE	978	1906	1670	3106	2554	4721	3627
	HUNA	748	1303	1155	2000	1624	2821	2104
	IMON	1068	1329	1165	1927	1546	2861	2061
	JINU	2595	3961	3407	5917	4767	8726	6531
	JINX	489	866	758	1333	1077	1817	1342
	NEPL	5301	8766	7427	11110	8825	15195	11315
	SHAN	770	1090	927	1628	1295	2250	1589
	SHEN	256	447	379	623	482	890	624
	SHGA	1173	2014	1724	3042	2415	4151	3101
	SHND	1219	2024	1755	3088	2502	4230	3060
	SHNX	1223	1996	1617	2853	2262	3770	2858
	SICH	1653	2949	2581	4299	3536	5757	4437
	TAIY	387	812	667	1182	920	1659	1198
	TIAN	607	1007	841	1559	1224	2153	1546
	WEST	774	1443	1251	2047	1671	2783	2122
	WUHA	487	614	542	827	678	1038	780
	YUNN	718	1584	1398	2440	1991	3466	2600
	ZHEJ	658	1088	932	1768	1399	2377	1710
HONG	WHOL	422	662	619	912	762	1211	980
INDI	ANPR	1592	2177	1911	3431	2669	5672	4123
	BENG	1012	1436	1279	2135	1722	3488	2592
	BIHA	1520	2075	1807	3165	2485	4878	3514
	BOMB	212	354	303	578	461	1018	758
	CALC	84	157	136	288	234	544	412
	DELH	107	213	182	475	392	1093	875
	EHIM	559	727	648	1022	811	1488	1091
	GUJA	881	1314	1140	2249	1792	4118	3088
	HARY	256	397	342	702	562	1322	999
	KARN	685	1041	919	1734	1419	3130	2459

COUNTRY	REGION	1990	2000		2010		2020	
			Base	Low	Base	Low	Base	Low
INDI	KERA	281	463	414	814	686	1536	1267
	MADR	79	157	125	298	228	513	376
	MAHA	1376	2059	1810	3427	2752	6165	4654
	MAPR	1547	2139	1881	3194	2541	5130	3722
	ORIS	1026	1353	1184	1981	1538	2915	2065
	PUNJ	502	813	728	1473	1249	2852	2351
	RAJA	683	1017	896	1722	1402	3269	2593
	TAMI	1230	1760	1552	2829	2279	4980	3781
	UTPR	1899	2749	2450	4416	3621	7622	5902
	WHIM	281	507	486	997	921	1888	1745
INDO	*JAKA*	293	462	424	691	557	1013	713
	JAVA	1933	3068	2905	4530	3849	6554	4902
	REST	769	1383	1298	2105	1752	3405	2527
	SUMA	799	1334	1251	1923	1610	2711	1997
JAPA	CHSH	2850	3502	3092	3788	3065	4046	3036
	CHUB	3229	4370	3893	5055	4062	5454	4050
	HOTO	2087	2684	2435	3082	2590	3412	2624
	KANT	4277	5401	4831	6290	5115	7692	5709
	KINK	3111	3844	3438	4335	3535	4857	3635
	KYOK	2313	2805	2497	3128	2546	3346	2483
KORN	WHOL	1764	3186	2862	4980	3923	7910	5455
KORS	NORT	562	846	776	1310	1065	1920	1380
	PUSA	1311	1691	1585	2628	2211	3803	2871
	SEOI	1052	2584	2390	3799	3050	5155	3593
	SOUT	668	1143	1063	1761	1468	2570	1899
LAOS	WHOL	38	56	55	82	79	121	108
MALA	*KUAL*	147	287	282	512	471	861	669
	PENM	728	1289	1279	2245	2066	3800	2955
	SASA	185	377	367	718	649	1369	1062
MONG	WHOL	151	193	178	260	212	361	266
MYAN	WHOL	309	426	421	577	567	737	719
NEPA	WHOL	270	357	336	467	425	615	514
PAKI	*KARA*	253	498	469	946	850	1711	1508
	LAHO	110	191	179	331	295	570	495
	NMWP	256	462	416	825	744	1411	1206
	PUNJ	580	936	877	1481	1336	2307	2010
	SIND	236	444	418	771	686	1362	1172
PHIL	BVMI	194	345	308	629	596	1075	846
	LUZO	252	530	470	961	921	1542	1206
	MANI	139	207	170	331	303	495	349
SEAL	WHOL	163	208	208	266	266	343	343
SING	WHOL	342	644	641	1130	1061	1731	1522
SRIL	WHOL	190	399	285	502	372	632	435

COUNTRY	REGION	1990	2000		2010		2020	
			Base	Low	Base	Low	Base	Low
TAIW	WHOL	2094	3334	2910	4796	4241	6843	5771
THAI	*BANG*	503	1111	987	1937	1515	3190	2262
	CVAL	419	863	731	1711	1407	3254	2395
	NEPL	323	472	419	669	522	915	646
	NHIG	286	555	503	898	652	1210	838
	SPEN	157	291	263	478	386	757	555
VIET	NORT	404	597	591	1018	926	1766	1566
	SOUT	367	589	585	1100	1000	2035	1793
TOTALS		83594	129465	114671	188527	154474	274116	207432

NOTE: The 22 italicized entries regions represent urban areas
Country and region abbreviations are defined in Table 3.2

Table 3.10 Primary Fuel Consumption in the Asia Region [in Petajoules]

Fuels	1990	2000		2010		2020	
		Base	Low	Base	Low	Base	Low
BC	396.29	770.20	687.46	1624.85	1329.19	2664.48	1917.35
HC	30881.99	49847.11	42182.05	73259.91	56654.28	102888.68	70671.04
DC	2641.69	3338.69	2897.78	4138.64	3309.00	4718.65	3522.37
OS	12335.72	15048.94	13844.15	18372.15	15055.83	21110.53	15498.99
HF	8591.14	11735.28	9930.23	14937.02	11888.20	19252.89	14179.41
MD	6813.56	11633.83	10294.04	18682.26	14896.00	31351.00	22792.32
LF	10421.95	16382.50	14987.78	25317.39	21076.97	39867.58	30733.35
GAS	5175.05	9573.52	8777.30	15127.25	13276.06	24835.88	20814.12
REN	130.06	424.43	413.78	795.20	776.48	1716.31	1675.71
HYD	3008.80	6403.83	6349.73	9675.29	9616.01	14873.98	14791.36
NUC	3169.21	4304.56	4304.56	6594.11	6594.11	10833.81	10833.81
ELE	28.75	2.43	2.33	2.45	2.32	2.30	2.32
HT	0.00	0.00	0.00	0.00	0.00	0.00	0.00
TOTAL	**83594.21**	**129465.32**	**114671.19**	**188526.52**	**154474.45**	**274116.09**	**207432.15**

BC = Brown Coal/Lignite
HC = Hard Coal
DC = Derived Coal (coke, briquettes)
OS = Other Solids
HF = Heavy Fuel oil
MD = Medium Distillates (diesel oil, light fuel oil)
LF = Light Fractions (gasoline, kerosene, naphthas, LPG)
GAS = Natural Gas
REN = Renewables
HYD = Hydro
NUC = Nuclear
ELE = Electricity
HT = Heat (steam and hot water)

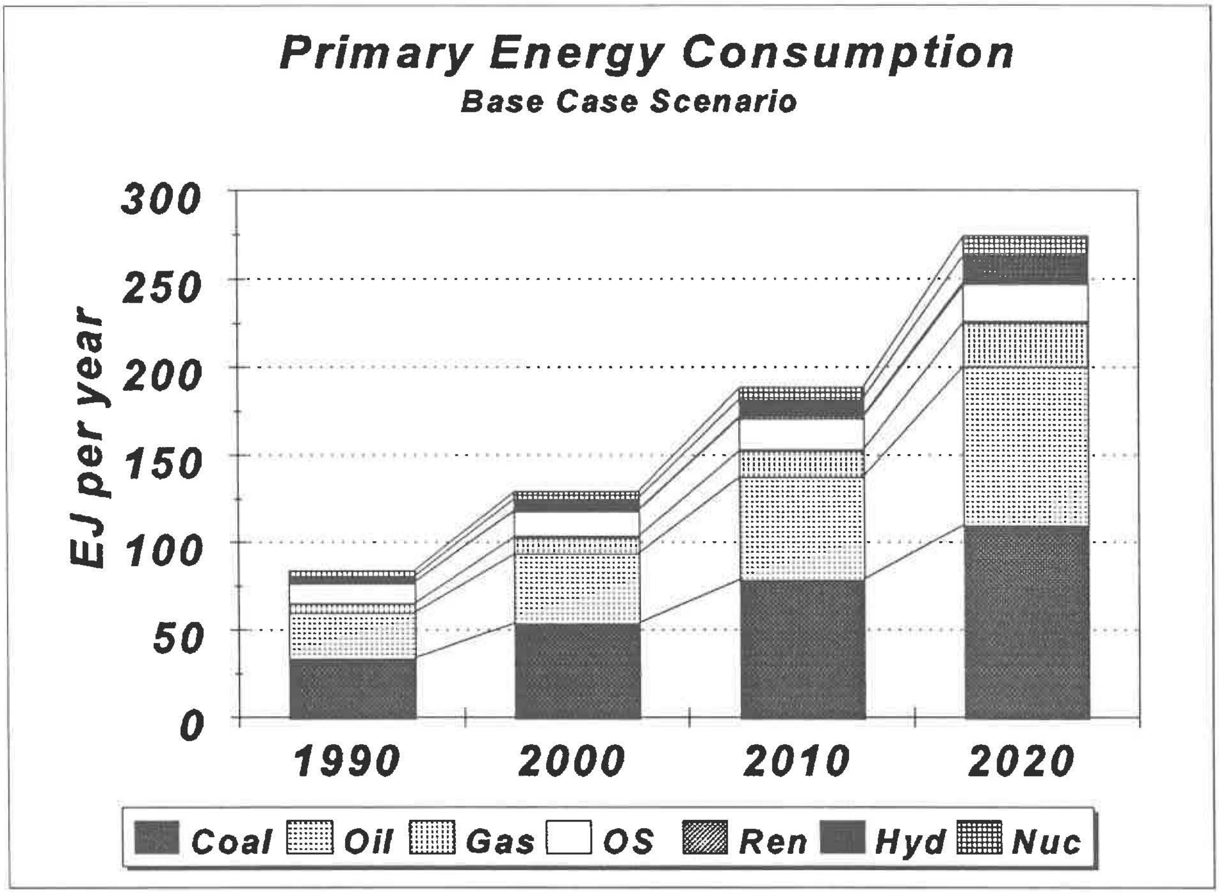

Figure 3.6 Asia Primary Fuel Consumption - Base Case

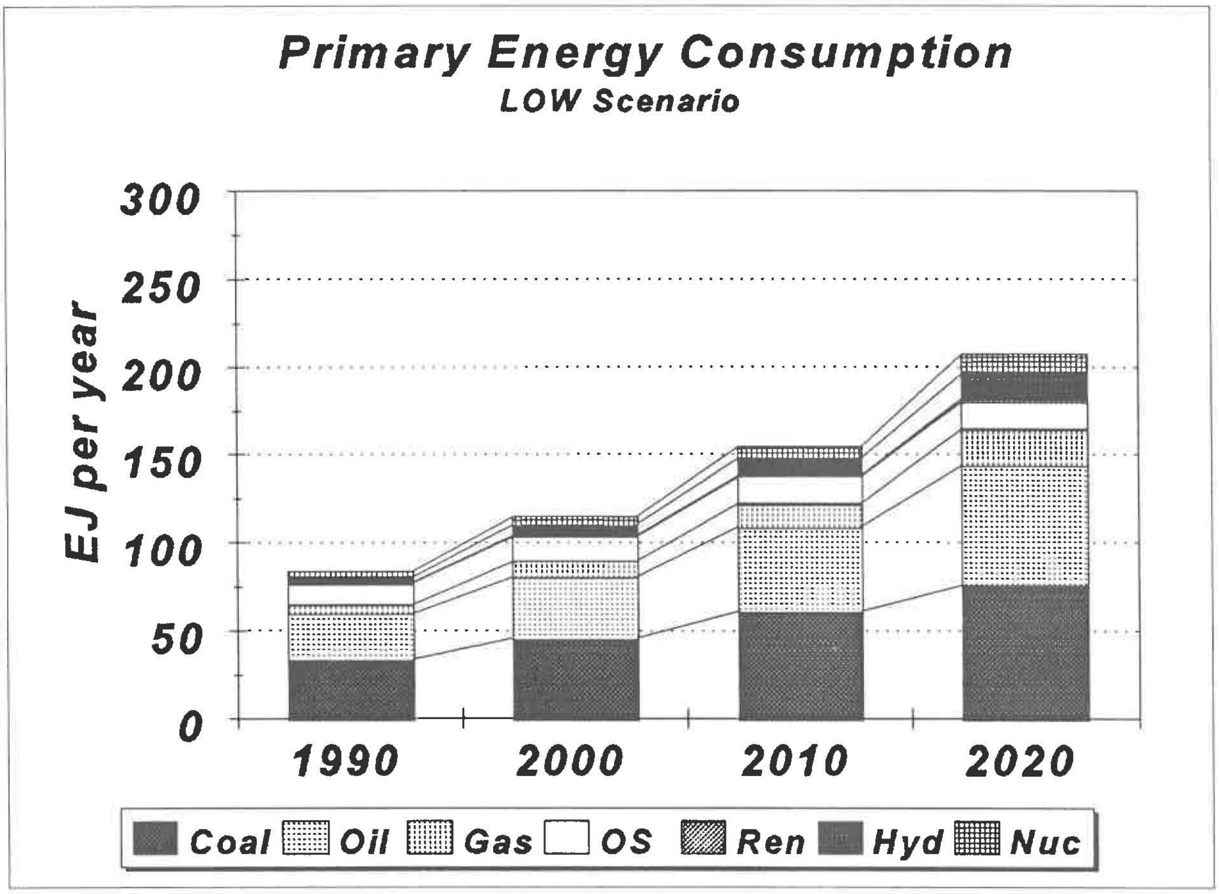

Figure 3.7 Asia Primary Fuel Consumption – Low Scenario

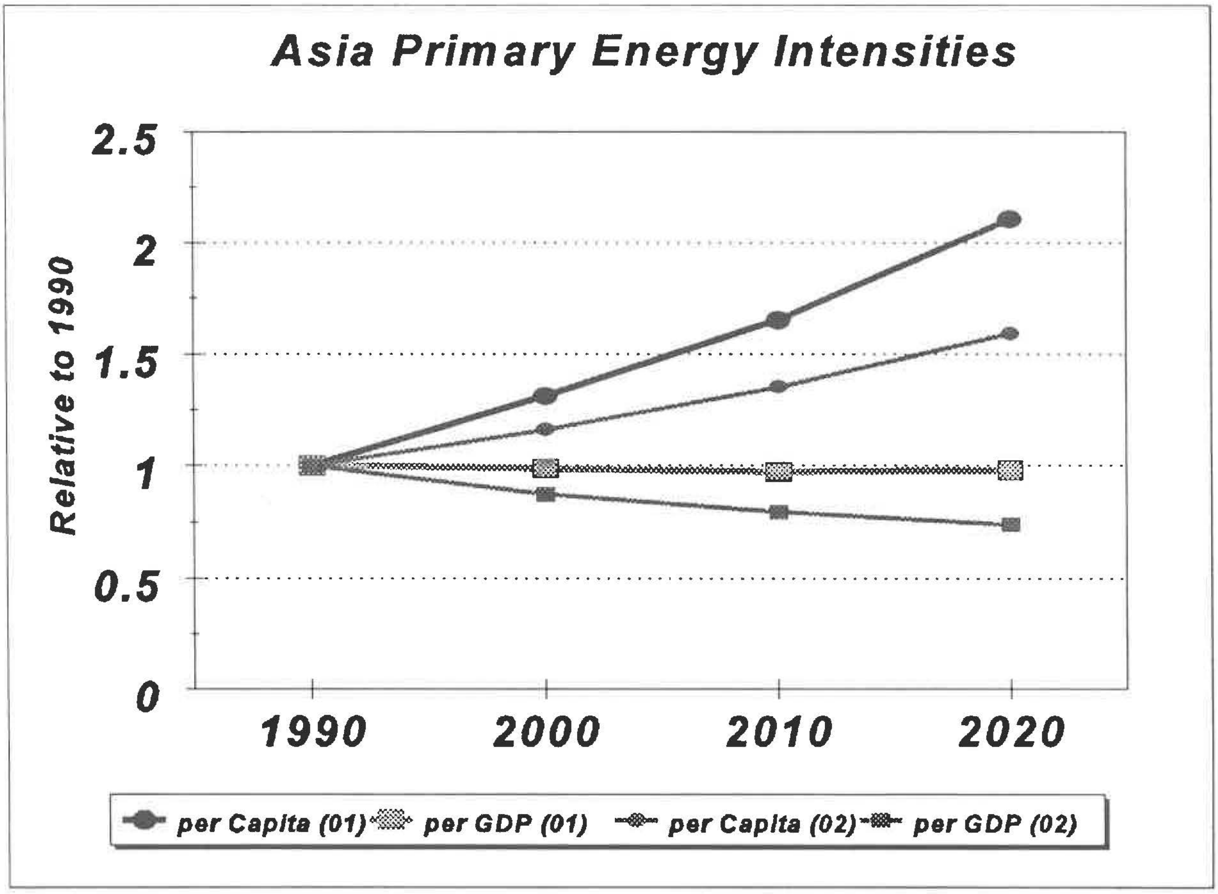

Figure 3.8 Asia Primary Energy Intensities

DOMESTIC = Residential Energy/per capita
INDUSTRIAL = Industrial Energy/GDP
TRANSPORT = Transportation Energy/per capita

01 = Base Case Energy Scenario
02 = Low Energy Scenario

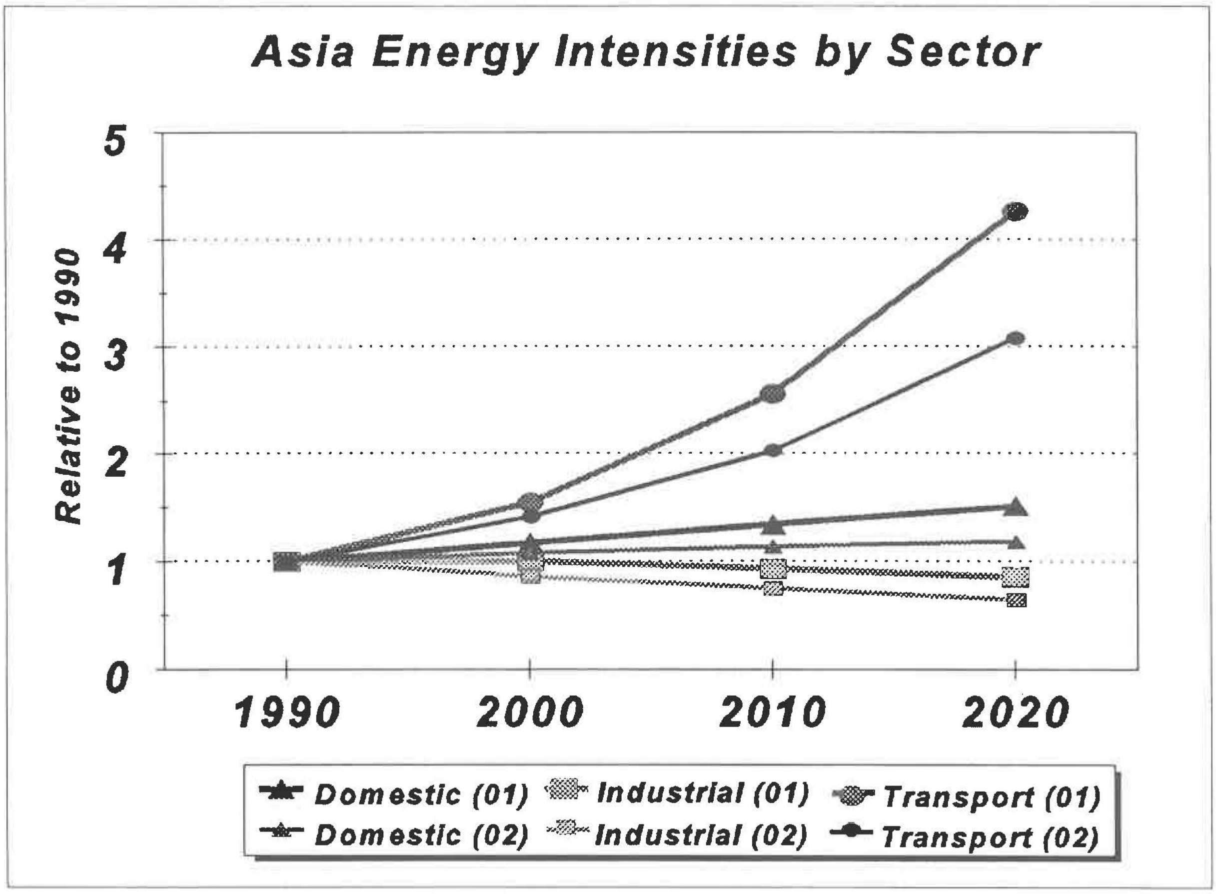

Figure 3.9 Asia Energy Intensities by Sector

DOMESTIC = Residential Energy/per capita
INDUSTRIAL = Industrial Energy/GDP
TRANSPORT = Transportation Energy/per capita

01 = Base Case Energy Scenario
02 = Low Energy Scenario

Over the scenario period in the Base Case, the domestic and transport energy use per capita grow by factors of 1.5 and 4.5 respectively; the industrial energy intensity decreases by about 15%. Increases in the energy intensity of the residential sector are driven by the growing affluence of the population and increased access to commercial fuels. Demand for electricity will grow faster than any other fuel. Transportation energy consumption per capita will increase strongly in all of the countries. Rising real income levels and removals of restrictions on private purchases of cars and two-wheelers will encourage private driving. Furthermore, booming trade will increase the demand for transport services. The increase in transportation fuel demand will be supported by improvements in road and highway infrastructures. The decline in industrial energy intensity follows the historic trend where industrial energy decreases at about 0.5% per year.

In the Low energy scenario (*Figure 3.7*), domestic and transport energy consumption per capita increase more slowly; by factors of 1.3 and 3.3 respectively by 2020. Industrial energy intensity, on the other hand, decreases more rapidly than in the Base Case scenario, declining 45% from the 1990 figure. High growth in output, in combination with a liberalization of the economy, will result in a modernization and a reduction in the average age of industrial capital equipment. Performance will also improve when more resources become available for maintenance. Furthermore, industries which in the past have been shielded from competitive pressure will improve operational performance as market reforms are implemented. Another reason for lower energy intensity is a change in the composition of industrial output. In the high growth scenario, industrial production growth will be strongest in high value added sectors like machinery and transport equipment, food processing and electronics, which are less energy intensive than base material transformation.

Growth in electricity demand results in a rapid growth in generation capacity. New generation capacities have a higher thermal efficiency than the existing. New capacities will be constructed with use of up-to-date technology, which has an efficiency close to that prevailing in the industrialized world. Institutional weaknesses and managerial problems that have plagued the electricity sector in developing countries will gradually be amended. For this reason, the average thermal efficiency of power generation will approach the efficiency in the industrialized world over the forecast period. Consequently, energy use in electricity generation will increase less rapidly than the demand for electricity.

The Asia-wide total primary energy intensities (per capita and per GDP) are shown for both the Base Case and the Low energy scenarios in *Figure 3.9*. In the Base Case scenario, average energy consumption per capita increases by a factor of about 2.25 over the scenario period reaching a value of 65 GJ per capita in 2020. Despite this increase, the figure is about 50% of the current average for Europe and only 20% of the current per capita energy consumption in the US. The energy intensity of the Asian economy as a whole, expressed in terms of energy consumption per unit of GDP, decreases modestly in the Base Case (3.5%) reflective of the business-as-usual characteristics of this scenario. All major countries, with the exception of Indonesia and the Philippines, will have an average growth in energy demand lower than the economic growth over the 30-year period. The decrease in energy intensity will be largest for China (55%) and India (33%). In Indonesia, energy intensity will increase by 10%. However, this will still be less than half the level of China's energy intensity in 2020. South Korea will see reductions in energy intensity of 36%. For the Low energy scenario, the overall energy intensity improves by about 26%, declining to levels close to those found in the industrialized countries in the 1980's. However, despite a significant decrease in both China and India in this scenario, their energy intensities remain nearly double the Asia-wide average in 2020, still several times the values recorded in the modern industrialized countries.

3.7 Summary and Conclusions

RESGEN provides a tool to generate regional energy scenarios with an output format consistent with the spatial- and time-dependent requirements of RAINS-ASIA. RESGEN interfaces directly with RAINS-ASIA by providing input databases for each scenario. The achievement of this specific objective required the following subtasks:

1. The RAINS-ASIA Energy Network was established in collaboration with AIT. This set of 12 research institutions supported the RAINS-ASIA team in the development of the regional databases and scenario development. This network served not only to facilitate the data collection process in the countries, but also served as a convenient vehicle for establishing ties to key institutions and potential RAINS-ASIA users.

2. With AIT and the RAINS-ASIA Energy Network, the first version of a regional, base-year, socioeconomic and energy database were developed for the 23 Asian countries. The generation of regional energy scenarios in Asia required the development of a new regional database which is consistent with the spatial- and time-dependent input data requirements of RAINS-ASIA. Because many of the countries in Asia did not have regional (subcountry) information readily available, it was necessary for the project to devote special attention to the creation of this database. A set of 94 subcountry regions was defined for Asia, including 22 megacities (metropolitan areas with populations greater than 2 million)

The database served to provide a workable source of input data to RAINS-ASIA, resulting in the generation of the first baseline regional energy scenario for all of Asia. Although the completeness and quality of this database varies considerably across the countries, this current version represents a unique database which can be upgraded and updated through a longer-term, iterative process. Integration and assimilation of collected data from Asia on regional energy use, point sources, and socioeconomic parameters for scenario development should be a continuing process.

3. A set of regional socioeconomic/energy scenarios was developed for the 23 Asian countries. The integration of this set of 23 country scenarios provided an initial Baseline Regional Energy Scenario which was used to test the RAINS-ASIA model. Despite shortcomings in current data, this initial energy scenario has also provided a first basis for examining in more detail the resulting sulfur emissions, dispersion, deposition, ecosystem impacts, and emission-reduction strategies. The scenarios can conveniently be modified and updated as additional data and regional information becomes available.

4. A Regional Energy Scenario GENerator (RESGEN) has been developed in the ©FOXPRO database language for generating regional energy scenarios and converting the output files of these scenarios into the specific data format required by RAINS-ASIA. RESGEN estimates energy use for six end-use sectors and two energy supply sectors; for 23 countries

and a sea lanes grouping; and for seventeen types of fuel. A methodology based on regional population and GDP distributions is used to allocate energy use to the 94 subcountry regions. A procedure for locating large point source emissions from power plants, oil refineries, and major industrial sources is included in RESGEN. The method produces an inventory of future point sources of emissions by latitude and longitude coordinates. User-friendly software has been developed for handling, reviewing, and modifying the large regional databases associated with the use of RESGEN.

NOTE:

Foxpro, RAINS-ASIA, and RESGEN are registered trademarks of their respective companies.

REFERENCES

Akimoto, H., & H. Narita, 1994, Atmospheric Environment, 29(2), pp 213-225.

Asian Development Bank, 1993, *Electric Utilities Data book for the Asian and Pacific Region*, ADB, Manila.

Asian Development Bank, 1992, *Energy Indicators of Developing Member Countries of ADB*, ADB, Manila.

Asian Institute of Technology, 1995, *Acid Rain and Emissions Reduction in Asia - Regional*, AIT, Bangkok.

Bertok, I., J. Cofala, Z. Klimont, W. Schöpp, M. Amann, October 1993, Structure of the RAINS 7.0 Energy and Emissions Database, IIASA Working Paper, WP-93-67.

ECON, 1994, *Energy Consumption in China, India, Indonesia, and South Korea* (by T. Haugland and K. Roland), ECON Energy, Oslo, Norway. Report No. 303/94.

Energy Map of China, 2nd edition, The Petroleum Economist LTD. London, Feb. 1994.

Energy Map of India, The Petroleum Economist LTD. London, Oct. 1993.

Foell, W.K., J.S. Buehring, W.A. Buehring, R.L. Dennis, M.E. Hanson, L.A. Hervey, A. Hötzl, K. Ito, R.L. Keeney, J.P. Peerenboom, E. Pönitz, J. Richter, A. Toifelhardt, The Wisconsin-IIASA Set of Energy/Environment (WISE) Models for Regional Planning Management: An Overview, IIASA, Laxenburg, Austria, August, 1981.

Foell, W.K., and C.W. Green, 1991, "Acid Rain in Asia: an Economic, Energy and Emissions Overview", Proceedings of 2nd Annual Workshop on Acid Rain and Emissions in Asia, AIT, Bangkok, November, 1990.

International Energy Agency, 1992, *Energy Statistics and Balances*, OCDE Publications, Paris.

Legler, John, et al., 1995, *RESGEN Software Manual*, Resource Management Associates of Madison, Inc., Madison, Wisconsin.

Mannini, A., M. Daniel, A. Kirchner, H. Soud, 1990, *World Coal-Fired Power Stations*, IEA Coal Research Publications, London.

Maude, C., A. Kirchner, M. Daniel, O. Montfort, 1994, *World Coal-Fired Power Stations - Africa, Asia, and Australasia*, IEA Coal Research Publications, London.

Oil and Gas Journal, PennWell Publishing Co., Tulsa, OK, Vol. 90, No. 51, Dec.21, 1992.

Regional Energy Development Programme (REDP), 1989, MEDEE-S: Energy Demand Model for the Developing Countries, UNDP/ESCAP.

Resource Management Associates of Madison, Inc. (RMA), September 1993, Database Structure for the Energy and Emissions (ENEM) Module of the RAINS-ASIA Model, Working Paper.

RAINS-ASIA:
AN ASSESSMENT MODEL FOR AIR POLLUTION IN ASIA

Chapter 4

Emissions and Control

David Streets, Markus Amann, Neelo Bhatti, Janusz Cofala, Collin Green

Report on the World Bank Sponsored Project
"Acid Rain and Emission Reductions in Asia"

December 1995

4. EMISSIONS AND CONTROL

Authors:
David Streets, Markus Amann, Neelo Bhatti, Janusz Cofala, Collin Green

TABLE OF CONTENTS

4.1 Introduction IV-1
4.2 The gridded emissions inventory (1987-88) IV-3
- 4.2.1 Methodology and assumptions IV-4
- 4.2.2 National emissions totals IV-9

4.3 Current and future emissions in ENEM IV-14
- 4.3.1 Methodology, data, and assumptions IV-14
- 4.3.2 Regional and national emission totals IV-20

4.4 Technical emission control options and costs IV-24
- 4.4.1 Low sulfur fuels and fuel desulfurization IV-26
- 4.4.2 Desulfurization during or after combustion IV-27
- 4.4.3 Control of process emissions IV-34
- 4.4.4 Cost curves for SO_2 reduction IV-35

4.6 Conclusions and recommendations IV-37
REFERENCES IV-38

LIST OF TABLES

Table 4.1 Assumptions for biomass emissions calculations for the Indian subcontinent IV-6
Table 4.2 Biofuels consumption in the Indian subcontinent (1987-88) IV-7
Table 4.3 Sulfur dioxide emissions from port traffic in Asia in 1988 . . . . IV-12
Table 4.4 Summary of anthropogenic sulfur dioxide emissions in 1987/1988 [tonnes/yr] IV-13
Table 4.5 Energy and emission sectors in the ENEM module IV-15
Table 4.6 Sulfur content by fuel and sector [%] IV-17
Table 4.7 Heat values of fuels by sector [GJ/metric ton] IV-18
Table 4.8 Sulfur retention in ash by fuel and sector [fraction] IV-18
Table 4.9 Calculated emission factors by fuel and sector [kt SO_2/PJ] IV-19
Table 4.10 Fuel characteristics and SO_2 emission factors in the power plant/boiler section of a large point source IV-20
Table 4.11 SO_2 emissions in 1990 from area sources and LPS [kt SO_2] IV-21
Table 4.12 Total SO_2 emissions by region (area sources plus LPS) in 1990 [kt SO_2] IV-22
Table 4.13 Technical options to reduce SO_2 emissions considered in ENEM IV-25
Table 4.14 Price differentials for low sulfur fuels IV-27
Table 4.15 Common parameters used for the SO_2 control cost calculation IV-32
Table 4.16 Country specific parameters IV-33
Table 4.17 Data used in the cost calculations for general parameters IV-33

Table 4.18 Technology specific data IV-34
Table 4.19 Control costs for process emissions IV-35

LIST OF FIGURES

Figure 4.1 RESGEN/RAINS-ASIA flow diagram IV-2
Figure 4.2 Crude oil seaborne trade in Asian waters: volumes and major routes IV-10
Figure 4.3 Dry bulk cargo seaborne trade in Asian waters: volumes and major routes IV-11
Figure 4.4 Example cost curves for the NHIG region of Thailand for the baseline energy scenario IV-36

Abbreviations used

Fuel types

BC1	Brown coal/lignite, high grade
BC2	Brown coal/lignite, low grade
HC1	Hard coal, high quality
HC2	Hard coal, medium quality
HC3	Hard coal, low quality
DC	Derived coal (coke, briquettes)
OS1	Other solids, low sulfur (biomass, waste, wood)
OS2	Other solids, high sulfur (incl. high S waste)
HF	Heavy fuel oil
MD	Medium distillates (diesel, light fuel oil)
LF	Light fractions (gasoline, kerosine, naphtas, LPG)
GAS	Gas

Sectors

CON	Fuel production and conversion
PP	Power plants, district heating
DOM	Households and other consumers
TRA	Transport
IN_BO	Combustion in boilers for electricity and heat
IN_OC	Other industrial combustion (furnaces)

4. EMISSIONS AND CONTROL

Authors:
David Streets, Markus Amann, Neelo Bhatti, Janusz Cofala, Collin Green

4.1 Introduction

Developing an accurate and detailed picture of sulfur dioxide emissions in Asia is a crucial component of the RAINS-ASIA project and serves multiple purposes. It is an output of the characterization of the energy and industrial situation that links the economic development of the region with the damage it causes to the environment. By studying the use of fossil fuels for provision of energy services and production levels in industrial manufacturing, it is possible to estimate the releases of sulfur dioxide to the atmosphere. These emissions then serve to drive the atmospheric transport, transformation, and deposition model, which calculates the temporal and spatial fate of the emissions. Subsequently, the impacts module estimates the vulnerability of ecosystems to these patterns of deposition. Also, by projecting future changes in energy and industrial development, future emissions can be estimated and future threats to the environment assessed.

The picture of current emissions from different types of facilities serves as a reference point for estimating the potential for reducing emissions. Figure 4.1 shows the flow diagram for the RESGEN/RAINS-ASIA model which highlights the ENEM (ENergy, Emissions and Control Module) components. The goal of the ENEM module is the development of regional and LPS emission scenarios for all 95 regions and 355 LPS included in the RAINS-ASIA model and the estimation of the incremental costs of pollution control associated with scenarios that reduce emissions. The emissions vectors produced by ENEM are available for input to the DEP (Atmospheric Transport and DEPosition) module, described in Chapter 5, to calculate the geographic distribution of acid deposition. By transforming the patterns of reduced emissions through the atmospheric deposition and impacts modules, a view of the consequent reduced environmental damage can be obtained in physical terms. If these physical measures could be converted to economic benefits, a full picture of the costs and benefits of different emission control options would be obtained.

The inputs to the ENEM model consist of a series of databases including:

- Regional and LPS energy consumption scenarios provided by the RESGEN model,
- Regional and LPS fuel characteristics databases (e.g., sulfur content, heating value and sulfur retention in ash) provided by the Asian Energy Network,
- Control technology and costs databases, and
- Model-user assumptions formulated into various "Control Strategies" which are developed by combining sector-, fuel-, and technology-specific control policy options for each region and LPS.

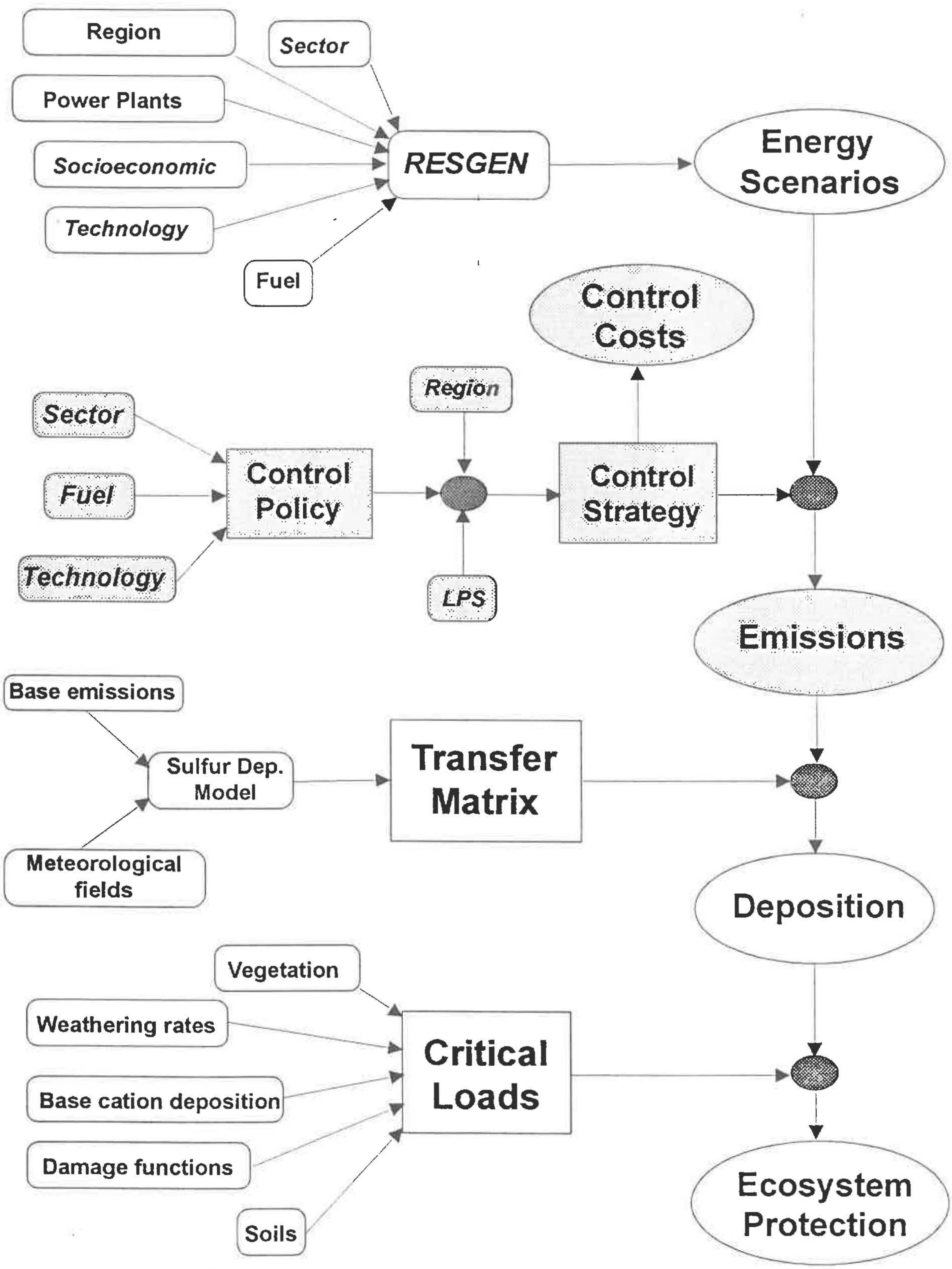

Figure 4.1 RESGEN/RAINS-ASIA flow diagram

Two distinct emission inventories were developed as part of the RAINS-ASIA project. Early in the project, a gridded 1^o x 1^o emissions inventory for the year 1987-1988 was compiled. The function of this inventory was primarily for the purpose of developing the atmospheric source/receptor relationship (see Chapter 5). This gridded inventory was used in certain specific studies and as a check on the more detailed base-year regional and LPS emissions inventory for 1990 developed later in the project.

The base-year regional and LPS emissions inventory was developed from databases constructed as part of the ADB-funded project. Detailed databases of energy use, industrial activity, and fuel characteristics for 95 regions were compiled by the network of Asian collaborators for the year 1990 (see Chapter 3). A thorough review of major point sources was also developed as part of this activity. Data for this phase of the project were collected in Asia and were developed, for the most part, independently from data gathered to construct the 1987-88 gridded emissions inventory.

As described in Chapter 3, the 1990 energy database was then used by the RESGEN model to develop future regional and LPS energy scenarios through the year 2020. These energy scenarios, including the base-year data for 1990, were combined with the regional fuel characteristics database in the ENEM module to calculate emissions scenarios for each energy scenario. The results were consistent regional and LPS emissions inventories for the base year, 1990, and three future years, 2000, 2010, 2020, for each energy scenario. Finally, a review of control technology conducted by IIASA and included in the ENEM module was used to compute alternative emission reduction scenarios and their associated costs. Each of these activities is reviewed in the sub-sections that follow.

4.2 The gridded emissions inventory (1987-88)

The gridded emissions inventory represents a snapshot in time of sulfur dioxide emissions in Asia in the late 1980's. It was prepared during the first year of the RAINS-ASIA project from the most recent data available. It was revised and extended during the second year of the project. The period of the data used in the inventory is best described as 1987-1988, reflecting minor differences in the years of the many data sources that were used to compile the inventory.

The inventory was originally compiled on a 1^o x 1^o grid for the entire Asian region and subsequently aggregated to 95 regions (reference Table 3.1) for use in developing the atmospheric transfer matrix and for evaluating the 1990 regional and LPS emissions inventory. All anthropogenic sources of emissions were included in the gridded inventory including both land-based emissions and emissions from international shipping. In contrast to some other inventories, sulfur dioxide emissions from the burning of agricultural wastes, dried animal wastes, and fuel wood were specifically included for many of the countries. Steady-state (non-eruptive) emissions from volcanoes were added towards the end of the project.

The gridded inventory is a combination of two main data sources. For Southeast Asia (10 countries) and the Indian subcontinent (6 countries), emissions were calculated specifically for this project using the methodology described below. Mongolia was added in the second year of the project also using this methodology. For the remaining six countries of East Asia

(China, Hong Kong, Japan, North Korea, South Korea, and Taiwan), the emission estimates of Akimoto and Narita (1994) were used.

For Southeast Asia, the Indian subcontinent, and Mongolia, information was initially compiled for major individual emission sources in the region. Fossil-fuel-fired power plants and industrial process sources that emit sulfur dioxide (e.g., copper smelters) were included. In all, 248 individual emission sources were included for these 17 countries, 94 of them being power generation facilities. Each individual emission source was assigned to its appropriate 1^{o} x 1^{o} grid cell. The contribution of these sources to total energy use and industrial production was then subtracted from national totals. The remaining energy use and industrial activity was then converted to sulfur dioxide emissions using standard emission factors and shared out to grid cells according to the methodology described below. A national summary of the emissions contained in the inventory is presented in Section 4.2.2.

4.2.1 Methodology and assumptions

The following procedures were used to develop emissions for Southeast Asia, the Indian subcontinent, and Mongolia. Emissions were estimated for three major categories: (1) emissions from energy consumption, (2) emissions resulting from industrial processes, and (3) emissions from international shipping. Emission estimates for the countries of East Asia (China, Hong Kong, Japan, North Korea, South Korea, and Taiwan) were taken from Akimoto and Narita (1994).

Emissions from energy consumption sectors

Emissions were initially calculated at the national level from energy/fuel consumption data for the following sectors: industrial, power generation, and other energy consumption. Energy use by fuel type and sector was obtained from IEA (1989). Emission factors for coal and oil were derived from data on the heating value of fuels, the sulfur content, and the sulfur retention in ash. For coal, the sulfur content and sulfur retention in ash was obtained from Spiro *et al.* (1992), supplemented by many other sources of information on sulfur contents of coals produced in Asia. The sulfur content of different types of oil products is difficult to obtain with any reliability. Refinery products are generally not reported by sulfur content, which is known to vary widely across product streams, especially for heavier refined products. For this work, oil consumption estimates from IEA 1989 were divided into four categories: light refined products for transportation uses (0.03%S), kerosene (0.3%S), middle distillates primarily for diesel generators (0.4%S), and residual fuel oil for industrial and power generating units. Sulfur contents for this latter category varied between 2.5%S and 3.5%S, depending on knowledge of practices in specific countries.

For the power generation sector, data were gathered on the location and fuel consumption at specific generating facilities. The size and location of coal-fired power generating facilities was obtained from IEA Coal Research (1990). Locations and types of oil-burning power generation facilities were obtained primarily from three sources: U.N. (1989), IAEA (1988), and IAEA (1991). Emissions calculated for these individual emission sources were assigned to their specific grid cells and were subtracted from the national emission total for power generation. Once all power generation emission sources had been identified and located, the remaining non-point source emissions were allocated to grid cells on the basis of population shares.

All other energy/fuel based emissions from the industrial sector and other energy consumption were treated as non-point source emissions. Non-point-source emissions were allocated to grid cells on the basis of population shares.

Biomass is an important fuel contributing to significant SO_2 emissions in many Asian countries. As such, it received special attention in this analysis. Biomass burning is a complex category for the Indian subcontinent because of the combined usage of animal wastes with fuel wood and agricultural waste. The approach used for countries in this region is described in Table 4.1. Emission factors used were: fuel wood, 0.6 kg SO_2/tonne fuel for residential cooking and 0.23 kg SO_2/tonne for residential heating; 6.0 kg SO_2/tonne fuel for animal wastes; and 0.52 kg SO_2/tonne for agricultural wastes (Smith, 1988). Table 4.2 lists the quantities of biofuels consumed. For the other countries of Southeast Asia, it was assumed that fuel wood and some agricultural wastes were the predominant fuel types; animal waste consumption was insignificant. Quantities of biofuels consumed in these countries were taken from World Resources (1992), and emission factors were taken from Spiro, et al. (1992).

Table 4.1 Assumptions for biomass emissions calculations for the Indian subcontinent

Country	Assumptions/Sources Used
Bangladesh	Assume that energy derived from biomass is distributed evenly among fuel wood, animal dung, and agricultural wastes. Total biomass energy production obtained from ADB (1991). Emission factor (E.F.) for SO_2 emissions from agricultural wastes same as E.F. for fuel wood. Assume most of biomass used in residential stoves.
India	Emission factor for SO_2 emissions from agricultural wastes same as E.F. for fuel wood. Assume most of biomass used in residential sector. Biomass consumption values obtained from Joshi (1991) and WEC (1989).
Sri Lanka	Assume that agricultural wastes and animal dung use each same (by weight) as that of fuel wood. Fuel wood consumption value obtained from WEC (1989). Assume most of biomass used in residential stoves. Emission factor for animal dung, agricultural waste, and fuel wood same as in other countries.
Nepal	Assume that agricultural wastes and animal dung use are each equal (by weight) to 1/4 that of fuel wood use. Fuel wood consumption figure obtained from WEC (1989). Emission factor for SO_2 emissions from agricultural wastes same as E.F. for fuel wood. Assume most of biomass used in residential stoves.
Bhutan	Assume no significant use of agricultural wastes and dung. Fuel wood consumption obtained from WEC (1989). Assume most of fuel wood used in residential stoves.
Pakistan	Assume that agricultural wastes and animal dung use are (by weight) each 1/8 that of fuel wood use. Fuel wood consumption values obtained from WEC (1989). Assume that equal amounts of fuel wood used in residential stoves and residential heating. Emission factor for SO_2 emissions from agricultural wastes same as E.F. for fuel wood.

Table 4.2 Biofuels consumption in the Indian subcontinent (1987-88)

Country	Fuel Consumed [10^6 tonnes/yr]		
	Fuel Wood	**Animal Wastes**	**Agricultural Wastes**
Bangladesh	44.37	44.37	44.37
Bhutan	2.10	-	-
India	164.39	126.46	83.79
Nepal	11.37	2.84	2.84
Pakistan	14.64	1.83	3.66
Sri Lanka	5.81	5.81	5.81

Emissions from industrial processes

The locations of industrial manufacturing facilities and production quantities by facility were taken from the 1989 Minerals Yearbook. Emission factors used for each process that emits sulfur dioxide are described below. For the metals and cement industries, it was assumed that no add-on pollution control devices were in place. For petroleum refining, steel production, and pulp and paper production, equivalence to 1980s U.S. practice was assumed. Almost all of the industrial plants were precisely located according to the maps provided in the Minerals Yearbook.

Emission factors used for industrial process emissions were of two types. When the process is simple and emissions derive basically from a single activity, process-specific emission factors were used. These were taken either from Spiro, et.al. (1992) or U.S. EPA (1987a). These emission factors are considered quite reliable, although some variation is to be expected depending on quality of the raw materials processed.

Primary copper smelting	1060 tonnes SO_2 per 1000 tons of Cu produced
Primary lead smelting	149 tonnes SO_2 per 1000 tons of Pb produced
Primary zinc smelting	490 tonnes SO_2 per 1000 tons of Zn produced
Aluminum smelting	20 tonnes SO_2 per 1000 tonnes of Al produced
Cement production	5.1 tonnes SO_2 per 1000 tonnes cement produced

For the more complex industrial processes, which have several sources of sulfur dioxide within the plant and considerable variation in process conditions and material inputs, process-specific emission factors are not recommended, especially for the development of regional or national inventories. In this case, emission factors were developed assuming equivalence to mid-1980s U.S. experience. The emission factors were developed by dividing U.S. industrial production figures by U.S. national process emissions published by the U.S. EPA (1987b). These latter estimates were built up from facility-level data for the U.S. and therefore embody a certain variety of facility and process types. It is implicitly assumed that facilities in the U.S. and Asia in the 1980s were somewhat similar. For the multinational industries such as petroleum refining, this is probably a reasonable assumption; however, in general we might expect emission factors developed in this way to be low. Pending a plant-specific survey of Asian facilities, however, this approach cannot be improved upon. Thus, the following emission factors were based on U.S. industry equivalence:

Petroleum refining:	48 tonnes SO_2 per 1000 bbd refining capacity
Steel production:	3.2 tonnes SO_2 per 1000 tonnes of steel produced
Pulp and paper production:	2.2 tonnes SO_2 per 1000 tonnes of pulp produced

Emissions from international shipping

An analysis was performed to quantify the emissions of sulfur dioxide from shipping in Asian waters. No estimates for this source category had previously been developed. These emissions estimates are subject to some uncertainty, however, because of the absence of detailed data in international publications on shipping routes and volumes, as well as a lack of data on the sulfur content of fuels burned.

The region covered by this analysis extends from the Indian Ocean eastward to the southern coast of Japan. The sources of shipping emissions have been divided into two categories: international shipping and major ports. The former category is further subdivided into two types of trade: crude oil and dry bulk cargo (primarily grain, coal, and iron ore). These four commodities together account for about 75% of seaborne trade worldwide (United Nations, 1984). The major international shipping routes of crude oil and dry bulk cargo and traded volumes are illustrated in Figures 4.2 and 4.3 taken from Fearnley's World Bulk Trades 1988. Note that direct shipments from Australia to Japan via the Pacific Ocean are not included in this analysis, as they are not considered relevant to the acidic deposition problem in continental Asia.

For the purpose of calculating emissions, crude oil is assumed to be carried by typical VLCC 200,000 dwt tankers consuming 120 tonnes of oil per day, while traveling at 15 knots. Dry bulk commodities are assumed to be carried by typical Panamax bulk carriers carrying 70,000 dwt and consuming 55 tonnes of oil per day while traveling at 15 knots (Stopford, 1988).

The sulfur content of bunker oil burned in shipping fleets in the 1980s varied considerably (up to 5%S), averaging between 2.5 and 3.5%S (Acid News, 1989; CONCAWE, 1993). This analysis assumes the use of 3%S oil, on average. The CONCAWE report assumed an average sulfur content of 3.3% for bunker oils manufactured currently in European refineries. All sulfur in the oil is assumed to be released as sulfur dioxide. Emissions of sulfur dioxide were calculated on an annual basis for each $1^o \times 1^o$ grid cell corresponding to the particular routes and commodity volumes. Routes within grid cells were approximated to either diagonal, horizontal, or vertical transects. Emissions in each grid cell were summed for each of the six routes, to produce aggregated emissions for all international shipping. These emissions were represented as a separate region in the RAINS-ASIA model inventory.

Traffic within major ports is known primarily in terms of total tonnage of cargo handled, with little information available on the distribution of types of commodities, types of ships, or sizes of ships. Clearly, traffic handled in these ports is a combination of local and foreign vessels transporting imported and exported goods and international vessels in transit. For the purposes of this analysis, only those ports handling more than 50 million tons of cargo in 1988 were included. This consisted of 12 ports, six of them in Japan. Table 4.3 lists these ports and the volumes of cargo handled (ISEL, 1992). All other ports -- including, for example, Indian ports, Indonesian ports, Port Kelang in Malaysia, Manila, and Bangkok -- handle significantly lower volumes of cargo. It is estimated that these twelve ports comprise 80% of all port traffic in the region.

For the purpose of calculating in-port emissions, both local and foreign cargo vessels were considered to represent total cargo traffic in the port. It was assumed that the typical vessel carries 70,000 dwt of cargo, averaging 11 knots and 18 tonnes of oil consumption per day, and travels in the port vicinity for 6 hours. This resulted in the emissions estimates shown in Table 4.3. Total port emissions are estimated to be approximately 10,000 tonnes of sulfur dioxide per year. These estimates may be low, but there is no information available on relative fuel consumption by vessel size and cargo volume in port conditions. It is unlikely that port emissions estimates could be improved without access to local information.

4.2.2 National emissions totals

Table 4.4 lists anthropogenic emissions of sulfur dioxide by country, together with emissions from international shipping that comprise the gridded base-year inventory. Total annual emissions for the period 1987-1988 are estimated to be 31.6 million tonnes, of which China alone is estimated to contribute 19.9 million tonnes, or 63%. India contributes 5.1 million tonnes (16%). The deposition patterns that result from this distributed array of sulfur dioxide emissions is discussed in Chapter 5.

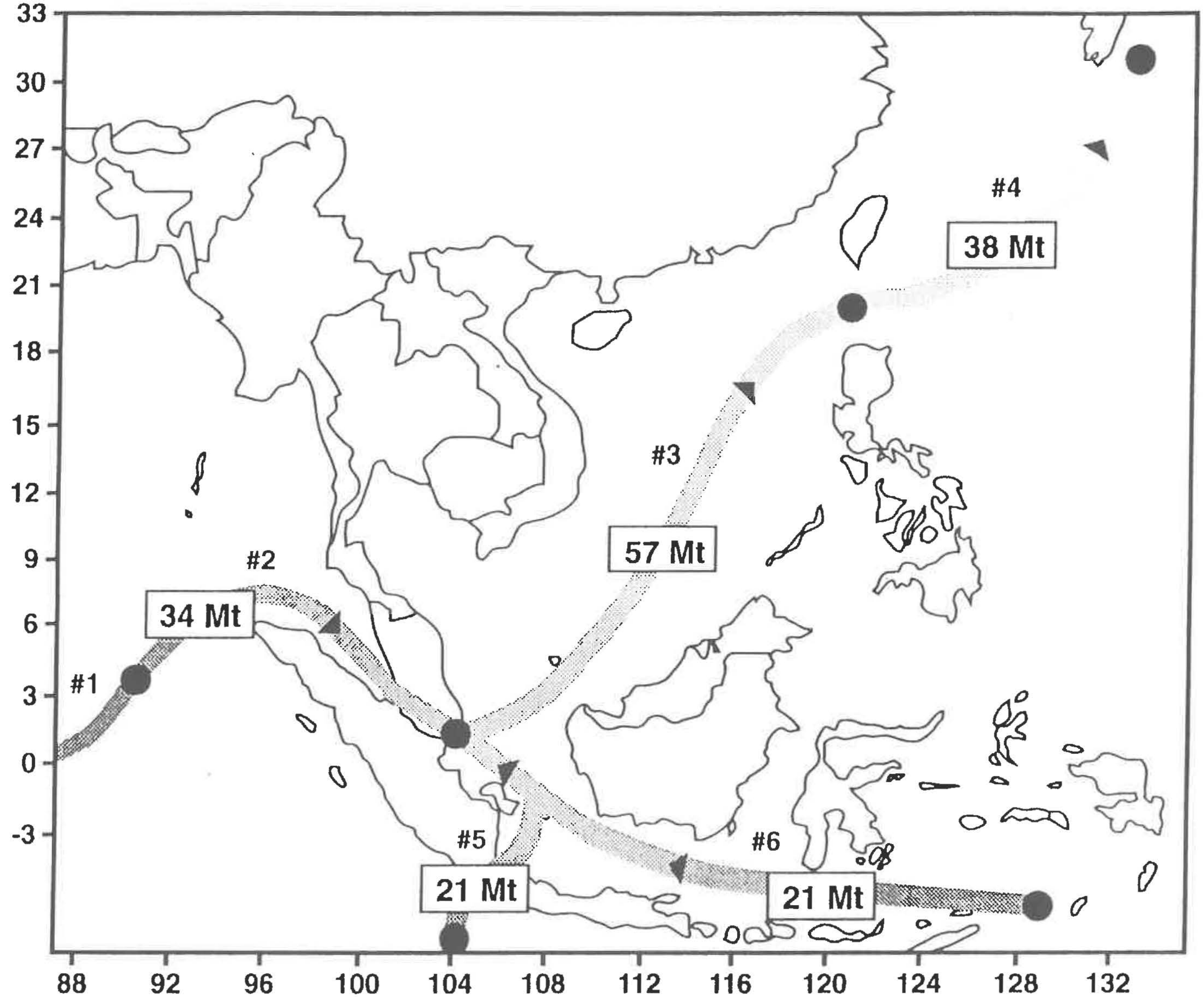

Figure 4.2 Crude oil seaborne trade in Asian waters: volumes and major routes

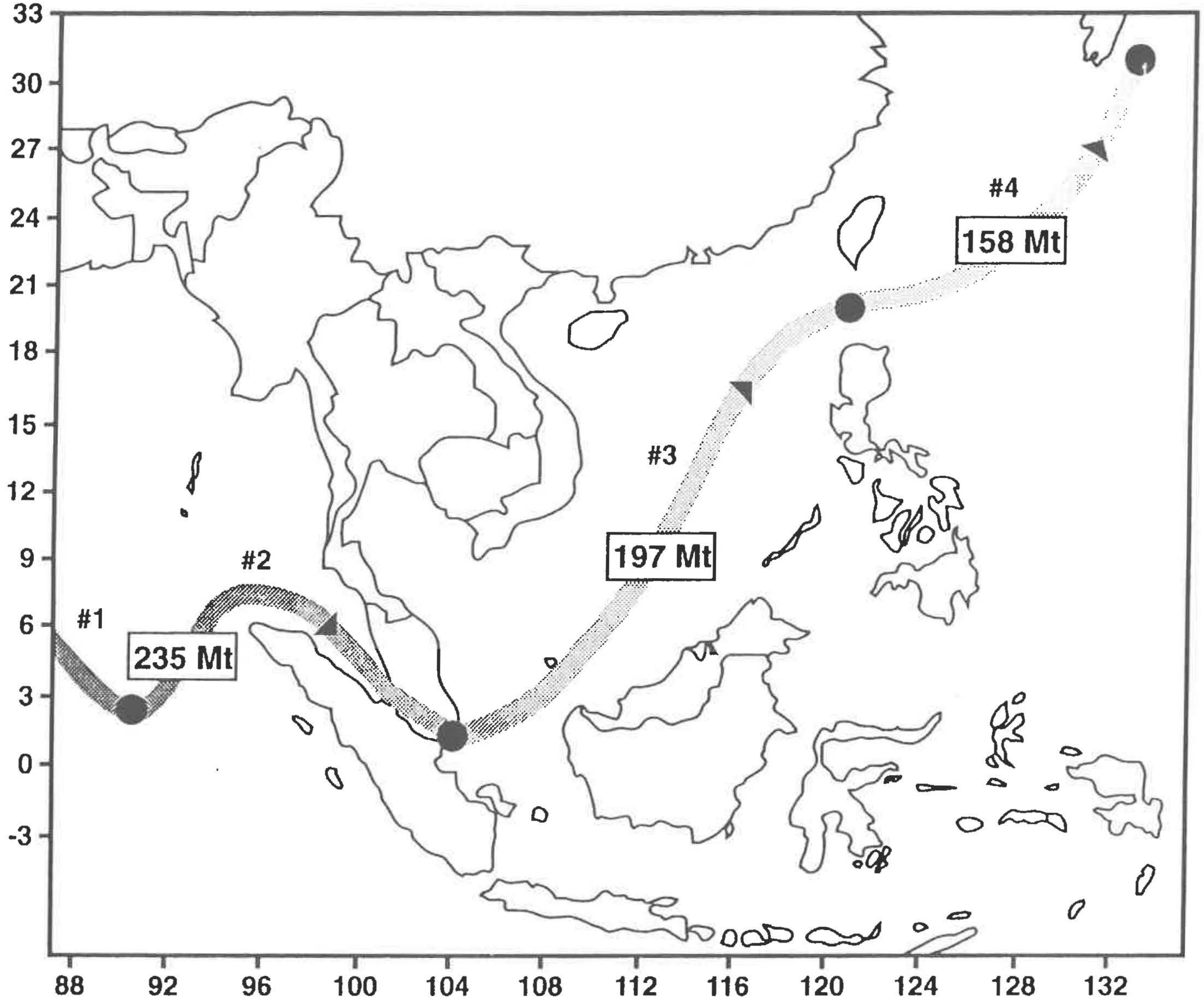

Figure 4.3 Dry bulk cargo seaborne trade in Asian waters: volumes and major routes

Table 4.3 Sulfur dioxide emissions from port traffic in Asia in 1988

Country	Emissions	Country	Emissions
Bangladesh	366,600	Malaysia	173,800
Bhutan	2,000	Mongolia	80,400
Brunei	600	Myanmar	14,600
Cambodia	2,800	Nepal	89,200
China	19,866,200	Pakistan	448,800
Hong Kong	133,400	Philippines	507,000
India	5,104,800	Singapore	169,600
Indonesia	396,100	Sri Lanka	89,100
Japan	977,900	Taiwan	545,200
Korea, North	407,000	Thailand	608,300
Korea, South	1,296,200	Vietnam	130,100
Laos	2,700	[Shipping]	225,600
		Total	31,638,000

Table 4.4 Summary of anthropogenic sulfur dioxide emissions in 1987/1988 [tonnes/yr]

Shipping Route	Emissions from Crude Oil Shipments	Emissions from Dry Bulk Shipments	Emissions from Oil and Bulk Shipments
1 Persian Gulf to Indian Ocean	62,100	neg.	62,100
2 Indian Ocean to Singapore	47,700	7,900	55,600
3 Singapore to Taiwan	44,500	14,500	59,000
4 Taiwan to Japan	31,500	8,700	40,200
5 Australia to Singapore (from S)	0	2,400	2,400
6 Australia to Singapore (from SE)	0	6,300	6,300
Totals	185,800	39,800	225,600

4.3 *Current and future emissions in ENEM*

Emissions of sulfur dioxide are calculated by the ENEM module of RAINS-ASIA for a base-year, 1990, and three future years, 2000, 2010, and 2020. For these years, RAINS-ASIA calculates area source emissions for 95 regions and point source emissions for 355 LPS. Area source emissions are calculated for three major end-use energy sectors (domestic, transportation, and industry), two energy conversion sectors (power plants and other energy conversion), and industrial processes. Emissions from LPS are calculated for both energy conversion facilities such as power plants, and large industrial facilities. Emissions from area sources and LPS are calculated for each fuel type and sector combination. Emissions estimates may be displayed at many different levels of aggregation (i.e., regional, country, and Asia-wide; as area sources, LPS, and combined total; by sector; and by fuel).

4.3.1 Methodology, data, and assumptions

Sectoral definitions

Energy consumption and emissions data in ENEM are aggregated into 5 major sectors. These sectors are shown in Table 4.5. The sectors displayed in ENEM differ slightly from those used in the RESGEN model and described in Chapter 3. For the most part, the sectors in ENEM are either aggregations of several of the RESGEN sectors, or they represent sub-sectoral divisions of specific sectors. The choice of sectors for the ENEM module was driven by the need to make the sectors consistent with international databases and to provide the flexibility to include additional pollutants, such as NO_x, in future phases of model development.

Table 4.5 Energy and emission sectors in the ENEM module

ENEM Energy/Emission Sector	Description
Domestic (DOM)	The domestic sector in ENEM is an aggregation of three sectors in RESGEN; residential, agricultural and commercial.
Industry (IN)	ENEM disaggregates the industrial sector into two subsectors: industrial energy consumption in boilers (BO), and other energy consumption (OC). Since RESGEN only calculates data for one industrial sector, all data are recorded in ENEM as industrial other energy consumption (IN-OC).
Transportation (TRA)	Energy consumption in the transportation sector.
Power Plants (PP)	Energy consumption in the power plant sector.
Other Conversion (CON)	Energy consumption in other energy conversion processes (i.e., oil refining, etc.).

Emissions estimates

Regional area source emissions resulting from the direct combustion of fossil fuels are estimated from regional data and projections of fuel consumption, fuel characteristics, and applied emission control technologies by the following equations.

$$SO2_{i,j}(t) = \sum_{k} \sum_{l} \sum_{m} E_{i,j,k,l,m}(t) \times EF_{i,j,k,l} \times (1 - ec_{i,j,k,l,m})$$

where:

$$EF_{i,j,k,l} = 2 \times \frac{sc_{i,j,k,l}}{hv_{i,j,k,l}} \times (1 - sr_{i,j,k,l})$$

and:

SO_2 ⇉ Sulfur emissions [kt SO_2]
E ⇉ Energy consumption [PJ]
EF ⇉ Uncontrolled emission factor [kt SO_2/PJ]
sc ⇉ Sulfur content [fraction]
hv ⇉ Heating value of fuel [PJ/ton]
sr ⇉ Fraction of fuel sulfur retained in ash after combustion

ec	⇉	Fraction of emissions removed by pollution control
I	⇉	Country
j	⇉	Region
k	⇉	Fuel type
l	⇉	Energy consuming sector
m	⇉	Abatement technology

A detailed database of regional fuel consumption by economic sector for the base year (1990) was developed for each of the 95 regions in the model. Future regional fuel consumption by sector is provided as output from the RESGEN model. These energy data are described in detail in Chapter 3.

In addition to detailed base-year energy data, the project developed detailed data on fuel characteristics necessary to calculate regional area source emissions of SO_2. Data were collected for all 95 regions and included the sulfur content and heating value of all fuels, and the fraction of sulfur retained in the ash after combustion for only solid fuels. An iterative process was employed for quality control which included considerable feedback among the institutions in the entire Asian Energy Network responsible for data collection.

In the event that data on regional fuel characteristics could not be found, national averages were used. In one instance, data were completely unavailable at the country level for the fraction of sulfur retained in the ash following combustion of solid fuels. In this case, data from the RAINS-Europe model, representing "typical" values for these parameters in Europe, were used until more suitable Asian-specific data can be developed.

Examples of fuel characteristics data for the five energy consumption sectors are provided in tables 4.6 through 4.9. These data are for the Jiangsu (JINU) region of China (CHIN). Similar data are available for display for all 95 regions in the RAINS-ASIA model and may be displayed using the features of the ENEM module. Fuel characteristics are considered to be temporal constants in the model and are not available for modification by the user.

Table 4.6 Sulfur content by fuel and sector [%]

Fuel*	Conversion	Power Plants	Domestic	Transport	Industry - Boilers	Industry - Other Combustion
BC1	1.00	1.00	1.00	1.00	1.00	1.00
BC2	3.00	3.00	3.00	3.00	3.00	3.00
HC1	0.50	0.50	0.50	0.50	0.50	0.50
HC2	1.46	1.03	1.46	1.46	1.46	1.46
HC3	1.50	1.50	1.50	1.50	1.50	1.50
DC	0.91	0.91	0.91	0.91	0.91	0.91
OS1	0.05	0.05	0.05	0.05	0.05	0.05
OS2	0.10	0.10	0.10	0.10	0.10	0.10
HF	0.53	0.53	0.53	0.53	0.53	0.53
MD	0.16	0.16	0.16	0.16	0.16	0.16
LF	0.03	0.03	0.03	0.03	0.03	0.03
GAS	0.02	0.02	0.02	0.02	0.02	0.02

* See table 3.3 for a description of fuel abbreviations.

Table 4.7 Heat values of fuels by sector [GJ/metric ton]

Fuel*	Conversion	Power Plants	Domestic	Transport	Industry - Boilers	Industry - Other Combustion
BC1	15.00	15.00	15.00	15.00	15.00	15.00
BC2	10.00	10.00	10.00	10.00	10.00	10.00
HC1	29.00	29.00	29.00	29.00	29.00	29.00
HC2	23.60	19.80	23.60	23.60	23.60	23.60
HC3	17.00	17.00	17.00	17.00	17.00	17.00
DC	28.50	28.50	28.50	28.50	28.50	28.50
OS1	16.00	16.00	16.00	16.00	16.00	16.00
OS2	12.50	12.50	12.50	12.50	12.50	12.50
HF	40.70	40.70	40.70	40.70	40.70	40.70
MD	43.10	43.10	43.10	42.70	43.10	43.10
LF	43.10	43.10	43.10	43.10	43.10	43.10
GAS	39.00	39.00	39.00	39.00	39.00	39.00

* See Table 3.3 for a description of fuel abbreviations

Table 4.8 Sulfur retention in ash by fuel and sector [fraction]

Fuel*	Conversion	Power Plants	Domestic	Transport	Industry - Boilers	Industry - Other Combustion
BC1	0.30	0.30	0.30	0.30	0.30	0.30
BC2	0.30	0.30	0.30	0.30	0.30	0.30
HC1	0.05	0.05	0.10	0.05	0.05	0.05
HC2	0.05	0.08	0.30	0.03	0.15	0.15
HC3	0.05	0.05	0.10	0.05	0.05	0.05
DC	0.05	0.05	0.10	0.05	0.05	0.05
OS1	0.00	0.00	0.00	0.00	0.00	0.00
OS2	0.00	0.00	0.00	0.00	0.00	0.00

* See Table 3.3 for a description of fuel abbreviations

Table 4.9 Calculated emission factors by fuel and sector [kt SO_2/PJ]

Fuel*	Conversion	Power Plants	Domestic	Transport	Industry - Boilers	Industry - Other Combustion
BC1	0.93	0.93	0.93	0.93	0.93	0.93
BC2	4.20	4.20	4.20	4.20	4.20	4.20
HC1	0.33	0.33	0.31	0.33	0.33	0.33
HC2	1.18	0.96	0.87	0.87	1.05	1.05
HC3	1.68	1.68	1.59	1.68	1.68	1.68
DC	0.61	0.61	0.57	0.61	0.61	0.10
OS1	0.06	0.06	0.06	0.06	0.06	0.06
OS2	0.16	0.16	0.16	0.16	0.16	0.16
HF	0.26	0.26	0.26	0.26	0.26	0.26
MD	0.07	0.07	0.07	0.07	0.07	0.07
LF	0.01	0.01	0.01	0.01	0.01	0.01
GAS	0.01	0.01	0.01	0.01	0.01	0.01

* See Table 3.3 for a description of fuel abbreviations

Point source emissions are estimated from fuel characteristics parameters and fuel consumption estimates specific to each source by a method similar to that described above for area sources. Data on fuel characteristics for the 355 LPS were initially collected by the Asian Energy Network and compiled by AIT as part of the ADB project. IIASA had the responsibility for final quality control. The process included considerable feedback and iteration among the institutions in the entire energy network. Missing data on LPS characteristics were developed by IIASA using information from the IEA Coal Research power stations directory (Manda *et al.*, 1994).

Examples of the fuel characteristics data for one LPS are provided in Table 4.10 for the Jianbi power plant (LPS26) located in the Jiangsu (JINU) region of China (CHIN). Similar data are available for all other large point sources and may be displayed using the features of the ENEM module.

Table 4.10 Fuel characteristics and SO_2 emission factors in the power plant/boiler section of a large point source

Country: CHIN **Region: JINU** **LPS: LPS26, Jianbi**

Fuel	GJ/ton	%Sulfur	% Sulfur Retention	Emission Factor ($ktSO_2/PJ$)
HC2	19.20	1.18	0.05	1.17
HF	40.70	0.53	0.08	0.24

4.3.2 Regional and national emission totals

National emissions of SO_2 for the year 1990 as calculated by RAINS-ASIA are listed in Table 4.11. Total Asia-wide emissions for the base year 1990 are estimated to be about 34 million tonnes, which is in reasonable agreement with the gridded emissions inventory for 1987/88 described in Section 4.2. Table 4.12 lists SO_2 emissions in 1990 by region. Regions with significant emission totals include several regions in China (HEHE, JINU, NEPL, SICH) whose current emissions exceed two million tons of SO_2.

Sulfur dioxide emissions results calculated from alternative scenarios using the Low energy scenario and emission abatement technologies are presented in Chapter 7 on scenario results.

Table 4.11 SO_2 emissions in 1990 from area sources and LPS [kt SO_2]

Country	Area sources	LPS	Total
Bangladesh	118	0	118
Bhutan	2	0	2
Brunei	6	0	6
Cambodia	22	0	22
China	18,548	3,360	21,908
Hongkong	31	108	140
India	3,273	1,199	4,472
Indonesia	541	89	630
Japan	818	17	835
Korea, North	343	0	343
Korea, South	1,542	98	1,640
Laos	3	0	3
Malaysia	149	57	206
Mongolia	78	0	78
Myanmar	18	0	18
Nepal	122	0	122
Pakistan	614	0	614
Philippines	382	9	391
Singapore	191	0	191
Sri Lanka	42	0	42
Taiwan	478	21	500
Thailand	569	469	1,038
Vietnam	113	0	113
International Shipping	243	0	243
Total	28,247	5,428	33,675

Table 4.12 Total SO_2 emissions by region (area sources plus LPS) in 1990 [kt SO_2]

COUNTRY	REGION	EMISSION	COUNTRY	REGION	EMISSION
Bangladesh	*Dhaka*	17.0	India (contd.)	Orissa	190.5
	Rest of Country	101.0		Punjab-Chandigarh	179.4
Bhutan		1.5		Rajasthan	161.0
Brunei		6.3		Tamil Nadu-Pondicherry	350.3
Cambodia		22.2		Uttar Pradesh	641.5
China	*Beijing*	270.3		Jammu-Kashmir-Himachal Pradesh	23.2
	Chongqing	974.2	Indonesia	*Jakarta*	24.9
	Fujian	297.9		Java	383.6
	Guangdong-Hainan	705.6		Rest of Country	109.2
	Guangxi	800.7		Sumatra	112.4
	Guangzhou	231.3	Japan	Chugoku-Shikoku	162.0
	Guiyang	340.2		Chubu	157.6
	Guizhou	785.6		Hokkaido-Tohoku	110.2
	Hebei-Anhui-Henah	3084.9		Kanto	167.9
	Hubei	426.4		Kinki	125.1
	Hunan	394.3		Kyushu-Okinawa	112.7
	Nei Mongolia-Ningxia	689.8	Korea-North		343.1
	Jiangsu	2108.6	Korea-South	Northern Province	246.2
	Jiangxi	334.6		*Pusan*	606.0
	Heilongjiang-Jilin-Liaoning	2491.1		*Seoul-Inchon*	499.1
	Shanghai	507.4		Southern Province	289.0
	Shenyang	102.3	Laos		3.4
	Shaanxi-Gansu	827.4	Malaysia	*Kuala Lumpur*	10.7
	Shandong	1061.9		Peninsula Malaysia.	162.2
	Shanxi	632.4		Sarawak-Sabah	32.7
	Sichuan	2336.1	Mongolia		77.7
	Taiyuan	199.8	Myanmar		18.1
	Tianjin	231.8	Nepal		122.3
	Tibet-Quinghai-Xinjiang Uygur	348.1	Pakistan	*Karachi*	105.1
	Wuhan	316.1		*Lahore*	20.7
	Yunnan	874.9		NW Frontier Provinces-Baluchistan	102.1

COUNTRY	REGION	EMISSION	COUNTRY	REGION	EMISSION
	Zhejiang	534.5		Punjab	285.1
Hongkong		139.6		Sind	101.1
India	Andhra Pradesh	388.1	Philippines	Bicol-Visayas.-Mindanao	85.5
	West Bengal	222.3		Luzon	172.6
	Bihar	363.1		*Metro Manilla*	132.7
	Bombay	140.7	Singapore		190.9
	Calcutta	39.4	Sri Lanka		41.9
	Delhi	44.6	Taiwan		499.5
	East Himalayas: Asam-NE Highlands	66.5	Thailand	*Bangkok Metro Region*	285.0
	Gujarat	388.9		Central Valley	124.2
	Haryana	101.5		NE Plateau	51.6
	Karnataka-Goa	134.1		N. Highlands	521.1
	Kerala	55.2		South Peninsula	55.8
	Madras	49.5	Vietnam	North	55.1
	Maharasthra-Dadra Nagar-Haveli-Daman-Diu	520.0		South	58.1
	Madhya Pradesh	412.1	International Shipping		243.3
			TOTAL		33,674.7

Note: Italicized regions indicate the 22 large urban areas, "megacities".

4.4 Technical emission control options and costs

A powerful feature of the RAINS-ASIA model is its capability to explore the effects and costs of emission reduction strategies. Defining a control strategy means prescribing certain emission control measures for specific emission sources. Reduction strategies can be oriented towards entire regions or countries, towards individual plants (e.g., for any of the 355 large point sources contained in the RAINS-ASIA database), to whole economic sectors considered in the database (e.g., for fuel use in the domestic sector, certain industries, etc.) or to specific fuel types (e.g., for high sulfur hard coal).

The following groups of emission control options are considered in the RESGEN and RAINS-ASIA models:

- energy conservation,
- substitution of fuels containing sulfur by those with less or no sulfur,
- desulfurization of fuels before combustion,
- desulfurization during and after combustion.

The first two emission control options, energy conservation and fuel substitution, relate directly to assumptions developed in the construction of energy scenarios. Hence, these options for emissions reductions are explored in the energy scenario generation module (RESGEN), and thus only receive brief treatment in this section (see Chapter 3).

Energy conservation is a strong and cost-effective option to reduce emissions. Often it produces a variety of other positive effects in addition to emission reductions, e.g., the replacement of ineffective capital stock and a reduction in overall energy demand that, in turn, have consequences on trade balances, etc. Energy conservation strategies are developed as part of the energy scenario development process in the RESGEN model. Alternative energy scenarios may be developed which can incorporate a wide variety of assumptions regarding energy consumption and more efficient use of energy. The result of such assumptions is lower energy demand, less fossil fuel combustion and lower emissions.

Similarly fuel substitution can also be a very effective means for reducing emissions. Substitution of low emission fuels such as natural gas for high emission fuels like coal in the energy consuming sectors has been demonstrated to be a very effective emissions control option in many industrialized countries. Fuel substitution options of this type are an integral part of the energy scenario development process and the means for implementing these assumptions is incorporated in the RESGEN model.

Desulfurization before, during or after combustion is directly related to reducing SO_2 emissions. Consequently, these types of options are treated in the energy and emissions (ENEM) module of RAINS-ASIA, neglecting, as a first order estimate, their feedbacks on the energy system.

This remainder of this section provides a brief description of the technical options to reduce SO_2 emissions available in the ENEM module. The measures include:

- using low sulfur hard coal, either by utilizing naturally occurring low sulfur coal grades or, to a certain extent, by coal washing,

- using heavy fuel oil with low sulfur content, again either produced from low sulfur crudes or oil desulfurized during the refining process,
- using gas oil (diesel oil) with lower sulfur content,
- introducing desulfurization during the combustion process, e.g., by injecting of limestone into the furnace or by various types of fluidized bed combustion,
- introducing desulfurization of the flue gas after combustion.

Since it is difficult - and not very useful - to describe dozens of commercially available processes without knowing the specific applicability to each individual emission source represented in RAINS-ASIA, the model groups the technologies into categories that describe their major technical and economic features. In practice, for each of the technology categories, one representative process has been selected and introduced into the model. The technical options to reduce SO_2 emissions included in ENEM are shown in Table 4.13.

Table 4.13 Technical options to reduce SO_2 emissions considered in ENEM

Technical SO_2 Control Option	**SO_2 Removal Efficiency or Final S% Achieved**
Oil Desulfurization / Heavy Fuel Oil	0.6 % S
Oil Desulfurization / Diesel	0.3-0.05 % S
Low Sulfur Coal	0.6 % S
Coal Washing	50 %
Limestone Injection or Fluidized Bed Combustion	50 %
Wet Limestone Scrubbing (FGD)	90 %
Regenerative Processes	98 %

The ENEM module also performs an economic assessment of emission reduction strategies, limited to the costs of applying emission control technologies. The purpose of this analysis is to provide a consistent basis for comparing of emission control costs:

- among various countries, and
- among different energy and emission control scenarios.

To enable international comparability of the cost estimates, the model uses the US dollar of 1990 as a common currency unit.

In summary, the computer implementation of ENEM enables the user to:

- review the energy balances for the various energy pathways developed with RESGEN;
- specify and store 'control strategies', i.e., combinations of emission control measures for any particular sector, fuel or individual large point source;

- develop 'emission control scenarios' by selective application of the various control strategies to any of the 95 regions considered in the RAINS-ASIA model, based on the specified energy pathway;
- explore SO_2 emissions for any of the emission control scenarios, aggregated by region, economic sector, fuel type or for individual large point sources;
- estimate emission control costs of the emission scenarios, for any combination of sectors, fuels and technologies; and
- identify the cost-minimal combination of control measures to reach certain emission limits in a particular region.

4.4.1 Low sulfur fuels and fuel desulfurization

A major group of measures to reduce SO_2 emissions focuses on reducing the sulfur content of fuels either by using naturally occurring low-sulfur fuels or through desulfurization treatment of the fuels. Despite the large number of currently commercially available and potential future processes for reducing the sulfur content in fuels, the RAINS-ASIA model restricts itself to the main technological and economic characteristics of the most relevant options. Without keeping track of eventually necessary investments, e.g., in the refinery sector, the model only takes account of the resulting price differentials for fuel grades with reduced sulfur contents. Because of the basic assumption of a free international market for energy and desulfurization technology, these price increments are considered valid for all countries throughout the region. In particular, RAINS-ASIA considers:

- low sulfur hard coal,
- low sulfur heavy fuel oil, and
- low sulfur gas oil.

In RAINS-ASIA, low-sulfur hard coal is assumed to have a minimum sulfur content of 0.6 percent. This definition might appear conservative. It is, however, justified by concerns about supply constraints for low-sulfur coal on the world market should this become a major long-term option for important world coal consumers. The costs related to this option are derived from an analysis of the long-term price differences on the world coal market (Amann, 1990). The model also enables the formulation of strategies aimed at less ambitious reductions of the sulfur content in coal, such as those achievable by coal washing.

Desulfurization of liquid fuels affects various oil products in different ways. The light fraction products (gasoline, jet fuel) contain a negligible amount of sulfur. For middle distillates (gas oil, diesel) two desulfurization steps are described in the model: a low-cost desulfurization bringing the sulfur content down to 0.3 percent, and a second step reducing it further to 0.05 percent at higher costs. The desulfurization of heavy fuel oil is considered to be economically competitive down to 0.6 percent sulfur content at costs determined by the refinery process. It is assumed that these costs will also determine the price difference of heavy fuel oil refined from low-sulfur crudes.

The actual cost data used in RAINS-ASIA are shown in Table 4.14. Basic data have been derived from OECD publications (OECD, 1987) and verified against current market observations (Pototschnig, 1993). Cost assumptions for desulfurization of gas oil and diesel oil have been confirmed by Kroon (1992).

Table 4.14 Price differentials for low sulfur fuels

Fuel type	Price difference (million US$/PJ/%S[1])	Typical heating value, GJ/t	Cost/t SO_2 removed (US$/t SO_2)
Hard coal and coke, 0.6 % sulfur	0.34	27.0	482[2]
Heavy fuel oil, 0.6 % sulfur	0.54	41.5	1111
Gas oil			
- reduction to 0.3 % sulfur	0.84	42.5	1784
- reduction to 0.05 % sulfur	2.52	42.5	5352

4.4.2 Desulfurization during or after combustion

Desulfurization during combustion and purification of the flue gases after fuel combustion require measures at the plant site (Amann, 1990). To represent the wide spectrum of currently available and future control technologies and the large variation in cost efficiencies, three techniques with different cost characteristics and removal rates have been selected for RAINS-ASIA:

- desulfurization during combustion with removal efficiencies of about 50 percent at relatively low investments and operating costs (e.g., limestone injection, fluidized bed combustion and various technological approaches that are currently under development in some Asian countries),
- the most commonly used wet flue gas desulfurization process with typical sulfur removal rates of 90 percent at comparably moderate costs (e.g., wet limestone scrubbing, spray dryer processes, etc.), and
- regenerative flue gas purification with emission reductions of up to 98 percent, at relatively high costs.

For each category, there are several competing technologies. To simplify the cost assessment in RAINS-ASIA, the model confines itself to the most commonly used technology in each category. In a competitive market, other potential technologies must overrule the market leaders at least in terms of cost and removal efficiencies, unless national preferences dominate these criteria. Such national considerations, however, should not be used for an international comparative assessment as envisaged in the RAINS-ASIA model.

[1] % S reduced compared to original fuel.

[2] Calculated on an assumption that 5 percent of S is retained in the ash.

Limestone injection

SO_2 can be captured as it forms during combustion if a SO_2 sorbent such as calcium carbonate (limestone) is present. Removal is usually accomplished by adding SO_2 sorbents to the coal pellets in stoker boilers, by injection of sorbents into pulverized coal-fired boilers, or by fluidized bed combustion. The most common process currently in use, the limestone injection process, was selected to represent the cost-efficiency ratio. This technology achieves emission reduction rates of 50 to 60 percent at moderate investments, making it an attractive option for countries with capital shortage or power plants designed to operate intermittently.

Characteristic to many of these technologies is that they require a high sorbent-to-sulfur ratio to achieve sufficient reduction rates. Consequently, such technologies produce large amounts of waste material, the disposal of which faces increasing difficulties.

The wet limestone flue gas desulfurization method and the Wellman-Lord process

A large variety of flue gas purification processes are available on a commercial basis. Over the last few years, the wet limestone scrubbing process has gained a dominant position on the world market. Flue gas is brought into close contact with a limestone suspension, which reacts with the sulfur in the flue gas to form gypsum as a by-product. Gypsum can be further used, e.g., for producing building material. Sulfur removal rates of between 90 and 95 percent are typical (IEA, 1988).

To mark the high-end of advanced SO_2 control options, the RAINS-ASIA model also considers the Wellman-Lord process as a characteristic high-efficiency regenerative technology without production of waste material. Using NaOH as a sorbent the captured sulfur can be further used in the chemical industry.

Cost evaluation

Common to all these desulfurization processes is that they require investments at the plant site. In the long-term analysis carried out in the RAINS-ASIA model, however, the emphasis lies on total life-cycle costs of the equipment rather than on short-term considerations of capital demand. Consequently, using the internationally recommended standard investment analysis method (OECD, 1986) as a guideline, the RAINS-ASIA model estimates life cycle costs from three components (I) investment related costs, (ii) fixed operating costs and (iii) variable operating and maintenance costs.

Investments

Investments include the expenditure accumulated until the start-up of an installation, such as delivery of the installation, construction, civil works, ducting, engineering and consulting, license fees, land requirement, working capital.

The model aggregates these items into an investment function *I*, providing for eventual economies of scale (Equation 1). The necessary size of an abatement installation for a certain plant capacity *bs* is derived from the fuel-specific flue gas volume *v* to be handled. The form of the function is described by its coefficients ci^f and ci^v. Additional costs due to site-specific difficulties for retrofit applications to existing plants can be reflected by the retrofit cost factor r. This factor determines a percentage increase of investments for the retrofit case compared to the cost of a new plant. The investment functions used in RAINS-ASIA are scaled to thermal input capacities of boilers/furnaces (MW_{thinp}).

$$I = (ci^f + \frac{ci^v}{bs}) \times v \times (1+r) \tag{1}$$

In order to derive life cycle costs of installations the investments are annualized over the plant lifetime lt, using the interest rate q(q is expressed as %/100):

$$I^{an} = I \times \frac{(1+q)^{lt} \times q}{(1+q)^{lt} - 1} \tag{4}$$

Fixed operating costs

The annual fixed expenditures OM^{fix} cover maintenance, taxes and administrative overhead. These cost items are not related to the actual use of the plant. As a rough estimate for such annual expenditures, most technical standards use a standard percentage f of the total investments:

$$OM^{fix} = I \times f \tag{5}$$

Variable operating costs

Variable operating costs OM^{var} are related to the actual operation of the plant and take into account

- additional labor requirement,
- increased energy demand for operating the device (e.g., for the fans and for reheating),
- sorbent material demand (e.g., limestone),
- waste disposal,
- etc.

These cost items are calculated based on the specific demand λ^x of a certain control technology and its (country-specific) price c^x:

$$OM^{var} = (\lambda^l c^l / pf + \lambda^e c^e) + ef \times x \times (\lambda^s c^s + \lambda^d c^d) \qquad (4)$$

$$ef = 2 \times \frac{sc}{hv} \times (1 - sr)$$

with

λ^l	labor demand
λ^e	additional electricity demand
λ^s	sorbents demand
λ^d	amount of waste
c^l	labor cost
c^e	electricity price
c^s	sorbents price
c^d	costs for waste disposal,
ef	implicit SO_2 emission factor
x	removal efficiency
sc	sulfur content
hv	heat value
sr	sulfur retention in ash

Unit costs of SO_2 control

Equation 5 relates all cost items to one unit of fuel input (c_{PJ}); in the case of investment related costs the capacity utilization factor pf (operating hours/year) is used. For individual plants (e.g., the large point sources distinguished in RAINS-ASIA the plant factor is modeled as a function of time, taking account of declining capacity utilization towards the end of the technical life time, when power stations are gradually phased out.

$$c_{PJ} = \frac{I^{an} + OM^{fix}}{pf} + OM^{var} \qquad (5)$$

Although the cost coefficient c_{PJ} is useful for the calculation of price effects on the product (e.g., on electricity), the cost efficiency of different control options can only be evaluated by relating the abatement costs to the amount of reduced SO_2 emissions (c_{SO2}). For this purpose Equation 6 is used:

$$c_{SO_2} = c_{PJ} \,/\, (ef \times x) \qquad (6)$$

Data for cost calculation

The parameters used in the equations above can be split into two groups:

- **Common parameters** are assumed to be equal for all countries under consideration. They can be divided into the *general* and *technology-specific* parameters (Table 4.15). General parameters are valid for all technologies. Technology-specific parameters describe the typical economic and technical properties of control technologies. This group comprises *technical* (removal efficiency, requirements for energy and sorbents material) and *economic* parameters (e.g., used in the investment function, and for calculating retrofit and maintenance costs).

- **Country-specific** parameters (Table 4.16) consider conditions in individual countries under which abatement technologies have to be applied. The most important parameters are the average capacity utilization of plants, the average boiler/furnace size and the prices for energy and material consumption.

Table 4.15 Common parameters used for the SO_2 control cost calculation

Symbol	Item	Unit
General parameters:		
v	Relative flue gas volume[3)]	-
lt	Lifetime of installation	years
Technology specific parameters:		
I	Investment function	US$/kW$_{thinp}$[4)]
ci^f	Intercept	US$/kW$_{thinp}$
ci^v	Slope	10^3 US$
f	Maintenance costs and overheads	%/100/year
λ^e	Specific demand for energy	GWh/PJ$_{thinp}$
λ^l	Specific demand for labor	man-yr/MW$_{thinp}$
λ^s, λ^d	Specific demand for sorbents and waste disposal	ton/t SO_2 removed
x	Sulfur removal efficiency	%/100
r	Retrofit cost factor	%/100

3)Relative to hard coal fired boilers.

4)kW$_{thinp}$ - kilowatt thermal (fuel) input to the boiler/furnace.

Table 4.16 Country specific parameters

Symbol	Item	Unit
sc	Sulfur content	%/100
hv	Heat value (lower)	GJ/t
sr	Sulfur retained in ash	%/100
bs	Average boiler size	MW_{thinp}
pf	Capacity utilization	hours/year
q	Real interest rate	%/100
c^e	Electricity price	US$/kWh
c^l	Labor price	US$/man-yr
c^s, c^d	Sorbents and waste disposal prices	US$/ton

Data sources

Although the cost evaluation method outlined above is based on international standard procedures, it still remains a difficult task to identify appropriate parameter values leading to accurate estimates of future SO_2 emission control costs in Asia.

After initial discrepancies in national cost estimates (for an early discussion of the differences among estimates for U.S., Japan and Germany see e.g., OECD, 1986), technology related data for world wide technologies are now converging (Dace *et al.*, 1986) and show a stabilizing trend (Schärer, 1993). Consequently, characteristic values confirmed for Western or Japanese technologies could be considered representative also for future applications in other Asian countries. General and technology specific data used in the RAINS-ASIA model are listed in Tables 4.17 and 4.18.

Table 4.17 Data used in the cost calculations for general parameters

Item	Value
Relative flue gas volume(*v*)	(Hard coal = 1)
Brown coal	1.2
Hard coal	1.0
Heavy fuel oil	0.9
Lifetime (*lt*)	(years)
- for existing power plants	20
- for new power plants	30
- for industry	20

Table 4.18 Technology specific data

Item	Symbol	Combustion Modification (limestone injection)		Wet Flue Gas Desulfurization		Regenerative Processes	Units
		new	retrofit	new	retrofit	new	
Investment function:							
Intercept	ci^f	22	29	44	57	116	US$/kW$_{thinp}$
Slope	ci^v	3,700	4,815	12,350	16,050	24,570	10^3 US$
Resulting specific investments for a 580 MW$_{thinp}$ plant[5)]		28	38	65	85	159	US$/kW$_{thinp}$
Operating costs:							
Annual maintenance costs	f	4.0		4.0		4.0	% of total investments/year
Labor demand	λ^l	10.8		10.8		25.2	man-year/GW$_{thinp}$
Additional energy demand	λ^e	0.5		1.0		2.2	GWh/PJ$_{thinp}$
Sorbents		Limestone		Limestone		NaOH	
Sorbents demand	λ^s	4.68		1.56		0.01	t/t SO_2 removed
By-product		Sludge		Gypsum		Sulfur	
Amount of by-product	λ^d	7.80		2.60		0.50	t product/t SO_2 removed
Sulfur removal efficiency	x	50.0		95		98.0	%

4.4.3 Control of process emissions

Process emissions[6)] are caused by various types of industrial sources. Thus it is difficult to estimate detailed control costs for this group of emitters. Therefore, a simplified approach has been adopted based on the assumption that process emissions can be removed up to a certain percentage of the uncontrolled emissions at step-wise increasing costs. Three such cost categories have been implemented. The costs for each step are shown in Table 4.19.

[5)] An equivalent of about 210 MW electric for a power plant.

[6)] For definition of process emissions in RAINS-ASIA, see Bertok et al., 1993.

Table 4.19 Control costs for process emissions

Control option	Removal efficiency, %	Unit cost, US$/t SO_2
Stage 1	50	432
Stage 2	70	503
Stage 3	80	633

4.4.4 Cost curves for SO_2 reduction

The RAINS-ASIA model also provides an option to calculate cost curves for reducing SO_2 in particular regions or countries. Such curves provide the minimum cost of achieving emission reductions for each abatement level, using the cost-optimal combination of abatement measures. Cost curves are compiled by ranking available emission control options for the various sources according to their cost-effectiveness and combining them with the potential for emission reductions determined by the properties of the fuel and the abatement technologies.

Consequently, the shape of such curves is influenced by the costs of applying the various emission control measures in a region (e.g., represented by cost coefficients according to Equation 6) and the potential for emission reductions determined by fuel characteristics and the selected energy pathway.

The RAINS-ASIA model computes two types of cost curves:

The '**total cost**' curve displays total annual costs to achieve certain emission levels in a region. These curves are piece-wise linear, with the slopes of the individual segments determined by the costs of applying the various technologies.

The **'marginal cost'** curve is a step-function, indicating the marginal costs (i.e., the costs for reducing the last unit of emissions) at the various reduction levels.

The current implementation of RAINS-ASIA creates cost curves only for the available emission control options, i.e., measures already implemented are excluded from the consideration. Thus, to obtain the overall costs of measures in a selected region, cost curves have to be based on the 'no-control' scenario, otherwise the costs of already existing installations would be ignored. An example cost curve for the N Highlands (NHIG) region of Thailand is presented in Figure 4.4.

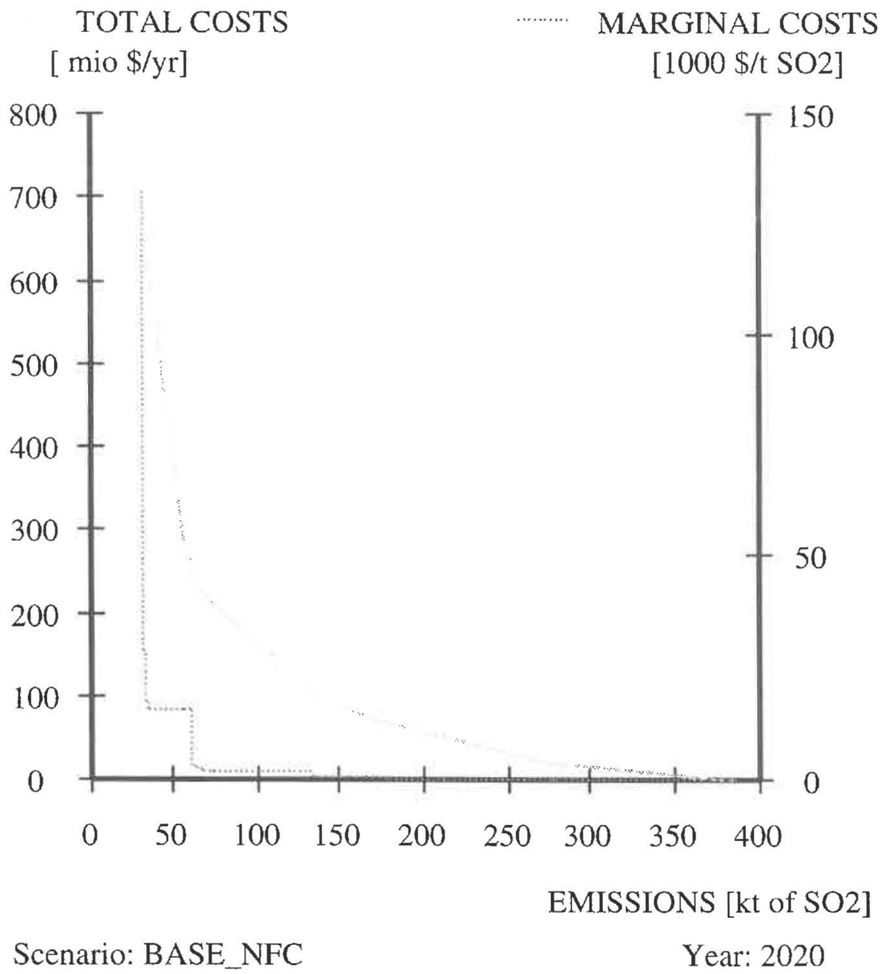

Figure 4.4 Example cost curves for the NHIG region of Thailand for the baseline energy scenario

4.6 Conclusions and recommendations

A comprehensive analysis of the current picture of sulfur dioxide emissions in Asia has been assembled for the RAINS-ASIA project. In addition, tools have been developed to project future emissions and the potential to reduce those emissions through application of control technologies and other methods. Having said this, there is still a critical need to improve, update, and extend the existing work.

In order to better anchor the future emissions forecasts, a revised, self-consistent, base-year inventory should be assembled for a more recent year, say, 1992. Any discrepancies between this work and the data of Akimoto and Narita need to be understood and reconciled. In addition, the energy data developed by the Asian network needs to be cross-checked and verified against the base-year inventory. In future work, it will be important to add emissions of nitrogen oxides, in order to obtain a complete picture of acidifying pollutants and to be able to assess the urban air pollution situation. This will necessitate new emphasis on the transportation sector. Finally, the emission factors used in the base-year inventory and in the RAINS-ASIA model need to be harmonized. Discussions have also taken place regarding extension of the methodology to include other pollutants or gases, such as carbon dioxide, methane, particulate matter, and ammonia. Decisions on these matters await resolution of future funding levels and direction of the project.

As the project moves into the phase of assessing costs and emissions under future scenarios, it is important that RAINS-ASIA uses appropriate technologies for the Asian context and also appropriate cost, performance, and application data for these technologies. Note that in Phase I the technology characteristics are largely based on European and North American experience. An Asian technology characterization data base is needed that could be used within the model and also for stand-alone analyses. At a minimum, this data base would include low-cost technologies that are not typically analyzed in the West (e.g., coal briquetting, CFBC, and wet particle scrubbers), low-cost adaptations of western technology, and appropriate technologies for Asian energy resources (Thai lignite, high-ash Indian coals, etc.). Costs would also reflect regional costs for labor and materials, as appropriate. The data base would include both energy production and emission control technologies.

REFERENCES

Acid News, 1989. Swedish NGO Secretariat on Acid Rain, Stockholm, Sweden. July.

Amann, M., 1990 Energy use, emissions and abatement costs in Europe. In: J. Alcamo, R.W. Shaw and L. Hordijk (eds), *The RAINS Model of Acidification, Science and Strategies in Europe*. Kluwer Academic Publishers, Dordrecht, The Netherlands.

Akimoto H., and H. Narita, 1994, *Atmospheric Environment 28* (2):213-225.

Asian Development Bank, 1991, *Environmental Considerations in Energy Development.*

Bertok, I., J. Cofala, Z. Klimont, W. Schöpp, M. Amann, 1993, *Structure of the RAINS 7.0 Energy and Emissions Database*. WP-93-67 IIASA, Laxenburg, Austria.

CONCAWE, 1993, *The European Environmental and Refining Implications of Reducing the Sulphur Content of Marine Bunker Fuels.* Report No. 1/93, Brussels, Belgium.

Dace, P.W. and D.R. Cope, 1986, *Flue gas desulphurization - system performance*. International Energy Agency, Coal Research, London, U.K.

Fearnresearch, 1988, *Fearnley's World Bulk Trades 1988*, Oslo, Norway.

Institute of Shipping Economics and Logistics, 1992, *Shipping Statistics Yearbook 1992*, Bremen, Germany.

International Atomic Energy Agency, 1988, *Experience with WASP and MAED Among IAEA Member States Participating in the Regional Co-operative Agreement (RCA) in Asia and the Pacific Region.* Report IAEA-TECDOC-528.

International Atomic Energy Agency, 1991, *Experience in Energy, Electricity, and Nuclear Power Planning with Emphasis on MAED and WASP Among Member States of the Regional Co-operative Agreement (RCA) in Asia and the Pacific Region.* Report IAEA-TECDOC-622.

International Energy Agency, 1988, *Emission Controls in Electricity Generation and Industry*. OECD, Paris

International Energy Agency, 1989, *World Energy Statistics and Balances*. OECD, Paris, France.

International Energy Agency, 1993, *Energy Prices and Taxes, fourth Quarter 1992*. OECD Paris, France.

Joshi, V., 1991, Biomass Burning in India. In: *Global Biomass Burning*, Joel S. Levine, *ed.* MIT Press, Cambridge, MA. pp. 185-193.

Kroon, P., 1992 *Notes about oil gasification and emission reduction of cars*. ESC - Energy

Studies, Netherlands Energy Research Foundation (ECN), Petten, The Netherlands. (manuscript)

Manda, C.W., A.T. Kirchner, M. Daniel, O. Monfort, 1994, *World Coal-fired Power Stations: Africa, Asia and Australia.* International Energy Agency Coal Research, London

Mannini, A., M. Daniel, A. Kirchner, and H. Soud, 1990, *World Coal-Fired Power Stations.* IEA Coal Research, London, U.K.

Minerals Yearbook, 1989.

Norwegian Meteorological Institute, 1990, *Calculated Budgets of Airborne Sulphur and Nitrogen over Europe.* EMEP MSC-W Report 2/90, Oslo, Norway.

OECD, 1986, *Understanding Pollution Control Cost Estimates.* OECD Environmental Monographs, Vol. 1, Paris.

Pototschnig, A., 1994, Economic instruments for the control of acid rain in Britain. In: G. Klaassen and F. Forsund (eds), *Economic Instruments For Air Pollution Control.* Kluwer Academic Publishers, Dordrecht, The Netherlands.

Schärer, B., 1993, Technologies to clean up power plants. Experience with a DM 21 Billion FGD and SCR retrofit programme in Germany, Part 1 and 2. *Staub - Reinhaltung der Luft 53*, 87-92 and 157-160.

Smith, K., 1988, Air Pollution. Assessing Total Exposure in Developing Countries. *Environment 30* (10):16-20, 28-35.

Spiro, *et al.*, 1992, *Journal of Geophysical Research 97*, 6023-6036.

Stopford, M., 1988, *Maritime Economics.* Unwin Hyman Ltd., London, U.K.

United Nations, 1989, *Electric Power in Asia and the Pacific 1985 and 1986.* ESCAP Report No. ST/ESCAP/720.

United Nations, 1984, *Statistical Papers.* Maritime Transport Study. Series D.

U.S. Environmental Protection Agency, 1987a, *Criteria Pollutant Emission Factors for the 1985 NAPAP Emissions Inventory.* Report EPA-600/7-87/015.

U.S. Environmental Protection Agency, 1987b, *National Air Pollutant Emission Estimates, 1940-1985.* Report EPA-450/4-86-018.

The World Bank, 1992, *World Development Report 1992.* Oxford University Press, New York, USA.

World Energy Council, 1989, *Survey of Energy Resources.*

World Resources Institute, 1992, *World Resources 1992-93*, New York, U.S.A.

RAINS-ASIA:
AN ASSESSMENT MODEL FOR AIR POLLUTION IN ASIA

Chapter 5

ATMOS Module

Long Range Transport and Deposition of Sulfur in Asia

Gregory Carmichael and Richard L. Arndt

Report on the World Bank Sponsored Project
"Acid Rain and Emission Reductions in Asia"

December 1995

5. ATMOS MODULE
LONG RANGE TRANSPORT AND DEPOSITION OF SULFUR IN ASIA

Authors:
Gregory R. Carmichael and Richard L. Arndt

TABLE OF CONTENTS

5.1 Summary V-1
5.2 Overview of ATMOS sub-project V-1
5.3. Acid deposition modeling V-2
5.3.1 Overview V-2
5.3.2 Modeling framework V-3
5.3.3 Policy issues V-6
5.4 Acid deposition modeling for Asia V-6
5.4.1 Description of the ATMOS model V-7
5.4.2 Transport calculation V-7
5.4.3 Concentration/deposition calculations V-10
5.4.4 Parameters used in model V-13
5.4.5 Input data V-15
5.4.6 Outputs V-20
5.5 ATMOS modeling results V-20
5.5.1 Sulfur deposition V-20
5.5.2 Source-receptor relationships V-24
5.5.3 Surface concentrations V-33
5.5.4 Preliminary model evaluation V-42
5.6 Monitoring and focal center activities V-42
5.6.1 Monitoring sulfur dioxide in East Asia V-42
5.6.2 Monitoring results V-43
5.6.3 Collaborations and focal center activities V-50
5.7 Other modeling activities V-52
5.7.1 Calcium deposition V-55
5.8 Uncertainty V-56
5.9 References V-57

LIST OF TABLES

Table 5.1 Dry deposition velocities used in the ATMOS model V-15
Table 5.2 Identification of Sources Contributions to Sulfur Deposition at Guiyang, China (106° E, 26°N). Region definition and LPS information is presented in Chapter 3. . . . . . V-29
Table 5.3.a Country-to-country source-receptor matrix. The columns represent the source country while the rows represent the receptor country. Shown is the total annual sulfur deposition expressed in tonnes-S/yr. V-30

Table 5.3.b	China's contribution to sulfur deposition in the region, expressed both as a percentage of China's total deposition in the region and as a percentage of the receptor- country's total deposition.	V-33
Table 5.4	Region-to-region source-receptor matrix for China. The columns represent the source region while the rows represent the receptor region. Shown is the total annual sulfur deposition expressed in tonnes-S/yr.	V-34
Table 5.5	SO_2 passive sampler monitor network for RAINS/ASIA	V-45
Table 5.6	Summary of sulfur dioxide passive sampler data.	V-46
Table 5.7	Activities related to ATMOS module	V-51

LIST OF FIGURES

Figure 5.1	The principal chemical and physical processes of acid deposition	V-5
Figure 5.2	Schematic of structure of acid deposition models	V-5
Figure 5.3	Summary of the ATMOS long range transport model	V-9
Figure 5.4	Multiple vertical layers used in the ATMOS model (from Heffter, 1983)	V-11
Figure 5.5	Branching and mixing in the ATMOS model (from Heffter, 1983)	V-11
Figure 5.6	Locations of upper-air meteorological stations	V-17
Figure 5.7	Annual precipitation amounts for 1990 from NMC analyzed fields	V-18
Figure 5.8	Spatial distribution of the sulfur dioxide emissions for Asia	V-19
Figure 5.9	Calculated annual sulfur deposition for the base year 1990	V-21
Figure 5.10	Fraction of sulfur deposition due to ships	V-22
Figure 5.11	Fraction of sulfur deposition due to large point sources	V-23
Figure 5.12a	Calculated sulfur wet deposition during the months December, January, and February (DJF). The total precipitation amounts during these months are also presented.	V-25
Figure 5.12b	Calculated sulfur wet deposition during the months June, July, and August (JJA). The total precipitation amounts during these months are also presented.	V-26
Figure 5.13	Fraction of total sulfur deposition due to volcanoes	V-28
Figure 5.14a	Calculated annual averaged sulfur dioxide surface concentrations for the base year 1990	V-38
Figure 5.14b	Calculated annual averaged sulfate surface concentrations for the base year 1990	V-39
Figure 5.15	Observed and predicted sulfate deposition (wet + dry) amounts (g-sulfate/m^2-yr) in Japan	V-40
Figure 5.16	Observed and predicted sulfate wet deposition at BapMon sites in India	V-41
Figure 5.17	Location of the SO_2 passive sampler monitoring sites	V-44
Figure 5.18	Observed and predicted SO_2 concentration at the passive sampler sites	V-49
Figure 5.19	Calculated daily values of SO_2 and sulfate at a receptor site in Japan	V-53
Figure 5.20	Urban application of the ATMOS model	V-54

5. ATMOS MODULE
LONG RANGE TRANSPORT AND DEPOSITION OF SULFUR IN ASIA

Authors:
Gregory R. Carmichael and Richard L. Arndt

5.1 Summary

A long range transport and deposition model (referred to as the ATMOS model) for sulfur in Asia has been developed. The model is a lagrangian parcel model with three vertical layers. The model calculates the ambient concentrations, and the wet and dry deposition of SO_2 and sulfate resulting from area and large point sources. The model also produces transfer matrices for use in the RAINS-ASIA model. Two matrices are produced: a region-to-grid matrix for the area sources; and a large point source-to-grid matrix for the elevated sources. These matrices are used by the RAINS-ASIA model to calculate future sulfur deposition under various emissions scenarios. Sulfur deposition for the base year 1990 was calculated and the transfer matrices were incorporated into the RAINS-ASIA model. Sulfur deposition from anthropogenic (including those from ships) and volcanic emissions were calculated and presented.

A monitoring network using passive samplers to measure SO_2 ambient concentrations was also established as part of the ATMOS activities. The design of the network and the observational results to date are presented. Other cooperative activities, including the establishment of an ATMOS focal center at the Indian Institute of Technology, Delhi, India, related to this task are also described.

5.2 Overview of ATMOS sub-project

The ATMOS module of RAINS-ASIA provides estimates of ambient levels of SO_2 and sulfate, and sulfur deposition loadings throughout Asia as a function of changing emissions. These estimates provide the link between emissions and deposition, and they are a major input into the RAINS-ASIA model. Specifically a matrix providing annual deposition of sulfur as a function of SO_2 emissions is the basic product of the ATMOS module. The calculation of this matrix requires the use of a long range transport model. Such a model was developed for this purpose as part of the Phase I project. In Phase-I it was decided to focus on the deposition of sulfur only and to not address the deposition of other acidifying species. This was motivated by the fact that sulfur is the dominant anthropogenic acid precursor emitted from energy use in Asia. It was further decided to modify and use the NOAA Branching Atmospheric Trajectory (BAT) model for this study. The terms of reference (TOR) for the ATMOS activities are described below.

<u>TOR</u>

1. Develop the ATMOS acid deposition model for use in Asia. The Asian domain should consist of the window bounded by 10 S latitude to 55 N; and 60 E longitude to 150 E, and should treat emissions from elevated large point sources (LPS) to

enable the evaluation of high stacks on acid rain in Asia.

2. Select model parameters (dry deposition velocities, reaction rates, dispersion parameters) which are appropriate for Asian applications. Asia-specific parameters must take into account high levels of dust, and tropical conditions. Sensitivity calculations will be performed to identify key input parameters.
3. Select base year for calculation of annual deposition.
4. Calculate annual sulfur deposition (wet, dry and total) on a grid-to-grid basis for a complete annual cycle. Sulfur dioxide and sulfate surface concentrations will also be calculated.
5. Develop appropriate post processing tools to calculate the transfer matrices needed by the RAINS-ASIA model and display the data on regional and sub-regional basis.
6. Identify observational data in Asia on sulfur dioxide and sulfate ambient concentrations, and precipitation sulfate, for use in model verification. Initiate preliminary model performance evaluation.
7. Obtain data on the base-cation composition of anthropogenic and natural aerosol components in Asian countries. Locate regions of natural emissions and identify seasonal dependence. This information will be used in future studies estimating base-cation deposition in Asia.
8. Establish a network of scientists and principal contacts in Asia to coordinate the development and application of the atmospheric model. The atmospheric modeling network in Asia will consist of principal contacts in each country responsible for providing regional specific information, and disseminating results within the country. The regional focal center for the atmosphere project is planned for India. The focal center would be the principal hub of communication of the Atmospheric Task.
9. Deliver the ATMOS model for use as a tool to study long range transport of air pollutants in the Asia region. This model can be used outside of the RAINS-ASIA model.

The project activities related to these terms of reference are discussed in the following sections.

5.3. Acid deposition modeling

5.3.1 Overview

An understanding of the detailed relationships between the emissions of primary pollutants and the resulting acid deposition is a requisite to designing effective actions for the maintenance of a healthy environment. Scientific efforts to understand acid deposition processes involve a combination of laboratory experiments, field experiments, and modeling analysis. Laboratory experiments provide the basic data on individual physical and chemical processes that, when combined, give rise to acid deposition. On the other hand, field experiments are usually designed to study a limited number of atmospheric processes under conditions in which a few processes are dominant. Unlike controlled laboratory experiments, however, field studies cannot be parametrically controlled. Since laboratory experiments and field studies by themselves cannot fully elucidate complex atmospheric phenomena like acid deposition, comprehensive models that allow multiple processes to occur simultaneously are required for data analysis and scientific inquiry.

The relationships between the emissions of primary emissions and the resultant acid deposition are difficult to determine because of the number and nature of the processes that occur. The principal chemical and physical processes involved in acid formation and deposition are illustrated in Figure 5.1. Sulfur and nitrogen containing species along with reactive hydrocarbons are emitted from a variety of anthropogenic and natural sources. These compounds are mixed, transported, reacted, and finally removed from the air back to the earth's surface. Sulfur dioxide may react immediately with hydroxyl radicals in the atmosphere to produce SO_3, which in turn reacts quickly with water vapor to produce sulfuric acid, or, depending on the meteorological conditions and the local availability of oxidizing substances, the SO_2 may be transported hundreds of kilometers before it reacts. Some SO_2 may also be deposited in gaseous form directly to the earth's surface. Some SO_2 may be absorbed into cloud droplets, where it may undergo chemical reaction with H_2O_2 or with O_3. Both reactions produce sulfuric acid in the liquid phase. This acid may be removed from the atmosphere through the formation of precipitation, or it may be injected into the gas phase through evaporation processes.

In a somewhat similar manner, NO and NO_2 can be transported, dry deposited, or reacted to form nitric acid. Gaseous nitric acid is usually absorbed immediately into available cloud water and is eventually returned to the earth as nitrate ion in precipitation. Organic acids, may also be formed from emitted reactive hydrocarbons, and end up in precipitation.

5.3.2 Modeling framework

Acid deposition models are computer-based models which calculate the distribution of trace gases in the troposphere from specified emissions distributions and meteorological scenarios. The basic component parts of such models are shown schematically in Figure 5.2. The major features consist of: 1) a transport component (or module) to describe the wind speed and direction, the eddy diffusivity and mixing layer height, the temperature, the water vapor, cloud water content, and the radiation intensity of each location as a function of time; 2) a chemical kinetic mechanism to describe the rates of atmospheric reactions, including homogeneous gas-phase, heterogeneous, and liquid phase reactions; and 3) removal modules to describe the dry deposition of material, and the in-cloud and below-cloud removal processes.

Each process incorporated into a model is itself a very complex and incompletely understood phenomenon. Therefore, in formulating such models it is necessary to incorporate the processes into the model framework by utilizing chemical, dynamic, and thermodynamic parameterizations. Furthermore, even processes that are quite well understood may require parameterization to maintain some balance of the details among the different processes that are treated in the model.

There are presently two basic approaches to modeling acid deposition. One approach (such as that taken by the US EPA) is to use comprehensive eulerian episodic acid deposition models. These models attempt to describe in detail the various physical and chemical processes involved in acid deposition. The ADOM model (Venkatram et al., 1988) developed by the Canadian and German governments; RADM (Chang et al., 1988), the US E.P.A. model; and the STEM-II model (Carmichael et al., 1986) developed by the Universities of Iowa and Kentucky are examples of such an approach. These models are extremely computational and data intensive, and provide information on acid deposition over periods up to one month. The second approach is such as that taken by the EMEP (European Monitoring and Evolution of Pollutants) program, which uses a less detailed chemical approach to the problem, and calculates, using a lagrangian framework, acid deposition on seasonal or annual basis. These models are typically less data and computer intensive for a given application.

Regardless of the approach the theoretical basis is the atmospheric advection-diffusion equations (i.e., the mass balance equations):

Gas phase:

$$\frac{\partial C_i}{\partial t} + \frac{\partial (U_j C_i)}{\partial x_j} = \frac{\partial}{\partial x}[K_{jj}\frac{\partial C_i}{\partial x_j}] + R_i + E_i + G_i \qquad (1)$$

(A) (B) (C) (D) (E) (F)

i=1,,....# of species

Cloud, Rain, and Snow Phases:

$$\frac{\partial (S_m C_{im})}{\partial t} + \frac{\partial}{\partial x_j}(U_j - V_{sm})S_m C_{im} = \frac{\partial}{\partial x_j}(K_{jjm} C_{im}\frac{\partial S_m}{\partial x_j}) + R_{im} + G_{im} \qquad (2)$$

i=1,..,#of species;

m=1 for cloud

m=2 for rain

m=3 for snow

where C_i denotes the gas phase concentrations, C_{im} denotes the liquid phase concentrations, U_j are velocity components, x_j represents the spatial coordinates, most generally three dimensional, S_m's are the liquid water contents, V_{sm}'s are the settling velocities of the hydrometers, K_{jj}'s are the eddy diffusivities, and R_i, G_i, and E_i are the rates of chemical reaction, mass transfer, and emissions, respectively.

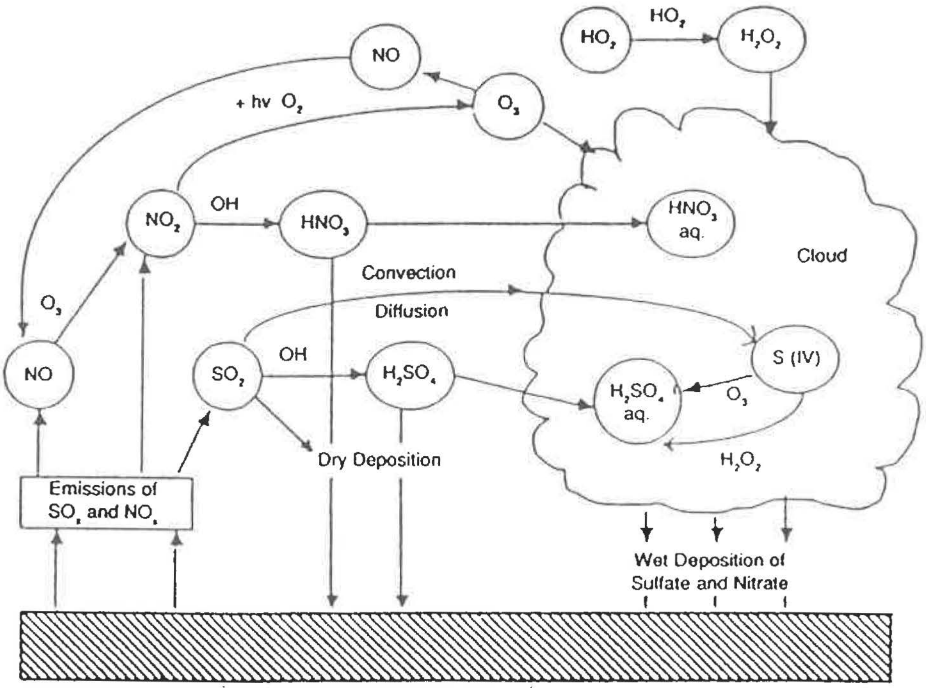

Figure 5.1 The principal chemical and physical processes of acid deposition

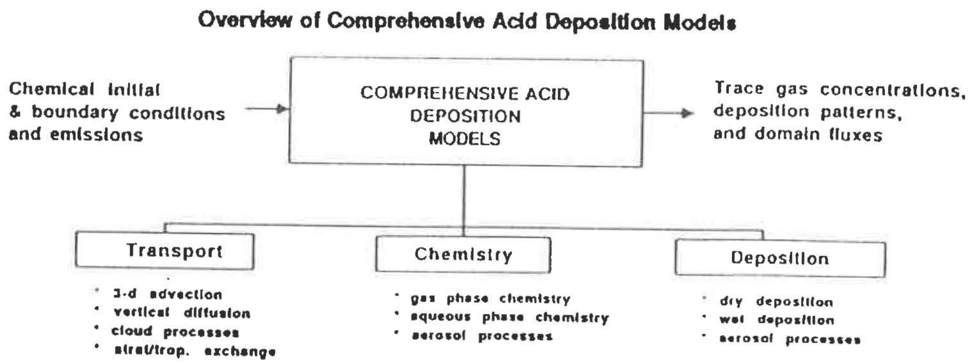

Figure 5.2 Schematic of structure of acid deposition models

In the above equations term (A) represents the unsteady accumulation of mass, (B) changes in mass due to advective fluxes, (C) changes in mass due to turbulent diffusive fluxes, (D) the rate of production/destruction due to chemical reaction, (E) the source term due to emissions, and (F) the rate of mass transfer between phases. These equations are nonlinear due to the nonlinear nature of the chemical processes, and are also highly coupled within a given phase, again due to the chemical processes, and coupled between phases through the inter-phase mass transfer processes (e.g., gas absorption, nucleation, and accretion processes).

5.3.3 Policy issues

Knowing the principal mechanisms of acid deposition provides guidance to policy makers as they develop emission control strategies. As discussed above, sulfate is the most important component of acidity in most of Asia. Sulfate is not a primary pollutant, but rather it is formed in the atmosphere by chemical reactions which oxidize sulfur dioxide (SO_2) to sulfate; i.e.,

$$SO_2 \quad + \quad \text{oxidants} \dashrightarrow \quad \text{sulfate} \qquad \text{(R-1).}$$

This reaction can take place in the gas, liquid or solid phase, and the oxidants include such species as ozone, hydrogen peroxide and hydroxyl radicals. The rate of sulfate formation in the atmosphere depends not only on the amount of sulfur dioxide, but also on the availability of the oxidizing agents. The levels of oxidants in the atmosphere vary with sunlight, temperature, and the presence of other pollutants such as nitrogen oxides and reactive hydrocarbons. Thus oxidant levels vary significantly from one location to another, and with season and time of day. Further complicating the picture is the fact that the acidic deposition at a specific point is determined by the combined effects of the chemical reaction rate, the general transport characteristics, and the emissions distribution.

Due to the complexity of the atmospheric processes, and the spatial and temporal variations in emissions and deposition patterns, it is very difficult to determine *a priori* how effective various control strategies will be. Acid deposition models are designed to predict the dynamic variation in the key species and the source-receptor relationships. Thus they are designed to evaluate acid deposition resulting from various emission scenarios.

5.4 Acid deposition modeling for Asia

For Phase-I it was decided to use a Lagrangian approach, and calculate the deposition fields using a modified version of the USA National Oceanic Atmospheric Administration, Branching Atmospheric Trajectory (BAT) model (Heffter, 1983). This modified model is referred to as the ATMOS model. The ATMOS model is similar in design to the EMEP model used in Europe to produce the deposition fields for RAINS-Europe. The ATMOS model calculates the dry and wet deposition of the species of interest from a particular source, as the pollutant is transported by the meteorological fields. The amount of deposition is calculated along trajectories determined by the meteorological conditions. Running these trajectories for a period of months or an entire year allows the calculation of seasonal and annual deposition throughout the region resulting from that particular source. Repeating the calculation for all sources allows the total deposition from the regional emissions to be calculated.

5.4.1 Description of the ATMOS model

The ATMOS model is a three-dimensional, multiple layer Lagrangian model. The ATMOS model was modified to include the calculation of SO_2 and sulfate surface concentrations, and wet and dry deposition amounts. It was also modified to include the capability for modeling both elevated and surface emission sources. The basic features of the ATMOS model are presented in Figure 5.3.

The ATMOS model provides a one by one degree resolution of the concentrations and deposition of SO_2 and sulfate. The model's meteorological domain is 20° South to 60° North latitude and 39° East to 155° East longitude. The sulfur species modeling domain is 10° South to 55° North latitude and 60° East to 150° East longitude. Within the modeling domain SO_2 emission plumes are modeled as puffs released every three hours from the emission source location. Each puff is assigned a mass proportional to the source strength, and is assumed to mix uniformly in the vertical throughout an assigned layer, and to diffuse with a Gaussian distribution in the horizontal. Area emissions are modeled as surface sources (released at the center of the grid) while large point sources and volcanoes are treated as elevated sources. Individual emission puffs are followed throughout their transport and deposition "lifetimes". Each puff's transport is followed for up to five days (or until the mass falls below a cut-off value). Puffs which are transported beyond the modeling domain are no longer tracked. As the puffs are being transported, SO_2 is chemically converted to sulfate, and SO_2 and sulfate are deposited to the surface. The deposition of the two pollutants is separated into wet and dry components. Details of the calculations are presented below.

5.4.2 Transport calculation

The puff's trajectory is calculated every three hours using the modified Euler advection technique (Carnahan et al., 1969). Each advection step is calculated as:

$$\text{step} = \frac{\sum_{i=1}^{M} w_i \, \Delta t \, d_i^{-2}}{\sum_{i=1}^{M} d_i^{-2}} \qquad (3)$$

where
- M = number of rawinsonde stations within a one degree radius.
- w_i = vertically averaged horizontal wind at station i
- t = advection step time interval
- d_i = distance from station i to step origin

The average horizontal winds in a layer are calculated from the meteorological data and are described in detail later.

The model separates the vertical dimension into two layers during the day (D) and three layers at night (N) (see Figure 5.4). The day layers are the boundary and upper layers. The night layers are the surface, boundary, and upper layers. The night surface layer extends from the ground to 300 meters. The boundary and upper layers are separated by the critical inversion which is determined from the vertical temperature profile. The maximum height for the model is 6000 meters. The following criteria determine the inversion height:

$$\frac{dQ}{dZ} \geq 0.005 \text{ K/m} \tag{4}$$

$$Q_{top} - Q_{bottom} \geq 2 \text{ K} \tag{5}$$

where dQ/dZ is the change in potential temperature (Q) with height (Z) and Q_{top} and Q_{bottom} are the top and bottom of the inversion layer, respectively. The boundary layer is given a maximum height of 2500 meters. Area sources emit into the surface layer at night or the boundary layer during the day. Elevated sources emit into the boundary layer at all times.

ATMOS Long Range Transport and Deposition Model

Features:

* Modification of BAT Model Developed by Hefter at NOAA

* 3-Layer Trajectory Model

* Forward or Backward Trajectories

* Concentrations at Sampling Sites or Grid Locations

* SO_2 & Sulfate Concentrations, Wet & Dry Deposition

* Source-to-Grid Matrices (1^{o} by 1^{o}) (surface & elevated)

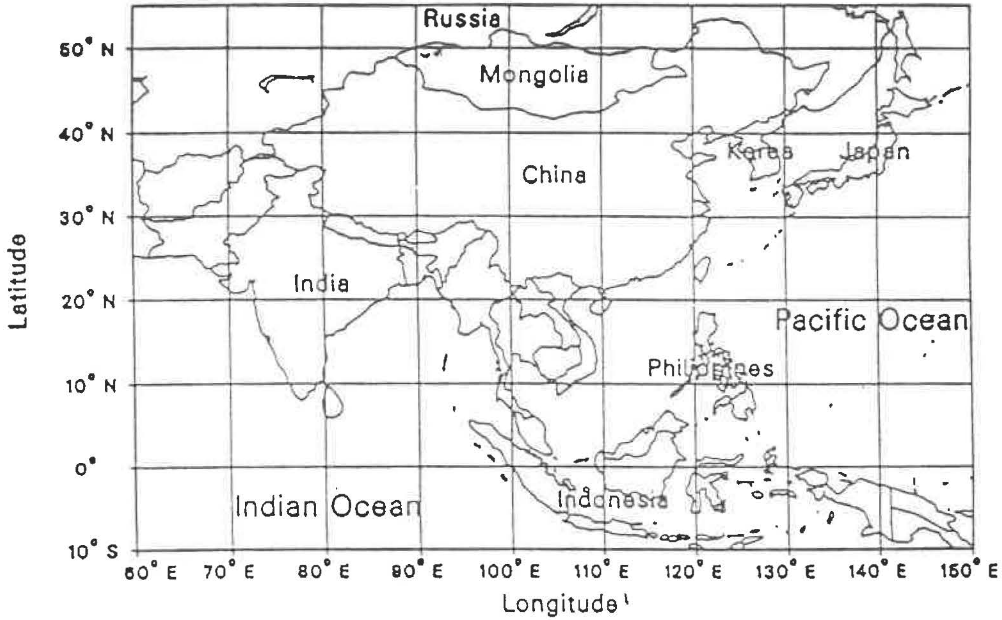

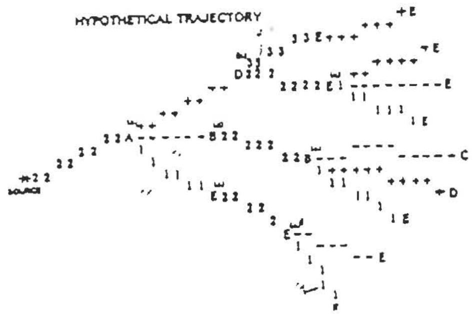

Figure 5.3 Summary of the ATMOS long range transport model

During day-to-night and night-to-day transitions the puff branches into multiple puffs. This action is performed to simulate vertical wind shearing of the puff. Up to 32 branches of the original puff may be tracked simultaneously after which branching ceases. Figure 5.5 illustrates the potential branching processes experienced during transition. During a day-to-night transition a puff in the boundary layer (2D) will branch into all three night layers (1N, 2N, and 3N) while a puff in the upper layer (3D) will stay in its nighttime counterpart (3N). During a night-to-day transition a puff in the surface layer (1N) will go into the boundary layer (2D), a puff in the boundary layer (2N) will stay in its daytime counterpart (2D), and the growing boundary layer will cause a puff in the upper layer (3N) to branch into the two day layers (2D and 3D). Puff mass following splitting is proportioned according to the post-transition layer thicknesses. A hypothetical branched layer is shown in Figure 5.3. The puff is released during the daytime, and at the first day/night transition is split into 3 layers (+,-,1). Each of these layers follows their own trajectories, and split again at the night/day transition. This continues for five days, or until the trajectories leave the modeling domain.

5.4.3 Concentration/deposition calculations

Two forms of sulfur are treated explicitly, gaseous SO_2 and aerosol sulfate. Sulfate is both emitted directly (estimated as 5% of the total sulfur emitted) and formed from the chemical conversion of SO_2. Deposition is separated into four components: dry and wet SO_2 and dry and wet sulfate.

The mass of sulfur, and the partitioning of sulfur between SO_2 and sulfate within each parcel j is calculated every hour by solving the mass balance equations. The mass of sulfur as SO_2 and sulfate in a parcel changes by the chemical conversion of SO_2 to sulfate, via removal by wet scavenging processes, and via surface removal by dry deposition. The mass balance equations for the total mass as SO_2 and sulfate within a parcel j are:

$$MSO_2(j, t+\Delta t) = MSO_2(j, t)Exp(-\Phi*\Delta t) \quad (6)$$

$$MSO_4(j, t+\Delta t) = \frac{k*MSO_2(j, t+\Delta t)}{(\Psi - \Phi)} + \left\{ \left[MSO4(j, t+\Delta t) - \frac{k*MSO2(j, t)}{(\Psi - \Phi)} \right] Exp(-\Psi * \Delta t) \right\} \quad (7)$$

where

$$\Phi = k + \frac{v_{d\text{-}so2}}{Zi} + k_{w\text{-}so2} \quad (8)$$

$$\Psi = \frac{v_{d\text{-}so4}}{Zi} + k_{w\text{-}so4} \quad (9)$$

and k represents the first order chemical conversion of SO_2 to suifate, k_w represents the wet removal rate constants, v_d the dry deposition velocities (these values are non-zero only for parcels in the surface layer), and Zi is the height of layer i.

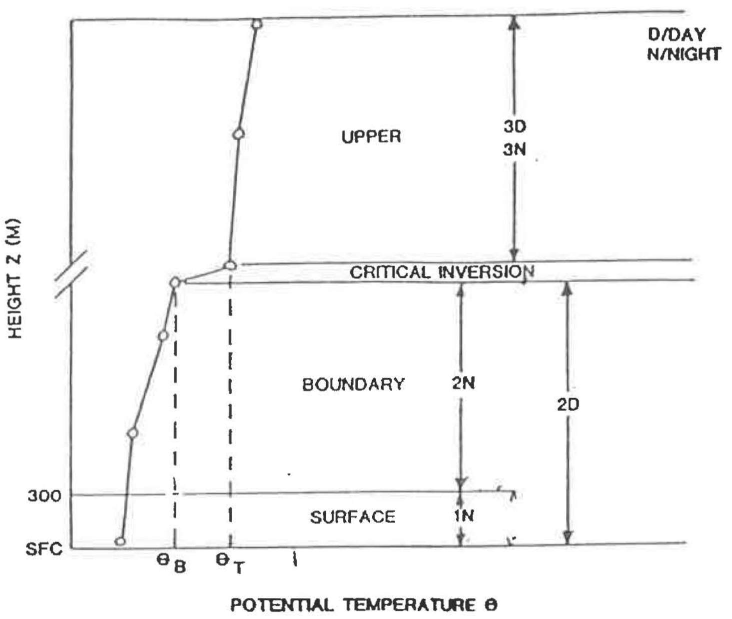

Figure 5.4 Multiple vertical layers used in the ATMOS model (from Heffter, 1983)

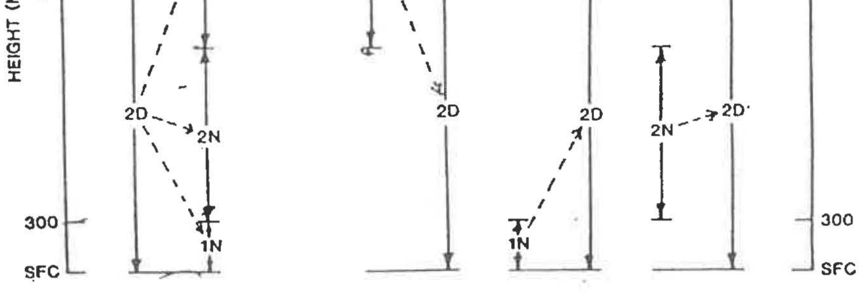

Figure 5.5 Branching and mixing in the ATMOS model (from Heffter, 1983)

The concentrations in a given layer, at each grid point within the model domain, are calculated based on the mass of each puff in that layer. (For example, only those puffs that come into contact with the surface contribute to the surface concentrations.) The mass is assumed to be uniformly mixed vertically within a layer and distributed in a Gaussian fashion horizontally. The concentration of the puff at a specific location is given by the Gaussian plume formula, which depends on the puff mass (proportional to the source strength), the horizontal dispersion, the height of the surface layer, and the distance from the puff center. Specifically, the concentration around the puff center is calculated from:

$$SO_2\,(\text{lat, long}, t + \Delta t) = \frac{MSO_2(j, t + \Delta t)}{(2*\pi*\sigma^2*L)V} \exp\left(\frac{-r^2}{2} * \sigma^2\right) \quad (10)$$

$$SO_4\,(\text{lat, long}, t + \Delta t) = \frac{MSO_4(j, t + \Delta t)}{(2*\pi*\sigma^2*L)V} \exp\left(\frac{-r^2}{2} * \sigma^2\right) \quad (11)$$

where:

σ = horizontal mass standard deviation

L = layer depth, weighted according to the square of inverse distance of the contributing rawinsonde , and

r = distance from the puff center

V = volume of the grid centered at lat, long with a layer thickness of Zi

The contribution of every puff to each grid cell is calculated, so that at the end of the desired period, concentrations in that layer can be calculated. In this study, σ was assumed to vary linearly with travel time. Minimum values of σ were 20 km and 40 km for elevated and area sources, respectively.

The model also explicitly calculates sulfur deposition and considers both dry and wet processes. Dry deposition results from the concentration puff coming into contact with the earth's surface. Hence, only those puffs in the lowest vertical layer contribute to dry deposition. For daytime deposition only the boundary layer contributes to dry deposition while at night only puffs in the surface layer contribute (see Figure 5.4). Dry deposition is dependent on several factors: surface type, latitude and season. Surface type is divided into terrestrial and marine. Terrestrial areas are further segregated by latitude and seasonal deposition rates. Wet deposition, the removal to the earth's surface of pollutant by precipitation, is what is most commonly thought of when discussing acid rain. In the ATMOS model this removal process takes place throughout the vertical column. All layers of the model contribute to wet deposition.

The dry and wet deposition amounts for SO_2 and sulfate are calculated as follows for each latitude and longitude point:

$$DRY_{SO2}\,(lat, long, t + \Delta t) = DRY_{SO2}\,(lat, long, t\,) + SO_2\,(lat, long, t + \Delta t) * v_{d\text{-}SO2} * \Delta t \qquad (12)$$

$$DRY_{SO4}\,(lat, long, t + \Delta t) = DRY_{SO4}\,(lat, long, t\,) + SO_4\,(lat, long, t + \Delta t) * v_{d\text{-}SO4} * \Delta t \qquad (13)$$

$$WET_{SO2}\,(lat, long, t + \Delta t) = WET_{SO2}\,(lat, long, t\,) + SO_2\,(lat, long, t + \Delta t) * k_{w\text{-}SO2} * Zi * \Delta t \qquad (14)$$

$$WET_{SO4}\,(lat, long, t + \Delta t) = WET_{SO4}\,(lat, long, t\,) + SO_4\,(lat, long, t + \Delta t) * k_{w\text{-}SO4} * Zi * \Delta t \qquad (15)$$

The above equations are summed over all parcels. The model implementation of these equations is formulated in a manner which takes special care to conserve mass.

The actual deposition calculation is done such that the deposition from each individual area and point source is calculated independently. The results are stored in two separate matrices. One which provides the deposition from each individual point source and the second in which the results are aggregated to provide the total deposition resulting from all area sources within a region. The regions are defined in Table 3.1 of Chapter 3.

5.4.4 Parameters used in model

Chemical reaction rate constant

Sulfate is formed chemically by homogeneous gas phase reactions via the mechanism (Stockwell, 1983):

$$SO_2 + OH <=> HSO_3^* --> HSO_3(M) \qquad (R\text{-}2)$$
$$HSO_3 + O_2 --> HO_2 + SO_3$$
$$SO_3 + H_2O --> H_2SO_4 \quad ;$$

and by heterogeneous reactions involving aerosol surfaces and clouds. The model lumps all these chemical processes into an overall reaction:

$$SO_2 -----> \text{sulfate} \qquad (R\text{-}3)$$

with the rate of reaction given as a first order expression

$$RSO_2 = k\,[SO_2] \qquad (16)$$

where k is the first order reaction rate constant.

The homogeneous gas phase reaction varies with the ambient levels of OH and thus changes with season and latitude. The heterogeneous reaction rate depends on ambient aerosol loading, the distribution of clouds, and the availability of liquid phase oxidants such as peroxides. Thus the heterogeneous rate is also expected to vary with season and latitude.

The first order reaction rate constant k is parameterized to account for these considerations. For the high latitude regions of Asia we used a parameterization developed by EMEP for use in Europe, (Eliassen and Saltbones, 1983). The parameterization was modified to take into account the higher levels of OH and clouds found in the tropical regions. The expressions used for k (in sec^{-1}) are as follows:

$$k = 7 \times 10^{-6} \tag{17}$$

{for latitudes between 20S and 20N}

$$k = 4 \times 10^{-6} + 2 \times 10^{-6} * \sin\left[\frac{2*\pi*(TOY-80)}{365}\right] \tag{18}$$

{for latitudes between 20N to 30N}

$$k = 3 \times 10^{-6} + 2 \times 10^{-6} * \sin\left[\frac{2*\pi*(TOY-80)}{365}\right] \tag{19}$$

{for latitudes greater than 30N}

where TOY represents the Julian day of the year.

Wet removal rate constants

The wet removal of SO_2 and sulfate is also treated as a first order process. Both in-cloud and below-cloud scavenging are considered. In the case of SO_2, scavenging is enhanced by in-cloud chemical conversion processes. Thus the rate expression varies with season and latitude. The expressions for the rate constants for SO_2 scavenging (kw) are (in units of sec^{-1}).

$$k_{W\text{-}SO2} = 1.0 \times 10^{-4} * P \tag{20}$$

{for latitudes between 20S and 20 N}

$$k_{W\text{-}SO2} = \{8.3 \times 10^{-5} + 2.7 \times 10^{-5} * \sin\left[\frac{2*\pi*(TOY-80)}{365}\right]\} * P$$

{for latitudes greater than 20N}, (21)

where P is the precipitation rate in mm/hr.

The wet scavenging of sulfate below cloud and in-cloud are treated differently:

$$k_{W\text{-}SO4} = 7.0 \times 10^{-4} * P^{0.7} \quad \text{\{for in-cloud\}} \tag{22}$$

$$k_{W\text{-}SO4} = 6.0 \times 10^{-5} * P \quad \text{\{for below-cloud\}} \tag{23}$$

again with P in mm/hr. The different exponent in the in-cloud expressions reflects the different physical properties at play in the removal of sulfate and is determined from studies by Okita (1994).

Dry deposition velocities

The dry deposition process of SO_2 and sulfate is also treated as a first order process. For those parcels of air which come into contact with the surface the removal is modeled as being proportional to the concentration times the dry deposition velocity (vd). The dry deposition velocities vary with many factors such as land type, land use, season (growing vs dormant), as well as the meteorological conditions. In the first phase of this study a simple parameterization for dry deposition was used. The values vary between land and sea, and with seasonal changes at the higher latitudes to account for growing season variations. The values used are summarized below (units cm/s):

Table 5.1 Dry deposition velocities used in the ATMOS model (Units in cm/s)

	$V_{d\text{-}SO2}$	$V_{d\text{-}SO4}$
land:		
Sept-Mar >20N	0.25	0.2
otherwise	0.5	0.2
sea:	0.318	0.1

5.4.5 Input data

The ATMOS model requires as inputs the emission rates of the species of interest and the location of the sources, meteorological winds, temperature, and precipitation rates. These inputs are discussed below.

Meteorology data

The meteorological data is used by the ATMOS model to calculate puff trajectories and to estimate inversion heights, which in turn are used in the determination of the heights of the three layers used in the model calculations. For Phase-I, 1990 was used as the base year and observed winds were used. Specifically we used the data from the upper air sondings for 1990 provided by the National Climatic Center (NMC) of the National Oceanic and Atmospheric Administration (NOAA). These data files contain rawinsonde and pipal vertical observations of wind speed and temperature from the surface to 500 mb. The location of the reporting stations are shown in Figure 5.6. The data is provided at six hour intervals. The meteorological data needed by the model at specific locations was obtained by interpolation between these observational points. If no rawinsonde data within a one degree radius is available, the information radius is increased at one degree intervals. Rawinsonde station wind data up to a radius of five degrees of the puff may be used in the trajectory calculation.

One problem with using observational data is the lack of values over the oceans. This is a particular problem in the south-east and in the far eastern regions of our study domain. In these regions we also used climatological winds to supplement the data set. If no wind data is available within the five degree radius, climatological values are used. These values are based on seasonal trends for the region. All winds are assumed to be constant for the six hour time period. If wind data for a six hour period is not available but data from the previous six hour period and/or the next six hour period are available, the average of these winds is then used. The necessary interpolations are done within the ATMOS model.

Precipitation data

Precipitation data used was NMC analyzed fields. This data was obtained from the USA National Center for Atmospheric Research (NCAR). The precipitation data consisted of accumulation values collected in six hour intervals throughout the region in 1990. This data was provided on a 1.4695° latitudinal by 1.4875° longitudinal grid spacing. Since these data are on a different grid than that used by the ATMOS model (i.e., 1° by 1°) it was necessary to interpolate the precipitation data. This was done inside the ATMOS model using a two-dimensional linear interpolation method (Carnahan et al., 1969). Figure 5.7 is a plot of the annual precipitation for 1990. Furthermore, the ATMOS model requires hourly precipitation rates. At present the six hour accumulated values were assumed to be uniformly distributed within the six-hour interval. Also the precipitation data is not separated into type (i.e. snow or rain); as a result precipitation removal rates are constant for all precipitation.

Emissions

The model traces sulfur emissions from both area (surface) sources and large point sources (LPS). Emission files from the RAINS-ASIA emissions module are used as the emission source files for the ATMOS model. Emissions from both natural and anthropogenic sources are included in the data files. Natural sources consist of the active volcanic sources in the region. Data for Japanese volcanic sources was provided by (Fujita, 1992). Other volcanic source data was taken from (Spiro et al., 1992). Anthropogenic sources are comprised of regional shipping activity emissions, area surface emissions, and elevated (LPS) sources. Shipping emissions include both emissions from regional shipping lanes and port activities. Area sources are separated into the 94 RAINS-ASIA region designations. Area sources include industrial , domestic and transportation emissions.

Area sources are provided on a one-by-one degree resolution. The emission location for surface sources is the center of the grid. The LPSs are electrical power plants and industrial sources which meet certain emissions criteria. Since elevated sources are individual facilities (e.g., electrical power plants) or volcanoes their emissions are designated at their actual location (on the hundredth of a degree resolution). The LPS data files are subdivided into existing and planned sources. Planned LPSs are those facilities that are not operational in 1990 but are expected to become operational by the year 2020. For the purpose of calculating the source-receptor relationship for planned LPSs, their emissions are given a standard emissions value for the base year. However, these planned facilities do not contribute to sulfur deposition until the year that they become operational.

A summary of the total emissions of sulfur treated in the model by country and region is presented in Chapter 4. The grided emissions are presented in Figure 5.8. Further details regarding the emissions are presented in Chapter 4.

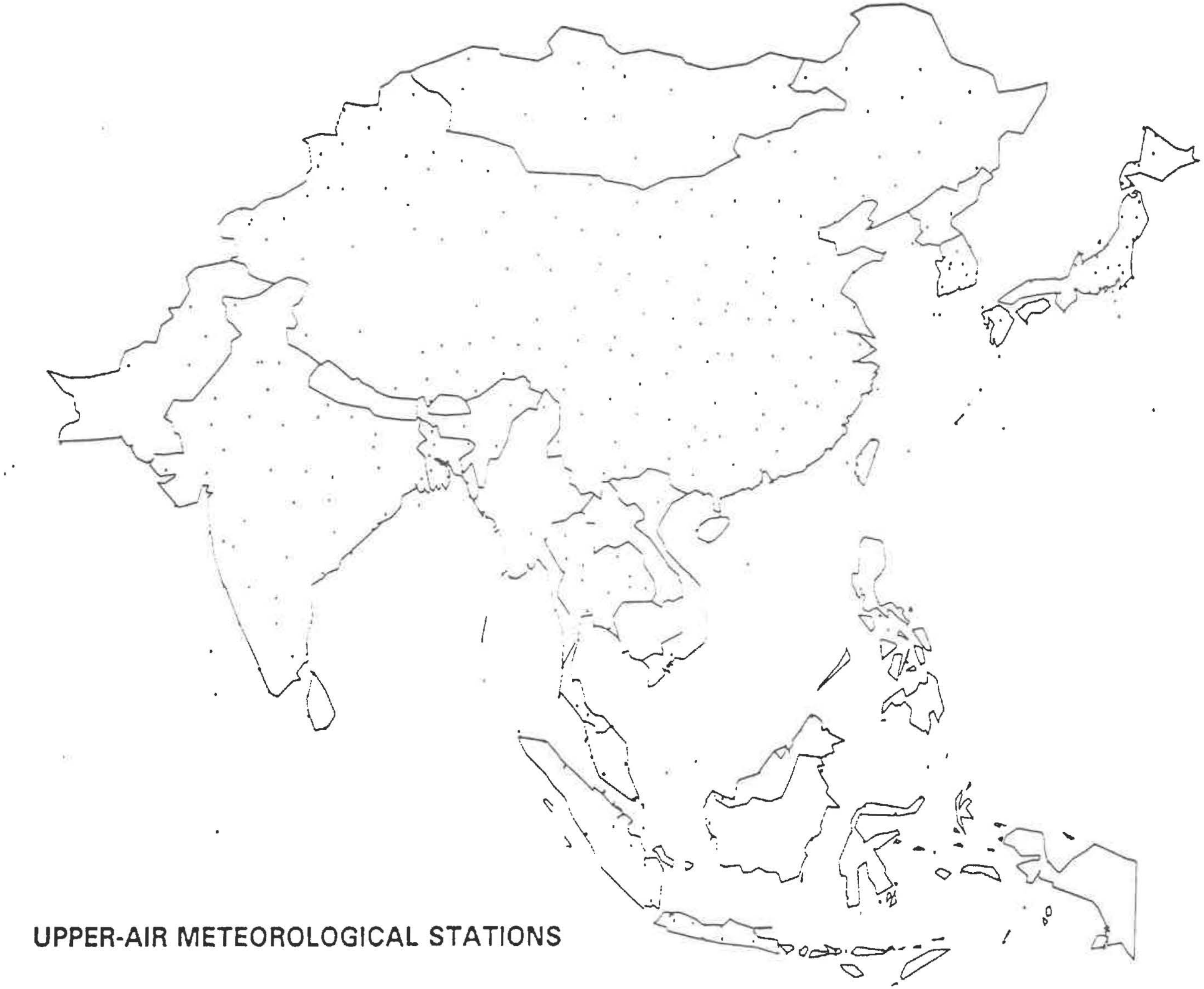

Figure 5.6 Locations of upper-air meteorological stations

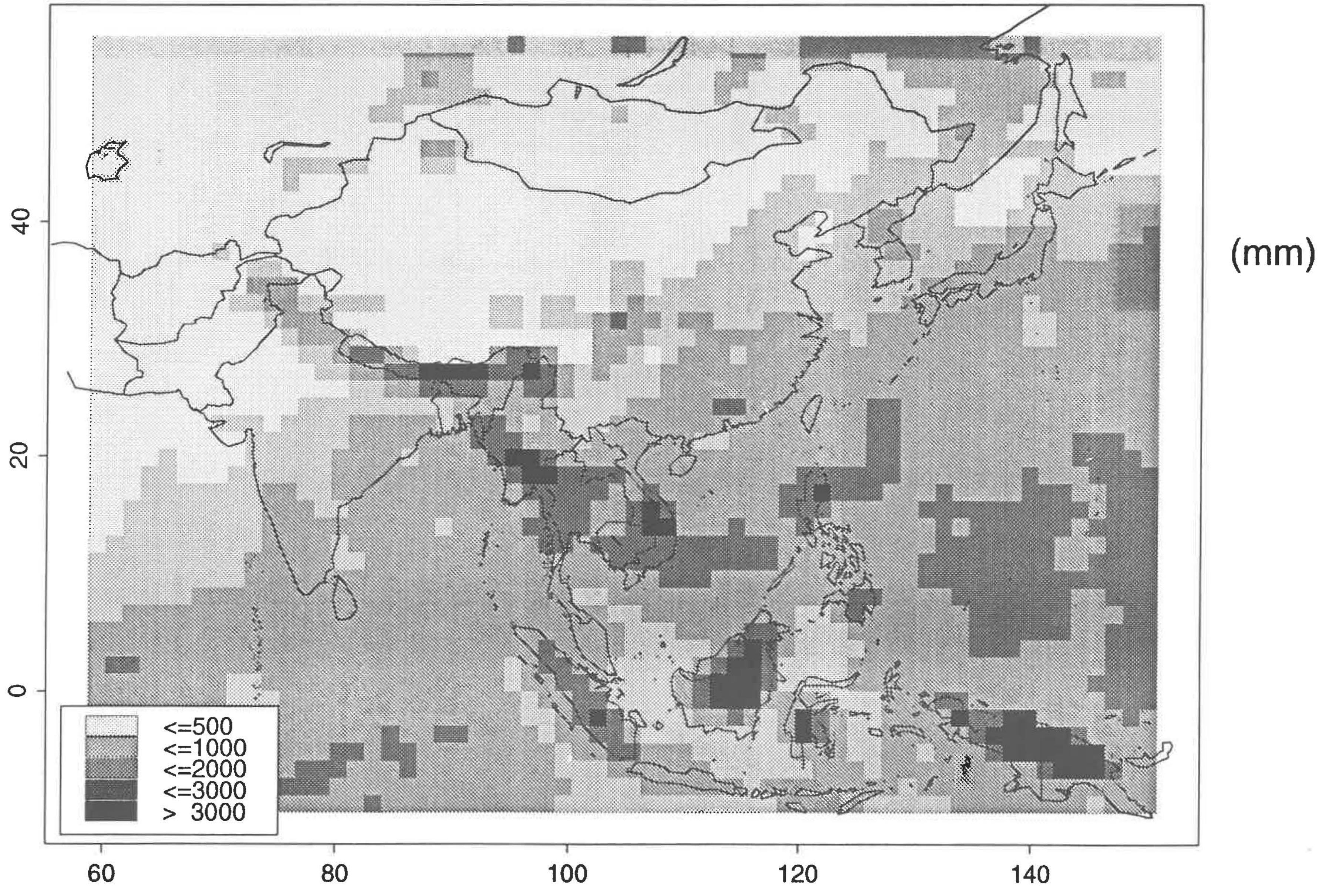

Figure 5.7 Annual precipitation amounts for 1990 from NMC analyzed fields

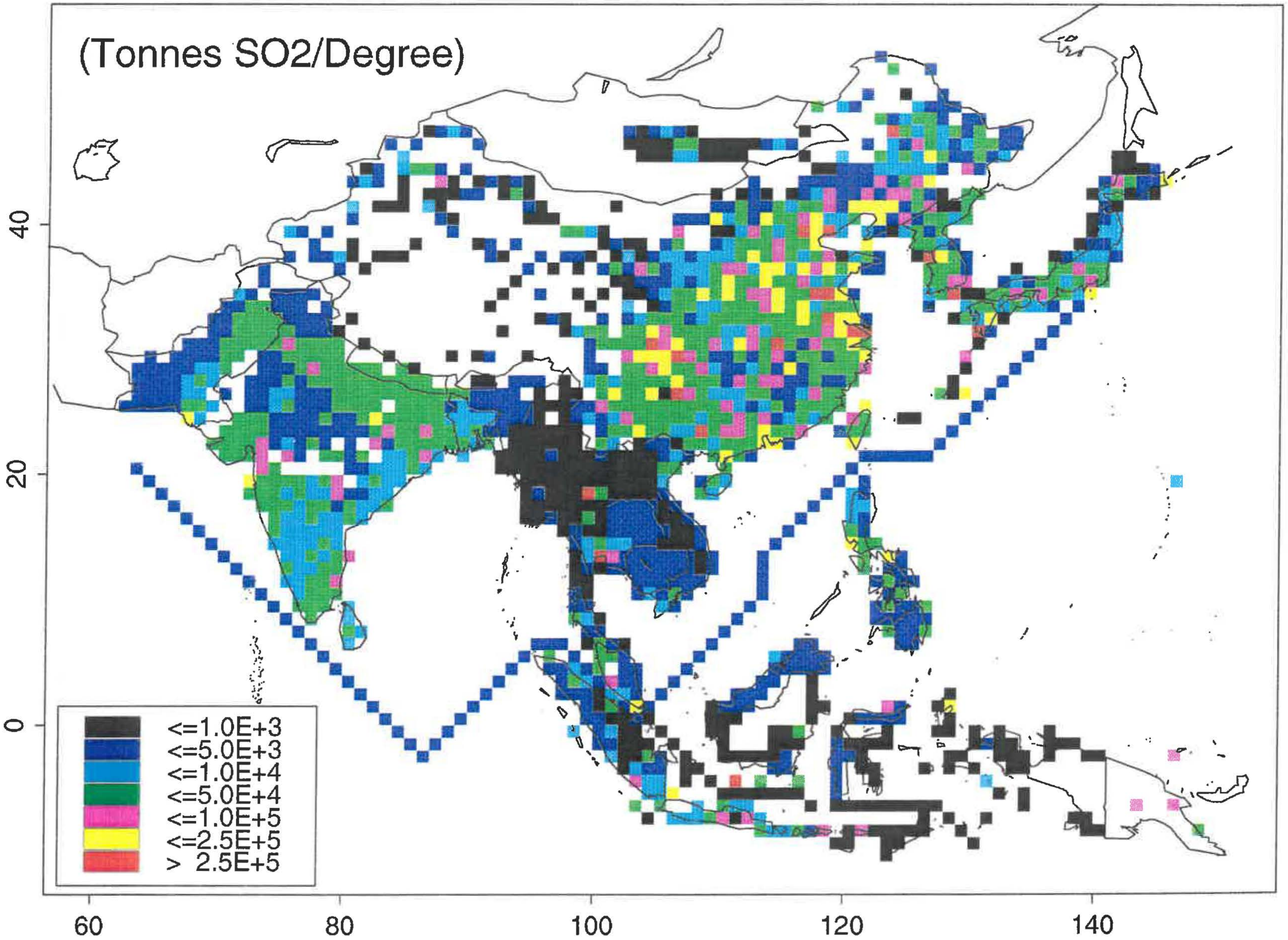

Figure 5.8 Spatial distribution of the sulfur dioxide emissions for Asia

5.4.6 Outputs

Deposition and concentration model output data are separately accumulated for LPS and area sources. Both sources contribute to the final deposition and concentration values for the region, but their contributions are provided in separate formats. For area sources, all deposition and concentration for an individual RAINS-ASIA region are accumulated together. From this data each region's contribution to the deposition of an individual grid cell is determined. The final output to the RAINS-ASIA model is then every region's deposition contribution to each grid cell in the RAINS-ASIA domain. For LPSs, each individual source's deposition and concentration data is output separately. The resulting data set is the contribution of every LPS to each grid cell in the study domain.

The ATMOS model also provides surface concentration and deposition data for the entire area under study. This data, on a one-by-one degree resolution or grid cell basis, contains both sulfur dioxide and sulfate concentrations and depositions. The concentration data are the average of one month's hourly concentrations for each grid cell determined by summing the hourly concentration values for all time periods and then dividing by the number of time periods.

5.5 ATMOS modeling results

5.5.1 Sulfur deposition

The ATMOS model described above was used to calculate sulfur deposition for the Base Year 1990. The annual-average concentrations of SO_2 and sulfate, and the dry and wet deposition of SO_2, sulfate and total sulfur deposition were calculated. Source-receptor matrices of total sulfur deposition were also produced. These consisted of a LPS-to-grid matrix and a region-to-grid matrix. The model calculated annual total deposition in g-S/m^2-yr is presented in Figure 5.9. Shown are the contributions from all anthropogenic sources included in the model (LPS and area sources) and volcanoes. There are very few regions in Asia which are not impacted by sulfur deposition. The high sulfur deposition regions follow closely the spatial distribution and the density of the emissions (See Figure 5.8 for comparison). For example, the dense emission regions in eastern and southern China, S. Korea, northern Thailand, and eastern India all show elevated sulfur deposition. The highest annual deposition ($\sim$10.5 g-S/m^2-yr) occurs around the city of Chongqing in Sichuan province. The strong continental outflow from east Asia is also clearly depicted. Sulfur emissions in the latitude band 20° to 40° N result in high sulfur deposition virtually throughout the western Pacific Ocean at these latitudes. Transport and deposition off the eastern coast of India over the Bay of Bengal is shown as is the high sulfur deposition around Malaysia, Singapore and the western parts of Indonesia. The total deposition patterns are also heavily influenced by the annual precipitation patterns (See Figure 5.7 for comparison). High annual precipitation amounts are found to occur in northern India, Nepal, southeastern China, and Southeast Asia.

Elevated sulfur deposition also occurs along the major shipping lanes. The emissions from ships is discussed in detail in Chapter 4. The contribution of ships to sulfur deposition is shown in Figure 5.10. The contribution of ships to sulfur deposition exceeds 10% for vast regions of the study area below 20° N latitude. In many oceanic regions the deposition due

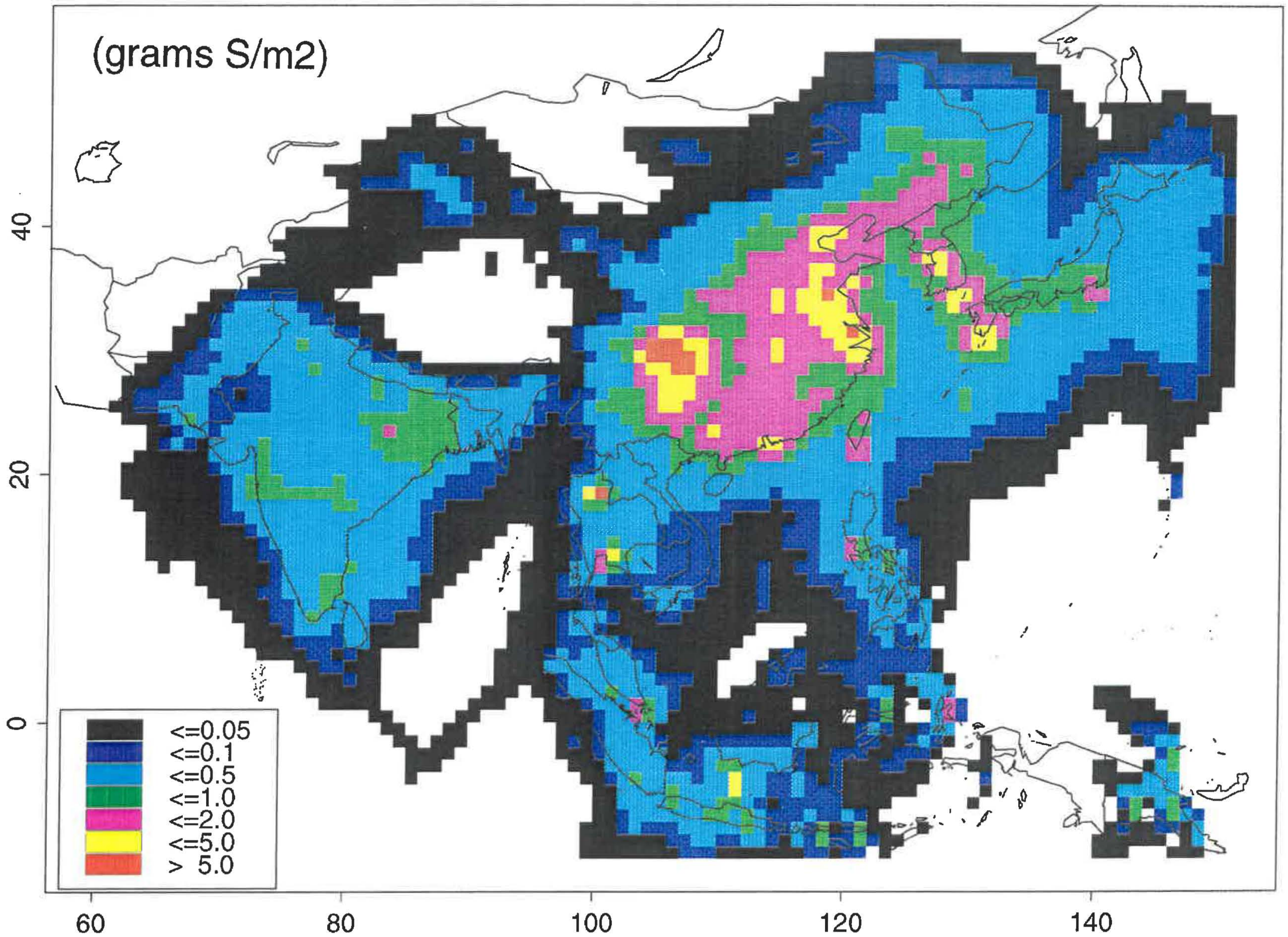

Figure 5.9 Calculated annual sulfur deposition for the base year 1990

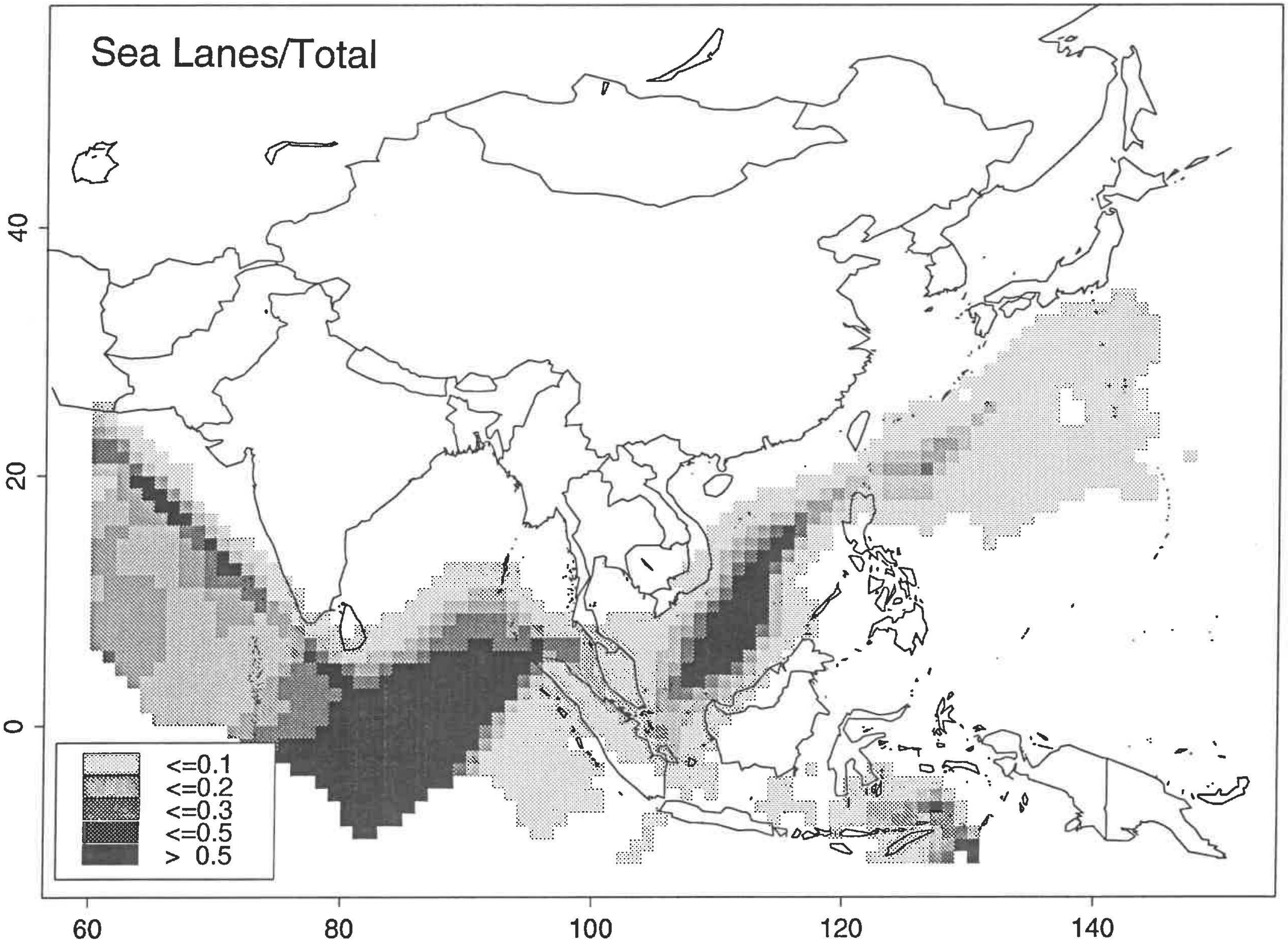

Figure 5.10 Fraction of sulfur deposition due to ships

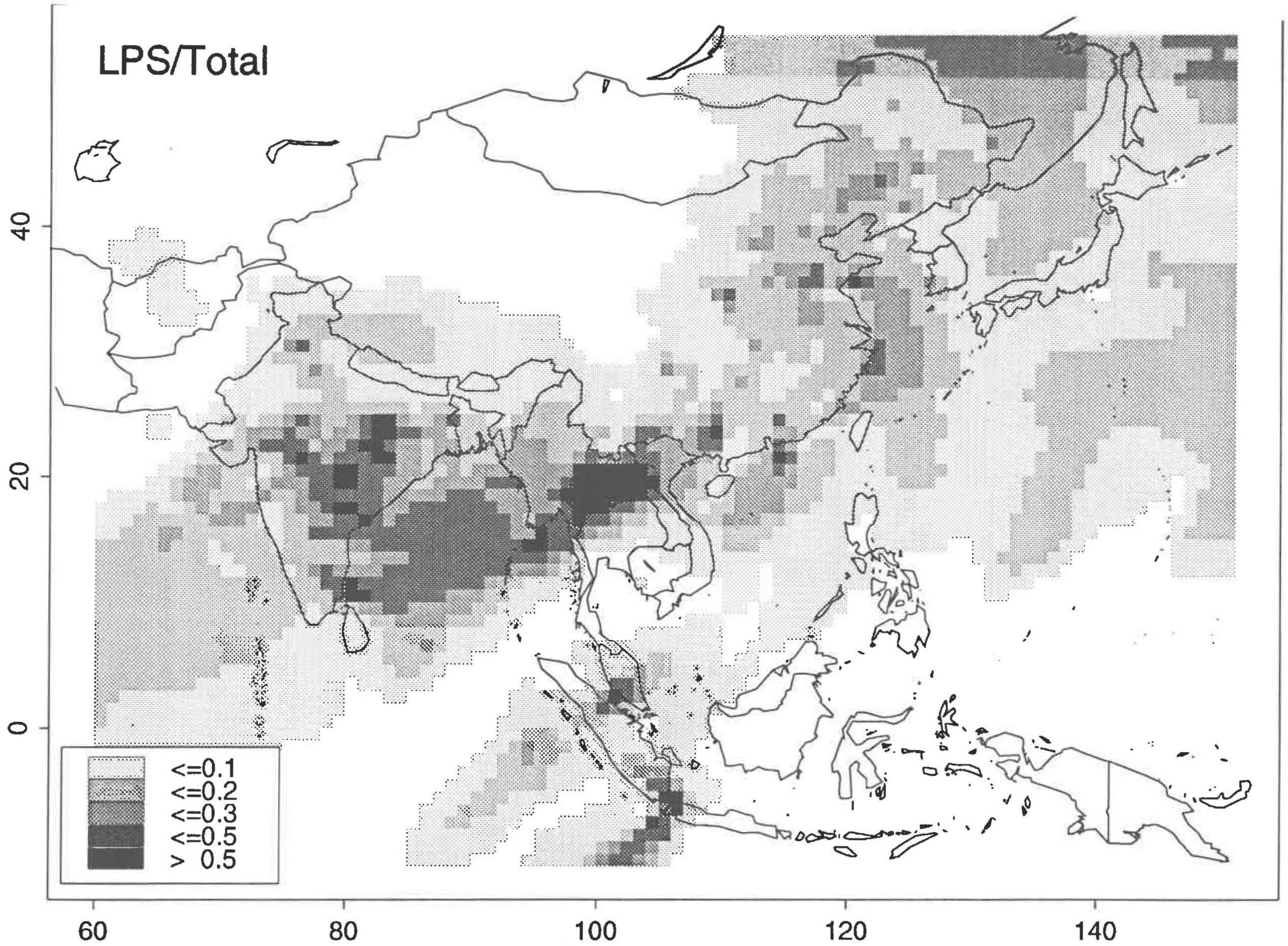

Figure 5.11 Fraction of sulfur deposition due to large point sources

to emissions from ships is the dominant source. Ships also contribute to the on-shore deposition throughout Malaysia, Indonesia, Vietnam and the Philippines.

Further insight into the sulfur deposition patterns are found by looking at the sulfur deposition arising from LPS separately. The fraction of sulfur deposition due to LPS is plotted in Figure 5.11 for the base year 1990. Most of the deposition from LPS occurs in eastern China, central India and northern Thailand. The maximum amount of deposition due to point sources is ~70%, where as on average LPS account for ~10% of the sulfur deposition. This is consistent with the LPS emissions comprising about 10% of the total anthropogenic sulfur emissions in Asia.

The deposition of sulfur due to dry and wet removal processes was also calculated. For the case of SO_2, the domain-integrated total deposition due to dry and wet removal mechanisms are of similar importance. In contrast, the wet deposition of sulfate dominates the sulfate deposition process. In most locations wet deposition of sulfate accounts for > 90% of the sulfate deposition. Wet removal processes account for 60% of the total sulfate deposition.

The deposition patterns in Asia have a strong seasonal variation. The seasonal variation is due to a combination of factors which include: seasonality of wind and precipitation fields; higher emissions due to domestic heating in the winter months in the northern parts of Asia; and changes in the dry deposition velocities, chemical reaction rates and wet removal rates with latitude and season. These features can be seen in the calculated deposition amounts for the months of December, January and February (DJF) contrasted with that for June, July and August (JJA) as shown in Figure 5.12. Also shown for reference are the precipitation amounts for these months. DJF represents dry months in India and most of China, but captures the winter monsoons in Indonesia and the heavy precipitation over the Japan Sea. In contrast, JJA captures the monsoon rains in the Indian sub-continent, and the rainy season in east Asia. The deposition patterns follow closely these seasonal changes in precipitation. This is shown in the deposition patterns in India, Indonesia, and east Asia. Over 30% of the total wet deposition over the Japan Sea and over Indonesia occurs during winter, while JJA deposition accounts for more that 30% of the total wet deposition in Southeast Asia and much of the India sub-continent.

The deposition from volcanoes was also calculated. Shown in Figure 5.13 is the fraction of total sulfur deposition due to volcanoes. Sulfur deposition from this natural source contributes significantly to sulfur deposition in Japan, Indonesia and the Philippines. Volcanoes account for ~30% of the total deposition in Japan, ~50% in Indonesia, and ~20% in the Philippines.

5.5.2 Source-receptor relationships

The ATMOS model calculates the deposition from each source directly and this information can be used to analyze a variety of policy-related questions. For example, the deposition from a specific LPS, region, or country can be viewed separately. The contribution of sulfur deposition from volcanoes and ships previously presented illustrate this capability. This information can also be used to identify which sources contribute to the deposition at a specified receptor. For example, the sources contributing to the deposition at Guiyang, China are listed in Table 5.2. Shown is a list of every source (area as well as LPS) which

Winter (DJF) Wet Sulfur Deposition (grams S/m2)

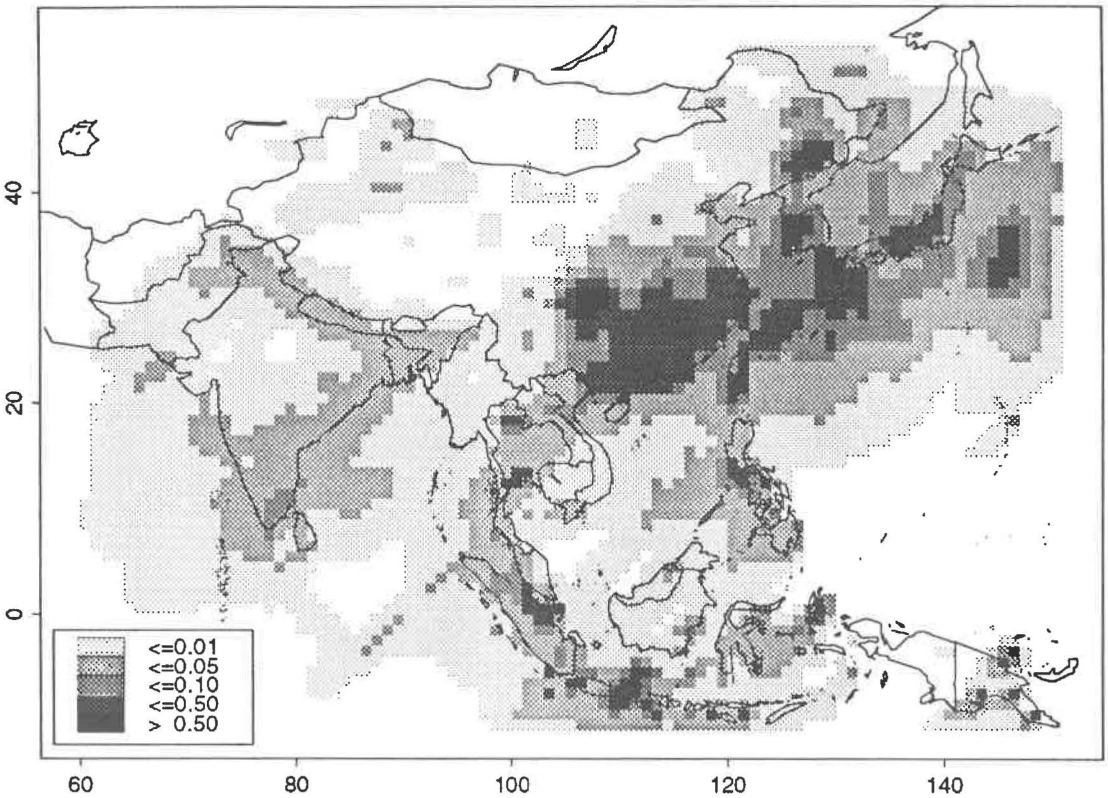

Winter (DJF) Precipitation (mm)

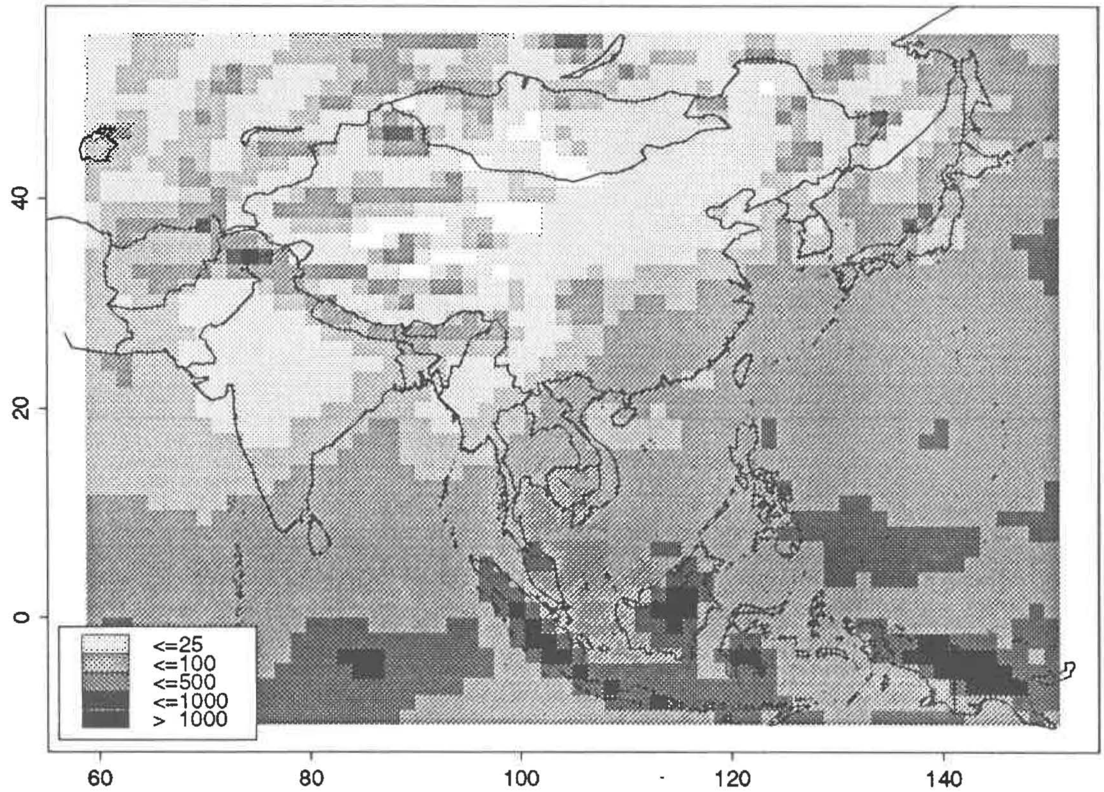

Figure 5.12a Calculated sulfur wet deposition during the months December, January, and February (DJF). The total precipitation amounts during these months are also presented.

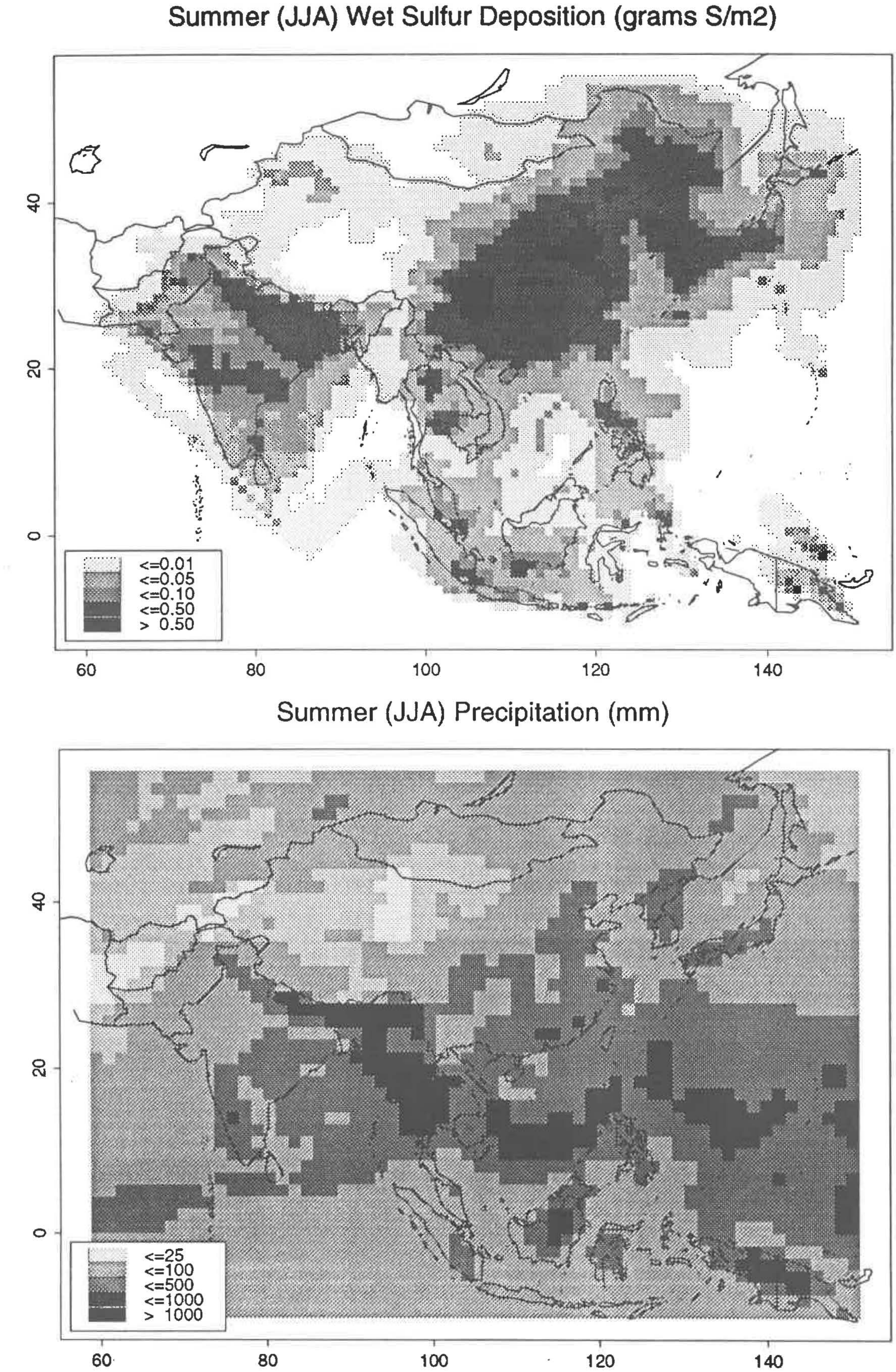

Figure 5.12b Calculated sulfur wet deposition during the months June, July, and August (JJA). The total precipitation amounts during these months are also presented.

contributes to the deposition at the selected receptor grid. The actual deposition attributed to each source is also presented.

This information can be aggregated to provide source-receptor information at a country-to-country or region-to-region level. (Please note that the source-receptor information presented is based on only one year of meteorology and must be considered preliminary.) The country-to-country source-receptor relationship calculated by the ATMOS model is presented in Table 5.3.a. The columns represent where the sulfur emitted from a specific country is deposited; while the rows represent where the deposition to a specified country comes from. For example, in the column CHINA, of the 7.22 Tg-S deposited in the region from China sources, 6 Tg-S are deposited on China, 1.03 Tg-S on the region's oceans, and the remaining 0.22 Tg-S is deposited on other countries of the region. The sources contributing to sulfur deposition for Japan can be read along the row indicated by JAPAN. In total, ~0.4 Tg-S are deposited in Japan in 1990. As shown, 38% of this deposition is due to anthropogenic emissions from Japan, ~10% is due to China's emissions, ~7% from S. Korea, and ~45% from volcanic sources.

Table 5.3.b demonstrates how this data can be interpreted to quantify the impact of a specific country's deposition on the region. For example, 83% and 14% of China's emissions which are deposited in the study region fall on China and the region's oceans, respectively. The remaining 3% falls on other nations (i.e. 0.8% on N. Korea and 0.5% on Japan). Column three presents the fraction of the receptor country's total deposition resulting from China. For example, 96% of the sulfur deposited in China is from Chinese sources while 35% and 22% of the sulfur deposited in N. Korea and Vietnam, respectively, is due to Chinese emissions. Table 5.4 provides an interesting perspective on the region's deposition. Although 97% of China's emissions deposited in the region fall either within China or on the region's oceans, the remaining 3% can account for significant percentages of the neighboring countries' total deposition.

The region-to-region deposition figures for China are presented in Table 5.4. This table summarizes the source-receptor relationships for the regions within China and accounts for all deposition in China resulting from China's emissions. The region definitions are defined in Chapter 3. Take the province of Guizhou for example. The annual deposition of sulfur to this region is ~0.29 Tg-S. Approximately 39% of this deposition arises from emissions in this province. However emissions from the Sichuan Basin (SICHUAN), Chongqing, Yunnan, and Guiyang account for 7%, 5%, 17%, and 19%, respectively, of the sulfur deposition in Guizhou.

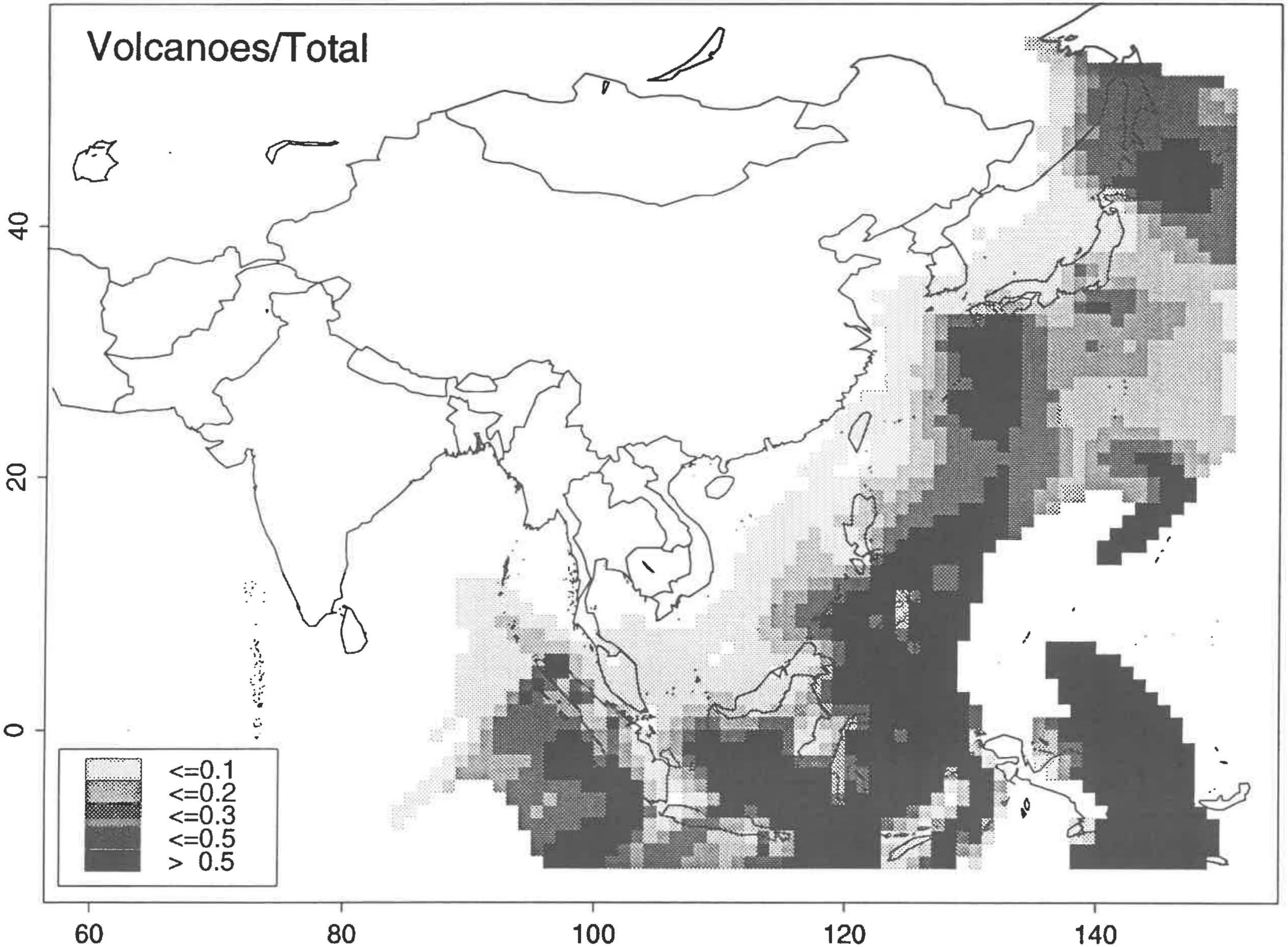

Figure 5.13 Fraction of total sulfur deposition due to volcanoes

Table 5.2 Identification of Sources Contributions to Sulfur Deposition at Guiyang, China (106° E, 26°N). Region definition and LPS information is presented in Chapter 3.

	Region	LPS Identification #	mg-S/m^2-yr
Area Sources:			
CHINA:	HEHE		3
	HUBE		7
	HUNA		13
	GUAH		2
	GUAX		119
	SICH		86
	CHON		83
	GUIZ		703
	GUIY		1320
	YUNN		216
INDIA	BIHA		1
VIETNAM	NORT		3
LPS Sources:			
CHINA:	CHON	4	38
	GUAX	11	8
	GUIZ	16	385
	SICH	114	28
	YUNN	126	29
THAILAND:	NHIG	252	2
TOTAL			**3046**

Table 5.3.a Country-to-country source-receptor matrix. The columns represent the source country while the rows represent the receptor country. Shown is the total annual sulfur deposition expressed in tonnes-S/yr.

SOURCE/ RECEPTOR	BANGLADESH	BHUTAN	BRUNEI	MYANMAR	CAMBODIA	CHINA	HONG KONG	INDIA	INDONESIA
OCEAN	3.47E+03	1.14E+00	2.11E+03	6.67E+02	1.09E+03	1.03E+06	1.37E+04	1.96E+05	9.47E+04
BANGLADESH	1.77E+04	1.27E+00	0.00E+00	6.80E+01	8.83E-04	2.68E+01	0.00E+00	1.64E+04	1.19E-05
BHUTAN	3.83E+02	1.63E+02	0.00E+00	6.66E-01	5.11E-09	4.55E+00	0.00E+00	8.14E+03	0.00E+00
BRUNEI	0.00E+00	0.00E+00	9.37E+01	3.04E-11	4.18E-09	1.01E-03	1.14E-05	0.00E+00	3.43E+00
MYANMAR	1.44E+03	3.38E+00	1.40E-02	4.41E+03	2.21E+01	4.70E+03	4.88E-01	1.09E+04	1.54E+00
CAMBODIA	1.33E-01	7.14E-06	3.05E-01	4.10E+00	5.37E+03	4.64E+02	4.72E+01	4.41E+00	3.17E+00
CHINA	2.00E+03	3.33E+02	5.36E-05	8.55E+02	6.99E+00	5.99E+06	2.83E+04	3.93E+04	7.29E-03
HONG KONG	3.86E+00	1.40E-03	3.50E-06	1.11E+00	2.17E-01	5.78E+03	9.63E+03	2.83E+01	4.01E-04
INDIA	1.58E+04	7.14E+01	0.00E+00	1.64E+02	1.57E-04	3.43E+02	0.00E+00	1.06E+06	4.61E-03
INDONESIA	6.00E-05	0.00E+00	3.50E+01	6.13E-03	1.36E+00	1.96E-02	1.59E-04	1.78E-04	1.11E+05
JAPAN	2.97E+00	1.95E-02	2.03E-14	1.59E+00	4.12E-04	3.88E+04	3.31E+01	3.62E+01	2.25E-14
N. KOREA	8.04E-01	3.70E-02	3.79E-15	6.09E-01	2.92E-06	5.96E+04	1.90E+00	7.19E+00	0.00E+00
S. KOREA	3.43E+00	2.69E-02	8.52E-14	1.04E+00	3.92E-05	2.80E+04	2.35E+00	1.80E+01	7.04E-15
LAOS	1.13E+02	1.43E-01	4.47E-03	1.08E+02	4.04E+02	6.57E+03	1.27E+02	1.16E+03	9.94E-02
MALAYSIA	1.04E-05	0.00E+00	3.18E+02	1.96E-03	8.41E-01	1.23E-01	4.24E-04	6.41E-05	2.66E+03
MONGOLIA	8.69E-04	7.30E-05	0.00E+00	7.32E-05	0.00E+00	1.38E+04	8.04E-06	1.77E-01	0.00E+00
NEPAL	3.22E+02	1.78E+00	0.00E+00	1.89E-01	2.71E-08	2.34E+01	0.00E+00	4.06E+04	0.00E+00
PAKISTAN	0.00E+00	3.46E-09	0.00E+00	0.00E+00	0.00E+00	9.77E+01	0.00E+00	1.73E+04	0.00E+00
PHILIPPINES	7.53E-02	6.38E-06	7.42E+00	1.53E-01	1.10E+00	4.24E+02	2.06E+01	3.13E+00	3.40E+01
SEA LANES	6.84E+00	8.38E-03	8.25E+00	2.18E+00	1.34E+01	9.01E+03	2.38E+02	4.31E+03	3.40E+04
SINGAPORE	0.00E+00	0.00E+00	2.66E-02	4.59E-10	6.98E-03	3.56E-07	0.00E+00	7.30E-10	1.55E+02
SRI LANKA	6.72E+00	4.99E-07	0.00E+00	7.76E-01	1.64E-03	8.78E-05	0.00E+00	2.97E+03	5.04E-04
TAIWAN	1.99E+00	4.93E-03	5.58E-05	6.89E-01	3.07E-01	3.98E+03	1.77E+02	1.46E+01	2.49E-05
THAILAND	6.19E+01	1.31E-02	2.27E-01	3.79E+02	7.37E+02	2.83E+03	5.56E+01	6.99E+02	1.61E+02
VIETNAM	1.80E+02	1.59E-01	1.30E+00	1.07E+02	1.70E+03	2.87E+04	4.21E+02	2.33E+03	7.92E+00
TOTAL DEPOSITION	4.15E+04	5.75E+02	2.57E+03	6.77E+03	9.35E+03	7.22E+06	5.28E+04	1.40E+06	2.43E+05

Table 5.3.a (Cont.)

SOURCE/ RECEPTOR	JAPAN	N. KOREA	S. KOREA	LAOS	MALAYSIA	MONGOLIA	NEPAL	PAKISTAN	PHILIPPINES
OCEAN	1.36E+05	3.49E+04	2.39E+05	1.24E+02	2.19E+04	1.48E+03	1.98E+02	1.73E+04	6.93E+04
BANGLADESH	0.00E+00	0.00E+00	0.00E+00	1.11E-04	2.81E-04	0.00E+00	1.77E+02	2.30E+02	2.96E-10
BHUTAN	0.00E+00	0.00E+00	0.00E+00	7.93E-05	4.76E-05	2.53E-08	4.37E+02	8.65E+01	5.09E-11
BRUNEI	6.92E-07	0.00E+00	1.33E-06	1.50E-06	5.66E+02	0.00E+00	0.00E+00	0.00E+00	2.35E+00
MYANMAR	3.16E-05	0.00E+00	0.00E+00	3.69E+00	1.45E+01	8.48E-03	3.01E+02	2.80E+02	1.19E-02
CAMBODIA	3.13E-03	2.89E-03	6.04E-02	8.29E+01	2.12E+01	0.00E+00	7.45E-02	6.53E-02	1.34E+01
CHINA	1.96E+02	2.16E+04	4.63E+03	9.66E+01	6.96E+01	5.19E+03	1.23E+04	3.43E+03	6.36E+01
HONG KONG	1.60E-01	7.44E-02	1.32E+00	4.17E-01	5.11E-02	3.97E-04	6.24E-01	4.54E-01	2.78E+00
INDIA	2.97E-09	0.00E+00	0.00E+00	2.95E-02	4.12E-02	7.94E-04	5.26E+03	1.88E+04	2.17E-08
INDONESIA	9.23E-07	0.00E+00	1.91E-08	1.35E-02	3.25E+03	0.00E+00	0.00E+00	0.00E+00	7.76E+01
JAPAN	1.49E+05	2.50E+03	2.88E+04	3.25E-01	8.57E-02	7.63E+01	3.12E-01	1.98E-01	1.57E-01
N. KOREA	8.55E+01	4.93E+04	6.28E+04	5.20E-02	1.79E-02	9.69E+01	1.23E-01	6.72E-02	1.75E-02
S. KOREA	1.16E+03	2.56E+03	1.75E+05	5.99E-02	2.13E-02	4.03E+01	1.14E-01	9.71E-02	5.70E-01
LAOS	3.13E-03	3.97E-03	6.70E-02	5.32E+02	3.47E+01	4.44E-06	3.37E+01	2.22E+01	5.67E+00
MALAYSIA	9.45E-04	0.00E+00	1.08E-05	7.79E-03	4.67E+04	0.00E+00	0.00E+00	0.00E+00	1.53E+02
MONGOLIA	4.44E-02	3.44E+00	2.95E+00	2.34E-06	5.05E-07	1.51E+04	5.45E-03	2.75E-01	0.00E+00
NEPAL	0.00E+00	0.00E+00	0.00E+00	3.62E-08	3.05E-14	0.00E+00	2.21E+04	1.04E+03	0.00E+00
PAKISTAN	0.00E+00	0.00E+00	0.00E+00	0.00E+00	0.00E+00	0.00E+00	3.97E+00	1.16E+05	0.00E+00
PHILIPPINES	9.05E+00	3.89E-01	1.98E+01	1.87E-01	2.69E+01	8.14E-04	5.45E-02	5.61E-03	8.47E+04
SEA LANES	4.21E+03	1.25E+02	2.41E+03	1.63E+00	6.01E+03	5.90E+00	1.60E+00	4.26E+02	2.67E+03
SINGAPORE	0.00E+00	0.00E+00	0.00E+00	6.39E-07	2.34E+02	0.00E+00	0.00E+00	0.00E+00	9.21E-03
SRI LANKA	0.00E+00	0.00E+00	0.00E+00	5.25E-06	5.05E-04	0.00E+00	5.70E-01	6.63E-01	0.00E+00
TAIWAN	1.79E+01	2.86E+00	2.00E+01	3.49E-01	3.62E-02	5.18E-02	3.55E-01	1.60E-01	3.43E+01
THAILAND	4.91E-04	6.14E-04	1.05E-02	1.05E+02	7.89E+03	0.00E+00	1.46E+01	1.15E+01	2.57E+00
VIETNAM	2.35E-02	2.51E-02	4.95E-01	4.07E+02	1.10E+02	4.02E-04	4.32E+01	4.39E+01	5.69E+01
TOTAL DEPOSITION	2.91E+05	1.11E+05	5.13E+05	1.35E+03	8.68E+04	2.20E+04	4.09E+04	1.58E+05	1.57E+05

Table 5.3.a (Cont.)

SOURCE/ RECEPTOR	SEA LANES	SINGAPORE	SRI LANKA	TAIWAN	THAILAND	VIETNAM	VOLC	TOTAL DEPOSITED
OCEAN	5.69E+04	1.72E+04	7.19E+03	1.16E+05	3.05E+04	9.03E+03	7.04E+05	2.80E+06
BANGLADESH	7.45E-01	0.00E+00	4.34E-03	0.00E+00	2.18E+00	6.81E-04	6.87E-05	3.46E+04
BHUTAN	1.16E-02	0.00E+00	5.57E-18	0.00E+00	8.95E-02	6.53E-04	0.00E+00	9.21E+03
BRUNEI	1.61E+00	4.43E+00	0.00E+00	1.45E-04	1.49E-02	4.67E-03	8.76E+00	6.80E+02
MYANMAR	6.01E+00	3.24E-02	2.67E-03	6.51E-02	1.49E+04	6.93E+01	4.28E+00	3.71E+04
CAMBODIA	5.88E+01	2.91E+00	0.00E+00	2.91E+00	1.10E+04	4.02E+03	8.68E+00	2.11E+04
CHINA	1.29E+02	0.00E+00	8.77E-09	7.07E+03	1.62E+04	5.37E+03	1.58E+03	6.14E+06
HONG KONG	5.14E+00	0.00E+00	0.00E+00	1.45E+02	1.01E+02	9.41E+00	1.24E+01	1.57E+04
INDIA	9.10E+02	0.00E+00	5.49E+02	0.00E+00	2.17E+01	2.14E-01	6.26E-02	1.10E+06
INDONESIA	1.82E+03	8.37E+03	0.00E+00	1.77E-05	7.99E+01	8.84E+00	1.56E+05	2.81E+05
JAPAN	9.72E+02	0.00E+00	0.00E+00	1.14E+02	6.28E+01	1.10E+01	1.85E+05	4.05E+05
N. KOREA	8.00E-01	0.00E+00	0.00E+00	2.15E+00	1.94E+01	2.53E+00	1.86E+02	1.72E+05
S. KOREA	1.16E+01	0.00E+00	0.00E+00	1.62E+01	2.32E+01	3.53E+00	4.42E+03	2.11E+05
LAOS	5.32E+00	1.29E-04	0.00E+00	5.85E+00	4.67E+04	8.22E+02	1.06E+00	5.66E+04
MALAYSIA	2.94E+03	1.86E+04	0.00E+00	3.28E-03	4.98E+01	1.74E+01	3.11E+03	7.45E+04
MONGOLIA	1.84E-08	0.00E+00	0.00E+00	0.00E+00	3.08E-03	1.00E-04	4.90E-02	2.89E+04
NEPAL	8.94E-02	0.00E+00	1.92E-20	0.00E+00	2.31E-05	1.11E-07	0.00E+00	6.41E+04
PAKISTAN	1.76E+01	0.00E+00	0.00E+00	0.00E+00	0.00E+00	0.00E+00	0.00E+00	1.33E+05
PHILIPPINES	2.39E+02	3.35E-01	0.00E+00	6.92E+02	7.77E+00	4.35E+00	4.08E+04	1.27E+05
SEA LANES	2.75E+04	2.00E+04	4.03E+02	7.41E+03	5.44E+02	8.02E+01	4.18E+04	1.61E+05
SINGAPORE	4.69E+02	1.88E+04	0.00E+00	0.00E+00	3.88E-02	1.24E-01	1.89E+02	1.98E+04
SRI LANKA	1.76E+02	0.00E+00	8.15E+03	0.00E+00	4.96E-02	3.35E-04	2.34E-04	1.13E+04
TAIWAN	1.05E+02	0.00E+00	0.00E+00	5.42E+04	4.33E+01	7.03E+00	3.20E+02	5.89E+04
THAILAND	3.64E+02	2.60E+01	0.00E+00	3.65E+00	2.84E+05	6.48E+02	1.87E+02	2.98E+05
VIETNAM	2.99E+02	3.91E+01	0.00E+00	3.93E+01	1.38E+04	2.57E+04	1.88E+01	7.40E+04
TOTAL DEPOSITION	9.29E+04	8.30E+04	1.63E+04	1.86E+05	4.18E+05	4.58E+04	1.14E+06	1.23E+07

Table 5.3.b China's contribution to sulfur deposition in the region, expressed both as a percentage of China's total deposition in the region and as a percentage of the receptor- country's total deposition.

COUNTRY-TO-COUNTRY SOURCE-RECEPTOR RELATIONSHIP

RECEPTOR	% OF CHINA'S DEPOSITION IN ASIA	% OF RECEPTOR'S TOTAL DEPOSITION
China	83	96
Oceans	14	36
North Korea	0.8	35
South Korea	0.4	13
Japan	0.5	10
Vietnam	0.4	22

5.5.3 Surface concentrations

Calculated annual-averaged surface concentrations of SO_2 and sulfate are presented in Figure 5.14. The distribution of surface concentrations follow closely the emission distribution and density. The SO_2 concentrations show more horizontal variability reflecting the fact that it is the primary pollutant. Sulfate shows a smoother and broader distribution reflecting the fact that it is a secondary product. Elevated SO_2 values are found throughout Asia. Direct environmental impacts to sensitive forest and crops can occur at levels of 20 to 30 $\mu g/m^3$. Vast areas of China and Korea exceed these levels.

Table 5.4 Region-to-region source-receptor matrix for China. The columns represent the source region while the rows represent the receptor region. Shown is the total annual sulfur deposition expressed in tonnes-S/yr.

SOURCE/ RECEPTOR	NE PLAIN	SHENYANG	HEBEI	BEIJING	TIANJIN	SHANDONG	SHANXI
NE PLAIN	4.58E+05	2.21E+04	5.02E+04	7.34E+03	8.02E+03	1.19E+04	4.63E+03
SHENYANG	8.75E+03	2.24E+03	9.71E+02	1.43E+02	1.88E+02	3.68E+02	8.65E+01
HEBEI	5.69E+03	1.21E+02	4.33E+05	3.42E+04	2.66E+04	3.47E+04	4.00E+04
BEIJING	7.98E+01	1.77E+00	7.09E+03	5.53E+03	1.29E+03	7.64E+02	1.22E+03
TIANJIN	2.36E+02	3.45E+00	1.18E+04	7.39E+03	8.01E+03	1.47E+03	9.09E+02
SHANDONG	6.59E+03	1.03E+02	6.36E+04	3.03E+03	2.76E+03	1.26E+05	6.94E+03
SHANXI	1.19E+02	1.33E+00	3.44E+04	4.02E+02	2.34E+02	2.19E+03	5.72E+04
TAIYUN	1.18E+01	9.60E-02	1.54E+03	3.52E+01	2.54E+01	1.65E+02	4.63E+03
SHAANXI-GANSU	3.07E+01	1.76E-01	8.52E+03	8.64E+01	7.50E+01	4.77E+02	1.20E+04
INNER MONGOLIA	5.84E+04	1.10E+03	2.85E+04	3.55E+03	1.81E+03	1.05E+03	1.81E+04
HUBEI	9.74E+01	3.07E+00	2.21E+04	7.78E+01	6.19E+01	1.67E+03	1.44E+03
WUHAN	1.07E+01	3.28E-01	2.71E+03	4.67E+00	4.27E+00	2.47E+02	6.78E+01
HUNAN	1.63E+02	7.35E+00	1.00E+04	4.61E+01	3.56E+01	1.28E+03	5.33E+02
JIANGXI	2.34E+02	5.44E+00	2.51E+04	2.49E+01	2.10E+01	2.25E+03	3.68E+02
JIANGSU	8.31E+02	2.49E+01	6.65E+04	4.12E+02	3.24E+02	1.22E+04	1.45E+03
SHANGHAI	1.20E+02	2.56E+00	1.14E+03	2.80E+01	2.05E+01	4.30E+02	6.91E+01
ZHEJIANG	4.01E+02	1.19E+01	7.50E+03	6.49E+01	5.67E+01	1.67E+03	4.02E+02
FUJIAN	1.79E+02	4.82E+00	3.95E+03	8.03E+00	9.14E+00	5.23E+02	1.26E+02
GUANGDONG	2.74E+01	8.53E-01	1.80E+03	3.09E+00	3.65E+00	2.49E+02	6.51E+01
GUANGZHOU	1.52E+00	3.78E-02	1.32E+02	2.50E-01	3.24E-01	1.92E+01	3.13E+00
GUANGXI	1.74E+01	8.33E-01	7.40E+02	5.99E+00	2.96E+00	9.69E+01	6.72E+01
SICHUAN	2.01E+01	3.07E-01	1.94E+03	2.96E+01	2.14E+01	1.21E+02	4.25E+02
CHONGQING	5.73E-01	6.25E-03	4.55E+01	5.21E-01	5.10E-01	3.62E+00	8.10E+00
GUIZHOU	1.12E+01	6.06E-01	8.32E+02	7.21E+00	6.03E+00	8.79E+01	6.74E+01
GUIYANG	1.22E-01	7.51E-03	4.30E+01	1.14E-01	5.76E-02	6.14E+00	3.08E+00
YUNNAN	6.84E-02	1.70E-04	4.07E+01	1.61E-01	2.51E-02	6.61E+00	3.21E+00
WEST	1.03E-01	0.00E+00	5.91E+00	1.74E-02	1.83E-02	3.17E-01	1.90E+01
TOTAL DEPOSITION	5.40E+05	2.57E+04	7.84E+05	6.24E+04	4.96E+04	2.00E+05	1.51E+05

Table 5.4 (cont.)

SOURCE/ RECEPTOR	TAIYUN	SHAANXI-GANSU	INNER MONGOLIA	HUBEI	WUHAN	HUNAN	JIANGXI
NE PLAIN	1.24E+03	1.75E+03	2.80E+04	1.12E+02	8.86E+01	2.79E+01	1.08E+02
SHENYANG	2.68E+01	3.25E+01	2.09E+02	1.95E+00	7.93E-01	3.79E-01	9.52E-01
HEBEI	1.78E+04	3.00E+04	2.05E+04	2.17E+04	2.40E+04	5.47E+03	1.11E+04
BEIJING	4.36E+02	2.23E+02	8.74E+02	5.86E+00	2.26E+00	5.91E-01	1.21E-01
TIANJIN	2.94E+02	1.72E+02	6.98E+02	6.44E+00	3.29E+00	8.06E-01	1.90E-01
SHANDONG	2.88E+03	2.16E+03	2.30E+03	1.06E+03	1.13E+03	3.18E+02	1.38E+02
SHANXI	1.80E+04	2.75E+04	4.27E+03	3.99E+02	1.07E+02	2.96E+01	1.03E+01
TAIYUN	3.72E+03	9.05E+02	2.13E+02	1.61E+01	4.69E+00	6.62E-01	2.38E-01
SHAANXI-GANSU	1.37E+03	1.25E+05	6.17E+03	6.25E+03	1.52E+02	4.26E+02	1.78E+01
INNER MONGOLIA	2.90E+03	1.87E+04	9.33E+04	3.91E+01	2.93E+00	2.28E+00	2.38E+00
HUBEI	3.21E+02	4.79E+03	2.36E+02	6.80E+04	4.04E+04	1.31E+04	3.40E+03
WUHAN	1.78E+01	1.07E+02	1.87E+01	5.63E+03	1.48E+04	1.17E+03	5.77E+02
HUNAN	1.41E+02	8.54E+02	9.33E+01	1.40E+04	8.71E+03	8.97E+04	8.79E+03
JIANGXI	8.35E+01	6.22E+02	1.01E+02	7.27E+03	9.64E+03	1.72E+04	7.33E+04
JIANGSU	4.14E+02	1.15E+03	3.76E+02	1.62E+03	2.65E+03	8.19E+02	1.55E+03
SHANGHAI	1.36E+01	6.34E+01	2.86E+01	7.46E+01	6.05E+01	3.85E+01	2.31E+02
ZHEJIANG	8.84E+01	6.89E+02	1.61E+02	1.31E+03	1.35E+03	1.12E+03	5.64E+03
FUJIAN	3.00E+01	3.08E+02	5.20E+01	6.21E+02	8.13E+02	1.13E+03	6.26E+03
GUANGDONG	2.01E+01	6.29E+01	1.29E+01	5.59E+02	7.74E+02	2.89E+03	3.63E+03
GUANGZHOU	1.37E+00	3.33E+00	7.00E-01	4.41E+01	5.65E+01	2.58E+02	3.74E+02
GUANGXI	1.99E+01	8.43E+01	1.07E+01	9.52E+02	5.05E+02	4.54E+03	7.06E+02
SICHUAN	5.43E+01	4.67E+03	2.38E+02	9.48E+03	2.45E+02	2.07E+03	6.43E+01
CHONGQING	1.03E+00	5.32E+01	3.66E+00	9.39E+01	5.94E+00	5.92E+01	4.25E+00
GUIZHOU	5.70E+00	1.90E+02	1.08E+01	1.47E+03	2.25E+02	3.20E+03	1.29E+02
GUIYANG	1.06E-01	9.08E+00	3.75E-01	8.53E+01	1.37E+01	1.58E+02	1.16E+01
YUNNAN	1.09E-01	2.84E+01	7.48E-01	8.75E+01	1.43E+01	1.86E+02	1.91E+01
WEST	7.90E-01	2.81E+03	1.01E+02	8.10E-01	2.89E-02	1.81E-01	3.01E-02
TOTAL DEPOSITION	4.99E+04	2.23E+05	1.58E+05	1.41E+05	1.06E+05	1.44E+05	1.16E+05

Table 5.4 (cont.)

SOURCE/ RECEPTOR	JIANGSU	SHANGHAI	ZHEJIANG	FUJIAN	GUANGDONG	GUANGZHOU	GUANGXI
NE PLAIN	3.93E+03	2.58E+02	1.72E+02	1.57E+01	1.86E+01	3.09E+00	4.97E+01
SHENYANG	8.96E+01	6.20E+00	9.54E-01	1.83E-01	1.72E-01	2.02E-02	5.80E-01
HEBEI	8.08E+04	6.47E+03	7.30E+03	3.95E+02	5.51E+02	2.25E+02	2.42E+03
BEIJING	2.07E+02	3.64E+00	8.88E-01	3.08E-03	5.48E-03	4.20E-05	1.70E-01
TIANJIN	3.40E+02	7.49E+00	1.40E+00	4.51E-03	6.27E-03	6.06E-04	2.88E-01
SHANDONG	1.42E+05	1.96E+03	3.10E+02	3.46E+00	3.01E+01	4.89E+00	1.24E+02
SHANXI	2.17E+03	3.34E+01	1.79E+01	4.00E-01	7.94E-01	5.59E-02	1.89E+01
TAIYUN	1.51E+02	1.54E+00	1.22E+00	6.78E-03	7.67E-03	2.04E-04	4.25E-01
SHAANXI-GANSU	5.40E+02	4.74E+00	6.68E+00	3.73E+00	2.81E+00	2.38E-01	2.35E+02
INNER MONGOLIA	3.88E+02	7.39E+00	3.34E+00	1.80E-01	7.18E-01	2.23E-01	4.44E+00
HUBEI	4.15E+03	1.69E+02	4.41E+02	1.09E+02	3.03E+02	9.66E+01	3.49E+03
WUHAN	8.33E+02	3.82E+01	1.01E+02	1.93E+01	5.70E+01	2.36E+01	3.62E+02
HUNAN	3.43E+03	2.57E+02	6.28E+02	1.05E+03	1.75E+04	4.57E+03	6.28E+04
JIANGXI	1.58E+04	2.10E+03	7.48E+03	1.29E+04	2.51E+04	1.44E+04	5.34E+03
JIANGSU	2.15E+05	2.78E+04	2.02E+04	7.22E+01	1.32E+02	6.17E+01	3.94E+02
SHANGHAI	8.96E+03	1.99E+04	6.58E+03	3.15E+01	2.13E+01	5.97E+00	4.30E+01
ZHEJIANG	2.13E+04	1.19E+04	6.74E+04	6.91E+03	1.45E+03	6.66E+02	1.34E+03
FUJIAN	5.88E+03	2.04E+03	8.06E+03	5.45E+04	1.65E+04	3.73E+03	1.29E+03
GUANGDONG	1.15E+03	2.20E+02	6.50E+02	6.57E+03	9.94E+04	3.46E+04	1.02E+04
GUANGZHOU	8.23E+01	1.31E+01	3.78E+01	3.20E+02	1.38E+04	1.15E+04	3.63E+02
GUANGXI	2.21E+02	1.74E+01	5.33E+01	3.03E+02	3.43E+04	2.21E+03	1.43E+05
SICHUAN	1.06E+02	7.17E-01	7.41E+00	9.54E+00	5.70E+01	7.20E+00	3.64E+03
CHONGQING	2.42E+00	5.20E-03	3.94E-01	3.15E-01	3.71E+00	5.19E-01	2.72E+02
GUIZHOU	5.55E+01	1.73E+00	2.85E+01	1.85E+01	4.72E+02	6.41E+01	2.90E+04
GUIYANG	2.74E+00	5.02E-03	3.48E+00	4.29E-01	1.77E+01	1.38E+00	1.53E+03
YUNNAN	7.70E+00	9.58E-02	1.89E+00	4.42E+00	1.22E+02	1.89E+01	3.53E+03
WEST	2.60E-01	1.04E-03	3.39E-03	4.17E-03	7.14E-03	5.67E-04	3.59E-01
TOTAL DEPOSITION	5.08E+05	7.32E+04	1.19E+05	8.32E+04	2.10E+05	7.22E+04	2.69E+05

Table 5.4 (cont.)

SOURCE/ RECEPTOR	SICHUAN	CHONGQING	GUIZHOU	GUIYANG	YUNNAN	WEST	TOTAL DEPOSITED
NE PLAIN	2.85E+02	1.06E+02	5.12E+01	2.22E+01	4.43E+01	3.67E+02	5.99E+05
SHENYANG	7.66E+00	4.11E+00	3.73E-01	7.64E-02	2.83E-01	4.50E+00	1.31E+04
HEBEI	4.59E+03	2.44E+03	2.69E+03	8.87E+02	1.55E+03	5.90E+02	8.16E+05
BEIJING	1.46E+01	9.49E+00	1.59E+00	1.38E-01	1.23E+00	1.24E+01	1.78E+04
TIANJIN	1.66E+01	1.24E+01	2.18E+00	1.71E-01	2.02E+00	1.09E+01	3.14E+04
SHANDONG	5.22E+02	2.85E+02	1.20E+02	2.67E+01	7.35E+01	1.09E+02	3.65E+05
SHANXI	8.12E+02	3.57E+02	1.33E+02	3.77E+01	5.53E+01	2.86E+02	1.49E+05
TAIYUN	5.51E+01	1.97E+01	4.66E+00	8.74E-01	1.44E+00	1.80E+01	1.15E+04
SHAANXI-GANSU	4.82E+04	9.66E+03	3.19E+03	8.07E+02	1.07E+03	7.49E+03	2.32E+05
INNER MONGOLIA	5.03E+02	7.90E+01	1.93E+01	3.21E+00	2.11E+01	2.60E+03	2.31E+05
HUBEI	1.23E+04	5.30E+03	1.00E+04	2.62E+03	3.87E+03	9.90E+01	1.99E+05
WUHAN	3.44E+02	1.35E+02	3.29E+02	1.18E+02	2.85E+02	5.10E+00	2.80E+04
HUNAN	1.27E+04	5.97E+03	3.12E+04	8.96E+03	1.70E+04	4.83E+01	3.00E+05
JIANGXI	1.81E+03	6.96E+02	1.79E+03	6.39E+02	2.20E+03	3.90E+01	2.27E+05
JIANGSU	7.25E+02	4.05E+02	2.30E+02	5.27E+01	2.80E+02	5.91E+01	3.56E+05
SHANGHAI	5.45E+01	2.76E+01	2.05E+01	5.66E+00	2.46E+01	5.15E+00	3.80E+04
ZHEJIANG	1.07E+03	4.53E+02	6.45E+02	1.94E+02	7.15E+02	3.17E+01	1.35E+05
FUJIAN	4.62E+02	2.84E+02	3.90E+02	1.15E+02	5.56E+02	1.52E+01	1.08E+05
GUANGDONG	2.56E+02	1.93E+02	6.37E+02	2.72E+02	7.43E+02	4.37E+00	1.65E+05
GUANGZHOU	1.58E+01	1.48E+01	4.37E+01	2.26E+01	5.58E+01	3.32E-01	2.72E+04
GUANGXI	2.18E+03	2.25E+03	1.62E+04	7.18E+03	1.89E+04	4.20E+00	2.35E+05
SICHUAN	6.68E+05	2.76E+05	6.43E+04	2.23E+04	6.25E+04	3.49E+03	1.12E+06
CHONGQING	1.85E+04	3.78E+04	4.76E+03	1.92E+03	2.88E+03	1.37E+01	6.64E+04
GUIZHOU	1.92E+04	1.53E+04	1.10E+05	5.39E+04	5.04E+04	1.79E+01	2.85E+05
GUIYANG	1.02E+03	1.10E+03	1.14E+04	1.46E+04	2.89E+03	6.76E-01	3.29E+04
YUNNAN	1.69E+04	1.98E+03	9.97E+03	3.80E+03	9.93E+04	4.73E+01	1.36E+05
WEST	4.97E+03	1.47E+01	2.60E+00	5.37E-01	4.31E+02	6.67E+04	7.51E+04
TOTAL DEPOSITION	8.16E+05	3.61E+05	2.68E+05	1.18E+05	2.66E+05	8.21E+04	6.00E+06

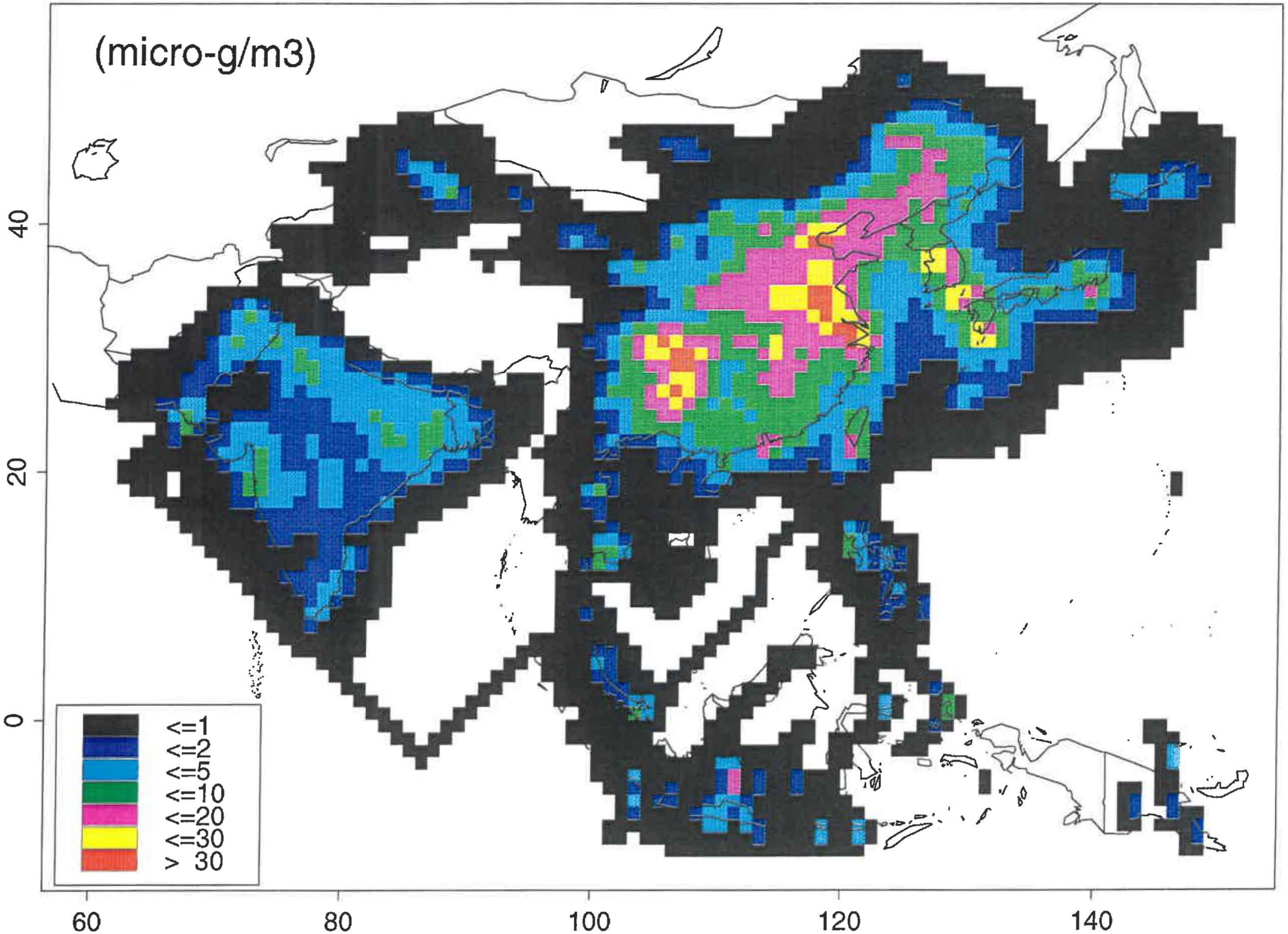

Figure 5.14a Calculated annual averaged sulfur dioxide surface concentrations for the base year 1990

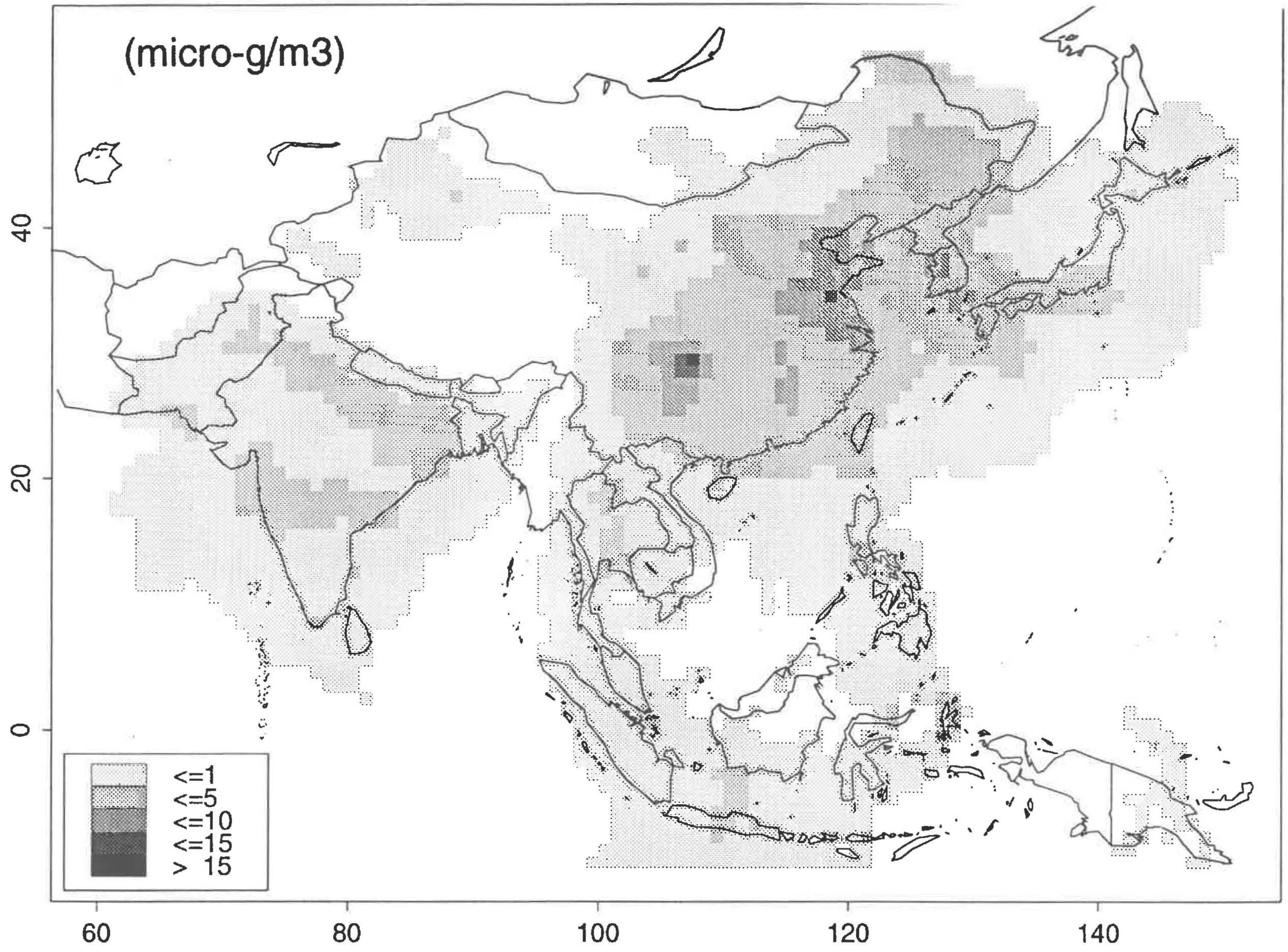

Figure 5.14b Calculated annual averaged sulfate surface concentrations for the base year 1990

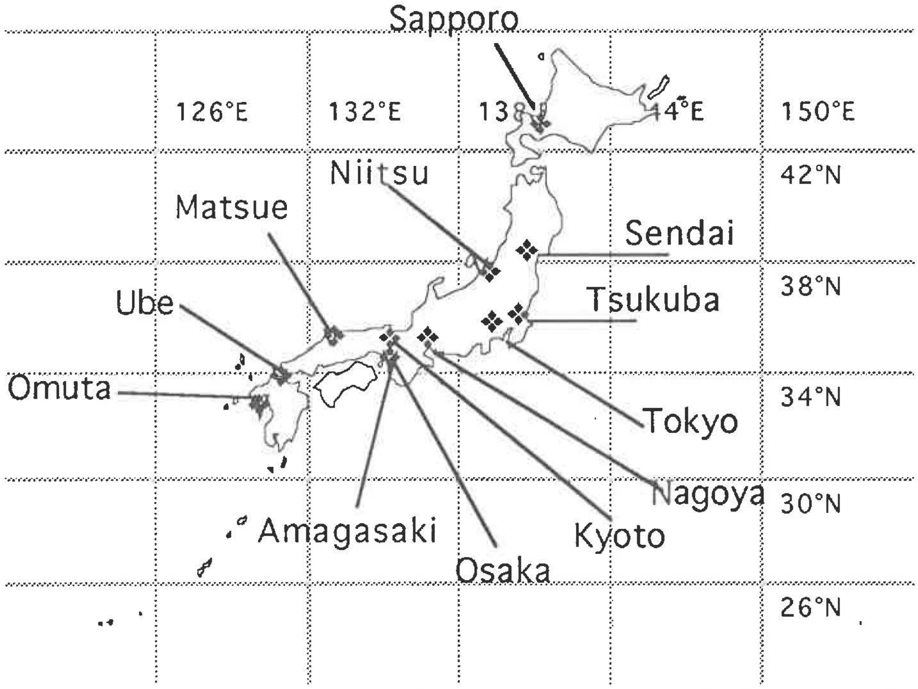

JAPANESE SULFATE DEPOSITION SAMPLING STATIONS

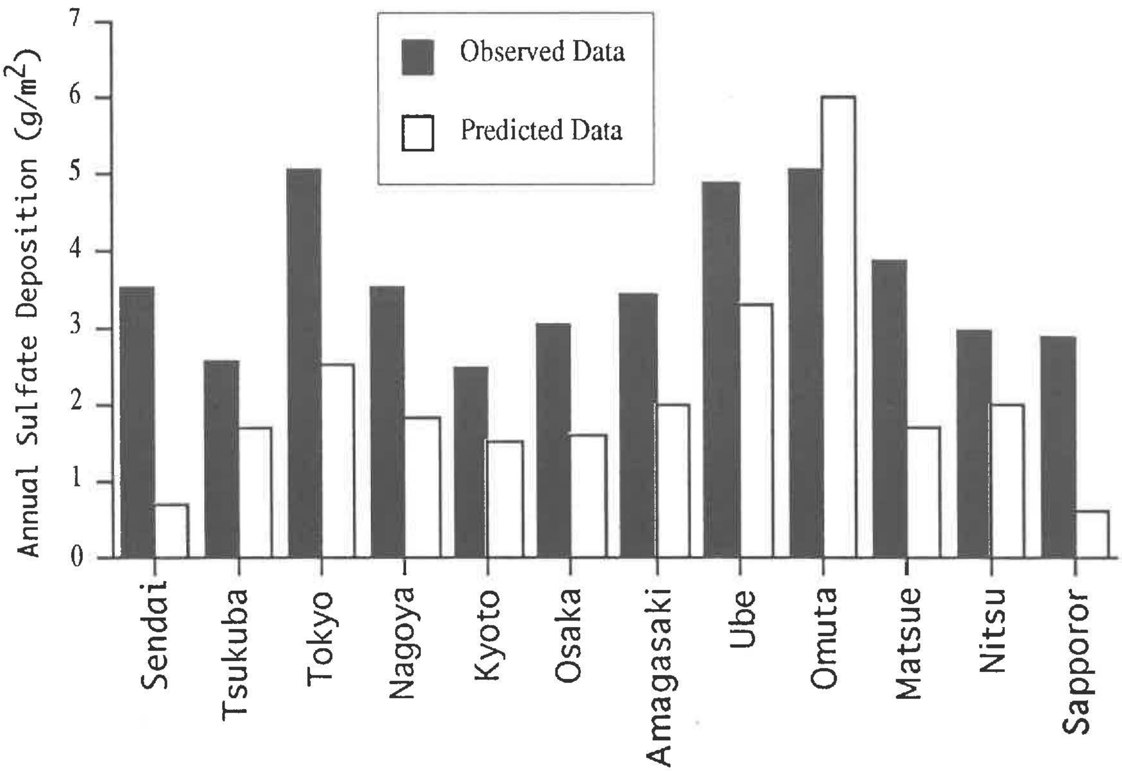

Figure 5.15 Observed and predicted sulfate deposition (wet + dry) amounts (g-sulfate/m^2-yr) in Japan

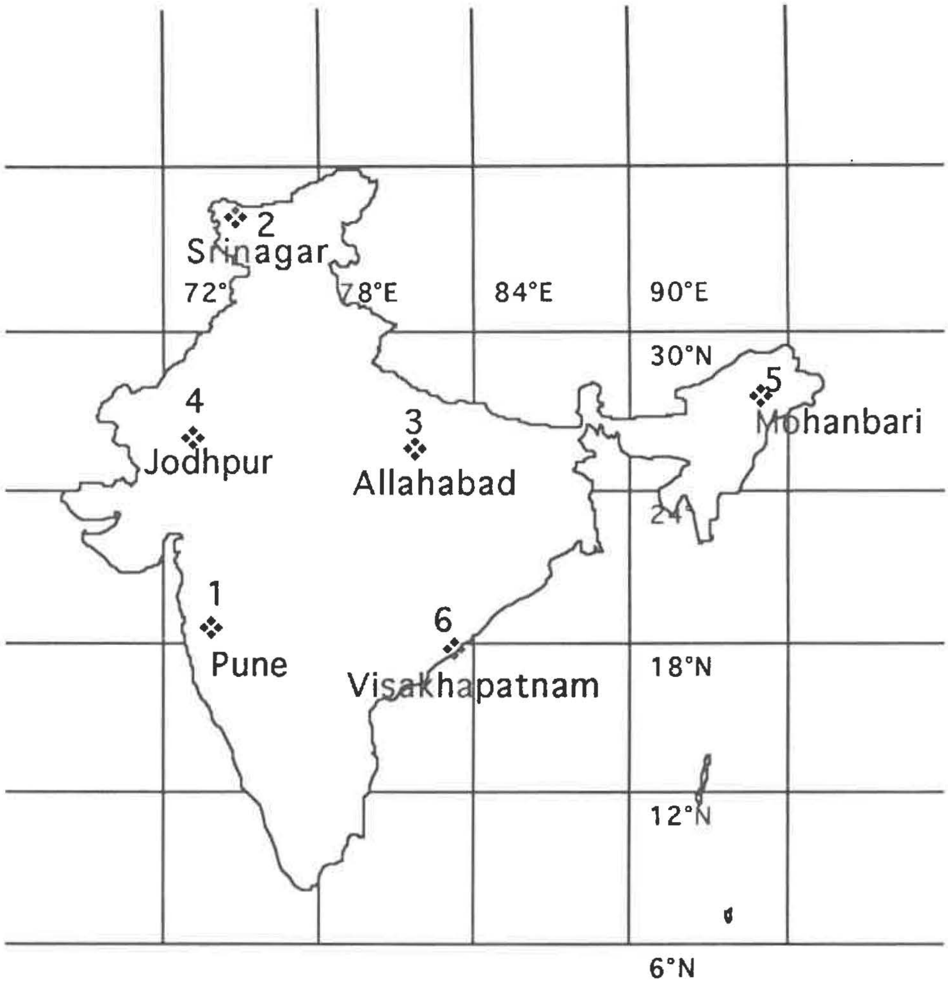

INDIAN SULFATE WET DEPOSITION MONITORING SITES

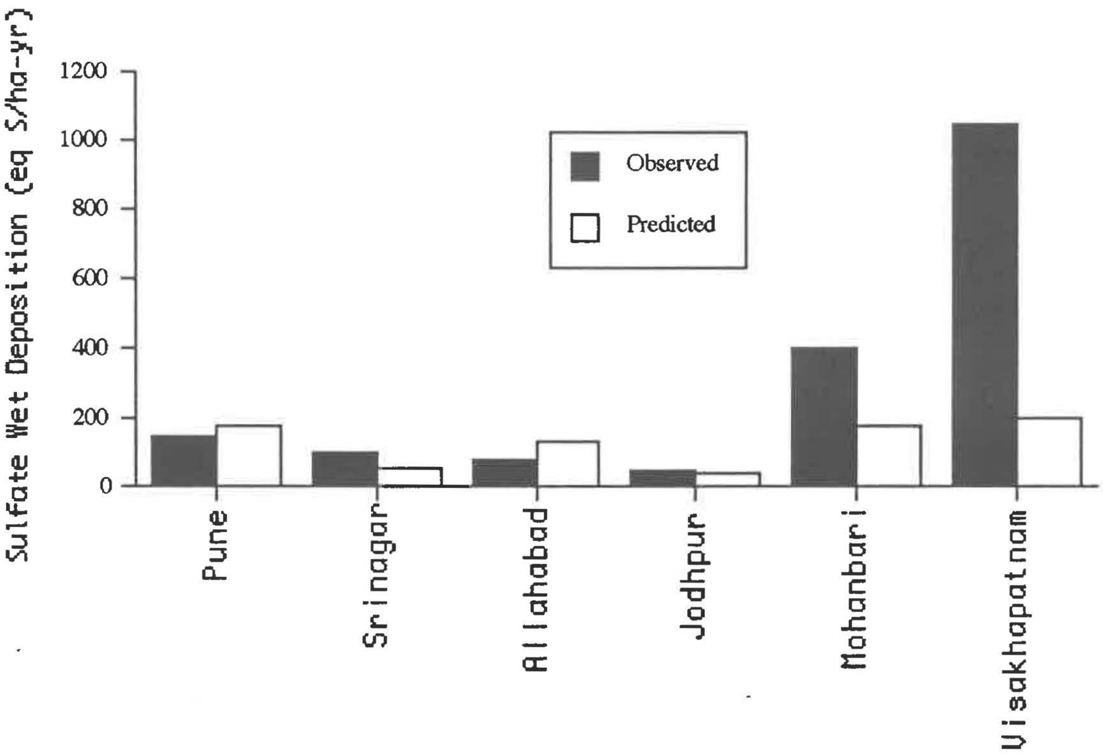

Figure 5.16 Observed and predicted sulfate wet deposition at BapMon sites in India

5.5.4 Preliminary model evaluation

Calculated annual sulfate deposition amounts can be compared with available observational data in Asia. While the data for direct comparison is limited, it is possible to undertake a preliminary comparison. The most comprehensive data set on acid deposition in Asia exists in Japan. Japan Environmental Protection Agency (Murano, 1994) has operated a country-wide network for many years. The observed annual sulfate total (wet + dry) deposition for the year 1989 is presented in Figure 5.15. As shown the values vary from 2 to 5.5 g-sulfate/m2/yr., with an average value of 3.8 g-sulfate/m2/yr. The predicted values are also shown for comparison. The calculated values are for the base year of 1990. The calculated values range from 0.6 to 6 g-sulfate/m^2/yr. The values also show a similar spatial distribution with high values in Kyushu, on the Japan Sea side of Honshu and the large metropolitan areas. The model tends to under predict the deposition. This is likely due in part to the fact that the monitoring sites are largely located in or near major urban areas, and in part to the model resolution of one-degree being too large to capture local influences.

The model calculated sulfate wet deposition is compared with available data from the WMO Background Air Pollution Monitoring Network (BAPMON) monitoring network (see Figure 5.16). This data has been summarized in Ayers and Hara (1994). Shown are data for India. In India the observed deposition varies from 80 to 1040 eq-S/ha-yr. The model calculated values range from 50 to 220 eq-S/ha-yr. The model again captures most of the spatial features including the high deposition in the far eastern regions of India and the high deposition on the eastern coast along the Bay of Bengal. The model over predicts the deposition in the industrial area in east-central India and under predicts on the east coast. Clearly a more complete model performance evaluation is needed.

5.6 Monitoring and focal center activities

5.6.1 Monitoring sulfur dioxide in East Asia

Verification of the ATMOS model is a critical component in the development of RAINS-ASIA, and is an essential step towards building confidence in the use of the model. It was recognized that a detailed model evaluation was beyond the scope of Phase-I. This was largely based on the fact that at present the data for a meaningful model performance evaluation is not available. For example, most data in the region on sulfur dioxide and sulfate concentrations are confined largely to urban centers. Thus rather than initiate a detailed model evaluation in Phase-I it was decided to work with scientists in the area to try to develop the data sets necessary to perform such evaluations. This approach was taken in recognition that a number of initiatives are ongoing in the area including many national measurement programs, and international coordinating activities exemplified by the International Global Atmospheric Chemistry (IGAC) Deposition of Biologically Important Trace Species (DEBITS) Project, and the Global Atmospheric Watch (GAW) network of the World Meteorological Organization (WMO). However it was decided that in Phase-I we would initiate a passive sampler network to obtain base-level data for future model evaluation. The specific tasks related to monitoring in Phase-I were:

1. Design a SO_2 monitoring network, using passive samplers, for the Asian study region. This includes establishing the location of the sites, the sampling/analysis protocols, identification of laboratories to perform the analysis, and establishment of QA/QC guidelines.

2. Implement SO_2 monitoring network and obtain one year of data.
3. Build ambient SO_2 data base, combining China-wide data with Asia-wide data.
4. Extend data base to include data on sulfate deposition, and other ambient data which may become available by other country or region-wide activities.

The new passive samplers offer a low-cost means of obtaining long-term ambient average sulfur dioxide concentrations throughout Asia. These simple inexpensive (~ $35 U.S./sampler including manufacturing, mailing and analysis) devices can obtain weekly to monthly average sulfur dioxide levels. Extensive testing in Asia and Europe has proven these devices to be accurate and reliable.

5.6.2 Monitoring results

Forty-three sampling sites were established in eleven countries. The samplers were prepared by Martin Ferm at the Swedish Environment Research Institute (SERI). Duplicate samples were exposed each month and then returned to SERI for analysis (all samples were analyzed at the same laboratory). The measurement sites were selected to provide information on the regional aspects of sulfur in Asia. Thus sites were chosen to be away from major local sources and to be distributed in highly sensitive regions as determined from the critical loads map. The location of the monitoring sites are shown in Figure 5.17 and the country contact persons are listed in Table 5.5. The results to date from the measurement program are shown in Table 5.6. Shown are the monthly values and annual means for each monitoring site. This data represents the first of its kind in the region, in terms of extent and in terms of being regional in focus. This activity has been extremely successful. It has provided critical data and has played the important role of institution building.

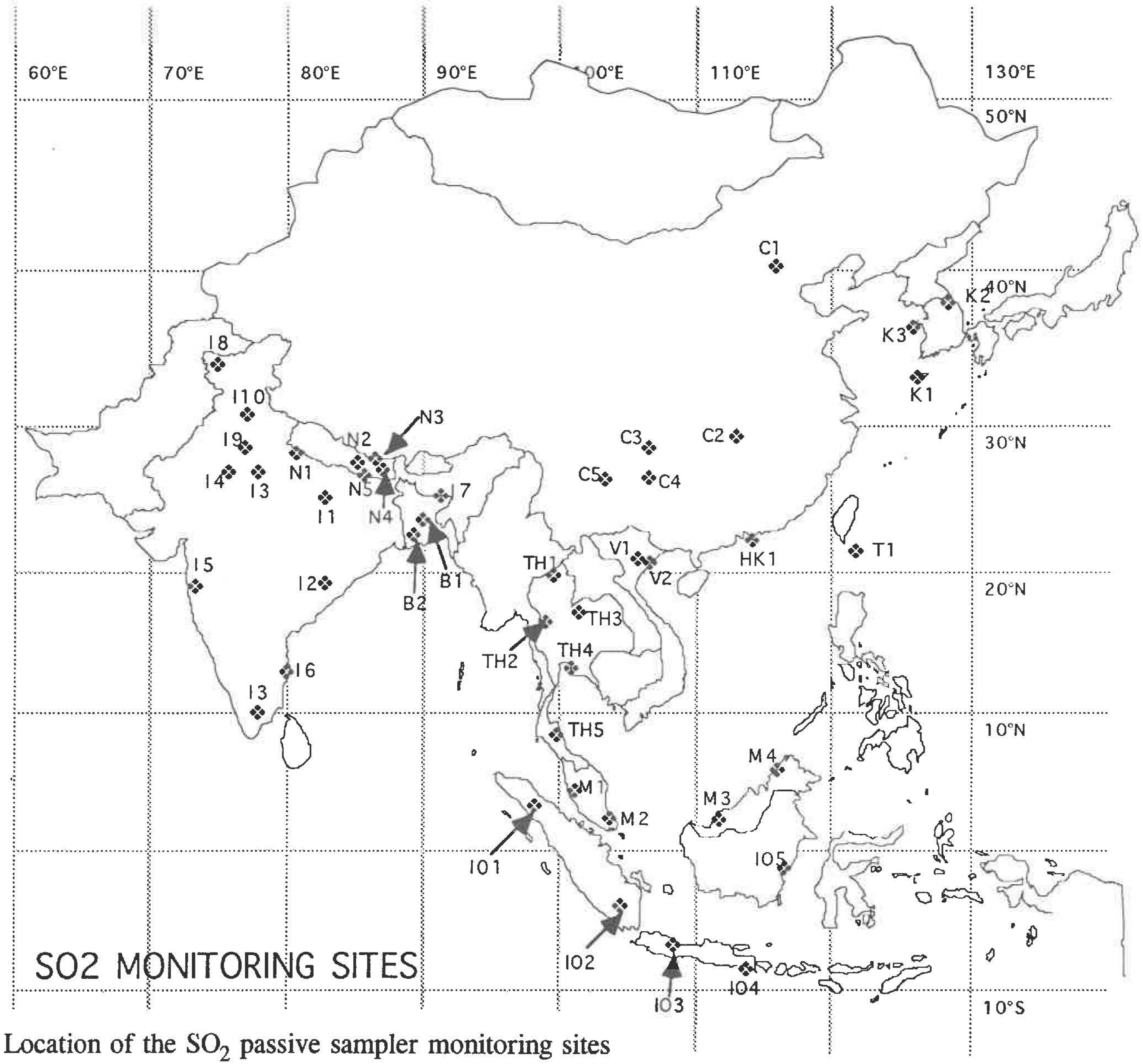

Figure 5.17 Location of the SO_2 passive sampler monitoring sites

Table 5.5 SO_2 passive sampler monitor network for RAINS/ASIA

Country	# Sites	Contact Person
India	10	Prof. Manju Mohan, Center for Atmospheric Sciences, IIT New Delhi
Nepal	5	Dr. S.P. Adhikary, Director General, Nepal Meteorological Services
Korea	3	Prof. M. Hong, Ajou University, Suwon
Thailand	5	Mr. Kanog Suksomsankh, Environmental Research & Training Center, Bangkok
Malaysia	5	Dr. Lim Fook, Malaysia Meteorological Agency
Indonesia	4	Prof. Soedomo, Inst. of Tech., Bandung
Taiwan	1	Prof. Liu, Taiwan National University
Hong Kong	1	Dr. Chan, Hong Kong Polytech University
Vietnam	2	Dr. Gian, Inst. of Chemistry, Hanoi
Bangladesh	2	Prof. Ahmad, Jahangirnagar University
China	5	Prof. Zhao, Eco-Environmental Center, Academia Sinica
Sweden		Dr. Martin Ferm, SERI

Table 5.6 Summary of sulfur dioxide passive sampler data. See Figure 5.17 for locations. Units are in ppb.

	Taiwan	Hong Kong	Korea			Malaysia				Bangladesh		Thailand		
	T1	HK1	K1	K2	K3	M1	M2	M3	M4	B1	B2	TH1	TH2	TH3
94-Jan	0.41	2.79												
Feb	0.22	67.77	0.46	1.94	3.82	0.12	0.28	1.17	0.21	3.14	4.54			
Mar	0.19	20.28	0.77	2.39	2.03	0.13	0.27	0.62	0.2	2.06	4.83			
Apr	0.33	2.21	1.35	2.66	3.43	0.13	0.33	0.8	0.1	2.47	5.05	0.61	0.55	
May	0.34	2.69	0.34	2.07	1.38	0.1	0.62	0.69	0.16	2.17	1.26			
Jun	0.22	1.87	0.74	1.63	1.01	0.15	1.64	0.23	0.18	2.93	1.05	0.95	0.64	0.49
Jul	2.04	3.16	2.91	0.74	1.35	0.21	0.83	0.28	0.08	2.87	0.88	0.84	0.6	0.31
Aug	0.82	3.9	2.82	0.68	1.45	0.1	1.05	0.29	0.08	4.115	0.845	0.58	0.89	0.32
Sep	0.21	1.68	1.59	0.83	1.53	0.24	1.16	0.48	0.14	2.405	1.055	0.86	0.41	0.67
Oct	0.42	1.78	1.38	1.66	2.4	0.11	0.47	0.2	0.06	1.86	1.66	0.34	0.72	1.2
Nov	0.63	1.02	1.91	2.3	3.94	0.05	0.14	0.22	0.09	0.99	0.905	0.44		1.53
Dec	0.16	0.74	2.16	4.33	2.43	0.01	0.24	0.21	0.05	3.45	2.515		0.35	2.65
95-Jan												0.56	0.62	2.59
Feb												0.76	0.8	1.66
Each station Annual mean	0.50	9.16	1.49	1.93	2.25	0.12	0.64	0.47	0.12	2.59	2.24	0.66	0.62	1.27
Each country Annual mean	0.50	9.16	1.89			0.34				2.41		0.82		

Table 5.6 (cont.)

	Thailand		Indonesia				China					Vietnam	
	TH4	TH5	IO1	IO2	IO4	IO5	C1	C2	C3	C4	C5	V1	V2
94-Jan							7.1	7.8		4.14	34.6	9.94	1.98
Feb									3.16			9.5	1.71
Mar							8.13	1.41	3.34	7.11	19.14	6.21	1.77
Apr	0.44	0.93	0.41		0.51	0.24	4.3	1.3	3.4	7.31	15.95	8.55	2.28
May	1.11		0.62	0.32	0.51	0.14	4.24	1.39	3.39	7.29		2.27	7.43
Jun	0.1	0.32	0.28	0	0.33	0.1	6.33	0.97		6.74	21.63	10.06	1.92
Jul	0.04	1.21	0.52	0.44	0.58	0.33	1.98	0.97		7.5	17.97		
Aug	0.06	0.41	0.49	1.54	0.65	0.43			4.11			9.2	
Sep	0.05	0.93					3.16	2.71	4.13	6.58		7.39	
Oct		1.48					6.17	3.83	4.64	7.6	12.73	5.79	5.2
Nov									5.77		29.36		
Dec		2.98					8.1	4.1	4.64	8.77	32.19		
95-Jan		1.38					2.27			7.67	26.67		
Feb		1.4											
Each station Annual mean	0.30	1.23	0.46	0.58	0.52	0.25	5.18	2.72	4.06	7.07	23.36	7.66	3.18
Each country Annual mean			0.45				8.48					5.42	

Table 5.6 (cont.)

	Nepal							India						
	N1	N4	N5	N6	N7	N8	N9	I1	I2	I5	I6	I7	I9	I11
94-Jan														
Feb	0.21	0.22		0.55		7.43								
Mar	0.82	0.39	0.96	0.76		9.4								
Apr	0.55	0.42	1.04			13.04								
May	0.52	0.19	0.63		7.88	6.62								
Jun	0.31	0.1	0.34			1.48								
Jul	0.15	0.06	0.29			0.46	0.07							
Aug	0.11	0.06	0.24			0.28	0.07							
Sep	0.21	0.05	0.28			0.34	0.05							
Oct		0.2												
Nov	0.27	0.18	0.37			0.43	0.14		0.58	2.58	0.73	1.01	10.24	0.48
Dec	0.28	0.21	0.43			0.8	0.27	0.65	0.92	3.33	1.68	0.51	10.45	0.66
95-Jan	0.28	0.27	0.48			6.26	0.72			2.2	1.26	0.62	6.67	1.21
Feb	0.28	0.19	1.24			5.82	0.89		0.44	1.36	0.8	0.36	10.16	
Each station Annual mean	0.33	0.20	0.57	0.66	7.88	4.36	0.32	0.65	0.65	2.37	1.12	0.63	9.38	0.78
Each country Annual mean	2.04							2.22						

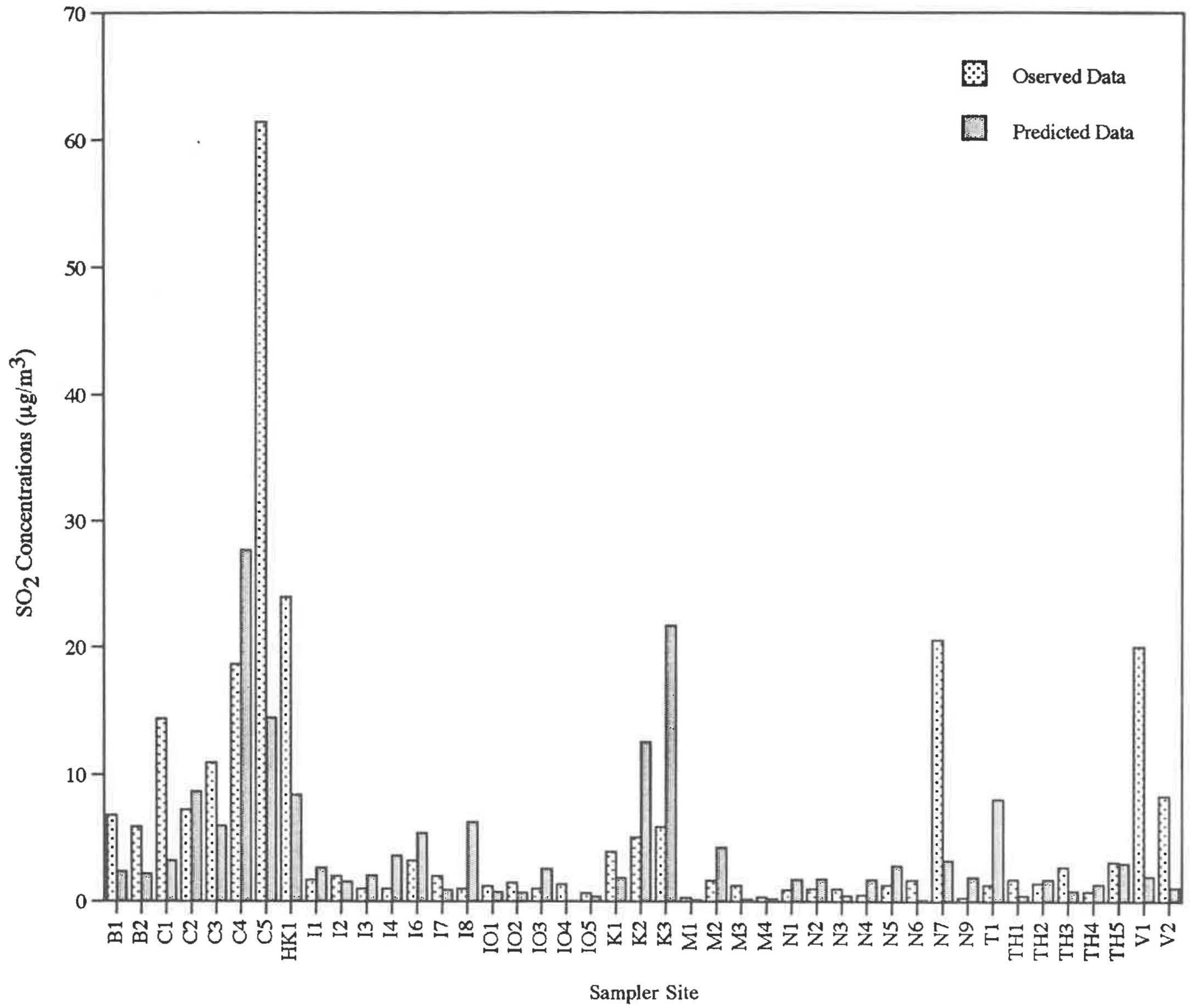

Figure 5.18 Observed and predicted SO_2 concentration at the passive sampler sites

B1: Jahangirnagar, Sava
B2: BIT, Khula
C1: Chongqing
C2: Yueyang
C3: Huittong
C4: Liuchongguan
C5: Fuye Ding, Beijing
HK1: Cape D'Aequier
I1: IIT Madras
I2: Berhampur Univers
I3: Cochin Univeersit
I4: BHU Varanasi
I5: Kashele
I6: IIT Bombay
I7: Nehu Shillong
I8: IIT Delhi
IO1: Medan
IO2: Palembang
IO3: Cisarua, Lembang
IO4: Balikpapan
IO5: Qjung Bandung
K1: Cheju
K2: Yangyang
K3: Taean
M1: Tanah Rata
M2: Mersing
M3: Sibu
M4: Lawa Mandau
N1: Dhangadi
N2: Phulchowki
N3: Dingboche
N4: Dhankuta
N5: Janakpur
N6: Budhanilakantha
N7: Babar Mahal
N9: Godawari
T1: Lan Hsü
TH1: Surat-Thani
TH2: ChiengRai
TH3: Tak
TH4: Phetchabun
TH5: Chongburi
V1: Hanoi
V2: Kien An

The model calculated SO_2 concentrations can also be compared to the measured SO_2 values from the passive sampler network described in the next section. Again no direct comparison is possible since the base year is 1990 and the observed values are for 1994. However this comparison provides important information regarding the spatial distribution of SO_2 and a check on the emissions used in the model. One would expect that SO_2 concentrations in 1990 to be systematically lower than those observed in 1994 (since there has been a rapid rise in emissions in Asia over the last few years). The predicted and observed SO_2 concentration are shown in Figure 5.18. The model predicted values capture quite well the spatial variability of the observed values. For example, the highest predicted and observed values are found in China and the lowest are found in Borneo.

5.6.3 Collaborations and focal center activities

Scientists and policy makers in Asian countries involved in Acid Rain and related policy analysis have worked closely on the ATMOS part of the project. These interactions have taken many forms including demonstration of the model at many international conferences, and specific visits to laboratories for same and in support of the monitoring activities. In addition many visitors have come to the University of Iowa to discuss and to assist in this project.

Networking for the ATMOS modeling activities has been extensive. Professor Carmichael has received visitors in his laboratory and has traveled to Korea, Japan, China, Nepal, Taiwan, Indonesia, Malaysia and India. The India trip consisted of participation at the CAAP (Characterization of Asian Acid Precipitation) meeting where some 30 scientists from Asia participated; and site visits to the Indian Institute of Technology (IIT)/Delhi to discuss the establishment of the ATMOS focal center. A working group meeting was organized at IIT during the International Meeting on Sustainable Development in Delhi in late January and early February of 1993. A preliminary design of the monitoring network took place at this meeting.

Two formal networks have been established for ATMOS activities. The monitoring network described previously, and the ATMOS focal center. The ATMOS focal center was established at IIT/Delhi. This focal center serves as the primary coordinating center for ATMOS related activities. The scope of activities for this task included:

* establishment of ATMOS Focal Center at the Center of Atmospheric Sciences at the Indian Institute of Technology, New Delhi, India. This includes purchase and installation of a computer to run ATMOS model and the RAINS-ASIA model in the Center.
* arrangement of training for research staffs of Indian Institute of Technology (IIT), New Delhi to develop expertise in ATMOS model.
* arrangement of training to scientists from China, India, Indonesia, Japan and South Korea in the use of the ATMOS model and associated databases.
* identification of site contact persons, establishment of terms of reference, provide progress reports of the monitoring activities, and to provide technical advice (when necessary) to the site operators in India on operation of SO_2 monitoring sites and to provide communications and coordination between all parties involved in this activity.

Table 5.7 Activities related to ATMOS module

Conferences where model was presented , demonstrated, and consultation occurred:

Characterization of Asian Acid Precipitation (CAAP) Workshop, Bombay, India

Sustainable Development Meeting, IIT Delhi, India

IGAC Atmospheric Chemistry and Climate Change Symposium, Taipei, Taiwan

Acid Deposition Conference, KL, Malaysia

Air Pollution 93, Monterey, Mexico

ASAAQ Meeting, Seoul, 1994

NASA/PRC Workshop on Atmospheric Chemistry, Beijing, China

American Meteorological Society, Annual Meeting, Jan. 1994, Nashville, TN

Institutional Visits:

S. Korea, EPA

Malaysia Met Service

Indonesia, Bandung, Univ.

ERTC- Thailand

Nepal, Department of Meteorology

Peking University, China

China Academy of Sciences - Eco Environ., China

Hong Kong Polytechnic University

Kyushu Univ., Japan

NIES, Japan

Jaipur State Agency for Pollution Protection, India

Banduras Univ., India

Agra Univ., India

Seoul National Univ., S. Korea

KIST, S. Korea

Visitors to the University of Iowa

Mr. Kim, Korea (Ihon Univ.)

Mr. Hui Xi, China Institute for Atmospheric Physics

Dr. Ichikawa, CRIEPI, Japan

Mr. H. Hiyami, CRIEPI, Japan

Prof. Singh, IIT Delhi

Prof. Adhikary, Nepal Meteorological Society

Special Training Sessions:

ATMOS Workshop IIT India - Jan 1992

IIT New Delhi, India, October 1994

* facilitator between the Swedish Environmental Research Institute (SERI) and persons for SO_2 monitoring.

The activities related to networking are summarized in Table 5.7.

5.7 Other modeling activities

Work was also initiated in Phase-1 to use the ATMOS model to look at the direct-effects of air pollution in the region. Two important environmental issues in Asia exacerbated by the expanding energy use in the region are forest damage due to high SO_2 gas phase concentrations and potential human health effects due to elevated levels of SO_2 in and around the urban centers. Each of these problems requires that SO_2 concentration data be considered. The annual average SO_2 concentrations for Asia were presented previously. But within the ATMOS model SO_2 concentrations are calculated every hour and this information can be used for studies on direct air pollution effects. Work was initiated to explore the feasibility of using the ATMOS model for such studies.

One activity was to modify the ATMOS model to output daily average concentrations. An example of the daily variation of predicted SO_2 and sulfate at a site in Japan is shown in Figure 5.19. The hourly concentrations show a large degree of variation with peak hourly values exceeding the mean value by a factor of 5 or greater.

Work was also initiated to use the ATMOS model to look at the air quality in and around mega-cities. The conceptual approach is shown in Figure 5.20. The resolution of the BAT model was reduced from 1 degree to 0.1 degree around a mega-city. A typical time series of hourly concentrations is shown in the right panel of Figure 5.20. This information can be used to construct concentration frequency distributions which in turn can be used to assess potential direct air pollution risk.

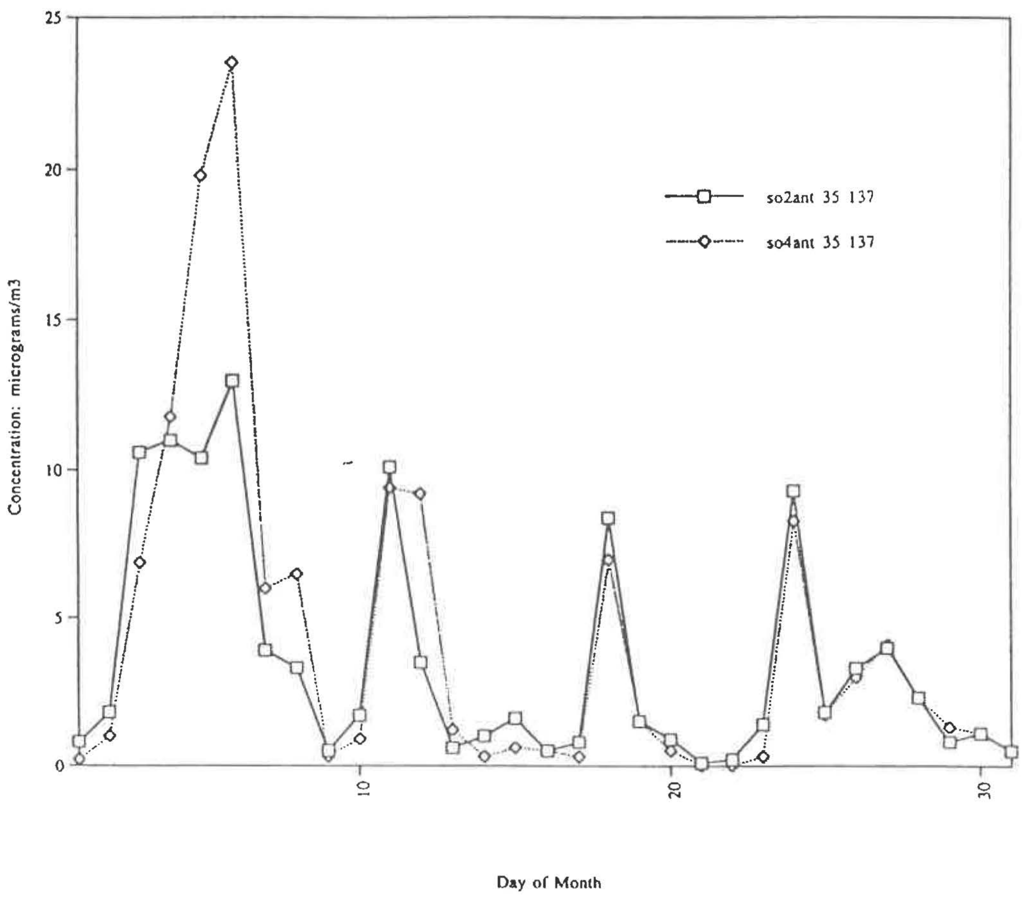

Figure 5.19 Calculated daily values of SO_2 and sulfate at a receptor site in Japan

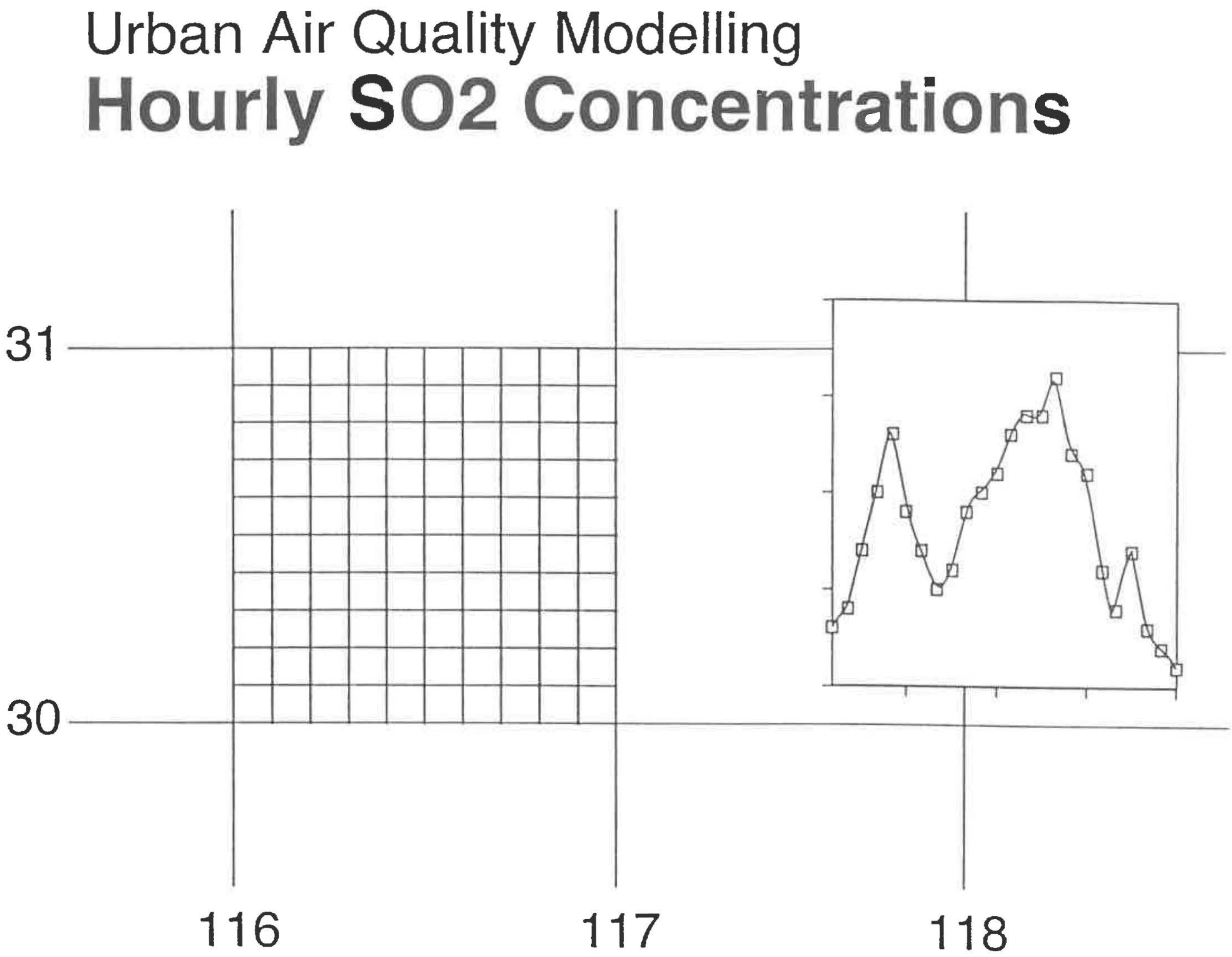

Figure 5.20 Urban application of the ATMOS model

5.7.1 Calcium deposition

Calcium is an important species in Asia because of its ability to neutralize the acidity of precipitation. For example in the springtime, the East Asia region, including China, Korea, and Japan, routinely experiences large-scale dust storms (so-called, Yellow Sand, Kosa, or Asian Dust) originating from the desert and Loess areas in China and Mongolia. These storms are associated with strong cold fronts which are accompanied by strong winds in Siberia and Southern Mongolia. During these storms, dust particles are uplifted as high as 6 km into the atmosphere (Iwasaka et al., 1988) and transported thousands of kilometers over East China, Korea, Japan, and out into the Pacific Ocean (Kotamarthi and Carmichael, 1993). The spring dust storms have significant influence on the regional energy balance and climate change, visibility impairments, health effects on humans, and on terrestrial and aquatic ecosystems.

Alkaline substances (Ca, Mg, K, and Na) can significantly influence precipitation acidity by neutralizing some fraction of the acids. Young et al. (1988) indicate that $SO_4^{=}$ in precipitation in the western U.S. is more closely correlated with Ca^{2+} than H^+, but the converse is true in the northeastern U.S. They concluded that calcium-containing mineral dust plays a significant role in the precipitation acidity in the western U.S. On an equivalent mass basis, calcium is the most important element, which accounts for two thirds of the alkalinity of four alkaline elements in U.S. (Gillette et al. 1992). Also, Gibson (1984) demonstrated that concentration levels of $SO_4^{=}$ and NO_3^- in rainwater in southern Saskatchewan, Canada were very high, but pH levels of precipitation were also relatively high, around 5. It was found that high concentration levels of Ca^{2+} exist and result in neutralization of acidity contributed by $SO_4^{=}$ and NO_3^- in that region.

Monitoring data for acid deposition throughout Asia show clearly that while the sulfate levels are similar to those found in North America and Europe, the pH values of the precipitation are much higher (typically 5.3 ~ 7 or higher). The difference is that wind-blown soil, rich in Ca^{2+}, is an important feature of the Asian atmosphere. Excess Ca^{2+} is greater than 20 meq/l in Japan and 40 meq/l in India and China. Throughout most of Asia, the values exceed 10 meq/l (Hara 1993).

As part of this project we helped in the estimation of Ca^{2+} deposition that was needed to assess the environmental impacts as discussed in Chapter 6. The procedures used are described in Chapter 6, Annex 2. However, we also investigated the use of the ATMOS model to directly calculate calcium deposition. Specifically, the long-range transport and deposition of calcium arising from three primary dust source areas (Takla Makan Desert, Gobi Desert, and Loess Region) was studied. For the calculation of dust transport and deposition, the ATMOS model was modified to allow for the on-line calculation of the dust emissions. A dust emission estimation procedure was placed within the ATMOS model and dust emissions for each 1° by 1° grid cell were estimated. These estimates made use of the observed wind speeds in the surface layer (~100 m). If the grid-cell friction velocity exceeded the threshold friction velocity, a dust emission was calculated. The total mass is divided equally among the three vertical layers to represent the vertical lifting of the dust that occurs during the passage of the cold fronts. Once in the air the airborne dust is transported and removed from the atmosphere in a manner similar to that described previously for sulfur. The model was used to provide an estimation of dust emissions driven by wind erosion at the source regions in the Takla Makan Desert, Gobi Desert, and Loess Region. In addition monthly average calcium concentrations, and dry and wet deposition rates over the Eastern Asia were estimated using the multi-layer trajectory model. These first estimates of calcium transport and deposition were found to be generally consistent with the limited observational data available. These results also demonstrate the importance of dust transport in east Asia. Further details are presented in Chang et al., 1995.

5.8 Uncertainty

It can not be stated strongly enough that the deposition patterns calculated in Phase-I have associated with them a high degree of uncertainty. The model itself has not been previously tested in Asia, and the model has made use of parameterizations which have largely been derived based on modeling studies at the mid-latitudes in North America and Europe.

No rigorous analysis was performed to characterize the sensitivity of the model results to changes in the input parameters. However, *preliminary* studies were performed in the course of this work. It was found that the maximum height of the model domain (presently set at 6 km) was not a very sensitive parameter. The ground level concentrations were highly sensitive to the choice of the σ value used in the Gaussian dispersion formula. Smaller σ values produced higher ground level concentrations near the source. In addition the location of the source within the grid had a large effect. For example, moving the area source location from the mid-point to the edge of the grid caused a similar effect as lowering the σ value. The model responded quite linearly to changes in conversion rates, dry deposition velocities and wet removal parameters. The wet removal rate constants for SO_2 and sulfate were also identified as critical parameters.

The meteorological fields also are a source of uncertainty. The method used in Phase-I was to rely on observed winds. However, missing (unreported data) as well as a non-uniform distribution of meteorological station in the region pose severe problems for this approach. One particular problem is the inability to follow trajectories out over the ocean and in and around Indonesia. A combination of observations with interpolated/analyzed 3-d fields should be pursued. Also it is imperative to investigate the interannual variability of the deposition. This requires that multiple years be simulated. The precipitation data is another source of uncertainty. We have used 6-hr accumulated precipitation. During this period it was assumed that the precipitation was uniformly distributed. Further work is needed to determine how precipitation is distributed as a function of time in the Asia study area.

Finally a critical component in the predictions is the quality of the emissions inventory. Both the magnitude and the location/distribution of the sources influence the model results. Any uncertainties in these inputs propagate directly to the calculated deposition fields.

5.9 References

Ayers, G. and H. Harn, Acid Deposition Assessment Report. Report to WMO, 1994

Carmichael, G.R., 1993, Modeling of Acid Deposition in Asia, Proceedings of the Third Workshop on Acid Rain in Asia, AIT Press, Bangkok, 21-43.

Carmichael, G.R., L.K. Peters, and T. Kitada, 1986. A second generation eulerian transport/chemistry removal model. Atmos. Environ. 20: 173-188.

Carnahan, B., H. Luther, and J. Wilkes, Applied Numerical Methods, John Wiley & Sons, New York, 1969.

Chang, J.S., R. Brost, I. Isaksen, S. Madranich, P. Middleton, W. Stockwell and C. Walec,1988. A three dimensional eulerian acid deposition model: physical concepts and formulation. J. Geophys. Res. 92:14681-14700.

Chang, Y., R. Arndt, and G. Carmichael, 1995, Mineral base-cation deposition in Asia, Atmos. Environ., accepted for publication.

Eliassen, A. and J. Saltbones, 1975, Decay and transpiration rates of transport of air pollutants as estimated for emission data, trajectories, and measured air concentration. Atmos. Environ., 17:1457-1473.

Fujita, S., Acidic Deposition in Japan, CRIEPI Report ET91005, October 1992, 90 pages.

Gibson, J.H., 1984, Evaluation of Wet Chemical Deposition in North America, Chapter 1 in Deposition both Wet and Dry, edited by B.B. Hicks, p.1-13.

Gillette, D.A., G.J. Stensland, A.L. Williams, W. Barnard, D. Gatz, P.C. Sinclair, and T.C. Johnson, 1992, Emissions of Alkaline Elements Calcium, Magnesium, Potassium, and Sodium from Open Sources in the Contiguous United States, Global Biogeochem. Cycles, 6(4):437-457.

Hara, H., 1993, Monitoring of Acid Deposition in Japan, Proceedings of the Expert Meeting on Acid Precipitation Monitoring Network in East Asia, Toyama, Japan

Heffter, J.L., 1983, Branching Atmospheric Trajectory (BAT) Model, NOAA Technical Memorandum, ERL ARL-121.

Iwasaka, Y., M. Yamato, R. Imasu, and A. Ono, 1988, Transport of Asian Dust (Kosa) Particles; Importance of Weak Kosa Events on the Geochemical Cycle of Soil Particles, Tellus, 40B:494-503.

Kotamarthi, V. R. and G.R. Carmichael, 1993, A Modeling Study of the Long Range Transport of Kosa Using Particle Trajectory Analysis, Tellus, 45B:426-441.

Martyn, D., 1992, Climates of the World, Elsevier Science Publishers B.V., Amsterdam.

Murano, K., Activity of JEA for East Asian Acid Precipitation Monitoring Network. Presented at Workshop on Acid Rain Network in South, East, and Southeast Asia, Malaysia, May 17-19, 1994.

Okita (1994) personal communications

Spiro, D. Jacob, and J. Logan, 1992. Global inventory of sulfur emissions with 1 x 1 resolution. J. Geophy. Res., 97:6023-6036.

Venkatram, A. P. Karamchandoni and P. Misra, 1988. Testing a comprehensive acid deposition model. Atmos. Environ. 22:737-748.

RAINS-ASIA:
AN ASSESSMENT MODEL FOR AIR POLLUTION IN ASIA

Chapter 6

Impact Module

Jean-Paul Hettelingh, Michael Chadwick, Harald Sverdrup, Dianwu Zhao

Report on the World Bank Sponsored Project
"Acid Rain and Emission Reductions in Asia"

December 1995

DISCLAIMER

The boundaries shown on any of the maps in this report do not imply official endorsement or acceptance by the World Bank.

6. ASSESSMENT OF ENVIRONMENTAL EFFECTS OF ACIDIC DEPOSITION

J.-P. Hettelingh, M.J. Chadwick, H. Sverdrup, D. Zhao (eds.)

TABLE OF CONTENTS

6.1 Introduction VI-1
6.1.1 Direct and indirect effects VI-2
6.1.2 Critical load approach VI-4
6.1.3 The RAINS-ASIA IMPACT project VI-6
6.1.4 Organization of the chapter VI-7
6.2 Establishing sensitivity criteria for Asian ecosystems using two approaches . . VI-7
6.2.1 Introduction VI-7
6.2.2 Steady state mass balance approach VI-8
6.2.3 Data for the derivation of BC/Al ratios VI-9
6.2.4 The basis of the relative sensitivity approach VI-17
6.3 Background data and mapping the sensitivity in Asia VI-28
6.3.1 Introduction VI-28
6.3.2 Background for the sensitivity mapping VI-28
6.3.3 Data for sensitivity and critical load mapping VI-29
6.3.4 Mapping sensitivity in Asia VI-40
6.4 Computation and mapping of critical loads in Asia VI-45
6.4.1 Introduction VI-45
6.4.2 The Steady State Mass Balance Model VI-46
6.4.3 Results VI-49
6.5 Conclusions and recommendations VI-52
6.6 References VI-59

LIST OF TABLES

Table 6.1 RAINS-ASIA Impact scientific meetings. VI-7
Table 6.2 Response type and estimated aluminum damage coefficients for spruce, pine and other conifers VI-13
Table 6.3 Proposed model entry values for calculation of critical loads (BC/Al values) using the Steady State Mass Balance Model (low values indicate high tolerance; high values, low tolerance to acidification) and other data input for SSMB VI-15
Table 6.5 Ecological factors influencing vegetation classification VI-23
Table 6.6 Summary of influential factors determining the method of classification for each vegetation type VI-25
Table 6.7 Classification of ecosystem sensitivity according to vegetation type characteristics VI-26
Table 6.8 GIS Manipulation by SEI VI-30
Table 6.9 The use of data sets within the RAINS-ASIA mapping programme VI-31

Table 6.10 Combination of the sensitivity from vegetation and the soil buffering conditions to give fourteen potential classes of overall sensitivity . . . VI-43

LIST OF FIGURES

Figure 6.1 The critical load concept consisting of: (1) iterating required emission reductions to meet critical loads and costs (short circle; dotted line), and (2) computing time horizons before ecosystems damage (continued critical load excess) or recovery (whenever excess ceases to exist). The computation of time horizons is represented by the solid line (long circle). . . . VI-5
Figure 6.2 The relationship between laboratory observations of shoot and root growth for Norway spruce (*Picea abies*) and BC/Al ratios in the rooting medium. Open symbols represent Norway spruce of Scandinavian provenances; solid symbols represent German provenances. There is no significant difference in response between Scandinavian and German provenances. . . . VI-11
Figure 6.3 The relationship between field and laboratory observations of growth and the rooting medium BC/Al molar ratio (for Norway and Red spruce) . . . VI-14
Figure 6.4 Map of critical base cation to aluminium ratios used in the application of the Steady State Mass Balance Model for the computation of critical loads (see Section 6.4) . . . VI-16
Figure 6.5 The classes of sensitivity derived from vegetation type (SEI based on Rutgers University data) . . . VI-27
Figure 6.6 Flow diagram of data use within the RAINS-ASIA impacts project . . . VI-34
Figure 6.7 Precipitation to Potential Evapotranspiration Ratio (SEI) . . . VI-35
Figure 6.8 Base cation deposition (University of Iowa; SEI; RIVM) . . . VI-36
Figure 6.9 Quantitative values of weathering rates and associated relative buffering rate classes (UL, SEI, RIVM, GEODAN) . . . VI-39
Figure 6.10 The % area of sensitivity classes and their combination . . . VI-44
Figure 6.11 The preliminary map showing relative sensitivity of terrestrial ecosystems in Asia to acidic deposition (SEI; RIVM; UL; RCEES; GEODAN) . . . VI-44
Figure 6.12 Critical loads for acidity in Asia. The red shaded areas represent the areas with the lowest critical load where sulfur deposition should not exceed 200 eq ha^{-1} yr^{-1} (approximately 0.32 g S m^{-2} yr^{-1}) (RIVM, SEI, RCEES, UL, GEODAN) . . . VI-51
Figure 6.13 5-percentile critical load map; Critical loads for acidity at which the risk of damage to about 95% of the ecosystems is decreased. The reliability of the 5-percentile critical load map varies over the region, especially in grid cells where the cover of the ecosystems is less than 25% of the grid cell. (RIVM, SEI, RCEES, UL, GEODAN). . . . VI-55
Figure 6.14 50-percentile critical load map; Critical loads for acidity at which the risk of damage due to acidification to 50% of the ecosystems is decreased. (RIVM, SEI, RCEES, UL, GEODAN) . . . VI-56

Figure 6.15 Computed excess of the 25-percentile critical loads of acidity by sulfur deposition in 1990. About 75% of the ecosystems in red shaded areas are subject to risk of damage because sulfur deposition exceeds critical loads. VI-57

6. ASSESSMENT OF ENVIRONMENTAL EFFECTS OF ACIDIC DEPOSITION

J.-P. Hettelingh, M.J. Chadwick, H. Sverdrup, D. Zhao (eds.)

6.1 *Introduction*

J.-P. Hettelingh, M. J. Chadwick, D. Zhao

Historical data in Europe provide evidence of increasing emission and transport of sulfate, up to a factor of 2 in 1950 and 3.5 in 1980 in comparison to pre-industrial levels. Emissions of SO_2 are transformed in the atmosphere to sulfate (SO_4^{2-}) which constitutes the main component causing acidic deposition. In Asia emissions of SO_2 are rapidly increasing due to high economic growth. Within the RAINS-ASIA project an initial attempt to include the impacts of sulfur deposition on Asian ecosystems has been made. Although knowledge of effects on many ecosystems in Asia is limited, this module has attempted to create maps of sensitivity and critical loads (environmental quality limits for acidic deposition). These are used in the RAINS-ASIA project to illustrate areas potentially at risk from acidic deposition induced damage. Air pollution, in the form of SO_2 and NO_x may cause adverse effects to the natural environment once concentration levels or deposition loads exceed certain limits. In the context of pollution abatement the question becomes increasingly relevant as to how much should be abated to obtain sufficient protection of natural resources such as soil and vegetation.

Knowledge is required concerning environmental quality limits if environmental quality objectives are to be set. "The ability of an ecosystem to assimilate a substance without degrading or damaging its ecological integrity" (Cairns, 1977) or, "the exposure to one or more pollutants below which significant harmful effects on the specific elements do not occur according to present knowledge" (Nilsson, 1986) are just two ways of expressing the ideas underlying environmental quality objectives: the first defines the assimilative capacity of an ecosystem, the second the critical load value that may be assigned. The two concepts are almost identical. The assimilative capacity concept, used mainly in relation to aquatic systems (Velz, 1976; Goubet, 1969), addresses the same concerns as the critical load concept enunciated a decade later (Nilsson, 1986). Both are environmentally centered. Assimilative capacity, like the critical load, was developed as a largely physico-chemical concept, having reference to the chemical and physical parameters of a system. However, it was related also to the ecological integrity of a system (the maintenance of the structural and functional attributes of the ecosystem). The structural integrity of the ecosystem refers to such features as species composition, diversity, autotrophic-heterotrophic ratios and saprobian designation; the functional integrity to features of nutrient transfer, energy dissipation, rate processes, maintenance efficiency and ecological efficiency. If the assimilative capacity was not exceeded the bounds of normal structure and functioning of the ecosystem would not be crossed. The question of how interdependent these two features of an ecosystem are is an important one as the critical loads approach does not deal with them directly. The concept of assimilative capacity has a number of variants: absorptive capacity, receiving capacity and environmental capacity (Pravdic and Juracic, 1988). They have been applied widely to ecological situations in one form or another (Pravdic, 1987; Pravdic and Juracic, 1988, Portmann and Lloyd, 1986; Preston and Portmann, 1981).

Quantitative estimates are difficult to establish accurately for either assimilative capacity or the critical load as in most situations relevant, reliable field measurements are of limited availability. Dose-response relationships of many target organisms, and populations of them, to the range of pollutants considered are not well established (see Chadwick and Nilsson, 1993). A reason is that organisms may be subject to a combination of stresses including excessive deposition and air concentration, for each of which critical limits are required.

The limit of air pollution *concentration* above which risks of damage can occur is known as **critical level**. The highest *deposition* of compounds that will not cause chemical changes leading to harmful effects on ecosystem structure and function is defined as the **critical load**. In this study emphasis was given to the computation of critical loads by applying two methods simultaneously. One method, the relative sensitivity approach, provides a non-parametric quantitative assessment of sensitivity based on climatic factors, factors relating to geology, soil characteristics, vegetation type and land use. The sensitivity approach has been used in regions outside Asia and accounts of its application can be found in Chadwick and Kuylenstierna (1991) and in Kuylenstierna and Chadwick (1989). The other method is based on a mathematical model (the Steady State Mass Balance Model) which computes the critical loads from the requirement that the supply of acidic compounds should not exceed the ability of a system to buffer the acidity (see Sverdrup *et al.*,1990; Hettelingh and De Vries, 1991; Hettelingh *et al.*, 1992; Sverdrup and de Vries, 1993; Downing *et al.*, 1993). The objective of applying two methods was to (1) combine biogeochemical considerations by means of the Steady State Mass Balance Model with other ecological aspects using the relative sensitivity approach, (2) assess the reliability of the computed critical loads by comparing the geographical distribution over the Asia region of critical loads to the distributional pattern of classes of relative sensitivity, and (3) ensure availability of an assessment of sensitivity in situations where lack of data would not have allowed computation of critical loads. This approach was considered to be an improvement over the identification of critical loads and sensitivity classes in Europe where both methods were applied independent of one another (see Hettelingh *et al.*, 1992). This comparison showed overall compatibility of the distribution of sensitive areas and areas with low critical loads. Thus, reliability of the results was increased in spite of the fact that the data uncertainty is high (there is large variation in the geographical resolution of available data - Section 6.3).

6.1.1 Direct and indirect effects

Sulfur deposition gives rise to acidification and, once critical loads have been exceeded, ecosystem damage may occur. In the first phase of the RAINS-ASIA project emphasis has been put on establishing critical loads for a large variety of soil and vegetation combinations in order to allow for the assessment of environmental effects of deposition patterns as computed with RAINS-ASIA.

The reasons for focussing on critical loads rather than critical levels include:

(1) the most serious direct effects occur on a local rather than a broad geographical scale; an appropriate assessment of local effects requires high resolution air concentration

data and models relating emission sources and concentration fields on a large geographic scale. The first phase of the RAINS-ASIA project has emphasised broad-scale dispersion of SO_2;

(2) episodic excessive concentrations may lead to acute, short-term damage including yield-loss, but may not necessarily affect the long-term sustainability of the ecosystem;

(3) the indirect effect of long-term excessive deposition, affects sustainability of a natural system rendering recovery less likely; the ultimate effect of excessive deposition may be a change of the soil chemical composition to an extent where there is a shift in the natural functions also.

Taking the considerations mentioned above into account, it is appropriate to give the emphasis to the indirect effects of sulfur deposition (acidification) in the first phase of the project. Soil acidification is defined as a decrease in the Acid Neutralising Capacity (ANC) of the soil and is directly dependent on the net supply of base cations (by weathering and deposition) and the net supply of anions (deposition minus retention) in the soil. Deposition of acidifying compounds such as H_2SO_4, HNO_3 and $(NH_4)_2SO_4$ leads to ecosystem acidification, to a degree which is dependent on biological transformations and ion leaching.

The dynamics of soil acidification are very site specific and depend on soil characteristics such as weathering rate, sulfate adsorption capacity and CEC. The acidification of soils ultimately leads to an increase in the soil solution of the aluminum concentration which increases the risk of vegetation damage. The acidification of the soil and the reduction in pH that this entails also leads to changes in nutrient availability (such as magnesium or phosphate) and form (such as nitrate or ammonium). These changes affecting the fertility of the soil also lead to impacts on vegetation structure and function. By defining the relationship between the chemical status (base cation and aluminum concentrations in the soil solution) and vegetation response, the critical load for that particular ecosystem may be derived.

Damage to forests in Europe, including defoliation, foliar discoloration, growth rate decreases and dieback have been reported over the last decades, and has been attributed, to a large extent, to soil acidification (Ulrich, 1983). Causes of tree damage are of course complex and involve the actions of other pollutants, action of climate and interactions with pests and pathogens. The long-term nature of changes in soil from acidification, interacting with other stresses, emphasises the importance of acidification relative to other causes. As well as changes in growth of individual plants, soil acidification also gives rise to changes in species composition and diversity (Falkengren-Grerup, 1990). Acidic deposition has caused acidification of surface waters, fish mortality and other ecological changes in large areas of central and northern Europe and eastern parts of North America. In Asia damage has been reported to forest and crops, although it is as yet undetermined whether these occurrences should be attributed to indirect pollution processes such as acidification.

Increased sulfate concentrations in runoff due to increased acidifying inputs are accompanied by an increase in base cation concentrations and a decrease in bicarbonates, resulting in acidification of surface waters. Knowledge about surface water acidification in Asia is limited. Xue and Schnoor (1993) have investigated acidification of surface waters in Sichuan concluding that the high deposition of base cations prevent acidification from occurring.

Nitrogen compounds have also contributed to acidification in Europe, but it has been established that sulfur is usually the dominant contributor. Due to the large difference between Asia and Europe in overall road traffic density, NO_x is likely to be a lesser contributor to acidification in Asia.

Critical loads for acidity computed as part of the RAINS-ASIA project refer to any acidifying deposition, whether this derives from sulfur or nitrogen compounds. The RAINS-ASIA model focusses on sulfur. Comparison of critical loads to sulfur deposition, as is done in the critical load approach (next section), should be made in the awareness that nitrogen deposition could further increase excess of critical loads of acidity. The inclusion of nitrogen would, on the other hand, also require the computation of critical loads for nitrogen from an ecosystem nutrient limit point of view (see Posch *et al.*, 1993). The RAINS-ASIA Impact model has not included nitrogen explicitly for reasons of simplification, and the fact that the computation and application of nutrient critical loads is still under scientific debate.

6.1.2 Critical load approach

The critical load approach is a methodology according to which critical loads are used as a criterion to assess whether emission reduction strategies are sufficient. In Europe this has taken the national cost of emission reduction into account (Hettelingh *et al.*, 1992a) and has been used with regard to the transboundary nature of the acid rain problem in Europe. In Asia the emphasis may be different, perhaps with concentration on national strategies. Figure 6.1 (dotted line) shows that the objective of the iterative procedure is to avoid sulfur deposition exceeding critical loads at the lowest possible national costs. Since reducing emissions to reach critical loads may be infeasible, the objective of meeting critical loads can be altered. Several strategies may be employed such as to reduce the overall excess of critical loads (exceedance minimisation) in any one region. In European negotiations an objective by which critical load excess should be reduced (gap closure) has been formulated. Then, the required emission reductions at minimum costs can be computed using RAINS-ASIA. Finally, the actual excess in different Asian regions is expressed in terms of (1) the area of 'protected terrestrial ecosystems' and (2) absolute values of the excess of deposition over a critical load in each of the 1^o by 1^o grid cells distinguished in RAINS-ASIA. This procedure is repeated by changing the objective finally leading to the identification of an appropriate starting point of emissions over the regions. In this procedure it is likely that parts of the region will continue to have depositions that exceed critical loads.

Since critical load exceedance may lead to "harmful effects", the question of when these harmful effects will occur becomes relevant. The answer to this question can be investigated by using dynamic soil models, which simulate the temporal changes in the balance of geochemical processes in a soil receiving acid deposition. The procedure of using dynamic models is also part of the critical load concept as illustrated in Figure 6.1 (solid line). The application of dynamic models is also useful to assess recovery time of an ecosystem once emissions have been sufficiently reduced. The dynamic part of the critical load concept has been initiated (Hettelingh *et al.*, 1992b; Hettelingh and Posch, 1993; Bleeker *et al.*, 1994) but has not yet been part of the integrated assessment of emission reduction strategies in Europe. However it is expected that the dynamic part of the critical load concept will become increasingly important as indications of target years for establishing required emission reduction vary over the region.

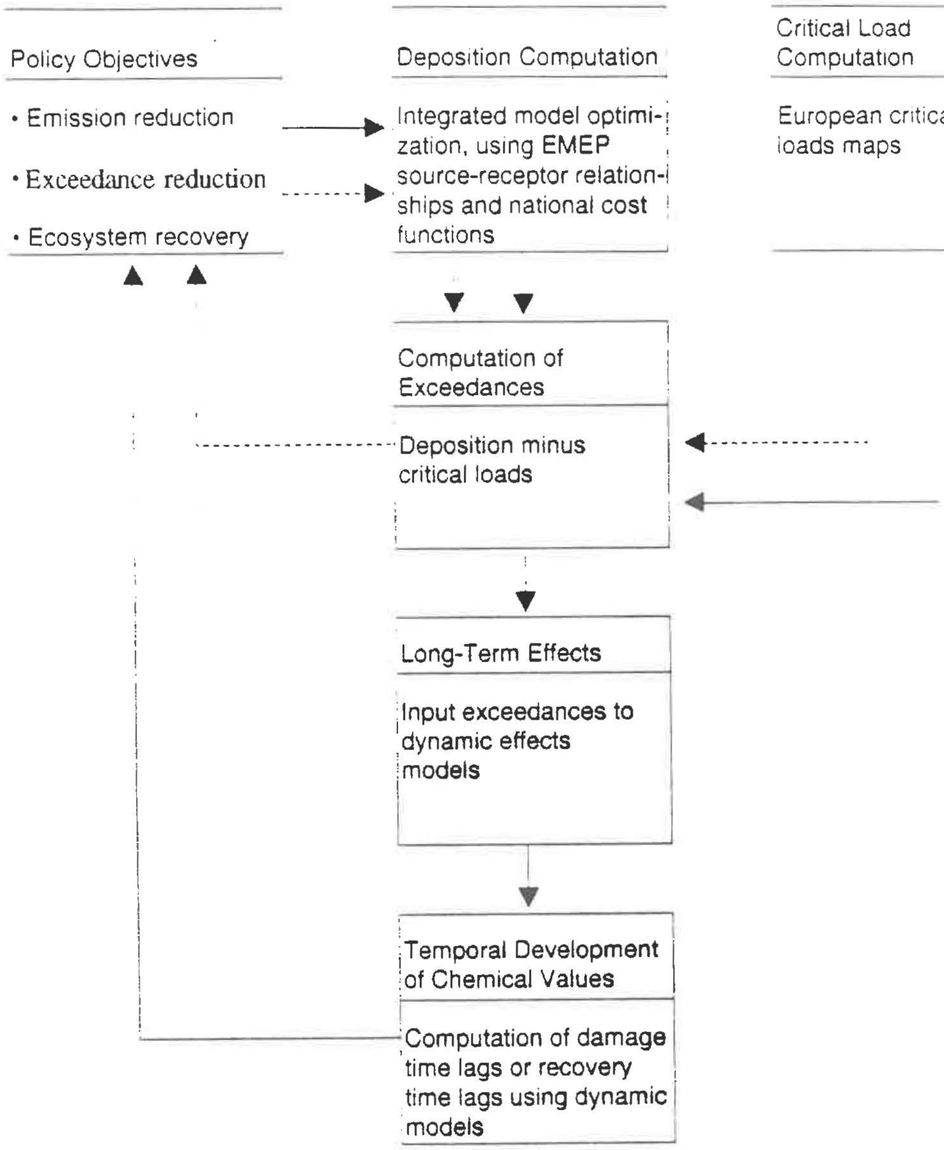

Figure 6.1 The critical load concept consisting of: (1) iterating required emission reductions to meet critical loads and costs (short circle; dotted line), and (2) computing time horizons before ecosystems damage (continued critical load excess) or recovery (whenever excess ceases to exist). The computation of time horizons is represented by the solid line (long circle)

In China, use of dynamic models have been made to compute the effect of excess sulfur deposition scenarios in heavily polluted regions (Zhao *et al.*, 1994). Recently, critical loads in China have been applied to assess allocation of pollution sources. This concept of the so-called rational distribution recognizes the need for assessing emission reduction in relation to environmental quality both by applying emission reduction techniques as well as locating heavy polluters in less sensitive areas. The RAINS-ASIA model allows for the analysis of effects due to regional shifts in regional pollution sources.

6.1.3 The RAINS-ASIA IMPACT project

The objectives of the RAINS-ASIA IMPACT project are:

(1) to establish critical loads for acidity for Asia;

(2) start a network of Asian scientific collaboration on impacts in general and critical loads in particular.

Summary of the project organization

The impact project team consisted of the National Institute of Public Health and Environmental Protection (RIVM, Netherlands), the Stockholm Environment Institute (SEI, United Kingdom and Sweden), the University of Lund (UL, Sweden), GEODAN Amsterdam (Netherlands), and the Research Center for Eco-Environmental Sciences (RCEES, China). RIVM was principal investigator, responsible for systems analysis, the Steady State Mass Balance (SSMB) modelling and computation of the critical loads including the interface with RAINS-ASIA; SEI was principal investigator for the development and application of the relative sensitivity method and responsible for geographical data production used by the SSMB and sensitivity methods involving data collection (digitizing) and derivation of data layers using a Geographical Information System (GIS); UL was responsible for systems analysis, the critical chemical limits used in the model and assessment of base cation weathering (together with SEI); GEODAN accounts for the application of the model in a GIS environment and provided GIS training to the Asian counterpart in China. RCEES became the official Asian counterpart of RIVM and the node of the participating institutes in Asia. GIS hard- and software, including the critical load model, was installed at RCEES and training provided at RIVM and GEODAN as well as at RCEES.

Other participating Asian institutes were invited to two impact workshops (see Annex 5 for meeting report) held in Beijing including Jahangirnar University (Dhaka, Bangladesh), the National Center for Research (Hanoi, Vietnam), Kyong-gi University (Korea), National Institute for Agro-Environmental Science (Tsukuba, Japan). In addition to participation from the 'focal' institutes also other scientists from China, Japan, India and Pakistan participated in one of the workshops. Maps of background data and critical load results were sent to these and other institutes for review. Provided the project will continue, increased participation is aimed at in the future by the installation of Geographic Information Systems and the critical load models at different sites in Asia. Several meetings were held which are summarized in Table 6.1.

Table 6.1 RAINS-ASIA Impact scientific meetings.

Date	Place	Objective
17-19 March 1992	RIVM	Outline of research activities
March 1992	SEI	Professor Zhao (RCEES) visited for 2 weeks to discuss methods
10-13 November 1992	RCEES	First IMPACT meeting; start network, propose methodology to Asian participants.
May 1993	RCEES	installation of hard and software GIS equipment and provide training.
November 1993	RIVM	Result exchange with RCEES; GIS continued training.
8-9 November 1993	RIVM	Verify critical load maps
10-14 October 1994	RCEES	Second IMPACT meeting; Exchange results with Asian participants; GIS training at RCEES.

6.1.4 Organization of the chapter

The method used to compute critical loads is described in several sections of this chapter. Section 6.2 describes how the compatibility between the most important assumptions of the steady state mass balance method and the method of relative sensitivity was increased. Section 6.3 describes the database of both methods and describes the method of relative sensitivity in some detail. Section 6.4 describes the steady state mass balance model and the critical load results which were made input to the RAINS-ASIA model. Maps of critical loads of Asia are presented and analyzed. Finally the Chapter gives some concluding remarks and recommendations for future work.

6.2 Establishing sensitivity criteria for Asian ecosystems using two approaches

H. Sverdrup, J.C.I. Kuylenstierna, J.-P. Hettelingh

6.2.1 Introduction

This section describes the basis for the two approaches used in this project, the Steady State Mass Balance (by the University of Lund) and Relative Sensitivity methods (by SEI). The methodologies and emphases are explained and aspects of compatibility between the projects are discussed.

The Steady State Mass Balance approach requires limit values relating the response of vegetation types to soil chemistry. In this text the theoretical basis for the limit values for soil acidity for a wide variety of plant species required by the Steady State Mass Balance approach is explained. The sensitivity approach is designed for use in situations where there is limited access to detailed data but where it is possible to apply data of a limited nature uniformly and widely. The method uses several datasets of relatively uniformly available ecological information, and combines them to derive a distribution of relative sensitivity. The use of different datasets in combination both reinforces the sensitivity assessment and incorporates different ecosystem attributes. The vegetation type is one of the major datasets and the theoretical basis for the use of the vegetation classes to determine sensitivity is explained in this chapter (see Section 6.3).

It is important to differentiate between concepts of sensitivity, buffering and tolerance with respect to the work described. The sensitivity refers to the degree of response of the entire ecosystem to a uniform dose. A sensitive ecosystem will respond to a greater degree than a relatively insensitive ecosystem. The buffering mechanisms in the soil influence the degree of change in the soil physical and chemical attributes for a given rate of acidic deposition. The amount of change in vegetation structure and function will be dependent on the tolerance of that vegetation to the changes induced in the soil. The SSMB model links an assessment of weathering rates with the tolerance of vegetation to changes in BC/Al ratios. The relative sensitivity method concentrates on the degree of buffering present in ecosystems and incorporates certain ecological features not included in the SSMB method. Thus a quantitative biogeochemical critical load assessment by means of the Steady State Mass Balance Method is used in combination with additional information on ecological features from the relative sensitivity method.

The Steady State Mass Balance Method has been applied within the Convention on Long Range Transboundary Air Pollution of the United Nations Economic Commission for Europe to compute critical loads for forest soils and ecosystems. The relative sensitivity method was applied as well, in the early course of the development of an impact methodology within the convention. The distribution of sensitivity classes and of critical loads was shown to be largely comparable (see Hettelingh *et al.*, 1991 and Kuylenstierna *et al.*, 1991). For the application in Asia an attempt has been made to use both methods simultaneously. One difference between the computation of critical loads in Europe and Asia is that, in Asia, different ecosystems with a range of structural and functional attributes are considered. Taiga, temperate forests, boreal deciduous forests, Mediterranean-type woodlands, steppe, savannah, deserts, alpine landscapes, tundra, tropical forests, mangrove swamps and rain forests are included.

The Steady State Mass Balance Method uses the response of single species to the balance between base cation nutrients and aluminum in the root zone as one of the inputs to the critical load computation: i.e. an ecosystem is subject to risk of damage whenever the ratio between base cations and aluminum is too low. Therefore, for each of the ecosystems mentioned above a critical limit has been derived, largely based on laboratory results, beyond which the risk of damage due to indirect effects of acidic deposition is negligible.

6.2.2 Steady state mass balance approach

The Steady State Mass Balance approach applies the basics of systems analysis and mathematical modeling to ecosystems such that distinct components, or indicators such as the base cation to aluminum (BC/Al) ratio, of an ecosystem are identified and isolated. In the following discussion reasons are described for the use of the BC/Al ratio as a critical soil parameter for which threshold values may be derived and, when these are exceeded, indicate where there is an increased risk of damage through acidification. The methodology and data which form the basis for the derivation of the threshold BC/Al values are summarised and the threshold values for a wide range of ecosystems are shown.

6.2.3 Data for the derivation of BC/Al ratios

A large literature review has been undertaken by Sverdrup and Warfvinge (1993) to investigate the relationship between the BC/Al ratio and changes in plant growth. The objective of the literature review was to identify the minimum values of BC/Al ratios for a large variety of species beyond which growth (of stem and/or root) diminishes. The study has included the derivation of mathematical relationships between BC/Al values and seedling shoot or root growth. These resulted in S-shaped relationships, some of which are illustrated in this section. All reviewed reports on (laboratory or field) experiments followed the same basic outline in their setup: plant material is grown in a medium, in series, with varying media composition. Growth, shoot length or root length was recorded. The experimental rooting medium varied between the different experiments, consisting of an aqueous solution, sometimes added as solution only, sometimes to sand culture; sometimes a complete soil culture was used. Growth was measured directly on the plant; the BC/Al ratio was varied in the bulk composition of the experimental medium. Thus any effects taking place in the boundary layer between the bulk of the solution and the root surface, is included in the response of growth versus solution composition. When one investigator reports significant growth changes at 2.5 mg/l, whereas another reports no change until 15 mg/l Al^{3+} or more, then this difference can often be traced back to differences in Ca, Mg and K concentrations of the soil or culture solution of the bioassay. It is a consistent pattern that the growth effect expressed as a function of (Ca+Mg+K)/Al ratio instead of Al concentration alone will generally remove most of the difference between such studies on the same plant species. Often K concentrations in the experiments will be several orders of magnitude larger than those measured in 'natural' soil solutions. This is caused by the use of "Ingestad ideal nutrient solutions" or similar compositions, rather than something similar to the natural soil solution composition.

Chemical limits and smb: response functions

The general equations for the damage functions can all be expressed in terms of the BC/Al ratio in order to show any extra effects. Several different types of response expressions can be derived from assuming antagonism between base cations and Al through different types of ion exchange at the root (equation (1)).

$$f(BC/Al) = \frac{[BC]^{n-m}(BC/Al)^m}{[BC]^{n-m}(BC/Al)+K(1+(n(H/Al))^m} \qquad (1)$$

where,
[BC] = Concentration of base cations Ca,Mg,K in soil solution
K = Response function coefficient
BC/Al = Base cation to aluminium ratio in soil solution
H/Al = Proton to aluminium concentration in soil solution

There are a number of special cases depending on the ion exchange mechanism utilized. For n=m=1, a valence unspecific reaction is assumed and the growth response to BC/Al is called unspecific. When n=3 and m=2 the exchange mechanism is of 'Vanselov' type and when n=1/3 and m=1/2 the response is of 'Gapon' type. See (Sverdrup and Warfvinge, 1993; Bult, 1982) for further details.

Use of the BC/Al ratio for critical load computation

The limit is used in the critical load equation (13) in Section 6.4, in which section the derivation of the full Steady State Mass Balance Model used in the study is provided. Indicator organisms are intolerant of acidification when their BC/Al ratio has a high critical limit (e.g. 10). A high critical BC/Al ratio implies a low aluminum requirement. The result is that the indicator organism cannot sufficiently meet its requirement for base cation nutrients whenever the aluminum concentration increases (due to acidification) to a level where the BC/Al ratio becomes lower than, in the example above, 10. In turn, the supply of aluminum becomes toxic. The computed critical load for such indicator organisms will tend to be low, as can be seen from equation (5) where BC/Al appears in the denominator. A low BC/Al critical limit (e.g. 1) indicates a relatively high tolerance of aluminium, and the converse of the above reasoning can be applied. Indicator organisms with a low BC/Al ratio are relatively tolerant of acidification and, for a given weathering rate, higher critical loads will be calculated with a low BC/Al than a high BC/Al ratio.

Laboratory results

Relations between growth and Al, Ca/Al and BC/Al were tested respectively. BC/Al was the parameter that gave the best correlation. This pattern remained consistent for a range of species studied, with the only exception being *Arnika* spp. Figure 6.2 show the results from laboratory assays for Norway spruce (*Picea abies*). Data show that there are no differences in response between trees infected with mycorrhiza and plants without.

Figure 6.2 shows that a significant decrease in growth begins to become evident for a BC/Al ratio (note:BC=Ca+Mg+K) lower than 10. A growth reduction of 20% (to compensate for other than acidifying effects) would, following Figure 6.2, lead to a critical limit of BC/Al of 1. A value of BC/Al = 1 has been used for forest systems in Europe. Different BC/Al ratios have been derived for many indicator species (Sverdrup and Warfvinge, 1993). Values for several tree species occurring in China are available, and from available data they generally appear to be less tolerant of aluminium than European species. The available data include very intolerant tree species such as Mandarin fir (*Schima superba*), Chinese fir (*Cunninghamia lanceolata*) and Japanese cedar (*Cryptomeria japonicas*), but also conifers slightly less tolerant than European species, such as Masson pine (*Pinus massoniana*) and Armand pine (*Pinus armandii*). Masson pine (*Pinus massoniana*) and Mandarin fir (*Schima superba*) occur commonly throughout China. Sverdrup and Warfvinge (1993) estimate from botanical relationships that other tree species are as insensitive as many common European species. East Siberian fir (*Abies nephroleptis*) occurs throughout northern Southeast Asia in the colder regions; Altai spruce (*Picea obovata*) occurs on the northern border of the area presently mapped; *Picea smithiana, Abies pindrow* and *Abies spectabilis* occur in the Himalayas; *Picea spinulosa* is found in Bhutan; *Abies squamata* is found in western China;

and *Abies recurvata* is found in central China. The recommended BC/Al value for these species is 1-1.5.

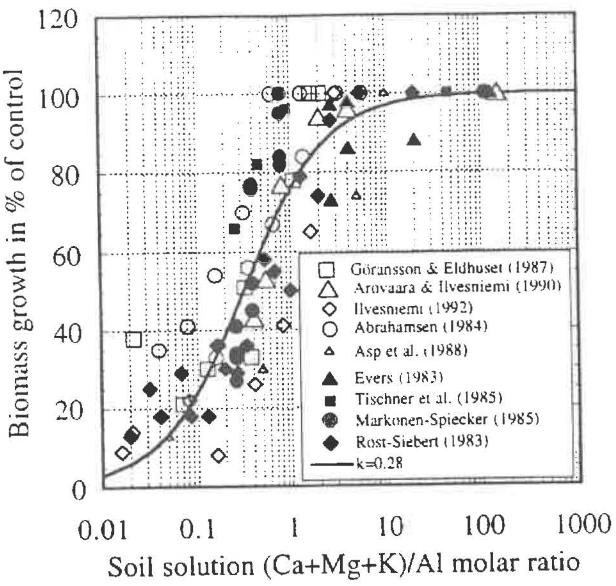

Figure 6.2 The relationship between laboratory observations of shoot and root growth for Norway spruce (*Picea abies*) and BC/Al ratios in the rooting medium. Open symbols represent Norway spruce of Scandinavian provenances; solid symbols represent German provenances. There is no significant difference in response between Scandinavian and German provenances.

Sverdrup and Warfvinge (1993) claim that due to biological relationships and the similar ecological distribution, a number of tree species are suspected of being as sensitive as Chinese fir (*Cunninghamia lanceolata*). Examples of such tree species occurring throughout Southeastern Asia are Chen fir, *Abies cheniensis* and *Abies delavayi* in southwestern China, *Abies fargesii* in western China, *Picea asperata*, *Picea likiangensis* and *Picea bractyla* in central China. For these the recommended limit is approximately BC/Al=10, considerably less tolerant than certain European species.

Response functions, as illustrated in Figure 6.2 have been derived for many species, and it has been shown that the uncertainty with which the response function can reproduce laboratory experiments is about 25% (see Sverdrup and Warfvinge, 1993). Table 6.2 provides an illustrative overview of plant species, the type of aluminum damage mechanism, the coefficient of the response function and the critical limit for BC/Al ratios at which growth has been reduced by 80% of normal. Other overviews of critical BC/Al ratios in general and for China in particular can be found in Annex 1. A complete overview can be found in Sverdrup and Warfvinge (1993).

Field responses

Field observations of tree growth decline in relation to soil chemistry are difficult to find. Often the growth data is semi-quantitative. The assessment of response curves to BC/Al ratios generally require: (1) data from different sources in order to generate sufficient data that adequately describes the response, (2) a wide range of studies from North America, France, Germany, Poland, Africa and China (3) datasets from experiments which were not completely controlled, or (4) data with an experimental design which was not fully described in the literature. Therefore, the data used are not all of the same quality and the accuracy and uncertainties involved may be large.

Growth response functions using field data have been based on an evaluation of French, North American, German, Polish, Liberian and Chinese data. The response curve based on field data has a similar shape to the response curve based on laboratory data for the same species. However, critical limits of BC/Al are often lower. This may indicate that the plant is subject to different BC/Al values in the rooting zone or that there is an interaction with other environmental factors. In the O- and E-layer, the BC/Al value may, under moderate acidification, be significantly different from the value in the B-horizon. Under laboratory conditions, the plants were generally exposed to uniform soil conditions, resulting in what is taken to be more conformable BC/Al values for all roots. Figure 6.3 shows the relation between field observations of growth decline and laboratory results for Spruce, indicating that the critical limit of BC/Al for spruce under field and laboratory conditions is about 0.5 and 1 respectively (80% growth of normal). This difference could be due to the heterogenous composition of BC/Al around roots under field conditions which increases the variability of critical limit estimates. Also, the data provides indications that the sensitivity may change over time as the plant grows older. Spruce appears to be intolerant when young, tolerant from 3-30 years and then intolerant again when the trees age. Orange, beech, oak and pine become less tolerant with age. However, care should be taken to clearly distinguish between the dynamic change of actual BC/Al values in the field (due to acidification) towards the critical limit BC/Al ratio, below which sustainability of an indicator organism is endangered.

Table 6.2 Response type and estimated aluminum damage coefficients for spruce, pine and other conifers[a]

Common name	Botanical name	Reaction type	K-value	BC/Al limit
Sitka spruce	*Picea sitchensis*	Unspecific	K=0.1	0.4
White spruce	*Picea glauca*	Unspecific	K=0.2	0.5
Black spruce	*Picea mariana*	Unspecific	K=0.25	0.8
East Siberian fir	*Abies nephroleptis*	n.d.	n.d.	1.0
Fir (China)	*Abies recurvata*	n.d.	n.d.	1.0
Fir (Himalaya)	*Abies pindrow*	n.d.	n.d.	1.0
Fir (Himalaya)	*Abies spectabilis*	n.d.	n.d.	1.0
Fir (Western China)	*Abies squamata*	n.d.	n.d.	1.0
Himalayan spruce	*Picea smithiana*	n.d.	n.d.	1.0
Spruce (Bhutan)	*Picea spinulosa*	n.d.	n.d.	1.0
Altai spruce	*Picea obovata*	n.d.	n.d.	1.0
Balsam fir	*Abies balsamea*	Unspecific	K=0.3	1.1
Norway spruce	*Picea abies*	Unspecific	K=0.35	1.2
Red spruce	*Picea rubens*	Unspecific	K=0.35	1.2
Fraser fir	*Abies fraseri*	Unspecific	K=0.35	1.2
Silver fir	*Abies alba*	n.d.	n.d.	1.4
Faber fir	*Abies fabri*	n.d.	n.d.	1.6-2.2
Chen fir (Sw. China)	*Abies cheniensis*	n.d.	n.d.	10
Fir (Southw. China)	*Abies delavayi*	n.d.	n.d.	10
Fir (Western China)	*Abies fargesii*	n.d.	n.d.	10
Spruce (Cent.China)	*Picea bractyla*	n.d.	n.d.	10
Spruce (China)	*Picea likiangensis*	n.d.	n.d.	10
Chinese fir	*Schima superba*	Unspecific	K=2	10
Mandarin fir	*Cunninghamia lanceolata*	Unspecific	K=6	20
White pine	*Pinus strobus*	Vanselow	K=0.000002	0.5
Aleppo pine	*Pinus halepensis*	Vanselow	K=0.000002	0.5
Slash pine	*Pinus elliottii*	Vanselow	K=0.000002	0.5
Sand pine	*Pinus clausa*	Vanselow	K=0.000004	0.6
Shortleaf pine	*Pinus echinata*	n.d.	n.d.	0.6
Monterrey pine	*Pinus radiata*	Vanselow	K=0.00008	0.8
Armand pine*	*Pinus armanii*	Vanselow	K=0.000015	1*
Cembra pine	*Pinus cembra*	n.d.	n.d.	1-1.2
Mountain pine	*Pinus mugo*	n.d.	n.d.	1-1.2
Scots pine	*Pinus sylvestris*	Vanselow	K=0.00002	1.2
Virginia pine	*Pinus virginiana*	Vanselow	K=0.00002	1.2
Pitch pine	*Pinus rigida*	Vanselow	K=0.00002	1.2
Jack pine	*Pinus banksiana*	Vanselow	K=0.00003	1.5
Loblolly pine	*Pinus taeda*	Vanselow	K=0.00003	1.5
Longleaf pine	*Pinus palustris*	Vanselow	K=0.00005	2
Ponderosa pine	*Pinus ponderosa*	n.d.	n.d.	2
Red pine	*Pinus resinosa*	n.d.	n.d.	2
Masson pine**	*Pinus massonii*	Vanselow	K=0.0001	4
Western red cedar	*Thuja plicata*	Vanselow	K=0.0000001	0.09
North. white cedar	*Thuja occidentalis*	n.d.	n.d.	0.1
Western hemlock	*Tsuga heterophylla*	Vanselow	K=0.0000003	0.2
Douglas fir	*Pseudotsuga menziesii*	Vanselow	K=0.000004	0.6
Japanese cedar	*Cryptomeria japonica*	n.d.	n.d.	0.8-1.2
Larch	*Larix decidua*	Vanselow	K=0.00005	2

[a]The BC/Al-limit represents growth reduced to 80% of normal. *: BC/Al - crit = 0.5,based on field estimate. **: BC/Al - crit = 2.0 under field conditions.

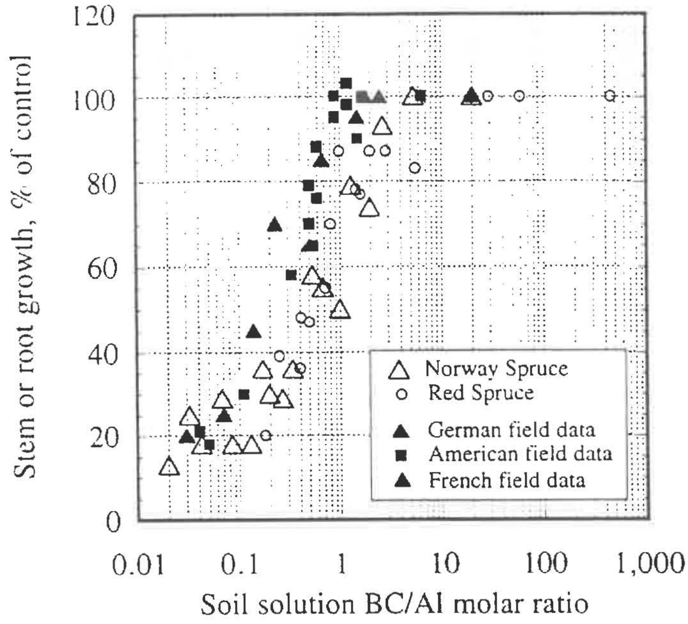

Figure 6.3 The relationship between field and laboratory observations of growth and the rooting medium BC/Al molar ratio (for Norway and Red spruce)

Results

Table 6.3 gives an overview of the BC/Al ratios which have been used as critical limits for each of the vegetation types distinguished in the study region. A map of the BC/Al ratios is displayed in Figure 6.4. High levels of BC/Al ratios indicate low tolerance to acidification.

Additional data required for applying the Steady State Mass Balance approach:

In order to calculate critical loads with the SMB, values for soil depth, gibbsite and base cation uptake coefficients are required. The values of the gibbsite coefficient vary with soil depth and organic content of the soil. The type of vegetation was used to estimate average rooting depth within each ecosystem class and the content of organic matter. Typically, a purely organic soil such as peat, will be given the value $pK_{gibb}=6.5$ ($K_{gibb}=3$). A soil consisting of pure mineral material without any organic matter is given the value $pK_{gibb}=9.2$ ($K_{gibb}=1500$). The values are shown in Table 6.3 for each vegetation type.

Table 6.3 Proposed model entry values for calculation of critical loads (BC/Al values) using the Steady State Mass Balance Model (low values indicate high tolerance; high values, low tolerance to acidification)and other data input for SSMB

Vegetation type	BC/Al limit suggested for use in SSMB approach	Rooting depth meter	Gibbsite coefficient	pK_{gibb}	BCu[1]
Polar or rock desert	6	0-0.1	150	8.1	0
Tundra	2	0-0.2	150	8.1	0
Cool semi-desert/ scrub	2	0-0.3	150	8.1	0
Montane cold scrub/grass	2	0-0.3	150	8.1	0
Cool scrub/Grassland	2	0-0.3	150	8.1	0
Main taiga	1	0-0.5	300	8.5	250
Southern taiga	1	0-0.5	300	8.5	250
Coniferous forest	1.5	0-0.5	300	8.5	250
Mixed forest	1	0-0.8	300	8.5	250
Temperate broadleaf forest	0.6	0-0.8	300	8.5	250
Interrupted temperate woods	1	0-0.5	300	8.5	100
Dry/highland woods	2	0-0.5	300	8.5	100
Mediterranean woodland	1	0-0.5	300	8.5	100
Interrupted tropical woods	2	0-0.5	150	8.1	0
Subtropical dry forest	2	0-0.5	300	8.5	100
Subtropical wet forest	1	0-0.2	150	8.1	0
Tropical dry forest	1	0-0.5	300	8.5	100
Tropical wet forest	0.6	0-0.2	150	8.1	0
Tropical savanna	10	0-0.5	300	8.5	100
General farmland	10	0-0.3	200	8.3	0
Irrigated paddy	10	0-0.3	200	8.3	0
Irrigated other farmland	10	0-0.3	200	8.3	0
Coastal wetland, cold	10	0-0.5	300	8.5	0
Coastal wetland, mangrove	10	0-0.5	300	8.5	0
Coastal wetland and hinterland	10	0-0.5	300	8.5	0
Hot scrub/Grassland	10	0-0.3	200	8.3	50
Succulents and thorn dry woods	10	0-0.3	200	8.3	50
Semi-arid forest	10	0-0.5	200	8.3	50
Non-polar rocky vegetation	10	0-0.2	300	8.5	0
Sand desert	10	0-0.5	300	8.5	0
Semi-desert	10	0-0.5	300	8.5	0

(1) A map of the of base cation uptake is given in Annex 1

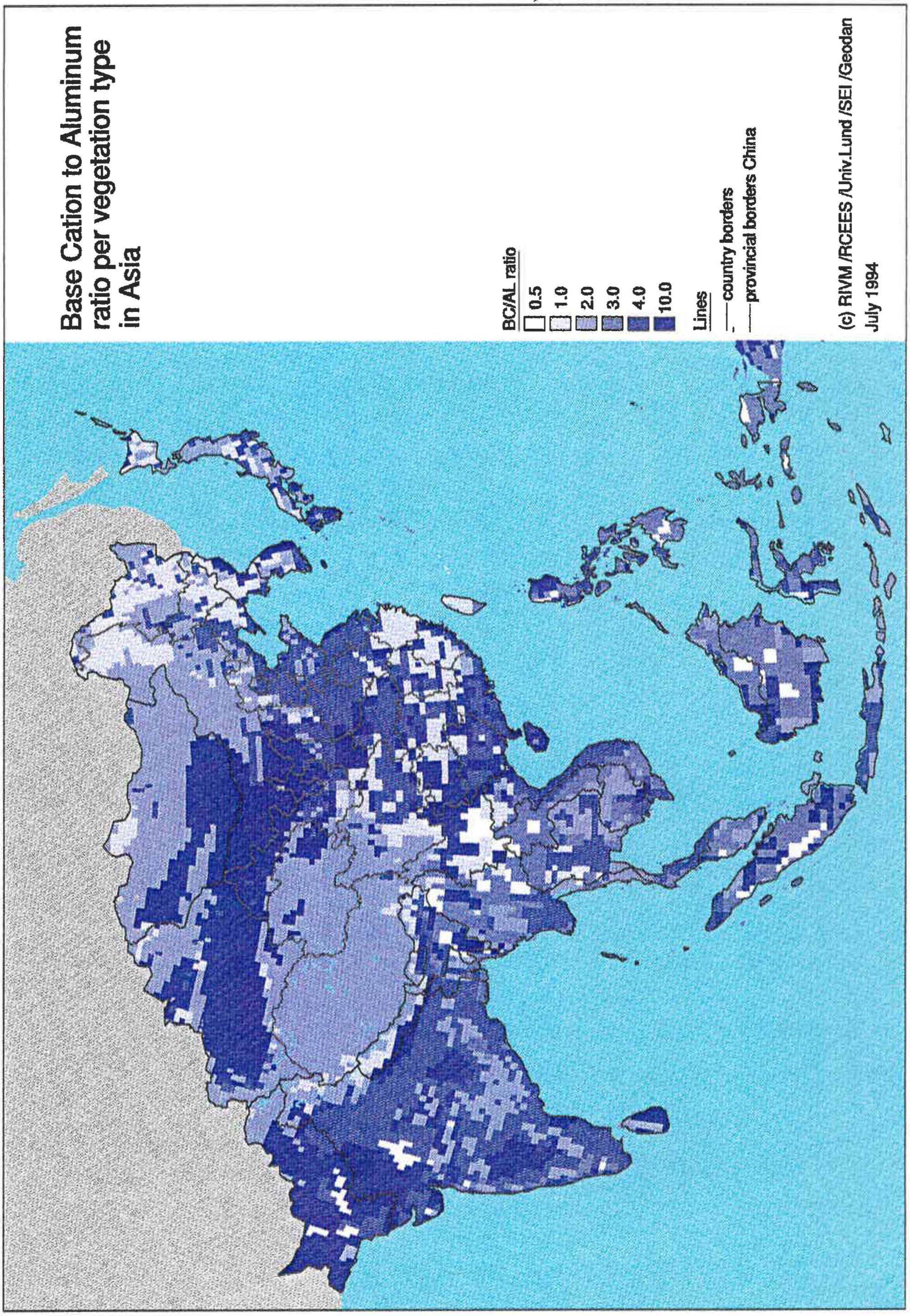

Figure 6.4 Map of critical base cation to aluminium ratios used in the application of the Steady State Mass Balance Model for the computation of critical loads (see Section 6.4)

6.2.4 The basis of the relative sensitivity approach

The method for the evaluation of the sensitivity of Asian ecosystems to acidic deposition is outlined in Section 6.3. In the following section the theoretical basis and background for the evaluation of vegetation types is discussed. The sensitivity method relies on ranking factors in order of their perceived effect on response to acidic deposition.

Defining sensitivity of ecosystems

The sensitivity of an ecosystem to indirect effects of acidic deposition relies upon changes in physicochemical characteristics of the soil that induce responses in ecosystem structure and function. Some of these buffering systems are related to the processes within the soil and these are covered in this project by a consideration of the relative rate at which acidic deposition is buffered by means of weathering processes (see Section 6.3.3 and Annex 2).

An understanding of certain ecosystem features is required for the sensitivity assessment. One feature is to determine the typical buffering rate of sites where vegetation types commonly occur and another to assess the changes in buffering conditions which will lead to change in ecosystem structure and function. The acidic deposition rate required to force the ecosystem soil reaction (the stable buffering condition) to the threshold buffering condition needs to be assessed as this acidic deposition rate is a measure of the sensitivity of the ecosystem. These features may be described in terms of buffering, vegetation tolerance and resulting ecosystem sensitivity. The buffering in the ecosystem will determine the degree of soil chemistry response. The vegetation tolerance will determine the degree to which biotic elements respond to a given change and the thresholds of response, and the sensitivity describes a synthesis of these features. These are considered to be fixed descriptive ecosystem features. An ecosystem where vegetation is tolerant of acidic conditions may well be very sensitive if the buffering rate is low. Alternatively, ecosystems where vegetation is intolerant of acidic conditions may well be insensitive due to high rates of buffering.

The time dependency of damage and recovery is a function of ecosystem response, which could be seen to be related to ecosystem sensitivity. Buffering processes and vegetation tolerance may change as the ecosystem acidifies, but this is considered to be a 'damaged' ecosystem which should be brought back to threshold buffering conditions by reductions in acidifying inputs.

Assessment of sensitivity from vegetation type distribution

The vegetation type present at a site integrates the different environmental factors at that site, the presence of that vegetation indicating the selection by site factors to maintain the existing vegetation. Thus, the vegetation present can be used to indicate the sensitivity of an ecosystem to the prevailing site factors. The vegetation type gives an indication of the buffering rate, considered to be a mixture of the buffering mechanisms in the soil (neutralizing acidic deposition), and the biological dynamics of the system that buffer (such as nutrient cycling rates). Different vegetation types have a typical tolerance to acidic conditions. The use of vegetation type to give indications of the buffering rate of the ecosystem overlaps with the use of soil data to give similar indications. Such a combination is designed to compensate for the poor data quality and increase confidence that ecosystem sensitivity may be reasonably identified.

Vegetation types are generally adapted to soils of a specific fertility and pH. This means that vegetation types can indicate the typical buffering rate of the soil. Another feature that readily delimits different vegetation types is the moisture status of the soil. In dry areas the soil will tend to have little organic matter and will not be heavily leached, entailing that there will still be a high mineral content of these soils. In the dry areas there is a net upward movement of water through the year leading to an accumulation of weathering products that buffer the ecosystem to acidic deposition. In contrast, soils in very wet areas may either be heavily leached and weathered or have a thick layer of acidic organic matter, shown in the extreme by peat formation in cold wet areas. All these aspects influence the ability to buffer acidifying inputs and are used to indicate ecosystem sensitivity.

In different ecosystems the flux of nutrients occurs at different rates through the ecosystem. In many tropical systems, such as tropical rain forests, the flux is very rapid. This increases the apparent concentration of nutrients so that the plants may not be so influenced by an increase in the acidity or aluminum concentrations. In contrast, vegetation in cold montane environments will have very slow nutrient circulation rates and will be more sensitive to changes as the buffering by this mechanism is relatively poor. Other factors that may be extracted from the type of vegetation includes flooding (by the sea or rivers) and also the influence of land use and anthropogenic management influences. The most drastic of these is the liming of agricultural land which will neutralize high rates of acidic deposition.

The threshold buffering point is related to a number of features. These include the response to aluminum in the soils, the response to changes in the nutrient status and to other stressing factors such as temperature. The additional stress of acidic deposition to the exposure of plants in a cold climate may tend to make the vegetation in these areas more prone to damage and therefore more sensitive to the changes caused by acidification.

Buffering is considered to play a greater role in controlling response than the tolerance because differences in buffering rates of ecosystems have a wider range than the tolerance to acidic conditions. This is related to the fact that the most dramatic changes in phytotoxic ion concentrations and the change in nutrient availability and form occur over a fairly small pH range, between about pH 5.0 and 4.2. At pH of about 4.2 there is an exponential rise in aluminum concentrations; the dominant form of nitrogen is ammonium rather than nitrate in soils of pH lower than 5.0; phosphate availability decreases drastically below pH of about 5.0 (Jordan, 1985). These are some of the main changes in soil water chemical composition that give rise to noticeable effects in vegetation structure and function. Buffering systems that will maintain ecosystems above pH of about 5.5 to 6.0 likely ensure that little change in ecosystem structure and function will occur.

In areas where buffering systems allow the pH to fall below 5 and particularly below 4.0-4.2 under the influence of acidic deposition effects are likely to be seen. There are ecosystems that naturally exist in acidic conditions with pH below 4.2. Plants in those sites are therefore naturally adapted to acidic conditions but, on addition of extra acidity there is an exponential change in soil conditions (such as the increase in aluminum) that will still lead to effects, irrespective of the fact that plants are tolerant.

In conclusion the allocation of vegetation types to classes indicating ecosystem sensitivity was made by considering a number of factors related to the buffering of the ecosystem against effects (Table 6.4).

Table 6.4 The factors that influence the assignment of vegetation types into classes that indicate ecosystem sensitivity

I	The likely mineralogy and soil buffering rate under different vegetation types and soil acidity;
II	The water regimes in relation to the soil group (dry = pedocal; wet = pedalfer);
III	Occurrence of flooding (by river or sea);
IV	The overall rate of nutrient circulation, decomposition and organic matter composition and depth under vegetation types and rooting depth of dominant species;
V	Occurrence of stressing factors such as exposure to wind and cold;
VI	Tolerance of vegetation to acidic conditions.

Most of the attributes of vegetation type used here refer to the buffering rate of the ecosystem although some refer to the tolerance of the vegetation to increasing soil acidity. In the following sections each of these factors is investigated and then the influence of these on the classification of Asian vegetation types is explained. It should be realised that this exercise is carried out with incomplete knowledge of Asian ecosystems requiring many assumptions using theoretical considerations synthesising experimental data, observations of vegetation distributions relative to physical and chemical factors and the response of ecosystems to acidic deposition. This experience is mainly from Europe and North America. It represents not a definitive classification, rather a framework that may be used to evolve and improve our understanding of Asian ecosystem response.

I Vegetation types and soil fertility

There are certain vegetation types which are readily associated with certain soil pH conditions. These include vegetation types such as dry calcareous grasslands, found on high pH, limestone containing soils, and conifer forests mainly found on acidic or moderately acidic soils. Deciduous forests tend to be found on less acidic soils. Naturally these represent generalisations, and do not apply to all species in all situations. Further, Asian specific data will allow for better approximations.

Over fifty per cent of wet tropical soils in Amazonia (as an example) are represented by highly weathered acid soils which are dominated by the minerals kaolinite, quartz and oxides of aluminium (such as gibbsite) and iron (hematite) (Kronberg *et al.*, 1979). Therefore, ecosystem types typical of these soils are considered to be sensitive due to very low weathering rates. These include lowland tropical rain forest exists to a large extent on very acidic, highly weathered soils with high aluminium contents and very low base saturation on the mineral colloids (cation exchange capacity (CEC) tends to be low). Therefore, additional acidic deposition could either lead to increased nutrient leaching (conditions for leaching are good due to the high water flux, but combated by efficient recovery by dense root mass in the organic horizons), or increased dissolution of aluminium which could be toxic to plant roots (even though rain forest tree species tend to have high tolerance to aluminium). Phosphate availability is low in these soils and additional acidification could make availability even lower. Monsoon forests are expected to have similar soil characteristics and are therefore expected to be sensitive.

In more temperate regions, with lower rainfall the weathering processes are not as rapid and soil is not as highly weathered and therefore these ecosystems will tend to be less sensitive. In the seasonal tropics and Mediterranean climates montmorillonite is common (Jordan, 1985). In drier or colder areas there are higher amounts of weatherable mineral of higher nutrient content and also on steep slopes in wet tropical areas, where there is constant removal of weathered material exposing the parent material to a greater extent than in lowland humid tropical areas. Soil conditions in very dry areas will have higher ability to buffer and this is explained in the next section.

II Vegetation types classified by soil water regimes

In dry areas there is a net upward rather than downward movement of water through the upper soil horizons. This is due to the relatively high evapotranspiration relative to precipitation rates. This net upward movement of water leads to the accumulation of the products of weathering which precipitate out in the upper soil crust (forming a "pedocal") and are available to buffer the acidic deposition. Ecosystems with such vegetation types will be insensitive to acidic deposition. The typical arid vegetation types which fall into this category include desert, semi-desert and dry scrub and dry grassland. Where soil moisture is higher leaching of base cations may occur and such ecosystems are potentially sensitive to acidification. As moisture increases the potential for base cation leaching will also increase leading to conditions more conducive for acidification.

III Vegetation types with frequent flooding

Certain vegetation types are subject to frequent flooding either by the sea or by rivers or by anthropogenic irrigation. This water often carries with it substantial amounts of silt and mud, high in pH, nutrients and weatherable materials. This will buffer the acidic deposition and lead to low sensitivity of these ecosystem types. These include irrigated farmland, paddy fields and flood plains.

Areas frequently flooded by the sea are also considered insensitive to acidic deposition. Seawater is of high pH and will neutralise any acidic deposition causing indirect effects to be irrelevant for the vegetation. Mangrove swamp is the main ecosystem type.

IV Nutrient circulation rates within ecosystems

In different ecosystems the circulation rates of nutrients and energy differs greatly. The rate of growth of plants depends on the availability of nutrients and energy and nutrient availability is controlled by the activity of the different ions rather than the concentrations. In ecosystems where there is a high rate of decomposition, nutrient uptake and high conservation of nutrients, the system may be more resilient to the acidic deposition. A very rapid circulation of a limited amount of nutrients is considered equivalent, in terms of the nutrient provision to the plants, to higher concentrations but with lower rates of circulation. Therefore, conifer forests have a lower buffering rate than deciduous forests due to the higher rates of transfer in deciduous forests (forming a mull instead of more humus). This is particularly related to the decomposition rate which is greatly influenced by the leaf substrate produced by different species and also on the soil temperature and moisture. In cold heathland and bog vegetation the decomposition rates are low due to cold temperatures, the high lignin content of the leaves, high C:N ratios of the leaf litter and presence of anaerobic conditions. Therefore, tundra and bog ecosystem will tend to have higher sensitivity due to nutrient limitations. The acidic deposition could result in even lower rates of decomposition and nutrient availability. Those vegetation types that have deep roots which reach as far as the less weathered material will be able to absorb nutrients from these horizons and these may eventually enrich surface soil horizons and tend to make the entire ecosystem less susceptible to acidification. For this reason the temperate deciduous forest ecosystem tend to be of lower sensitivity than temperate conifer forests due to the deeper roots. A low proportion of nutrients in tropical rain forests derive from the soil (in acidic soils) and these plants tend to have shallow roots.

In tropical rain forests the net primary productivity is very high, but the soil organic carbon level is much lower than in cooler climates (Jordan, 1985). This rapid decomposition and nutrient cycling will tend to make the tropical rain forest less sensitive than would be expected from the very acid soil conditions that these forests tend to exist.

V Interacting stress factors

It is considered that ecosystems of highly stressed environments, and which are sensitive due to low buffering rates will have increased sensitivity to acidic deposition. Plant species growing at the limit of their range will have decreased tolerance to any external stress. The main stress linked to this is due to conditions in cold environments such as high altitude non-tropical areas. These ecosystems include tundra, boreal forests and the Himalayan region.

VI Tolerance of acidic conditions

Ecosystems where vegetation types indicate acidic soils will generally contain vegetation tolerant of acidic conditions. and conversely vegetation adapted to alkaline soils will be intolerant of acidic conditions. This is taken into account in the assessment but it is held that the information concerning the buffering ability of the ecosystem that the vegetation type imparts has greater influence than the relative tolerance of the vegetation to the acidic conditions. However, the tolerant vegetation types modify the classification of sensitivity by causing these to have lower sensitivity. For this reason, vegetation types such as conifer forest and tropical rain forest are not in the highest class of sensitivity (Table 6.7) as might be expected from buffering conditions.

Classification

Table 6.5 shows the influence of the six factors in the classification of vegetation types into classes that represent different sensitivity to acidic deposition. Not all factors were used to classify every vegetation type but the table shows which factors influenced the classification of different vegetation types and some information as to how these factors influenced the classification. For each vegetation type the information is summarised in Table 6.6.

Table 6.5 Ecological factors influencing vegetation classification

Vegetation type	Factors Soil buffering ability	Soil moisture	Occurrence of flooding	Influence of nutrient circulation rooting depth/ organic matter type	Stressing factors (temperature)	Tolerance of aluminium	Sensitivity	Class
Desert/ semi-desert	very high	very dry		-		-	insensitive	6
Mangrove	-	-	flooding by sea	-	-	-	insensitive	6
Irrigated land/ paddy land	high	-	seasonal flooding	-	-	-	insensitive	6
Thorn woods/ semi-arid woods	high	dry	-	deep roots allow access to high buffering soil layers	- -	- -	slightly sensitive	5
Dry tropical/ sub-tropical woods/savannah	medium	medium/ dry	-	deep roots	-	-	moderately sensitive	4
Agriculture	mediumj/ high	moist	-	addition of nutrients/ management (liming not always used)	-	may be relatively intolerant	moderately sensitive	4
Cool scrub/ grassland	medium	moist	- -	moderate circulating rates decomposition rates	-	-	sensitive	3
Temperate broad-leaved	medium-poor	moist	-	moderate circulation of nutrients and mull humus. Deep roots - access to nutrients in lower soil horizons	-	moderate tolerance	sensitive	3

Table 6.5 (Cont.)

Vegetation type	Soil buffering ability	Soil moisture	Occurrence of flooding	Influence of nutrient circulation rooting depth/ organic matter type	Stressing factors (temperature)	Tolerance of aluminium	Sensitivity	Class
Tropical montane forests	medium (thinner less weathered soils on steep slopes	moist	-	relatively rapid circulation rates	-	moderate	sensitive	3
Conifer forest/ mixed forest	poor	moist	-	low decomposition; mor humus; shallow roots	-	moderate/ high	very sensitive	2
Heath/moor-land/bog	poor	moist/ wet	-	low decomposition; mor humus; shallow roots	-	moderate/ high	very sensitive	2
Wet tropical forest	very poor	very wet	-	rapid decomposition; shallow roots	-	high	very sensitive	2
Tibetan cold grass	poor	wet	-	slow decomposition	very cold - stressed vegetation	-	very sensitive	2
Main/ southern-northern Taigo	poor	moist/wet	-	mor humus; low decomposition rates	cold - additional stress	moderate/ high	highly sensitive	1
Tundra	poor	wet		mor humus; low decomposition	cold stress	moderate		1

- = not included in assessment

Table 6.6 Summary of influential factors determining the method of classification for each vegetation type

Vegetation type	Relevant ecological factors
Desert/semi-desert	Buffering rates of desert soils is very high and dry conditions restrict leaching of base cations; insensitive
Mangrove	Flooding by sea; anaerobic conditions - indirect effects of acidic deposition unimportant
Irrigated land/paddy	Seasonal flooding with silt laden waters; insensitive
Semi-arid and thorn woods	High buffering rate; deep rooting; relatively insensitive. Higher water availability gives rise to seasonal leaching; more sensitive than desert vegetation
Dry tropical/sub-tropical woods/ savanna	Soils may be of varying buffering quality; seasonal rain results in leaching. Deeper rooting give access to deeper soil horizons; moderately sensitive
Agriculture	Generally on moderately to fertile soils - high buffering ability; possibility of acidification where liming not practised; Poor management of moderately fertile soils and low tolerance to acidic conditions - potentially sensitive in Asia.
Cool scrub/grassland	Wetter conditions implies possibility of leaching; medium buffering conditions; sensitive conditions.
Temperate broadleaf woodland	Mesic soil conditions; medium to poor buffering conditions; sensitive to acidic deposition (relatively rapid decomposition and circulation rates; mull humus and deep roots render it less sensitive than conifer forest (next class)
Tropical montane forest	Moderate soil buffering ability - exposure of higher buffering soils on steep slopes in tropics; montane tropical forest less sensitive than other wet tropical forest
Other conifer trees	Soil buffering ability low; decomposition and nutrient circulation rates are low - mor humus formation makes nutrients unavailable; generally shallow roots - limited access to lower, well buffered horizons; very sensitive.
Bog/mire/moor/heath	Poor, acid soil; low decomposition rates - mor humus with low nutrient availability; wet conditions - rapid nutrient leaching; very sensitive.
Wet tropical forest	very acid soils - extremely low weathering rates; very wet conditions ideal for nutrient leaching - ecosystem already nutrient poor; tight nutrient cycling, rapid decomposition rates and high tolerance to aluminium decreases sensitivity; very sensitive
Tibetan cold grass	Assumed poor soil quality, slow decomposition rates and low nutrient availability; exacerbated by the exposure to extreme conditions; very sensitive
Northern/main/southern Taiga	Sensitivity of the Taiga conifer woods is high as for conifer trees; exacerbated by the additional stress of the harsh climate; highly sensitive
Tundra	Assumed to grow on acidic soils; slow decomposition rates as for bog and moorland; higher sensitivity due to the extreme climate; highly sensitive

The classification of the main vegetation types found in Asia from the reasoning in Table 6.5 and 6.6 is summarised in Table 6.7. The reclassified vegetation map showing the distribution of sensitivity according to distribution of vegetation types is shown in Figure 6.5.

In order to use vegetation type alone to determine sensitivity a very detailed description of the distribution of ecosystems would be required. For example the distribution of eutrophic, mesotrophic and oligotrophic rain forest would be required. However, the data available only show the distribution of "rain forest". This is also true of other vegetation types. However, the vegetation type classification does give valuable information concerning the sensitivity of ecosystems to acidic deposition but in order to gain more detailed information it is also necessary to look at the buffering ability of the soil in the different regions. A more detailed soil map is available than vegetation map and data exist that can link different soil types to buffering rates and mechanisms operating in different areas. This is further described in Section 6.3.

Table 6.7 Classification of ecosystem sensitivity according to vegetation type characteristics

Class	**Ecosystem Types**
Ecosystems of low sensitivity	
6	desert; semi-desert; irrigated/paddy land
5	thorn woods; semi-arid woods
4	dry tropical/sub-tropical forest; savanna; agricultural land
3	cool scrub; grassland; temperate broadleaf woodland; tropical montane forests;
2	conifer forest; mixed forest; tibetan cold grass; moor; bog; mire; wet tropical forest
1	tundra; main Taiga; northern and southern Taiga
Ecosystems of high sensitivity	

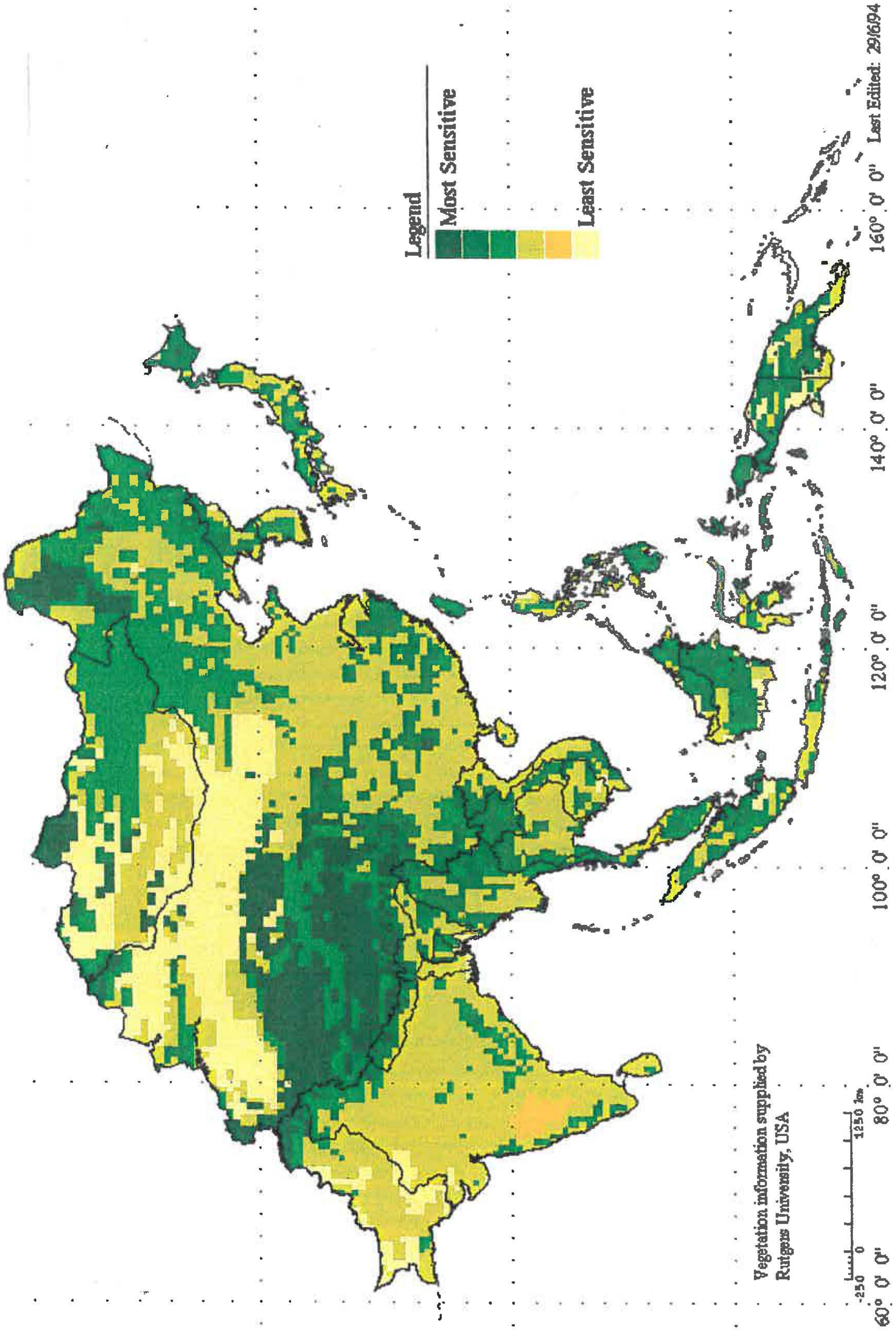

Figure 6.5 The classes of sensitivity derived from vegetation type (SEI based on Rutgers University data)

6.3 Background data and mapping the sensitivity in Asia

S. Cinderby, J.C.I. Kuylenstierna and M.J. Chadwick

6.3.1 Introduction

The effects of acidic deposition have been widely studied in Europe and North America and it has been possible to make predictions about the effects on structure and function of both terrestrial and aquatic ecosystems. This has been carried out both by the application of process models on detailed data and by simpler methods applied on a wider area where information is not so readily available. One of the methods used in Europe has been to assess the relative sensitivity of ecosystems to acidic deposition which has been used in the RAINS-ASIA project in combination with the Steady State Mass Balance Model to produce a critical loads map. In the development of the IMPACT module of the RAINS-ASIA model the role of the sensitivity mapping has been to assess (1) data inputs to both the Method of Relative Sensitivity and the Steady State Mass Balance Model, (2) include ecological considerations in addition to the biogeochemical basis of the Steady State Mass Balance Model, and (3) the geographic distribution of sensitivity as an aid to verify the distribution of critical loads over Asia thus enhancing the reliability of the results.

It has been possible to determine the main factors that control acidic deposition induced changes. Reactions of plant communities are difficult to predict but experiments and observation have shown changes in ecosystem function; acidification entails a reduction in the growth rate of key species of plant communities due to decreases in nutrient availability and increases in toxic ion concentrations. Differential changes in the growth of species would be expected to give rise to changes in plant community structure (species composition and diversity). The same ecological principles which determine the sensitivity in Europe and North American ecosystems will apply to ecosystems in Asia. However, Tropical ecosystem dynamics will result in differences in response than predicted from temperate ecosystems (McDowell, 1988). There have been studies into the potential effects of acidification in Asia and on tropical ecosystems in general (Rodhe and Herrera, 1988; McDowell, 1988; Galloway, 1988; Sanhueza *et al.*, 1988; Moreira *et al.*, 1988; Isichei and Akerdolu, 1988; Liping and Chuying, 1991; Chuying *et al.*, 1991; Fuzhu *et al.*, 1991; Zongwei and Yunfeng, 1991; Rodhe, 1989) and preliminary attempts at mapping sensitivity to acidic deposition have been made for parts of Asia (Bhatti, Streets and Foell, 1991; Wada, Iwasa and Arimitsu, 1983; Kuylenstierna, Cinderby and Chadwick, 1992).

Section 6.3 outlines the data and methods required to identify areas where the terrestrial ecosystems will be susceptible to changes in structure and function i.e. are sensitive to acidic deposition. The method outlined here refers to a relatively simple assessment of sensitivity in Asia, but the data described is both used in the assessment of sensitivity and in the calculation of SMB critical loads.

6.3.2 Background for the sensitivity mapping

The aim of mapping sensitivity is to create a distribution of ecosystems that have different relative reactions to a given rate of acidic deposition, and to do this with relatively limited, generally available small-scale (continental) spatial data. Methods are available that allow determination of the sensitivity of both terrestrial and aquatic ecosystems. Initially, however, only the sensitivity of terrestrial ecosystems has been assessed. This is due to the difficulty in obtaining mapped data describing the quality of the baseflow influencing the buffering capability of aquatic ecosystems. In many areas of Asia old acidic soils overlie calcareous bedrock which will provide a heavily buffered baseflow to lakes even though the terrestrial ecosystem is poorly buffered and sensitive to acidic deposition.

Theory of sensitivity mapping

The sensitivity assessment is based upon the existence of buffering systems in ecosystems that partially resist changes induced by acidic deposition and the environmental characteristics determining the different distribution of plant species as discerned by observation, analysis and experimentation. These features are combined in the methodology to determine the distribution of terrestrial ecosystems that have different relative sensitivity.

The sensitivity assessment used in Asia uses information concerning the distribution of vegetation and soil types and then combines the information imparted from these sources of data. These factors are used as surrogates for other ecosystem information known to be relevant in the buffering of acidic deposition.

The sensitivity method could attempt to map vegetation type alone to give an approximate assessment of the distribution of sensitivity but experience in the development of the sensitivity methodology in Europe and elsewhere suggest that one data layer alone is insufficient (Kuylenstierna and Chadwick, 1989; Lucas and Cowell, 1984). The reasons for this include the fact that few current vegetation types have distributions unaltered by anthropogenic influence and also because the disaggregation of the vegetation and land use data available for the Asian continent is too poor for this to be used alone to determine sensitivity distribution. The land cover classification (Section 6.3.3; vegetation data) is limited (there is no indication of species composition and it shows only dominant land use in relatively large grids, about 50x50 km at the equator). Therefore, both in Europe and in Asia, buffering system characteristics are also estimated from edaphic characteristics and climatic data and inclusion or further data layers enhances the eventual distribution of sensitivity.

6.3.3 Data for sensitivity and critical load mapping

The IMPACTS group of the RAINS-ASIA project focused on delimiting the environmental effects of acidic depositions in the Asian region. The production of maps showing the relative sensitivity of ecosystems, Steady State Mass Balance computations of critical loads and their geographical distribution all required the collection and modelling of a large number of spatial data sets. The inputs to the modelling procedure describe the areal distribution of parameters influencing the soil weathering conditions and the sensitivity distribution indicated by the vegetation characteristics. These spatial data were obtained from a number of different sources and in a variety of formats. The data were first entered into a geographic information system (GIS). This procedure constrained the data to a common map projection and spatial extent. The base data were then modified and combined within the GIS to produce the derived data needed to construct the various result maps. These basic data sets utilised for the mapping programme will be described in this section. Details about the datasets and derivation methods are described in Annex 2.

The data inputs to the mapping programmes can be seen in Table 6.8. The use of the various data sets by the relative sensitivity assessment and the Steady State Mass Balance estimation of critical loads can be seen in Table 6.9 and in Figure 6.6. The inputs can be subdivided into four main groups: climate data, soil data, geological data and vegetation data. The data

Table 6.8 GIS Manipulation by SEI

Data Type	**Source Format**	**Original**	**GIS Manipulation**
Climatic Data:			
Precipitation (P)	WMO and ASEAN Institute Climatic Atlases	1:10 000 000 scale paper maps	Combined within the GIS to form complete regional cover
Potential Evapo-transpiration (PE)	FAO Climate Data	Point Measurements	Interpolated points data to contour maps
P:PE Ratio	SEI	SPANS GIS File	Produced by division of the two input layers
Ground Water Flux	SEI	SPANS GIS File	Reclassification of P:PE
Effective Tempera-ture Sum	FAO	Point Measurements	Variable modelled and interpolated within GIS
Base Cation Deposition	G. Carmichael, University of Iowa	Paper diagrams	Variable modelled within GIS
Soil Data:			
Soil pH	FAO	1:5 000 000 Arc/Info GIS Files	Soil types reclassified into pH units within the GIS
Soil Texture	FAO	1:5 000 000	Soil types reclassified into
Arc/Info GIS Files	texture classes within the GIS		
Geology Data:			
Geology	UNESCO	1:10 000 000 scale paper maps	Selectively digitised by SEI
Soil Buffering Ability Data:			
Weathering Rates	University of Lund	1:10 000 000 scale SPANS GIS File	Derived from the above data through GIS modelling
Relative Soil Buffering Ability	SEI	1:10 000 000 scale SPANS GIS File	A reclassification into relative classes of the above numeric data layer
Vegetation Data:			
Vegetation and Land Use	Rutgers University	0.5^o*0.5^o GRASS GIS raster file	Converted into SPANS GIS file format
Sensitivity from Characteristics	SEI	SPANS GIS File	Reclassification of Vegetation map

Table 6.9 The use of data sets within the RAINS-ASIA mapping programme

Data Type	Implemented by Relative Sensitivity Method	Implemented by Simple Mass Balance Method	Application of Data
Climatic Data:			
Precipitation (P)	✓	✓	Used in calculation of P:PE
Potential Evapo-transpiration (PE)	✓	✓	Used in calculation of P:PE
P:PE Ratio	✓	✓	Effectiveness of precipitation
Ground Water Flux (Q)		✓	Estimates groundwater flows
Effective Temperature Sum	✓	✓	Estimates effect of temperature on rate of chemical weathering
Base Cation Deposition		✓	Estimates amount of base cations entering soil system from the atmosphere
Soil Data:			
Soil pH	✓	✓	Initial base weathering rates set from soil pH
Soil Texture	✓	✓	Weathering rate modified by soil texture
Geology Data:			
Geology	✓	✓	Modifies weathering rate of lithosols
Vegetation Data:			
Vegetation and Land use	✓	✓	Dominant land cover
Sensitivity from Vegetation Characteristics	✓		Distribution of the sensitivity of vegetation to acidic deposition
BC/Al Ratio		✓	Distribution of plant tolerance to aluminium in solution
BC Uptake		✓	Uptake of BC nutrients by vegetation
K Gibbsite		✓	Dissolution coefficient of aluminium containing minerals in the rooting zone

sources are briefly described below. For a more detailed discussion of the accuracy and reliability of the information contained in these layers readers should refer to Annex 2.

Climatic data

a. Precipitation Map (P)

The SEI Asian Precipitation map was produced with information from two main sources. Firstly, the World Meteorological Organisations (WMO) Mean Annual Precipitation map and, secondly, the ASEAN map of similar data for the southeast Asian region. The original paper maps were manually digitised by SEI and combined to create a region-wide coverage. Its accuracy is described in Annex 2. The precipitation map was employed in the calculation of the precipitation to potential evapotranspiration ratio.

b. Potential Evapotranspiration (PE)

The data were obtained as point location weather station readings for the entire world. The annual measurements of potential evapotranspiration were made using the Penman formula. This is regarded as the most reliable method for estimating potential evapotranspiration (see Annex 2). The information for the Asian region was extracted from the global file and input into the GIS database at SEI. From the point measurements a triangulated irregular network (TIN) interpolation algorithm with smoothing was applied to produce a coverage of the entire region. This was needed for the calculation of the P:PE ratio.

c. P:PE Ratio

The P:PE ratio was calculated by a division of the precipitation and potential evapotranspiration maps within the GIS. The resultant map was then reclassified into ranges such that there was a clear differentiation between Asian soil moisture regimes. The ratio represents the effectiveness of precipitation and is used to assess the moisture regime across the Asian region. The distribution of P:PE ratio can be seen below in Figure 6.7.

d. Estimated Runoff (Q)

This map is a reclassification of the P:PE ranges through a visual comparison between P:PE ratio map and groundwater flux data for Europe (see Annex 2 for details). The estimated values represent the sum of infiltration, groundwater movement and surface runoff. The potential errors in this data layer are discussed in the Annex 2. The map was used in the calculation of the Steady State Mass Balance critical load values.

e. Effective Temperature Sum (ETS)

This variable is an aggregate of the daily mean temperature exceeding a threshold. The information on daily temperatures was estimated from monthly mean weather station readings held by the FAO. The calculated point values of ETS were then interpolated within the GIS to produce a complete spatial coverage. These values were employed in the calculation of weathering rates as inputs to the Arhenius equation which approximates the relationship between temperature and speed of chemical reactions.

f. Base Cation Deposition

This map is an estimation of the sum of wet and dry base cation deposition. It was derived from global estimates of predicted air concentrations of minerals near the surface for four months and the SEI precipitation map for the Asian region. The methodology and air concentrations data for this layer were supplied via the ATMOS module of RAINS-ASIA by the University of Iowa. The base cation deposition values were used in the calculation of the Steady State Mass Balance critical loads by influencing the base cation concentration in the soil solution and thus the BC/Al ratio. The values of base cation deposition for the region can be seen in Figure 6.8 below.

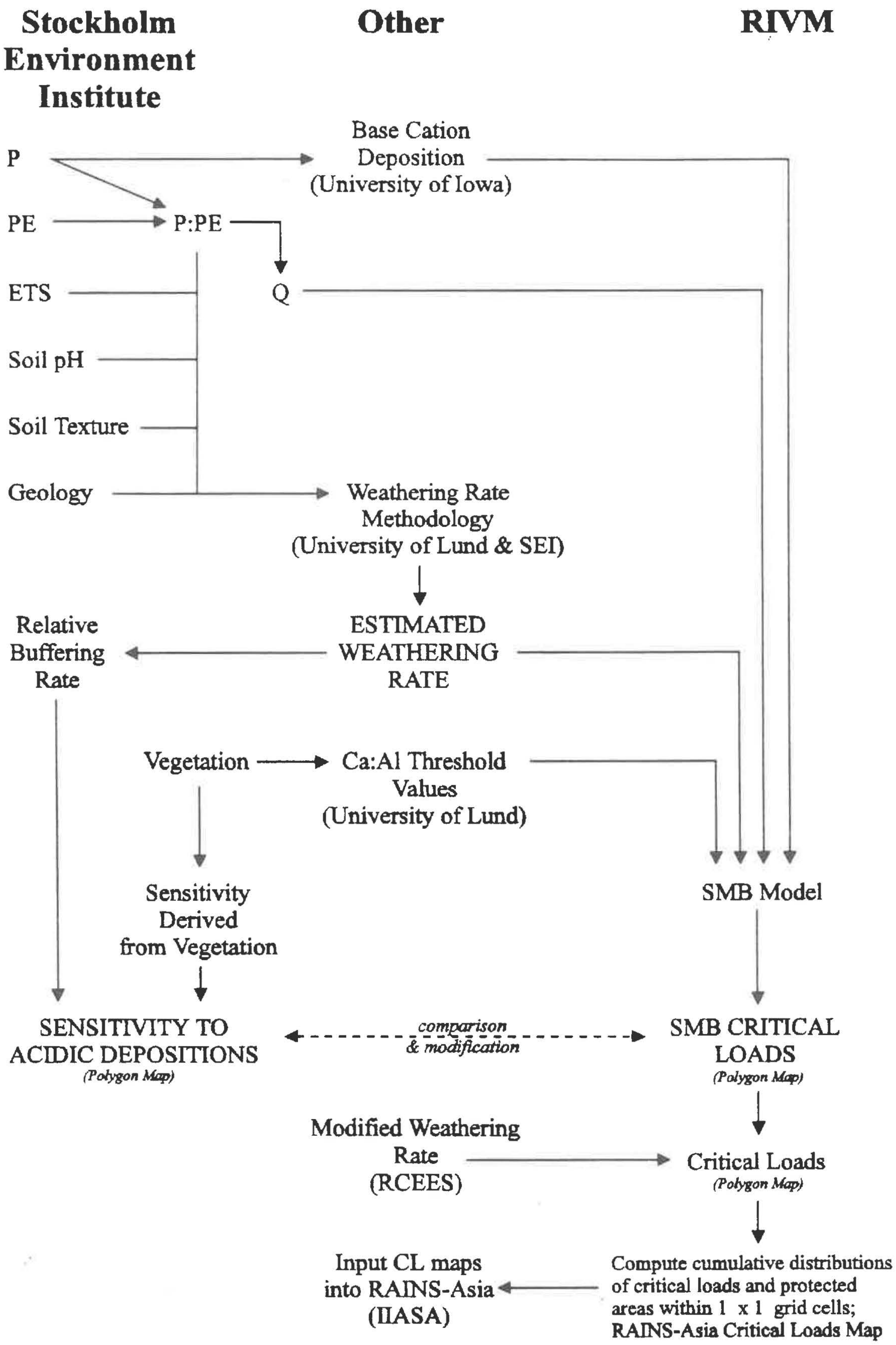

Figure 6.6 Flow diagram of data use within the RAINS-ASIA impacts project

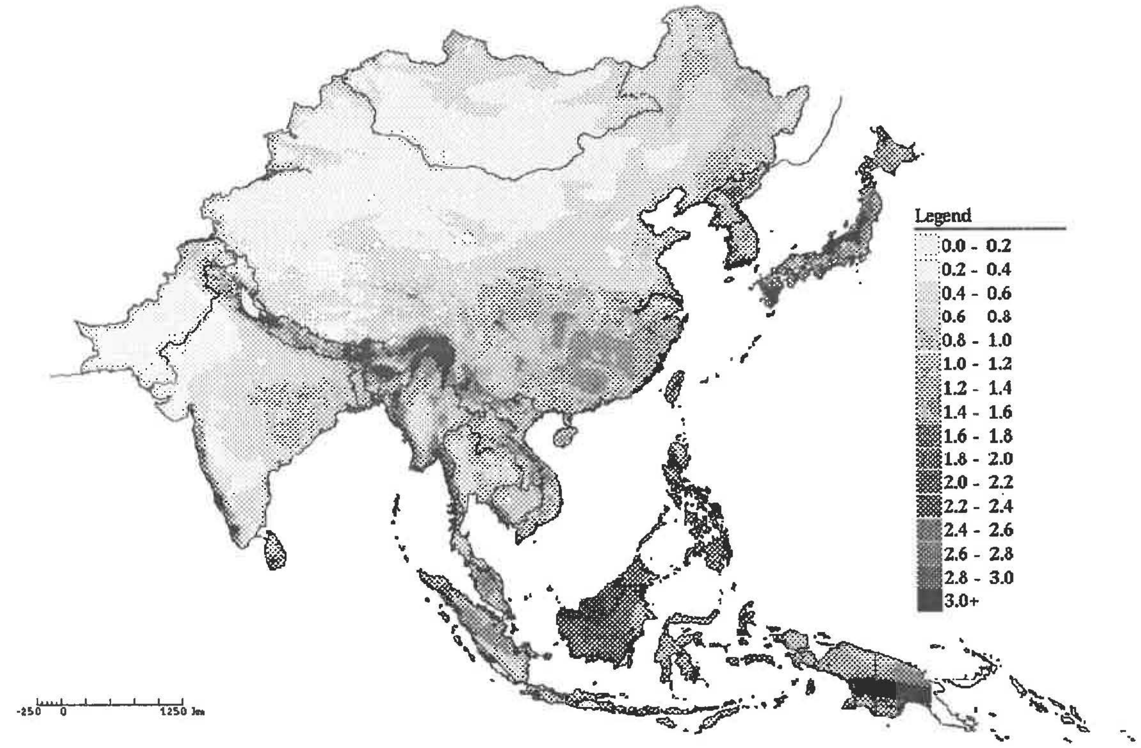

Figure 6.7 Precipitation to Potential Evapotranspiration Ratio (SEI)

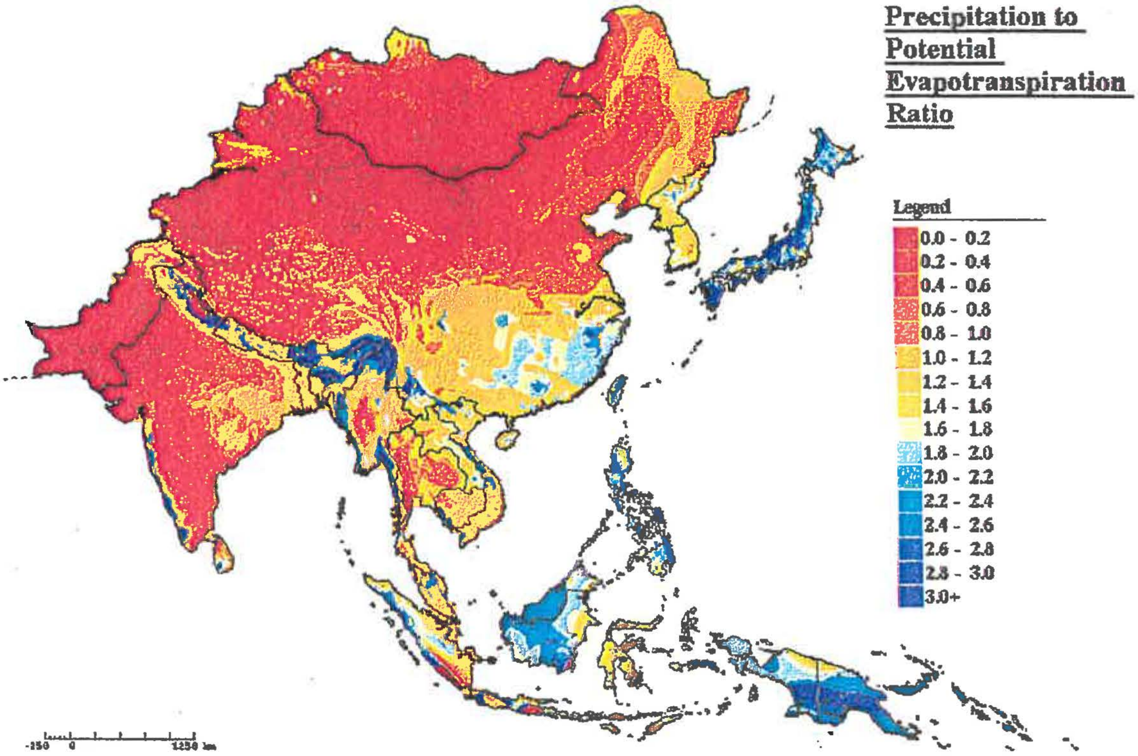

Figure 6.8 Base cation deposition (University of Iowa; SEI; RIVM)

Soil data

a. Soil pH

The initial soil type data was supplied by the FAO in digital ArcExport format. A database of average pH units for the various soil types for Asia was then compiled by SEI from FAO information and additional data held in pedological texts. The FAO soil types map was then reclassified into a map of average pH units for the top 50cm of the soil profile. Uncertainties exist in this information they include problems with the reliability of the surveying of the FAO soil type distribution and difficulties in assigning average pH units to soil types which were not mapped on the basis of their pH.

b. Soil Texture

As with the pH map this is a reclassification of the FAO 'Soil Map of the World'. The soil types have been reclassified into the mean texture class for that soil unit. The original data contained three classes of texture - fine to coarse, and mixed units. The process of assigning the mean texture value to the soil has resulted in the creation of five classes. The texture of the soil particles influences the rate of weathering reactions.

Geology data

This information was derived from the UNESCO World Geology map. The derived map shows the distribution of the acidity of metamorphic and igneous rocks. For sedimentary rocks the differentiation is based on age rather than acidity. This group has been subdivided into two classes, the Precambrian and Cambrian and all younger rocks. This split was made on the basis of the potential carbonate content of the rocks. Older rocks are assumed to have low carbonate content and younger rocks an indeterminate amount. The underlying geology modifies the buffering ability of thin soils; however, this factor had limited effect due to the low coverage of identifiable rock types in areas where soils were thin.

Weathering data

This map shows the estimated distribution of weathering rates for Asia. The map was derived from a decision tree classification (see Annex 2 Figure A2.7). Base rates of weathering were estimated from model calculations (Sverdrup, 1990) and assigned to soil types. These base rates are initial estimates of weathering rate which are then further modified by the physical characteristics occurring at a site. The first branch of the model differentiates highly leached lateritic soils which are assigned to a low initial base rate and only further modified by the moisture regime function described below. The other soils are assigned an initial base rate depending on the soil pH. Low pH soils have a low initial base rate with increasing rates set for soil groups with higher pH.

Lithosols, thin soils with rock deposits within 10cm of the surface, have their base rate adjusted dependent on the nature of the underlying geology. Acid rocks release few weathering products and may reduce the base rate assigned from pH alone. Basic and ultrabasic rocks are more easily weathered potentially increasing the buffering ability of the overlying soils.

In cool regions weathering will be slower than in warmer climates. Colder areas have therefore had their weathering rates reduced. The texture of soil particles will also influence the rate at which weathering processes occur. The particle diameter determines the size of the surface upon which chemical reactions can occur. Finer particled soils have had their weathering rate increased relative to coarser soils in the decision tree process.

The moisture regime operating in a region will affect the potential for chemical reaction processes and also the transport of minerals within the soil profile. In wet areas leaching processes will dominate causing soluble minerals to become washed out of soils with a subsequent reduction in buffering abilities. In dry areas alkali minerals have a tendency to accumulate in the upper horizons. This build-up will increase the base saturation (the proportion of basic cations relative to acidic cations) of the soils. A modifying function based on moisture regime has influenced the weathering rate of all the soils.

a. Relative Buffering Rates

For the assessment of sensitivity, relative units of buffering rate were used rather than quantitative values of weathering rate. The reason is to accommodate for the variability of the data and uncertainties in weathering rate values. The weathering rate map was therefore reclassified into relative classes, high to low, of buffering rate. The distribution of estimated values of weathering rate and the associated classes of relative buffering can be seen in Figure 6.9.

Nine classes of relative buffering rate were employed in the relative sensitivity mapping. The delimitation of nine classes evolved from two factors: firstly, being calculated from interval data, the distribution of weathering rate values approximately formed nine classes. Secondly, the physical extent of the study region justified the use of this number of classes. The identification of nine classes is therefore the result of the data used in the estimation and a methodological decision. These classes of buffering ability were then employed in the generation of the distribution of the relative sensitivity of ecosystems to acidic depositions.

Vegetation data

a. Land Use and Vegetation

The Rutgers University 'Major World Ecosystems' map was employed in the project to assess the land cover types of Asia. The map shows dominant landuse on an 0.5^{0} x 0.5^{0} longitude/latitude grid. The original map has thirty-eight vegetation classes.

b. Sensitivity derived from Vegetation Cover

The Landuse map was reclassified into classes based on the sensitivity of the vegetation to acidic depositions. The rationale for this classification is discussed in Section 6.2.4 The classes of sensitivity derived from vegetation can be seen in Figure 6.5.

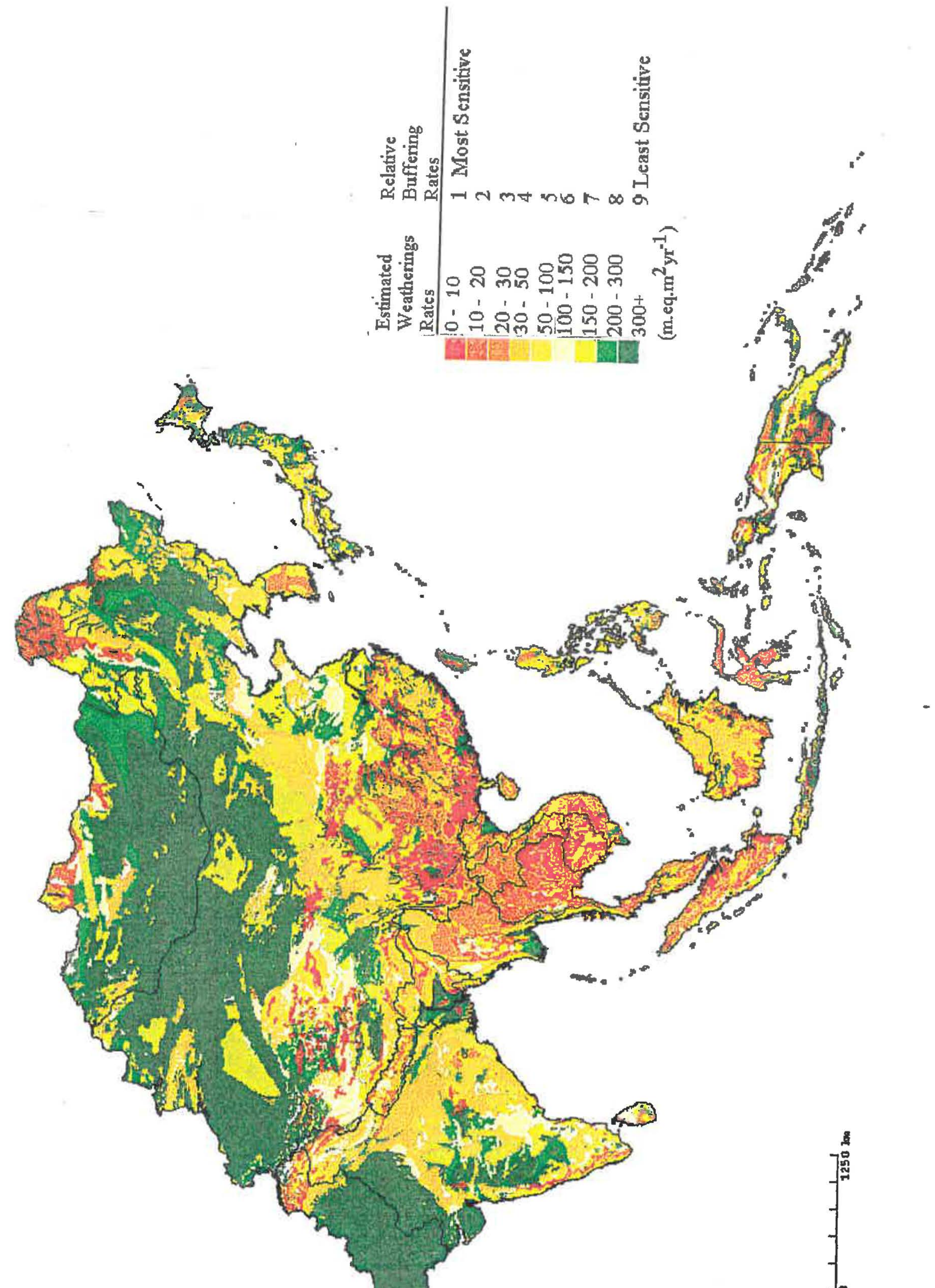

Figure 6.9 Quantitative values of weathering rates and associated relative buffering rate classes (UL, SEI, RIVM, GEODAN)

6.3.4 Mapping sensitivity in Asia

The sensitivity of terrestrial ecosystems in Asia to acidic deposition links different databases (soil, vegetation and climate) and serves to impart more detailed information than may be gained from one layer alone. It also compensates for the inaccuracy of the information available in the different layers. The sensitivity assessment focuses on the effects on vegetation as it is assumed that changes in fauna will be dependent on the changes in the vegetation structure and function, or closely correlated to them.

Two main aspects determine the sensitivity of ecosystems to acidic deposition: one is the buffering ability, and the other the vegetation tolerance range to changes in soil physico-chemical characteristics. It is considered that for the production of a sensitivity map that evaluation of the distribution of buffering ability is of primary importance and the methods described here concentrate on assessing its distribution. There are aspects of ecosystem structure and function that may be deduced from the vegetation type indicating the ability of the ecosystem to buffer acidic deposition. As this gives insufficient detail the buffering systems are also derived from soil and climatic information. Buffering mechanisms within the soil help to maintain the pH and buffer the ecosystem from indirect effects associated with acidic deposition. These two data layers are combined to indicate the degree of change that will occur in ecosystem under different deposition rates.

Detailed methodology

The methodology is based on three main aspects: how to allocate vegetation types to classes that indicate the sensitivity of ecosystems to acidic deposition; how to determine the buffering ability from soil type attributes and climatic factors, and finally how to link the vegetation categories to the soil (buffering) characteristics.

a. Allocation of Vegetation Types to Classes

The allocation of vegetation types was made by considering a number of attributes related to the buffering of the ecosystem against effects. These are described in detail in Section 6.2.4. Each vegetation type has been assessed in terms of the six factors, as described in Table 6.4, and assigned to one of six categories as shown in Tables 6.5 to 6.7.

The categories in Table 6.7 show an indication of the sensitivity of ecosystems as derived from the vegetation type and this is mapped in Figure 6.5. In the European work four classes of vegetation were distinguished (Kuylenstierna and Chadwick, 1989). However, it seemed reasonable to distinguish six classes of vegetation in Asia given the greater range of buffering represented by ecosystems in the Asian region. It can be seen that the resolution of sensitivity according to vegetation is coarse and, as explained earlier, this is due to the poorly disaggregated classification of vegetation type and to the resolution of these data. This emphasises the importance of the buffering ability deduced from the soil processes.

b. Buffering Ability of the Soil

The buffering ability of the soil is related to buffering processes. The most important long-term buffering process is the rate of weathering of base-rich soil minerals. The weathering process neutralises acidity and therefore resists increases in soil acidity. Other, capacity based buffering mechanisms are not specifically covered in this methodology as rate based processes are considered more important. This means that the sulphate adsorption capacity has not been included. This capacity may be large in highly weathered tropical soils. According to Australian research it has been found that sulphate adsorption capacity increased with amount of rainfall in tropical regions (Harward and Reisenauer, 1966). Areas which may have high sulphate adsorption capacity have been delimited in Asia (Sanchez, 1976). In these areas the additional buffering may result in a delayed response.

The method for determining the buffering rate (relative weathering rate) is described in Section 6.3.3 (under weathering data), and in more detail in Annex 2 and the result of this process is a map showing the relative ability of the soil in different regions to buffer acidic deposition. For the Steady State Mass Balance method quantitative weathering rate estimates have been used for each area. For the assessment of sensitivity it is the relative buffering rate that is of importance as the distribution of sensitivity is the end-point of the method. Figure 6.9 shows the distribution of relative buffering ability which has nine classes. Only a limited number of classes of relative buffering rate could be reasonably described and the representation of a greater number could not be justified by the available data.

c. Combination to Form Classes of Sensitivity

In applying the relative sensitivity method to Europe (Kuylenstierna and Chadwick, 1989) weights were assigned to the different factors in order of the perceived importance of the factors. In this Asian work the combination method has been kept simple. The nine classes of soil buffering ability have been summed to the six classes of sensitivity according to vegetation type as shown in Table 6.10. The method is one of ranking the factors in order of increasing sensitivity to acidic deposition and then linking these rankings together. The numbers associated with the classes of weathering or vegetation are not necessarily of equal interval weight and do not convey information as to the degree to which one class buffers relative to another, except by rank. Therefore, class nine of the soil buffering rate represents a soil that has higher buffering ability than any of the classes below, but no linear quantitative relationship is implied. Both datasets, the sensitivity according to vegetation class and buffering rate of the soil are designed to give a geographical representation of which areas are more relatively sensitive than others. Desert areas (vegetation Class 6 and soil Class 9) in North-western China, for example, give the lowest class of sensitivity. If desert areas were associated with class 1 soils then this would imply that one of the databases was erroneous and the combination would create a compromise sensitivity class which does rely too heavily on one or other dataset. In this way the method of combination allows for reasonable estimates of sensitivity from a combination of two databases.

Weights have not been explicitly applied that indicate whether one factor (soil or vegetation type) is more important than another (Table 6.10). However, as there are nine classes of soil buffering ability compared to the vegetation classification, the soil will have a greater influence on the sensitivity. This emphasis on the soil data is largely due to the quality and resolution of the data compared to the land use data.

Fourteen possible classes of sensitivity result from the combination (Table 6.10). This number of classes is untenable given the uncertainties in the methods and data and so these have been collapsed to form five final classes of sensitivity to acidic deposition. The method used is to sum the insensitive classes as there seems little point for great differentiation in areas unlikely to be affected by acidic deposition. More emphasis has been placed on the differentiation of sensitive areas. Therefore small areas of sensitive ecosystems have been kept distinct. The area of final sensitivity classes, created by addition of higher classes, is shown in Figure 6.10 and the final sensitivity map is shown in Figure 6.11.

Table 6.10 Combination of the sensitivity from vegetation and the soil buffering conditions to give fourteen potential classes of overall sensitivity

		Relative soil buffering classes								
		1	**2**	**3**	**4**	**5**	**6**	**7**	**8**	**9**
Sensitivity according to vegetation	**1**	2	3	4	5	6	7	8	9	10
	2	3	4	5	6	7	8	9	10	11
	3	4	5	6	7	8	9	10	11	12
	4	5	6	7	8	9	10	11	12	13
	5	6	7	8	9	10	11	12	13	14
	6	7	8	9	10	11	12	13	14	15

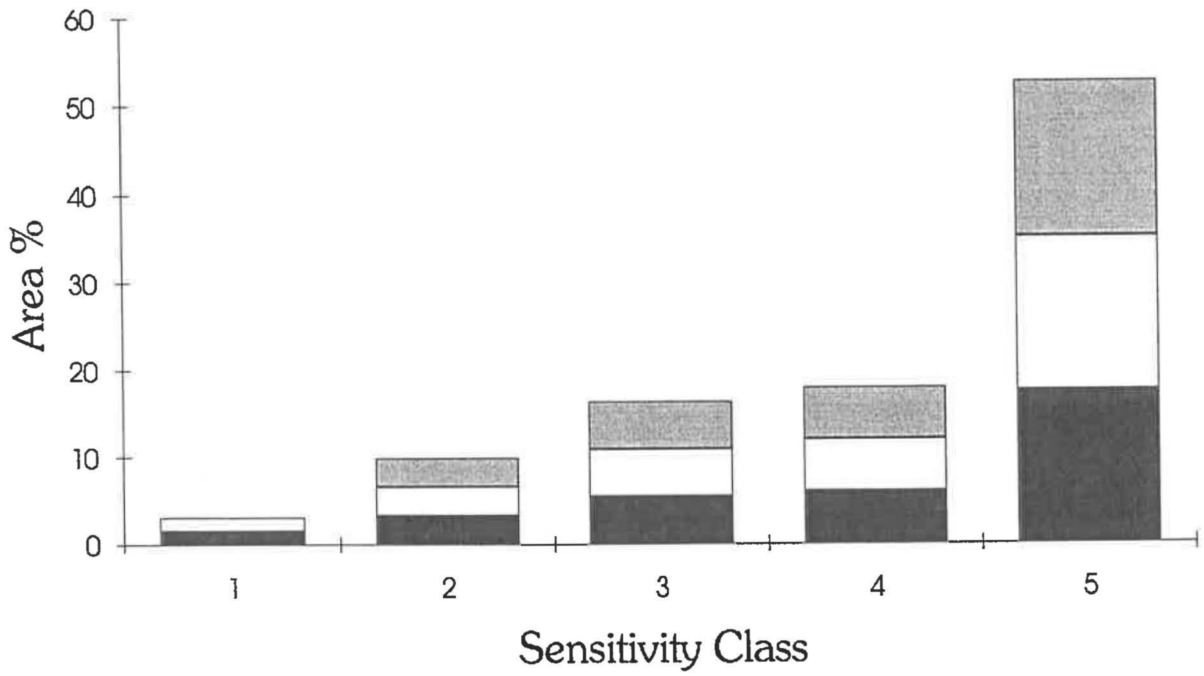

Figure 6.10 The % area of sensitivity classes and their combination

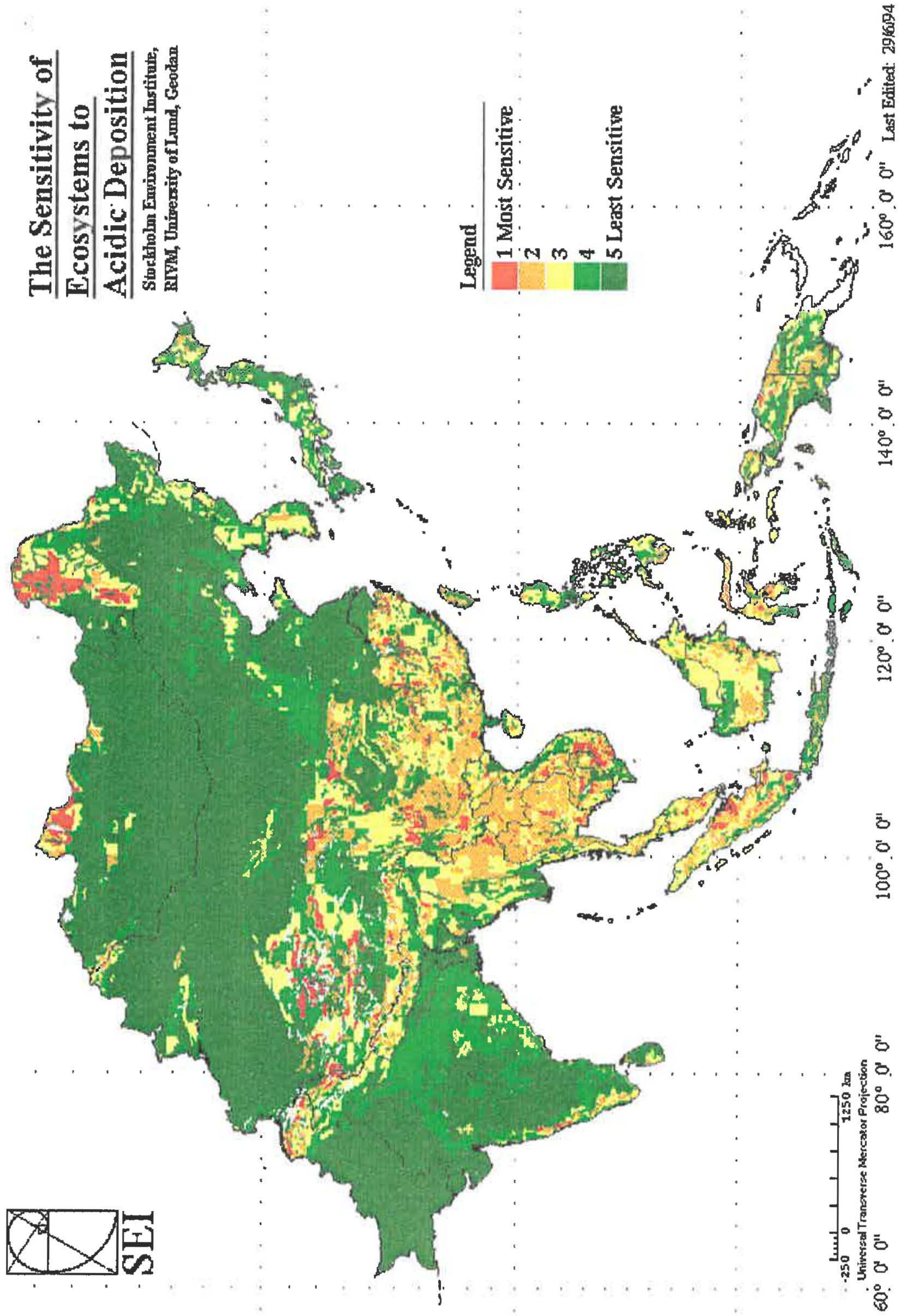

Figure 6.11 The preliminary map showing relative sensitivity of terrestrial ecosystems in Asia to acidic deposition (SEI; RIVM; UL; RCEES; GEODAN)

It can be seen from Figure 6.11 that the most sensitive areas are found in south-eastern Asia, parts of the Himalayan range, parts of the Tibetan plateau and in the southern part of the boreal forest that dips into northern China. There are other small areas of high sensitivity such as in parts of Japan and the rain forest strip in south-western India. The high sensitivity regions are largely found on acidic soils and the ecosystem shows a low ability to buffer acidic deposition in the long term. In the relatively short term the old tropical soils may not be acidified due to the large sulphate adsorption capacity that some of these soils have been shown to exhibit. The insensitive areas cover the mainly dry, desertified regions and the rich agricultural lands. It is clear that most of India and north western China are not sensitive to acidic deposition. It should be noted that the map shows the small scale distribution of sensitivity giving a broad overview of the continental picture. Within areas designated sensitive there are likely to be pockets of land relatively insensitive to acidic deposition (such as paddy fields in south eastern China). These are not picked out due to the resolution of the input databases. The map in Figure 6.11 is considered a preliminary assessment and will be improved as methods and data are refined in response to comments during the review process.

6.4 Computation and mapping of critical loads in Asia

J.-P. Hettelingh, H. Sverdrup, D. Zhao, E. Meijer, M.J. Chadwick, J.C.I. Kuylenstierna, S. Cinderby.

6.4.1 Introduction

The Steady State Mass Balance Model computes the critical load from the mass balance for acidity. This model computes an equilibrium between acidifying processes (due to sulfur deposition or base cation uptake by plants) and buffering processes (such as by weathering reactions or base cation deposition). The model computes the critical load as the acid deposition for which critical limits for plant response (BC/Al ratio; Section 6.2) stability (aluminum leaching) are not violated.

Critical load models have also been applied by individual national counterparts in the RAINS-ASIA Impact network. In China site specific research was done (1) using the Steady State Mass Balance Model, and (2) assessing the development of the BC/Al ratio due to a variety of sulfur deposition scenarios (Zhao *et al.*, 1995; see Annex 4). In Japan a very detailed analysis of different versions of Steady State Mass Balance Models on a regional scale were implemented and tested (Shindo *et al.*, 1994; see Annex 3).

This section describes the mathematical formulation of the Steady State Mass Balance Model which was used for the computation of critical loads in Asia. Results of the application of the model, including the maps which have been implemented in RAINS-ASIA, are provided.

6.4.2 The Steady State Mass Balance Model

Plant response criteria

$$CL(Ac) = ANC_w - ANC_{l,crit} \qquad (2)$$

The critical value of alkalinity leaching is defined from the, maximum allowable, critical hydrogen ion leaching and critical aluminum ion leaching as follows:

$$ANC_{l,crit} = -H_{l,crit} - Al_{l,crit} \qquad (3)$$

with,

$$H_{l,crit} = Q[H]_{crit} = Q\left(\frac{[Al]_{crit}}{K_{gibb}}\right)^{1/3} \qquad (4)$$

and

$$Al_{l,crit} = Q[Al]_{crit} = 1.5\frac{BC_{l,crit}}{(BC/Al)_{crit}} \qquad (5)$$

where[1],

ANC_w = alkalinity produced by weathering
$ANC_{l,crit}$ = critical alkalinity leaching
$H_{l,crit}$ = critical value of proton leaching ($mol_c\ ha^{-1}\ yr^{-1}$)
$Al_{l,crit}$ = critical value of aluminum leaching ($mol_c\ ha^{-1}\ yr^{-1}$)
$[Al]_{crit}$ = critical value of aluminum concentration ($mol_c\ m^{-3}$)
K_{gibb} = gibbsite solubility constant (200 to 300 $m^6\ eq^{-2}$)
Q = runoff ($^3ha^{-1}yr^{-1}$)
$BC_{l,crit}$ = critical leaching of base cations (mol_c ha-1 yr^{-1})
$(BC/Al)_{crit}$ = critical molar base cation to aluminum ratio (see Section 6.2).

[1]Note that the factor 1.5 is derived from the ratio of molar charges of 2 for base cations and 3 for aluminum, which ratio appears in the denominator of equation 5.

The critical leaching of base cations is computed from a mass balance of the weathering rate of calcium (Ca), Magnesium (Mg) and potassium (K) as follows:

$$BC_l = BC_{w,(Ca+Mg+K)} + BC_d - BC_u \tag{6}$$

where,

BC_d	= base cation deposition (mol_c ha-1 yr^{-1})
$BC_{w(Ca+Mg+K)}$	= weathering rate of Ca+mg+K (mol_c ha-1 yr^{-1})
BC_u	= base cation uptake (mol_c ha-1 yr^{-1})

Note that BC_w is different from alkalinity weathering (ANC_w in equation (2)) in that ANC_w includes in the release of cations about 30% sodium (Na) which is not used by plants as a nutrient and does not protect against Aluminum. The weathering rate thus becomes:

$$BC_{w,(Ca+Mg+K)} = x_{Ca+Mg+K}\, ANC_w \tag{7}$$

where,

$x_{Ca+Mg+K}$	= fraction of weathering as Ca, Mg and K= 0.7 (mol_c ha-1 yr^{-1})

The base cation uptake in equation (7) has to meet the requirements that (1) a minimum leaching of base cations is taken into account ($[BC]_{min}$ = 0.002 eq m^{-3}), and (2) base cation uptake does not exceed the availability of base cations. Condition 1 leads to:

$$BC_{min} = Q[BC]_{min} \le x_{Ca+Mg+K}\, ANC_w + BC_d \tag{8}$$

Condition 2 yields:

$$BC_u \le x_{Ca+Mg+K}\, ANC_w + BC_d - BC_{min} \tag{9}$$

Conditions 1 and 2 are implemented in the model as:

$$BC_u = \min[\max(x_{Ca+Mg+K}\, ANC_w + BC_d - BC_{min}, 0), BC_u] \tag{10}$$

Substitution of equations (7), (6) and (5) in (4) yields the following expression for $H_{l,crit}$:

$$H_{l,crit} = Q^{2/3}\left\{\frac{1.5\ \left(BC_d^* + (1 - X_{Na})BC_w - BC_u\right)}{(BC/Al)K_{gibb}}\right\}^{1/3} \tag{11}$$

Substitution of $H_{l,crit}$ and $Al_{l,crit}$ in equation (3) gives:

$$ANC_l = -(1.5\frac{x_{Ca+Mg+K}\ ANC_w + BC_d - BC_u}{(BC/Al)_{crit}K_{gibb}})^{1/3}\ Q^{2/3} - 1.5\frac{x_{Ca+Mg+K}\ ANC_w + BC_d - BC_u}{(BC/Al)_{crit}} \tag{12}$$

Substitution of equation (12) in equation (2) gives the Steady State Mass Balance equation based on the plant response (BC/Al) criterion:

$$CL = ANC_w + (1.5\frac{x_{Ca+Mg+K}\ ANC_w + BC_d - BC_u}{(BC/AL)_{crit}K_{gibb}})^{1/3}\ Q^{2/3} + 1.5\frac{x_{Ca+Mg+K}\ ANC_w + BC_d - BC_u}{(BC/Al)_{crit}} \tag{13}$$

Soil stability criteria

Acid deposition may lead to aluminum leaching in excess of aluminum produced by weathering or other processes in high precipitation area. Therefore aluminum leaching has to meet the following requirement:

$$Al_l \leq Al_w + Al_d + Al_b \tag{14}$$

It is assumed that Al_d and Al_b can be neglected and that the production of aluminum through weathering of minerals is related to the production of base cations from weathering through the stoichiometry of minerals as follows:

$$A_{l,crit} = AL_w = 2ANC_w \tag{15}$$

From equations (15), (4), and (5) it is derived that

$$H_{l,crit} = \left(\frac{2ANC_w}{K_{gibb}}\right)^{1/3} Q^{2/3} \tag{16}$$

Substitution of equation (15) and (16) in (3) leads via equation (2) to

$$CL = 3ANC_w + \left(2\frac{ANC_w}{K_{gibb}}\right)^{1/3} Q^{2/3} \tag{17}$$

6.4.3 Results

The critical load is finally computed as the minimum of the result of equations (13) and (17). The result is obtained in combination with a Geographical Information System. Each of the explanatory variables have been mapped (see Sections 6.2 and 6.3). A map of critical loads is obtained (Figure 6.12) by running the model on the geographical overlays of the regionally distributed explanatory variables.

From Figure 6.12 it can be seen that the areas with lowest critical loads (until 200 eq $ha^{-1}yr^{-1}$), i.e. which are most sensitive to acidic deposition, are located in south China, in the area covering the south east of Thailand covering Cambodia and the southern part of south Vietnam. Critical loads ranging to 500 eq ha^{-1} yr^{-1} are found in the whole of south east Asia. Areas which are sensitive (critical loads ranging from 500 to 1000 eq ha^{-1} yr^{-1}) are found in the south and south west of the study region. Figure 6.12 is to a large extent similar to Figure 6.11 (Section 6.3.4) which map was derived using the Method of Relative Sensitivity.

Input of the critical load map in RAINS-ASIA

The geographical representation of the critical loads has to meet the requirement of being consistent with the resolution by which modelled acid deposition is mapped in RAINS-ASIA. The atmospheric sub module of RAINS-ASIA computes sulfur deposition in $1^{o}x1^{o}$ grid cells. Critical loads similarily need to be represented in grid cells in order to allow for a comparison with sulfur deposition

The cover of a $1^{o}x1^{o}$ grid cell may contain more than one combination of vegetation classes and biogeochemical characteristics. In mapping critical loads for each grid cell a decision is needed about which ecosystem to represent. As solution a cumulative distribution (CDF) has been computed of critical loads in grid cell.

The cumulative distribution of critical loads

The aim of this section is to describe how a single critical load value and a single exceedance function is obtained in a $1^o x 1^o$ grid cell which contains a variety of ecosystems. The principle is to construct a cumulative distribution of critical loads. Cumulative distributions for the mapping of critical loads have been described elsewhere (Hettelingh *et al.*, 1991; Posch *et al.*, 1993). A cumulative distribution function (CDF), is used to describe the cumulative occurrence of an ascending sequence of critical loads $x_1 < \ldots < x_n$ in a $1^o x 1^o$ grid cell, is defined as

$$F(x) = \begin{cases} 0 & \text{for } x < x_1 \\ \sum_{k=1}^{i} w_k & \text{for } x_i \leq x < x_{i+1} \\ 1 & \text{for } x \geq x_n \end{cases} \qquad (18)$$

where:
$F(x)$ = the probability of a critical load being smaller than x
w_i = the weight assigned to critical load x_i $(i = 1,\ldots,n)$
The weight w_i represents the "importance" of the ecosystem with critical load x_i. This may reflect the area of an ecosystem or its intrinsic value.

All ecosystems in a grid cell are protected by taking the minimum critical load value in this cell. To discard outliers, it has been agreed to use a (low) quantile of the CDF $F(x)$ rather then the minimum critical load. The qth quantile ($0 \leq q \leq 1$) is denoted by x_q and is the critical load satisfying $F(x_q) = q$. Taking the qth quantile critical load protects a $(1-q)$th percentage of the ecosystems. Percentiles are obtained by scaling quantiles to 100, i.e. the pth percentile corresponds to the $(p/100)$th quantile.

Figure 6.13 shows the 5 percentile map of critical loads. Grid cells are shaded according to the range which contains the critical load value which, when not exceeded, will reduce the risk of damage to 95% of the ecosystems in each grid cell. A $1^o x 1^o$ grid cell is entirely shaded because, similarly to sulfur deposition, it is assumed that the 5-percentile critical load in each grid cell is homogeneously applicable in the whole grid cell. Effects of throughfall or orographic deposition effects are not taken into account in the $1^o x 1^o$ grid cell. From Figure 6.13 it can be seen that rather large areas in Asia fall in the most sensitive range of 0-200 eq ha^{-1} yr^{-1}. When a less stringent protection criterion is used, i.e. protection of 50% of the ecosystems is required (Figure 6.14), it is clear that areas with very low critical loads (between 0-200 eq ha^{-1} yr^{-1}) cover much smaller areas.

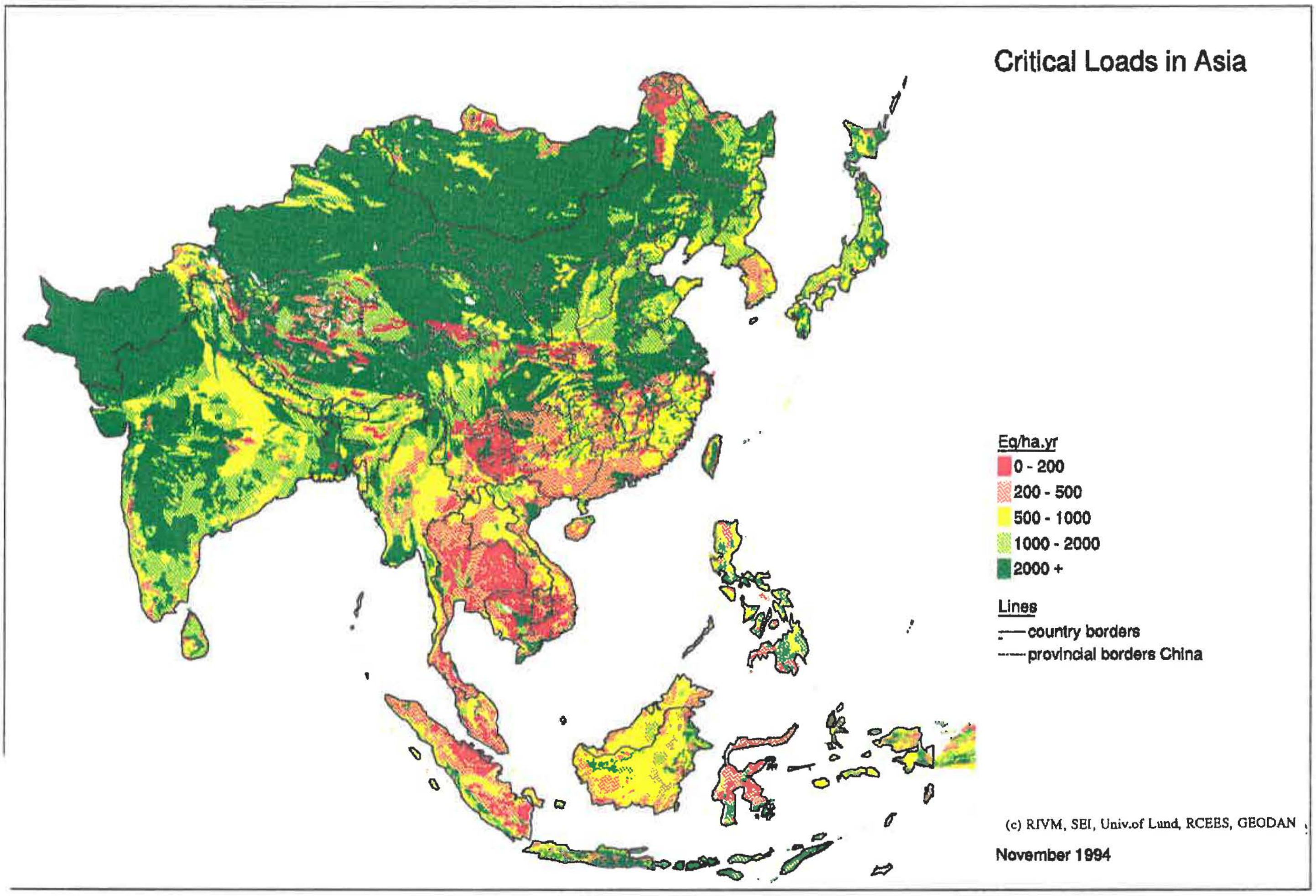

Figure 6.12 Critical loads for acidity in Asia. The red shaded areas represent the areas with the lowest critical load where sulfur deposition should not exceed 200 eq ha^{-1} yr^{-1} (approximately 0.32 g S m^{-2} yr^{-1}) (RIVM, SEI, RCEES, UL, GEODAN)

The RAINS-ASIA model includes a database of critical loads and the estimated percentage of the ecosystems protected. Thus, if a 5 percentile (p5) critical load is chosen about 95% of the ecosystems in each grid cell will have a low risk of being damaged when acid deposition does not exceed this 5 percentile critical load. At p10 this percentage protection is reduced to 90%, at p25 to 75% etc. In fact, for each grid cell a cumulative distribution of critical loads is available to the user.

However, a low percentile has a rather high uncertainty because of the reliability of the basic data in general and data resolution in particular. The lowest current resolution available for ecosystems is 0.5 by 0.5 degrees, displaying dominant ecosystem in each grid cell. Other variables in the critical load computation model have a higher resolution. Taking these limitations and current data quality into account it is recommended to us p25 as the basis for the analysis of deposition excess. Lower percentiles should not be used as the critical load values will not reliably represent the damage thresholds for the chosen ecosystem if small areas are considered. For more information on the accuracy of the ecosystem database see Annex 2.

Exceedance of critical loads

Figure 6.15 shows the excess of critical loads for acidity due to sulfur deposition in 1990. The areas with the largest excess are located in south east China with peaks ranging from 3000 eq ha^{-1} yr^{-1} to 5000 eq ha^{-1} yr^{-1} (4.8 to 8 g S m^{-2} yr^{-1} respectively), Thailand, parts of Indonesia, Korea, the south of Japan and small areas in the Philippines. The 25-percentile critical loads were used for this comparison, meaning that in areas where no excess occurs at least 75% of the natural systems are 'protected'. The use of lower percentiles would show a larger area of critical load excess.

6.5 *Conclusions and recommendations*

J.-P. Hettelingh, M.J. Chadwick, D. Zhao

The critical load approach, in combination with integrated assessment models, has been applied to some effect to guide and direct European and national policy formulations to reduce sulfur emissions. The present and projected high rates of economic growth in Asia, and the consequent increase in emissions of SO_2 and the excess of critical loads that would result, suggest that many natural and associated systems in Asia may eventually be at risk from acidification. Thus, the use of critical load values, as indicators of deposition limits, should enable some of the adverse effects, encountered in European lakes and forests, to be avoided. Already in China, the critical load approach is being investigated as a means of identifying how emitting sources could be located in order to maintain environmental quality below the thresholds at which adverse effects would be manifested.

The calculation of critical load values for much of Asia, however, is a considerable undertaking. The range of environmental conditions and ecosystems in an area of Asia considered in the RAINS-ASIA project exceeds that of Europe by far: the range encompasses tropical rain forest to near desert conditions and mangroves to areas of taiga: there is an associated range of soil type and a wide range of cropping systems and land use. Thus, the level of information called for, the experience in interpreting it and the range of applicability required by model systems are much greater than for the more restricted land area and conditions encountered in Europe. Similarly, validation procedures will need to be more extensive.

Deposition alone is not the only cause of increased risk of damage. Atmospheric concentrations (of sulfur dioxide, nitrogen oxides and ozone) have been shown to cause direct damage to natural ecosystems and crops, as well as having health effects in large urban areas. In fact, in many parts of Asia, the concern for urban air quality is increasing and air concentrations of SO_2 may already reach dangerous levels. Determination of critical levels for SO_2, along the lines of European work, needs to be undertaken. Critical levels (concentrations below which no damage is expected) have been formulated for ozone (Fuhrer and Achermann, 1993), sulfur dioxide and nitrogen oxides (UN ECE, 1993). The assessment of environmental benefits of emission reductions should include both levels and loads simultaneously. As more pollutants, each causing specific effects, are addressed in developing environmental policies, it is likely that the critical load approach as applied to sulfur will be extended. A suite of threshold values, supported by an iterative procedure of emission reductions of various pollutants might appropriately be called a <u>critical threshold approach</u>. Its objective would be not to exceed thresholds which put ecosystem sustainability at risk nor exceed health guidelines.

In trying to establish targets, based on critical load and level values, to ensure sustainability of environmental systems, the complication caused by interacting pollutants and various exposure routes does not provide policy makers with simple options. A critical threshold approach might enable policies to be developed with the aim of avoiding:

i) the excess of the critical load of acidity from sulfur and nitrogen simultaneously;

ii) the excess of the critical load of nutrient nitrogen by nitrogen oxides and ammonia;

iii) the excess of the critical level of ozone by the interaction of nitrogen oxides with volatile organic compounds;

iv) the excess of critical levels of sulfur dioxide and nitrogen oxides;

v) exceeding WHO health guidelines for different pollutants.

Interactions between pollutants are likely, such as acidity with heavy metals (see Gian *et al.*, 1991) and the possibility of climate change and associated changes in cropping systems and vegetation land cover may add to this complexity.

Additive and synergistic relationships between direct and indirect effects of pollutant concentrations and depositions respectively are likely to exist and to these may be added additive effects and synergisms between pollutants. Consideration of this led, two decades ago (Butler, 1978), to the suggestion that, in effect, multiple pollutant dose-response relationships are, overall, very close to a non-threshold one and essentially follow a linear non-threshold model (LNTM). The implications of this could be far-reaching for abatement policy responses.

Nevertheless, as a starting point, the RAINS-ASIA model can be applied in combination with the critical load approach to support policies which are aimed at reducing sulfur oxide emissions such that the excess of critical loads can be controlled. Further development of RAINS-ASIA and the threshold approach will support the development of policies which, while stimulating continued economic growth, will be able to anticipate pollution risks.

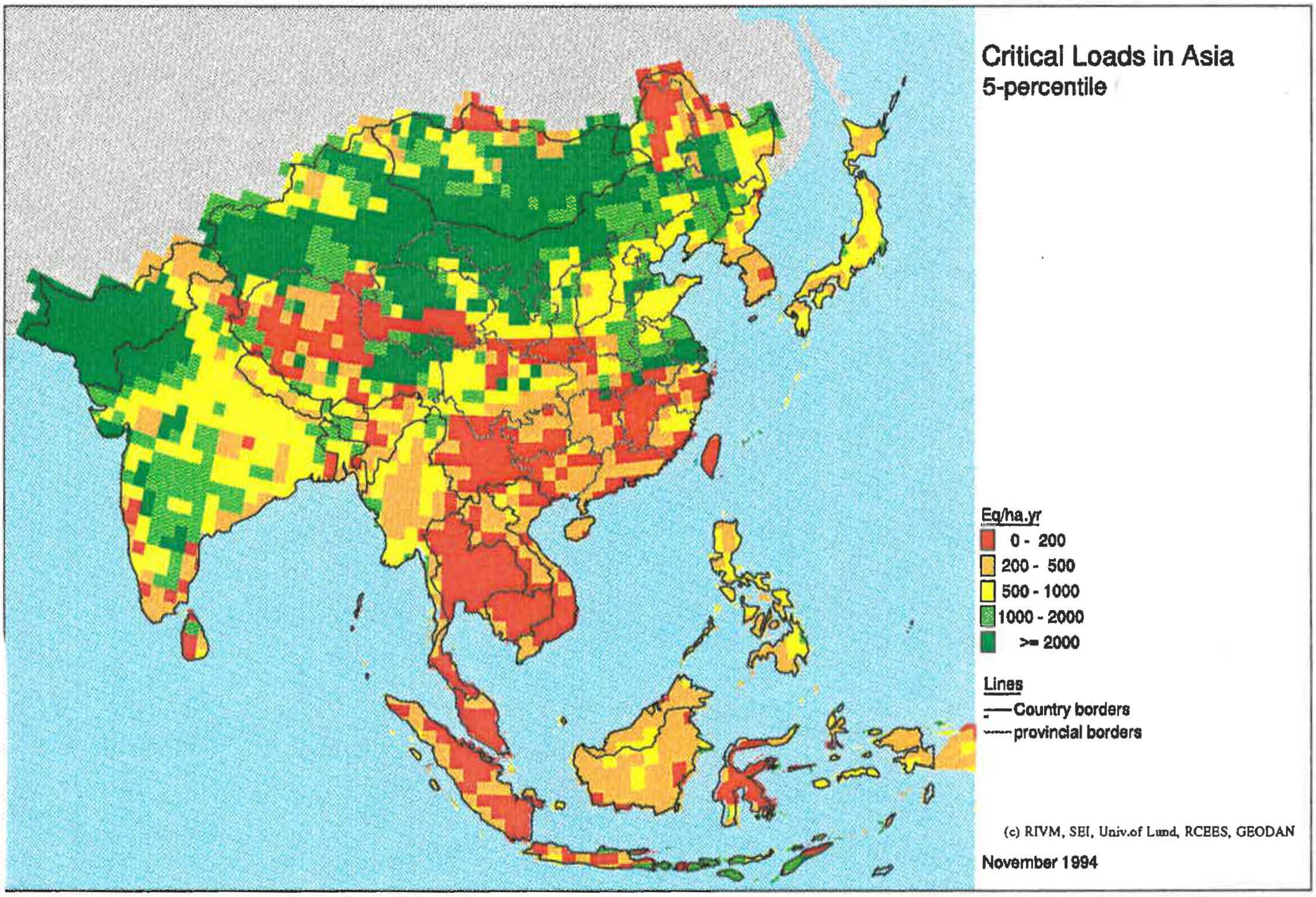

Figure 6.13 5-percentile critical load map; Critical loads for acidity at which the risk of damage to about 95% of the ecosystems is decreased. The reliability of the 5-percentile critical load map varies over the region, especially in grid cells where the cover of the ecosystems is less than 25% of the grid cell. (RIVM,SEI,RCEES,UL,GEODAN).

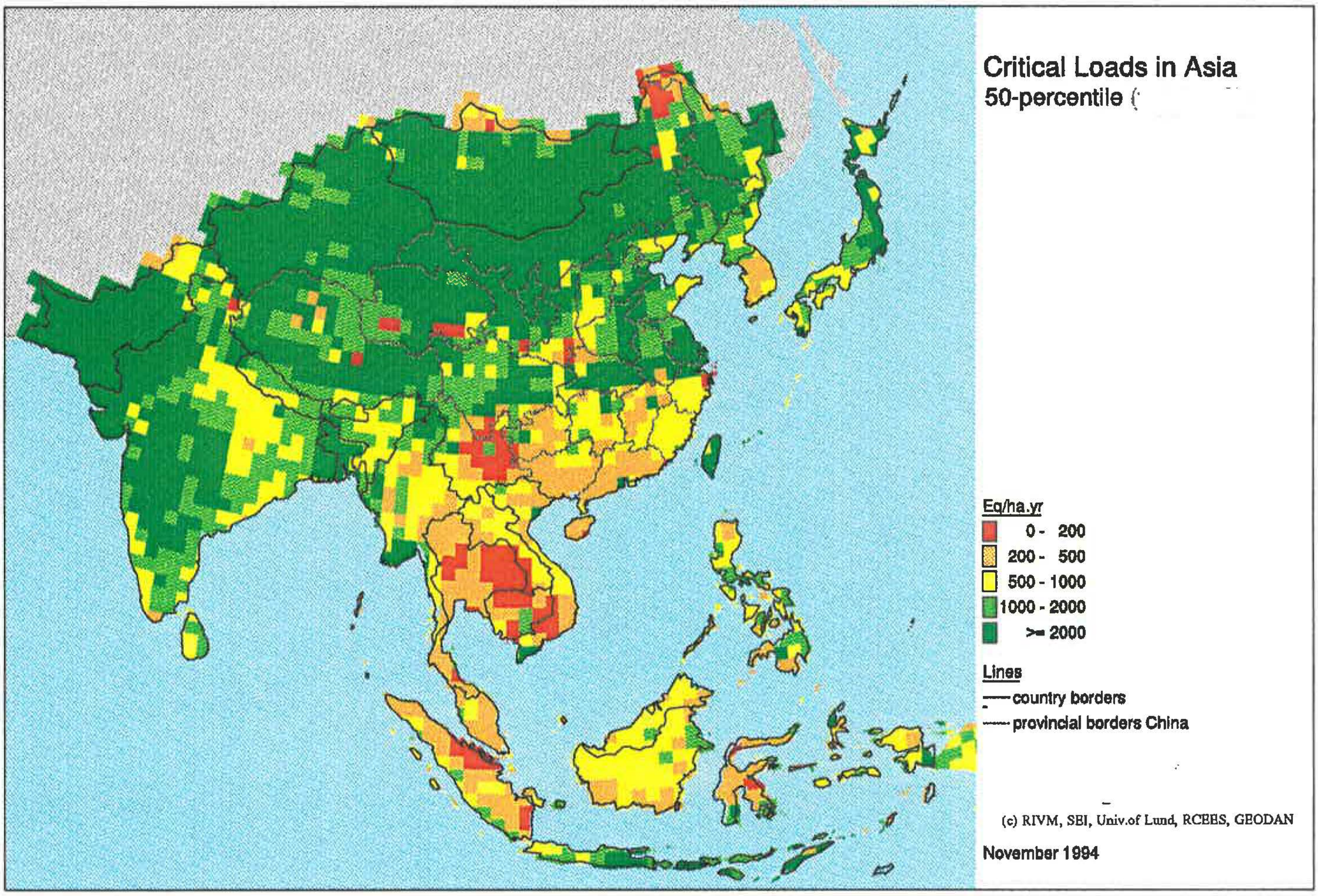

Figure 6.14 50-percentile critical load map; Critical loads for acidity at which the risk of damage due to acidification to 50% of the ecosystems is decreased. (RIVM, SEI, RCEES, UL, GEODAN)

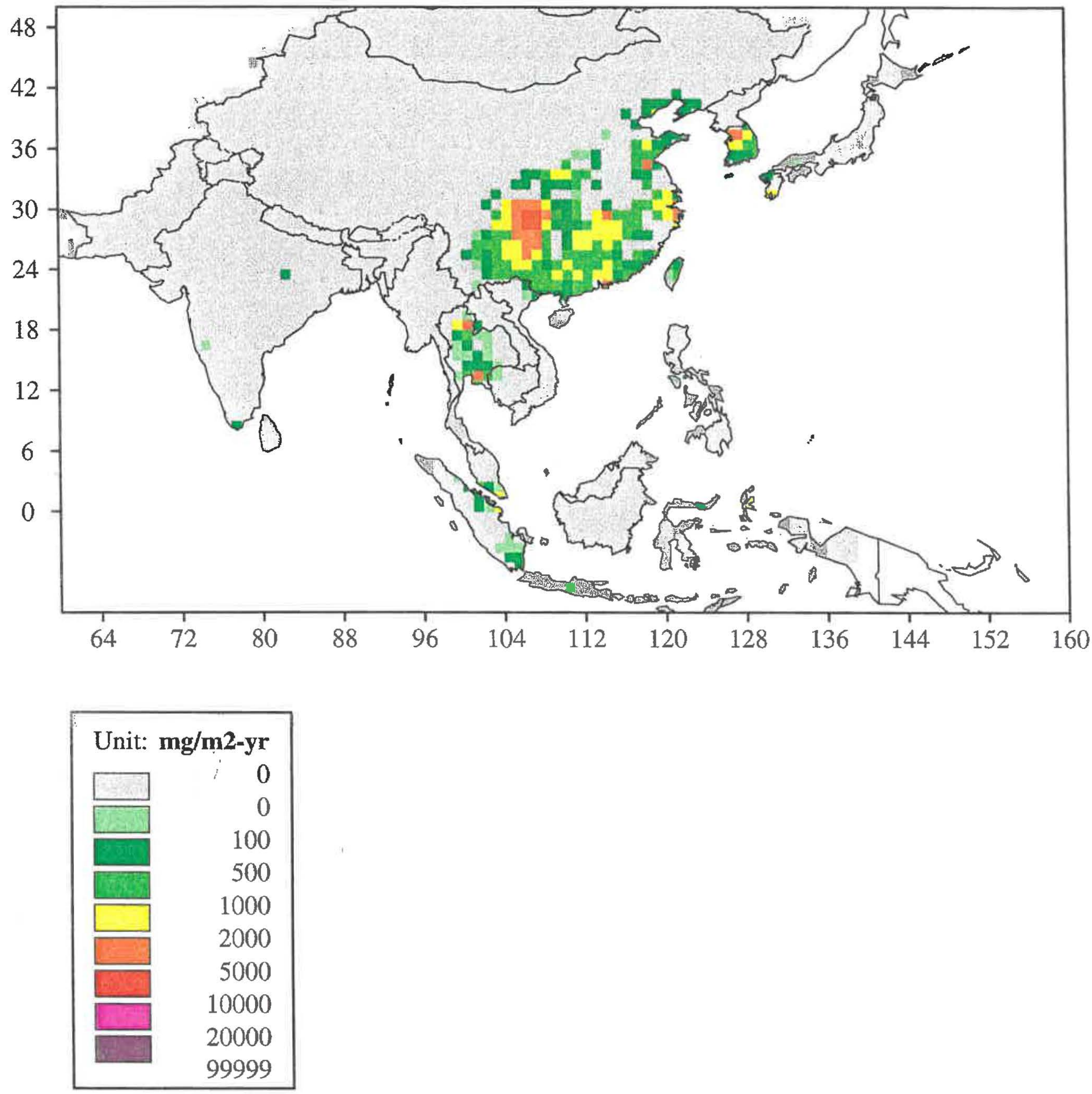

Figure 6.15 Computed excess of the 25-percentile critical loads of acidity by sulfur deposition in 1990. About 75% of the ecosystems in red shaded areas are subject to risk of damage because sulfur deposition exceeds critical loads.

Further research requires the further development of critical loads and levels in combination with an assessment of the benefits of avoiding a pollution excess of such thresholds. The pollutants that need to be addressed will have to include NO_x and tropospheric ozone.

The collaborating network of Asian scientists which has been initiated during the first phase of the project has the potential to identify damage and its causes and forecast environmental effects in relation to national and international policies. With extension of the network this potential can be further enhanced. The RAINS-ASIA impact module may serve as an interface which can hasten the exchange of data, results and experience with respect to environmental effects and indicate ways of increasing protection.

6.6 References

Abrahamsen, G., 1984, Effects of acidic deposition on forest soil and vegetation, *Phil. Trans. R. Soc. Lond. B 305*, 369-82.

Arovaara, H., H. Ilvesniemi, 1990, The effect of soluble inorganic aluminium and nutrient imbalances on *Pinus sylvestris* and *Picea abies* seedlings. In *Acidification in Finland* (ed. by P. Kauppi), Springer-Verlag, Berlin. pp. 715-33.

Asp, H., B. Bengtsson, P. Jensen, 1988, Growth and uptake in spruce (*Picea abies*) grown in sand culture with various aluminium contents, *Plant and Soil 111*, 127-33.

Barrow, N.J., K. Spencer, W.H. McArthur, 1969, Effects of rainfall and parent material on the ability of soils to adsorb sulfate, *Soil Science 108*, 120-6.

Bhatti, N., D.G Streets, W.K. Foell, 1991, Acid rain in Asia. In *Proceedings of the Second Annual Workshop on Acid Rain and Emissions in Asia* (ed. by W.K. Foell and D. Sharma), Asian Institute of Technology, Bangkok, Thailand. pp. 5-33.

Bleeker, A., M. Posch, M., Forsius, J. Kämäri, 1994, Calibration of the SMART acidification model to selected IM-catchments. In *International Cooperative Programme on Integrated Monitoring of Air Pollution Effects on Ecosystems, Annual Synoptic Report 1994.* National Board of Waters and the Environment, Helsinki.

Bormann, F.H., 1985, Air pollution and forests: an ecosystem perspective, *Bioscience 35*, 434-41.

Bult, G.H., 1982, Soil Chemistry, Vol. B, Physical Chemical Modelling Development. In *Soil Science 5B.*

Butler, G.C., 1978, Approaches for protection standards for ionizing radiation and combustion pollutants, *Environmental Health Perspectives 22*, 13-5.

Cairns, J., 1977, Aquatic ecosystem assimilative capacity, *Fisheries 2*, 5-7 and 24.

Chadwick, M.J., J.C.I. Kuylenstierna, 1991a, The relative sensitivity of ecosystems in Europe to acidic depositions. A preliminary assessment of the sensitivity of aquatic and terrestrial ecosystems, *Perspectives in Energy 1*, 71-93.

Chadwick, M.J., J.C.I. Kuylenstierna, 1991b, Critical loads and critical levels for the effects of sulphur and nitrogen compounds. In *Acid Deposition* (ed. by J. Longhurst), Springer-Verlag, Berlin.

Chadwick, M.J., J. Nilsson, 1993, Environmental quality objectives - assimilative capacity and critical load concepts in environmental management. In *Clean Production Strategies* (ed. by T. Jackson), Lewis, Boca Raton.

Chuying, C., Z. Jiawu, X. Guangshan, Z. Chonglian, L. Liping, 1991, Effects of acid rain on forest ecosystem in southwestern China, *Journal of Environmental Sciences (China) 3(2)*, 27-36.

Downing, R.J., J.-P. Hettelingh, P.A.M. de Smet (eds.), 1993, *Calculation and Mapping of Critical Loads in Europe: Status Report 1993.* Coordination Center for Effects, National Institute of Public Health and Environmental Protection, Bilthoven.

Evers, F.H., 1983, Ein Versuch zur Aluminiumtoxizität bei Fichte, *Der Forst- und Holzwirt 12*, 305-7.

Falkengren-Grerup, U., 1990, Distribution of field layer species in Swedish deciduous forests in 1929-54 and 1979-88 as related to soil pH, *Vegetatio 86*, 143-50.

Fuhrer, J., B. Achermann (eds.), 1993, *Critical Levels for Ozone: a UN-ECE Workshop Report*, Swiss Federal Research Station for Agricultural Chemistry and Environmental Hygiene, No. 16, Liebefeld-Bern, Switzerland.

Fuzhu, Z., T. Hongshou, Y. Xiaofeng, C. Yugu, 1991, An evaluation of the effects of acid rain on yield of main crops and vegetables and associated economic losses in southwestern China. In *Proceedings of the Third Annual Conference on Acid Rain and Emissions in Asia* (ed. by W.K. Foell and C.W. Green), Asian Institute of Technology, Bangkok, Thailand. pp. 175-80.

Galloway, J.N. (1988). Effects of acid deposition on tropical aquatic ecosystems. In *Acidification in Tropical Countries (ed. by H. Rodhe and R. Herrera).* SCOPE 36, J. Wiley and Sons. pp. 141-66.

Gian, X.T.X., N.T. Van, N.H. Ninh, 1991, Air pollution and acid rain in Vietnam. In *Proceedings of the Third Annual Conference on Acid Rain and Emissions in Asia* (ed. by W.K. Foell and C. Green), Asian Institute of Technology, Bangkok, Thailand. pp. 196-200.

Göransson, A., T.D. Eldhuset, 1987, Effects of aluminium on growth and nutrient uptake of *Betula pendula* seedlings, *Physiol. Plant 69*, 193-9.

Goubet, A., 1969, The cooling of riverside thermal-power plants. In *Engineering Aspects of Thermal Pollution* (ed. by F.L. Parker and P.A. Krenkel). Vanderbilt University Press, Nashville, TN.

Harward, M.E., H.M. Reisenauer, 1966, Reactions and movement of inorganic soil sulfur, *Soil Science 101(4)*, 326-35.

Hettelingh, J.-P., W. de Vries, 1991, *Mapping Vademecum*, National Institute of Public Health and Environmental Protection, Coordination Center for Effects, Bilthoven, The Netherlands.

Hettelingh, J.-P., R.J. Downing, P.A.M. de Smet, 1991, *Mapping Critical Loads for Europe*, RIVM, Bilthoven.

Hettelingh, J.-P., M. Posch, 1993, Critical loads and a dynamic assessment of ecosystem recovery. In *Predictability and Nonlinear Modelling in Natural Sciences and Economics* (ed. by J.Grasman and G.van Straten). Kluwer Academic Publishers, Dordrecht, The Netherlands.

Hettelingh, J.-P., R.J. Downing, P.A.M. de Smet, 1992, The critical load concept for the control of acidification. In *Acidification Research: Evaluation and Policy Applications* (ed. by T. Schneider), Elsevier Studies in Environmental Science 50, Amsterdam, pp. 161-174.

Hettelingh, J.-P., R.H. Gardner, L. Hordijk, 1992b, A statistical approach to the regional use of critical loads, *Environ. Pollut. 77*, 177-183.

Ilvesniemi, H., 1992, The combined effect of mineral nutrition and soluble aluminium on *Pinus sylvestris* and *Picea abies* seedlings, *Forest Ecology and Management 51*, 227-38.

Isichei, A.D., F. Akeredolu, 1988, Acidification potential in the nigerian environment. In *Acidification in Tropical Countries (ed. by H. Rodhe and R. Herrera)*. SCOPE 36, Wiley, Chichester. pp. 297-316.

Jordan, C.F., 1985, *Nutrient Cycling in Tropical Forest Ecosystems*, Wiley.

Kuylenstierna, J.C.I. M.J. Chadwick, 1989, The relative sensitivity of ecosystems in Europe to the indirect effects of acidic depositions. In *Regional Acidification Models* (ed. by J. Kämäri, D. Brakke, A Jenkins, S. Norton and R.F. Wright), Springer-Verlag, Heidelberg.

Kuylenstierna, J.C.I., C.A. Gough, M.J. Chadwick, J.-P. Hettelingh, R.J. Downing, P.A.M. de Smet, 1991, Comparison of the Stockholm Environment Institute critical loads map and the CCE critical loads map based on European and national data. In *Mapping Critical Loads for Europe* (ed. by J.-P. Hettelingh, R.J. Downing and P.A.M. de Smet), Coordination Center for Effects, Technical Report No. 1, Bilthoven, The Netherlands. pp. 58-75.

Kuylenstierna, J.C.I., S. Cinderby, M.J. Chadwick, 1992, A preliminary mapping of relative sensitivity of terrestrial ecosystems to acidic deposition in Asia. In *Proceedings of the Third Annual Conference on Acid Rain and Emissions in Asia* (ed. by W.K. Foell and C.W. Green), Asian Institute of Technology, Bangkok, Thailand. pp. 46-76.

Kronberg, B.I., W.S., Fyfe, O.H. Leonardos, A.M. Santos, 1979, The chemistry of some Brazilian soils: element mobility during intense weathering, *Chemical Geology 24*, 211-29.

Liping, L., C. Chuying, 1991, Effects of simulated acid rain on root growth of *Cunninghamia lanceolata* and *Schima superba* saplings planted in acidified soil, *Journal of Environmental Sciences (China) 3(2)*, 45-52.

Lucas, A.E., D.W. Cowell, 1984, Regional assessment of sensitivity to acidic deposition for eastern Canada. In *Geological Aspects of Acid Deposition* (ed. by O.P. Bricker), *Acid Precipitation Series 7*, Ann Arbor, Boston. Butterworth. pp. 113-29.

McDowell, W.H., 1988, Potential effects of acid deposition on tropical terrestrial ecosystems. In *Acidification in Tropical Countries (ed. by H. Rodhe and R. Herrera).* SCOPE 36, Wiley. pp. 117-40.

Makkonen-Spiecker, K., 1985, Auswirkungen des Aluminiums auf junge Fichten (*Picea abies* Karst.) verschiedener Provenienzen, *Forstwissenschaftliches Zentralblatt 104*, 341-53.

Moreira-Nordemann, L.M., M.M. Forti, V.L Di Lascio, C.M Do Espírito Santo, O.M. Danelon, 1988, Acidification in southeastern Brazil. In *Acidification in Tropical Countries* (ed. by H. Rodhe and R. Herrera). SCOPE 36, Wiley. pp. 257-96.

Nilsson, J. (ed.), 1986, Critical loads for nitrogen and sulphur, *Miljörapport* 1986:*11*, Nordic Council of Ministers, Copenhagen.

Nilsson, J., P. Grennfelt (eds.), 1988, Critical Loads for sulphur and nitrogen. Report from a workshop held at Skokloster, 19-24 March 1988. Nordic Council of Ministers, *Miljørapport* 1988:*15*, Copenhagen.

Posch, M., J.-P., Hettelingh, H.U. Sverdrup, K. Bull, W.de Vries, 1993, Guidelines for the computation and mapping of critical loads and exceedances of sulphur and nitrogen in Europe. In *Computation and Capping of Critical Loads in Europe* (ed. by R.J. Downing, J.-P. Hettelingh, P.A.M. de Smet), RIVM, Bilthoven.

Portmann, J.E., R. Lloyd, 1986, Safe use of the assimilative capacity of the marine environment for waste disposal - is it feasible? *Water Sci. Technol. 18*, 233.

Pravdic, V., 1987, Environmental capacity: an approach for prevention of water pollution, *Water Qual. Bull. 12*, 137-40, 166.

Pravdic, V., M. Juracic, 1988, The environmental capacity approach to the control of marine pollution: the case of copper in the Krka river estuary, *Chem. Ecol. 3*, 105.

Preston, A., J. Portmann, 1981, Critical path analysis applied to the control of mercury inputs to United Kingdom coastal waters, *Environ. Pollut. Ser. B 2*, 451.

Rodhe, H., 1989, Acidification in a global perspective, *Ambio 18(3)*, 155-60.

Rodhe, H., R. Herrera (eds.), 1988, *Acidification in Tropical Countries*. SCOPE 36, Wiley.

Sanchez. P.A., 1976, *Properties and Management of Soils in the Tropics*, Wiley, New York.

Sanhueza, E., G. Cuenca, M.J., Gómez, R. Herrera, C. Ishizaki, J. Martí, J. Paolini, 1988, Characterization of the Venezuelan environment and its potential for acidification. In *Acidification in Tropical Countries (ed. by H. Rodhe and R. Herrera).* SCOPE 36, Wiley. pp. 197-256.

Shindo, J., A.K. Bregt, T. Hakamata, 1994, Application and evaluation of critical load methods for acid deposition in Gunma, Japan.

Sverdrup, H.U., 1990, *The Kinetics of Base Cation Release due to Chemical Weathering*, Lund University Press, Lund.

Sverdrup, H., W. de Vries, 1993, Calculating critical loads for acidity with the simple mass balance method, *Water, Air and Soil Pollution 72*, 143-162.

Sverdrup, H., W. de Vries, A. Henriksen, 1990, Mapping critical loads: a guidance manual to criteria, calculation, data collection and mapping. Nordic Council of Ministers, *Miljørapport* 1990:*14*, Copenhagen.

Sverdrup, H., P. Warfvinge, 1993, *Effect of Soil Acidification on Growth of Trees and Plants as Expressed by the (Ca + Mg + K)/Al Ratio*, Report 2:1993, Department of Chem. Eng. II, Lund University, Lund, Sweden.

Tischner, T., U. Kaiser, A. Hueltermann, 1985, Untersuchungen zum Einfluss von Aluminium-Ionen auf das Wachstum von Fichtenkeimlingen in Abhängigkeit vom pH-Wert, *Forstwissenschaftliches Zentralblatt 104*, 329-36.

Ulrich, B., 1983, An ecosystem-orientated hypothesis on the effect of air pollution on forest ecosystems. In *Ecological Effects of Acid Deposition* (ed. by G. Persson and A. Jerretöv), Environmental Protection Board, SNV-DM 1636, Stockholm, 221-31.

Ulrich, B., M.E. Sumner (eds.), 1991, *Soil Acidity*, Springer-Verlag.

Wada, H., Y. Iwasa, K. Arimitsu, 1983, *Map for Assessing Susceptibility of Japanese Soils to Acidic Precipitation*, Kokudo Mapping Company, Tokyo.

Wellburn, A. (1988). *Air Pollution and Acid Rain.* Longman, Harlow.

UN ECE, 1993, *Manual on Methodologies and Criteria for Mapping Critical Levels/Loads and Geographic Areas where they are Exceeded.* Convention on Long-range Transboundary Air Pollution, Task Force on Mapping, Geneva. Federal Environmental Agency, Texte 25/93, Berlin.

Velz, C.J., 1976, Stream analysis - forecasting waste assimilative capacity. In *Water Resource and Pollution Control* (ed. by H.W. Gehm and J. I. Bregman). van Nostrand Reinhold, New York.

Xue, H.B., J.L. Schnoor, 1994, Acid deposition and lake chemistry in southwest China, *Water Air and Soil Pollution*, 75: 61-78.

Zhao, D, J. Xiong, 1988, Acidification in southwestern China. In *Acidification in Tropical Countries* (ed. by H. Rodhe and R. Herrera). Scope 36, J. Wiley & Sons. pp. 317-47.

Zhao, D., J. Mao, J. Xiong, X. Zhang, J. Yang, 1995, The assessment of critical loads in China (forthcoming).

Zongwei, F., S. Kyunfeng, 1991, Relative sensitivities of woody plants to acid deposition in south areas of China, *Journal of Environmental Sciences (China)*, *3(2)*, 61-8.

RAINS-ASIA:
AN ASSESSMENT MODEL FOR AIR POLLUTION IN ASIA

Chapter 7

Scenarios of Future Acidification in Asia: Exploratory Calculations

Markus Amann, Janusz Cofala

Report on the World Bank Sponsored Project
"Acid Rain and Emission Reductions in Asia"

December 1995

7. SCENARIOS OF FUTURE ACIDIFICATION IN ASIA: EXPLORATORY CALCULATIONS

Authors:
Markus Amann, Janusz Cofala

TABLE OF CONTENTS

7.1 Introduction VII-1
7.2 Energy pathways VII-2
7.3 A reference emission scenario: base case energy path without additional measures to control emissions VII-4
7.3.1 Sulfur deposition VII-7
7.3.2 Achievement of critical loads for acid deposition VII-8
7.4 Exploring the technical potential for reducing SO_2 emissions: The BAT (Best Available Technology) scenario VII-12
7.5 An advanced emission control technology (ACT) scenario VII-14
7.6 A 'basic control technology' (BCT) scenario VII-17
7.7 A scenario with local applications of advanced technologies (LACT) . . . VII-21
7.8 Relocation of plants in sensitive regions VII-25
7.9 Implications of the energy efficiency pathway VII-30
7.10 Conclusions VII-31
References VII-33

LIST OF TABLES

Table 7.1 SO_2 emissions in 1990 and for the reference scenario in the year 2020 (in thousand tons of SO_2) VII-6
Table 7.2 Cost-effectiveness of available measures for area sources in the North Highlands region in Thailand VII-16
Table 7.3 Emissions and control costs for the BAT, ACT and BCT scenarios in the year 2020 . . . . . VII-20
Table 7.4 Emissions and control costs in 2020 for China, India and Pakistan in the LACT scenario VII-22
Table 7.5 Contribution of sulfur deposition to two grids for the reference scenario for the year 2020 in milligrams sulfur/m^2/year VII-26
Table 7.6 Comparison of emissions and emission control costs for the base case energy pathway and the energy efficiency pathway VII-31

LIST OF FIGURES

Figure 7.1 Primary energy consumption in the region, Base case energy pathway (1000 PJ) VII-3
Figure 7.2 Primary energy consumption in the region, Energy efficiency pathway (1000 PJ) VII-3

Figure 7.3	SO_2 emissions by fuel, reference scenario (million tons of SO_2) . .	VII-5
Figure 7.4	SO_2 emissions by sector, reference scenario (million tons of SO_2) .	VII-5
Figure 7.5	Sulfur deposition in 2020, Reference scenario (base case energy pathway, no further measures beyond current legislation assumed) .	VII-7
Figure 7.6	Growth in sulfur deposition between 1990 and 2020, Reference scenario (base case energy pathway, no further emission control measures current legislation assumed)	VII-8
Figure 7.7	Excess deposition above critical loads (all ecosystems) in 2020, Reference scenario (no further emission control beyond current legislation assumed).	VII-9
Figure 7.8	Excess deposition above critical loads for agricultural ecosystems in 2020, Reference scenario (no further emission control beyond current legislation assumed).	VII-10
Figure 7.9	Ambient levels of SO_2 concentrations in Asia, 2020, reference scenario (no emission control beyond current legislation assumed)	VII-11
Figure 7.10	Excess of critical loads for the BAT scenario in 2020	VII-13
Figure 7.11	Excess deposition for the ACT strategy in the year 2020	VII-17
Figure 7.12	Excess sulfur deposition for the basic control technology (BCT) scenario for the year 2020	VII-21
Figure 7.13	Excess sulfur deposition for the LACT scenario (local application of advanced control technologies) for the year 2020	VII-24
Figure 7.14	Sulfur deposition from the Lampang power station for the reference scenario (no emission control assumed) for the year 2020	VII-27
Figure 7.15	Excess sulfur deposition for a scenario in which some new power stations in China and Thailand are moved to ecologically less sensitive regions	VII-29

7. SCENARIOS OF FUTURE ACIDIFICATION IN ASIA: EXPLORATORY CALCULATIONS

Authors:
Markus Amann, Janusz Cofala

7.1 Introduction

This chapter presents the results of an initial application of the Regional Air Pollution Information and Simulation (RAINS) model to explore the potential impacts on acidification of future scenarios of energy development in Asia. The purpose of these initial applications is twofold.

First, these scenarios provide the first regionally-disaggregated and integrative picture of the consequences of emissions and acid deposition under potential economic development and technological conditions for Asia during the coming two to three decades based on currently available knowledge.

Second, the scenario development provides a first practical test of the RAINS-Asia model, a new tool for the integrated assessment of sulfur emissions' impacts and abatement strategies for Asia.

The database upon which the scenarios are based represents an extensive collection and compilation effort carried out by a large number of institutions in Asia and Europe. The scenario generation process has provided an important step in sorting, organizing, assimilating, and updating that data - a process which is still underway and, in fact, never ends.

This chapter is organized as follows: Section 7.2 describes the baseline development of future energy use in Asia according to national expectations (the *base case* energy pathway). As an alternative, a scenario has been developed that explores the potential for increased energy efficiency and use of renewable resources (the *energy efficiency* pathway). Section 7.3 projects future sulfur emissions for the baseline energy scenario without further measures to control SO_2 emissions and analyzes regional sulfur deposition with critical loads, which have been defined in Chapter 6 of this report. Motivated by the serious threat imposed to many ecosystems by the uncontrolled growth of emissions, various features of the RAINS model are used to explore alternative strategies to keep sulfur deposition closer to critical loads. Section 7.4 examines costs and environmental impacts of a hypothetical strategy applying western emission standards to all Asian countries. Because of the high costs involved in such a policy, Section 7.5 applies advanced emission control measures only to the largest emission sources throughout the region. Since currently advanced control technologies are not legally required in most Asian countries, Section 7.6 investigates the costs and levels of ecosystem protection, if only domestically available emission control techniques would be applied. It will be shown that by selectively applying advanced measures to those areas, which have significant impacts on sensitive ecosystems, similar environmental impacts could be achieved at lower costs (Section 7.7). Section 7.8 demonstrates the capability of the RAINS model to identify impacts of individual emission sources and to relocate large point sources to less sensitive sites. Section 7.9 explores the implications of energy efficiency strategies. Conclusions are drawn in Section 7.10.

7.2 Energy pathways

To provide a basis for the analysis of emissions and emission control strategies, the RESGEN module of the RAINS model was used to develop two alternative energy pathways:

- The base case energy pathway, resembling 'business as usual' practices. This pathway assumes that each country would continue the current trends in energy policies, without strong promotion of energy efficiency measures or fuel substitution to reduce the emissions of acidifying pollutants. Efforts were made to utilize energy demand forecasts made by the government planning organizations or research institutions in each country. This pathway is the basis for the emission (control) scenarios analyzed in the following sections 7.3 to 7.8.

- An energy efficiency pathway. This pathway explores the possible reduction of emissions through a strong effort to use energy more efficiently. The efficiency improvements possible through to 2020 are based primarily on the experiences of the industrialized countries during the period 1973 – 1983 including the response to the sharp rise in energy prices, general improvements in technology, and increased use of renewable resources. The consequences of an energy efficiency pathway on SO_2 emissions and control costs are further explored in Section 7.9.

These two pathways are based on a variety of assumptions on socio-economic development, population growth, technological progress, etc., which are documented in Chapter 3 of this report. RESGEN was used to develop energy pathways for all 23 countries considered in RAINS-Asia. Furthermore, the data of the largest countries was disaggregated into sub-national regions, totalling 94 over all of Asia. Chapter 3 provides details on the RESGEN model.

Figures 7.1 and 7.2 display total primary energy consumption by fuel for the two pathways. Reflecting the current expectations in the countries, total primary energy consumption in the base case grows by 230 percent between 1990 and 2020 with a proportional increase in coal consumption. In the efficiency case, primary energy consumption grows by about 150 percent in the same period, with an even lower increase in coal use.

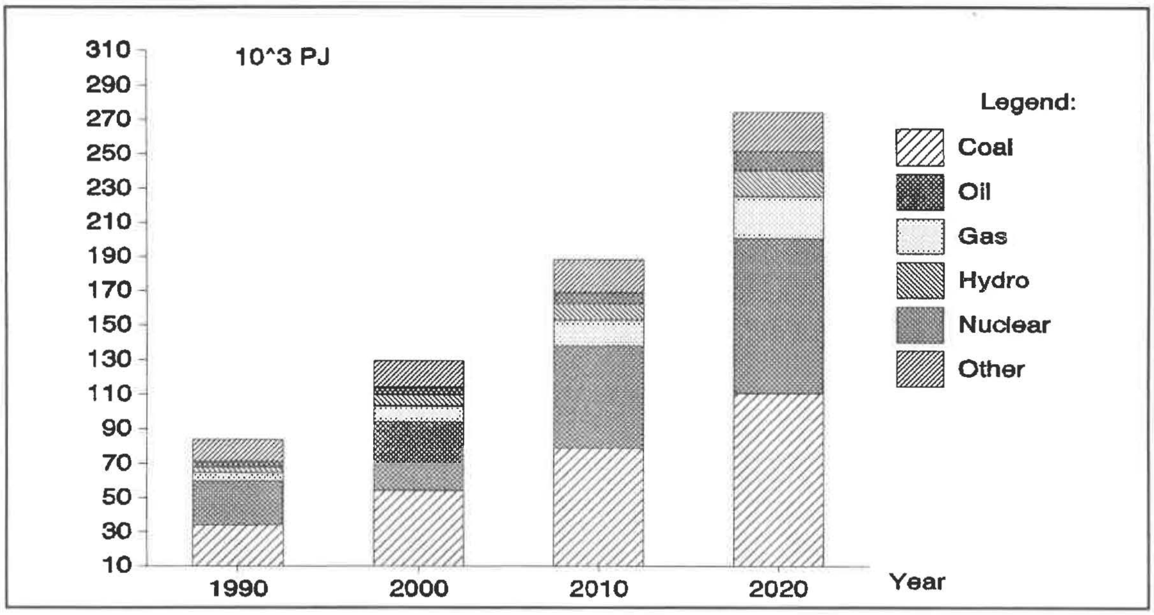

Figure 7.1 Primary energy consumption in the region, Base case energy pathway (1000 PJ)

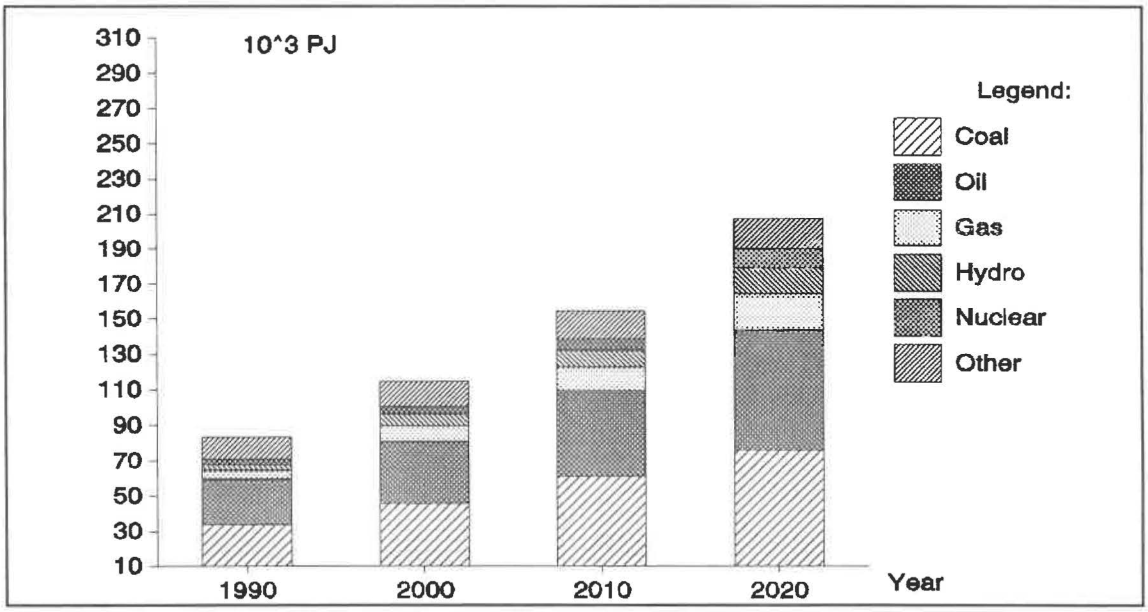

Figure 7.2 Primary energy consumption in the region, Energy efficiency pathway (1000 PJ)

7.3 *A reference emission scenario: base case energy path without additional measures to control emissions*

In order to provide a reference for the further analysis, an emission scenario has been developed based on the assumption that economic and energy development will follow the base case pathway and that -beyond the control measures required by current legislation in Japan and Taiwan - no further action will be taken for reducing SO_2 emissions. Due to the strong growth in economic activities and, subsequently, energy consumption assumed in the base case energy path, the lack of measures to limit emissions would lead to a significant increase in SO_2 emissions in the region: from 33.6 million tons in 1990 to more than 110 million tons in 2020, i.e., by about 230 percent. The increase in SO_2 emissions is strongly connected to the use of coal. Coal combustion is responsible for about three quarters of the total emissions over the whole period under study. About 20 percent of the emissions originate from the combustion of liquid fuels; the balance is a result of biomass combustion (Figure 7.3).

Figure 7.4 shows the development of emissions by economic sector. The highest growth in emissions comes from the power plant sector, due to the increased use of coal-based electricity generation. This sector's contribution to total emissions increases from 30 percent in 1990 to 37 percent in 2020. Thereby, also the relative importance of the various emission sources experiences an important change: whereas in 1990 about 16 percent of total SO_2 emissions in the region originated from the large point sources considered in the RAINS model (i.e., power stations with large boilers), in 2020 this share is expected to constitute about 25 percent of total emissions.

Differences among countries in the rates of economic development and the anticipated structures of the energy supply cause a regionally inhomogeneous picture of future emissions growth. In Japan, SO_2 emissions would increase by about 30 percent, whereas, e.g., in India, Indonesia, Philippines and Thailand the predicted expansions reach typically a factor of four to five (compare Table 7.1). For Pakistan, the expected growth in the consumption of high sulfur lignite would increase SO_2 emissions by a factor of 12, although compared to a low level in 1990.

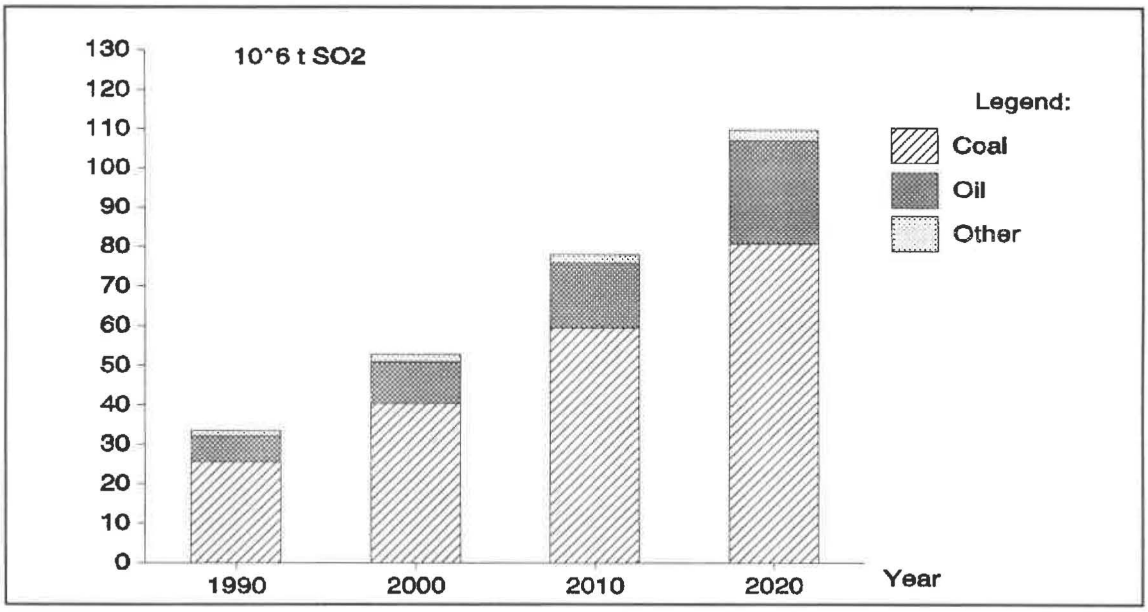

Figure 7.3 SO_2 emissions by fuel, reference scenario (million tons of SO_2)

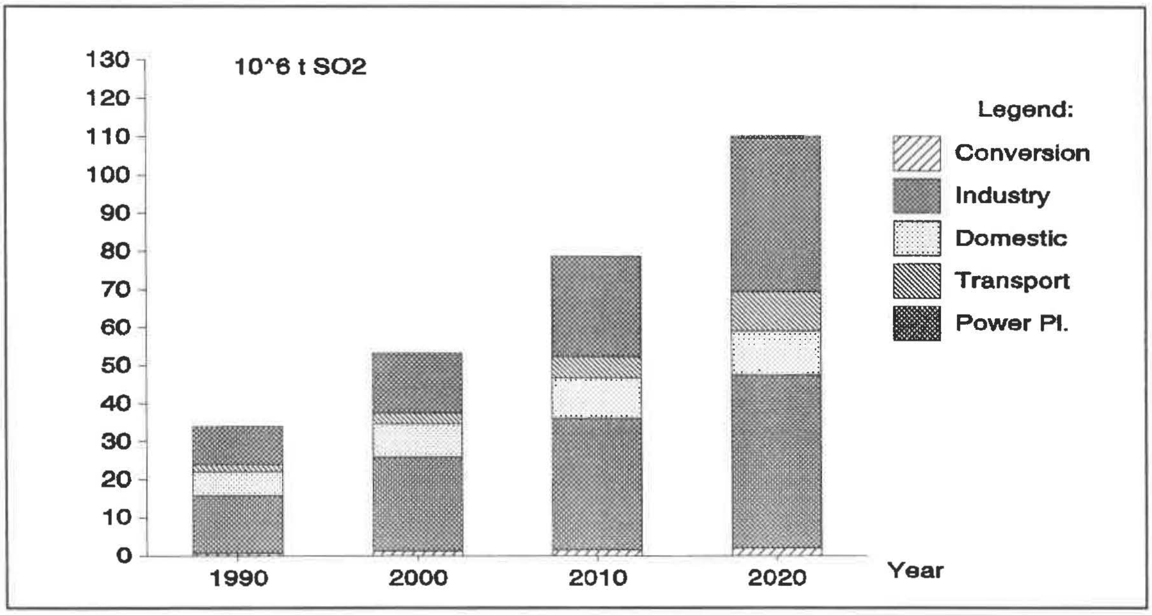

Figure 7.4 SO_2 emissions by sector, reference scenario (million tons of SO_2)

Table 7.1 SO_2 emissions in 1990 and for the reference scenario in the year 2020 (in thousand tons of SO_2)

	1990	Reference scenario, 2020	Increase
Bangladesh	118	524	344 %
Bhutan	2	12	500 %
Brunei	6	18	200 %
Cambodia	22	147	568 %
China	21908	60687	177 %
Hong Kong	140	378	170 %
India	4471	18549	315 %
Indonesia	630	3162	402 %
Japan	835	1120	34 %
Korea, north	343	1345	292 %
Korea, south	1640	5537	238 %
Laos	3	12	300 %
Malaysia	205	409	100 %
Mongolia	78	168	115 %
Myanmar	18	40	122 %
Nepal	122	247	102 %
Pakistan	614	7527	1126 %
Philippines	390	2037	422 %
Sea lanes	243	511	110 %
Singapore	191	1033	441 %
Sri Lanka	42	239	469 %
Taiwan	500	1478	196 %
Thailand	1038	4637	347 %
Vietnam	113	654	479 %
TOTAL	33674	110477	228 %

7.3.1 Sulfur deposition

The boost in SO_2 emissions resulting from the high growth in energy consumption will cause a strong increase in sulfur deposition throughout the region. In 2020, virtually all eastern parts of China and large regions in India would experience deposition between two and five grams. In many industrialized and metropolitan areas in Thailand, the Philippines and Malaysia sulfur deposition will exceed five grams to ten grams per square meter and year. Peak deposition of sulfur would escalate in some industrialized areas in China to about 26 grams per square meter and year (Figure 7.5). For comparison, sulfur deposition observed in the well-known industrial areas of Central and Eastern Europe peaked at about 15 grams per square meter and year.

Figure 7.6 reveals a significant change in deposition for almost all of Asia: In major areas in eastern and southern China and in some parts of Japan, sulfur deposition will increase by a factor of two to three, with places with increases of up to a factor of five. A factor of five is also observed in many regions India, Korea and Thailand. There are, however, also several sites in Asia for which an increase in sulfur deposition up to a factor of ten has to be expected. It should be mentioned that changes in emissions from outside the region (e.g., from Siberia) are not taken into account for this analysis.

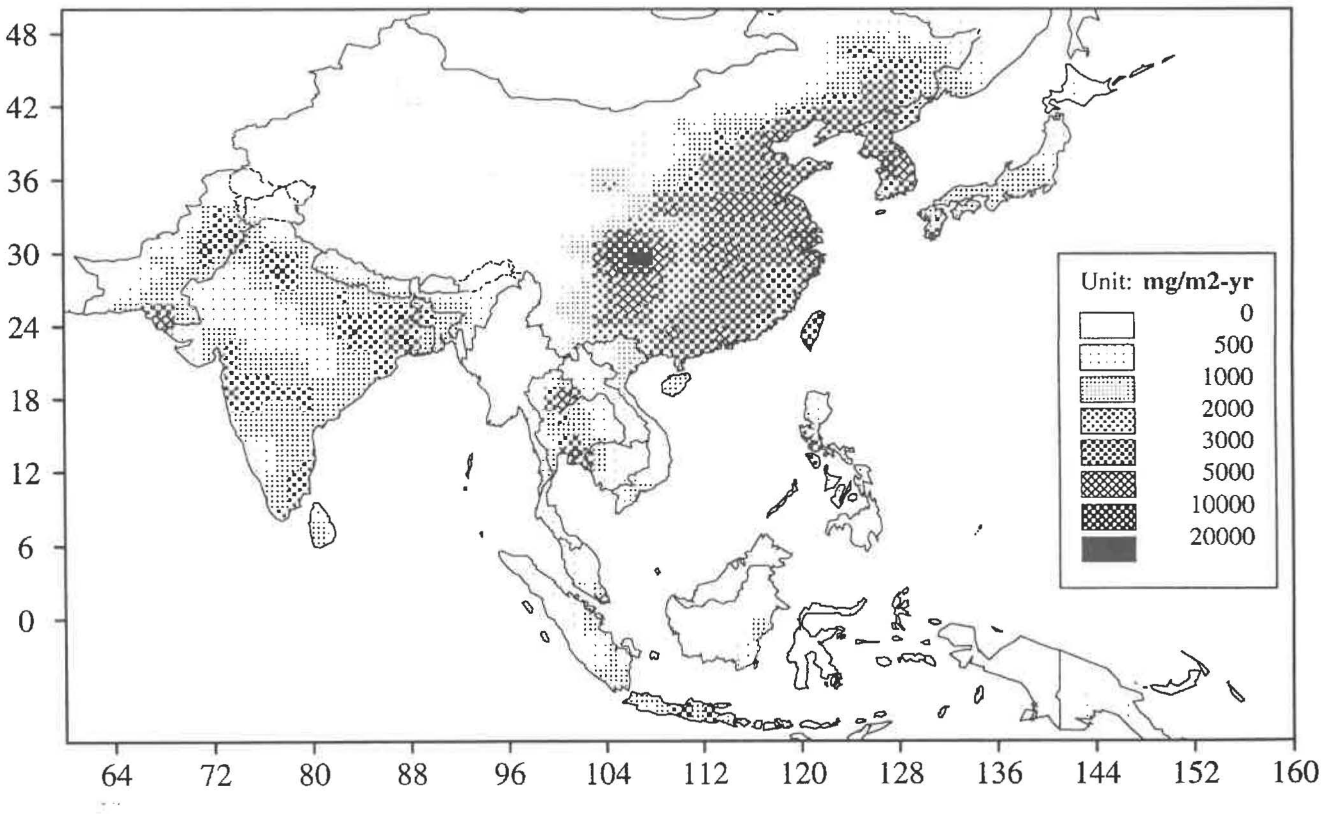

Figure 7.5 Sulfur deposition in 2020, Reference scenario (base case energy pathway, no further measures beyond current legislation assumed)

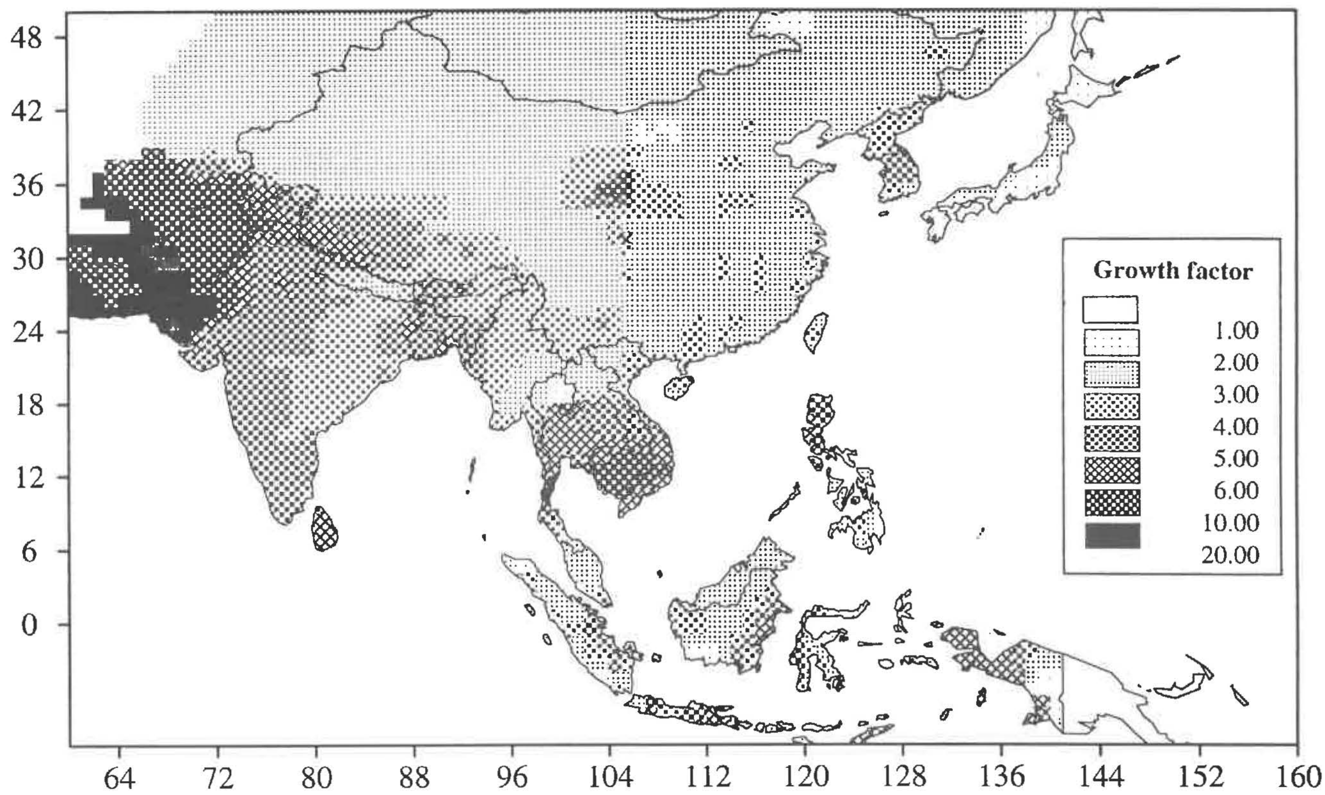

Figure 7.6 Growth in sulfur deposition between 1990 and 2020, Reference scenario (base case energy pathway, no further emission control measures current legislation assumed)

7.3.2 Achievement of critical loads for acid deposition

One way to judge the potential environmental damage caused by increased sulfur deposition is to compare deposition with critical loads, which resemble the maximum deposition that will not cause chemical changes leading to harmful effects on ecosystem structure and function. A detailed description of how critical loads have been estimated and how excess deposition can be interpreted is provided in Chapter 6 of this report. Figure 7.7 displays excess deposition, i.e., sulfur deposition above the critical loads, for the reference scenario for the year 2020. As a conservative assumption the 25 percentile of critical loads database has been used for this analysis, allowing for eventual uncertainties and data inaccuracies in the quantitative estimates of the critical loads.

Figure 7.7 shows that under the reference emission scenario, i.e., in the do-nothing case, critical loads will be exceeded in many regions in Asia, although not everywhere. Pakistan, the western and central parts of India, western China, Myanmar and parts of Indonesia experience no or only little excess deposition even under the highest emission scenarios considered in this paper. In other areas, e.g., in southern and eastern China, in Korea and in northern Thailand, widespread serious excess deposition has to be expected. In addition, many 'hot spots' occur on the local scale.

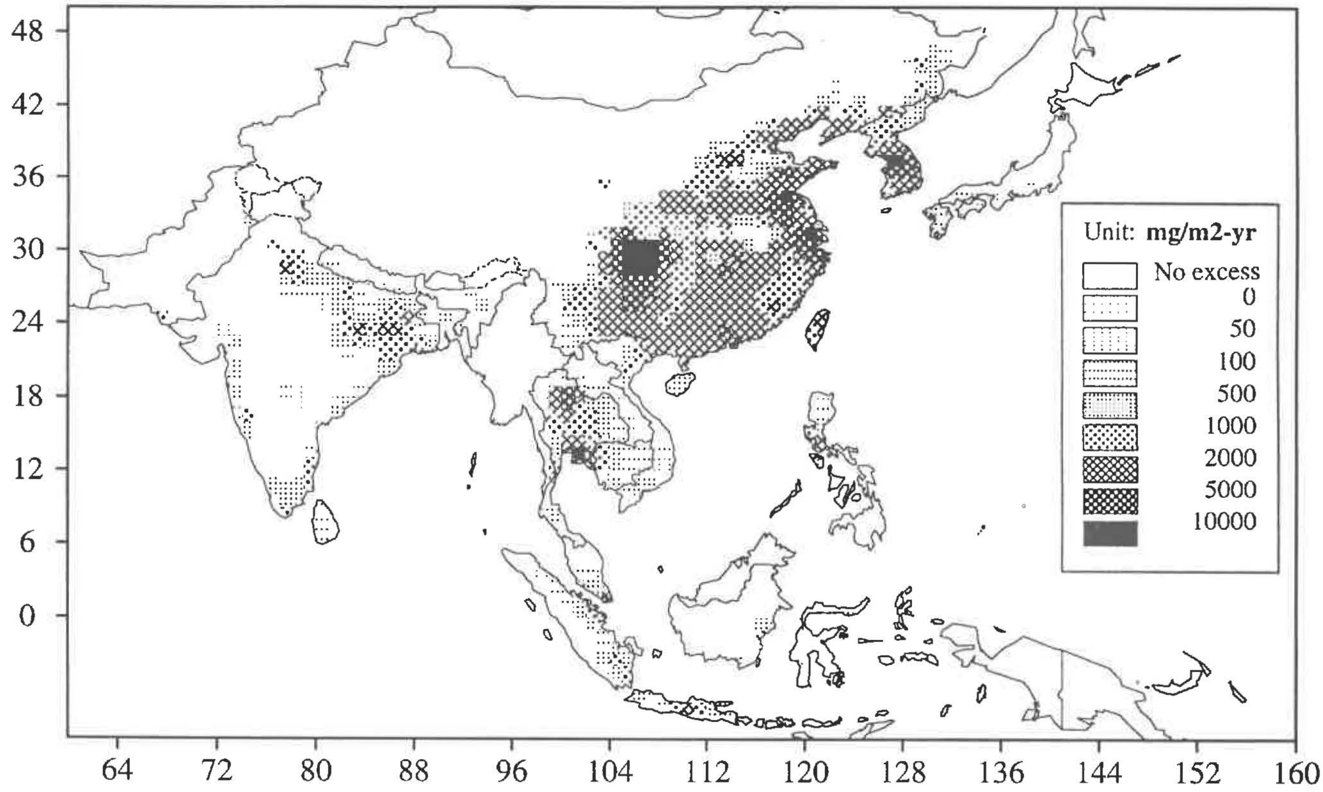

Figure 7.7 Excess deposition above critical loads (all ecosystems) in 2020, Reference scenario (no further emission control beyond current legislation assumed).

It must be emphasized that - under the assumptions of this scenario - excess deposition will reach unprecedented levels in some regions: The RAINS model calculates that critical loads will be exceeded by between two and five grams sulfur per square meter per year in large parts in central and eastern China, in northern Thailand. Highest excess deposition (up to 15 to 20 grams sulfur per square meter per year) is calculated for some ecosystems in Korea, the Bangkok metropolitan region, and in the Sichuan and Shanghai provinces. For comparison, total sulfur deposition in many of these areas is currently in the range of two to three grams.

Although the current state of scientific knowledge does not yet allow drawing conclusions about the environmental damage implied with such excess deposition, the fact that sulfur deposition will be more than ten times above the sustainable levels in large areas may give reason for serious concern. To derive more specific information on potential environmental threats, the RAINS model enables the examination of conditions for various types of ecosystems individually. To illustrate this feature, Figure 7.8 displays excess deposition only for agricultural ecosystems. Calculations show that the growth of sulfur deposition could have a severe negative influence on the conditions of many important agricultural crops in Asia. The fact that the major rice growing areas in Asia (e.g., in China, India and Japan) will experience excess deposition up to 15 grams per square meter and year may also give reason for serious concern.

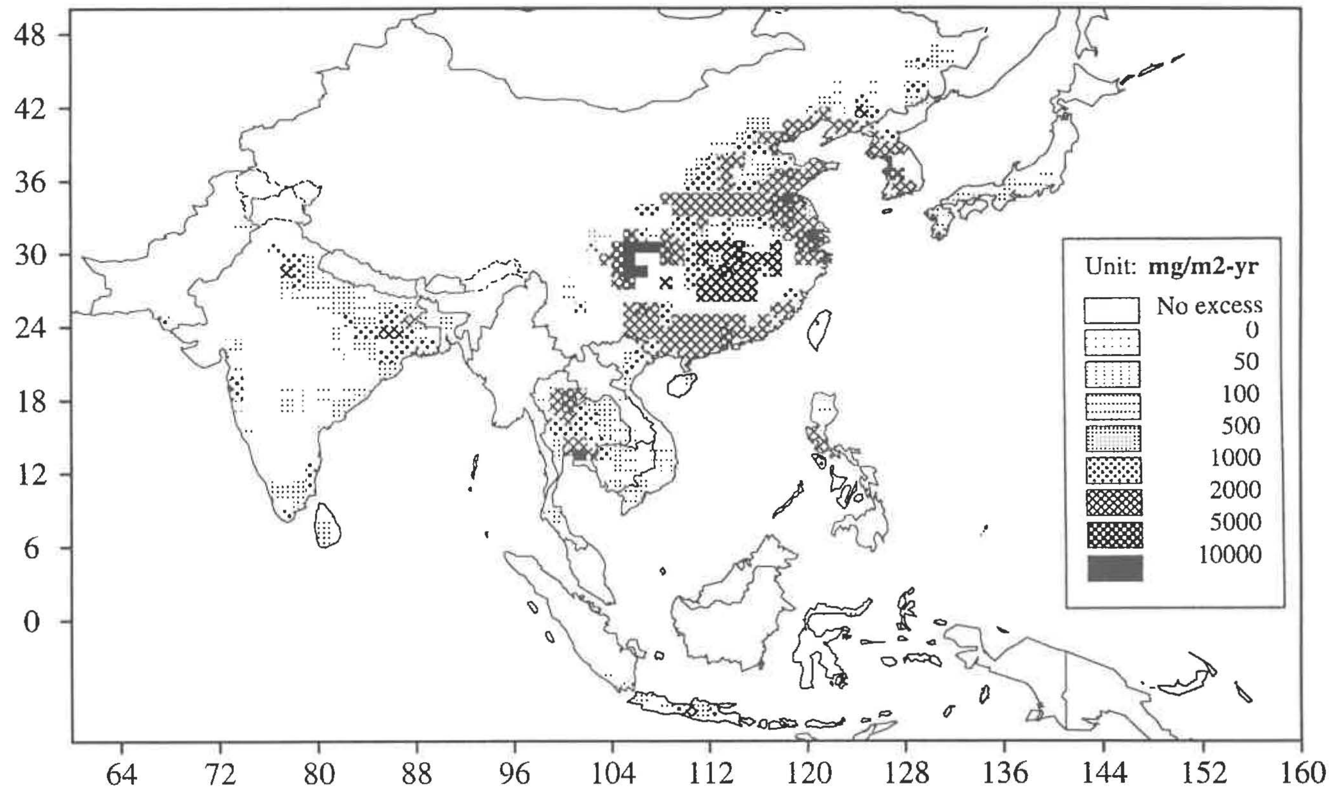

Figure 7.8 Excess deposition above critical loads for agricultural ecosystems in 2020, Reference scenario (no further emission control beyond current legislation assumed).

Obviously, deposition of air pollutants influencing the soil chemistry represents only one potential cause for environmental damage. Analysis shows, however, that high deposition is always linked to sufficiently high levels of ambient concentrations. The associated ambient SO_2 levels in the rice growing regions in China are estimated to reach in this scenario up to 60 micrograms SO_2/m^3 (Figure 7.9). Although specific analysis of dose-response relationships for rice paddies is still lacking, a rough extrapolation of the threshold levels for similar ecosystems (which range usually from 20 to 30 micrograms/m^3, see e.g. IUFRO, 1978) would suggest an excess of these levels by a factor of two to three.

High ambient levels of SO_2 concentrations resulting from this scenario do not only imply serious risks to natural and agricultural ecosystems, but impose also serious threat to human health. One of the first and most visible signals is the deterioration of urban air quality in large metropolitan agglomerations in Asia. Although the assessment of urban air pollution was excluded from the first phase of the RAINS-Asia work, Figure 7.9 suggests the unabated scenario to exceed the WHO guideline of 40-60 micrograms SO_2/m^3 (annual average - WHO, 1979) in many Asian regions, even calculated as an average over grids with a size of one degree longitude by one degree latitude resolution. Although a direct link to actual air quality in cities is not yet possible, experience shows that actual concentrations in the urban centers of a grid are usually substantially higher than the grid average. Calculated on the same spatial resolution the model shows that ambient levels of SO_2 concentrations increase in many regions in Asia by a factor of four to five compared to the 1990 levels.

As outlined above it can be expected that the growth in SO_2 emissions associated with the envisaged evolution of energy use gives reason for serious concern about maintaining sustainable conditions for natural and agricultural ecosystems in Asia. Sulfur deposition will cause significant changes in the soil chemistry over wide areas in Asia, affecting growing conditions for many natural ecosystems and agricultural crops. Ambient levels of SO_2 will exceed WHO health guidelines not only in cities, but also in many rural regions. If no countermeasures were taken, a degradation of the environmental quality to unprecedented levels has to be anticipated.

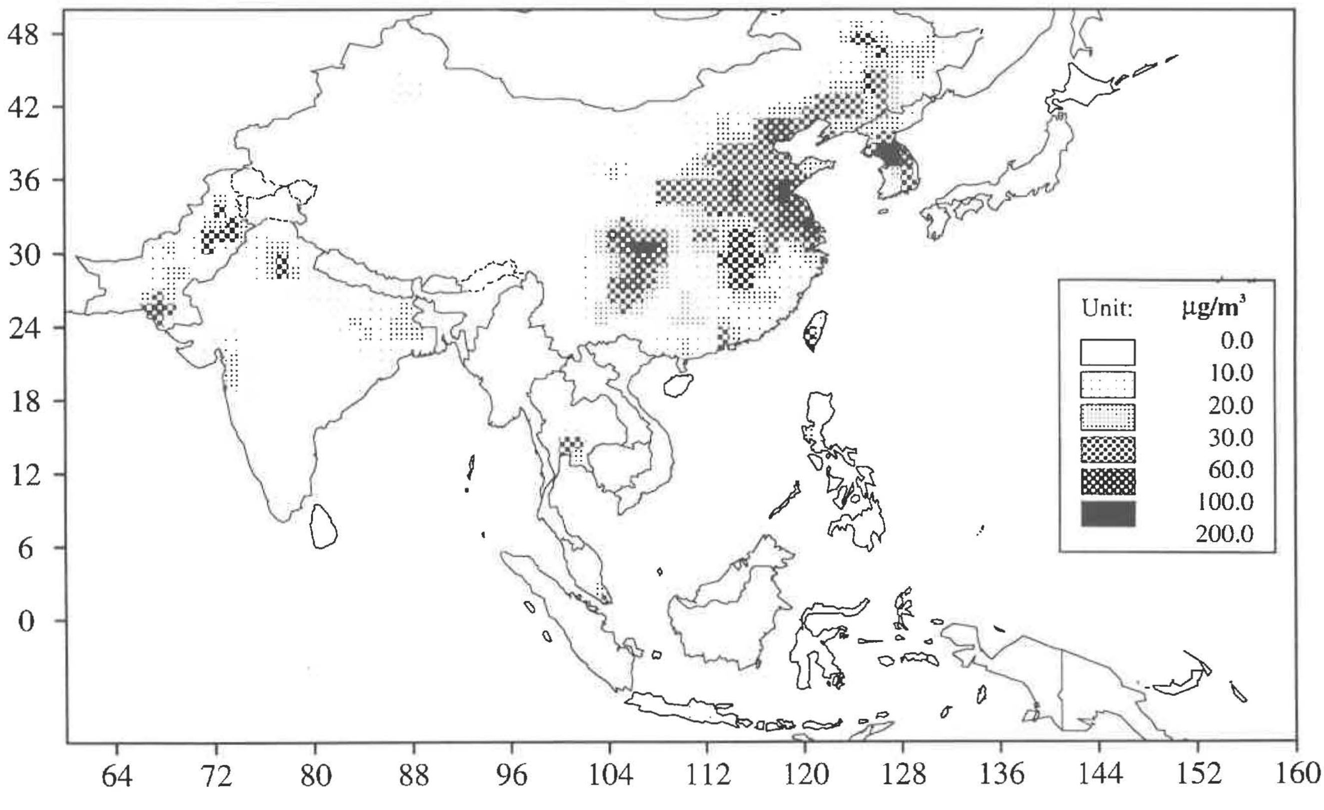

Figure 7.9 Ambient levels of SO_2 concentrations in Asia, 2020, reference scenario (no emission control beyond current legislation assumed)

A major feature of the RAINS model is its capability to simulate SO_2 emission control strategies and explore their costs and their regional environmental benefits in physical terms. In the model, emissions can be reduced by prescribing specific measures at selected sources, i.e., at specific economic sectors in individual regions or countries. Details of how emission control measures and costs have been modelled in RAINS are provided in Chapter 4 of this report.

In response to the finding of the previous section, i.e., that realizing the officially anticipated energy development without any measures to control emissions might cause dramatic negative environmental impacts, the following sections explores costs and environmental benefits of alternative strategies for reducing SO_2 emissions. Sections 7.4 and 7.5 discuss the impacts of applying certain packages of emission control measures throughout the region. Thereafter, Sections 7.6 to 7.8 explore the potential for cost savings offered by selective application of technologies guided by the different levels of environmental sensitivities.

7.4 Exploring the technical potential for reducing SO_2 emissions: The BAT (Best Available Technology) scenario

To explore the potential, costs and ecological improvements offered by advanced technological means to reduce emissions a scenario has been developed which simulates for the base case energy pathway the application of advanced emission control technologies to all relevant emission sources throughout Asia. The measures considered in this scenario represent the current technological standards in many industrialized countries. In particular, wet flue gas desulfurization (WFGD) processes are assumed for all industrial and power plant boilers burning coal and oil, including retrofits of the existing boiler stock. Since, for obvious technical reasons, in the residential/commercial (domestic) sector and in the transport sector the use of flue gas desulfurization is not possible, the use of low sulfur fuels (low sulfur coal, low sulfur oil) has been assumed for all small sources (Box 1).

Box 1: Measures assumed for the 'best available technology' (BAT) scenario

The Best Available Technology (BAT)-scenario

- Flue gas desulfurization (wet limestone scrubbing) for all (existing and new) large power stations (LPS) burning coal and oil
- Flue gas desulfurization (wet limestone scrubbing) for all large industrial boilers
- Use of low sulfur fuels (coal, heavy fuel oil, gasoil) for all other users

The RAINS model shows that advanced emission control methods applied to the fuel consumption levels as suggested by the reference energy scenario could drastically reduce SO_2 emissions in Asia below the current levels. Between 1990 and 2020, SO_2 emissions from the region would decline from 33.6 to 16.3 million tons, i.e., by 51 percent, despite the assumed growth in energy consumption by 230 percent. Since control technologies work most effectively at large sources, the relative contribution from large point sources declines from 16 percent in 1990 to less than nine percent in 2020. Note, that this is much in contrast to the unabated scenario, in which the share of large point sources increases to 25 percent.

Different structural compositions in the emission sources create also a wide span in the evolution of national emissions. For instance, as a result of such a policy, emissions from China, the Philippines and Thailand would decline by 60 to 70 percent, whereas India's emissions would still increase by about one third compared to 1990 (Table 7.1).

Not surprisingly, declining emissions will also result in reduced sulfur deposition. Most interesting, however, is a comparison between the diminished deposition and the critical loads. As displayed in Figure 7.10, a general use of advanced emission control technologies will bring down sulfur deposition below the critical loads almost everywhere in the regions. A major exception is the border area between the Hunan and Jiangxi provinces in China, where sensitive ecosystems are located in regions with intense economic activity. Additional isolated 'hot spots' occur in India, Thailand and Korea.

The scenario shows that, despite the more than three-fold increase in energy consumption expected for the next few decades, sustainable conditions - at least in terms of sulfur deposition - could be achieved by advanced technologies for most of the Asian ecosystems.

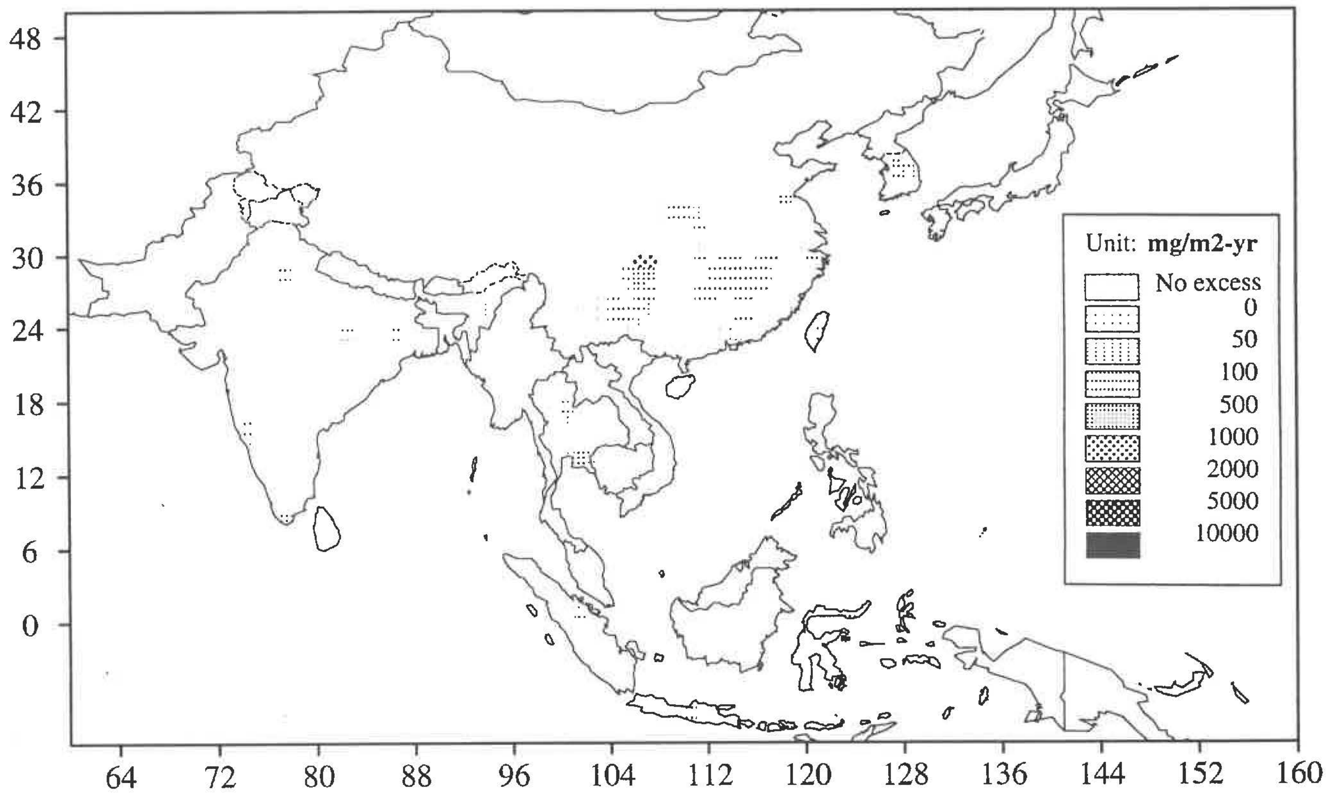

Figure 7.10 Excess of critical loads for the BAT scenario in 2020

The success in ecosystem's protection achievable with advanced control technologies, however, has its price. The RAINS model also enables analysis of the costs involved in various emission control technologies. As discussed in Chapter 4, the cost evaluation of the RAINS model has been restricted to the incremental costs caused by emission control measures and does not include the total costs of the energy system. Furthermore, as outlined before, cost estimates reflect annualized full life cycle costs (including investments and operating costs).

In the year 2020 full application of advanced emission control technologies would require 90 billion US $ per year, which is about 0.59 percent of the regional GDP assumed for the underlying energy scenario. For comparison, the relative costs for the latest agreement on reducing sulfur emissions in Europe (the Oslo protocol) were only about one third of this level (0.21 percent of the GDP; Amann *et al.*, 1994). It should be pointed out that there exists a wide range in burdens to the various national economies: Whereas for some countries with low consumption of fossil fuels (e.g., Myanmar) or highly developed economies (e.g., Japan) the abatement costs are comparably low (0.05 and 0.06 percent, respectively), developing countries with a heavy reliance on coal face substantially higher burdens (e.g., China, 1.7 percent). In Europe, the highest share of GDP for the latest agreement was 0.79 percent.

Since the environmental benefits of such a strategy cannot yet be quantified in monetary terms, a definite answer about the cost-benefit ratio of fully applying western emission control standards cannot be derived yet. It has to be observed, however, that the costs associated with such a strategy would put significant burdens on many developing economies in the region. Consequently, the following sections use the RAINS model to search for alternative, perhaps more cost-effective, solutions to reduce source emissions in Asia.

7.5 An advanced emission control technology (ACT) scenario

Section 7.4 has explored a scenario that applies best available emission control technologies to all emission sources in Asia. As a consequence, emissions would be greatly reduced, resulting in a fall in sulfur deposition levels below the critical loads for most of Asia. An obvious option for cost-savings would be to reduce the overachievement of the critical loads by selecting only the most cost-effective measures to reduce emissions. If structural changes in the energy system, such as energy conservation measures and fuel substitution, are left aside for a moment, the remaining technologies show a wide range of cost-effectiveness, i.e., they reduce different amounts of sulfur for the same amount of money (Table 7.2). A rational policy could therefore request only the most cost-effective measures, thereby reducing the achieved emission reductions to some degree, but to a greater extent also the involved costs.

To follow this idea further, a scenario has been developed which assumes the application of advanced control technologies (wet flue gas desulfurization WFGD) only for new, large emission sources in the power plant, the industrial and refinery sectors. Emissions from existing power stations and from small sources in the industry are assumed to be controlled through the use of low sulfur fuels[1] (50 percent share of low sulfur coal and oil). Also in the domestic and transport sectors low sulfur fuels are prescribed (see Box 2). For Japan and Taiwan, however, the scenario assumes compliance with current national legislation.

Box 2: Measures for the advanced emission control scenario

The Advanced Control Technology (ACT)-scenario

- Flue gas desulfurization (wet limestone scrubbing) for all new power stations
- Flue gas desulfurization (wet limestone scrubbing) for all large industrial boilers in refineries
- Low sulfur fuels for boilers in industry (100% of liquid fuels and 50% of coal consumption)
- Low sulfur fuels for the domestic and transport sectors (100% of total consumption)

As expected, restricting advanced measures to certain sources lowers the emission reductions. Whereas the BAT strategy will be able to cut total SO_2 emissions in Asia by half up to 2020, the ACT scenario produces a 50 percent increase of emissions at a level of 50.4 million tons. However, this level is still less than half of the unabated level of 110 million tons.

Selecting only the most cost-effective measures cuts down costs. From more than 90 billion US $/year (costs for the BAT scenario in 2020) costs drop to 39 billion US $/year, i.e., by about 57 percent. Consequently, compared to GDP the strategy would only take a share of 0.25 percent, which is already close to the 0.21 percent level currently discussed in Europe.

It has been pointed out earlier that, due to country-specific structural differences, the actual situation varies considerably among countries. In China, where the BAT strategy would consume 1.7 percent of GDP, limiting measures to the more cost-effective technologies will reduce the share to 0.59 percent of the GDP. Thereby, the burden is comparable to other countries such as India, Indonesia, the Philippines and Thailand, which all are in a range betwеen 0.51 to 0.57 percent of GDP.

[1]For gasoil the limit adopted in the ACT strategy is 0.3 percent. Limits for other fuels are as for the BAT strategy.

Table 7.2 Cost-effectiveness of available measures for area sources in the North Highlands region in Thailand

Fuel	Sector	Control technology	Cost, US \$/ton SO_2 removed	
			Unit costs	Marginal costs
Brown coal	Power plants	WFGD	208	208
Heavy fuel oil	Power plants	WFGD	403	403
Heavy fuel oil	Conversion Industry	WFGD	468	468
Brown coal	Industry	WFGD	689	689
Heavy fuel oil	Domestic Transport	LSHF	1084	1084
Gasoil	All sectors	LSMD1	1823	1823
Hard coal	Industry	WFGD	2710	2710
Brown coal	Power plant	RFGD	287	2792
Heavy fuel oil	Power Plant	RFGD	732	11150
Gasoil	All sectors	LSMD2	5469	15677
Heavy fuel oil	Industry Conversion	RFGD	997	17742
Brown coal	Industry	RFGD	1565	29311
Hard coal	Industry	RFGD	6720	133729

Legend:

Control technologies:
WFGD - Wet flue gas desulfurization
RFGD - Regenerative flue gas desulfurization
LSHF - Low sulfur heavy fuel oil
LSMD1, LSMD2 - Low sulfur medium distillates (0.3% S and 0.05% S respectively)

Unit cost shows the average cost of reducing one ton of SO_2 if a given technology is applied from the unabated case. Marginal cost shows the incremental cost of reducing additional ton of SO_2 if technologies are applied according to their cost - effectiveness.

Of course, reduced costs are accompanied by higher emissions. For instance in China, the ACT strategy results in a 37 percent increase of SO_2 compared to a 70 percent decrease of the BAT scenario.

Obviously, the ACT strategy reduces emissions at lower costs than a BAT scenario. To judge the environmental effectiveness, however, a comparison of the resulting deposition patterns with the critical loads is necessary. Figure 7.11 shows that areas with serious excess deposition occur in the ACT strategy in Korea and some Chinese provinces, whereas in most other regions the critical loads could be achieved.

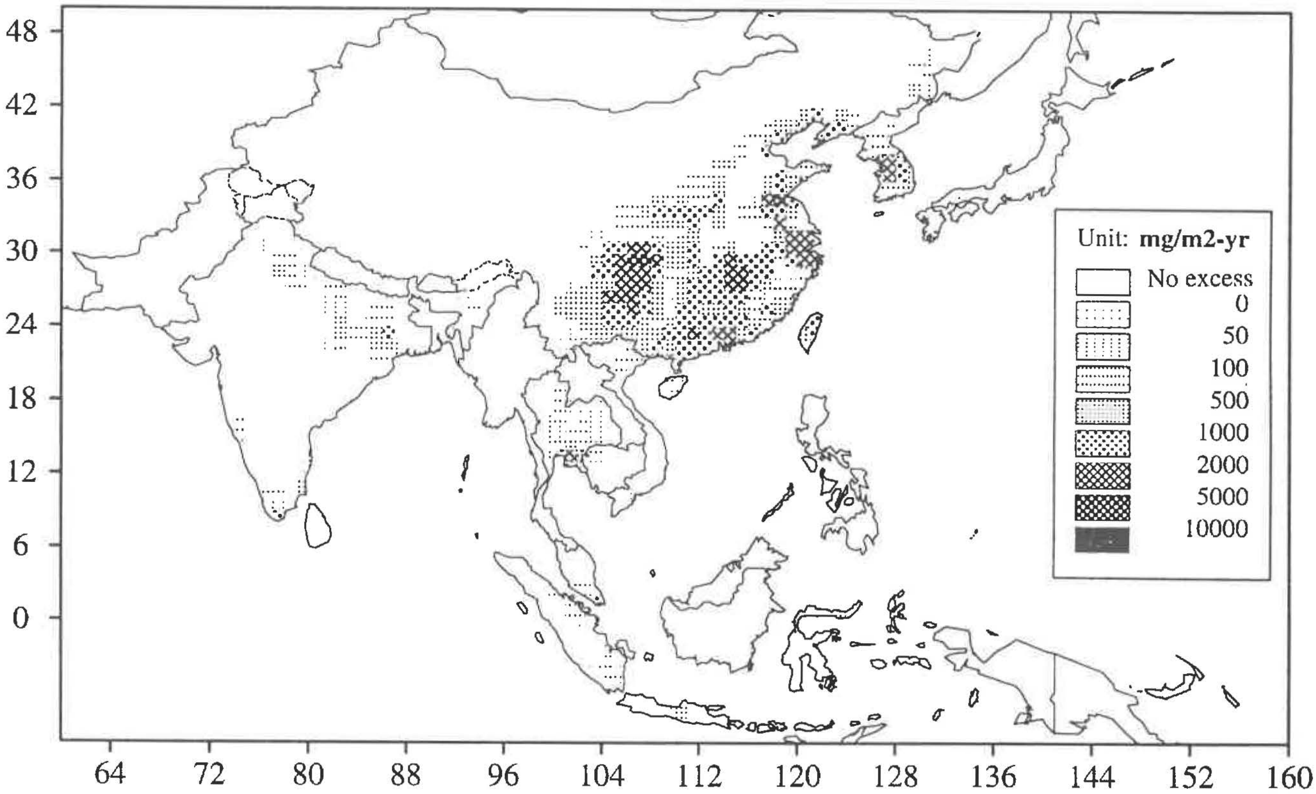

Figure 7.11 Excess deposition for the ACT strategy in the year 2020

7.6 A 'basic control technology' (BCT) scenario

Although emission control costs are reduced significantly in the 'advanced control technology' (ACT) scenario, the construction of such emission control devices according to world standards requires substantial technical know-how and capital investments. Experience shows that developing countries often have limited access to the necessary technical and financial resources needed to implement advanced technological solutions. Consequently, preference is often given to less advanced approaches readily available on the domestic market, which are also often less capital intensive.

To explore the economic and ecological features of strategies that give preference to domestic technologies an example scenario was constructed, in which use is made of domestically available control technologies. Therefore, instead of installing standard flue gas desulfurization units at large power stations, emissions from these sources would be controlled through more basic technologies with low capital requirements. As an example for such technical solutions, the RAINS model considers the lime stone injection process, which achieves emission reductions of about 50 percent. Investment requirements are low but, due to the significant amount of waste material to be handled, operating costs may be higher than for the standard flue gas desulfurization method.

The 'basic control technology' (BCT) scenario assumes that in China, India and Pakistan emissions from new large point sources are controlled by domestic technology (with a typical removal efficiency of about 50 percent) rather than by advanced flue gas cleaning methods (with efficiencies of more than 90 percent). For small sources in the industrial and domestic sector the use of low sulfur fuels is assumed (Box 3).

Due to the application of less efficient control technologies, the remaining emissions in all three countries will be higher than in the advanced technology scenario. For China, SO_2 emissions in the year 2020 would amount to 38.1 million tons (i.e., an increase of 77 percent), for India 13 million tons (+190 percent) and for Pakistan 3.6 million tons (+490 percent). In the ACT scenario comparable growth rates are 37 percent in China, 135 percent in India and 210 percent in Pakistan, respectively.

Box 3: Measures assumed for the basic technology scenario

The Basic Control Technology (BCT) - scenario

- China, India and Pakistan:
  - Domestic technologies with low capital requirements (e.g., lime stone injection) for all new coal fired power stations
  - Use of low sulfur fuels as in the ACT (Advanced Controls) scenario for the industrial and domestic sector

- All other countries:
  - Controls as in the ACT scenario

Most interesting, however, is the fact that total costs are close to the levels of the ACT scenario. This can be explained by the fact that the RAINS model calculates and compares total life cycle costs of emission control equipment: in the case of the currently used domestic control technologies the lower investments are compensated by higher operating costs, in particular for the treatment and disposal of waste material. Obviously, costs for waste disposal are strongly influenced by local conditions and legislation. Therefore, the RAINS model can only provide generic estimates of such costs, which in fact reflects the situation in developed countries. Lower legal standards for waste disposal facilities may reduce the costs considerably, however at higher environmental hazards caused by the deposits. To avoid a transfer of the air pollution problem to other media, such as a contamination of soils and ground water, the RAINS model bases its cost estimates on standards which strive to minimize such risks.

Figure 7.12 shows excess deposition for the basic technology scenario. Compared to the ACT scenario the increase in emissions from the large point sources results in a situation whereby many parts of eastern China face excess deposition of more than two grams per square meter and year, with peak exceedances in the Sichuan and Shanghai provinces of about ten grams. Consequently, it can be concluded that in the long run a strategy relying solely on control technologies with modest removal efficiencies will not be able to preserve important agricultural areas from serious excess deposition.

Table 7.3 summarizes emissions and costs from the three emission control scenarios discussed up to now. Obviously, there is a clear trade-off between emission levels, control costs and ecosystem's protection.

Table 7.3 Emissions and control costs for the BAT, ACT and BCT scenarios in the year 2020

Country	SO_2 Emissions (thousand tons of SO_2)			SO_2 Control Costs (million US $/yr)		
	BAT	ACT	BCT	BAT	ACT	BCT
Bangladesh	165	258	258	475	228	228
Bhutan	3	4	4	7	9	9
Brunei	15	17	17	15	2	2
Cambodia	22	69	69	487	123	123
China	6672	29932	38124	34230	11975	12712
Hong Kong	24	68	68	574	255	255
India	5906	10522	13054	17055	6328	6213
Indonesia	438	785	785	6121	2255	2255
Japan	393	1047	1047	6132	3458	3458
Korea, north	75	7075	7075	3087	1089	1089
Korea, south	552	1469	1469	3769	3214	3214
Laos	5	7	7	9	6	6
Malaysia	66	246	246	843	163	163
Mongolia	13	81	81	138	56	56
Myanmar	32	37	37	32	5	5
Nepal	218	230	230	53	12	12
Pakistan	606	1907	3609	4333	3095	3703
Philippines	146	440	440	1201	1063	1063
Sea lanes	102	307	307	445	222	222
Singapore	65	221	221	860	635	635
Sri Lanka	37	53	53	222	173	173
Taiwan	245	827	827	2999	1249	1249
Thailand	336	813	813	6485	2916	2916
Vietnam	183	345	345	853	338	338
TOTAL	16321	50396	62822	90424	38877	40108

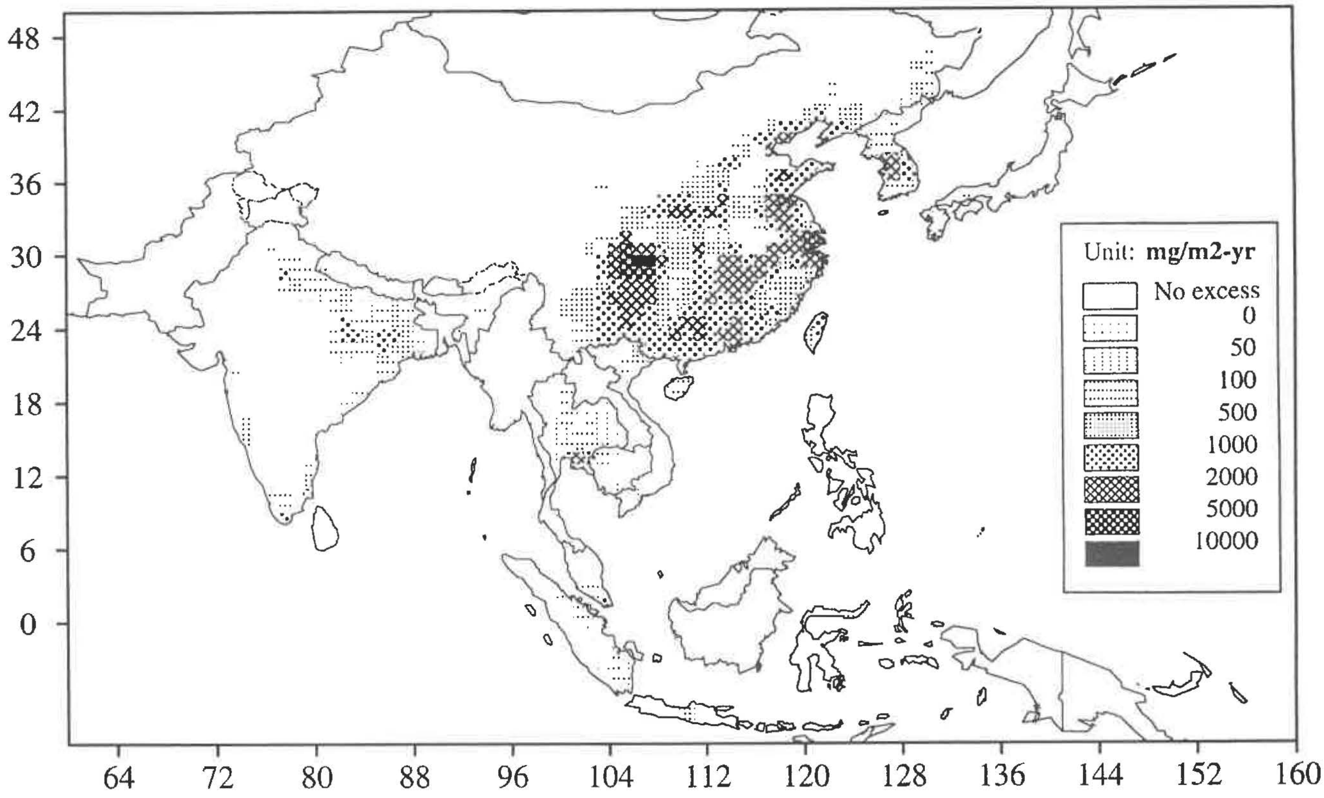

Figure 7.12 Excess sulfur deposition for the basic control technology (BCT) scenario for the year 2020

7.7 A scenario with local applications of advanced technologies (LACT)

The analyses carried out in the preceding sections shows that there is a clear trade-off between ecosystem protection and emission control costs. Furthermore, it became clear that different strategies have different cost-effectiveness, i.e., some of them achieve different protection levels for similar costs. The important question arises of how the cost-effectiveness of strategies could be further increased.

Ultimately, the integrated assessment process enables the optimization of emission control measures, e.g., in order to minimize costs for achieving exogenously specified target deposition or ecosystems protection levels. Earlier versions of the RAINS model implemented for Europe contain such optimization procedures and have been used to identify optimized abatement scenarios as a starting point for international negotiations (Amann *et al.*, 1993).

Although the present implementation of the RAINS model for Asia does not provide this capability, the model can already be used to search for cost-effective strategies. Section 7.4 (the advanced control technology scenario) made a step towards increasing cost-effectiveness in comparison to the best available technology (BAT) scenario by selecting only the most effective measures. A further reduction of costs, without increasing environmental damage, could be achieved by directing advanced control measures to ecologically sensitive areas and relaxing control requirements at less sensitive locations. It should be mentioned that China is currently exploring similar approaches by requesting only power stations in ecologically sensitive regions to reduce emissions (rational siting of plants, Zhao *et al.*, 1995).

As an illustrative example, a scenario is constructed for China, India and Pakistan that applies advanced emission control measures to only those provinces where significant excess deposition would occur without such measures (compare Box 4). Emissions and control costs for these three countries in the LACT scenario are shown in Table 7.4. In this scenario the emissions from low-income countries (e.g., Bangladesh, Cambodia or Sri Lanka) remain uncontrolled. Countries with higher per capita income (e.g., Indonesia, Japan, South Korea or Thailand) control their emissions as in the ACT scenario.

Table 7.4 Emissions and control costs in 2020 for China, India and Pakistan in the LACT scenario

Country	Emissions (thousand tons SO_2)			Costs, million US $		
	LACT	BCT	ACT	LACT	BCT	ACT
China	37904	38124	29932	8505	12609	12063
India	13434	13054	10522	3870	6214	6386
Pakistan	5592	3609	1908	857	3702	3102
Sum	56930	54787	42362	13232	22535	21551

Box 4: Regional emission control strategies for the Local ACT scenario in China, India and Pakistan

NO CONTROL	ADVANCED EMISSION CONTROL (ACT)
China:	
Fujian	Beijing
Guandong-Hainan	Chongquing
Guanxi	Guangzhou
Hebei-Anhui-Henah	Guyang
Inner Mongolia	Guizhou
North-eastern plain, Heilongjiang	Hubei
Shenyang	Hunan
West Tibet-Quinghai	Jiangsu
Yunnan	Jianxi
	Shanghai
	Shaanxi-Gansu
	Shandong
	Shanxi
	Sichuan
	Taiyuan
	Tianjin
	Wuhan
	Zhejiang
India	
Andra Pradesh	West Bengal
Bombay	Bihar
Karnataka-Goa	Calcutta
Kerala	Delhi
Madras	Eastern Himalaya-Assam
Maharasthra-Dadra-Nagar	Guijarat
Punjab-Chandigarh	Haryana
Western Himalaya-Jammu-Kashmir	Madhya Pradesh
	Orissa
	Tamil Nadu-Pondicherry
	Uttar Pradesh
Pakistan	
Lahore	Karachi
North-western frontier provinces	
Punjab	
Sind	

From Table 7.4 it can be derived that focusing advanced emission control measures on ecologically sensitive regions would result, for China and India, in emissions roughly comparable to the basic technology case, however, at only two thirds of the costs. Avoiding expensive - and environmentally less effective - controls in a group of low-income countries would save about 3 billion US $ in the year 2020.

As shown before in Figure 7.11, the ACT scenario reduces excess sulfur deposition in large areas of Asia, i.e., ecosystems would not be under threat. In the LACT case, ecosystems protection is slightly lower than in the ACT scenario, while costs decline substantially (Figure 7.13).

The scenario demonstrates that targeting emission control measures could substantially increase the cost-effectiveness of strategies. Taking China as an example, focusing measures to the ecologically sensitive regions could achieve environmental impacts roughly comparable to the Basic Control Technology (BCT) case while costs declining to 0.41 percent of GDP.

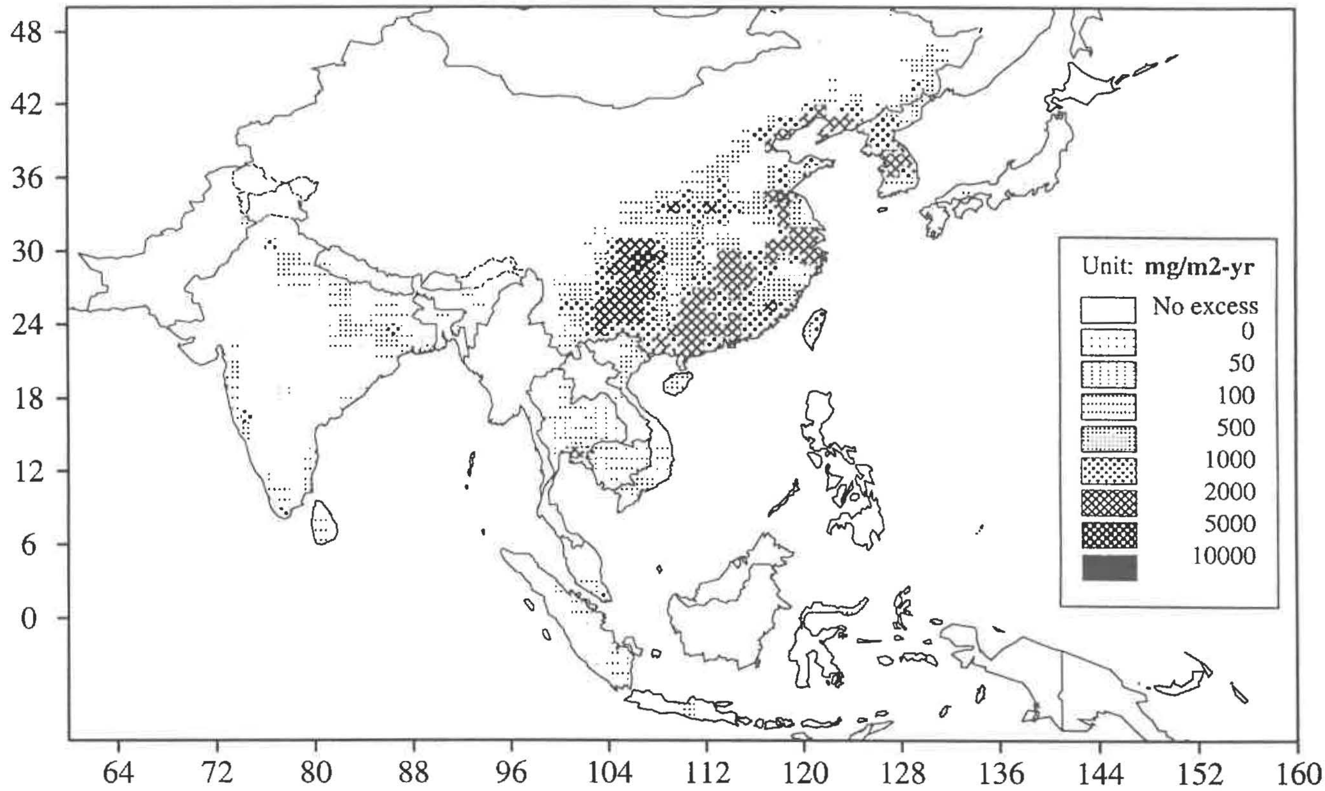

Figure 7.13 Excess sulfur deposition for the LACT scenario (local application of advanced control technologies) for the year 2020

7.8 Relocation of plants in sensitive regions

An alternative approach to protect sensitive ecosystems - or to avoid the occurrence of 'hot spots', i.e., areas with peak excess deposition - would be to locate new power stations in less sensitive regions. The RAINS model facilitates the analysis necessary for such strategies in various ways:

- The DEPOSITION module of RAINS provides an easy option to explore the dispersion of pollutants for each individual emission source considered in the model, i.e., the spread of emissions could be displayed for each of the 94 area sources and the 355 large point sources separately. Thereby, it is possible to identify whether a specific source has strong impacts on sensitive ecosystems.

- The DEPOSITION module of RAINS also enables the identification of the sources contributing to the deposition at a specific location.

- By using the energy module RESGEN the user can create new energy scenarios with a different regional allocation of newly built power station capacities, while maintaining the internal consistencies of the regional energy balances.

- To enable fast exploration of the environmental impacts of re-located power stations, the DEPOSITION module of RAINS offers the option to change the location of individual power stations without performing consistency checks on the energy balances.

This section provides examples of model use, aimed at a re-location of power stations with strong impacts on sensitive ecosystems to less sensitive regions. Excess deposition of the reference scenario (base case energy pathway, no further emission control beyond current legislation, year 2020) has been shown in Figure 7.7. 'Hot spots', with exceedance of critical loads of more than ten grams sulfur/m^2/year occur, inter alia, in the Chinese Sichuan province and in the central and northern part of Thailand. Table 7.5 lists the contributions to deposition in the year 2020 for two grids, based on the RAINS calculations.

Table 7.5 shows that some point sources make a significant, and often dominant, contribution to local deposition (e.g., the Chengdu power station contributes about 30 percent of total deposition to grid 105/30). Consequently, measures that focus on a few specific sources could significantly improve the local situation. However, emissions do not only have a local impact, but are dispersed via the atmosphere to a larger area. To explore this feature, the RAINS model has been used to create Figure 7.14, displaying the spread of emissions and the resulting deposition from the Lampang power station expected for the year 2020 under the reference scenario.

Table 7.5 Contribution of sulfur deposition to two grids for the reference scenario for the year 2020 in milligrams sulfur/m^2/year (note that some of the power stations are only foreseen for the year 2020 and do not yet exist!)

Grid 105/30 (Sichuan)		Grid 100/18 (Northern Thailand)	
Area sources:			
China, Sichuan	10324	Thailand, Northern Highlands	1047
China, Chongquing	1085	Thailand, Bangkok	18
China, Yunnan	115	Thailand, other area sources	14
China, Shaanxi-G.	47		
China, Guizhou	94	India (all sources)	15
China, Guiyang	28	China (all sources)	27
China, West Tibet	16	Bangladesh (all sources	3
China, Hubei	16	Other countries	3
China, Hebei	8		
China, Hunan	5		
China, Other Provinces	11		
India, all sources	6		
Large Point Sources			
China, LPS N25 (Chengdu)	5901	Thailand, LPS 1 (Lampang)	2696
China, LPS N24 (Jianqou)	993	Thailand LPS 2 (Mae Moh)	4231
China, LPS 56 (Baima)	189	Thailand, 2 other LPS	10
China, LPS 4 (Chongqing)	129		
China, LPS N1 (Luohang)	118		
China, LPS N65 (Douba)	89		
China, LPS N66 (Huayinshan)	65		
China, LPS N59 (Xigu)	13		
China, LPS 11 (Qinzhen)	13		
China, LPS N22 (Jingyuan)	11		
China, 10 other LPS	27		
TOTAL	**19303**	**TOTAL**	**8064**
Critical load (25 percentile)	4035	Critical load (25 percentile)	490

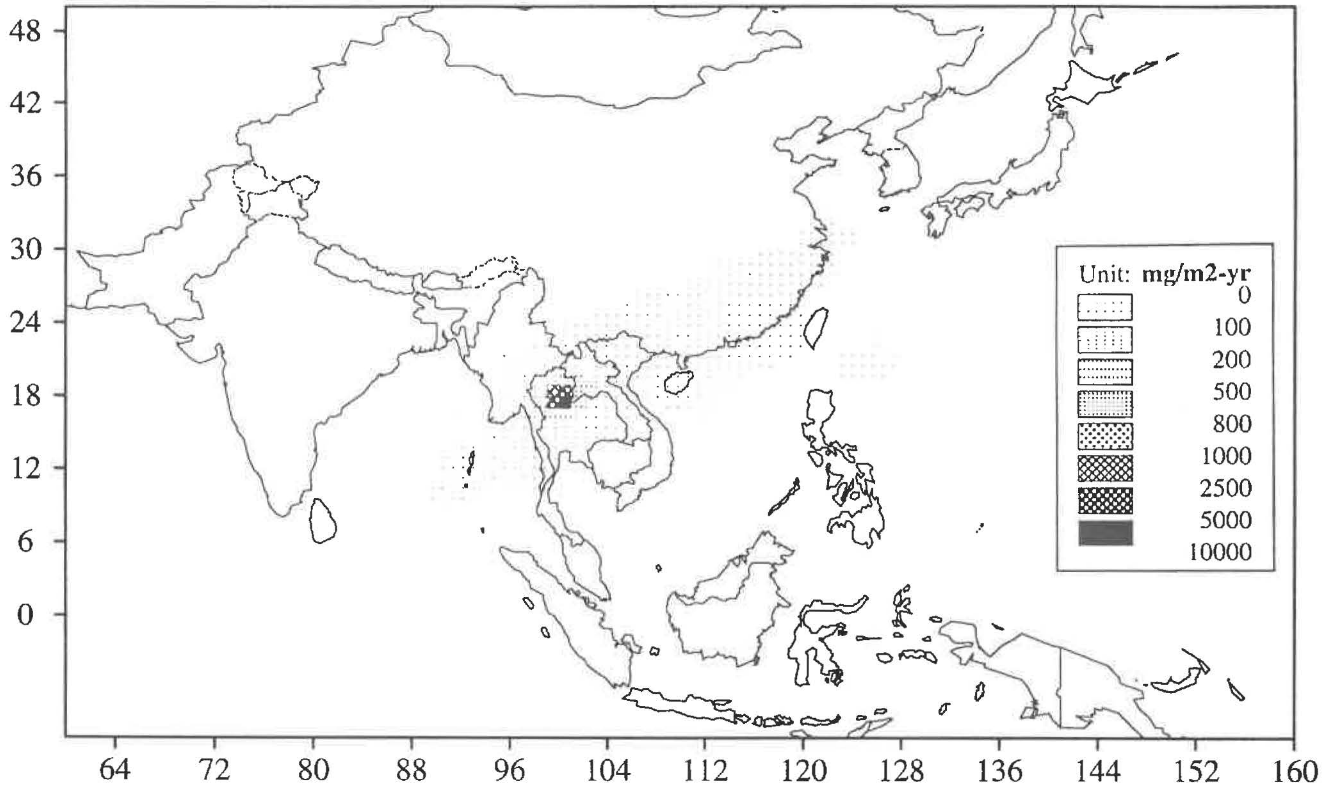

Figure 7.14 Sulfur deposition from the Lampang power station for the reference scenario (no emission control assumed) for the year 2020

The RAINS model could be used to explore the impact of reducing emissions at these power stations by introducing various emission control options. Another way to limit environmental impacts could be to move individual stations to less sensitive areas. To illustrate the capacity of the model, this scenario assumes that some coal power stations, which make significant contributions to excess deposition in sensitive ecosystems in the baseline scenario, are moved to less sensitive regions in the same country. Starting from the baseline scenario (no further emission control beyond current legislation) such moves have been assumed in China and Thailand (Box 5). In China, four sources planned for construction in the heavily polluted region of the Sichuan province have been moved to the northern part of the country. For Thailand, the scenario explores the effects of moving two large point sources from the north of the country to the southern peninsula. One of those sources has been simultaneously switched from lignite to imported hard coal. It should be stressed that this scenario only illustrates the capabilities of the RAINS model: it does not suggest the technical, economic or political feasibility of such moves. To answer such questions, more detailed case studies on local energy supply, demand and power transmission options will be necessary.

Box 5: Relocations of power plants assumed in the scenario

	Emissions in 2020, thousand tons of SO_2	Location (long/lat)	
		before move	after move
China:			
Sichuan, LPS N24 (Jianqou)	330	104/31	106/39
Sichuan, LPS N25 (Chengdu)	406	104/30	109/40
Sichuan, LPS 56 (Baima)	469	105/29	112/39
Sichuan, LPS N65 (Douba)	333	104/28	113/40
Thailand:			
Centr. Valley, LPS 3 (Ao Phai)	542	100/13	98/8
North Highlands, LPS 1 (Lampang)	617	99/18	99/9

It is outside of the scope of the RAINS model to determine the costs of such modified expansion plans. The model can, however, explore the environmental improvements, in terms of critical loads achievement, of such measures. Even under the assumption that the relocated power stations would not be equipped with desulfurization technologies, excess deposition in the hot spots declines compared to the baseline reference scenario. For instance, in the Sichuan province in China excess deposition in the grids affected by the moved sources decreased by about five to six g/m^2-yr, whereas, due to the large tolerance of acid deposition of the ecosystems in the new locations, no major areas would experience excess deposition as a result of this measure (Figure 7.15). Environmental improvements also occur in Thailand, where excess deposition in the northern part declines by about 50 percent.

It should be stressed again that this scenario has only an illustrative character, since the necessary support studies on the site conditions of the energy supply systems have not been carried out.

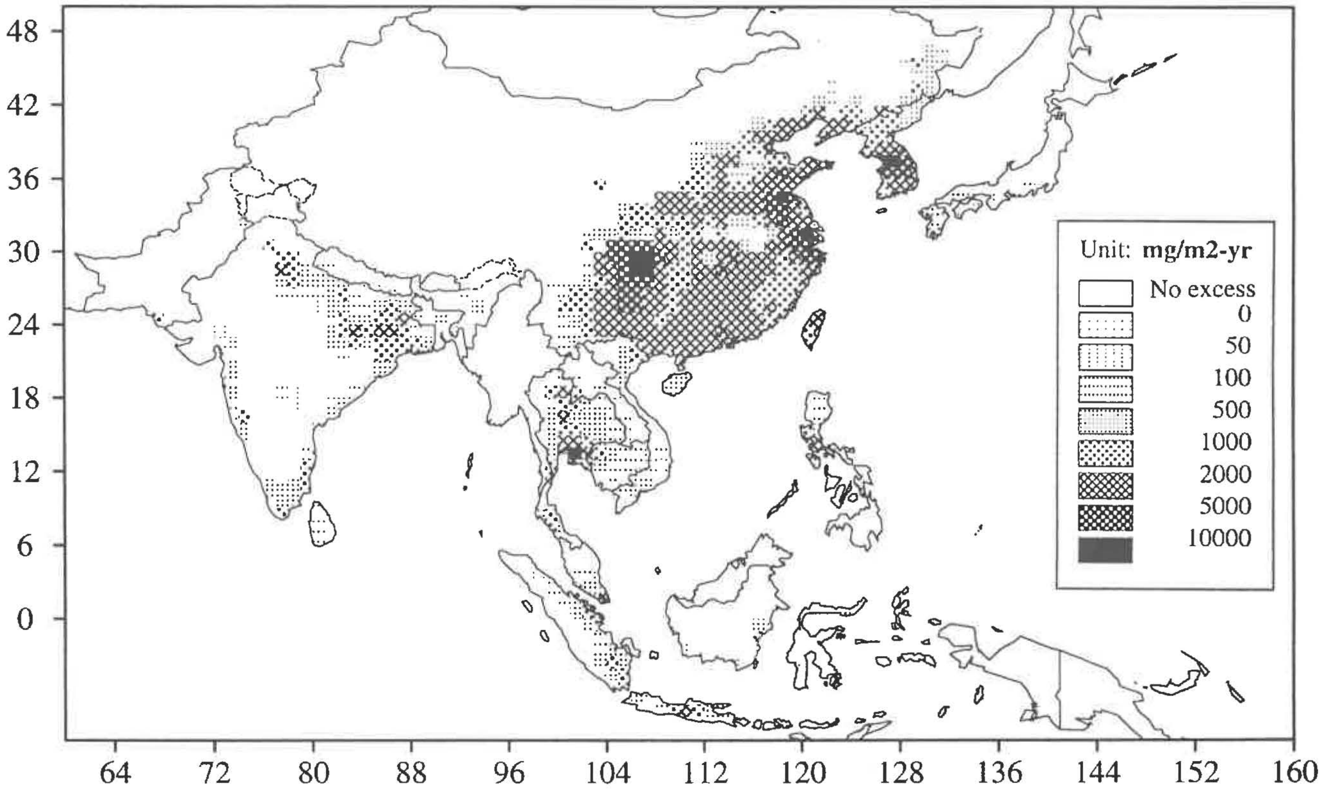

Figure 7.15 Excess sulfur deposition for a scenario in which some new power stations in China and Thailand are moved to ecologically less sensitive regions

7.9 Implications of the energy efficiency pathway

All the six scenarios discussed above are based on certain assumptions about the development of the economies and of energy intensities. As will be shown, however, the volumes and the structural composition of energy supply have a critical influence on the level of emissions. This means that not only will emission levels be crucially dependent on the energy scenario, but also that energy policies promoting energy efficiency and use of cleaner fuels are important instruments to reduce pollution and pollution control costs.

To illustrate this fact this section compares calculations for some of the emission control scenarios discussed above, which are all based on the reference energy pathway, with control strategies based on the energy efficiency pathway. Table 7.6 shows that, due to a lower consumption of fuels, SO_2 emissions in the energy efficiency pathway are consistently lower than in the base case energy path. Consequently, emission control strategies based on the energy efficiency pathway provide better protection for the ecosystems than would result from the base case.

Furthermore, the table shows that, despite the lower emission levels resulting from the various control scenarios, the costs for achieving the (lower) emissions are also about 30 percent below the costs of the base case energy pathway. Since, as has been pointed out in Chapter 3 of this report, both energy pathways are based on the same economic development assumptions (e.g., the growth of GDP), the energy efficiency pathway would also alleviate the burdens imposed by SO_2 control measures on the national economies. To carry the example case further, the cost of the abatement measures for the focused application of advanced control technologies (LACT) scenario based on the energy efficiency pathway in China, would amount to 0.29 percent of GDP instead of the 0.41 percent calculated for the base case. At the same time China would face less excess deposition than in the reference case.

Table 7.6 Comparison of emissions and emission control costs for the base case energy pathway and the energy efficiency pathway

		Emission control scenario			
	Energy pathway	**No Further Control (NFC)**	**Basic Control Technology (BCT)**	**Advanced Control Technology (ACT)**	**Best Available Technology (BAT)**
Emissions (million tons SO_2)	Base case	110.5	62.8	50.4	16.3
	Efficiency	80.1	47.1	39.1	12.4
Costs (billion US $/yr)	Base case	3.9	40.1	38.8	90.4
	Efficiency	2.0	26.9	25.5	65.6

7.10 Conclusions

If no countermeasures were taken, an initial analysis with the RAINS-Asia model indicates that currently observed trends in energy consumption will impose significant environmental threats to a variety of ecosystems in large parts of Asia. Within the next two to three decades, regional SO_2 emissions are expected to triple in Southeast Asia. In many areas, sulfur deposition will increase by more than a factor of five and exceed the levels observed in the most polluted areas in central and eastern Europe.

This increase in SO_2 emissions, which is strongly connected with the presently observed and expected future growth of economic activities and energy consumption, will severely threaten the sustainable basis of many natural and agricultural ecosystems in the region. Taking the critical loads estimated in this study as an indicator for sustainable levels of acid deposition, future sulfur deposition will exceed critical loads by more than a factor of ten in wide parts of Asia.

The exploratory analysis carried out for this study demonstrates that there is a variety of measures that can be taken to reduce SO_2 emissions and thereby avoid widespread excess deposition in the region. Advanced emission control technologies could reduce emissions below current levels even in a high growth energy scenario, albeit at extremely high costs. Illustrative scenarios demonstrate the potential for an increase in the cost-effectiveness of strategies if measures are focused on specific fuels, technologies, economic sectors, emission sources or ecologically sensitive regions.

The analysis shows that energy planning is also an important factor for controlling adverse environmental effects, in particular acidification. The development of carefully designed energy systems is of particular importance for controlling emissions in those countries considering an expansion or replacement of the present energy infrastructure.

RAINS-Asia is now available as a tool for the integrated assessment of strategies to keep SO_2 emissions from energy use at acceptable levels. The model enables the comparison of regional emissions, deposition and ecosystem protection levels resulting from different energy development pathways and from different emission control strategies. It simulates the effects of specific technologies and measures for a variety of fuel types and economic sectors, applicable to any of the 94 regions and 355 large point sources considered in the RAINS-Asia model. The model provides estimates of the emission control costs for each source, and assesses protection levels for up to 31 types of different ecosystems in Asia.

The analysis presented in this study has to be seen as an initial attempt to develop the necessary tools required for an integrated assessment of regional energy development that takes environmental impacts at different spatial and temporal scales into consideration. Although major progress towards this goal has been achieved, several aspects have to be further improved or added into the analysis. Special attention should be devoted to validation of the various models and databases developed in the first phase of the project. An important element currently missing is the development of the huge urban agglomerations in Southeast Asia, which may put severe pressure on local and regional air quality. Furthermore, refined methods of uncertainty and robustness analysis will have to be developed to assess the accuracy and reliability of model results.

References

Amann M., Klaassen G., Schoepp W., 1993: Closing the Gap Between the 1990 Deposition and the Critical Sulfur Deposition Values. Background Paper for the UN/ECE Task Force on Integrated Assessment Modelling, UN/ECE, Geneva, Switzerland.

IUFRO (International Union of Forest Research Organizations), 1978: Resolution über Maximale Immissionsraten zum Schutze der Wälder. Fachtagung Laibach/Jugoslawien 18 - 23 September 1978.

WHO (World Health Organization), 1979: Environmental Health Criteria 8 - Sulfur Dioxide. Geneva, Switzerland.

Zhao D., Mao J., Xiong J., Zhuang X., Yang J., 1995: Critical Load of Sulfur Deposition for Ecosystem and its Application in China. Research Center for Eco-Environmental Sciences, Academia Sinica, Beijing, China, pp.23.

ANNEX 1

Annex 1 **CRITICAL BC/Al RATIOS**

(H. Sverdrup)

A1.1 *Introduction*

This annex provides a more extensive overview of plant species and their critical BC/Al ratio derived from Sverdrup and Warvfinge (1993). These data in general and the Chinese data in particular have been used to establish the relationship between growth response and the value of the BC/Al ratio on one hand and critical loads on the other. Critical loads for ecosystems containing the species listed in the Tables are computed by using critical BC/Al ratio

A1.2 *Overview of selected species and their critical BC/Al ratios.*

Table A1.1 Response type and estimated aluminium damage coefficients for different species of deciduous trees and shrubs ordered according to relative sensitivity. The BC/Al-limit represents growth reduced to 80% of normal (Sverdrup and Warfvinge, 1993)

English name	Species	Reaction type	K-value	BC/Al(crit)
Honey locust	*Gleditsia triacantos*	Vanselow	K=0.0000005	0.4
Grape	*Vitis vinifera*	n.d.	n.d.	0.5
Sugar maple	*Acer saccharum*	Vanselow	K=0.000004	0.6
Norway maple	*Acer platanoides*	n.d.	n.d.	0.6
Oak	*Quercus robur*	Vanselow	K=0.000004	0.6
Red oak	*Quercus rubra*	Vanselow	K=0.000004	0.6
Pin oak	*Quercus palustris*	Vanselow	K=0.000004	0.6
Fire cherry	*Prunus cerasus*	n.d.	n.d.	0.6
Birch	*Betula pendula*	Vanselow	K=0.000006	0.8
Teak	*Tectona grandis*	Vanselow	K=0.000006	0.8*
American beech	*Fagus grandifolia*	Vanselow	K=0.000004	0.6
Beech	*Fagus sylvatica*	Vanselow	K=0.000004	0.6
Rowan	*Sorbus aucuparia*	n.d.	n.d.	0.6-1
Cotton	*Gossypium hirsutum*	Unspecific	K=0.3	1.2
Tea	*Camellia sinensis*	Unspecific	K=0.4	1.4
Peach	*Prunus persica*	Unspecific	K=0.4	1.4
Guapira	*Guapira olfersiana*	Vanselow	K=0.000002	1.4
False acacia	*Robinia pseudoacacia*	n.d.	n.d.	1-1.4
Hornbeam	*Carpinus betulus*	n.d.	n.d.	1.2-1.6
Lime	*Tilia cordata*	n.d.	n.d.	1.2-1.6
European alder	*Alnus glutinosa*	Vanselow	K=0.0002	5
Paper birch	*Betula papyrifera*	Vanselow	K=0.00005	2
Gray birch	*Betula populifolia*	Vanselow	K=0.00005	2
Yellow birch	*Betula alleghaniensis*	Vanselow	K=0.00005	2
Orange	*Citrus aurantium*	Vanselow	K=0.00005	2
Wattle	*Acacia spp.*	n.d.	n.d.	1.4-2
Black elder	*Sambucus nigra*	n.d.	n.d.	1.2-2.2
Ash	*Fraxinius exelsior*	n.d.	n.d.	1.8-2.2
Eucalyptus	*Eucalyptus gummifera*	Vanselow	K=0.00006	2.8
Mandarin orange	*Citrus natsudaidai*	Vanselow	K=0.0003	3
Rhododendron	*Rhododendron ponticum*	Vanselow	K=0.0004	4.5
Willow	*Salix fragilis*	Gapon	K=0.08	5
Aspen	*Populus tremula*	Vanselow	K=0.0005	6
Autumn olive	*Elaeagnus umbellata*	Vanselow	K=0.0005	6
Coffee	*Coffea arabica*	Gapon	K=0.2	75

*BC/Al=0.35 based on a field value for stem growth. n.d. represents values derived from a combination of the quantitative and semi-quantitative data.

(allowing a growth reduction of 80% at most) as input to the Steady state mass Balance Model.

Table A1.2 Response type and estimated aluminium damage coefficients for different species of herbs and legumes. The limiting BC/Al-value represents root growth for laboratory results reduced to 80% of normal (Sverdrup and Warfvinge, 1993)

English name	Species	Reaction type	K-value	BC/Al(crit)
May lilly	*Maianthemum bifolium*	n.d.	n.d.	0.3
Wood sorrell	*Oxalis acetosella*	n.d.	n.d.	0.3
Heath bedstraw	*Galium saxatile*	unspecific	K=0.08	0.3
Foxglove	*Digitalis purpurea*	unspecific	K=0.08	0.3
Bilberry	*Vaccinium myrtillus*	n.d.	n.d.	0.2-0.6
Lowland heather	*Erica cinerea*	n.d.	n.d.	0.5-0.8
Wintergreen	*Trientalis europaea*	n.d.	n.d.	0.8
Heather	*Calluna vulgaris*	Unspecific	K=0.2	0.8
Cowberry	*Vaccinium vitis-idea*	n.d.	n.d.	1.2
American cranberry	*Vaccinium macrocarpon*	unspecific	K=0.4	1.5
Black medick	*Medicago lupulina*	n.d.	n.d.	1.5
Arnika	*Arnica montana*	Unspecific	K=0.6	2.5
Yellow wood anemone	*Anemone ranunculoides*	n.d.	n.d.	3
Lilly of the valley	*Convallaria majalis*	n.d.	n.d.	3
	Corydalis lutea	n.d.	n.d.	3
	Lathyrus nigra	n.d.	n.d.	3
Vetch	*Vicia sepium*	unspecific	K=1.2	4.5
Yellow Lupin	*Lupinus luteus*	unspecific	K=1.2	4.5
Marjoram black vetchling	*Origanum vulgaris*	unspecific	K=1.2	4.5
Lucerne	*Medicago sativa var. falcata*	n.d.	n.d.	5
Wood anemone	*Anemone nemorosa*	n.d.	n.d.	5
Crocus	*Crocus* spp	n.d.	n.d.	5
Wild strawberry	*Fragaria vesca*	n.d.	n.d.	5
Zig-zag clover	*Trifolium medium*	n.d.	n.d.	5
Cowslip	*Primula veris*	n.d.	n.d.	15
Wood avens	*Geum urbanum*	unspecific	K=12	45
Colombine	*Aquilegia vulgare*	n.d.	n.d.	50
Bellflower	*Campanula persicifolia*	n.d.	n.d.	50
Sand leek	*Allium scorodoprasum*	n.d.	n.d.	50
Autumn hawkbit	*Leontodon autumnalis*	unspecific	K=12	80
Buttercup	*Ranunculus* spp	n.d.	n.d.	100
Wall lettuce	*Mycelis muralis*	unspecific	K=40	120
Common chickweed	*Stellaria media*	unspecific	K=40	120
Common valerian	*Valeriana officinalis*	n.d.	n.d.	150
Mouse-ear chickweed	*Cerastium fontanum*	unspecific	K=70	300
Selfheal	*Prunella vulgaris*	unspecific	K=200	800
Common dandelion	*Taraxaccum officinale*	unspecific	K=200	800

n.d. represents values derived from a combination of quantitative and semi-quantitative data.

Table A1.3 Response type and estimated aluminium damage coefficients for different species of grasses. The limiting BC/Al-value represents root growth reduced to 80% of normal (Sverdrup and Warfvinge, 1993)

English name	Species	Reaction type	K-value	BC/Al(crit)
Heath rush	*Juncus squarrosus*	unspecific	K=0.08	0.3
Wavy hair-grass	*Deschampsia flexuosa*	unspecific	K=0.13	0.5
Perennial ryegrass	*Lolium perenne*	unspecific	K=0.13	0.5
Creeping bent	*Agrostis stolonifera*	unspecific	K=0.2	1
Common bent	*Agrostis capillaris*	unspecific	K=0.2	1
Rough crabgrass	*Digitaria sanguinalis*	unspecific	K=0.2	1
Tufted hair-grass	*Deschampsia cespitosa*	n.d.	n.d.	2
False brome	*Brachypodium sylvaticum*	unspecific	K=1.2	6
Erect brome	*Bromus erectus*	unspecific	K=1.2	6
Meadow foxtail	*Alopecurus pratensis*	unspecific	K=1.2	6
Yorkshire fog	*Holcus lanatus*	unspecific	K=1.5	8
Large meadow-grass	*Poa remota*	n.d.	n.d.	10
Meadow-grass	*Poa supina*	n.d.	n.d.	10
Brown bent	*Agrostis vinealis*	n.d.	n.d.	10
Mat-grass	*Nardus stricta*	n.d.	n.d.	10
Smooth crabgrass	*Digitaria humifusa*	unspecific	K=8	15
Meadow fescue	*Festuca pratensis*	unspecific	K=8	20
Rencote sedge	*Carex remota*	unspecific	K=12	45
Tawny sedge	*Carex hostiana*	n.d.	n.d.	45
Wood sedge	*Carex sylvatica*	n.d.	n.d.	45
Trembling sedge	*Carex aigilata*	n.d.	n.d.	45
Smooth meadow-grass	*Poa pratensis*	unspecific	K=50	250
Annual meadow-grass	*Poa annua*	unspecific	K=70	300
Wood meadow-grass	*Poa nemoralis*	n.d.	n.d.	300

n.d. represents values derived from a combination of the quantitative data in this study and semi-quantitative data.

Table A1.4 Response type and estimated aluminium damage coefficients for different species of grasses, cereals, herbs and legumes. The limiting BC/Al-value represents root growth forlaboratory results reduced to 80% of normal (Sverdrup and Warfvinge, 1993)

English species	Species	Reaction type	K-value	BC/Al(crit)
Subterranean clover	*Trifolium subterraneum*	Vanselow	K=0.000004	0.6
Lucerne	*Medicago sativa*	Vanselow	K=0.000002	1.2
Soya bean	*Glycine max*	Unspecific	K=0.4	1.5
Tyler wheat	*Triticum aestivum*	Vanselow	K=0.00005	2
Potato	*Solanum tuberosum*	Vanselow	K=0.00002	2
Tomato	*Lycopersicon esculentum*	n.d.	n.d.	2.5
Rye	*Secale cerale*	Vanselow	K=0.0005	6
Atlas wheat	*Triticum aestivum*	Vanselow	K=0.0005	6
Rice	*Oryza sativa*	Vanselow	K=0.0005	6
Cowpea	*Vignia unguiculata*	Vanselow	K=0.0005	6
White clover	*Trifolium repens*	Vanselow	K=0.0.01	20
Grana wheat	*Triticum aestivum*	Vanselow	K=0.02	40
Lettuce	*Lactuca sativa*	Vanselow	K=0.001	40
Sweet corn, Maize	*Zea mays*	Unspecific	K=12	45
Horse bean	*Vicia faba*	Vanselow	K=0.1	80
Sorghum	*Sorghum vulgare*	Vanselow	K=0.1	80
Barley	*Hordeum vulgare*	Vanselow	K=2.0	400

n.d. represents values derived from a combination of quantitative and semi-quantitative data.

Table A1.5 Critical limits and tolerance classification (see Zhao *et al.*, 1994)

Plant type	n	I	II	III	IV	V	VI	VII	VIII
			-critical BC/Al limit-						
Conifers	35	0.3	0.5	1.2	2	10			
Deciduous	36		0.6	1.4	2	6		75	
Grasses	39		0.5	1.0		10	45		300
Herbs	25	0.3		1.0	3	5	50	100	800
Crop plants	17				2	6	50	80	400
Average		0.3	0.5	1.1	2.2	9	50	90	500
Chinese tolerance	80	Strong	Rel. strong	Sl. sens.	Sens.	Very sens.	Very sens.	Very sens.	Very sens.

Table A1.6 Relative tolerance of coniferous trees to acid deposition as screened in Chinese bioassays (BA) and as derived from field surveys (F). * represents values estimated in accurate laboratory experiments (Sverdrup and Warfvinge, 1993)

English name	Species	Method	Sensitivity class	Est. BC/Al (crit)
Oriental thuja	*Thuja orientalis*	F&BA	Strong	0.3
Chinese juniper	*Juniphorus chinensis*	F&BA	Strong	0.3
Morning cypress	*Chamaecyparis funebris*	F&BA	Strong	0.3
Japanese black pine	*Pinus thunbergii*	F&BA	Relatively strong	0.7
Masson pine	*Pinus massonii*	F	Slightly sensitive	4*
Mandarin fir	*Cunnighamia lanceolata*	F	Slightly sensitive	20*
Deodor cedar	*Cedrus deodora*	F	Slightly sensitive	1.4
Japanese cedar	*Cryptomeria japonica*	F	Slightly sensitive	1.4
Chinese yew	*Taxus chinensis*	F	Slightly sensitive	1.4
Loblolly pine	*Pinus taeda*	F	Slightly sensitive	1.5*
Swamp cypress	*Taxodium distichum*	F	Sensitive	2
Dawn redwood	*Metasequoia glypsstroboides*	F	Very sensititve	6

Table A1.7 Relative tolerance of decideous trees to acid deposition as screened in Chinese bioassays (BA) and as derived from field surveys (F), part 1. * represents values estimated in accurate laboratory surveys (Sverdrup and Warfvinge, 1993)

English name	Species	Method	Sensitivity class	Est. BC/Al (crit)
Chestnut	*Castanopis sclerophylla*	F&BA	Strong	0.3
	Michelia macclurei		Strong	0.3
Horsetail	*Casuarina aquisetifolia*	F&BA	Strong	0.3
Assam rubber tree	*Ficus elastica*	F&BA	Strong	0.3
Tall fig	*Ficus altissima*	F	Strong	0.3
Chinese sabinia	*Sabina chinensis*	F&BA	Strong	0.3
Chinese privet	*Ligustrum lucidum*	F&BA	Strong	0.3
Forest osman	*Osmantus forrestii*	F&BA	Strong	0.3
Podocarp	*Podocarpus macrophyllus*	F&BA	Strong	0.3
Japanese tea	*Camellia japonicum*	F&BA	Strong	0.3
Chinese tea	*Camellia sinensis*	F&BA	Strong	1.4*
Oil tea	*Camellia oleifera*	F&BA	Strong	0.3
Orange	*Citrus deliciosa*	F&BA	Strong	0.3
Sweet orange	*Citrus sinensis*	F&BA	Strong	2*
Ebony	*Diospyros kaki*	F&BA	Strong	0.3
Sharon rose	*Hibiscus syriacus*	F	Strong	0.3
Tarim poplar	*Populus simonii*	F	Strong	0.3
Bougainvillea	*Bougainvillea spectabilis*	F	Strong	0.3
Persian lilac	*Melia azedarach*	F	Strong	0.3
	Palbergia hypeana	F&BA	Relatively strong	0.7
Chinese catalpa	*Catalpa ovata*	F&BA	Relatively strong	0.7
	Gardenia szechuanensis	F&BA	Relatively strong	0.7
Jasmin	*Gardenia jasminoides*	F&BA	Relatively strong	0.7
Magnolia	*Magnolia denudata*	F	Relatively strong	0.7
Eucalyptus	*Eucalyptus tereticornis*	F&BA	Relatively strong	0.7
Olive	*Olea europaea*	F&BA	Relatively strong	0.7
Pomegranate	*Punica granatum*	F&BA	Relatively strong	0.7
Windmill palm	*Trachycarpus fortunei*	F&BA	Relatively strong	0.7
Snowball elder	*Viburnum awabuki*	F&BA	Relatively strong	0.7
	Rhapis excelsa	F&BA	Relatively strong	0.7
Oleander	*Nerium indicum*	F&BA	Relatively strong	0.7
Oriental berryelm	*Celtis orientalis*	F	Relatively strong	0.7
Chinese sassafras	*Sassafras tzuma*	F	Relatively strong	0.7
Indian erythrina	*Erythrina indica*	F	Relatively strong	0.7
Camphotek tree	*Camphotheca acuminta*	F	Relatively strong	0.7
Cycad	*Cycas revoluta*	F	Relatively strong	0.7

Table A1.7 continued

English name	Species	Method	Sensitivity class	Est. BC/Al (crit)
Winter sweet	*Chimonanthus praecox*	F	Slightly sensitive	1.4
Camphor tree	*Cinnamomum camphora*	F	Slightly sensitive	1.4
Japanese cinnamon	*Cinnamomum japonica*	F	Slightly sensitive	1.4
Persian cinnamon	*Cinnamomum*	F	Slightly sensitive	1.4
	parthenoxylum	F	Slightly sensitive	1.4
Liguster	*Ligustrum quihoui*	F	Slightly sensitive	1.4
Chinese locust	*Gleditsia sinensis*	F	Slightly sensitive	1.4
Confederate rose	*Hibiscus mutabilis*	F	Slightly sensitive	1.4
Loquat	*Eriobotrya japonica*	F	Slightly sensitive	1.4
Emperor tree	*Paulownia catalpifolia*	F	Slightly sensitive	1.4
	Bauhinia variegata	F	Slightly sensitive	1.4
Paper mulberry	*Broussonetia papyrifera*	F	Slightly sensitive	1.4
	Grevillea robusta	F	Slightly sensitive	1.4
White jasmin	*Jasminum nudiflorum*	F	Slightly sensitive	1.4
Oriental mahogany	*Melia toosendan*	F	Sensitive	2
Chinese mahogany	*Toona sinensis*	F	Sensitive	2
Formosan sweet gum	*Liquidambar formosana*	F	Sensitive	1.4*
Peach	*Prunus persica*	F	Sensitive	2
Oriental plane	*Platanus orientalis*	F	Sensitive	2
Heavenly bamboo	*Nandina domestica*	F	Sensitive	2
Chinese fig	*Ficus sublanceolata*	F	Sensitive	2
Corkscrew willow	*Salix matsudana*	F	Sensitive	2
Pagoda tree	*Sophora japonica*	F	Sensitive	2
Alibissa	*Alibizza julibrissin*	F	Sensitive	2
Chinese wingnut	*Pterocarya stenoptera*	F	Sensitive	3*
Eucalyptus mhahogany	*Eucalyptus robusta*	F	Very sensitive	6
False acacia	*Robinia pseoudoacacia*	F	Very sensitive	6
Worm willow	*Salix tortuosa*	F	Very sensitive	6
	Ormosia nosici	F	Very sensitive	6
White mulberry	*Morus alba*	F	Very sensitive	6
Chinese maple	*Acer buergerianum*	F	Very sensitive	6
Chinese elm	*Ulmus parviflora*	F	Very sensitive	6
Chinese redbud	*Cercis chinensis*			

ANNEX 2

Annex 2 DATA PRODUCTION AND RELIABILITY; RELATIVE BUFFERING RATES AND ESTIMATED WEATHERING RATES

A2.1 *Data production and reliability*

S. Cinderby; J.C.I Kuylenstierna

The work of the Impacts group within the RAINS-ASIA project involved the production of maps showing the distribution of relative sensitivity of ecosystems to acidic deposition and the distribution of simple mass balance critical load values. These maps were eventually combined to produce the final critical loads map for acidic depositions for the southern and eastern Asian regions. These maps were produced by combining and modelling various data layers within a geographic information system (GIS).

The inputs to this process were a large number of spatial datasets of differing types and resolutions. This Annex describes the various input layers to the mapping and modelling procedure. This will include the origin of the data layers, their modification and combination within the GIS and their role in the spatial modelling which was performed. An indication of the accuracy of the input data layers will also be given. The quality of the data used in the preparation of the various resulting maps provides an informed opinion as to the accuracy of the information the maps portray.

A2.1.1 Climatic data

Precipitation map (P)

The SEI Precipitation Map (see Map 1) was derived by digitising the isolines of equal precipitation from two sources; the map of Mean Annual Precipitation (WMO-UNESCO-UNEP, 1981) produced by the World Meteorological Organisation (WMO) for the majority of the region and the similar map produced by the ASEAN Institute for Indonesia, Malaysia, southern Thailand and the Philippines (ASEAN Secretariat, 1982). These were compiled into maps within the geographic information system and then combined to form a single cover for the entire region. The scale of the original maps is 1:10,000,000.

The WMO map was produced from 6600 weather stations with data averaged over a 30-year period (or longer in high variability areas). The number of stations in some areas is, however, very sparse. For example, the Chinese provinces of Xizang Zizjqu and Xinjiang Uygur Zizhiqu have very few weather stations. This means that the accuracy of the precipitation data across the region is spatially variable. The location of weather stations used to produce the WMO map can be seen in Figure A2.1.

The ASEAN region data was produced from 799 weather station sites. The location of these stations can be seen in Figure A2.2. The period over which these data were averaged was generally greater than 20 years but for 247 locations, where coverage was sparse, stations recording over a time scale of as little as 10 years were included. The number of stations used from each category can be seen in Table A2.1 below. Obviously the accuracy of the data used by the WMO is of a higher overall quality than the ASEAN data, but the area covered by the data set is much larger. Overall, both data sources are of high accuracy and reliability.

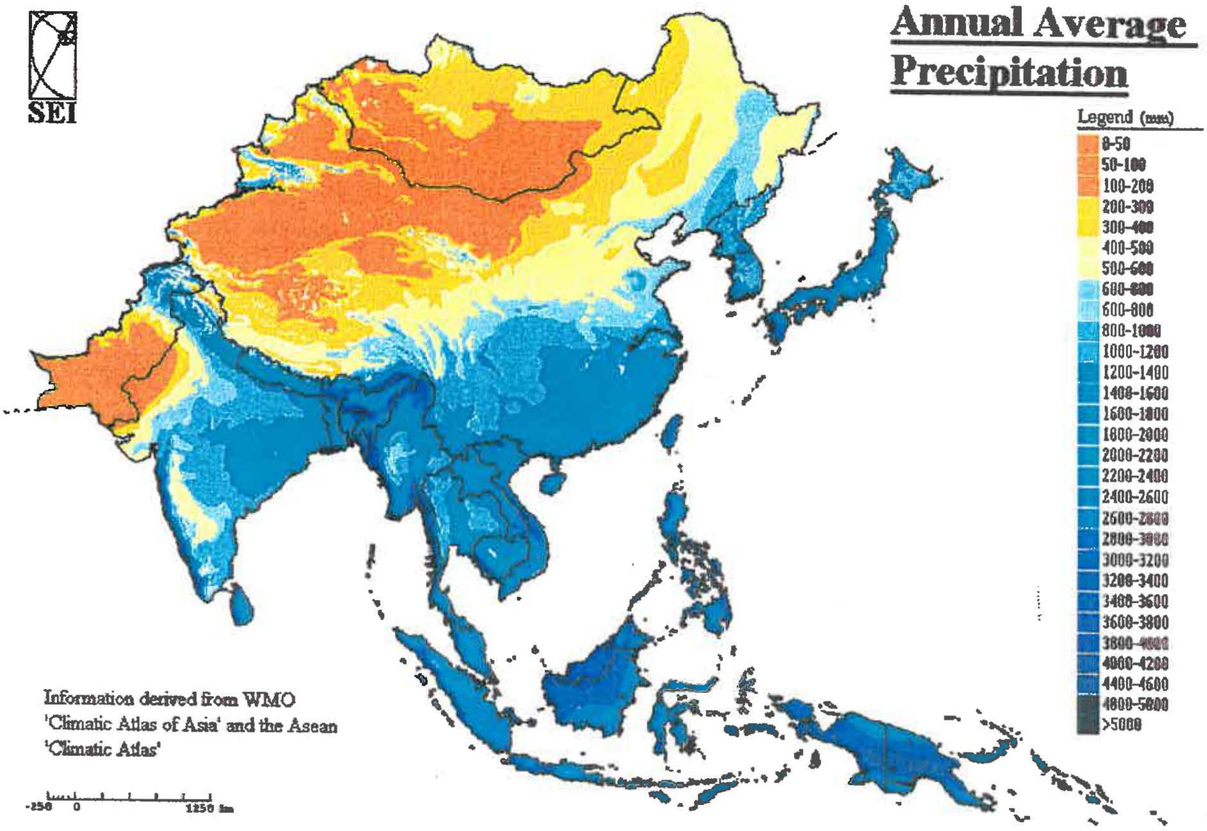
SEI
Annual Average Precipitation
Legend (mm)
0-50
50-100
100-200
200-300
300-400
400-500
500-600
600-800
600-800
800-1000
1000-1200
1200-1400
1400-1600
1600-1800
1800-2000
2000-2200
2200-2400
2400-2600
2600-2800
2800-3000
3000-3200
3200-3400
3400-3600
3600-3800
3800-4000
4000-4200
4400-4600
4800-5000
>5000
Information derived from WMO 'Climatic Atlas of Asia' and the Asean 'Climatic Atlas'
-250 0 1250 km

Map 1

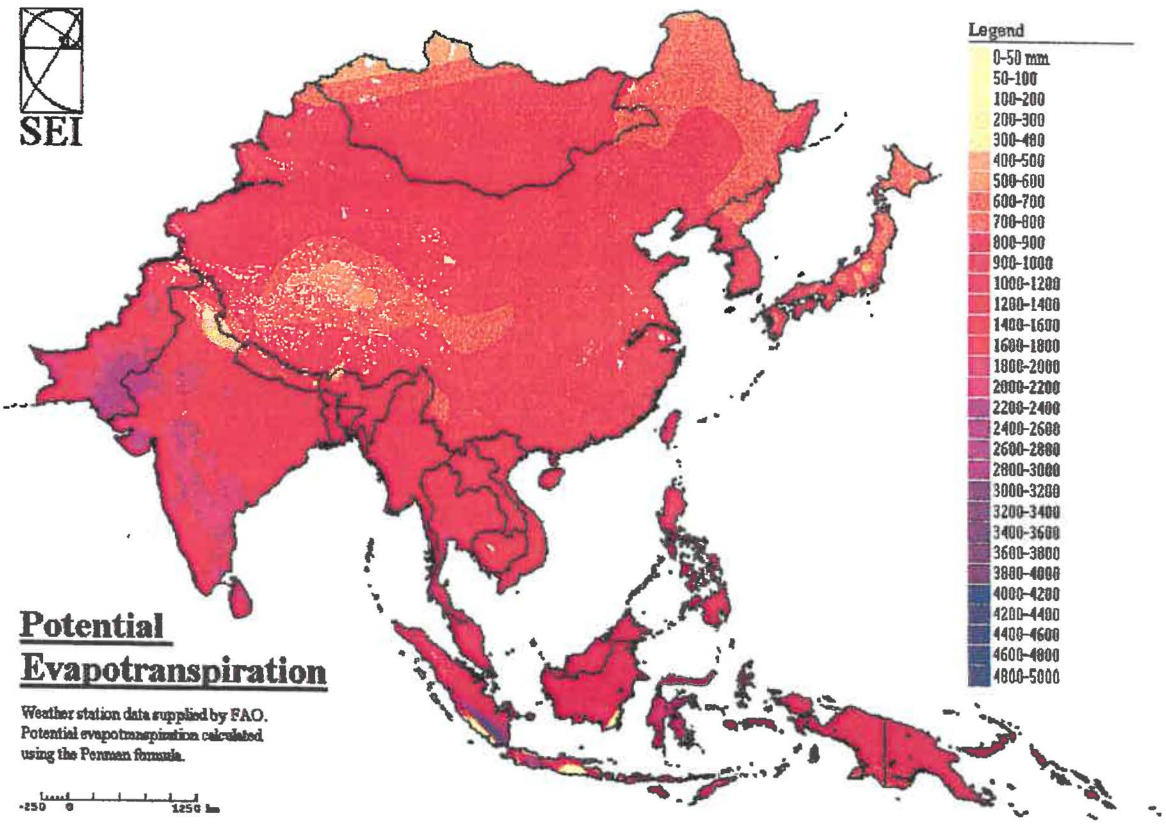
SEI
Legend
0-50 mm
50-100
100-200
200-300
300-400
400-500
500-600
600-700
700-800
800-900
900-1000
1000-1200
1200-1400
1400-1600
1600-1800
1800-2000
2000-2200
2200-2400
2400-2600
2600-2800
2800-3000
3000-3200
3200-3400
3400-3600
3600-3800
3800-4000
4000-4200
4200-4400
4400-4600
4600-4800
4800-5000
Potential Evapotranspiration
Weather station data supplied by FAO.
Potential evapotranspiration calculated using the Penman formula.
-250 0 1250 km

Map 2

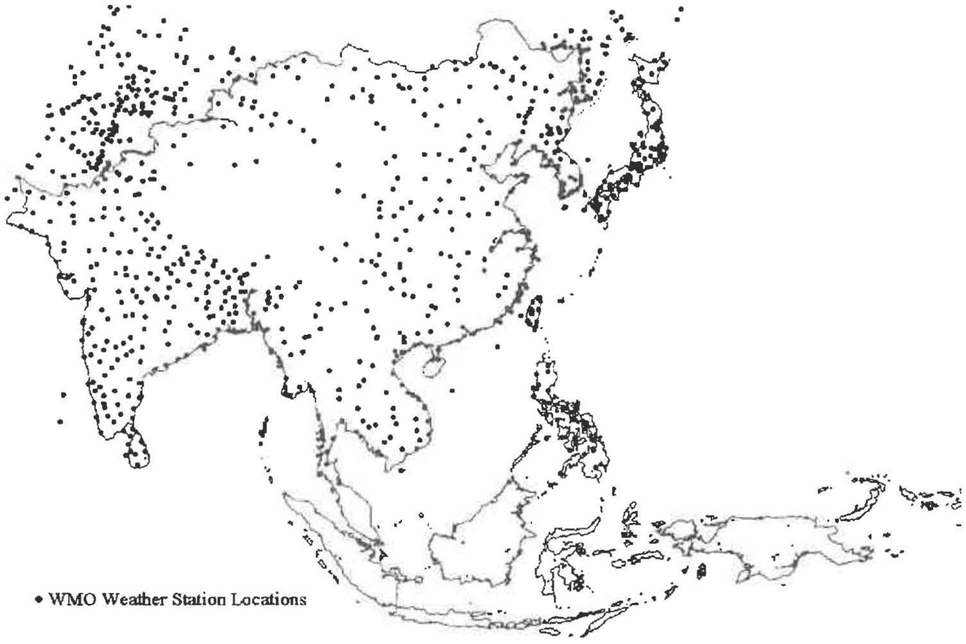

Figure A2.1 The location of WMO weather stations

Figure A2.2. The location of ASEAN weather stations.

Table A2.1 The duration (years) of records for ASEAN weather stations.

COUNTRY	Class 1	Class 2	Class 3
Indonesia	109	191	141
Malaysia	127	23	35
Philippines	48	1	67
Singapore	9	0	3
Thailand	43	1	1

Class 1: Stations with > 20 years of complete data within the standard period

Class 2: Stations with < 20 years of complete data but with > 20 years of data in total

Class 3: Stations with <20 years of complete data.

Potential Evapotranspiration (PE)

Climatic parameters for a number of weather stations were supplied by the FAO. The subset of this information for the Asian region was extracted and the point data for 833 sites entered into the GIS. An areal surface was then produced by interpolating the values using a triangulated irregular network (TIN) algorithm. This looks at groups of three points in turn and works out the location of isolines based on the class boundaries desired and the data values at the points (Intera Tydac Technologies, 1993). A smoothing option was applied during the interpolation procedure. This results in more aesthetically pleasing isolines but does not improve the accuracy of the interpolated map. In order to produce a full coverage for the region it was necessary to interpolate outside the extent of the weather stations. This region only covers a small area of the map and has been checked for any obvious anomalies.

The FAO information on potential evapotranspiration was derived using the Penman formula (Frère and Popov, 1979). Potential evapotranspiration is defined as the maximum quantity of water which may be evaporated by a uniform cover of dense short grass when the water supply to the soil is not limited (Jones and Thomasson, 1985). Obviously by taking a uniform cover type of short grass the specific physiological capabilities of the actual vegetation cover at a site are ignored. The Penman formula is however regarded by meteorologists as the most accurate technique available for estimating PE (Shaw, 1988). The formula used is as follows:

$$PE = \frac{\frac{Po}{P}.\frac{\Delta}{\gamma}.[0.75R_A(a+b\frac{n}{N}) - \sigma T_K^4(0.56-0.079\sqrt{e_d})(0.1+0.9\frac{n}{N})] + 0.26(e_a-e_d).(1+0.54U)}{\frac{Po}{P}.\frac{\Delta}{\gamma}+1.0}$$

PE	=	estimation of potential evapotranspiration in mm
Po	=	mean atmospheric pressure in millibars at sea level
P	=	mean atmospheric pressure in millibars as a function of altitude
Δ	=	rate of exchange with temperature of the saturation vapour pressure in millibars per °C
γ	=	psychometric coefficient for a psychometer with forced ventilation
R_A	=	short wave radiation received at the limit of the atmosphere expressed in mm of evaporable water and taking account for the solar constant value of $2.00 cal.cm^{-2}.min^{-1}$
a & b	=	coefficient for the estimation of total radiation from sunshine duration
n	=	sunshine duration in hours and tenths for the given period
N	=	sunshine duration astronomically possible for the given period
σT_K^4	=	blackbody radiation in mm of evaporable water for the prevailing air temperature
e_a	=	saturation vapour pressure in millibars
e_d	=	saturation vapour pressure for the period under consideration in millibars
U	=	mean wind speed at an elevation of 2m above ground for the period expressed in ms^{-1}

The accuracy of this interpolated map appears reasonably good in most areas however, once again, the density of the weather station network leads to some areas of questionable accuracy. The location of the weather stations used tointerpolate the potential evapotranspiration values can be seen in Figure A2.3 and the final interpolated contours in Map 2.

Precipitation to Potential Evapotranspiration (P:PE) ratio

This map (see Map 3) was derived within the GIS by performing a map modelling procedure dividing the precipitation levels by the evapotranspiration values. The mean value of the precipitation class from the SEI precipitation map was used in the calculation. The calculated ratios on the derived map were then reclassified into ranges. By using a ratio some of the possibility for error has been eliminated as inaccuracies in the data will be compensated for by the division process and by the classification of the values generated into ranges. The index represents an index of the effectiveness of precipitation which gives an indication of the moisture levels within the soil (Parry, Carter and Konijn, 1988).

Ground water flux (Q)

This map (see Map 4) is an estimation of ground water flux at a site including infiltration, ground water movement and surface runoff. The correlation between P:PE ratio and runoff was estimated from visual comparison between the SEI European P:PE ratio map (Kuylenstierna, 1993) and the 'Runoff Map for Europe' (Hydrometeorological Service, 1976)

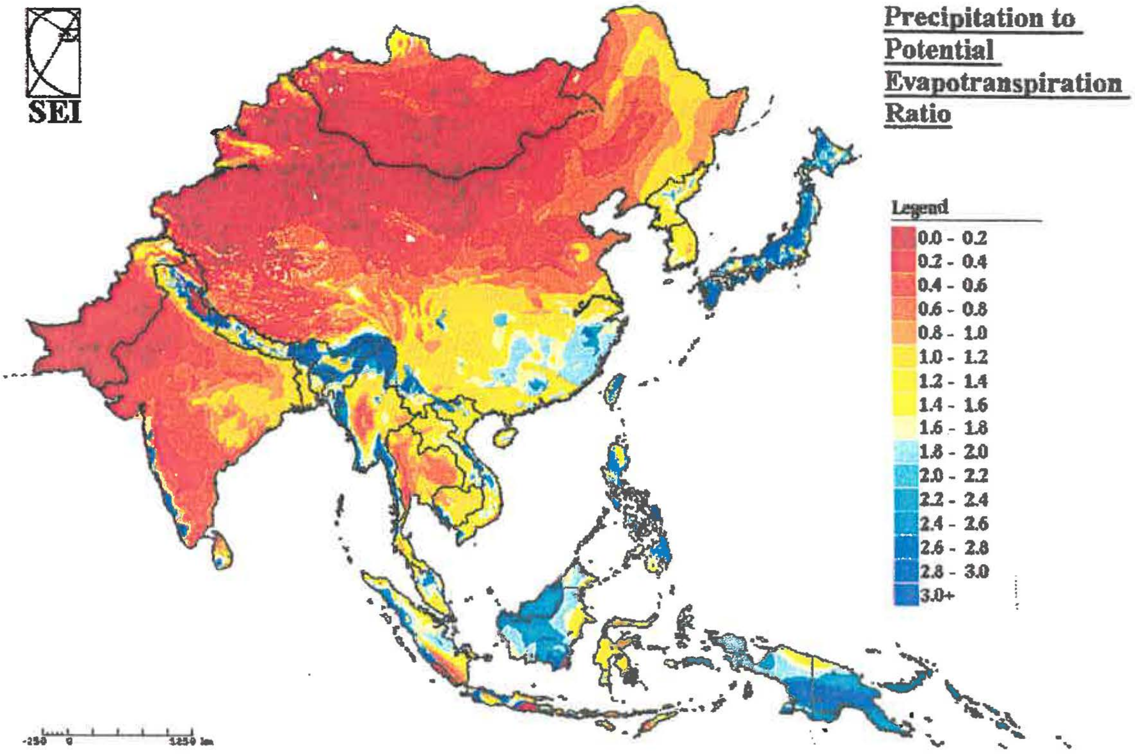
SEI
Precipitation to Potential Evapotranspiration Ratio
Legend
0.0 - 0.2
0.2 - 0.4
0.4 - 0.6
0.6 - 0.8
0.8 - 1.0
1.0 - 1.2
1.2 - 1.4
1.4 - 1.6
1.6 - 1.8
1.8 - 2.0
2.0 - 2.2
2.2 - 2.4
2.4 - 2.6
2.6 - 2.8
2.8 - 3.0
3.0+

Map 3

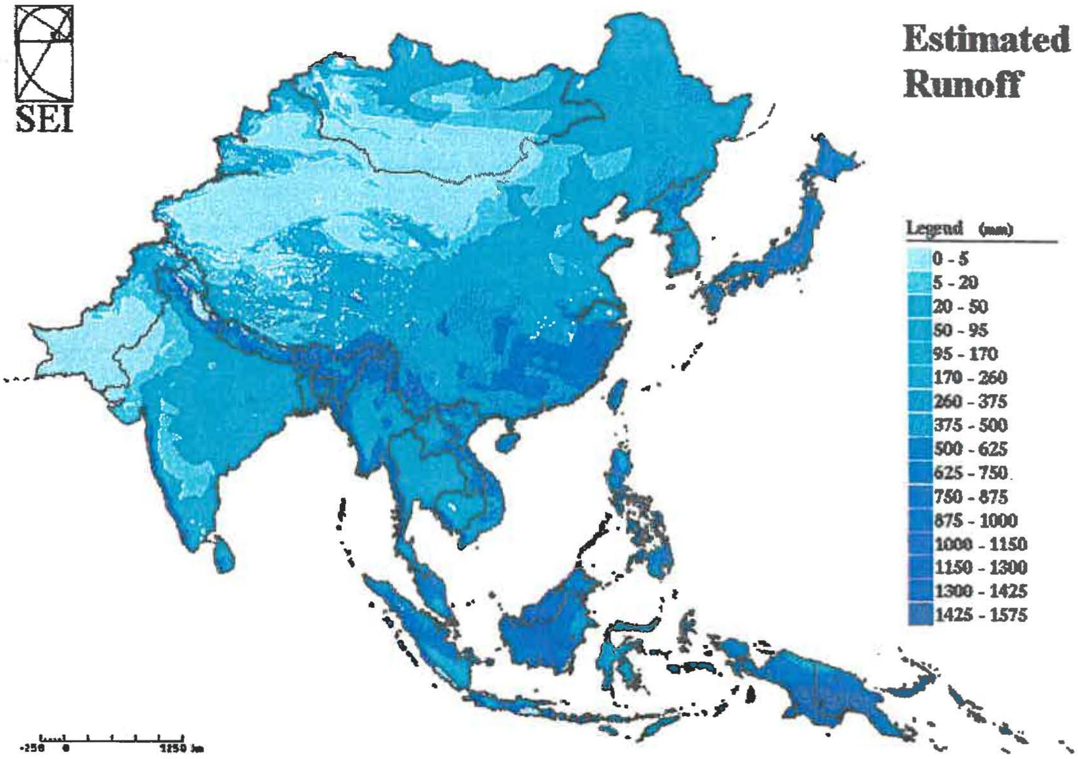
SEI
Estimated Runoff
Legend (mm)
0 - 5
5 - 20
20 - 50
50 - 95
95 - 170
170 - 260
260 - 375
375 - 500
500 - 625
625 - 750
750 - 875
875 - 1000
1000 - 1150
1150 - 1300
1300 - 1425
1425 - 1575

Map 4

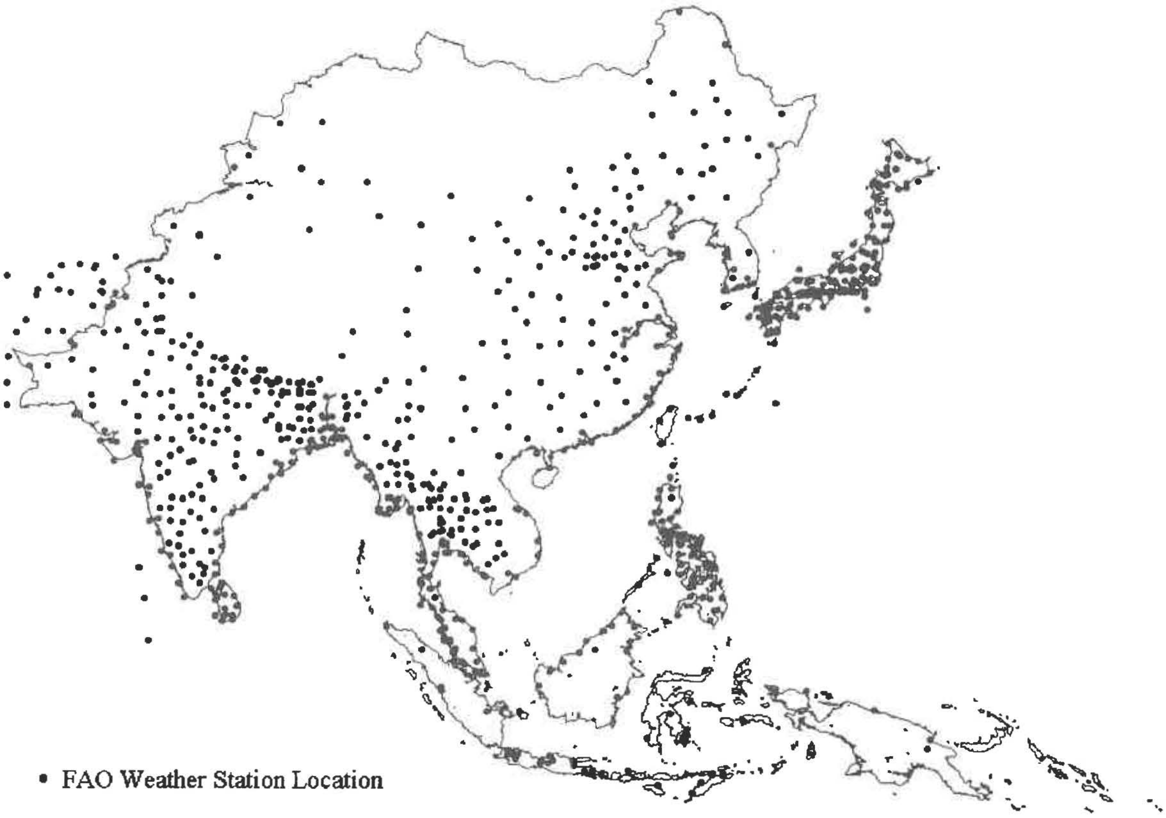

Figure A2.3 The location of the FAO weather stations

produced by the Hydrometeorological Service of Moscow. The correlation was used to reclassify the P:PE map into estimations of ground water flux. The accuracy of this map is uncertain due to a number of factors. Firstly, the inaccuracies inherent in the visual correlation. Secondly, in the simple mass balance equation Q is defined as flow rate through a system (Hettelingh, Downing and de Smet, 1991). It should ideally be calculated from precipitation minus actual evapotranspiration minus surface runoff. In Asia the final two inputs to this calculation were absent so the correlation between P:PE and Q was used instead. The correlation was estimated from European moisture regime conditions and it is unclear whether the relationship, between these two factors, holds for the Asian environment.

Effective Temperature Sum (ETS)

The input data for this map (see Map 5) was once again supplied by the FAO as a point layer of weather station readings. The effective temperature sum (ETS) is the aggregate of the daily mean temperature exceeding a threshold (Alcamo, Shaw and Hordijk, 1990). (Its use in the estimation of weathering rates will be explained later.) The daily temperatures were interpolated from mean monthly readings. The TIN algorithm, with smoothing, was again used to create an areal coverage. The spatial accuracy of this map is similar to that of the potential evapotranspiration map.

Base cation deposition

This map was derived using the following formula (Carmichael, 1992):

$$\text{Base Cation Deposition} = F^{dry}{}_{calcium} + F^{wet}{}_{calcium}$$

where:

$F^{dry}{}_{calcium}$ = Dry Deposition of Calcium

$F^{wet}{}_{calcium}$ = Wet Deposition of Calcium

$$\text{Dry Deposition of Calcium} = C_{pa} \cdot Vd \cdot X_{Ca}$$

where

C_{pa}	= Concentration of Aerosols ($mg.m^{-3}$)
Vd	= Dry Deposition Velocity (1 $cm.s^{-1}$)
X_{Ca}	= Mass Fraction of Calcium in Aerosol (g Ca: g Dust) (value taken as 0.041)

$$\text{Wet Deposition of Calcium} = P.S.C_{pa}.c^{-1}.X_{Ca}$$

where

P	= Precipitation ($mm.yr^{-1}$)
S	= Scavenging Ratio (1000 $g.Ca.m^3$ water : $g.Ca.m^3$ air)
c^{-1}	= Density of Air ($1200 g.m^{-3}$air)

This map was derived from a number of input datasets. Firstly, contour maps of predicted air concentrations of minerals near the surface for the months of January, April, August and November were digitised. The maps were combined and used to calculate annual averages of air concentrations of aerosols for the Asian Continent. Annual average values for the calculation were taken from the SEI-produced precipitation map. The maps were combined within the GIS and a modelling equation written to perform the calculation. Estimates of the other parameters were supplied by Greg Carmichael of the University of Iowa, USA. A range of values were supplied for each of the other parameters and a number of result maps were produced by varying the values of the parameters used in the calculation within the range specified. Ultimately, after discussions with Greg Carmichael values from the low end of the possible range were employed in the calculations (these are shown above; for resulting distribution see Map 6).

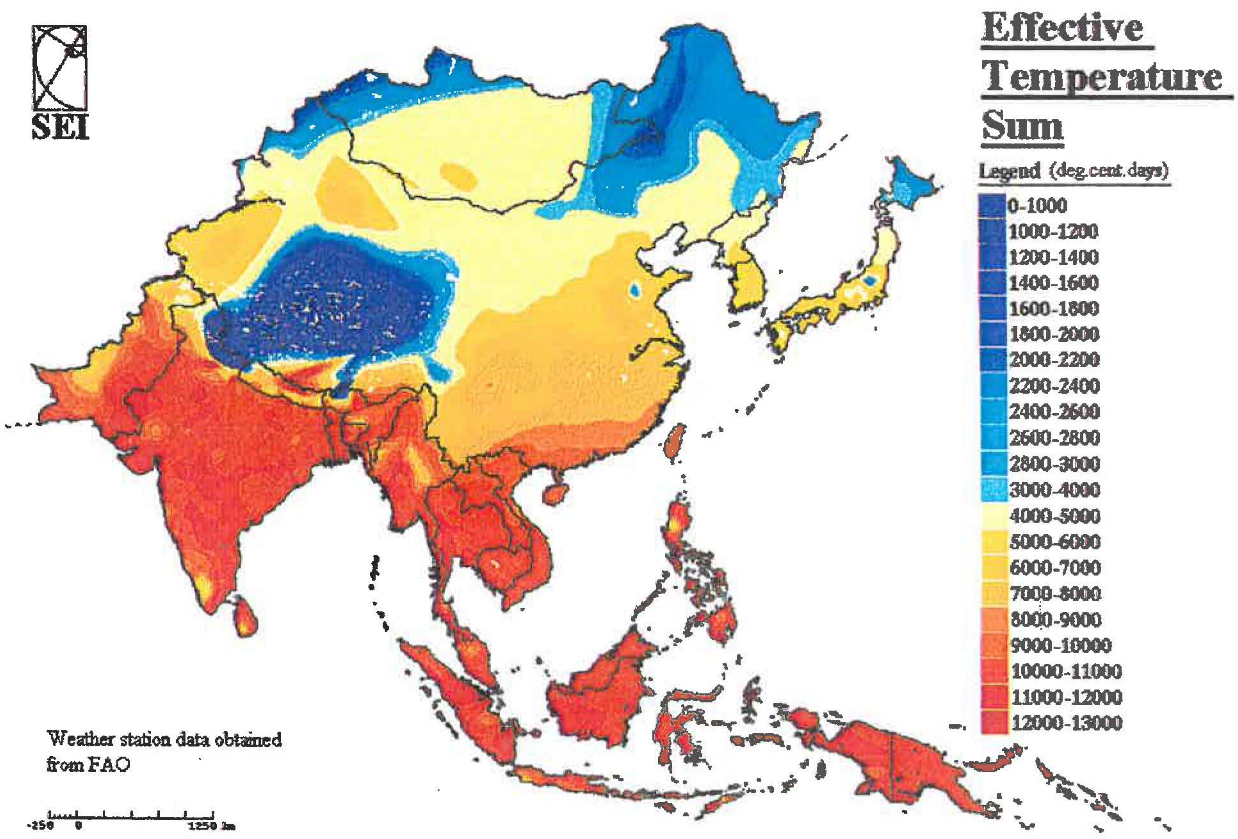
SEI
Effective Temperature Sum
Legend (deg.cent.days)
0-1000
1000-1200
1200-1400
1400-1600
1600-1800
1800-2000
2000-2200
2200-2400
2400-2600
2600-2800
2800-3000
3000-4000
4000-5000
5000-6000
6000-7000
7000-8000
8000-9000
9000-10000
10000-11000
11000-12000
12000-13000
Weather station data obtained from FAO
-250 0 1250 km

Map 5

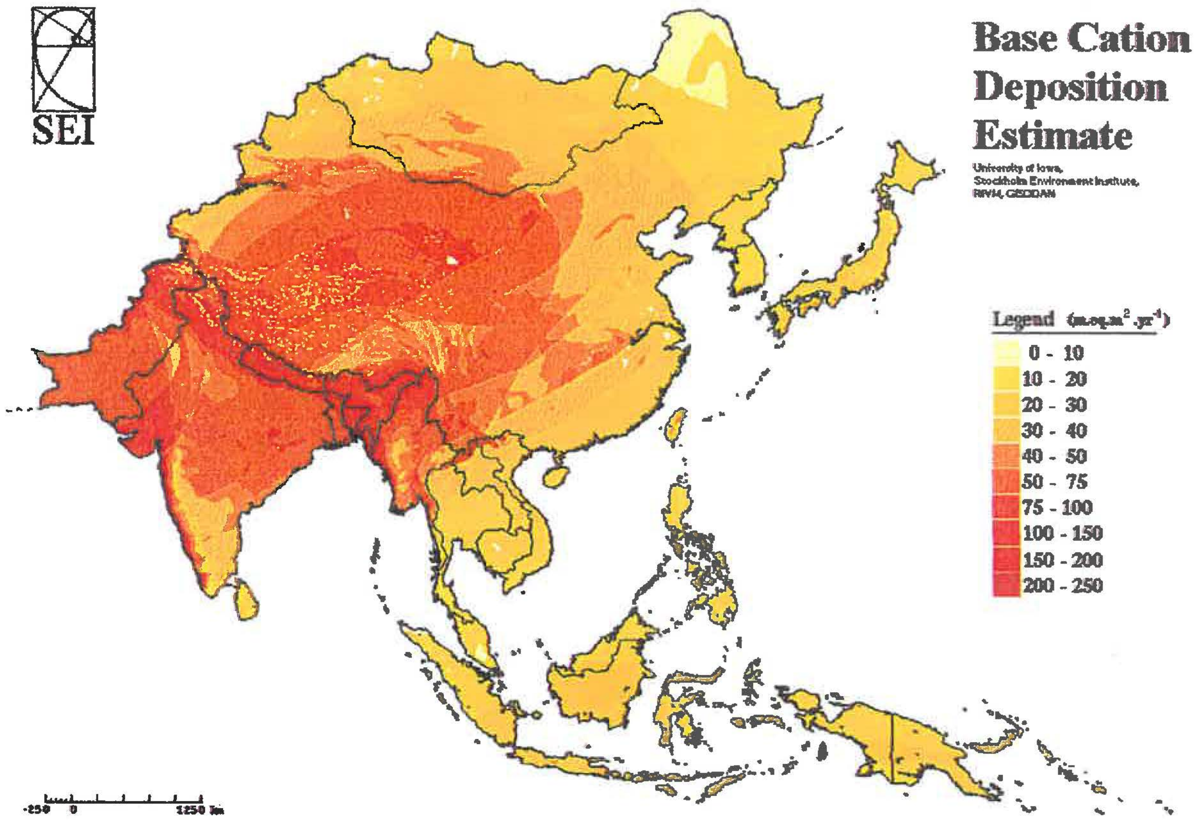
SEI
Base Cation Deposition Estimate
University of Iowa, Stockholm Environment Institute, RIVM, GEODAN
Legend (m.eq.m^2.yr^-1)
0 - 10
10 - 20
20 - 30
30 - 40
40 - 50
50 - 75
75 - 100
100 - 150
150 - 200
200 - 250
-250 0 1250 km

Map 6

The accuracy of this map layer was initially uncertain. The input maps of the air concentrations of minerals were produced by a coarse global resolution model and digitised from poor quality paper reproductions of the model output. Only four months' data, representative of the climatic conditions prevalent in their season, were used to produce an annual estimate; ideally monthly estimates should have been utilised. The values of precipitation were annual.

The estimates provided by this calculation have since been largely ratified by modelled base cation depositions provided by the atmospheric experts within the RAINS-ASIA project. The base cation depositions have now been assessed using four months of air concentrations of dust and corresponding monthly precipitation values. The results correspond well with those produced by the first approximation used in the critical loads estimation.

A2.1.2 Soil data

Soil pH

This map (see Map 7) was produced by SEI by reclassifying the FAO soil types (FAO-UNESCO, 1977; 1978; 1979; 1981; 1988) based on their average pH unit value. This information was obtained from a number of sources including data held by the FAO and published in the text accompanying the map sheets. Additional data were obtained from other pedological texts to supplement and verify the FAO information (Fitzpatrick, 1980; 1971). The FAO soil classification system does not differentiate on the basis of soil pH. Soil acidity is only a diagnostic characteristic for a limited number of soil types and many soils are difficult to classify according to pH. This means that the certainty with which pH is able to be predicted varies with soil type. For some soil types the variation in pH can be quite wide covering more than one of the classes shown on the map; for these soils the mean pH was taken. This may have resulted in some soils being shifted into the wrong class but without more detailed national data this was inevitable. The measurement of pH is for the top 50cm of the soil profile. The accuracy of the original FAO soil surveying can be seen in Figure A2.4. The surveying inaccuracies are in addition to those resulting from assigning soils into pH classes.

The definition of the three reliability classes is as follows:

Class 1: areas covered with sufficient ground control to be of high reliability. Amongst these maps some variation in accuracy occurs because of varying scales and classification schemes based on varying concepts of soil units;

Class 2: areas delimited by soil reconnaissance. These regions have their soil boundaries delimited by changes in vegetation pattern, geomorphology, lithology or climatic characteristics;

Class 3: areas which are unexplored or have occasional soil studies within them. The FAO soil boundaries represent a rough sketch of the soil units in these areas.

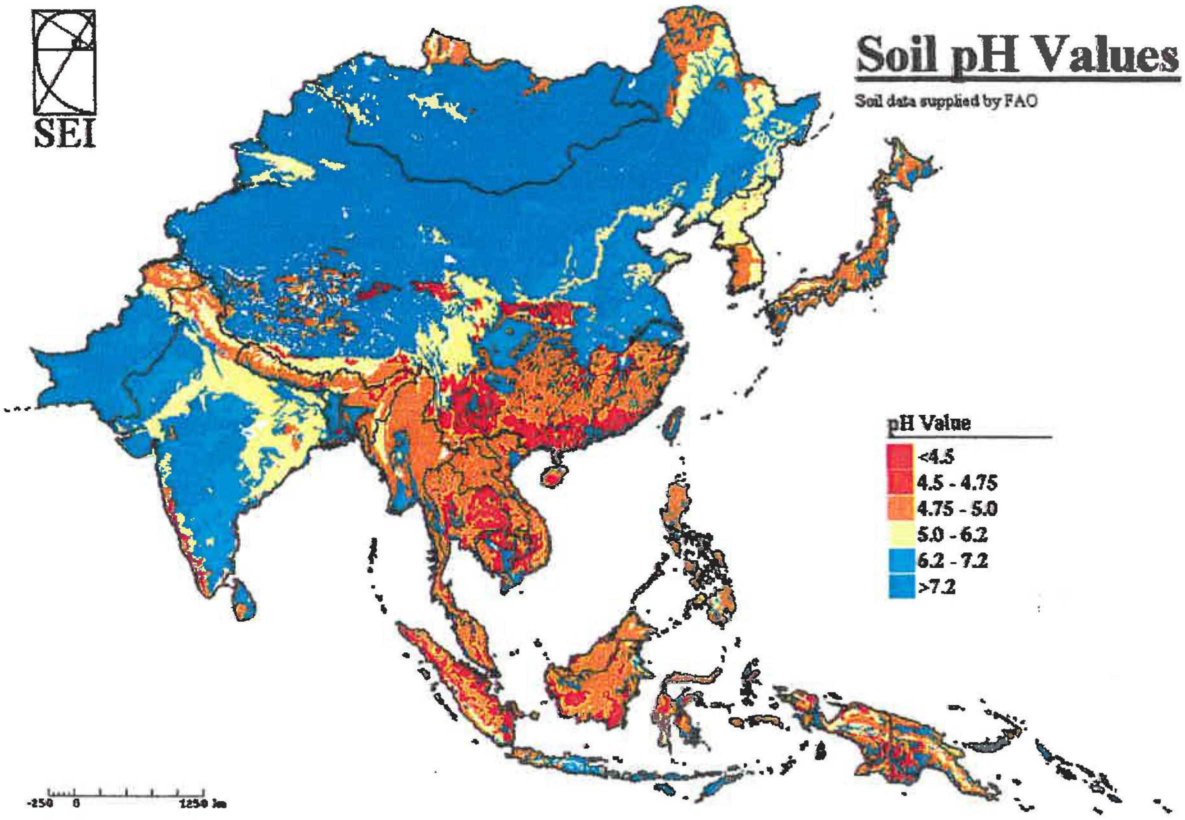
SEI
Soil pH Values
Soil data supplied by FAO
pH Value
<4.5
4.5 - 4.75
4.75 - 5.0
5.0 - 6.2
6.2 - 7.2
>7.2

Map 7

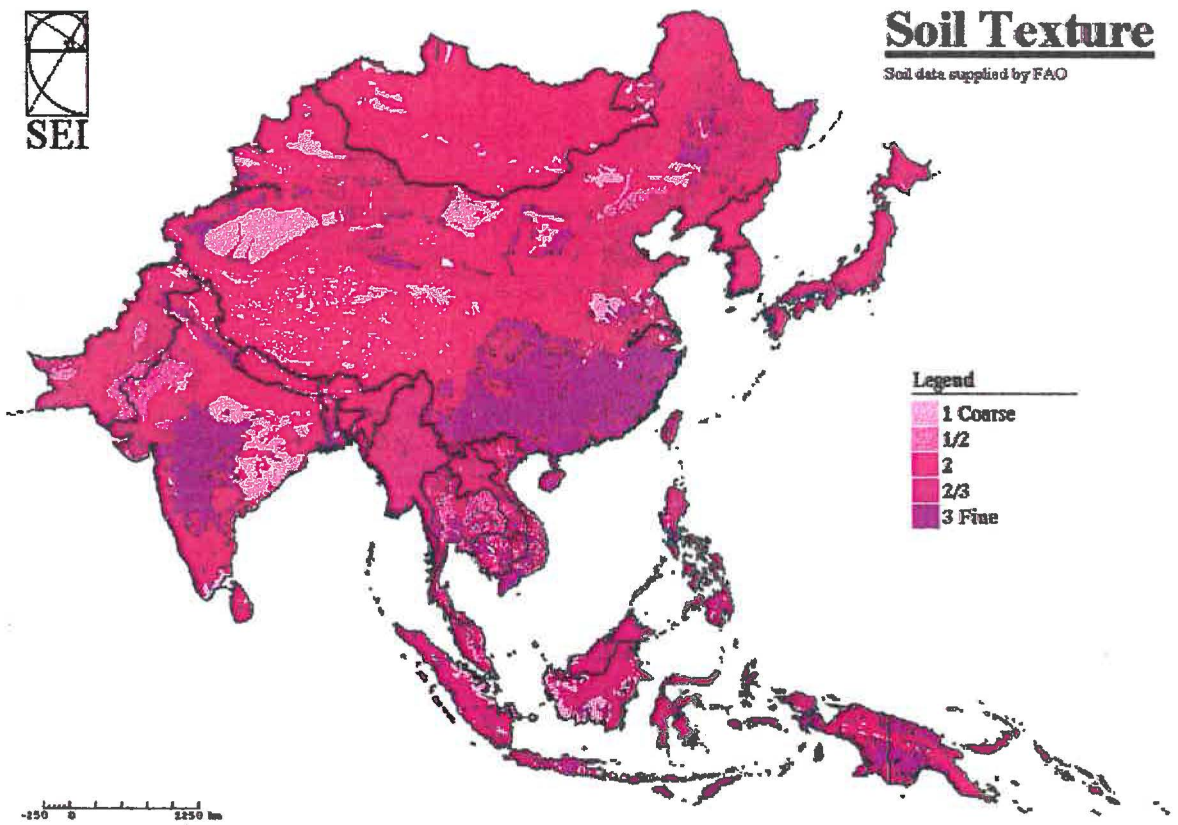
SEI
Soil Texture
Soil data supplied by FAO
Legend
1 Course
1/2
2
2/3
3 Fine

Map 8

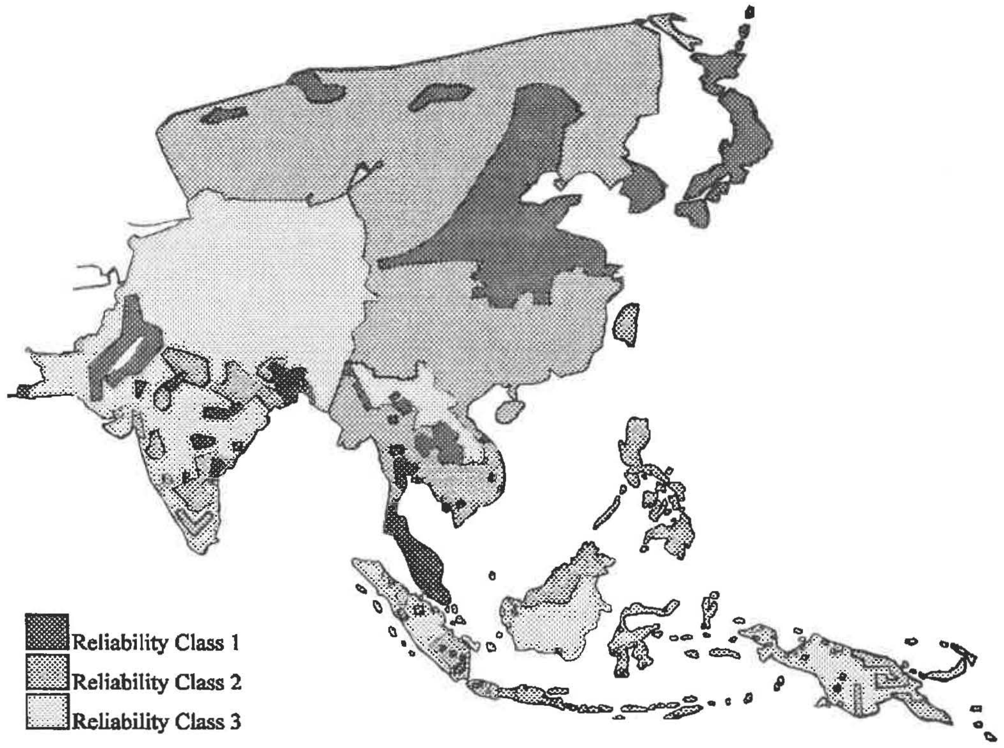

Figure A2.4 The reliability classes of the FAO soil map data (FAO, 1977-81)

Obviously, the data for the class 3 areas are potentially poor and so the derived distribution of soil pH may be equally uncertain. The benefits of using the FAO soil data are, however, that it has been collected and compiled in a consistent manner for the entire region avoiding problems with differing national soil classifications. The problems of accuracy within the soil data can only be overcome at a later stage by employing national scale datasets in the mapping procedure.

Soil texture

As with the soil pH map this is a reclassification of the FAO soil types based on the map units associated texture class. The FAO map has three classes of texture, fine to coarse (see Table A2.2). The classification scheme employed by the FAO includes soil units where some of the soils in the area are of texture class 1 and some are of class 2 (similarly with classes 2 and 3). During the reclassification the mean texture for that mapping unit was assigned to the whole unit. This results in the derived map (see Map 8) having five classes of texture. This process means that none of the soils in the intermediate units will in reality have the texture class assigned.

Table A2.2 FAO Texture class and particle size (FAO, 1977-88)

Texture Class	Particle Diameter (mm)
Class 1 - Coarse (Sand)	2 - 0.02
Class 2 - Intermediate (Silt)	0.02 - 0.002
Class 3 - Fine (Clay)	< 0.002

A2.1.3 Geology data

Rock type

This map (see Map 9) was derived by SEI from the UNESCO World Geology map produced at a scale of 1:10,000,000. The legend on the original map shows metamorphic and igneous rocks divided by their relative acidity. Sedimentary rocks are subdivided based on their age rather than their type. For the purposes of assessing buffering and weathering rates the division was made between Precambrian and Cambrian sedimentary rocks and all younger rocks. The Cambrian period (530±40 m.yr BP to 460 m.yr BP) contains sedimentary rocks with the first unequivocal shelled fossils (Whittow, 1984). However, it was decided that rocks of such age would generally be well weathered of carbonate material and would, therefore, have lower buffering rates than younger rocks. Precambrian rocks being even older were combined with the Cambrian rocks into a low buffering ability class. Obviously, this is not ideal as the classification scheme tells one nothing about the nature of the sedimentary rocks across Asia, only their age. This means that whilst the information included in the map is essentially accurate some detail is lacking which could move some of the 'other' classes into different groups and, potentially, move some of the Cambrian rocks into a higher buffering ability class. The World Geology map was chosen as it was the only regional data set available. Unfortunately the 'other' category covers the largest area on the map and, therefore, bedrock geology could only be used in a limited way in the assessment of weathering. Ideally more detailed maps showing the type of all the rocks would have been utilised but this information was unavailable to the project. No reliability information for the data contained on the map is available. As an estimate 1:10,000,000 scale maps can be said to have a detection resolution of approximately 1000m, so only rock bodies of this size or greater will be differentiated on the map (Tobler, 1988).

A2.1.4 Vegetation

Land use and vegetation

The Rutgers University 'Major World Ecosystems Map' was used to obtain information on landuse and vegetation cover (see Map 10). The map was originally produced by the Oak Ridge National Laboratory, USA, to assess global vegetation carbon content (Olson, 1982).

The map has a maximum resolution of 0.5 by 0.5 degrees (giving an equatorial ground resolution of approximately 55*55 km). A facet of the map being supplied with equal longitude/latitude (lola) raster cells is that the apparent ground resolution of the cells increases

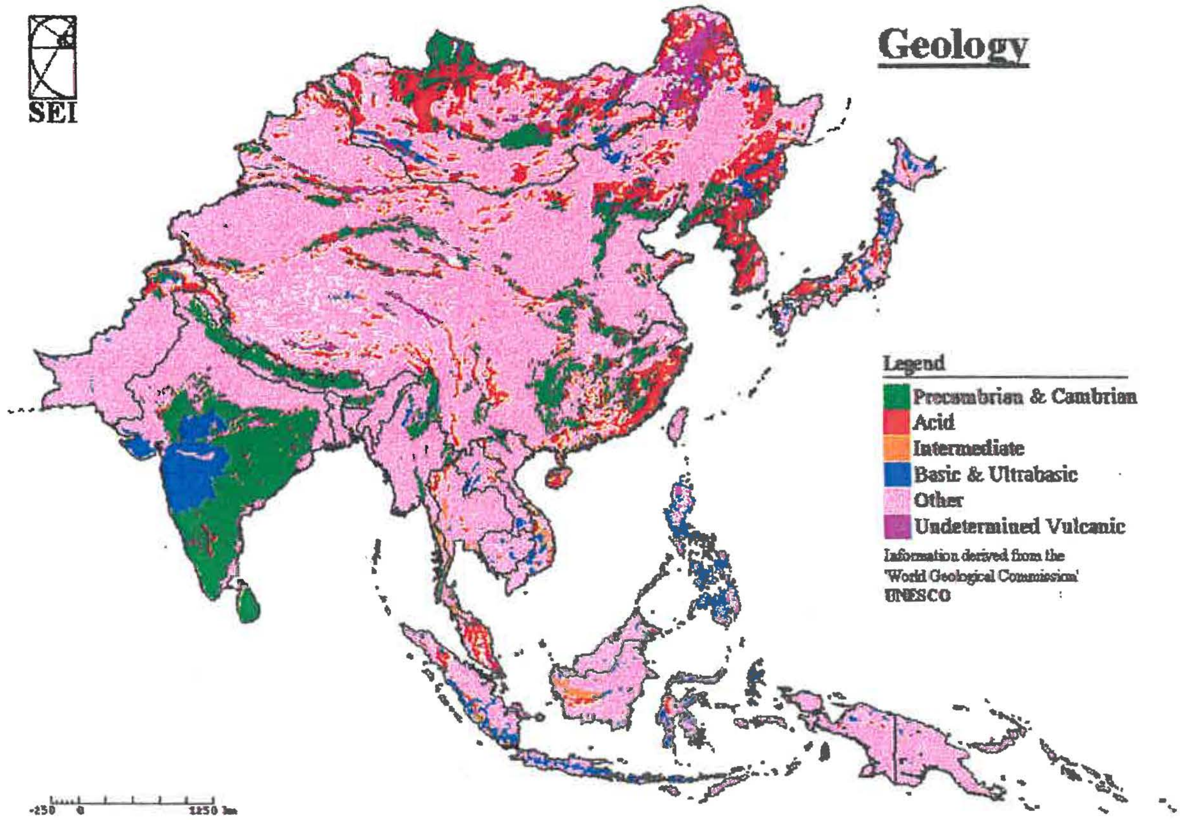
SEI
Geology
Legend
Precambrian & Cambrian
Acid
Intermediate
Basic & Ultrabasic
Other
Undetermined Vulcanic
Information derived from the
'World Geological Commission'
UNESCO
-250 0 1250 km

Map 9

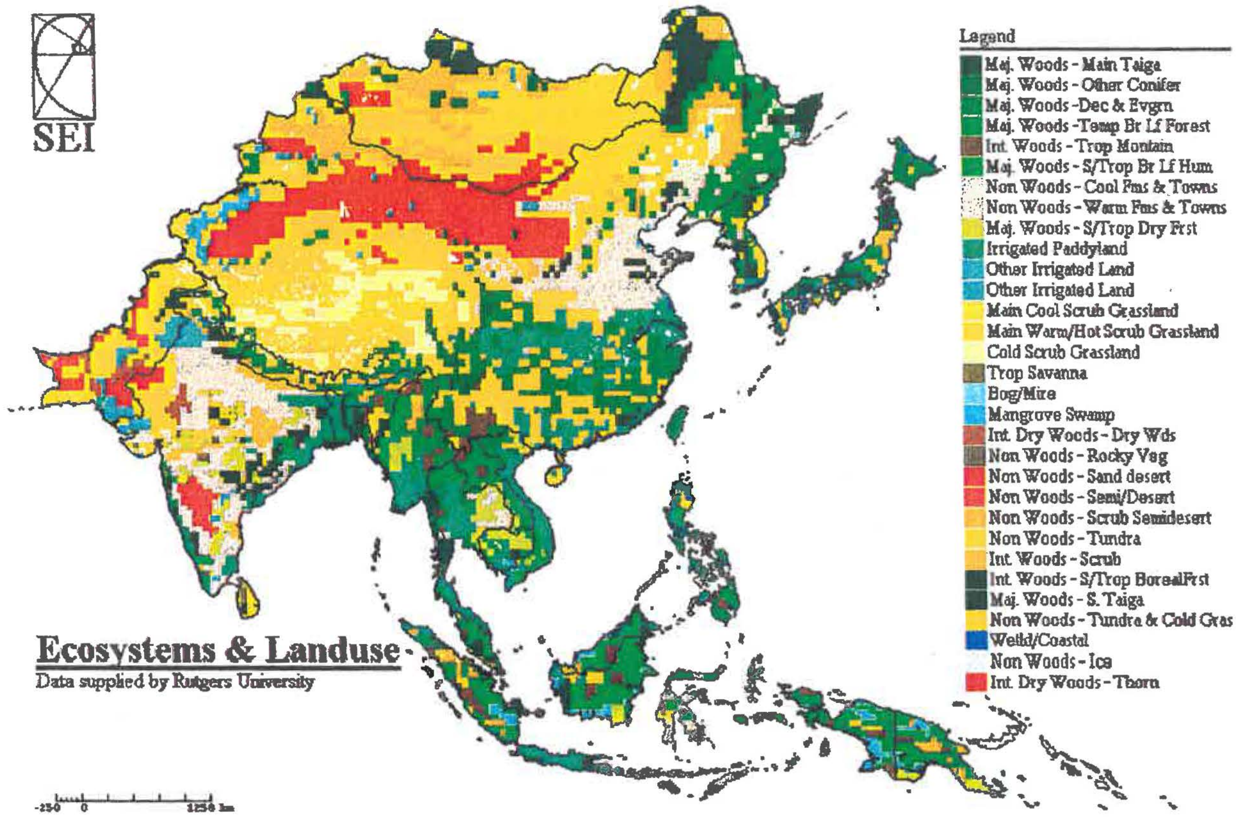
SEI
Legend
Maj. Woods - Main Taiga
Maj. Woods - Other Conifer
Maj. Woods -Dec & Evgrn
Maj. Woods -Temp Br Lf Forest
Int. Woods - Trop Montain
Maj. Woods - S/Trop Br Lf Hum
Non Woods - Cool Fms & Towns
Non Woods - Warm Fms & Towns
Maj. Woods - S/Trop Dry Frst
Irrigated Paddyland
Other Irrigated Land
Other Irrigated Land
Main Cool Scrub Grassland
Main Warm/Hot Scrub Grassland
Cold Scrub Grassland
Trop Savanna
Bog/Mire
Mangrove Swamp
Int. Dry Woods - Dry Wds
Non Woods - Rocky Veg
Non Woods - Sand desert
Non Woods - Semi/Desert
Non Woods - Scrub Semidesert
Non Woods - Tundra
Int. Woods - Scrub
Int. Woods - S/Trop BorealFrst
Maj. Woods - S. Taiga
Non Woods - Tundra & Cold Gras
Wetld/Coastal
Non Woods - Ice
Int. Dry Woods - Thorn
Ecosystems & Landuse
Data supplied by Rutgers University
-250 0 1250 km

Map 10

with latitude. That is the area covered by each equal lola cell decreases with increasing latitude, providing more spatial detail.

The class in each cell represents the dominant cover type in that location (Olson, Watts and Allison, 1983). The distribution shown on the map was derived from a number of different data types. Potential vegetation maps were used and modified by modern regional estimates of current vegetation, landuse practices, forestry surveys and agricultural yields. Many paper map sources were incorporated and remotely sensed data used where available, for example, in parts of Thailand. These data sets were interpreted by experts using personal judgement as to the type and extent of ecosystems in each lola cell. A facet of placing the dominant ecosystem class in each cell is that in mixed areas the actual area of that cover type may be considerably less than 50% of the whole cell. The map represents vegetation patterns for 1980.

The map was used in this project as it represented the only regional study of recent origin. The relatively coarse nature of the data, in comparison with some of the other coverages, results in the 'blocky' appearance of the resultant sensitivity and critical loads maps. The coarse scale of this gridded information was only applicable when considering the resolution of data produced by the other collaborative researchers within RAINS-ASIA; for example the deposition data is produced on a 1 by 1 degree grid. As the ultimate aim of the critical loads map was its use in an integrated assessment model, with other coarser data, it was defensible to use low resolution information, such as the landuse map, within the mapping project. The accuracy of the information within the grids is reasonably high; however, its coarse resolution does make it one of the weaker data sets used in the project. National studies could increase the resolution of the land use distribution; however, only recently produced data should be considered due to the potentially large changes in vegetation and land use which could have occurred in this rapidly developing region. A further disadvantage of turning to national data for a regional assessment is the differing types of classifications employed to produce land use maps. This can lead to problems because of inconsistencies across country borders or even between different national survey areas which a regional data base, such as the Oak Ridge map, hopefully avoids.

Sensitivity assessment from vegetation distribution

This map (Map 11) was derived by reclassifying the landuse map into new ranges of vegetation sensitivity. This map formed one of the two layers in the final formulation of the distribution of the relative sensitivity of Asian ecosystems to acidic depositions. The assignment of sensitivity classes to the vegetation types is explained in Section 6.2.4.

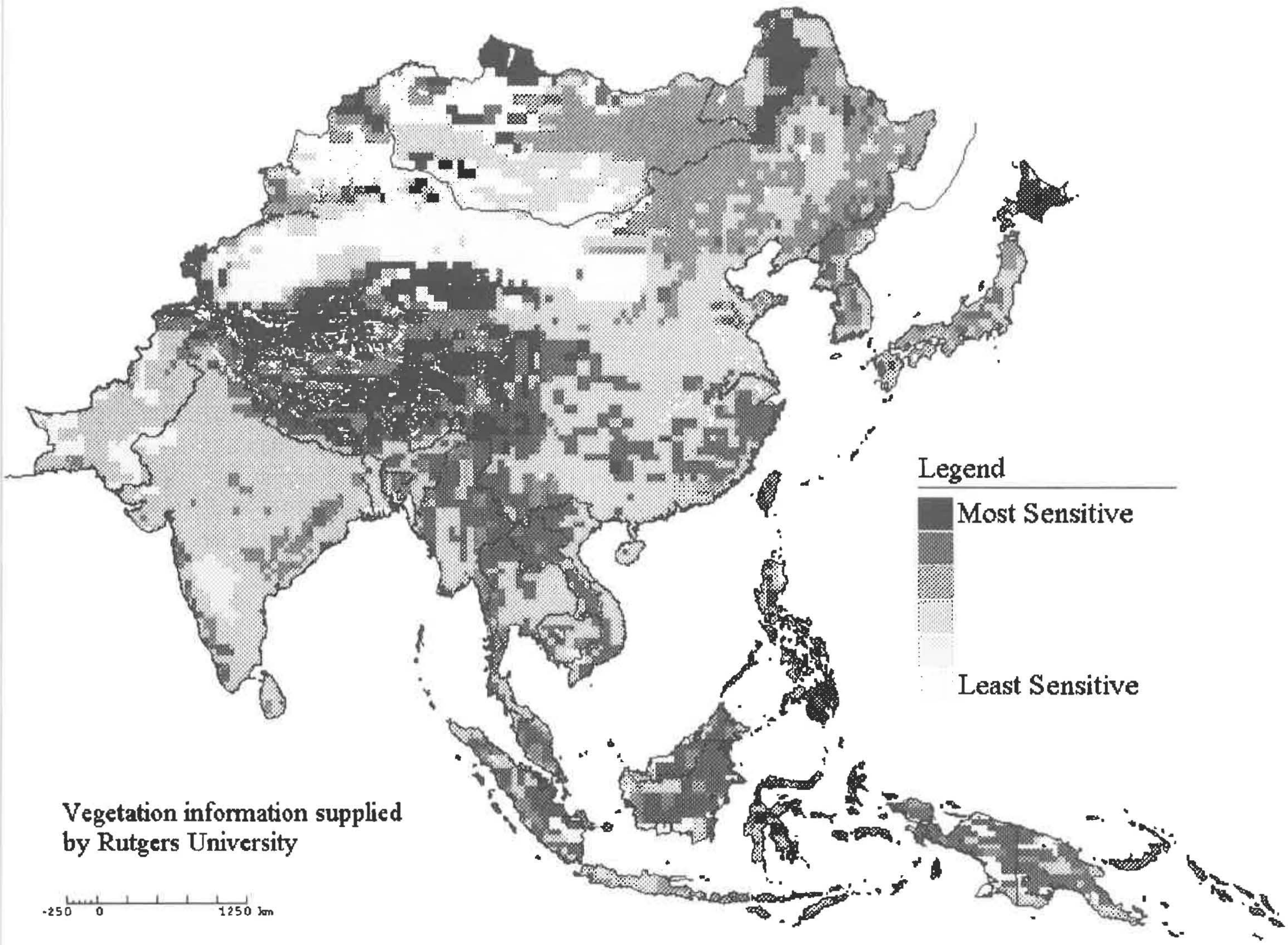

Map 11 The classes of sensitivity derived from vegetation type (SEI based on Rutgers University data)

A2.2 ***Relative buffering rates and estimated weathering rates***

H. Sverdrup, S. Cinderby, J.C.I. Kuylenstierna

The indirect effects of acidic deposition on ecosystems are primarily related to changes in soil chemistry. The sensitivity of an ecosystem to acidic deposition is, therefore, partially related to the ability of the soil to neutralise, by internal processes, external inputs of acidity. The neutralisation process will cause a lowering in the base saturation and a drop in the pH. Initially the buffering of acidic inputs will be through the existing capacity of the primary minerals present in the soil; however this capacity is finite. In the longer term the ability of the soil to buffer against a drop in its pH will be dependent on the replenishment of exchangeable base cations. One source of replenishment results through the weathering and release of the material and rock within and underlying the soil. In the longer term, the weathering rate represents the maximum neutralisation capacity rate of Acid Neutralisation Capacity (ANC) production. In order to assess the ability of the soil to buffer acidic depositions it was decided to attempt to model the rate of weathering in the Asian region.

Rates of weathering are dependent on a number of factors. These include:

- i) initial soil mineralogy
- ii) nature of underlying rock
- iii) temperature regime of the region
- iv) soil texture
- v) soil moisture regime.

A2.2.1 Initial estimation of weathering conditions

The initial soil mineralogical conditions have been inferred from the estimated pH level of the upper horizons. The pH level is a measure of production rate in the soil exchangeable ions; low pH values represent low rates of ANC product ions. For example, soils formed from an alkali parent material, such as dolomite will have a high pH. Soils formed above granitic material would have a lower pH. Soils formed in wet areas will be affected by leaching of base cations and will generally have low pH, as opposed to soils formed in dry regions where base cations have a tendency to accumulate in the upper horizons, making them alkaline.

From the pH level of the upper horizons an initial base weathering rate has been assigned to each of the soil types (Table A2.3). The estimated base rates applied have been derived from work on soil weathering carried out in Europe (Sverdrup and Warfvinge, 1993; Sverdrup and Warfvinge, 1990) and North America (Sverdrup, 1990). No Asia-specific estimates have been used. The relationship between the rate of weathering and the soil pH can be seen in Figure A2.5

A particular soil group, the laterites, was set a specific initial base rate, assigned on the basis of their unique mineralogy and genesis. These consist of indurated clays composed primarily of iron, aluminium and manganese oxides (Money, 1965). They are formed by intense chemical weathering, or over very long periods of time, and involve the leaching of silica and bases from the original soil (Goudie, 1984). The process of laterization is more intense and exceptional than general pedological development to the extent that laterites must not be

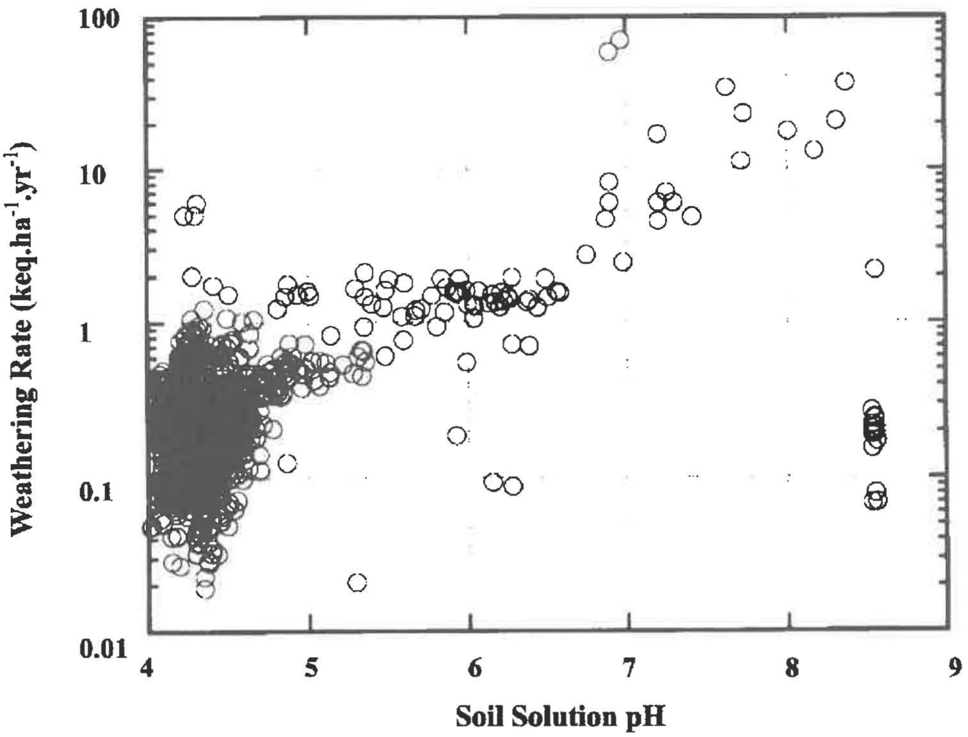

Figure A2.5 Swedish soil pH and their related weathering rate values calculated using the PROFILE model (Sverdrup, 1993)

considered simply as soils (Whittow, 1984). The exact cause of laterite formation is uncertain although large fluctuations in the groundwater table level have been cited as the most likely process (Goudie, 1984). This fluctuation causes rapid leaching of the upper horizons and deposits large quantities of dissolved ferrous material. These soil types have a low buffering potential and general weathering will not affect the base saturation in the soil. For these reasons these soil types have been assigned a low base rate and have only been further modified, in the modelling procedure, by the soil moisture regime as general pedological processes do not apply to lateritic deposits.

Table A2.3 Relationship between soil pH and initial base rate (Sverdrup, 1993)

Soil pH	Initial Base Rate ($meq.m^{2}.yr^{-1}$)
< 5	35
5 - 6.2	150
6.2 - 7.2	350
>7.2	650

A2.2.2 Modifications to the Initial Weathering Rate Estimations

Soil chemistry is a dynamic process and locally the soil mineralogy and geochemistry undergo continual change (Hunt, 1972). The FAO assessment of pH represents the base saturation which has resulted from recent weathering conditions and relates to the initial base rate. In order to assess the future replenishment of base cations within the upper horizons of the soil it is necessary to consider the current environmental conditions influencing soil development. These conditions will affect the current rate of weathering and may result in a modification of the base saturation.

One influence on the nature of the soils is their underlying geology. In Asia a large number of soils have formed from transported deposits such as loess or alluvium. The region has not undergone the extensive glaciations of Europe although glacial deposits are present in Himalaya, Altai and Hindu-Kush regions (Goudie, 1984). A result of this lack of glaciation is that soils formed *in situ* above bed rock tend to be old and, potentially, deep so that their current mineralogy and weathering potential has little relationship to the deposits from which they were derived. For these reasons the nature of the bedrock has only been allowed to influence lithosols in the estimation of weathering rates.

Lithosols are connotative of young stony soils of limited depth with hard rock within 10cm of the surface (Fitzpatrick, 1980). They are characteristically formed in mountainous areas but may occur in other areas where soil material has been removed. As they are recently formed and contain a large percentage of clastic material their mineralogy and nature are best inferred from the underlying rock.

The rock types have been classified in two ways. For igneous rocks, where some indication of their chemical composition was known, the classification is based on the likely resistance of the rocks to the processes of chemical and physical weathering. For example, granitic rocks are dominated by quartz, microcline and plagioclase feldspars, with only small contents of mafic minerals. They are chemically stable and resistant to physical abrasion (Whitten and Brooks, 1972). Basic and ultrabasic rocks such as basalt or diorite in comparison contain less quartz and more plagioclases and easily weatherable mafic minerals. These minerals are much more susceptible to weathering processes (Sverdrup and Warfvinge, 1988). Metamorphic rocks have been classified in the same way based on their geochemistry. The relative rate of mineral weathering can be seen below in Table A2.4.

Table A2.4 The weathering rate of different minerals in soil, 50cm depths in $keq.km^{-2}.yr^{-1}$ (Sverdrup and Warfvinge, 1988)

Mineral	**Average content of mineral classes (%)**			
	100	**30**	**3**	**0.3**
Carbonates	++	++	1000	300
Fast Weathering (garnet, anorthite, olivine, pyroxenoids, epidote)	++	>1000	300	30
Intermediate Weathering (amphiboles, biotite, pyroxenes)	1000	300	30	3
Slow Weathering (feldspars, muscovite, plagioclase)	60	20	2	-
Inert Group (quartz)	10	1	-	-

The sedimentary rock types have been classified relative to their age due to the nature of the stratification employed on the original data. For the purposes of assessing the release of base cations into the soil, the oldest sedimentary rocks are presumed to be well weathered with low reserves of basic minerals which are highly soluble, and consequently easily removed. The younger rocks are of indeterminate nature and do not modify the base rate assigned from the soil pH. With improved geological data the differentiation within this class could be greatly enhanced to separate the calcareous rocks from the sandstones and shales.

The new base rates (seen in Table A2.5) have only been assigned to those lithosols where the rate derived from pH is higher than that inferred from the underlying geology. This was done in an attempt to remove over-estimations in the weathering rates set from the soil pH. This procedure was applied because it was felt that the geological data, where available, were of a higher spatial accuracy than the soil pH information.

Table A2.5 The relative susceptibility to weathering of rock types

Rock Type	**Base Rate ($meq.m^{-2}.yr^{-1}$)**
Acid Igneous/Metamorphic	35 (Few weathering products)
Intermediate Igneous/Metamorphic	150
Basic & Ultrabasic Igneous/Metamorphic	350 (Most weathering products)
Precambrian & Cambrian Sedimentary	35
Other Sedimentary	No Modification

For chemical weathering to occur, and for many types of physical weathering processes, the presence of water is essential. It is therefore necessary to assess the water regime within a system to predict its effect on the rate of weathering. An indication of the moisture regime is given by the ratio of precipitation to potential evapotranspiration (P:PE ratio shown in Figure A2.6. This ratio represents an index of the effectiveness of precipitation, which is equivalent to moisture surplus, and gives an indication of the excess or deficit of water in the soil profile (Parry, Carter and Konijn, 1988). The ratio can be used to assess the soil water flux within an area. The increase of available moisture in the soil will lead to an increase in the rate of chemical reactions occurring in the profile. When soil moisture is in excess the downward movement of water will result in the leaching of soluble minerals from the upper soil horizons. This leads to a net increase in the acidity of the upper horizons by a reduction in the base saturation (Hunt, 1972).

In periods of water deficiency, when leaching does not occur, soluble decomposition products derived from organic matter and weathering in the upper horizons will not be removed leading to their increase (Fitzpatrick, 1971: Goudie, 1984). Additionally, when water is deficient from the system, plant transpiration and evaporation may cause the uptake of vadose (ground and soil) water into the upper soil horizons through capillary action. This may potentially lead to the deposition of soluble alkaline salts dissolved from lower in the soil profile. This process can operate to depths of 0.5m or greater depending on the nature of the soil and vegetation (Cruickshank, 1972). For example, the capillary rise in coarse silt (diameter 0.02mm) may be as great as 2.5m (Hunt, 1972). The build up of soluble minerals in the upper horizons reduces the acidity of the soils by increasing the base saturation.

The influence of moisture regime on the weathering of soils has been modelled using the SEI-derived function shown in Figure A2.6. Soils which are very dry (P:PE <0.25) are assumed to have a net base cation increase in the upper horizons through their build up and influx from deeper sources. This high base cation content is included in the initial base weathering rate set from the soil pH, and therefore the moisture regime has not been allowed to modify this value.

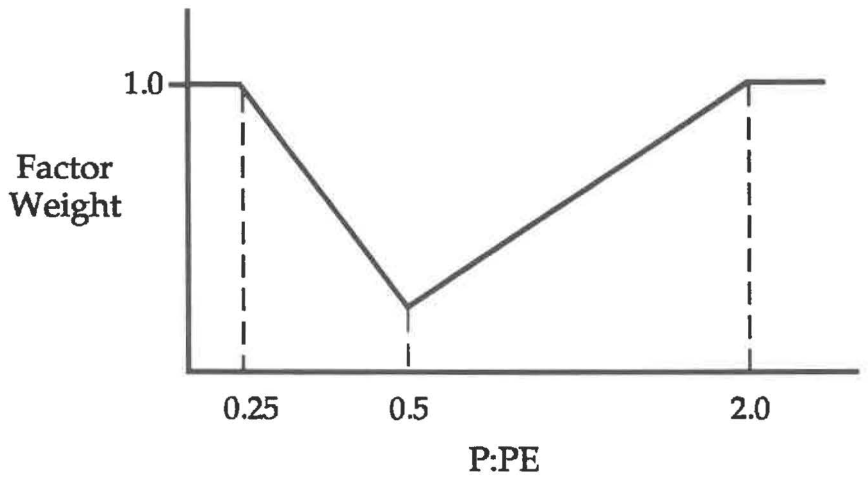

Figure A2.6 The relationship between moisture and weathering rate

As the amount of water entering the soil increases the quantity of these soluble minerals decreases as additional leaching occurs. It has been assumed that this process operates until the P:PE ratio is 0.5, that is, precipitation is half the level of potential evapotranspiration. Above this level the additional moisture in the environment allows more chemical reactions to occur and the weathering rate to increase. This rise continues until the addition of more water in the soil has no further effect on increasing the potential of chemical reactions occurring. This can be seen in the upper limit of the function (Figure A2.6), above which increasing moisture does not increase the rate of weathering. The effects of excess moisture which cause leaching have not been included in the assessment of weathering rates. These were considered to have been included in the initial base rate estimations derived from the soil pH and the presence of laterites.

The size of the surface upon which chemical reactions can occur will also affect the rate with which weathering occurs. In general, fine grained particles have a larger surface area than coarser particles per unit of volume (Hunt, 1972). The size of this reaction surface is important as weathered crusts can form through oxidation or combination on particles which prevent or slow down the rate of further weathering. The rate of reaction has therefore been modified preferentially for finer grained soils. The modification weights can be seen in Table A2.6

Table A2.6 Modification factor of base rates by soil texture

Texture	**Weight**
Coarse	0.25
Coarse/Medium	0.5
Medium	1.0
Medium/Fine	2.0
Fine	4.0

The rate of geo-chemical reactions is also governed by the temperature at which they occur. For example with a 10°C rise in temperature the speed of chemical reactions increases by a factor of two or three (Cruickshank, 1972). The hydrolysis of primary silicates is the principal soil reaction to which this applies. Whilst it is true that surface air temperatures are not necessarily representative of within soil temperature, for the top 50cm of the profile there is a diurnal temperature cycle with a damping effect on the minimum and maximum values caused by the thermal insulating properties of the soil (Hunt, 1972). Therefore, in the uppermost horizons air temperature can be used to indicate the soil temperature. Below 1m there is little daily variation; however, seasonal variation is represented. At depths greater than 2.5m there is no annual variation in temperature; the soil conditions represents the mean annual temperature.

The standard equation for assessing increases in the rate of chemical reactions with temperature is the Arhenius equation (Sverdrup, 1990). This was used to determine the temperature function describing the influence of temperature on weathering:

$$\text{Temperature Function} = 10^{(12.455-3500/(273+T))}$$

where;
T is the mean annual air temperature

Monthly mean air temperatures were not used directly for assessing soil temperature. Instead the number of days with a temperature above a threshold value were summed as it was considered more indicative of soil conditions for two reasons. Firstly the threshold value more accurately represents the soil thermal damping. Secondly, the threshold of 5°C was applied as below this temperature the rate of reaction is very low (Hunt, 1972). This threshold factor is termed the effective temperature sum (ETS) and is calculated using the following formula:

$$ETS = \sum_{1}^{365} ({}^{o}C - t^{o}C)$$

where;
°C is the daily mean temperature
t°C is a threshold temperature which in this case is 5°C

The ETS was then correlated with a mean annual air temperature to derive values from the Arhenius equation of changes in the rate of reactions.

The modification by temperature in the model only operates in cool regions and has the effect of lowering the weathering rate. The cool regions have been delimited as those areas having an ETS equivalent to a mean annual air temperature of less than 8°C. In the hot equatorial regions the Arhenius equation predicted large increases in chemical reaction rates. These increases may be possible if the supply of weatherable minerals was infinite. In these areas the Arhenius equation was indicating the potential chemical reaction rate. However, it was decided that the pool of available minerals to weather in tropical regions is too small for large increases in the amount of base cations released into the soil. Even though weathering in these areas will be quicker than in cooler areas the supply of minerals will limit the release of bases.

The full model of weathering rates can be seen in Figure A2.7 (see Map 12). The majority of the base rate approximations was supplied by the soil pH status with only small modifications made by environmental conditions and soil attributes. However, it must be recognised that the results generated by the model have been produced from existing small scale data of varying reliability. The base weathering rates assigned to the soil mineralogy are based on the best available research of Europe and North America and have not been verified for Asia.

In order to reduce the perceived accuracy of the quantitative model results, the values generated by the modelling process were classified into ranges (see Table A2.7). These estimated classified values, generated by the model, have been used directly in the Simple Mass Balance (SMB) equation for generating critical load values. For the mapping of ecosystem sensitivity to acidic depositions the numeric values, associated with these estimated weathering rates, were removed and classes assigned in their place to produce the relative buffering rate map (see Map 13).

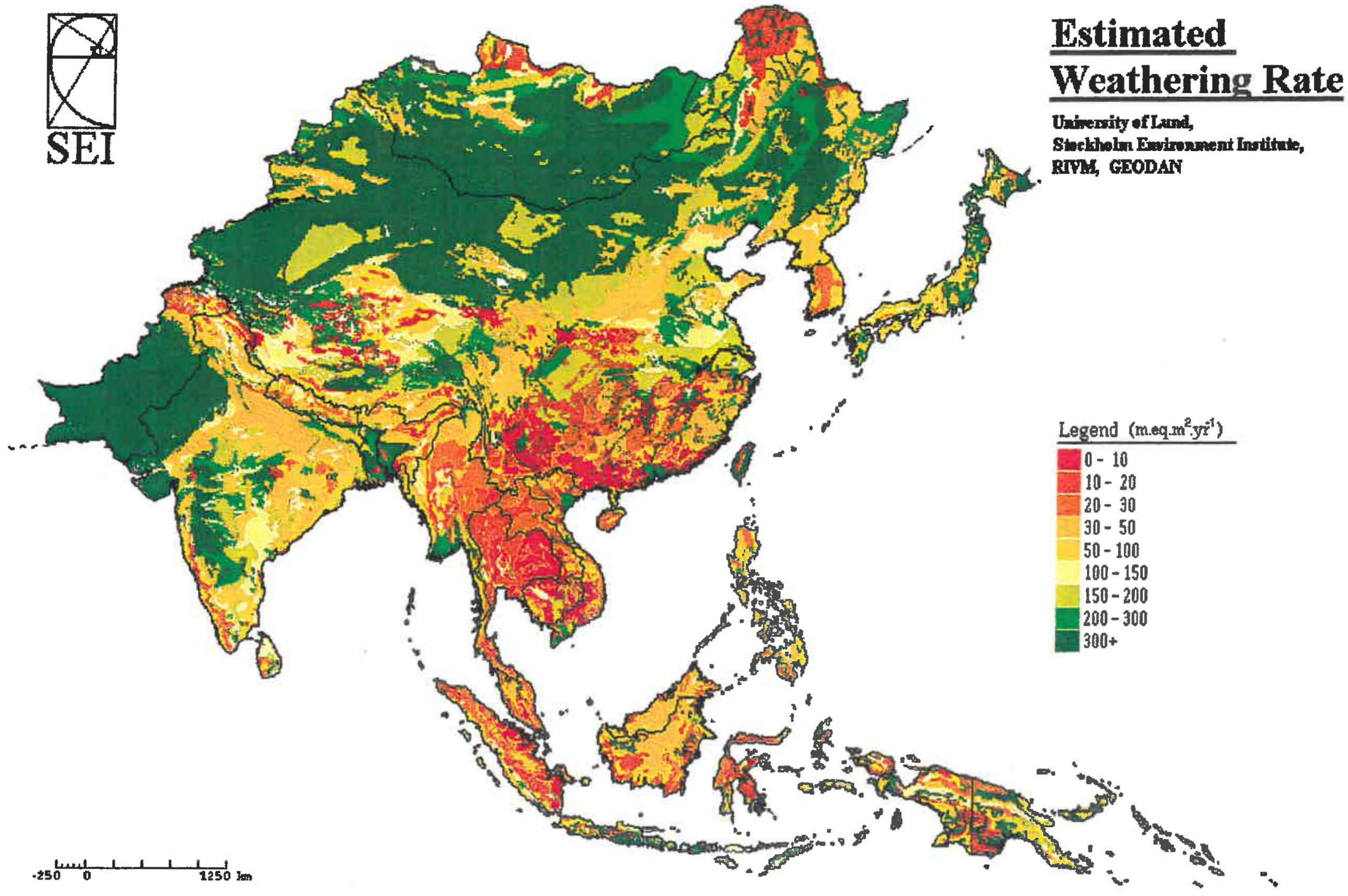
SEI
Estimated Weathering Rate
University of Lund,
Stockholm Environment Institute,
RIVM, GEODAN
Legend (m.eq.m^{2}.yr^{1})
0 - 10
10 - 20
20 - 30
30 - 50
50 - 100
100 - 150
150 - 200
200 - 300
300+
-250 0 1250 km

Map 12

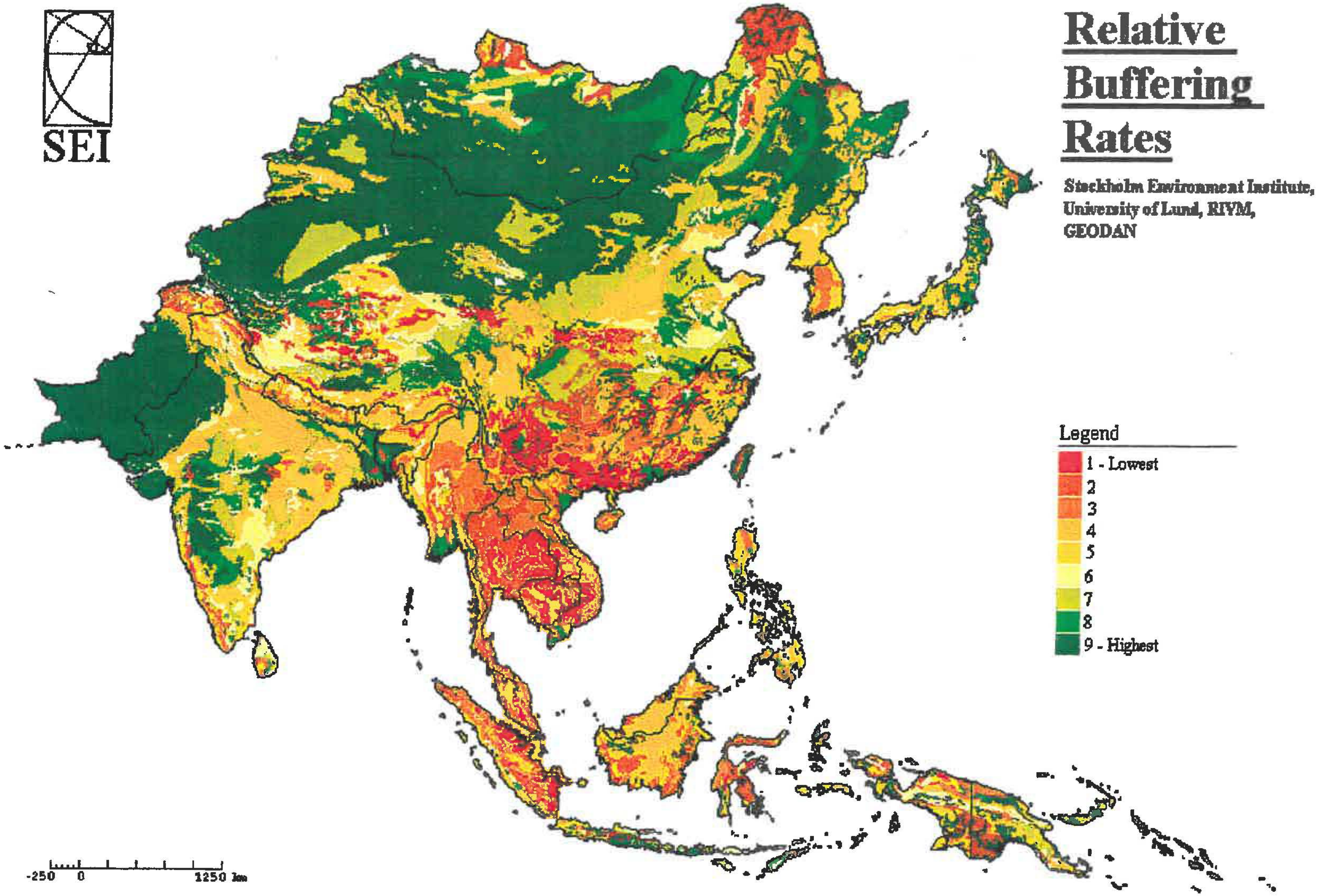
SEI
Relative Buffering Rates
Stockholm Environment Institute, University of Lund, RIVM, GEODAN
Legend
1 - Lowest
2
3
4
5
6
7
8
9 - Highest
-250 0 1250 km

Map 13

Table A2.7 Estimated weathering rates and their associated relative soil buffering classes. (Numeric values used in SMB critical load derivation and relative classes used by the relative sensitivity methodology)

Estimated Weathering Rate (meq.m^{-2}.yr^{-1})	**Relative Buffering Rate**
0 - 10	1 - Low
10 -20	2
20 - 30	3
30 - 50	4
50 -100	5
100 - 150	6
150 - 200	7
200 - 300	8
> 300	9 - High

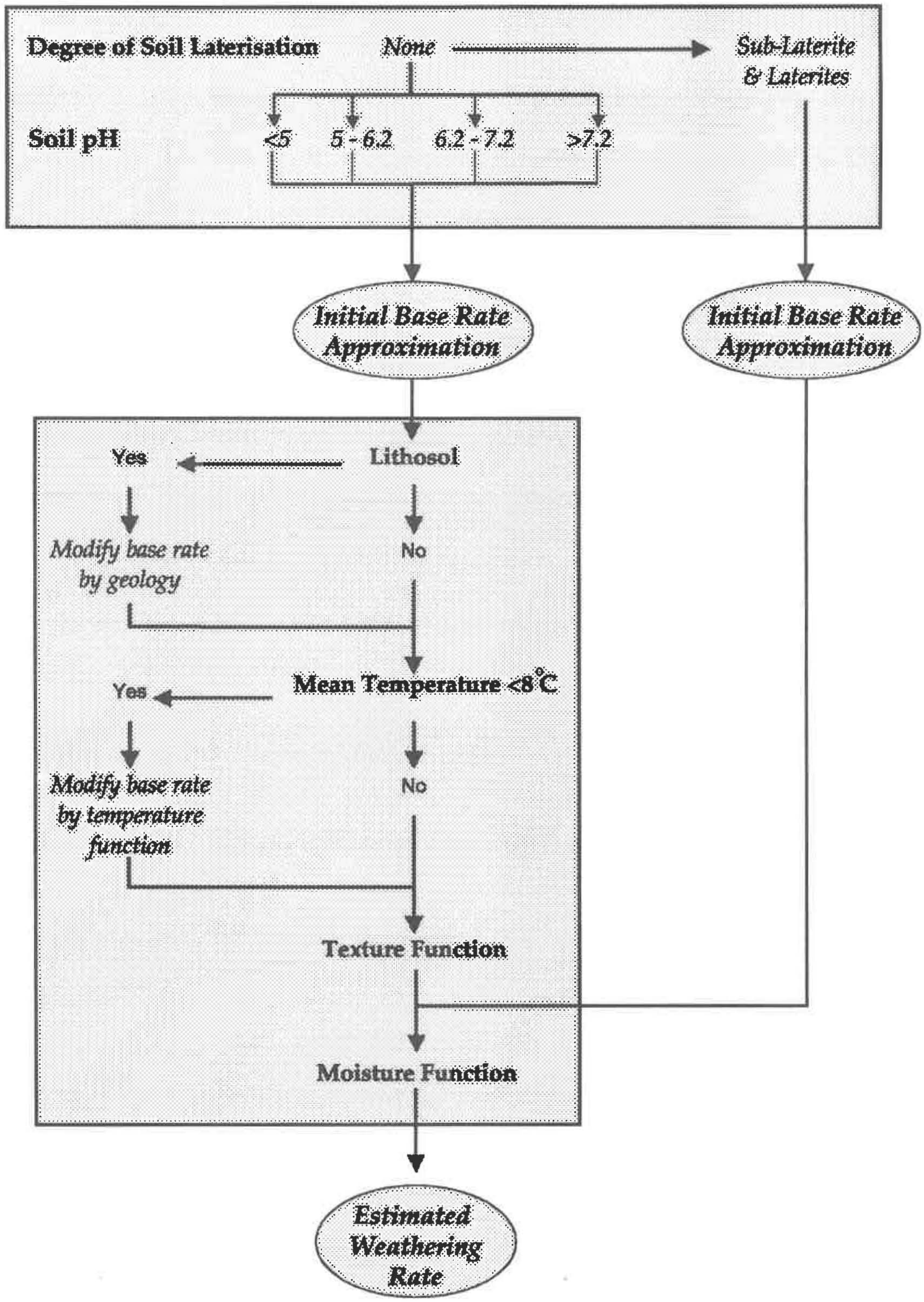

Figure A2.7 Overview of the weathering rate model.

References

Alcamo, J., R. Shaw, L. Hordijk, 1990, *The RAINS Model of Acidification*, IIASA, Kluwer Academic Publishers.

ASEAN Secretariat, 1982, *The ASEAN Climatic Atlas, Maps of Mean Annual Precipitation.* Directorate of ASEAN Committee on Science and Technology, ASEAN, Directorate of National Mapping, Kuala Lumpar, Malaysia.

Cruickshank, J.G., 1972, *Soil Geography*, Newton Abbot.

FAO-UNESCO, 1977, *Soil Map of the World, Volume VII, South Asia,* UNESCO, Paris.

FAO-UNESCO, 1978, *Soil Map of the World, Volume VIII, North and Central Asia,* UNESCO, Paris.

FAO-UNESCO, 1979, *Soil Map of the World, Volume IX, South East Asia,* UNESCO, Paris.

FAO-UNESCO, 1981, *Soil Map of the World, Volume V, Europe,* UNESCO, Paris.

FAO-UNESCO, 1988, *Soil Map of the World, Revised Legend,* UNESCO, Paris.

Frère, M., G.F. Popov, 1979, *Agrometeorological Crop Monitoring and Forecasting.* FAO Plant Production and Protection, Number 17, Plant Production and Protection Division, FAO, Rome.

Fitzpatrick, E.A., 1971, *Pedology: A Systematic Approach to Soil Science,* Oliver and Boyd, Edinburgh.

Fitzpatrick, E.A., 1980, *Soils: Their Formation, Classification and Distribution,* Longman Press. England.

Goudie, A., 1984, *The Nature of the Environment*, Basil Blackwell, New York.

Hettelingh, J.P., R.J. Downing, P.A.M. de Smet, 1991, *Mapping Critical Loads for Europe,* CCE Technical Report Number 1, RIVM, Netherlands.

Hunt, C.B., 1972, *Geology of Soils. Their Formation, Classification and Uses*, W.H. Freeman and Company, San Francisco.

Hydrometeorological Service, 1976, *Runoff in Europe*, Hydrometeorological Service, Moscow.

Intera Tydac Technologies, 1993, *SPANS GIS Reference Manual, 6th edition for SPANS 5.3 for OS/2.*

Jones, R.J.A., and A.J. Thomasson, 1985, *An Agroclimatic Databank for England and Wales, Technical Monograph Number 16,* Soil Survey. Harpendon.

Kuylenstierna, J.C.I., 1993, *Assessment of Ecosystem Sensitivity to Acidic Depositions: Critical Load Estimates, Detriment and Damage*, Stockholm Environment Institute at York, York.

Money, D.C., 1965, *Climate, Soils and Vegetation*, Univerity Tutorial Press, England.

Olson, J.S., 1982, Earth's vegetation and atmospheric carbon dioxide. *Carbon Dioxide Review.*

Olson, J.S., J.A. Watts, L.J. Allison, 1983, *Carbon in the Live Vegetation of Major World Ecosystems. ORNL-5862,* Oak Ridge National Laboratory, Oak Ridge, Tennesse.

Parry, M.L., T.R. Carter, N.T. Konijn, 1988, *Impact of Climatic Variations on Agriculture. Volume 2: Assessments in Semi-Arid Regions*, IIASA-UNEP, Kluwer Academic.

Shaw, E.M., 1988, *Hydrology on Practice*, Van Norstrand Reinhold, London

Sverdrup, H.U., 1990, *The Kinetics of Base Cation Release Due to Chemical Weathering,* Lund University Press, Lund, Sweden.

Sverdrup, H.U., 1993, Data taken from Swedish forest inventory database, Lund University, Lund.

Sverdrup, H.U., P. Warfvinge, 1988, Chemical weathering of minerals in the Gårdsjön catchment in relation to a model based on laboratory rate coefficients. In *Critical Loads for Sulphur and Nitrogen* (ed. by J. Nilsson and P. Grennfelt), Miljørapport 1988:15, Nordic Council of Ministers, Copenhagen.

Sverdrup, H.U., P. Warfvinge, 1990, On the geochemistry of chemical weathering. In *Report from a Nordic Seminar: Chemical Weathering under Field Conditions* (ed. by K. Rosén). *Reports in Forest Ecology and Forest Soils 63*, Sveriges Lantbruksuniversitet, Uppsala, 79-118.

Sverdrup, H.U., P. Warfvinge, 1993, Calculating field weathering rates using a mechanistic geochemical model PROFILE, *Applied Geochemistry* 8, 273-83.

Tobler, W., 1988, *Resolution, Resampling and All That. Building Databases for Global Science.*

Whitten, D.G.A., J.R.V. Brooks, 1972, *The Penguin Dictionary of Geology*, Penguin Books, London.

Whittow, J., 1984, *The Penguin Dictionary of Physical Geography*, Penguin Books. London.

WMO-UNESCO-UNEP, 1981, *Climatic Atlas of Asia, Maps of Mean Annual Precipitation*, Goscongidromet, Gidrometeoizdat, Leningrad.

ANNEX 3

Application and evaluation of critical load methods for acid deposition in Gunma, Japan

Junko Shindo*, Arnold K. Bregt and Tomoyuki Hakamata***

* National Institute of Agro-Environmental Sciences, Kannondai 3-1-1, Tsukuba Ibaraki 305 Japan
** The Winand Staring Centre for Integrated Land, Soil and Water Research, Wageningen, The Netherlands

INTRODUCTION

Recently, the concept of critical loads has got great attention of scientists and decision makers in the field of air pollution and acid deposition abatement in Japan. Yearly averages of rain pH and deposition rates of sulphate and nitrate ion are at the same level as in Europe and North America. Forest decline has been observed in several areas in the latest decade, though its cause is not cleared up yet. In such situation, quantitative estimation of ecosystem sensitivity to acid deposition is required and the concept of critical load appears to be useful for this objective.

We applied the several implementation based on simplified mass balance model to a test area in Japan to evaluate applicability of these methods for the Japanese situation.

MATERIALS AND METHODS

(1) Methods for critical load calculation

The following simplified steady-state mass balance (SMB) model is most widely used for calculation of critical load CL:

$$CL = BC_w + H_{l(crit)} + Al_{l(crit)} = BC_w + [\{Al_{l(crit)}/Q\} / K_{gibb}\}^{1/3} Q + Al_{l(crit)} \quad (1)$$

where BC_w : acid neutralizing capacity produced by weathering, $H_{l(crit)}$ and $Al_{l(crit)}$: critical hydrogen and aluminum ion leaching, K_{gibb} : gibbsite equilibrium constant and Q : runoff.

Based on this model, several formulas have been proposed to calculate critical loads depending on the different definition of critical aluminum leaching. We applied 6 formulas shown in Table 1 to a test area in Japan. CL1 to CL5 were used in the European and Asian application and CL6 is proposed by us as a modification of CL3.

In our study, we used the same critical values as those proposed by the European researchers, as Japanese data on the relation between critical chemical values and forest decline are lacking. We are however not sure if these values are also applicable for the Japanese situation.

(2) Input data

Gunma prefecture was selected as a test area which is located about a hundred kilometers north-west of Tokyo. It covers an area of 6,363 km^2 and about 70 % of the area is covered with forest.

The data used for the calculation of the critical loads are derived by the following methods based on the Digital National Land Information data base and other national data base whose spatial resolution are about 1 square kilometer. All data are stored in the GIS-package ILWIS as raster maps.

Table 1. Methods used for estimation of critical loads for Gunma.

	Criterion and critical values	Formula to express $Al_{l(crit)}$	Study area	Reference
CL1	$[Al^{3+}]_{crit}$ = 0.2 eq m^{-3}	$[Al^{3+}]_{crit}\,Q$	Europe	(1)
CL2	$((Ca+Mg+K+Na)/Al)_{crit}$ * = 1 mol mol^{-1}	$\frac{1.5(BC_w+BC_d-BC_u)}{((Ca+Mg+K+Na)/Al)_{crit}}$	Europe	(1)
CL3	$((Ca+Mg)/Al)_{crit}$ = 1 mol mol^{-1}	$\frac{1.5\max\{f_{BC1}BC_w+BC_d-BC_u-[BC]_{l(nor)}Q,\ [BC]_{l(min)}Q\}}{((Ca+Mg)/Al)_{crit}}$	Asia	(2)
CL4	$(Al_l/Al_w)_{crit}$ =1 mol mol^{-1}	$f_{Al/BC}\,(Al_l/Al_w)_{crit}\,BC_w$	Asia	(2)
CL5	$((Ca+Mg+K)/Al)_{crit}$ = 1 mol mol^{-1}	$\frac{1.5\{f_{BC2}BC_w+BC_d-BC_u-[BC]_{l(min)}Q\}}{((Ca+Mg+K)/Al)_{crit}}$	Europe (Alpine area)	(3)
CL6	$((Ca+Mg)/Al)_{crit}$ = 1 mol mol^{-1}	$\frac{1.5\max\{f_{BC1}BC_w+BC_d-BC_u,\ [BC]_{l(min)}Q\}}{((Ca+Mg)/Al)_{crit}}$		(4)

BC_d: Base cation deposition(eq $ha^{-1}yr^{-1}$)

$[BC]_{l(nor)}$:Normal concentration of BC leaching(eq m^{-3}) =0.5(CL3)

$[BC]_{l(min)}$:Minimum concentration of BC leaching(eq m^{-3}) =0.002(CL3,CL6) or 0.015(CL5)

$f_{BC1}=(Ca_w+Mg_w)/BC_w$=0.7 eq eq^{-1}, $f_{BC2}=(Ca_w+Mg_w+K_w)/BC_w$=0.8 eq eq^{-1}, $f_{Al/BC}=Al_w/BC_w$=2.0 eq eq^{-1}

* $H_{l(crit)}$ is derived from the criterion, $[Al^{3+}]_{crit}$ = 0.2 eq m^{-3}

Weathering rates

Weathering rates were estimated based on the acidity of parent material and soil texture data according to the method described by De Vries (5). Surface geology data was used to classify the parent material into acid, intermediate and basic and soil types were used to derive texture classes. Weathering rates corrected with temperature ranged from 99 to 2440 eq ha^{-1} yr^{-1}.

Runoff

Runoff was calculated by Nogami (6) as the difference between the annual precipitation and the annual evapotranspiration estimated from annual temperature by the Thornthwaite method. Runoff data in the area were extremely high, ranged from 1,460 to 24,770 $m^3ha^{-1}yr^{-1}$

Base cation deposition

We used 473 eq ha^{-1} yr^{-1} as the base cation deposition rate for every grid cell of the test area. This value was an average of yearly base cation deposition (including wet and soluble dry deposition) measured at two locations in 1983.

Base cation uptake

In the natural forest the net uptake of base cations was assumed to be zero, as the uptake by the trees is in equilibrium with the release of cations due to litter decomposition. In the secondary and planted forest, cation uptake was calculated from net growth rate and concentration of base cations in the tree. Net growth was calculated from net primary production (NPP) rate estimated from temperature through an regression equation and ratio of net growth to NPP. All parameters were derived from literature for each forest type (deciduous broad leaf, deciduous needle and evergreen needle). Base cation uptake ranged from 0 to 2664 eq ha^{-1} yr^{-1} whose average was much higher site specific information such as nutrient and water condition of soils. Quantitative data on weathering rate and mineralogy data are lacking in the national scale in Japan. We especially need more accurate data or estimation methods on it. In order to compare the critical load values to deposition data, we also need data on acid deposition as well as the data on nitrogen uptake, immobilization, denitrification and other data depending on the acidification and neutralization processes taking place in each ecosystem.

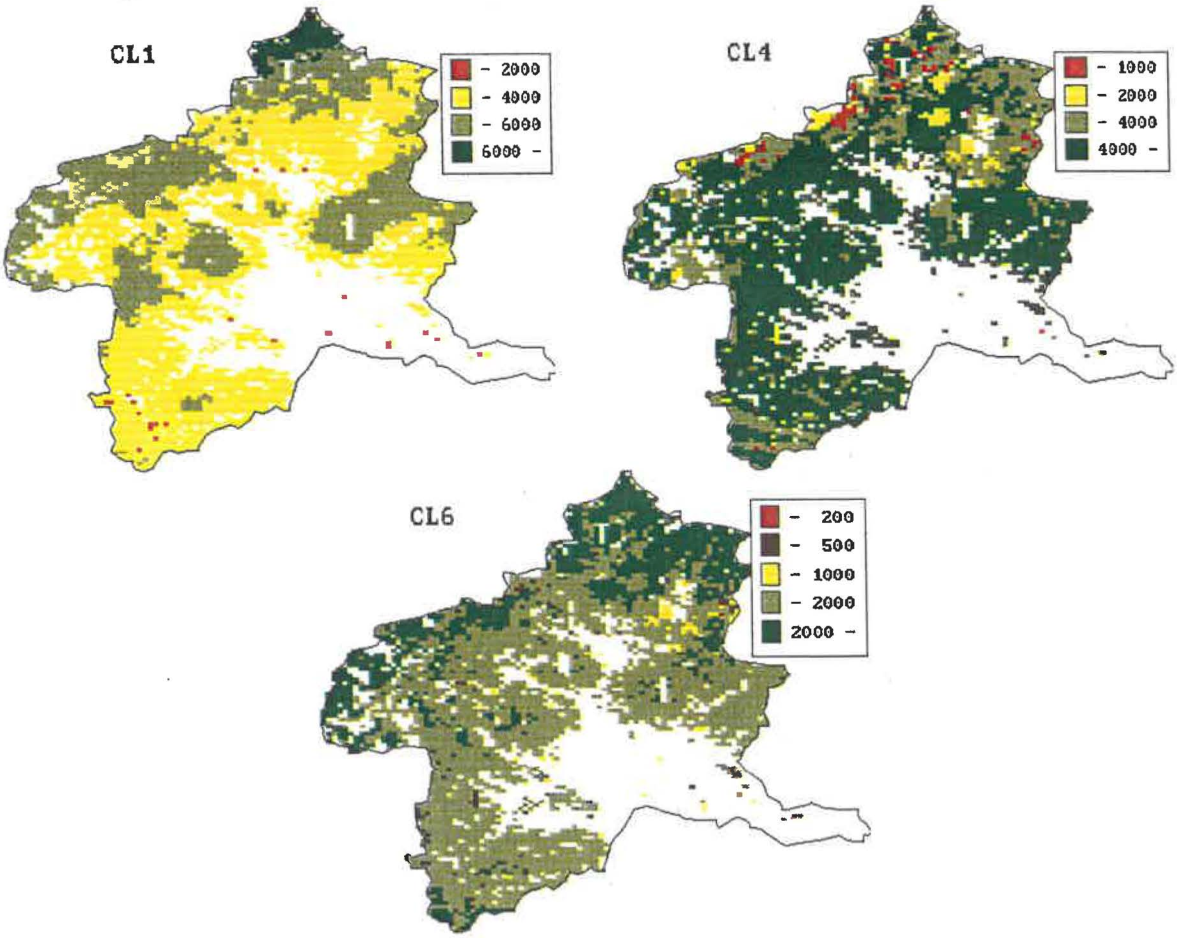

Fig.2 Spatial distribution of critical loads based on different formulas

REFERENCES

1 Hettelingh, J.P., Dowing, R.J. and De Smet, P.A.M. 1991. Mapping critical loads for Europe. CCE Technical report 1, RIVM, Bilthoven.

2 Dowing, R.J., Hettelingh, J.P. and de Smet, P.A.M. 1993. Calculation and mapping of critical loads in Europe: Status Report 1993. Coordination Center for Effects, RIVM, the Netherlands.

3 Hettelingh, J.P., Sverdrup, H. and Meijer, E. 1992. RAINS Asia impact module. In: Papers of the RAINS Asia effects task force meeting, Beijing, China.

4 A.K. Bregt, J.Shindo and T.Hakamata, Evaluation of critical load methods for acid deposition in Gunma, Japan. submitted to AMBIO.

5 De Vries, W. 1991. Methodologies for the assessment and mapping of critical loads and the impact of abatement strategies on forest soils. Report 40, DLO the Winand Staring Centre, Wageningen.

6 Nogami, M. 1992. Files in Japan environmental data base (JEDB). News letter GIS for environmental change, 14.

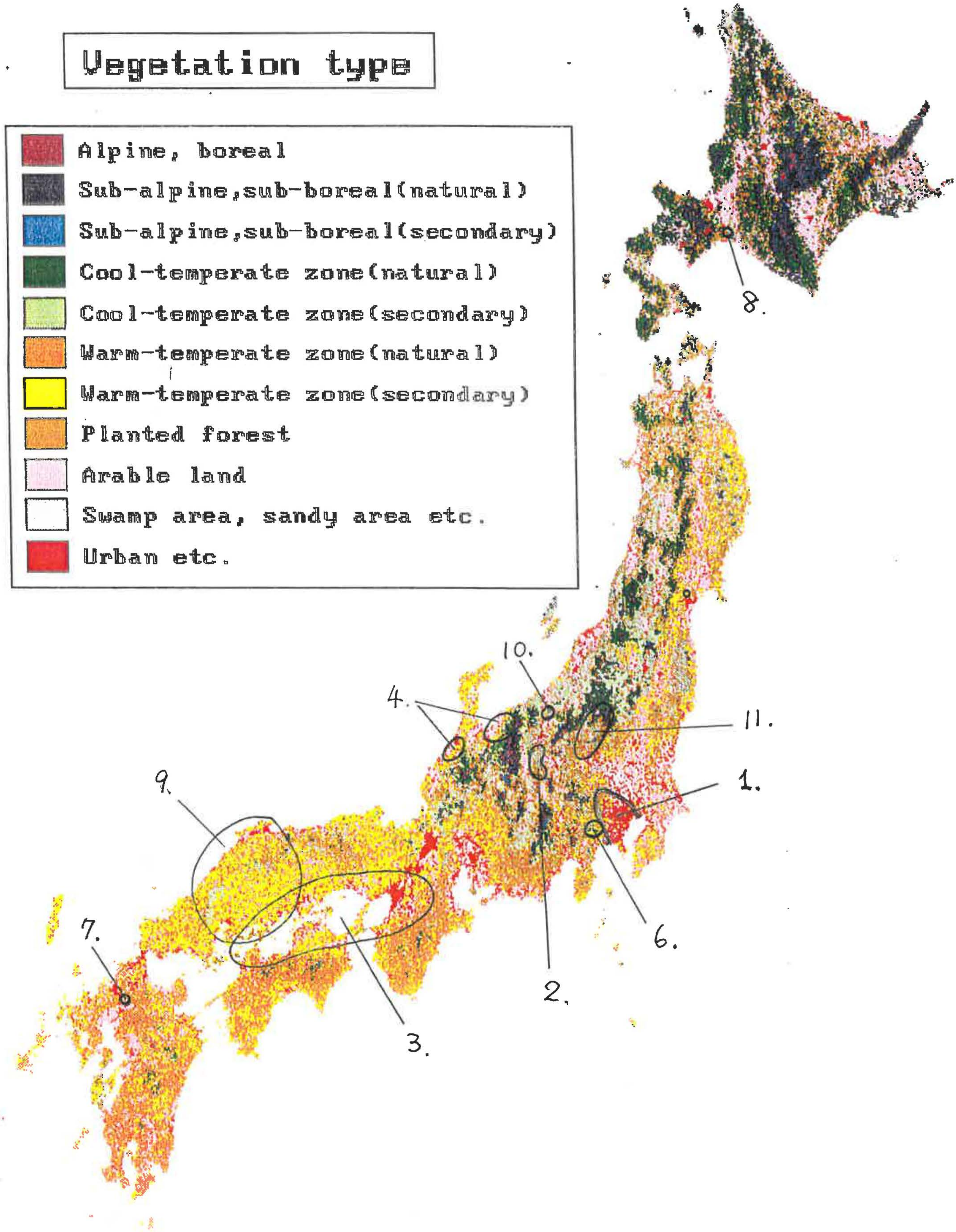

Vegetation type
Alpine, boreal
Sub-alpine, sub-boreal (natural)
Sub-alpine, sub-boreal (secondary)
Cool-temperate zone (natural)
Cool-temperate zone (secondary)
Warm-temperate zone (natural)
Warm-temperate zone (secondary)
Planted forest
Arable land
Swamp area, sandy area etc.
Urban etc.
1.
2.
3.
4.
6.
7.
8.
9.
10.
11.

ANNEX 4

APPLICATION OF CRITICAL LOADS IN CHINA

ZHAO Dianwu* MAO Jietai** XIONG Jiling***
ZHUANG Xiaoshan* YANG Jianxin*

* Research Center for Eco-Environmental Sciences, Academia Sinica
** Department of Geophysics, Peking University
*** Guizhou Institute of Environmental Sciences

ABSTRACT

Current situation of air pollution of China is introduced. Critical loads for 4 soil species in sensitive areas of China have been calculated using methods of SSMB, PROFILE Model and MAGIC Model. A case study for applying critical load map for abating acidification has been made for Guizhou Province with respect to 4 scenarios of control. Finally, an attempt for combining critical loads and critical levels on one map was made. The result showed that emission reduction of whole province evenly is not necessary, if critical loads are taken into consideration. Instead, reducing emissions from three big cities or moving LPS from these cities could also meet the requirement of environmental protection satisfyingly.

1. ENERGY-RELATED AIR POLLUTION IN CHINA

Coal consumption reached 1.05 billion tons in 1990. It is estimated that about 40% were used in cities covering only 10% of the total area of the country. Coal consumption for power generation accounted for about 25% of the total. Therefore, severe air pollution mainly occurred in cities, particularly in megacities, i.e. LOCAL AIR POLLUTION. Contribution to air pollution of power sector currently is relatively in a secondary position. Most of the damages to forests and crops mainly happening around cities can be thought as a strong evidence of the situation.

However, general survey did discover some places far from cities with soil pH being decreased markedly in 30 or more years. Obviously, REGIONAL AIR POLLUTION did exist and play some role in this respect.

Moreover, projection showed that coal consumption would be 2 billon tons with a share of 40% for power generation by the year 2010. Consequently, SO_2 emission at that time will approach the current level. It is speculated that in the coming decade regional air pollution will inevitably become a widespread threat to environment.

2. ABATEMENT OF AIR POLLUTION IN CHINA

China has a large area with a great varieties of topography, vegetation, climate, soil etc. Under different conditions, detrimental effects brought about by same emissions of air pollinates could be quite different, heavy in some regions, light or negligible in some other regions.

There has been a principle of pollution control in China: ALL-ROUND PLANNING, RATIONAL DISTRIBUTION. Now that some regions are more sensitive to acid deposition, naturally, more emission should be reduced relative to those non-sensitive regions. Let us call this idea as RATIONAL REDUCTION.

There must be criteria for realizing the rational distribution or reduction. This criteria is the well-known CRITICAL LOAD or CRITICAL LEVEL.

Even though great efforts having been made, obviously, it is impossible decreasing emissions of air pollutants from energy use to an unharmful level. In this case, cost-effective ways are to avoid siting power plants and industrial parks at sensitive regions, i.e. regions with low critical loads or critical levels, or to allocate the limited funds for pollution control to those sources which emissions mainly deposit at areas with low critical loads or levels. From the viewpoint of sustainable development, this is one of the key principles that should be taken into consideration when making energy planning together with other economic and politic principles.

3. COLLECTION OF BASIC DATA

Environment is a most complex system and, too, is the effect process to the ecosystem by pollution. Appropriate planning and decision can only come from reliable basic data. Unfortunately, it is very often ignored.

In China, heavy attention has been paid to collection of basic data in many aspects:

A. Collecting specialised maps, atlas, reports, articles. Such as Soil Atlas of China, Meteorological Maps, Agricultural Maps, Provincial Maps of Natural Resources, books on soil, forest, energy, etc.

B. General survey of forest growth, collecting and analyzing soil samples mainly at sensitive regions.

C. Setting up SO_2 and NO_2 samplers at rural and remote areas. Until now, 12 sampling sites have been set up for half a year. Work is easy, but, maintenance is difficult.

D. Comprehensive study of acidification of soil and surface water. A small catchment of about 1.5 km^2 has been established at suburbs in Guiyang, Guizhou Province with heavy air pollution and acid rain. There are 7 sampling sites for soil water, soil and throughfall, one bulk rain collector, one low volume aerosol collector, and SO_2 and NO_2 samplers, a weir for measuring discharge and collecting water samples. Work at this small catchment has been conducted for two years. A interim report has just been completed. Discussion with Norwegian friends indicated that it is a successful experiment. This catchment is located at sensitive soil---yellow soil. It is planned to set up second and third small experiment catchments at other regions with sensitive soil species---red soil and lateritic soil.. Carefully gathered data at this site can serve for checking data from other places.

4. VERIFICATION OF CRITICAL LOADS

On the basis of basic data collected in China, critical loads were calculated for major sensitive soil in China: yellow, red soil, lateritic soil and latosol using three models: SSMB, PROFILE, MAGIC, and compared with critical loads calculated using data from publications of international organizations, such FAO, etc.

A. SSMB

Steady state modeling approaches assume a time-independent state of chemical interactions involving an equilibrium between the soil solid phase and soil solution. The steady state mass balance (SSMB) method computes the maximun acid input to the system that will not cause exceedance of the critical alkalinity value. The method can be used to compute critical loads for forest soils, surface waters and groundwater. The steady state mass balance method has been used in the European application to derive critical loads of actual acidity for forest soils.[Mapping Critical Loads for Europe. CCE Technical Report No. 1]

We tried our best to collect actually measured or best estimated data. Weathering data were taken from PROFILE's results. The calculation of critical loads is for four sensitive soil species in southern China: yellow soil, red soil, Lateritic red soil, latosol . Results obtained are as follows:

Table 1. Results Obtained from SSMB Method

Item	Unit	Yellow soil	Red soil	Lateritic red	Latosol
Weathering rate	keq/ha/yr	0.593	0.502	0.398	0.351
Deposition	keq/ha/yr	1.4	1.31	1.08	0.96
Uptake	keq/ha/yr	0.352	0.273	0.3	0.25
Runoff	m	0.6	0.9	1.3	1.6
BC/Al		1.5	1.5	1.5	1.5
pK(gibssite)		-8.42	-8.45	-8.5	-8.63
Leaching	ueq/L	412	198.8	117.8	47.5
Critical load	keq/ha/yr	0.723	0.691	0.664	1.036

B. PROFILE MODEL

PROFILE is designed to calculate the steady-state chemistry of soils, groundwater recharge as well as surface waters. The soil profile itself is divided into compartments corresponding to the natural soil stratification. In each of the soil compartments, a number of chemical reactions are included, represented either by equilibrium relationships or kinetic equations. The reaction systems considered are soil solution equilibrium reactions, silicate weathering, uptake of nutrient cations, NO^{-}_{3} and NH_4, nitrification and cation exchange reactions. All processes interact via the soil solution. [Per Warfvinge and Harald Sverdrup]

Table 2-9 show basic data and basic parameters for calculating critical loads of yellow soil, red soil, lateritic red soil and latosol. The soil parameters were based on sampling and analyzing recently carried out in southern provinces. Detailed calculations are displayed in Table 10. Major results are listed as Table 11.

Table 11. Results Obtained from PROFILE Model

Soil	Yellow	Red	Lateritc red	Latosol
Weathering rate	0.593	0.502	0.389	0.351
ANC	-0.524	-0.363	-0.291	-0.091
Uptake of N	0.287	0.205	0.250	0.200
Uptake of cation	0.352	0.273	0.300	0.250
C. L. of potential acidity	1.052	0.797	0.639	0.392
C. L.of acidity	1.117	0.865	0.689	0.442

C. MAGIC MODEL

MAGIC was developed for assessing the long-term acidification of surface water based on the assumption that surface water quality is controlled by atmospheric deposition and some important chemical reactions that take place while the water is in contact with the rocks and soils of the terrestrial system. The model uses lumped parameters over a catchment or region and may be used to assess regional responses of soil and water chemistry to changes in patterns of acid deposition. The current version splits the soil profile into two horizontal layers. [B.J. Cosby, G.M. Hornberger, J.M. Galloway]

Basic data for MAGIC are carefully measured at a small catchment at Liuchongguan, Guiyang City, Guizhou Province. This small catchment has been working for more than two years and a quite lot of all-round data have been collected. These are relatively sufficient and reliable information now we have got. Some of the important parameters are as follows:

S-wet deposition	4.0 g $S/m^2/yr$		
S-dry deposition	2.1 g $S/m^2/yr$		
Runoff coefficient	0.5		
Rainfall	1.173 m/yr		
Rain chemistry	pH 4.3,		
(1992---1993)	SO_4 213 ueq/L,	NO_3 19.0 ueq/L,	Cl 11 ueq/L,
	F 3.3 ueq/L,	K 6.5 ueq/L,	Na 8.3 ueq/L,
	Ca 132 ueq/L	Mg 27 ueq/L	

Soil parameters, see Table 12.

Table 12. Important Soil Parameters for MAGIC

Layer	CEC	BS	$pK[Al(OH)_3]$	Al_i	Al^{3+}	H^+
A	26.19	29.63	8.35	170.5	110.8	79.3
B	17.99	13.59	8.44	140.8	85.2	67.8
C	8.5	13.00	8.80	127.06	71.3	48.2

Five scenarios of SO_2 emissions have been made for calculating using MAGIC Model, see Figure 1.

Results from MAGIC are demonstrated on Figure 2-5. Some conclutions could be drawn from these figures as follows:

A. Scenarios 1-4, $Al^{3+}/(Ca+Mg)$ of surface layer of soil (Soil 1) is greater than 1, except for scenario 4 being approaching 1. $Al^{3+}/(Ca+Mg)$ is still greater than 1. Therefore, all these four scenarios are unacceptable.

B. For scenario 5, i.e. 70% reduction, $Al^{3+}/(Ca+Mg)$ for Soil 1 and 2 decreases to below 1, Al^{3+} reduces to 150 ueq/L, H^+ of soil water to about 50 ueq/L, and alkalinity goes up to about -200 ueq/L. Parameters of this levels can meet the demand of environment protection. From this point of view, the deposition of scenario 5 is thus taken as critical load for this area with yellow soil. That is 0.6 keq/ha/yr.

C. A comparison between critical loads from different method can be made, see Table 13.

Table 13. Critical Loads from Different Method
(in keq/ha/yr)

Method	SSMB	PROFILE	MAGIC	RIVM Map*
Yellow	0.723	1.052, 1.117	0.6	0.5--1.0
Red soil	0.691	0.797, 0.865	---	0.2--0.5
Lateritic red	0.664	0.639, 0.689	---	0--0.2
Latosol	1.036	0.392, 0.442	---	0--0.2

Note: 1. * Estimated from RIVM etc's map.
2. The first figure of PROFILE is Critical of potential acidity, the second critical load of acidity.

Generally speaking, RIVM etc's map gives far low critical loads. It seems there is no large difference between other methods, except for latosol from SSMB. It is not surprising for this discrepancies, since no calculation can announce reliable and sufficient data have been used.

By the way, an interesting phenomenon appeared in the course of MAGIC calculation. the Al concentration in soil water decreased along with decreasing of uptake of cations, see Figure 6. As is well-known, cations are uptaken by trees as nutrients. Then, the more trees, the more uptake of cations, and consequently, the higher concentration of Al. In other words, the more trees the more sensitive the soil. Is this correct?

5. A CASE STUDY---- APPLICATION OF CRITICAL LOADS IN GUIZHOU PROVINCE OF CHINA

Guizhou Province is located in southwest China. Due to being situated in a basin surrounding by mountains with unfavourable meteorological condition for air pollutants to disperse, and rich in high sulfur coal, air pollution and acid rain are among the most severe in China. In the central part of this province, three big cities, Guiyang the capital, Zunyi and Anshun are relatively industrialised and densely populated. Sulfur contents of coal mined and used there can be as high as 3-5%. in the western part, Liupanshui region, is another industrial park. Fortunately, coal sulfur content generally is below 1%. in the eastern, particularly southeastern part, is a region almost undeveloped with only very few small industry. The whole province mainly covers with sensitive yellow, most sensitive soil spreads in the southeastern part. Figure 7 shows critical load map of Guizhou Province.

Research on acid rain and air pollution have been conducted for more than ten years and, naturally, a lot of basic data have been gathered. For this reason, it is belived that this is a suitable area for carrying out a case study of applying critical loads for energy planning. Taking 1992 as base year, 2010 as target year. Four scenarios have been made, see Table 14.

Table 14. SO_2 Emissions of Scenarios of Energy in Guizhou (in 10^4T)

Area	1992		2010 (BAU)		2010 (-50% Wholly)		2010 (-50% at 3 areas*)		2010 (3 LPS moved)	
	Areal	**LPS**	**Areal**	**LPS**	**Areal**	**LPS**	**Areal**	**LPS**	**Areal**	**LPS**
Guiy	10.63	3.83	18.67	11.50	9.34	5.75	9.34*	5.75*	18.67	moved to Bijie
Liu	6.68	1.1	10.62	2.51	5.31	1.26	10.62	2.51	10.62	35.51
Gui S	6.47	---	10.93	---	5.47	---	10.93	---	10.93	---
Bijie	4.56	0.12	7.90	---	3.95	---	7.90	---	7.90	19.72
Zunyi	5.0	4.73	15.65	0.78	7.83	0.39	7.83*	0.39*	7.83*	0.39* half moved to Bijie
Tong	1.23	0.3	2.58	---	1.29	---	2.58	---	2.58	---
Gui SW	1.91	0.29	3.71	---	1.86	---	3.71	---	3.71	---
An	4.79	16.5	19.44	33.0	9.72	16.5	9.72*	16.5*	19.44	moved to Liu
GuiSE	2.24	0.86	5.23	---	2.62	---	5.23	---	5.23	---
Sub-T	43.51	27.73	94.73	47.79	47.39	23.9	67.86	25.15	86.91	55.62
Total	**71.24**		**142.52**		**71.29**		**93.01**		**142.53**	

Note: Guiy--Guiyang, Liu--Liupanshui, Gui S--Southern Guizhou, Tong--Tongren, Gui SW--Southwestern Guizhou, An--Anshun, Gui SE--Southeatern Guizhou.

SO_2 concentrations and sulfur depositions for 1992 and for four scenarios of 2010 are demonstrated on Figure 8-17. Maps of exceedance of deposition to critical load are shown in Figures 18-22

From the exceedance maps, some conclusions can be drawn up:

A. In 1992, regions with deposition exceeding critical load are Guiyang City and Zunyi City and surrounding areas. See Figure 18.

B. In 2010, the region with deposition exceeding critical load expands significantly, and what is more, it merges with region exceeding critical load around Chongqing City, Sichuan Province. Regional pollution really does occur. See Figure 19.

C. Figure 20 shows exceedance area after emission of the whole province being reduced by half. Then the exceeding areas only around three big cities, Guiyang, Anshun and Zunyi. The exceedance areas contract with the highest value decreasing from 10 to 6 g m^2/yr.

D. If only reduce emission of three cities, Guiyang, Zunyi and Anshun, the highest exceeding value also decreases from 10 to 6, even though the exceedance area is a region including all these three cities. In fact, there is no big difference between reducing all provincial emission and only three big cities', see Figure 21.

E. Figure 22 demonstrates the result of moving some LPS to less sensitive area with less emissions. The exceedance area splits to 4 areas, but the situation is again about the same as emission reductions.

F. The conclusion is that the best way is, if possible, to move LPS to less sensitive area with relatively less emission or only reduce emission from a few densely populated big cities. It seems that smoothly lower down emission from whole province is not a cost-effective option.

6. ATTEMPT OF COMBINING CRITICAL LOAD AND CRITICAL LEVEL ON ONE MAP

As stated above that air pollution situation now in China, a developing country, is of a mixed nature, i.e. there are both LOCAL POLLUTION and REGIONAL POLLUTION existing together. Even though local pollution dominant currently, but, since the consideration of energy planning should be on the coming few decades, REGIONAL POLLUTION should by no means be ignored. Now we al ready have CRITICAL LOAD MAP, and we will have CRITICAL LEVEL MAP as well soon. It can perhaps be imagine that, for decision-makers, two different maps might create confusing sometimes. Thus an attempt of combining these two maps into one has been made.

Two ideas for this purpose have been drawn up. Firstly, determine which one is the decisive factor for protecting ecosystem, critical load or critical level? Secondly, try to transfer the critical load to equivalent SO_2 concentration..

From the current critical load map, Chinese provinces can be grouped into 5 categories, see Figure 23.

Category 1: Critical load 0-0.32 g/m^2/yr, Yunnan Province.
Category 2: Critical load 0.31-0.8 g/m^2/yr, Guangdong, Guangxi, Hainan, Guizhou, Hunan, Jiangxi Provinces.
Category 3: Critical load 0.8-1.6 g/m^2/yr, Zhejiang, Fujian, Shaanxi Provinces.
Category 4: Critical load 1.6-3.2 g/m^2/yr, Shanxi, Henan, Shandong Provinces.
Category 5: Critical load > 3.2 g/m^2/yr, remaining Provinces.

In addition, following are four assumptions needed:

Assumption 1: Precipitation is equal throughout whole China and washout ratio is also equal to deposition velocity.
Assumption 2: Deposition velocity for SO_2 be taken as 0.5 cm/sec.
Assumption 3: Cations is able to neutralize 40% of acid in rainwater.
Assumption 4: Critical level for forest and crops are 30 ug/m^3.

Based on assumptions mentioned above, critical loads can thus be transferred into equivalent SO_2 concentrations as follows:

Category 1: SO_2 0-13 ug/m^3
Category 2: SO_2 13-36 ug/m^3
Category 3: SO_2 36-66 ug/m^3
Category 4: SO_2 66-130 ug/m^3
Category 5: SO_2 > 130 ug/m^3

Then hereby come to conclusion:

A. For categories 1 and 2, critical loads are the decisive factor, SO_2 concentration in this range seems do not injure forest and crops.

B. For categories 3, 4 and 5, the decisive factor is critical level, i. e. SO_2 concentration. There is no necessary to worry about the deposition. These regions are clearly with non-sensitive soils. Direct effects will still do harm to vegetation, even though soil acidification will not happen in a rather long period.

In this way, the advantages are that certain regions should mainly take care of only critical load (deposition) or only critical level (SO_2 concentration). Combining two maps into one will likely be convenient to decision-makers for PRELIMINARY planning purpose.

Of course, the above mentioned assumptions are not totally rational and some problems, such as washout ratio, remain to be solved.

7. CONCLUSION REMARKS

A. Map of critical loads is an useful tool helping decision-makers to achieve cost-effective rational distribution of LPS or rational reduction of emissions. This has already been proved by European experience. The case study in this paper seems to support this idea as well.

B. Considering the current situation of energy-related air pollution, i. e. both local pollution and regional pollution exist. Therefore, map of critical level should be worked out at the same time.

C. With mentioning, maps of the kind should be reliable. Reliability of results comes from reliable basic data. Carefully collecting enough and representative basic data is of course of crucial importance.

D. It is suggested that several methods be used simultaneously, in order to cross check the final results.

E. For policy analysis of energy planning or economic planning, obviously, maps of critical load and level are far from enough. Among other things, a decision can by no means be made and accepted without making a cost-benefit analysis.

REFERENCES

Cosby, B. J., Hornberger, G. M., Wright, R. F. and Galloway, J. N., Modeling the Effects of Acid Deposition, Water Resources Research, 22, 1283-91, 1986.

Larssen, Thorjorn, Studies of soil and water in small catchments in Guiyang and Nanchang, 1994 (unpublished).

Miljorapport, Critical Loads for Sulphur and Nitrogen, Report from a workshop held at Skokloster, Sweden, 19-24 March, 1988.

UN-CCE, Mapping Critical Loads for Europe, CCE Technical Report No. 1, July 1991.

Warfvinge, P. and Sverdrup, H., Calculating Critical Loads of Acid Deposition With PROFILE - A Steady-State Soil Chemistry Model, Water, Air, and Soil Pollution 63: 119-143, 1992.

Zhao Dianwu and Hans Martin Seip, Assessing Effects of Acid Deposition in Southwestern China Using the MAGIC Model, Water, Air, and Soil Pollution 60: 83-97, 1991.

Figure 1. CHANGES OF WET DEPOSITION OF SULFUR
1900-2050, Guiyang catchment

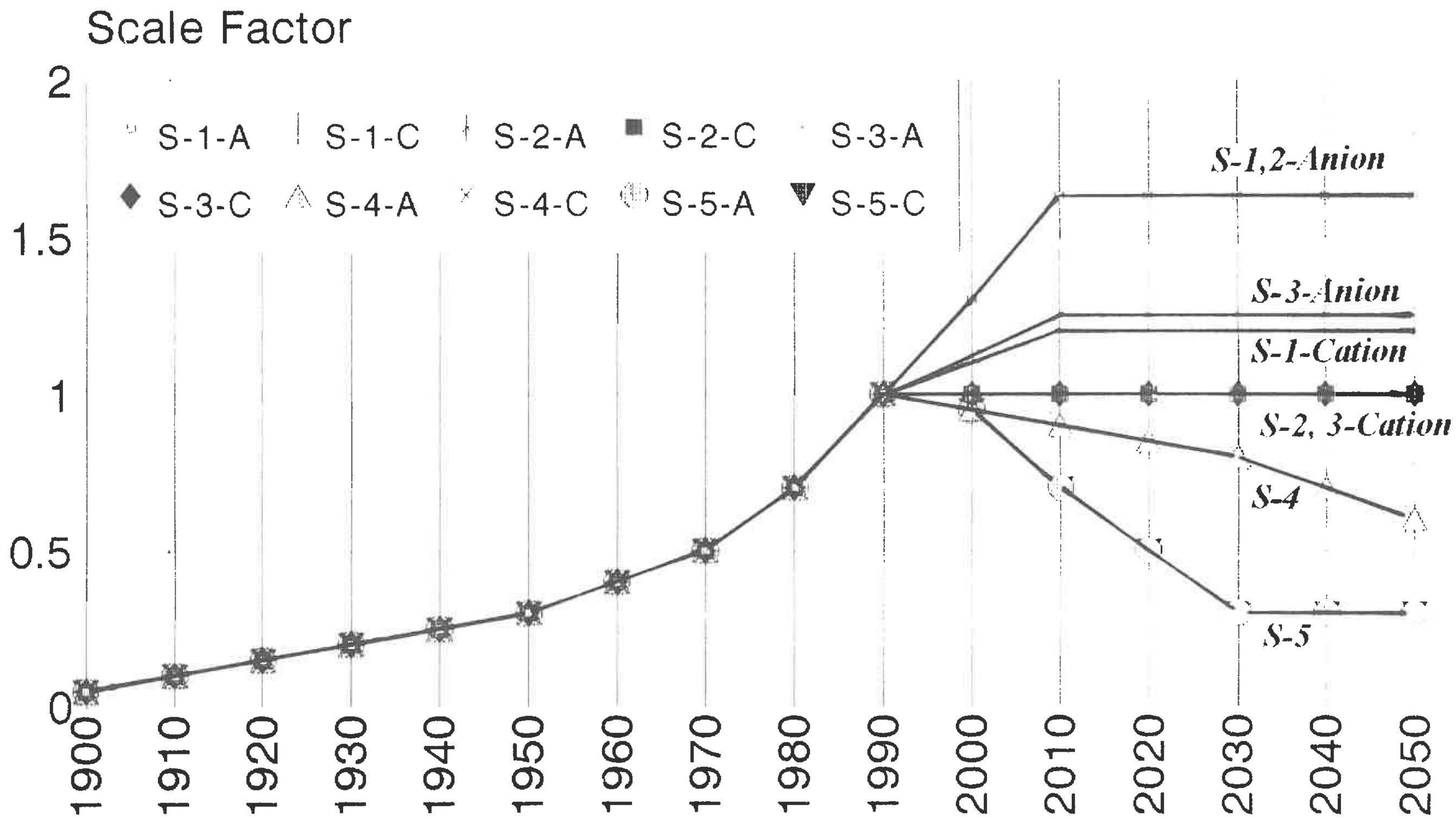

Scenarios 4,5,anion and cation are same, others different
S-1-A, S-1-C etc, an-&cat-ion deposition, scenario 1, etc

MAGIC RESULTS

Figure 2.

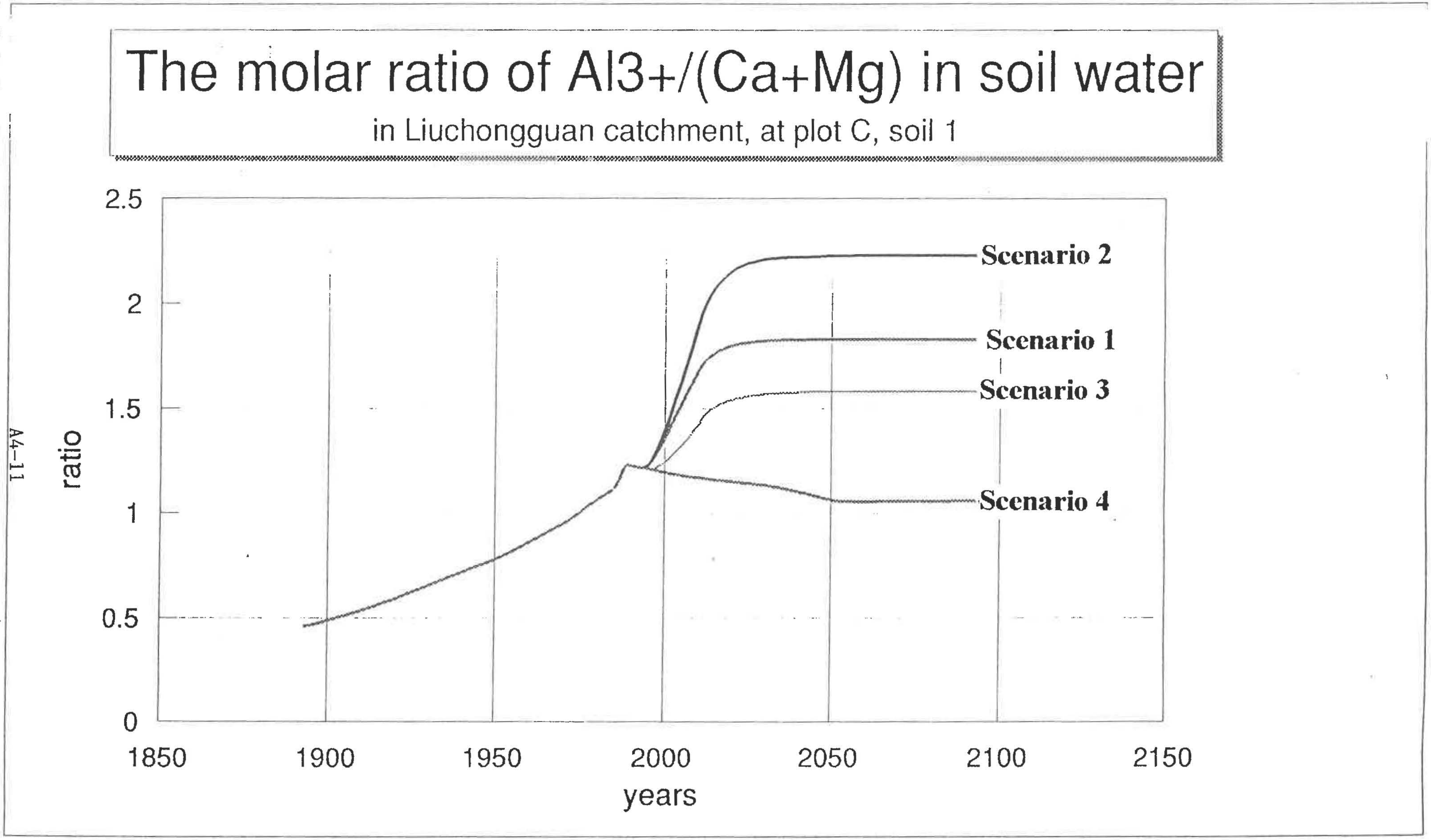

A4-11

MAGIC RESULTS

Figure 3.

The molar ratio of Al3+/(Ca+Mg) in soil water

in Liuchongguan catchment, at plot C, soil 2

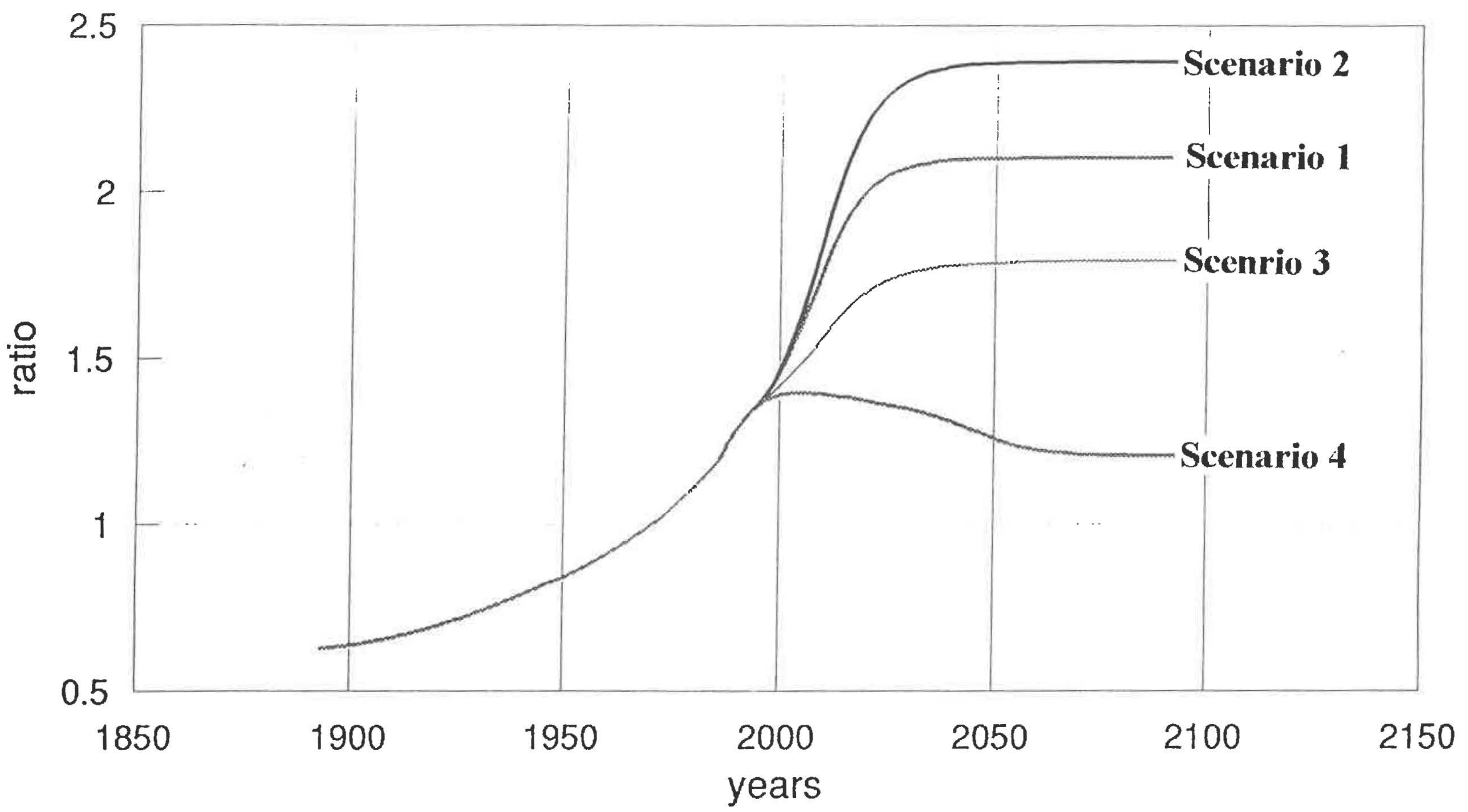

A4–12

MAGIC RESULTS **Scenario 5** **Figure 4.**

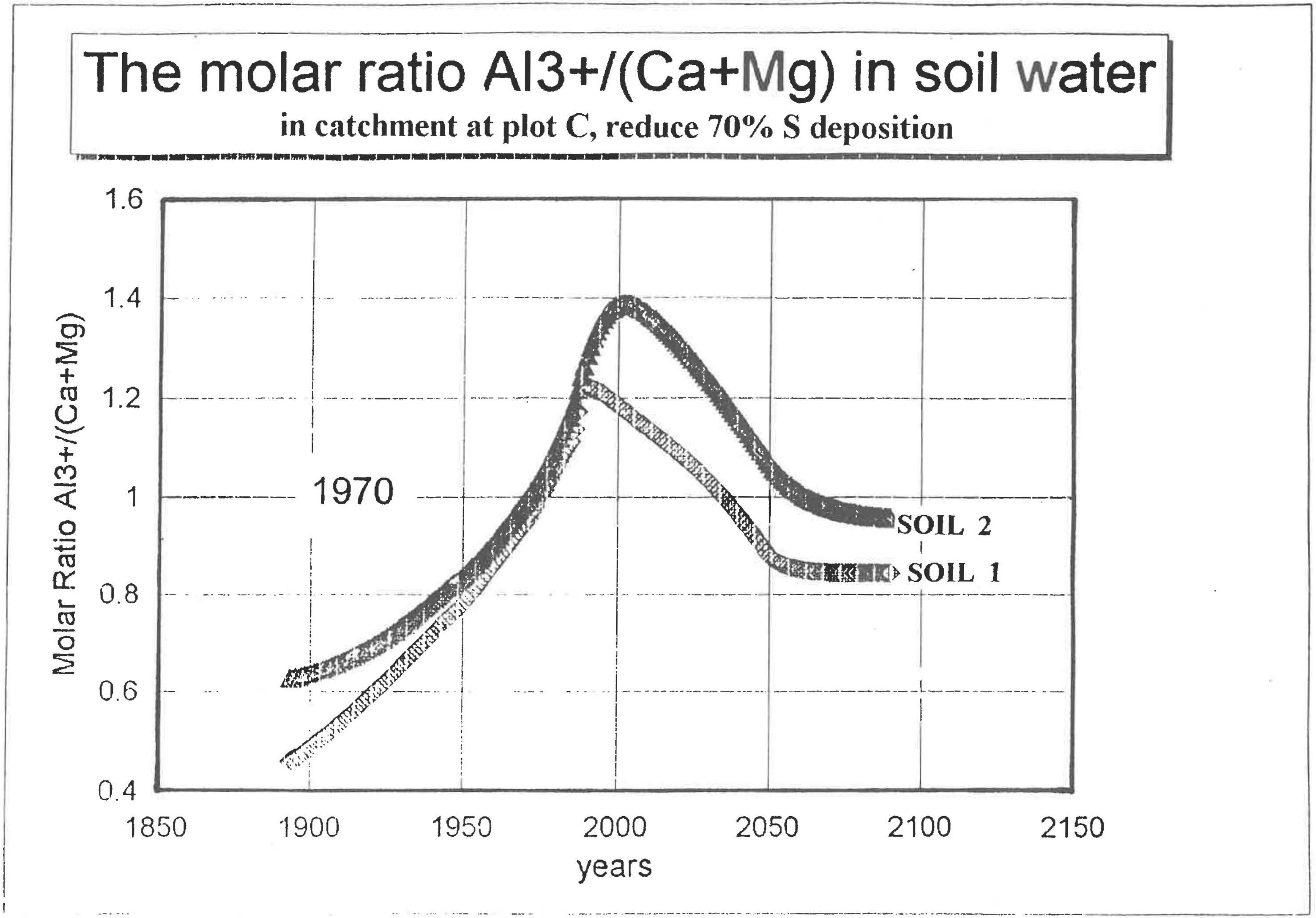

A4-13

MAGIC RESULTS **Scenario 5** **Figure 5.**

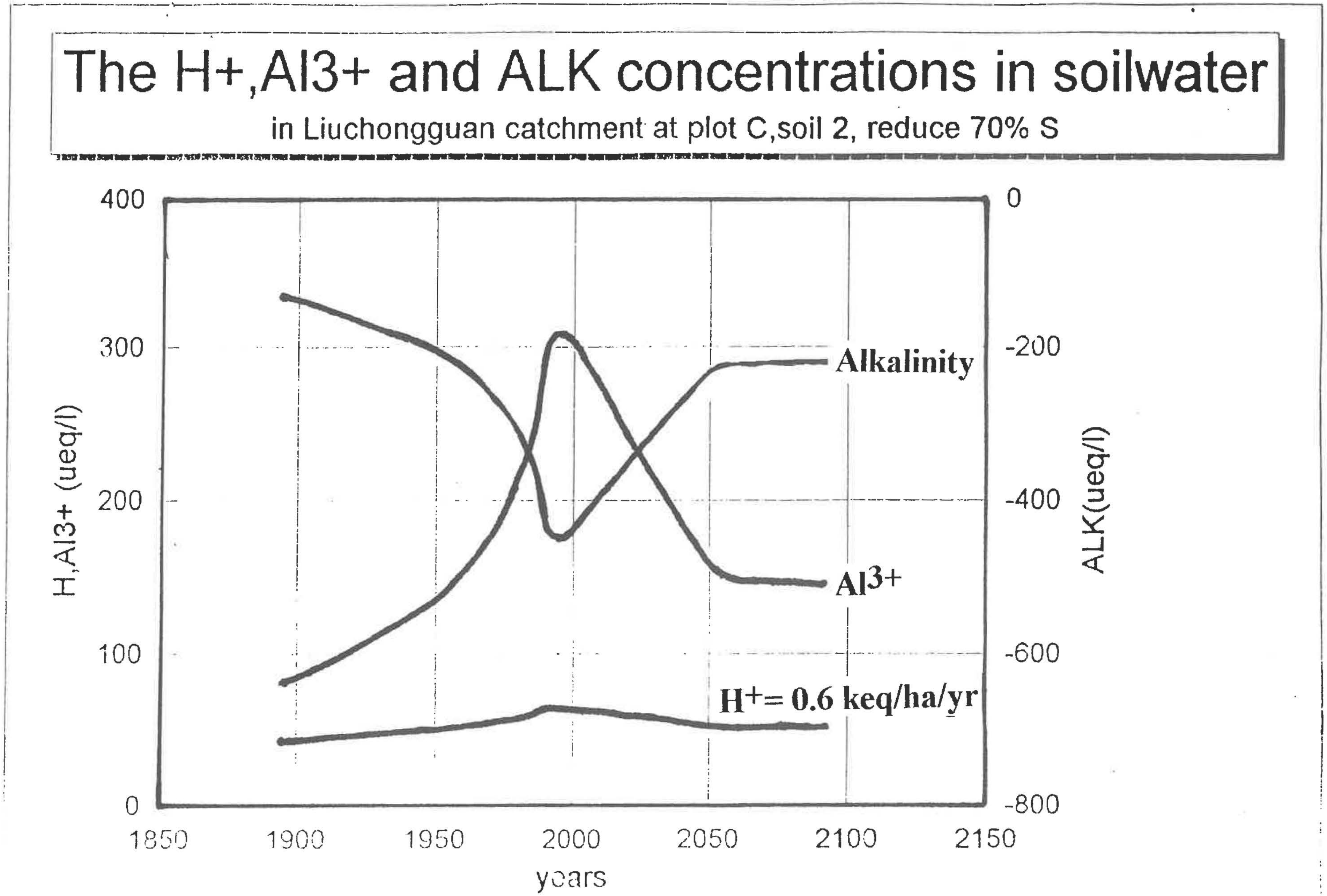

The variation of ratio Al/(Ca+Mg) when reduce uptake

in Liuchongguan catchment at plot C, Scenario 1

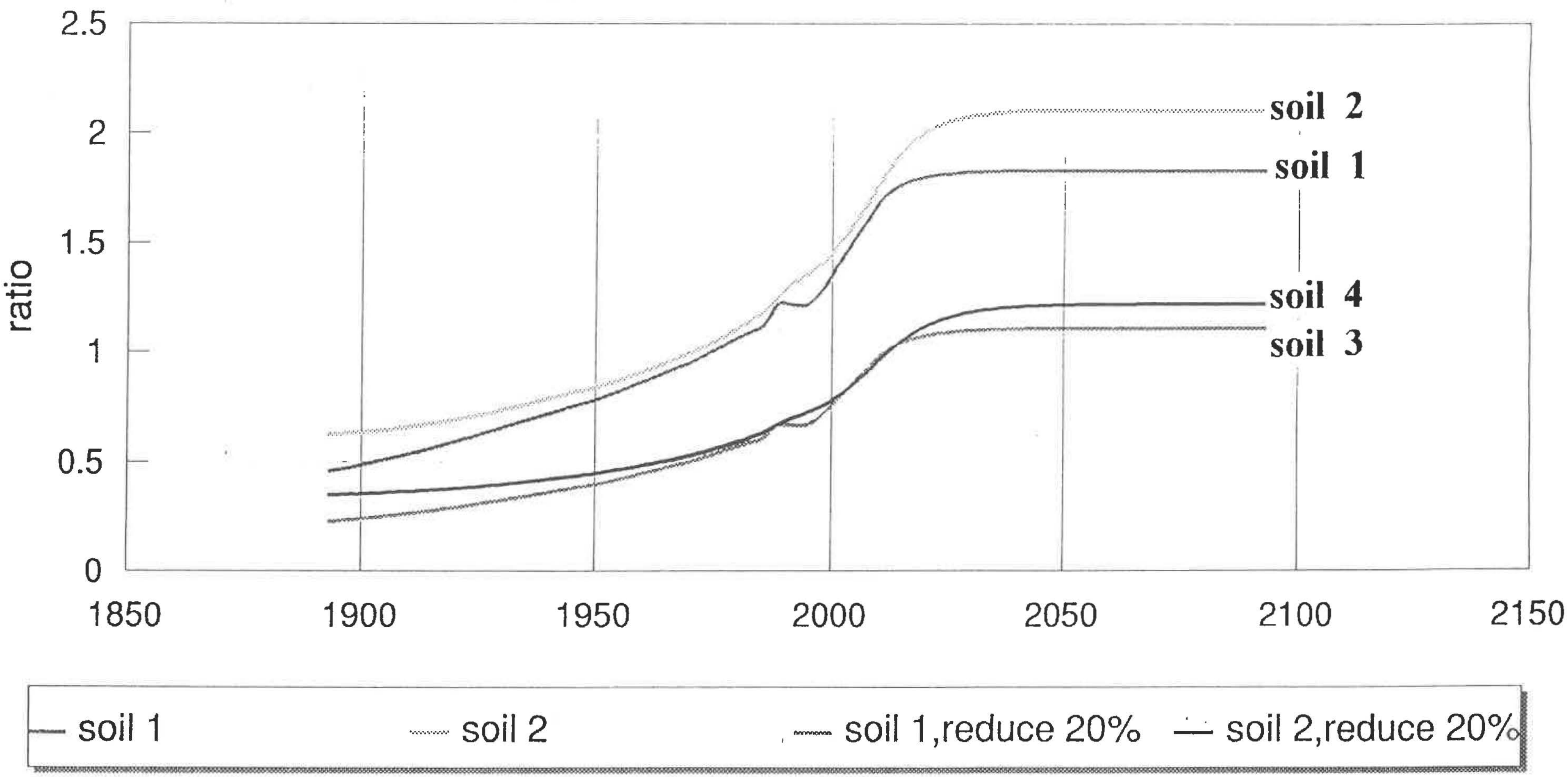

PROFILE RESULTS

Table 2.

INPUT DATA FOR SOIL LAYERS

for yellow soil in southern China

DATA	UNIT	LAYER 1	LAYER 2	LAYER 3	LAYER 4
Layer height	m	0.09	0.11	0.35	0.5
Moisture content	m3/m3	0.2	0.2	0.2	0.2
Soil bulk density	kg/m3	800	1110	1450	1550
Specific surface area	m2/m3	9.15E+05	1.2E+06	1.25E+06	1.25E+06
CO2	atm	3	5	20	20
Inflow	% of rain	100	80	70	60
percolation	% of rain	80	70	60	60
Ca+Mg+K uptake	% of max	30	50	20	0
N uptake	% of Max	30	40	30	0
DOC	mg/l	2	1	0.5	0.1
log K gibbsite		7.5	8.4	8.6	8.8
Muscovite	%	9.7	9.7	9.7	9.7
Vermiculate	%	0	0	0	0
Chlorite	%	3.5	3.5	3.5	3.5
K-feldspare	%	4.6	4.6	4.6	4.6

PROFILE RESULTS

Table 3.

BASIC PARAMETERS FOR CRITICAL LOADS

for yellow soil in southern China

PARAMETERS	UNIT	VALUE
Soil layers		4
precipitation	m/yr	1.173
Runoff		0.6
Deposition		
SO4	keq/ha/yr	2
NO3	keq/ha/yr	0.08
NH4	keq/ha/yr	0.22
Cl	keq/ha/yr	0.15
Ca	keq/ha/yr	1
Mg	keq/ha/yr	0.2
K	keq/ha/yr	0.1
Na	keq/ha/yr	0.1
Non-marine fraction	%	95
Maximum uptake		
Ca+Mg+K	keq/ha/yr	0.4
NO3+NH4	keq/ha/yr	0.35
Temperature	C	17.3
Nitrification rate		high

PROFILE RESULTS

Table 4.

INPUT DATA FOR SOIL LAYERS

for red soil in southern China

DATA	UNIT	LAYER 1	LAYER 2	LAYER 3	LAYER 4
Layer height	m	0.09	0.11	0.35	0.5
Moisture content	m3/m3	0.2	0.2	0.2	0.2
Soil bulk density	kg/m3	800	950	1100	1200
Specific surface area	m2/m3	1.56E+06	2.1E+06	2.1E+06	2.1E+06
CO2	atm	3	5	20	20
Inflow	% of rain	100	80	70	60
percolation	% of rain	80	70	60	60
Ca+Mg+K uptake	% of max	30	50	20	0
N uptake	% of Max	30	40	30	0
DOC	mg/l	1	0.5	0.1	0.1
log K gibbsite		7.5	8.4	8.6	8.8
Muscovite	%	4.1	4.6	4.6	4.6
Vermiculate	%	1.8	2	2	2
Chlorite	%	0.9	1	1	1
K-feldspare	%	2.4	2.7	2.7	2.7
Albite	%	0.9	1	1	1
Biotite	%	0.9	1	1	1

Table 5.

BASIC PARAMETERS FOR CRITICAL LOADS

for red soil in southern China

PARAMETERS	UNIT	VALUE
Soil layers		4
precipitation	m/yr	1.5
Runoff	m	0.9
Deposition		
SO_4	keq/ha/yr	1.6
NO_3	keq/ha/yr	0.06
NH_4	keq/ha/yr	0.22
Cl	keq/ha/yr	0.15
Ca	keq/ha/yr	0.9
Mg	keq/ha/yr	0.2
K	keq/ha/yr	0.1
Na	keq/ha/yr	0.1
Non-marine fraction	%	95
Maximum uptake		
Ca+Mg+K	keq/ha/yr	0.35
NO_3+NH_4	keq/ha/yr	0.3
Temperature	C	19
Nitrification rate		high

PROFILE RESULTS

Table 6.

INPUT DATA FOR SOIL LAYERS

for lateritic red soil in southern China

DATA	UNIT	LAYER 1	LAYER 2	LAYER 3	LAYER 4
Layer height	m	0.09	0.11	0.35	0.5
Moisture content	m3/m3	0.2	0.2	0.2	0.2
Soil bulk density	kg/m3	800	900	1000	1100
Specific surface area	m2/m3	1.81E+06	2.1E+06	2.1E+06	2.1E+06
CO2	atm	3	5	20	20
Inflow	% of rain	100	80	70	60
percolation	% of rain	80	70	60	60
Ca+Mg+K uptake	% of max	30	50	20	0
N uptake	% of Max	30	40	30	0
DOC	mg/l	1	0.5	0.1	0.1
log K gibbsite		7.5	8.4	8.6	8.8
Muscovite	%	4.7	5.2	5.2	5.2
Chlorite	%	0.9	1	1	1
K-feldspare	%	2.9	3.2	3.2	3.2

PROFILE RESULTS

Table 7.

BASIC PARAMETERS FOR CRITICAL LOADS

for lateritic red soil in southern China

PARAMETERS	UNIT	VALUE
Soil layers		4
precipitation	m/yr	1.8
Runoff	m	1.3
Deposition		
SO4	keq/ha/yr	1.3
NO3	keq/ha/yr	0.04
NH4	keq/ha/yr	0.22
Cl	keq/ha/yr	0.15
Ca	keq/ha/yr	0.8
Mg	keq/ha/yr	0.18
K	keq/ha/yr	0.1
Na	keq/ha/yr	0.1
Non-marine fraction	%	95
Maximum uptake		
Ca+Mg+K	keq/ha/yr	0.3
NO3+NH4	keq/ha/yr	0.25
Temperature	C	19
Nitrification rate		high

PROFILE RESULTS

Table 8.

INPUT DATA FOR SOIL LAYERS

for latosols in southern China

DATA	UNIT	LAYER 1	LAYER 2	LAYER 3	LAYER 4
Layer height	m	0.09	0.11	0.35	0.5
Moisture content	m3/m3	0.2	0.2	0.2	0.2
Soil bulk density	kg/m3	800	850	900	1000
Specific surface area	m2/m3	1.84E+06	2.1E+06	2.1E+06	2.1E+06
CO2	atm	3	5	20	20
Inflow	% of rain	100	80	70	60
percolation	% of rain	80	70	60	60
Ca+Mg+K uptake	% of max	30	50	20	0
N uptake	% of Max	30	40	30	0
DOC	mg/l	1	0.5	0.1	0.1
log K gibbsite		7.5	8.4	8.6	8.8
Muscovite	%	0.9	1	1	1
Chlorite	%	0.9	1	1	1
K-feldspare	%	0.9	1	1	1

PROFILE RESULTS

Table 9.

BASIC PARAMETERS FOR CRITICAL LOADS

for latosols in southern China

PARAMETERS	UNIT	VALUE
Soil layers		4
precipitation	m/yr	2
Runoff	m	1.6
Deposition		
SO4	keq/ha/yr	1
NO3	keq/ha/yr	0.03
NH4	keq/ha/yr	0.22
Cl	keq/ha/yr	0.15
Ca	keq/ha/yr	0.7
Mg	keq/ha/yr	0.16
K	keq/ha/yr	0.1
Na	keq/ha/yr	0.1
Non-marine fraction	%	95
Maximum uptake		
Ca+Mg+K	keq/ha/yr	0.25
NO3+NH4	keq/ha/yr	0.2
Temperature	C	20
Nitrification rate		high

PROFILE RESULTS

Table 10.

For yellow soil:

Depth	pH solution	pH Atm Eq	ANC ueq/l	Mg+Ca+K ueq/l	Total Al umol/l	ALR	KGIBB	NO3 ueq/l	NH4 ueq/l	BC+Na keq/ha/yr	Si umol/l	Mg ueq/l	Ca ueq/l	K ueq/l	Na ueq/l
0.000	4.283	4.283	-52.003	59.676	0.000	0.000	-6.848	6.820	18.755	0.000	0.000	17.100	85.300	8.530	8.530
0.045	4.175	4.176	-97.319	68.923	13.617	2.591	-7.544	14.967	4.864	0.026	3.920	21.400	97.600	9.400	10.700
0.145	4.344	4.345	-125.487	68.101	33.121	3.737	-8.418	5.136	0.000	0.045	11.600	25.100	94.500	8.290	12.200
0.375	4.413	4.419	-116.834	94.468	32.299	2.184	-8.619	0.000	0.000	0.206	51.400	51.500	107.000	15.200	14.500
0.800	4.559	4.574	-72.846	121.629	19.932	0.421	-8.831	0.000	0.000	0.316	110.000	86.300	107.000	25.000	14.800
			-412.486							0.593					

uptake of N= 0.287 keq/ha/yr BC+Na= 0.593 keq/ha/yr CL of potential acidity= 1.052 keq/ha/yr
uptake of cation= 0.352 keq/ha/yr ANC= -0.524 keq/ha/yr CL of acidity= 1.117 keq/ha/yr

For red soil.

Depth	pH solution	pH Atm Eq	ANC ueq/l	Mg+Ca+K ueq/l	Total Al umol/l	ALR	KGIBB	NO3 ueq/l	NH4 ueq/l	BC+Na keq/ha/yr	Si umol/l	Mg ueq/l	Ca ueq/l	K ueq/l	Na ueq/l
0.000	4.615	4.615	-24.000	43.333	0.000	0.000	-7.844	4.000	10.000	0.000	0.000	13.300	60.000	6.670	6.670
0.045	4.385	4.388	-48.126	50.345	3.617	0.761	-7.662	7.344	2.278	0.024	4.270	16.500	68.900	7.650	8.560
0.145	4.490	4.493	-62.563	50.691	13.082	1.292	-8.448	0.000	0.000	0.043	12.900	18.800	67.600	7.500	10.300
0.375	4.551	4.569	-56.891	70.157	13.220	0.308	-8.646	0.000	0.000	0.172	52.100	33.200	79.100	14.000	14.200
0.800	4.715	4.763	-31.179	87.098	8.121	0.283	-8.887	0.000	0.000	0.263	109.000	50.400	79.400	22.200	17.700
			-198.759							0.502					

uptake of N= 0.205 keq/ha/yr BC+Na= 0.502 keq/ha/yr CL of potential acidity= 0.797 keq/ha/yr
uptake of cation= 0.273 keq/ha/yr ANC= -0.363 keq/ha/yr CL of acidity= 0.865 keq/ha/yr

For lateritic red soil:

Depth	pH solution	pH Atm Eq	ANC ueq/l	Mg+Ca+K ueq/l	Total Al umol/l	ALR	KGIBB	NO3 ueq/l	NH4 ueq/l	BC+Na keq/ha/yr	Si umol/l	Mg ueq/l	Ca ueq/l	K ueq/l	Na ueq/l
0.000	5.211	5.211	-5.000	32.778	0.000	0.000	0.000	2.222	12.222	0.000	0.000	10.000	44.400	5.560	5.560
0.045	4.616	4.625	-24.500	38.416	1.119	0.424	-8.009	7.467	5.060	0.022	3.120	12.500	51.200	6.570	6.960
0.145	4.585	4.591	-41.665	38.683	7.663	1.016	-8.489	6.018	0.000	0.031	8.130	14.100	50.200	6.570	7.990
0.375	4.643	4.681	-35.412	50.288	7.713	0.244	-8.684	0.062	0.000	0.136	32.800	23.800	54.600	11.100	9.480
0.800	4.817	4.933	-16.249	63.154	4.663	0.219	-8.961	0.047	0.000	0.209	69.000	36.400	54.600	17.700	9.720
			-117.826							0.398					

uptake of N= 0.250 keq/ha/yr BC+Na= 0.398 keq/ha/yr CL of potential acidity= 0.639 keq/ha/yr
uptake of cation= 0.300 keq/ha/yr ANC= -0.291 keq/ha/yr CL of acidity= 0.689 keq/ha/yr

For latosols soil:

Depth	pH solution	pH Atm Eq	ANC ueq/l	Mg+Ca+K ueq/l	Total Al umol/l	ALR	KGIBB	NO3 ueq/l	NH4 ueq/l	BC+Na keq/ha/yr	Si umol/l	Mg ueq/l	Ca ueq/l	K ueq/l	Na ueq/l
0.000	5.956	5.966	5.000	26.500	0.000	0.000	0.000	1.500	11.000	0.000	0.000	8.000	35.000	5.000	5.000
0.045	4.949	4.988	-8.507	31.095	0.294	0.182	-8.868	6.034	5.289	0.019	1.170	10.300	40.500	5.730	6.260
0.145	4.745	4.756	-22.797	31.573	3.313	0.678	-8.626	6.278	0.147	0.029	3.320	12.100	40.000	5.510	7.160
0.375	4.788	4.901	-15.964	40.154	3.451	0.169	-8.799	1.681	0.000	0.121	13.300	22.100	43.700	7.230	8.420
0.800	5.003	5.564	-0.224	48.761	1.859	0.137	-9.217	0.992	0.000	0.182	27.600	35.000	43.700	9.390	8.510
			-47.492							0.351					

uptake of N= 0.200 keq/ha/yr BC+Na= 0.351 keq/ha/yr CL of potential acidity= 0.392 keq/ha/yr
uptake of cation= 0.250 keq/ha/yr ANC= -0.091 keq/ha/yr CL of acidity= 0.442 keq/ha/yr

Figure 7

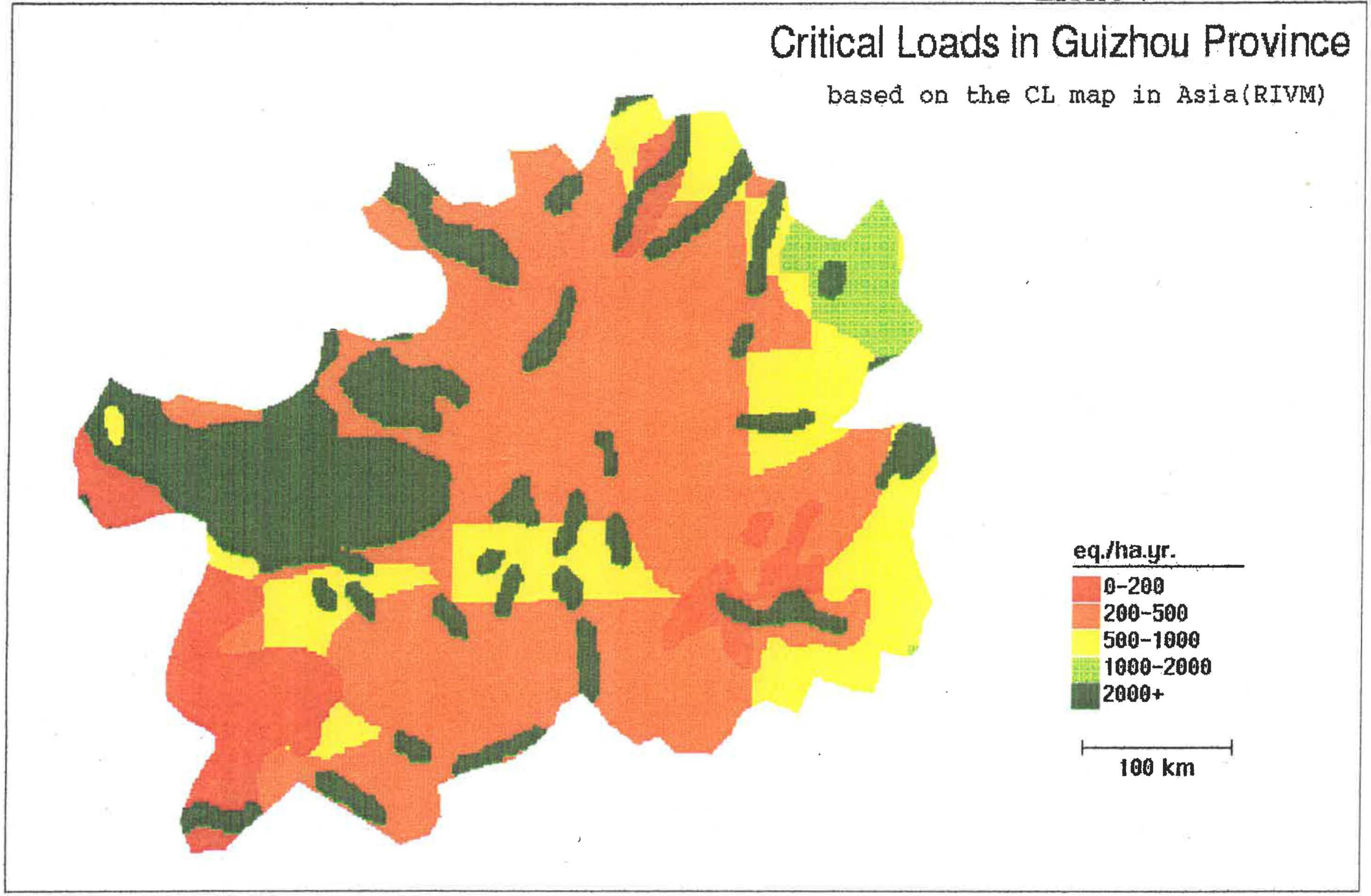
Critical Loads in Guizhou Province
based on the CL map in Asia(RIVM)
eq./ha.yr.
0-200
200-500
500-1000
1000-2000
2000+
100 km

Figure 9

S Deposition 1992 (g/m2/year)

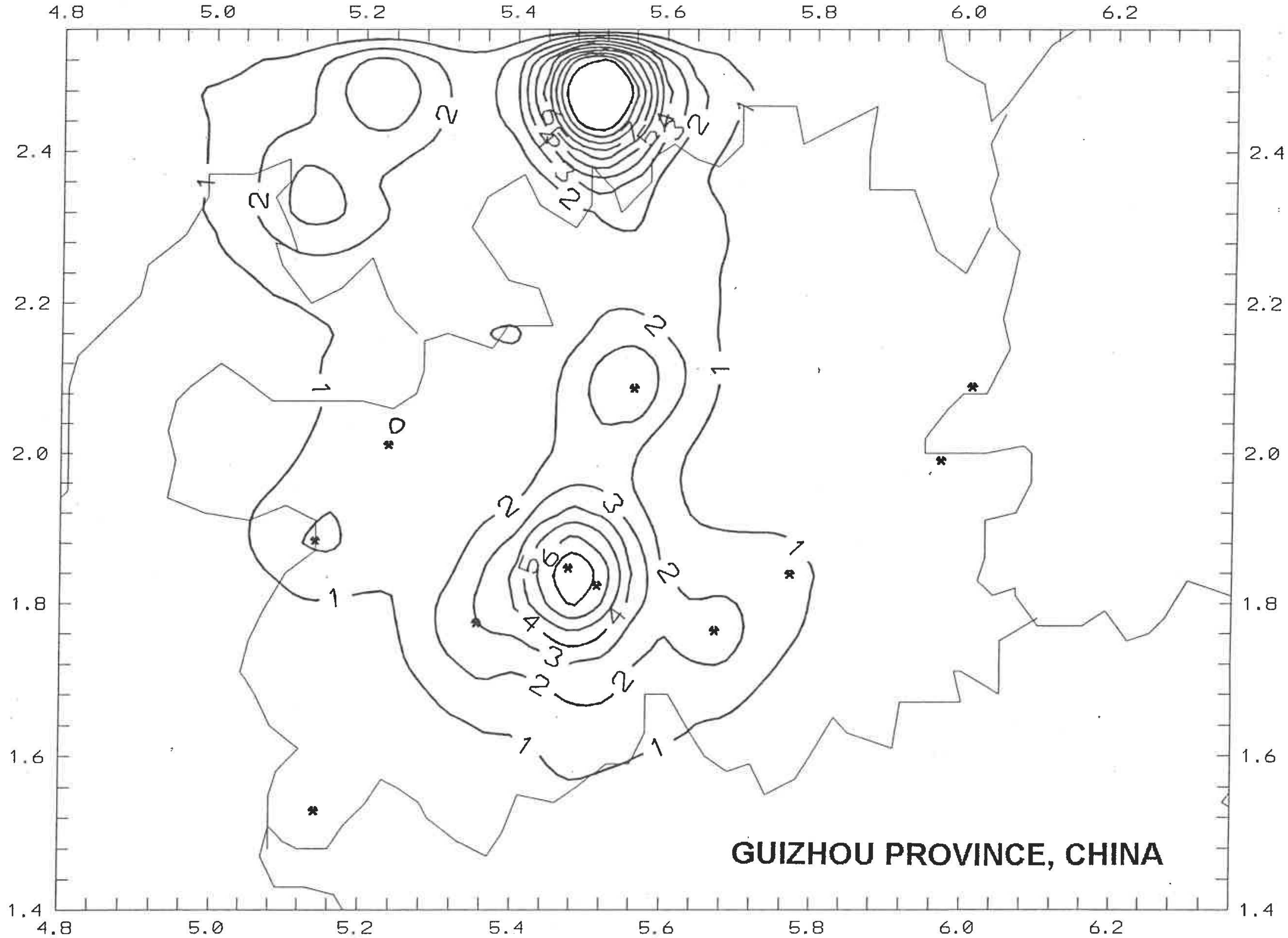

Figure 10

SO2 Concentration 2010 (µg/m3)

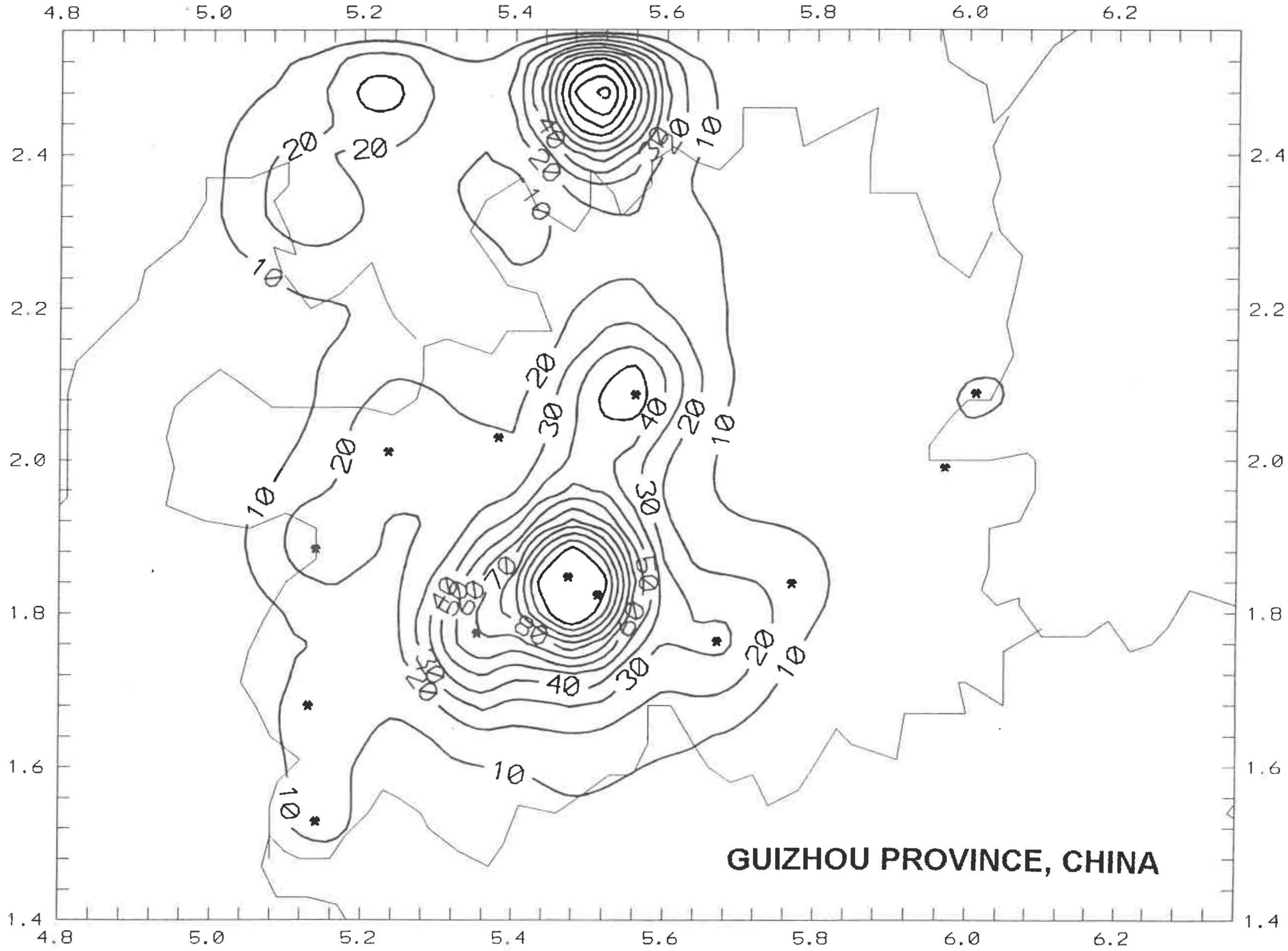

Figure 11

S Deposition 2010 (gS/m2/year)

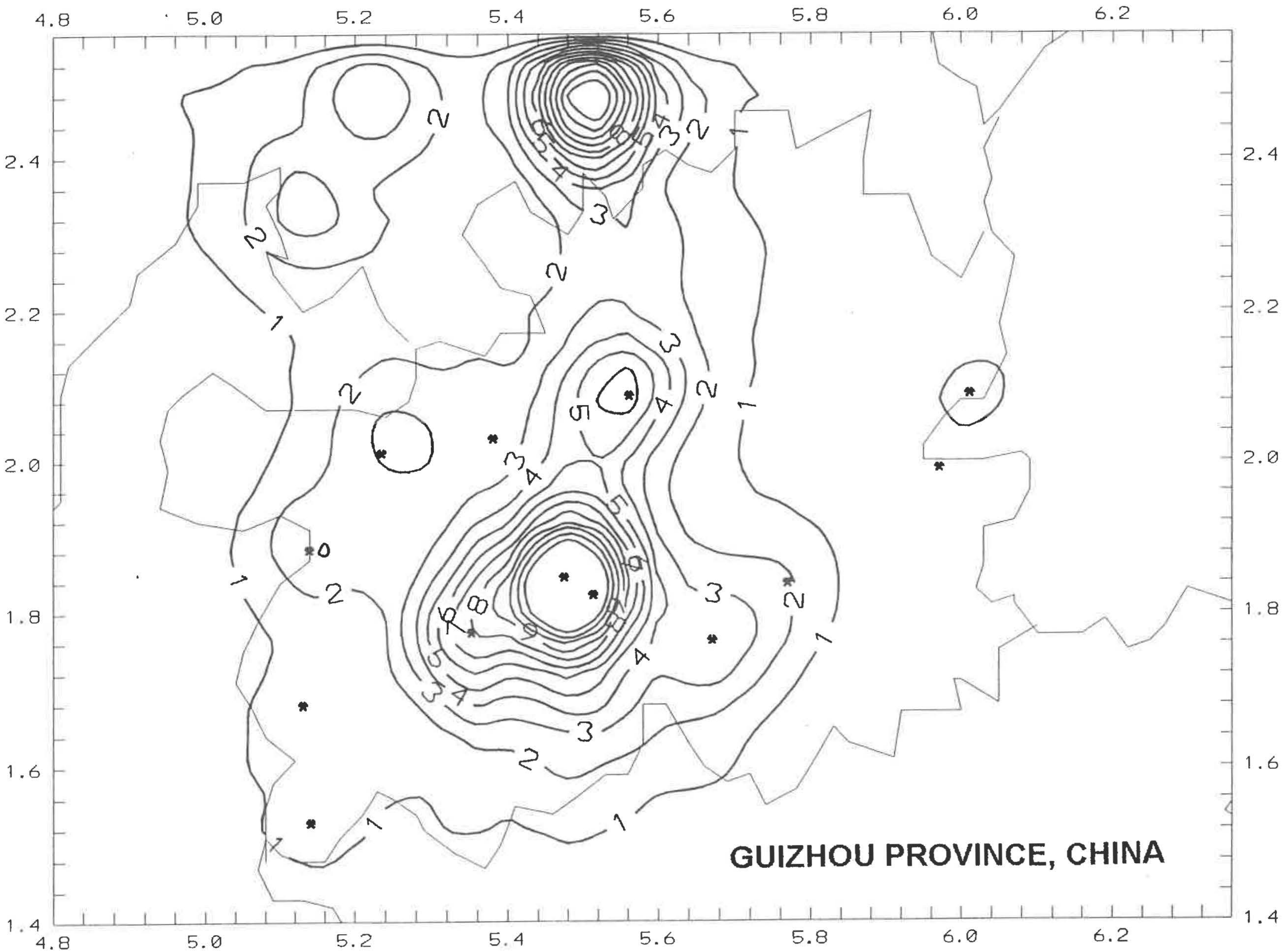

Figure 12

All, -50%

SO2 Concentration (ug/m3)

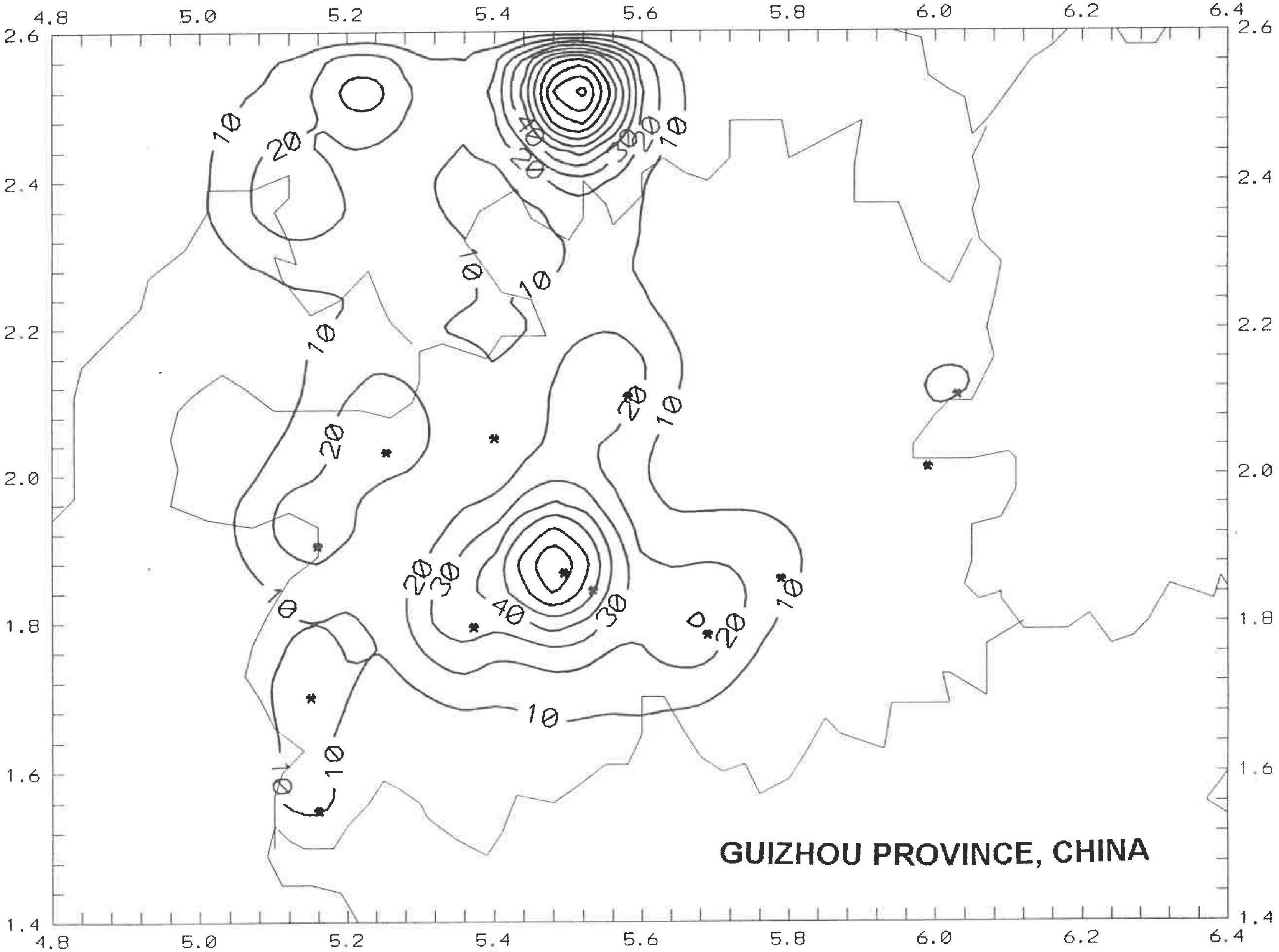

Figure 13

All, -50%

S Deposition (gS/m2/year)

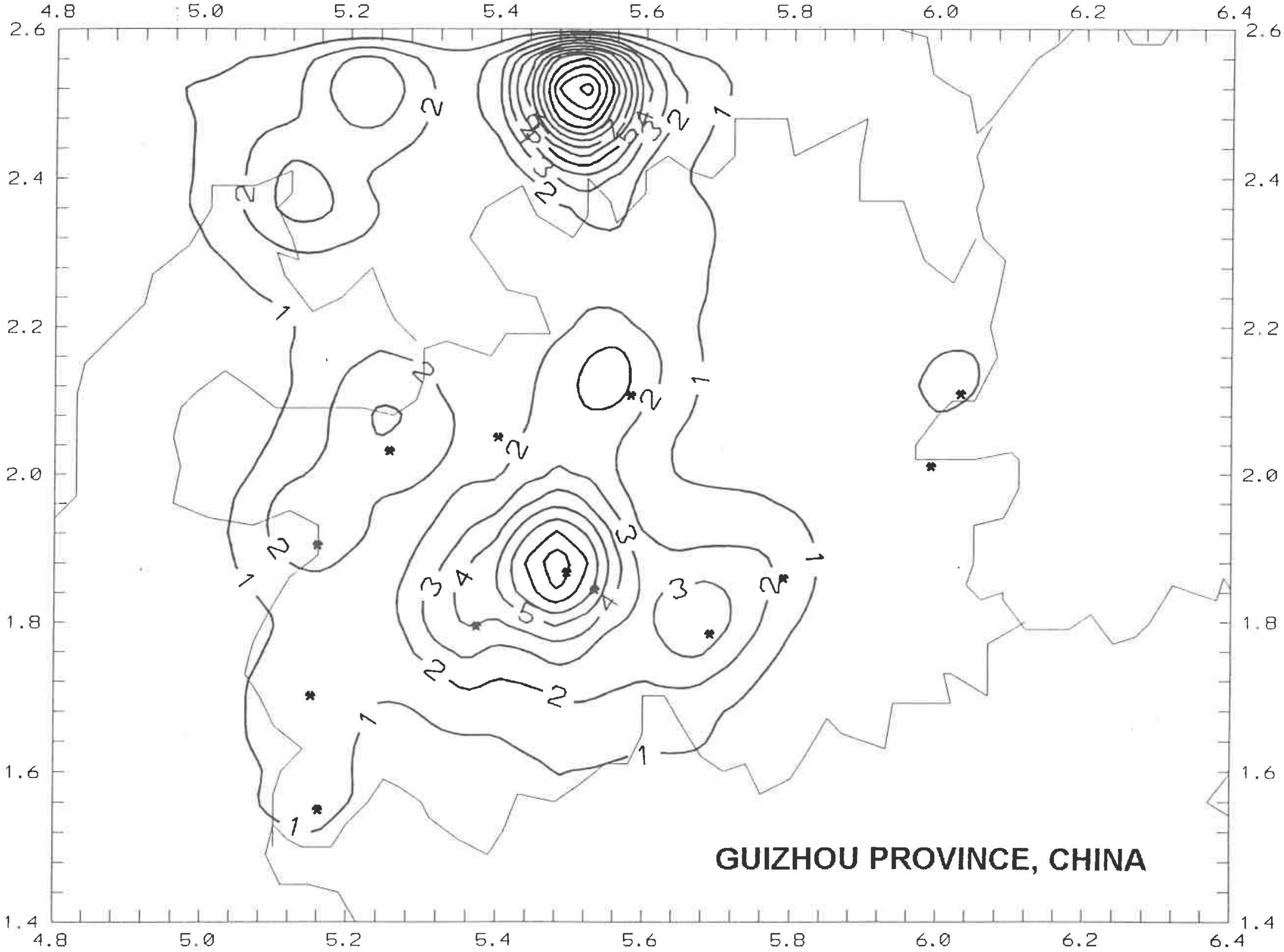

Figure 14

3 regions, -50%

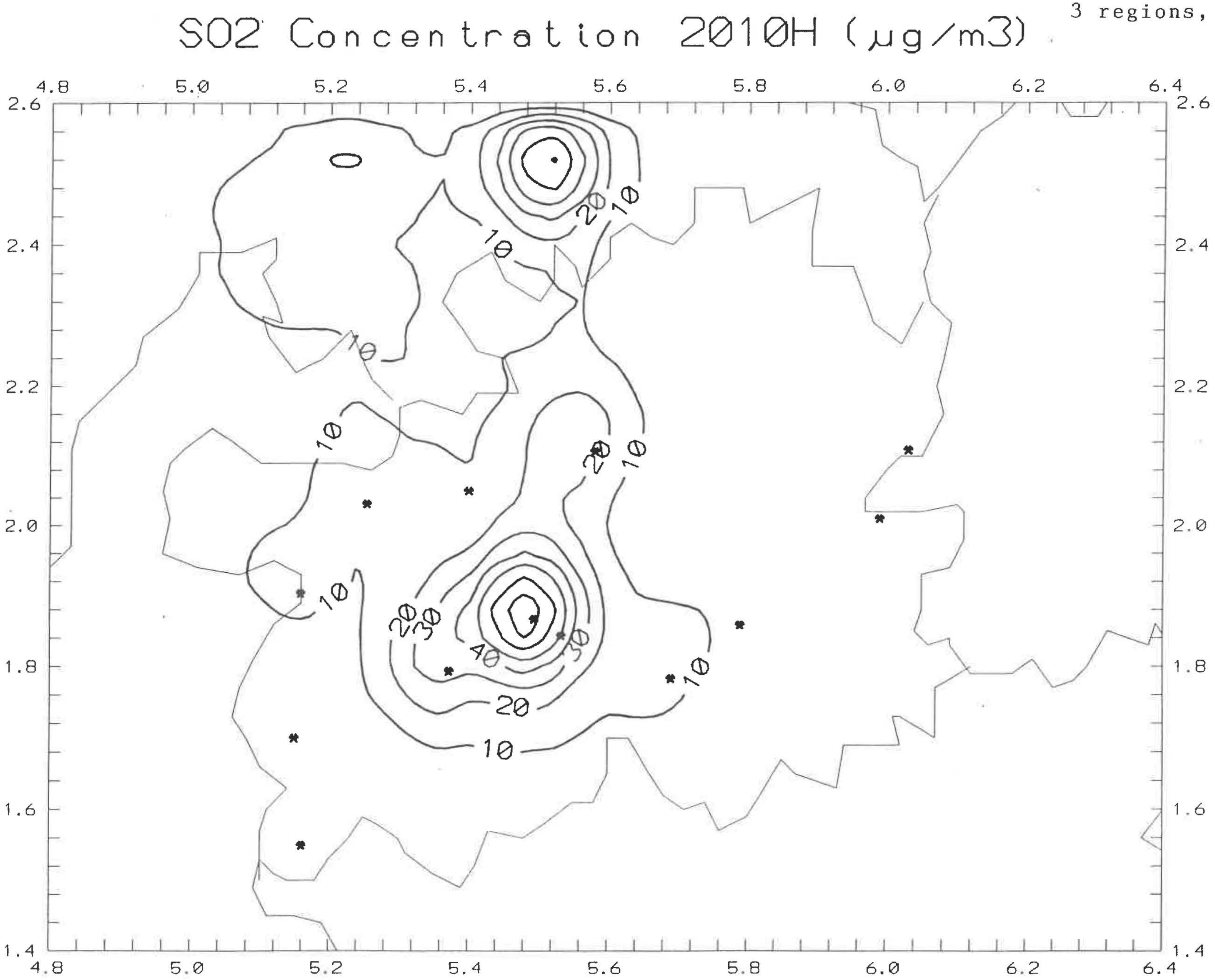

Figure 15

3 regions, -50%

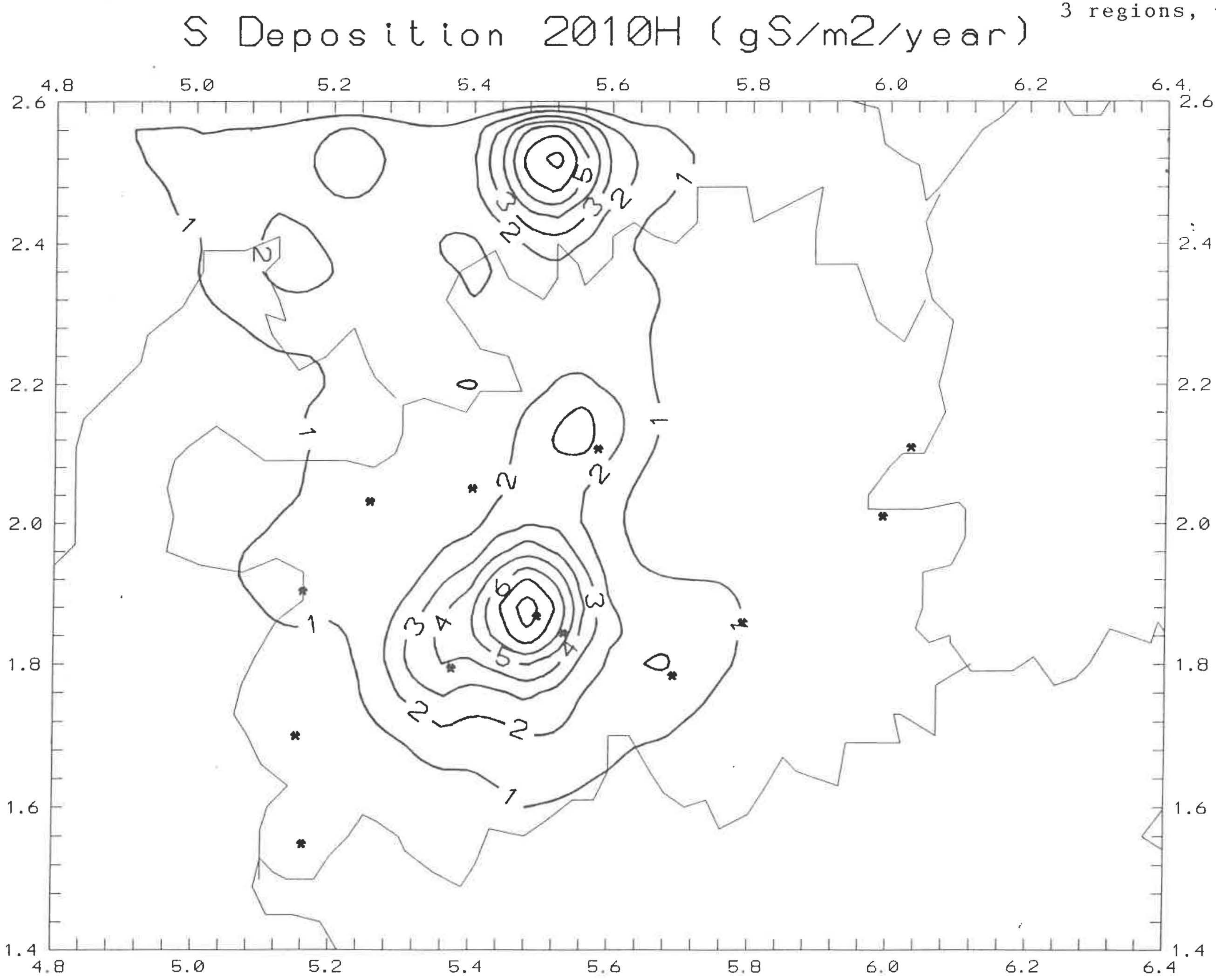

Figure 16

3 LPS moved

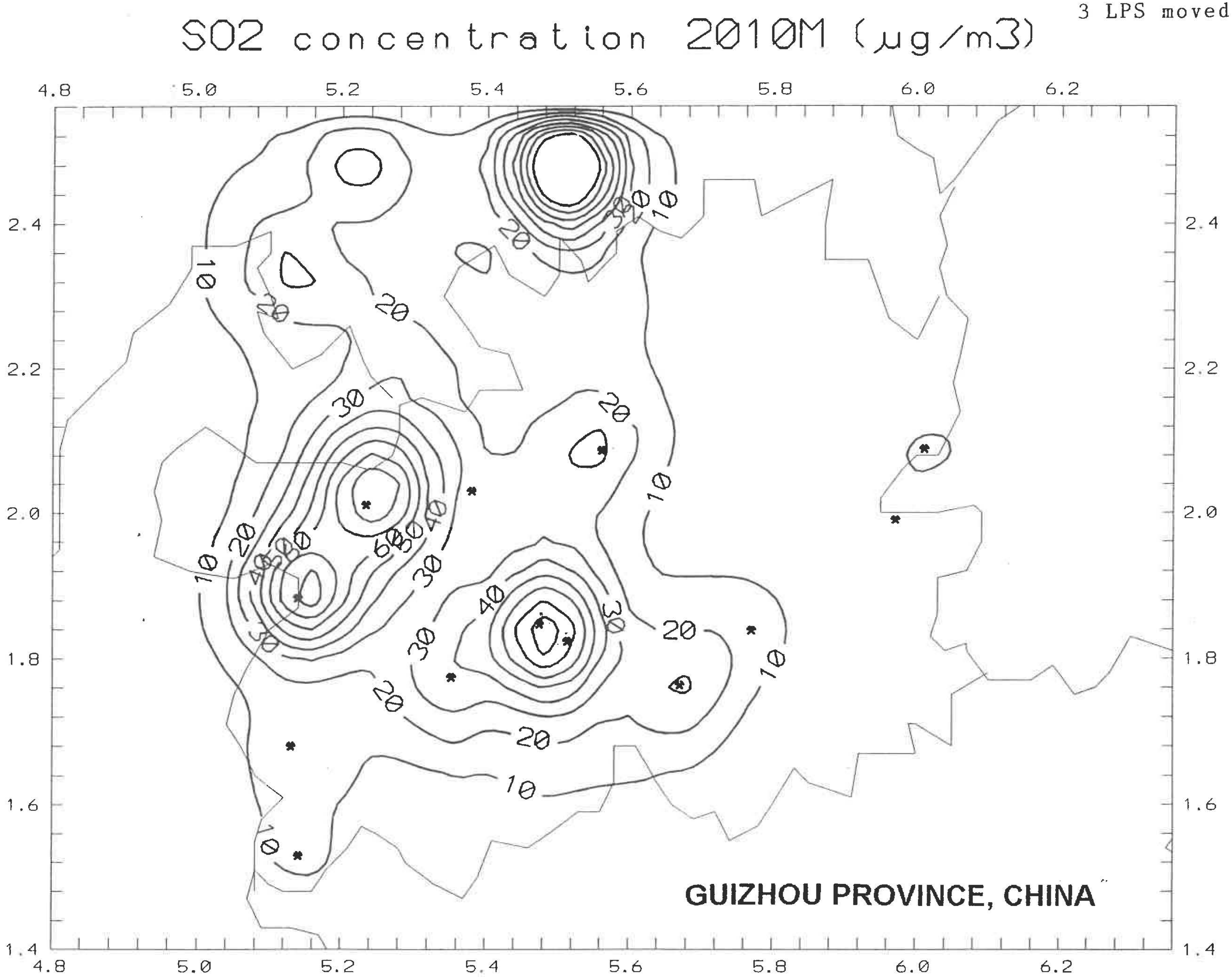

Figure 17

3 LPS moved

S Deposition 2010M (g/m2/year)

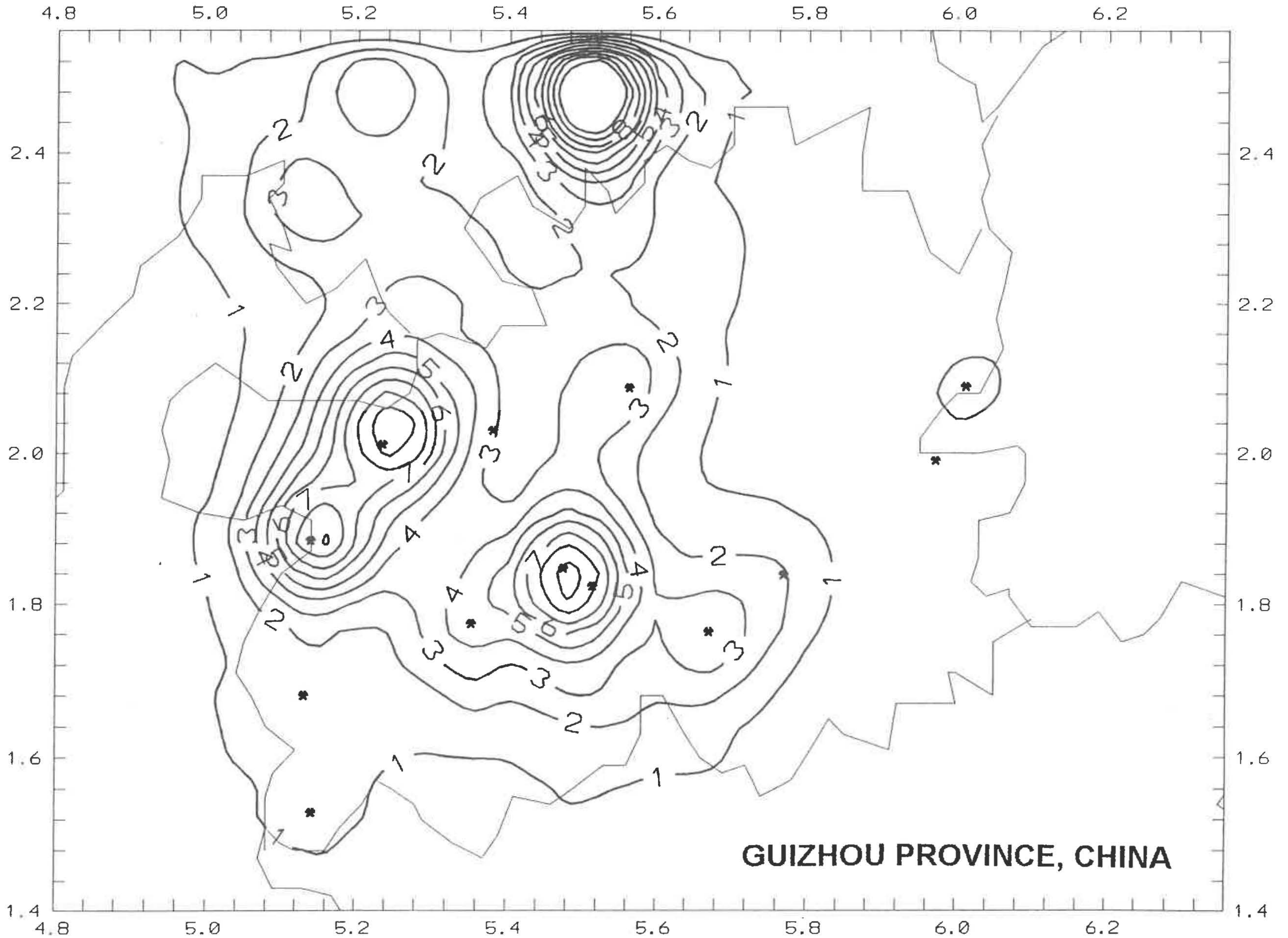

Figure 18

EXCESS TO CRITICAL LOAD (gS/m2/year) 1992

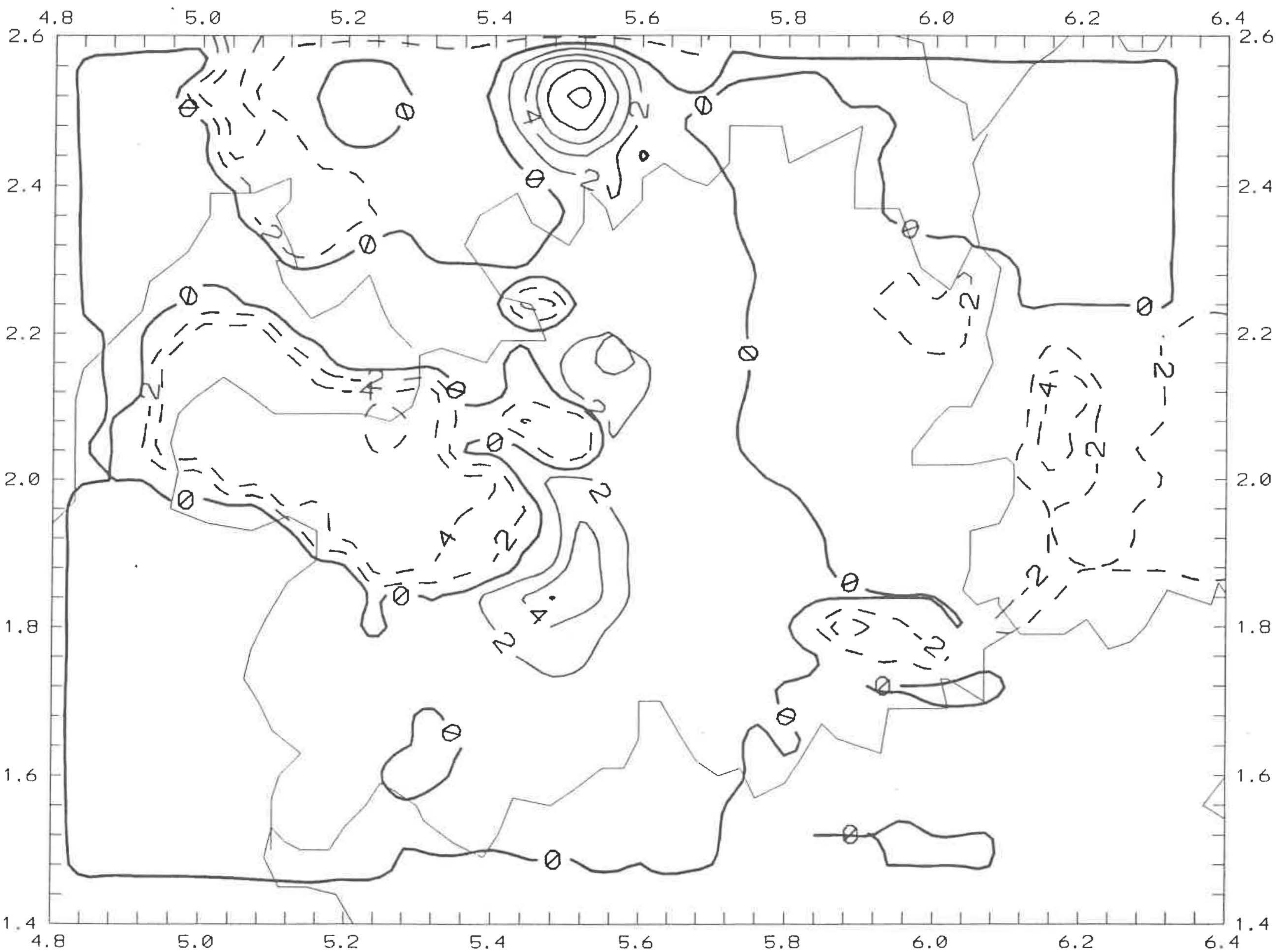

Figure 19

EXCESS TO CRITICAL LOAD (gS/m2/year) 2010

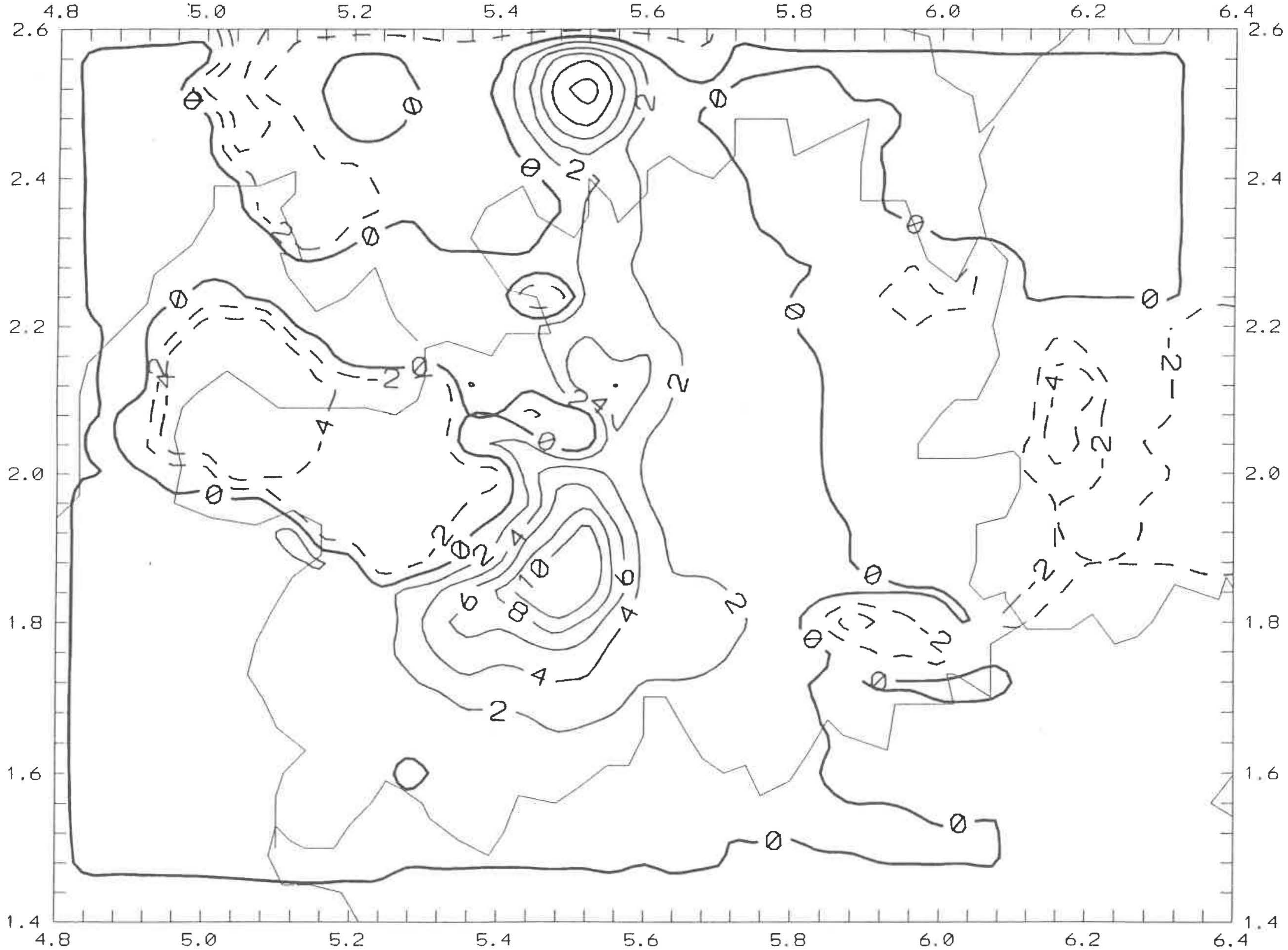

Figure 20

All, -50%

EXCESS TO CRITICLE LOAD (gS/m2/year)

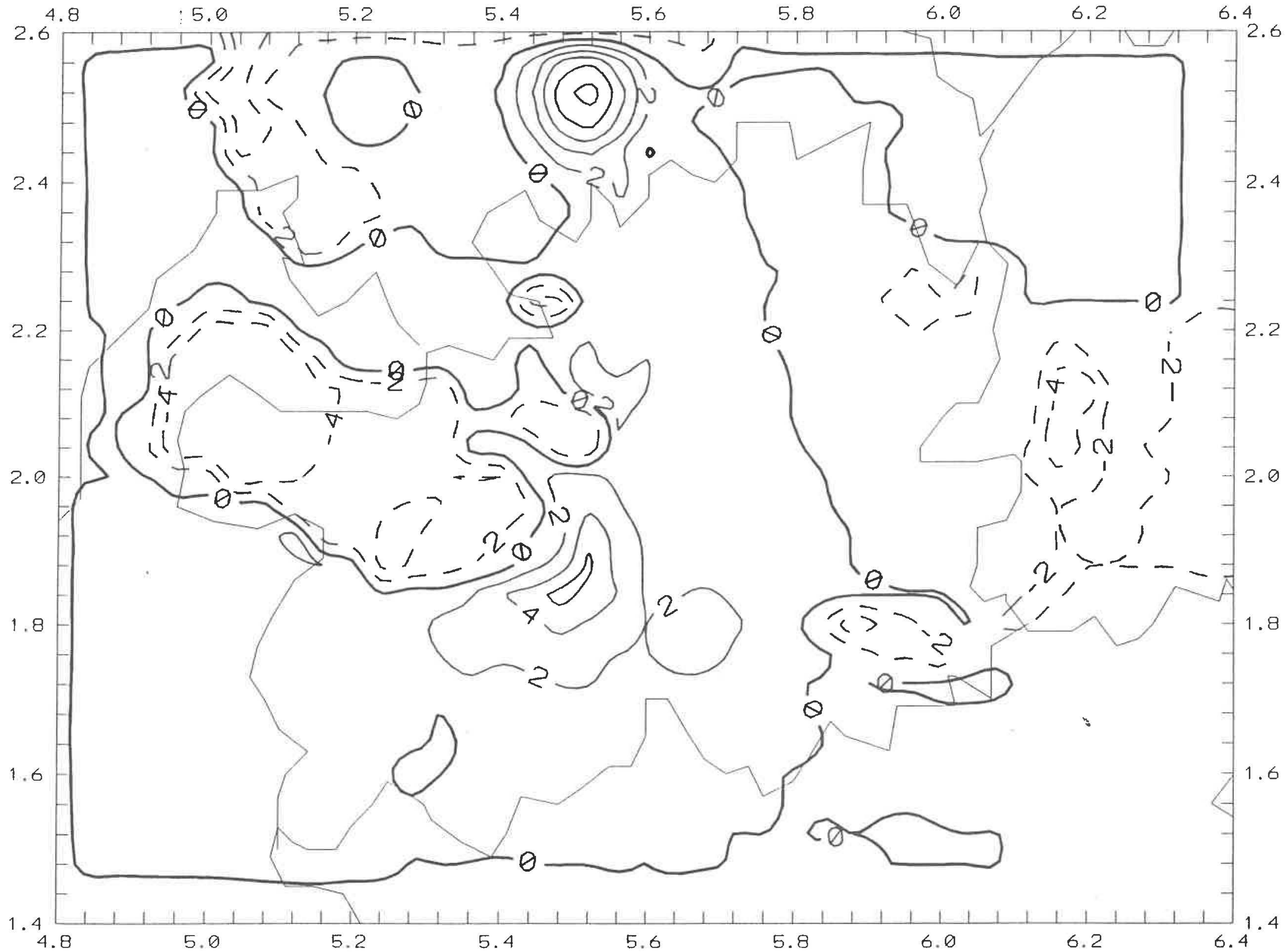

Figure 21

EXCESS TO CRITICAL LOAD 2010H (gS/m2/year) 3 regions,-50%

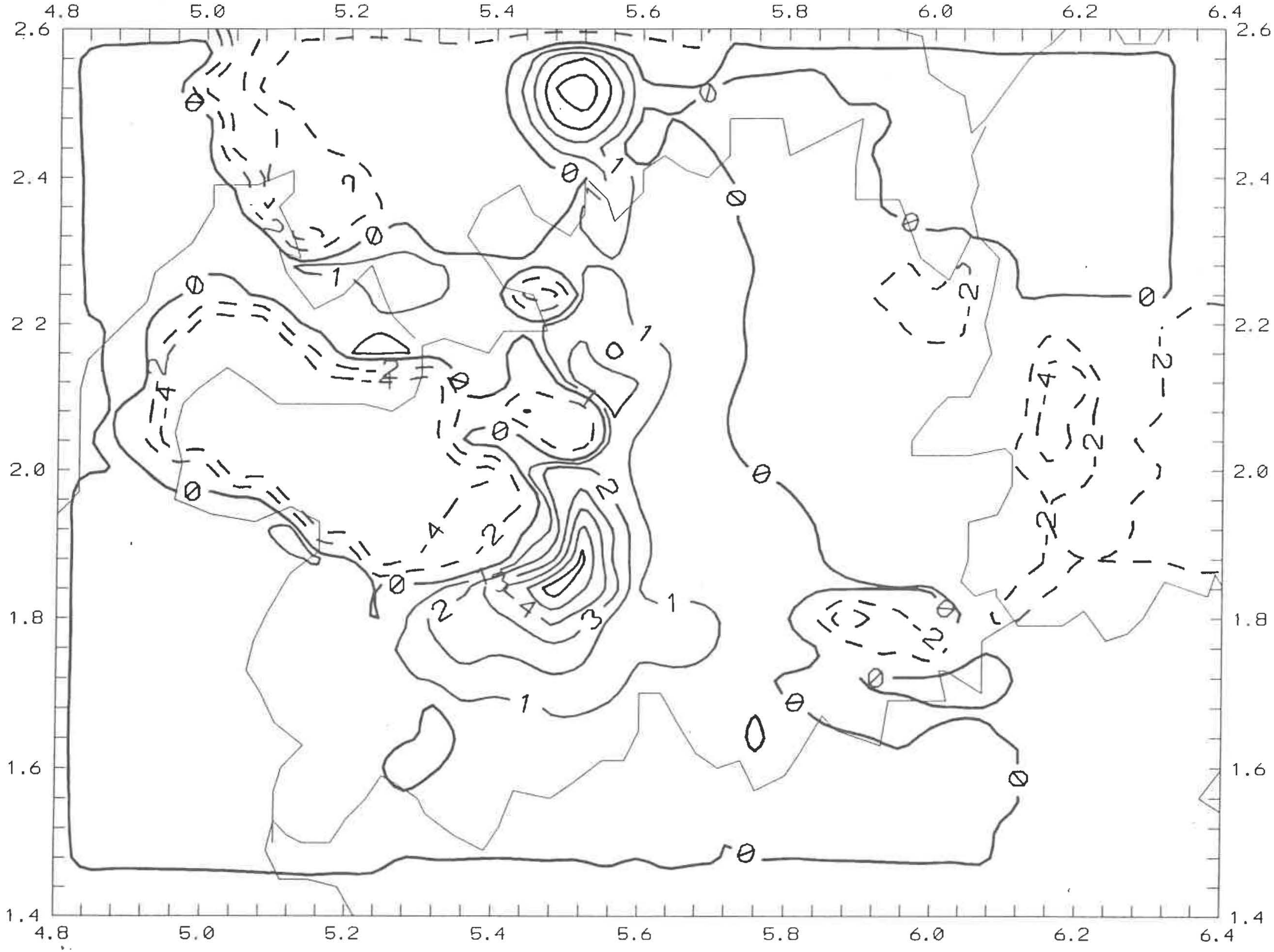

A4-38

Figure 22

EXCESS TO CRITICAL LOAD (gS/m2/year)

3 LPS moved

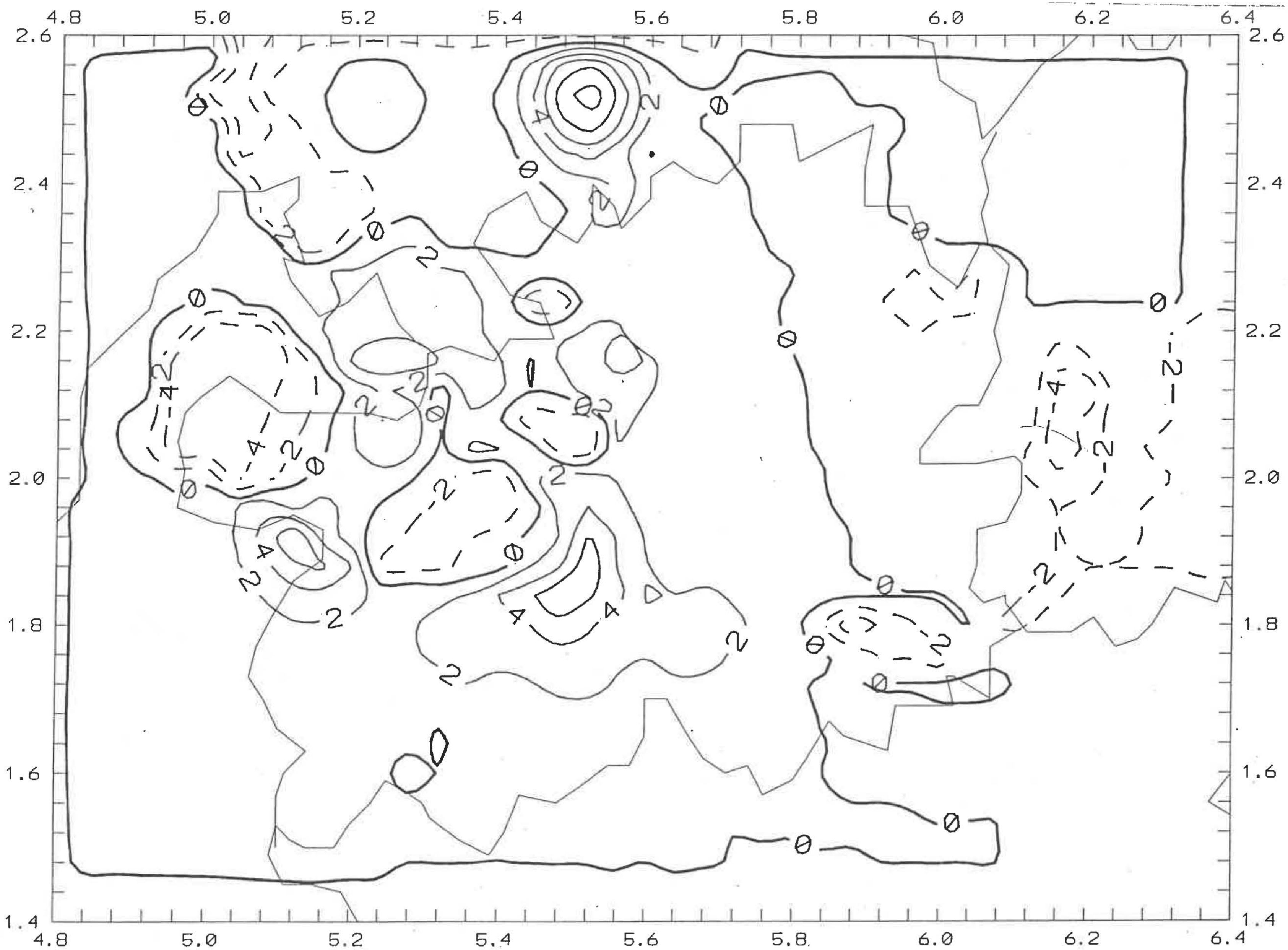

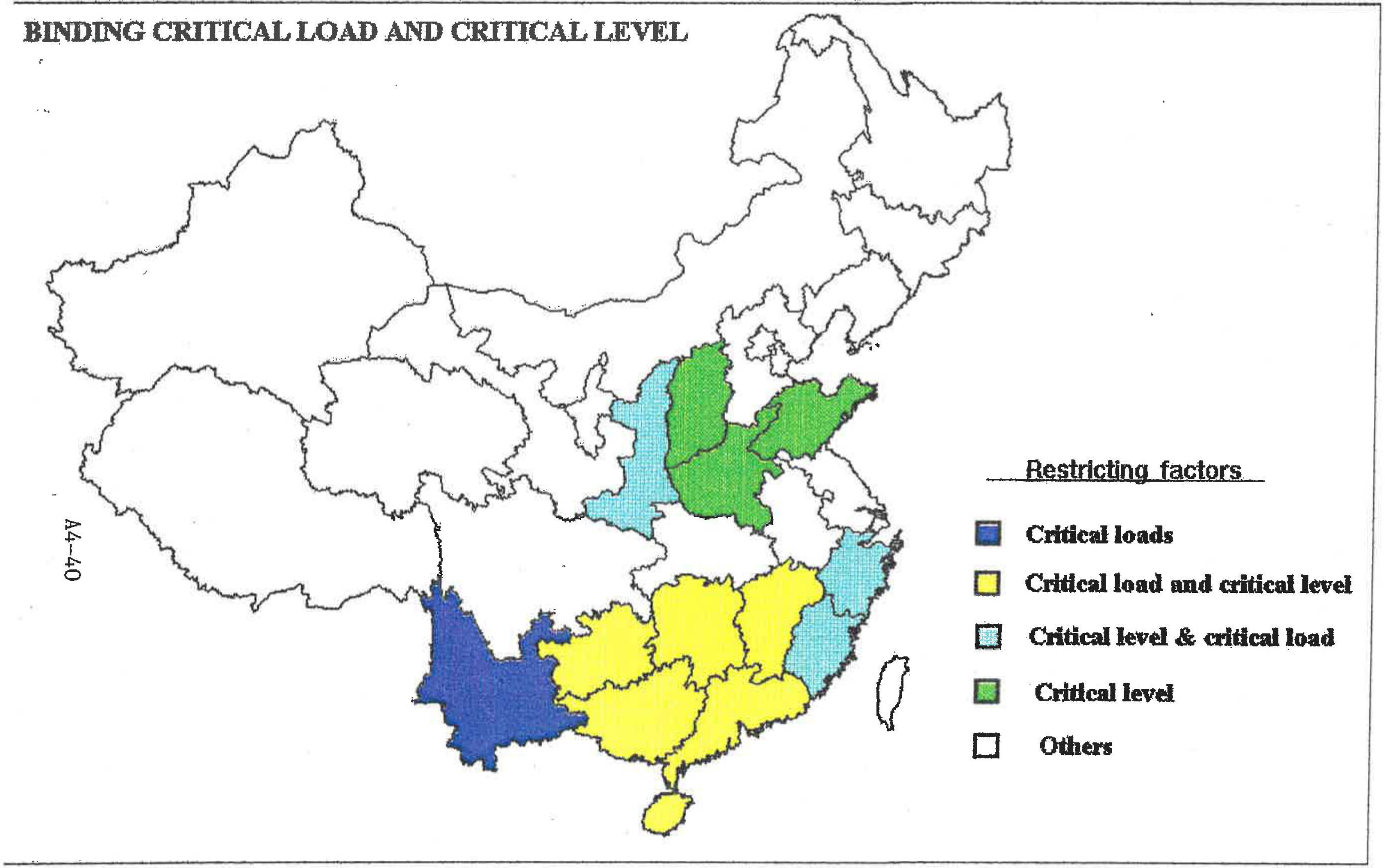
BINDING CRITICAL LOAD AND CRITICAL LEVEL
Restricting factors
Critical loads
Critical load and critical level
Critical level & critical load
Critical level
Others

ANNEX 5

SUMMARY REPORT OF THE IMPACT TASK MEETINGS
10-13 November 1992; 9-13 October, 1994
Research Center for Eco Environmental Sciences
Beijing China.

by
Jean-Paul Hettelingh, Ph.D.
Head RIVM-Coordination Center for Effects
P.O.Box 1, 3720 BA Bilthoven, The Netherlands
Tel. ..-31-30-743529: Fax 250740
email: jean-paul.hettelingh@rivm.nl

1. **Background**

The RAINS-ASIA project aims at the establishment of a national and regional policy analysis model for acid rain in Asia. The Regional Acidification, INformation and Simulation (RAINS) model for Asia enables the assessment of a variety of sulfur emission reductions schemes by investigating (1) energy demand and related SO_2 emissions, (2) atmospheric transport and deposition of SO_2, and (3) effects on vegetation-soil types. Three sub-projects, i.e. energy and emissions (ENEM), atmospheric transport (ATMOS) and environmental effects (IMPACT) are preparing the submodules of RAINS-ASIA.

The first phase of the RAINS-ASIA project, which is financed by the World Bank and the Asian Development Bank (ADB), has started in mid 1992. Evaluations of existing research material on acidification in Asia were made in yearly workshops organized at the Asian Institute of Technology (AIT) in Bangkok since 1989. These workshops established contacts between Asian and European institutes active in the field of energy and environmental sciences. These contacts are increasingly being strengthened by the organization of a network of Asian institutes.

For each of the three subprojects a network is built consisting of a Coordination Center (CC) and National Focal Centers (NFC). The tasks of the NFC's include verification, validation and improvement of the results obtained from a RAINS-ASIA submodule. The tasks of the CC is to help improve communication with and among NFC's about scientific methods and data and to help produce generalized Asian geographical representations of module results.

The Research Center for Eco-Environmental Sciences (RCEES) has been appointed Coordination Center for Effects in Asia. In collaboration with the National Institute of Public Health and Environmental Protection (RIVM) a second RAINS-ASIA impact meeting has been organized by RCEES in Beijing (China) from 9 to 13 October 1994. The first RAINS-Asia impact meeting was held from 10 to 13 November 1992. The last meeting gathered European and Asian scientists, most of whom also attended the first impact meeting The major aim of both meetings was to involve Asian scientists with the development of the critical load methodology, establish contacts between effect oriented scientists of Asian countries and review results of the impact module, i.e. critical load maps and critical load distributions. The focus of the first impact meeting is summarized below:

a. Provide guidelines and criteria for the identification of (potential) National Focal Centers: National Focal Centers could include (i) centers with knowledge of ecosystem or soil sensitivity to pollutants in general and to acid pollution in particular (ii) geological survey centers (iii) environmental research institutes. Most importantly should potential institutes be willing and able to organize a local network of scientists specialized in areas which are relevant to environmental impact assessments. Such areas include meteorology, biology, hydrology, environmental chemistry, and others involved in the investigation of the pathway of (acid) pollutants from their sources through the environment.

b. Agree on methodologies for the estimation and assessment of the sensitivity of ecosystems in Asia and Asian countries: The sensitivity of Asian ecosystems to acid pollution can be established using quantitative and semi-quantitative methods. Quantitative methods apply mathematical models (e.g Steady State Mass Balance; MAGIC; PROFILE etc.) and other methods (Method of Relative Sensitivity) for the computation of critical loads and assessment of ecosystem sensitivity. A critical load is interpreted as the value of deposition below which no damage (i.e. changes of the chemical balance) will occur to a soil-ecosystem combination.

c. Provide insight in available data: An overview of currently available data to be used in both methods is presented to allow for preliminary evaluation

d. Establish a plan of action for the current and further work: A workplan is made For (i) the incorporation of the involvement of NFC's in the project, (ii) dissemination of geographical maps of background data, maps of preliminary critical loads and sensitivity (iii) identification of NFCs, and (iv) a second IMPACT meeting.

The objectives of the first meeting were met to a satisfactory extent. An active involvement of National Focal Centers should be improved for example by the installation of Geographical Information Systems at the NFC sites.

The objectives of the second impact meeting were chosen to be a logical follow up of the goal of the first meeting.

2. **Objectives of the second impact meeting**

Objectives of the second RAINS ASIA impact meeting included:

1. A scientific discussion about the importance and relevance of environmental effects in general and indirect and direct effects in particular: Attention was given to the potential risk of exceeding a critical load for an extensive period of time in comparison to the immediate risk of having too high air concentrations of SO_2 (i.e. exceeding critical levels). It was the general opinion that current damage found in China was most probably related to exceeding air concentrations. The need was expressed to include critical levels for vegetation and crops in future work of a potential second phase of the project. It was recognized that damage that is currently found due to concentration excess can be considered an early warning for the more important, because irreversible, damage which may occur due to critical load excess.
2. A detailed review by Asian specialists of the current RAINS-ASIA IMPACT results:

Geographical displays and a data diskette of the results of the RAINS-ASIA impact work were sent to participants for their review before mid August 1994. The results were found to be in accordance with current expectations of the distribution of sensitive areas and ecosystems. However, it was stressed that future work would have to include funded participation of national scientists to verify the results in the field.

3. Demonstration and training of the RAINS-ASIA model: A full day was dedicated to enable scientists of becoming familiar with the RAINS-Asia model. The session consisted of a demonstration given by IIASA followed by hands on participation of the workshop attendants. The demonstration and use of the model was welcomed with great enthusiasm. It lead to discussions between participants of the causes of excess of critical loads and increased awareness of the importance of long range transport of SO2.
4. An inventory of the future work that country participants expect to undertake and the funding requirements.: In view of future work a call was made for research program requirements which National Focal Centers could take on in the future support of RAINS Asia impact work. Proposals were requested in writing and in relation to continuation of the project. Until now only Vietnam has responded (December 1994). All countries will be prompted for a follow up as soon as the future of the project becomes more transparent.

3. Overview of presentations and the critical load methodology at the second meeting.

The opening of the meeting included an overview of the objectives of the RAINS-Asia impact module and its results. These results were made available to the participants in advance in the form of maps and a data diskette. GIS software was used on the spot to allow insight in background data used to compute critical loads. Special attention was drawn to the regional distribution of sensitive areas in relation to the actual vegetation. With respect to the assumptions behind the critical load computation a presentation was given about the relationship between the base cation to aluminum ratio and growth reduction.

Following these general presentations the floor was given to national presentations.

Zhao, Xiong and Yang (China) presented the importance of air concentrations for damage assessment. It was concluded that the inclusion of critical levels in addition to critical loads should be an important focus of the RAINS-Asia impact module follow up. The Chinese presentation also included a comparison of different methods for the computation of critical loads and the temporal analysis of base cation to aluminum ratios as function of deposition scenarios. The Chinese paper is included as Annex 4 to the final report.

Shindo (Japan) presented, for a region in Japan, the results of a comparison between different mathematical formulations of critical load models which have been developed, mainly in Europe, over the past decade. A choice was made for one model which was expected to be best applicable in Japan (see Annex 3). It was concluded that the current RAINS-Asia impact model reflected the requirements for Japan.

Ahmad (Bangla Desh) showed results of recent investigations into the importance of humic acid to root systems. It was carefully suggested that the indirect effect of acidity could become a cause of concern for future yields.

Gian (Vietnam) stressed the importance of large point sources for the excess of environmental quality thresholds. Emphasis was given to the exorbitant air concentrations of

SO2 which exceed WHO air quality guidelines by far. The conclusion was that further investigation of the importance of effects due to air concentrations (direct effects) was required in addition to the current emphasis on indirect effect. It was obvious that concern for human health exceeds the importance of environmental thresholds. It was pointed out that the need for application of appropriate abatement techniques is stepped up as far as current resources in Vietnam allow.

Kahn (Pakistan) presented a literature overview of the importance of direct effects in general for different pollutants. The conclusion was that a pollutant such as ozone may prove to be of great additional importance in explaining the causes of currently identified damage to i.e. crops in Asia. The conclusions were supported by other scientists at the workshop.

4. Conclusion

The main conclusions of the workshop, as described above, can be summarized as follows:

a. There is need to extent the application of critical loads (sustainable threshold above which indirect environmental effects occur) with critical levels (sustainable threshold above which direct effects may occur).
b. There are indications that currently found damage to vegetation (e.g. crops in China; a picture was shown) is due to direct effects which are related to episodic peaks of air concentrations of SO_2.
c. There was consensus over the hypothesis that episodic damage due to exceeding air concentrations should be considered an early warning for the potential risk of soil chemical changes (indirect effects) due to the excess of critical loads in the long run.
d. The current maps of critical loads as included in the RAINS-Asia module are state of the art. Further improvement by national contributions based on carefully designed field work should be included as an aim for future continuation of the project.
e. The RAINS-Asia model was generally concluded to be an excellent tool to enhance scientific collaboration on Long Range Transboundary causes of current changes of environmental quality. The hands on training proved to be an excellent mechanism to stimulate discussions on air pollution and critical loads.
f. The need was expressed for National Focal Centers to become more acquainted with Geographic Information Systems (GIS). The installation of GIS soft and hard ware at NFC-sites would improve the exchange of information (i.e. maps) with respect to environmental effects in Asia.
g. Participants were requested to formulate a proposal for further NFC involvement in a future RAINS-Asia continuation.